Palaeozoic Ammonoidea:
Ontogeny, Hydrostatics, Palaeoecology and Stratigraphy

Dissertation

zur

Erlangung der naturwissenschaftlichen Doktorwürde
(Dr. sc. nat.)

vorgelegt der

Mathematisch-naturwissenschaftlichen Fakultät

der

Universität Zürich

von

Carole Meier

aus

Frankreich

Promotionskommission

Prof. Dr. Christian Klug (Leitung der Dissertation)

Prof. Dr. Hugo Bucher

Dr. Kenneth De Baets

Zürich, 2018

This PhD thesis is dedicated to my four grandparents:
Françoise and Valentin Naglik,
Henriette and André Albert

View of the northern flank of the Devonian Bursykhirman Mountain, from the Geological Reserve of Kitab, Uzbekistan. This picture was taken during the field investigations of 2012

"I tell you folks
It's harder than it looks
It's a long way to the top…"
(AC/DC 1975)

Contents

ACKNOWLEDGEMENTS

ACKNOWLEDGEMENTS

First, I would like to thank my supervisor Prof. Dr. Christian Klug (Zürich) for his support, his kindness and patience. I would have never been able to complete this dissertation without his enthusiasm and encouragements. He found the right words when I was at my worst and put me back on tracks. I greatly appreciate all the discussions we had, I have learned a lot on many scientific topics but also about various other subjects.

I am grateful to Kenneth De Baets (Erlangen) who helped me a lot when I started my PhD, who shared his experience in the field in Uzbekistan with enthusiasm, and who spent some extra-time at the end to discuss a lot about our article related to Uzbekistan.

I would like to thank Prof. Dr. Hugo Bucher also in my PhD committee for sharing his knowledge and providing interesting discussions during my PhD.

I am grateful to all the colleagues I have met through all along this enriching experience that constitutes my PhD, especially:

- Dieter Korn (Berlin): I would not have applied to this PhD if I did not have the chance to meet him in Berlin in 2010. I thank him for his encouragement to contact Christian Klug at that time.
- Claude Monnet (Lille I) for is huge help with 3D modelling when I started my PhD and later for interesting scientific discussions and help about the Unitary Associations method.
- Dominik Hennhöfer and Enric Pascual Cebrian (Heidelberg) for their help with grinding tomography.
- The Uzbek colleagues Utkir J. Rakhmonov, Firuza Salimova, Natalya Meshchankina and all the people we met there, for their kindness, hospitality and help during our fieldwork in 2012.
- Rene Hoffmann (Ruhr-Universität Bochum) for great improvements of my manuscripts before their publication and for sharing his expertise in 3D-modelling.
- Sebastien Clausen (Lille I) for his encouragements to start a PhD, bringing me in contact with Dieter Korn, and for helping me later with logistics to get thin sections.
- David Ware (Berlin) who shared his great knowledge on ammonoids, for the great scientific discussions in too many fields to be listed here, and also for being a good friend, with whom I had disputes but also great conversations.
- Nicolas Goudemand and Severine Urdy (Lyon) for their scientific advice, which helped me a lot when I started, and for their encouragements, kindness and support when I encountered some hard times.
- Alik Huseynov (Max Planck) and Farhad Rikhtegar (MIT) whom I met in Zürich (UZH/ETH) and who helped me with the 3D software, and who provided access to work stations.
- Markus Hebeisen and Jérôme Gapany (PIM Zürich) for being very friendly and helpful with work-related issues.
- Heike Götzmann and Heinrich Walter (PIM Zurich) for great help in solving administrative and technical problems I encountered.
- All the professors, Postdocs and technicians from the PIM for sharing their knowledge with me.

I would like also to thank all my PIM fellows that I met during my PhD and shared very good times with me: it was a great pleasure to get to know Linda and Christian Kolb and I hope to see them again later; especially Amane, Borhan and Thodoris helped and supported me during the

last weeks of my PhD; they kept me motivated. I greatly appreciate their support and availability to answer administrative questions; I hope to stay in touch.

Moreover, I would like to thank my "Ch'tis" friends Benjamin, Aurélien, but also Léa and Gaël (Boy) for their true friendship we carry on even though we are all distributed over different countries, as we are *so close, no matter how far*… They inspired me to retrieve my motivation to finish my dissertation.

I am very grateful to my family, my brothers Olivier and Vincent as well as my parents who always supported my choices, even when I decided to leave them for Switzerland. I thank them for their help, their kindness, their patience and love, they always believed in me even when I was down.

Finally, I am deeply indebted to my husband Max and my lovely daughter Elizabeth. They supported me with love and endless patience. It has been sometimes hard, but they really empowered me to ensure the completion of my thesis…

FUNDING

The completion of this dissertation would have been impossible without the financial support of the Swiss National Science Foundation (Project numbers 200020_132870 and 200020_149120).

ABSTRACT

ABSTRACT

In Phanerozoic sedimentary rocks, fossils document many important evolutionary and macroecological events that shaped today's ecosystems. Among the Palaeozoic periods, the Devonian (419.2 ±3.2 Ma to 358.9 ± 0.4 Ma) was a time of major changes and evolutionary innovations both in marine and terrestrial life. Concerning the marine realm, new cephalopod groups such as the ammonoids and bactritoids appeared during the Early Devonian. Phylogenetically, the bactritoids are important because they represent the stemgroup of both the Ammonoidea and the Coleoidea (squids and octopuses). The ammonoids were widely distributed, highly diverse, abundant in many localities and had high evolutionary rates, which is reflected in their great morphological disparity. Moreover, their conchs grew by accretion, thereby producing a record of their entire ontogeny. All these aspects make ammonoids an important group for stratigraphic and evolutionary studies. For this thesis, both classical methods (systematic descriptions, stratigraphy) and state-of-the-art methods such as tomographies were employed.

In the first parts of this thesis (Chapters I and II), I present pioneering research on how empirical volumetric data of ammonoid conchs obtained from tomographic data can yield new palaeobiological information about ammonoids. Three-dimensional models of several specimens were reconstructed using grinding tomography. Based on these models, the ontogenetic growth of chamber and septal volumes are documented and compared among three major Palaeozoic ammonoid clades, namely the agoniatitid *Fidelites clariondi*, the anarcestid *Diallagites lenticulifer* (both Middle Devonian) and the goniatitid *Goniatites multiliratus* (Early Carboniferous). These volumetric data have also been plotted against usual 2D conch parameters, which are traditionally used as proxies for growth. I discovered a good correlation between 2D and 3D measurements. Concerning the record of growth stages, mature modifications are well reflected in the ontogenetic trajectories of the examined 3D parameters whereas data from early ontogenetic stages are poor due to the insufficient voxel-size and recrystallization.

In addition to the documentation of conch growth, hydrostatic properties of these three ammonoid species were reconstructed. Using the volumetric information in combination of known and estimated values of the various body and shell parts, aperture orientations were reconstructed. Accordingly, their conchs were oriented differently from the living *Nautilus*, which can be explained by different conch geometries. Remarkably, my results agree with previous published mathematical models, which, in turn, were tested with living *Nautilus*. These mathematical models, established some decades ago, suggested for example that the longer the body chamber, the poorer was the hydrodynamic stability of the animal. These results have implications concerning the reconstruction of the modes of life of the extinct ammonoids. These results were also included in a review of ammonoid locomotion, which was included in the the book *Ammonoid Paleobiology* (Chapter III).

In the last part of my thesis, I present a study of the most diverse early Emsian ammonoid faunas from the Zeravhan-Gissar Mountains in Uzbekistan (Chapter IV). In the Kitab State Geological Reserve in this region, the transition from a late Pragian reefal facies to an early Emsian pelagic facies rich in dacryoconarids and ammonoids is well exposed. I documented facies changes of this stratigraphic interval in order to better understand the regional geological processes. Sedimentological analyses of two ammonoid-bearing localities were carried out, mainly in the Dzhaus Beds (late Emsian, *inversus* zone).

In addition to this sedimentological study, the highly diverse ammonoid assemblages were analysed. In the sections of the Kitab State Geological Reserve, a faunal turnover of ammonoid species was documented, which is consistent with the base of the *cancellata* dacryoconarid Zone (traditionally used to define the base of the Daleje Event, a phase of global sea – level rise). The palaeobiogeographically peculiar situation of Uzbekistan is also discussed by comparing the composition of the Uzbek ammonoid assemblages with coeval assemblages from Central Europe and South China. Remarkably, many species found in the Kitab State Geological Reserve are endemic. Some new taxa have been introduced after revision of the cephalopod fauna. A first cluster analysis suggests that there are closer palaeobiogeographic affinities to Europe, while a closer look at some of the ammonoid species reveals great similarities with South China. In the future, South Chinese and Vietnamese Emsian ammonoid localities should be investigated in greater detail to compare the taxa in these regions with those of Uzbekistan.

Concerning volumetric studies, more specimens from other clades should be investigated in the future in order to further our knowledge of growth processes, hydrostatic and hydrodynamic properties of ammonoid conchs across all major clades and conch morphologies. For example, buoyancy and hydrostatics of heteromorph ammonoids could be examined through ontogeny in order to better understand changes in their mode of life through their life history.

INTRODUCTION

Palaeozoic Ammonoidea: Ontogeny, Hydrostatics, Palaeoecology and Stratigraphy

INTRODUCTION

During the Phanerozoic, several major evolutionary and macroecological events occurred, that shaped modern ecosystems. In the Palaeozoic for example, the "Cambrian Explosion" (Morris 1989), the "Great Ordovician Biodiversification Event" (Webby et al. 2004) and the "Devonian Nekton Revolution" (Klug et al. 2010) belong to the most important pulses of increases in biodiversity. These events are developed further herein. Understanding the complex mechanisms and interactions between faunas/ floras and their environment is nowadays a central topic of research in biology (from the origin of life to today) since it is widely accepted that we are now facing a new mass extinction (Barnosky et al. 2011 and references therein). Three of the five most important mass extinction events took place in the Palaeozoic (Raup and Sepkoski 1982; Alroy et al. 2008 and references therein; Fig.1).

In order to correctly analyse the nature of such extinction events and particularly the ongoing loss of biodiversity, it is of great importance to understand how extinctions affect organisms and which taxa may play central roles in their course. Moreover, comprehending the rediversification of biota and the involved evolutionary processes is crucial. In order to carry out such research, the autecology of the involved organisms needs to be assessed.

Consequently, I aimed at contributing to the increase in knowledge about the origination, evolution and palaeobiology of an important extinct group. I chose ammonoids because they are abundant, diverse and played an important role in Palaeozoic as well as Mesozoic food webs.

In particular, I studied growth, conch geometry, buoyancy and hydrostatic properties of some representative Palaeozoic ammonoids. I carried out most of this research employing tomographic data. Although the methodology itself is not new, it represents pioneering work when it comes to ammonoid palaeobiology. My 3D-models are based on image stacks obtained by serial grinding tomography (Naglik et al. 2015a, 2015b; Chapters I and II). With these data, I could reconstruct shell and chamber volumes, which in turn allowed me to assess ammonoid buoyancy, hydrostatic and hydrodynamic properties.

Additionally, I contributed two chapters to the new edition of the book *Ammonoid Palaeobiology*. One of the chapters is dedicated to the topic "Ammonoid Locomotion" (Naglik et al. 2015c; Chapter III).

I co-authored two additional chapters on "Describing Ammonoid Conchs" (Klug et al. 2015; Appendix I-A) and "Ammonoid Buoyancy" Hoffmann et al. 2015; Appendix I-B).

In chapter IV, I documented the sedimentology and ammonoid stratigraphy of the early Emsian in the Kitab area in Uzbekistan.

In parallel to my main PhD projects briefly listed above, I collaborated with several colleagues on their own projects such as the 3D – reconstructions of the Jurassic ammonite *Normannites* (Tajika et al. 2015a – Appendix I-C and Tajika et al. 2015b) and various other publications linked on the palaeontology and sedimentology of the Devonian of Morocco (Tessitore et al. 2013; Frey et al. 2014 – Appendix I-D; Klug et al. 2014 – Appendix I-E; Tessitore et al. 2016).
In the following introduction, I outline the general context of these research topics.

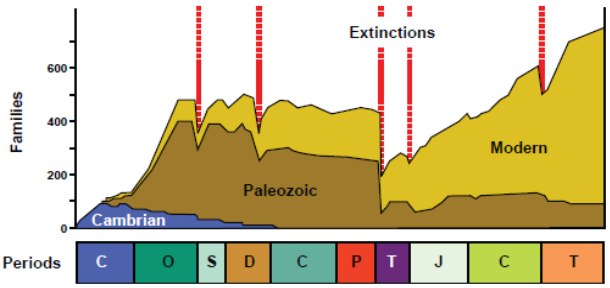

Figure 1. The classical diversity curve of marine invertebrate families through Phanerozoic time from Raup and Sepkoski (1982; in Sheehan 1996), documenting the Cambrian, Palaeozoic and modern evolutionary faunas as well as the "Big Five" mass extinctions of marine invertebrates. Geological periods, from left to right: C—Cambrian; O—Ordovician; S—Silurian; D—Devonian; C—Carboniferous; P—Permian; T—Triassic; J–Jurassic; C—Cretaceous; T—Tertiary. Modifed after Servais et al. (2009).

THE DEVONIAN PERIOD

The Devonian period lasted from 419.2 ±3.2 Ma to 358.9 ± 0.4 Ma according to the International Chronostratigraphic Chart v. 2017/02 (Cohen et al. 2013; 418.1 to 360.7 Ma according to Kaufmann, 2006). This was a time of several "firsts" as McGhee (2005) pointed out. It is classically known as the age of fishes with an explosive proliferation of both marine and freshwater fishes (e.g., McGhee 2005; Benton

2005) as well as the time when the first tetrapods conquested the terrestrial biome. Speaking of life on land, the Devonian period plays a key role in the evolution of terrestrial plants: although pioneering land floras are known from older intervals (Wellman et al. 2003; Knauth et al. 2009), the first expanded forests with high trees appeared (Algeo and Scheckler 1998; Scheckler 2001, McGhee 2005).

This increasing land vegetation (e.g. Goldring 1927; Meyer-Berthaud et al. 1999; Stein et al. 2012) globally altered atmosphere and hydrosphere during the Devonian. There is some good support for the hypothesis that the rapidly spreading vegetation contributed much to the two Late Devonian mass extinctions (Kellwasser and Hangenberg Events) or even triggered them. Remarkably, they both belong to the most severe mass extinctions of the Phanerozoic if we refer to the study of McGhee et al. (2013).

It is widely accepted now that the rapid spread of large vascular plants on land caused the intensification of weathering and formation of soils (Algeo et al. 1998). In turn, weathering increased and ever more organic matter was transported into the sea by erosion. As a consequence, ever more organic matter reached the seas and caused an eutrophication including phytoplankton blooms, eventually leading to oxygen depletion and the corresponding formation of black-shale deposits during and after the Kellwasser events, i.e. near the Frasnian/ Famennian boundary (Walliser 1996; Algeo et al. 2001; House 2002; McGhee 2005). Absorption of carbon dioxide by terrestrial plants, marine burial of organic matter and deeper weathering on land significantly reduced atmospheric CO2 (Algeo et al. 1998; Rye and Holland 1998; Berner et al. 2003). The lower CO2-levels then caused a global cooling (Icehouse period) and associated global regressions during the Late Devonian (Berner et al. 2003; Haq and Schutter 2008), particularly around the Kellwasser and Hangenberg Events (Haq and Schutter 2008).

Thus far, the Late Devonian mass extinctions are the only among the most severe extinctions where evidence for an essential role of Large Igneous Provinces (LIPs) is poor (Algeo et al. 1998; Barash et al. 2016; McGhee 1996).

On the other hand recent studies suggest that, after all, high volcanic activity might have caused the Late Devonian extinction events (e.g. Kravchinsky et al. 2002; Ricci et al. 2013; Racki et al. 2018 and references therein). Particularly, Racki et al. (2018) bring new arguments in favour of the volcanism-hypothesis with Mercury (Hg) measurements in favour of LIPs from rocks dated to 372 Ma, just before the Frasnian/ Famennian boundary. The authors measured Hg peaks in different localities and lithologies, which were apparently not related to increased bioproductivity in an anoxic setting.

Ultimately, whatever really was the main culprit for the Late Devonian mass extinctions, scientists agree that these extinction events represent a multi-steps crisis lasting several million years.

In the course of these crises, many carbonate platforms perished despite their particularly high growth rates reaching 200m/Ma in the Late Devonian (Bosscher and Schlager 1993). The Late Devonian is marked by high-order eustatic changes (Haq and Schutter 2008). In contrast, the Early Devonian was affected rather by low-order eustatic events, also called Bio-events (House 1996; Walliser 1996), such as the Zlíchov and the Daleje Events.

Nevertheless, the Devonian period cannot be comprehended in full when limiting ones view to the rise of land plants and the major mass extinctions. Regarding macroevolution and macroecology, an important event occurred during the Devonian, the so-called "Devonian Nekton Revolution" (Klug et al. 2010). At that time, a number of macroecological changes happened including the diversification of gnathostomes and the origin of important cephalopod groups such as ammonoids and bactritids. These groups of nektonic animals (freely swimming as opposed to benthic – on the sediment – and demersal – above but close to the sediment) then increasingly occupied the free-water column (Fig. 2). As a result, the proportion of nektonic animals increased to the detriment of planktonic animals (e.g. cephalopods with orthoconic conchs, dacryoconarids etc.).

The Devonian is an interesting interval in earth history because it saw the apparition and diversification of the ammonoids, which is an important clade both in biostratigraphy and increasingly in invertebrate palaeobiology. Ammonoids have been quite intensively studied for several centuries now (e.g. Breyn 1732; Sowerby 1812) as they represent one of the most valuable stratigraphic tool thanks to their high evolutionary rates and their worldwide distribution. Still, some evolutionary and biological aspects of these cephalopods remain incompletely understood; with the results presented in my PhD-thesis, I hope to shed more light on some open questions regarding the palaeobiology of early ammonoids.

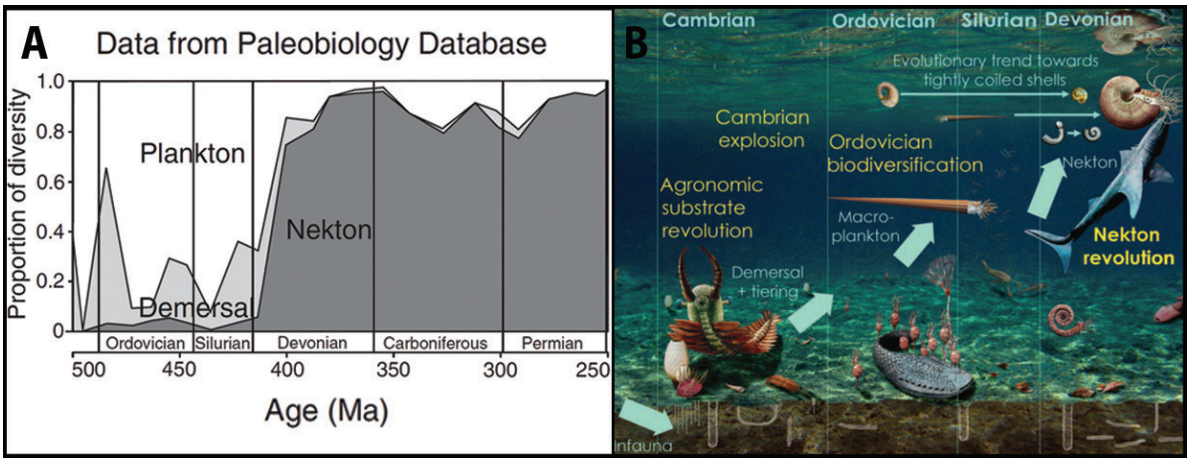

Figure 2. Palaeozoic diversity of marine animals. A - Proportional abundance of demersal, planktonic and nektonic animals in the Palaeozoic. B – Macroecological evolution of Early to Middle Palaeozoic marine food webs such as occupation of the free-water column and evolution in coiling strategies (modified from Klug et al. 2010).

AMMONOIDS AND THEIR ORIGIN

The subclass Ammonoidea is an extinct group of animals belonging to the class Cephalopoda. Cephalopods appeared in the Late Cambrian (e.g. Dzik 1981; Mutvei et al. 2007; Kröger et al. 2011). They belong to the Mollusca and like many of their relatives, many cephalopods have a calcareous external conch (ectocochleate). Although there were likely many similarities in the anatomy of their soft parts, it is mainly the conch that usually became fossilized. Therefore, systematic and taxonomic researches are limited to their study; normally, it is a number of conch-parameters that are measured to assess phylogenetic relationships and also palaeoecology. Other body parts of the animal such as the soft parts and buccal apparatuses are only rarely preserved (e.g. Kruta et al. 2014). An ammonoid conch is composed of the following parts (Fig. 3):

The protoconch or initial chamber is a minute more or less spherical structure formed in the egg; this is where the conch begins its growth. It is also the first part of the phragmocone, which consists of a more or less conical tube that is subdivided into numerous chambers separated by septa; the body chamber, which is the last part of the long conch tube, contained the soft-parts of the animal. Further details about shell-parameters used in ammonoid research can be found in Appendix I-A (Klug et al. 2015).

Most modern cephalopods, namely the coleoids, have an inner shell (endocochleate). The only extant externally shelled cephalopods with a phragmocone are the nautilids, represented today only by the two genera *Nautilus* and *Allonautilus*. Due to some similarities in conch morphology between extant nautiloids and extinct ammonoids, they have often been comparatively studied in order to improve our understanding of ammonoid palaeobiology and palaeoecology (e.g. Ward 1987; Saunders and Landman 2009). Despite this morphological resemblance,

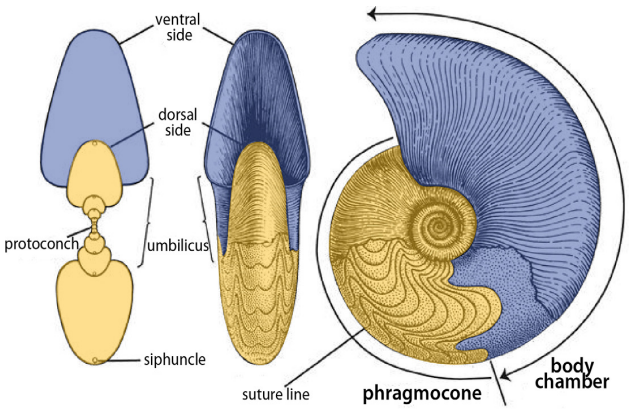

Figure 3. Technical terms used to describe ammonoid conchs, here illustrated using a conch of the Late Devonian genus *Manticoceras*. The body chamber, which was occupied by the soft tissues, is highlighted in blue. The phragmocone is shown in yellow (modified from Miller et al. 1957)

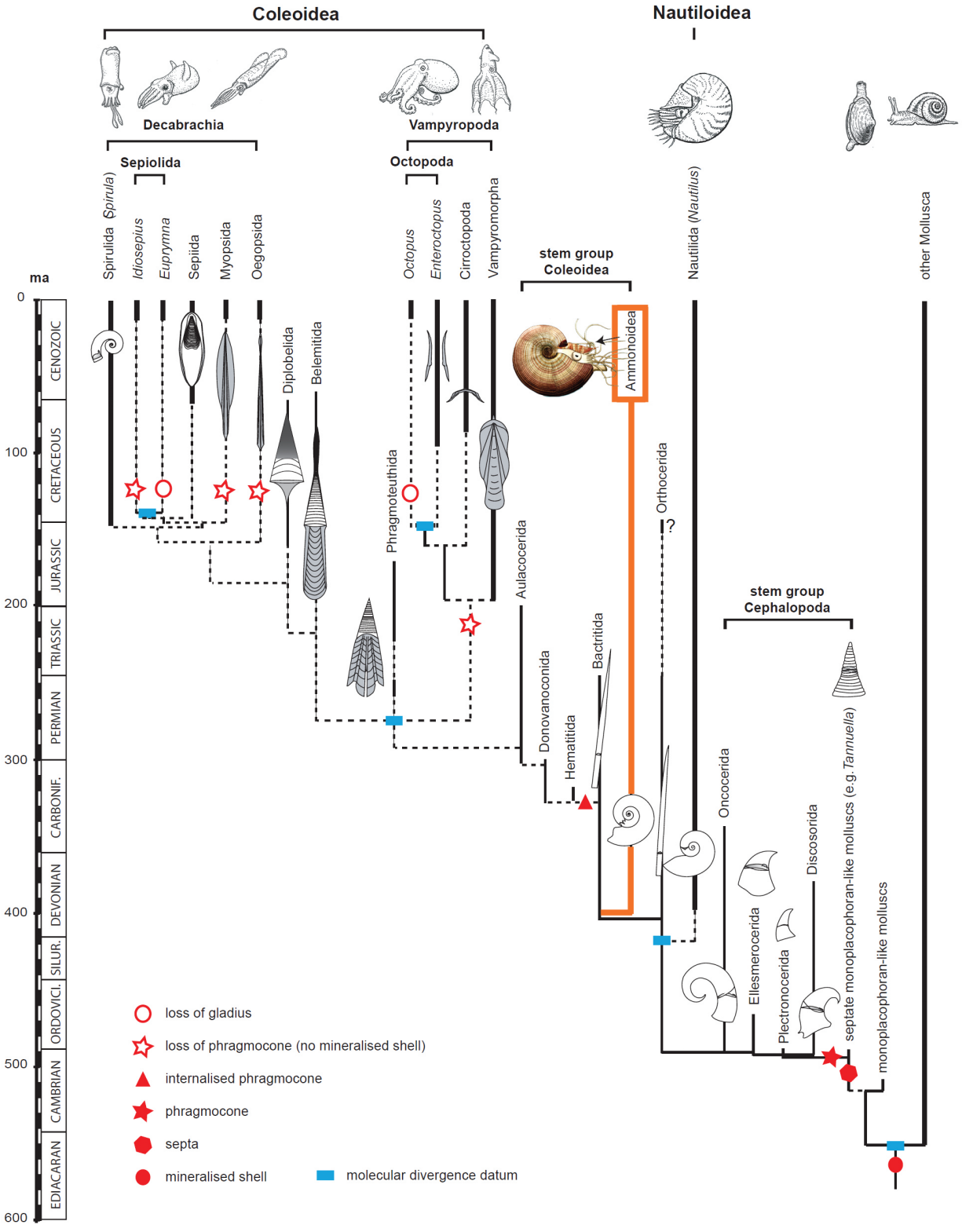

Figure 4. Molecularly calibrated timetree of cephalopod evolution (modified after Kröger et al. 2011).

however, ammonoids are phylogenetically more closely related to coleoids than to nautiloids (e.g. Jacobs and Landman 1993; Keupp 2000; Kröger et al. 2011; Fig. 4); according to Kröger et al. (2011), ammonoids evolved from bactritoids in the Early Devonian, which, in turn, root in the Orthoceratida (Kröger et al. 2011).

Like all cephalopods, ammonoids underwent a direct development. Within the egg, the embryonal conch formed (= ammonitella; Ward and Bandel 1987). Hatching occurred at the end of this first growth stage. The end of this growth stage can usually be recognized by the so-called nepionic constriction. After hatching, most ammonoids underwent two to three additional growth changes before adulthood, which are usually reflected in changes in conch geometry (Klug 2001). The growth stages are (Bucher et al. 1996):

- Ammonitella
- Neanoconch
- Juvenile
- (Preadult)
- Adult

Like most other mollusc conchs, those of ammonoids grew by accretion, which means that their conchs grew by adding narrow increments of carbonatic shell around the aperture (or peristome). Thereby, these molluscs recorded their entire ontogeny, thus making them ideal tools to study evolutionary patterns in a developmental context (e.g. Erben 1962; 1964; 1965; 1966; Klug 2001a; De Baets et al. 2013; Chapter I). Moreover, their high evolutionary rates and great diversity as well as morphologic disparity made them one of the most important and reliable index fossils for a period covering about 320 million years (House 1989). Thereby, the famous quote by Seilacher (1988), claiming that "*ammonoids are for palaeontologists what Drosophila is for biologists*" describes their importance for invertebrate palaeontology quite accurately. Palaeozoic ammonoid phylogeny is presented in Fig. 5.

Historically, fossil cephalopods have been studied early on, but in greater detail starting in the 19th century with the works of e.g. Barrande (1865; 1877) on the Devonian of the Czech Republic. Further ammonoid studies of the Devonian followed at a more or less constantly increasing rate. In the 20th century, several important publications focusing on materials from various European countries including the Czech Republic, Germany, or France with important works by, e.g. Erben (1954; 1960; 1962; 1964; 1965 and 1966) or Chlupàč (1976). Additional discoveries followed being described from other countries such as Canada (House and Pedder 1963), Russia (Bogoslovsky 1969; 1972; Yatskov 1990; Yolkin et al. 2000; Nikolaeva 2007), France (Feist 1970), China (Shen 1975; Ruan 1996), Uzbekistan (Bogoslovsky 1980; 1984; Becker et al. 2010), Algeria (Göddertz 1987), Spain (Montesinos-Lopez and Truyols-Massoni 1987; Montesinos & García-Alcalde 1996; Carls 1999), Germany and Turkey (Göddertz 1989), Alaska and Morocco

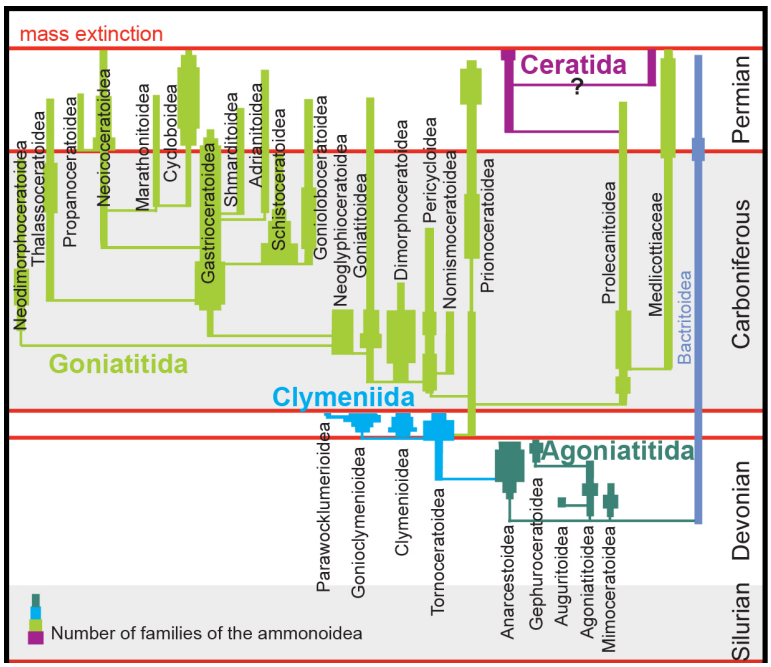

Figure 5. Phylogeny of Palaeozoic ammonoids. The red lines mark the "Big Five" mass extinctions. The thicknesses of the lines for each order represent the number of families (modified after House and Senior 1981 as well as Ernst and Klug 2011).

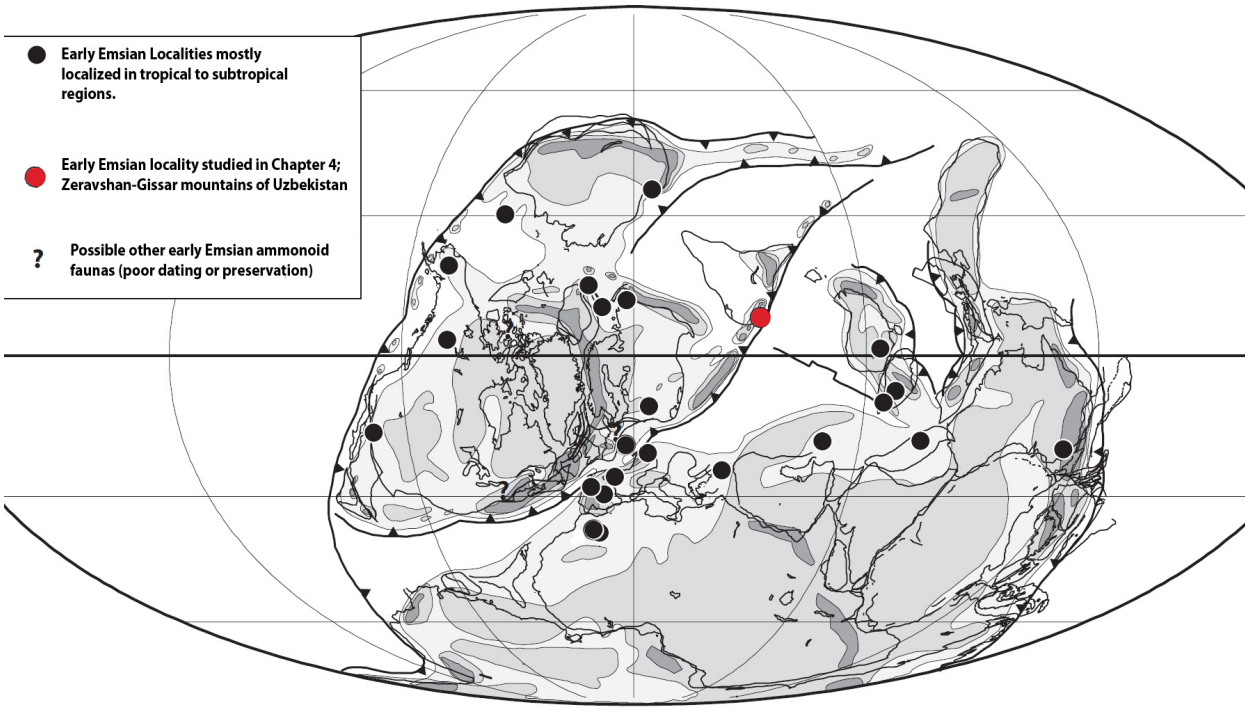

Figure 6. Palaeogeographic occurences of Emsian ammonoid faunas. Map modified from De Baets et al. (2011) after the palaeogeographic map of Scotese (2001).

(Becker and House 1994; Klug 2001b) and Tajikistan (Bardashev et al. 2005). Most of these localities are located in tropical to subtropical palaeolatitudes of the Early Devonian as shown in figure 6.

The locality highlighted in red (fig. 6) represents the study area in Uzbekistan that yields abundant early Emsian ammonoids (Chapitre 4). It represents one of the most diverse ammonoid faunas of early Emsian age and is located in the Zeravhan-Gissar Mountains (Bogoslovsky 1980; 1984; Yatskov 1990).

VIRTUAL PALAEONTOLOGY

Rapid developments in various technologies (e.g. computer tomography/ CT, synchrotron tomography, grinding tomography, etc.) and computer sciences (e.g. segmenting software) over the last decades boosted research in many fields of research and undoubtedly produced many important new insights (e.g. Donoghue et al. 2006; Hoffmann and Zachow 2011; Garwood et al. 2010). In palaeontology, virtual reconstructions of fossils became a standard method during the last two decades as they bring several advantages compared to traditional two-dimensional studies.

Indeed, virtual 3D-models of fossils nowadays allow:

- to obtain numerical data, which can be shared with scientists all around the world without moving the fossil specimen itself if it has been processed using non-invasive methods;

- sometimes, if the use of physical abrasive tools can be avoided to separate the fossil from the matrix; this can reveal finest details in weakly articulated or highly fragile specimens and erases the risk of mechanical damage to very fine structures (e.g. Garwood et al. 2010; Sutton et al. 2014);

- non-invasive methods can reveal internal structures without destroying the fossil;

- virtual 3D-models of fossils can be dissected in several directions; by sectioning specific parts of the fossil, structures such as organs, shell parts or bones can be isolated to better understand its form and function (Sutton et al. 2014);

- adding a third dimension to a dataset potentially yields volumetric data. In the case of ammonoids, these are shell volumes, septum volumes, body chamber volume and phragmocone chamber volumes through ontogeny; I quantified the latter in my first article (Chapter 1);

- ultimately, the obtained 3D-models may be further used to produce 3D-prints.

Many more examples could be listed to demonstrate the broad range of interesting applications and case studies that became possible due to virtual

reconstructions. These methods became commonly used first in vertebrate palaeontology, but slightly more recently also to examine invertebrates such as brachiopods. In its beginnings, it was physical-optical tomography by serial grinding. This method was first applied by the vertebrate palaeontologist William J. Sollas in 1903. Even though these tomographic methods were of lesser importance in the first part of the 20th century, they started to become more and more widely used in the second-half of the 20th century and even more so since the beginning of the 21st century, as Sutton et al (2014) show in their seminal book *Virtual Palaeontology* (Fig. 7).

Various methods exist to obtain a virtual 3D-model of a fossil. As there are many such methods, I only outline the two main categories of tomographic methods, namely the destructive and non-destructive methods. Depending on the structure of interest that has to be visualized in the material and the physical properties of the material (density, density contrast, size), the one or another kind of method is chosen. Instead of listing all methods, a flow chart of recommendations for tomographic methods is presented, in which the preferred method is mentioned, depending on a series of questions concerning the material (Fig. 8; Sutton et al. 2014).

If correctly chosen, virtual palaeontological techniques overcome the disadvantages of physical isolation methods and bring a broad range of possible

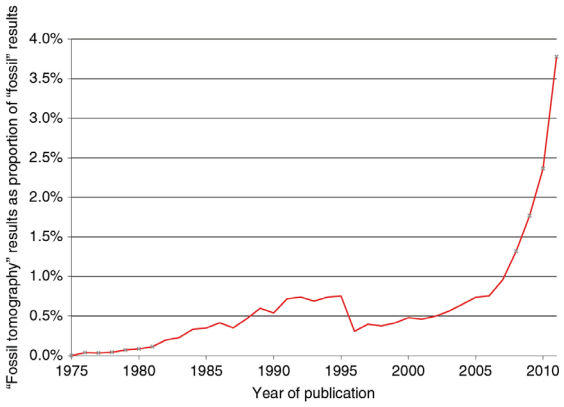

Figure 7. Rising use of tomographic methods in palaeontology. This graph represents the proportion of this kind of scientific articles searched in "Google Scholar"; the general trend shows an exponential increase of publications over the last two decades. The drop in 1996 is interpreted as an artefact caused by the search engine (Sutton et al. 2014).

investigations to many groups of fossils (e.g. Sutton et al. 2001; Hutchinson et al. 2007; Kruta et al. 2011; Goswami et al. 2011; Goudemand et al. 2011; Neenan and Scheyer 2012; Lukeneder 2012; Loza et al. 2017).

Concerning ammonoid research, the first attempt to examine internal structures using a non-destructive method with X-ray photographs was carried out by Lehmann (1932).

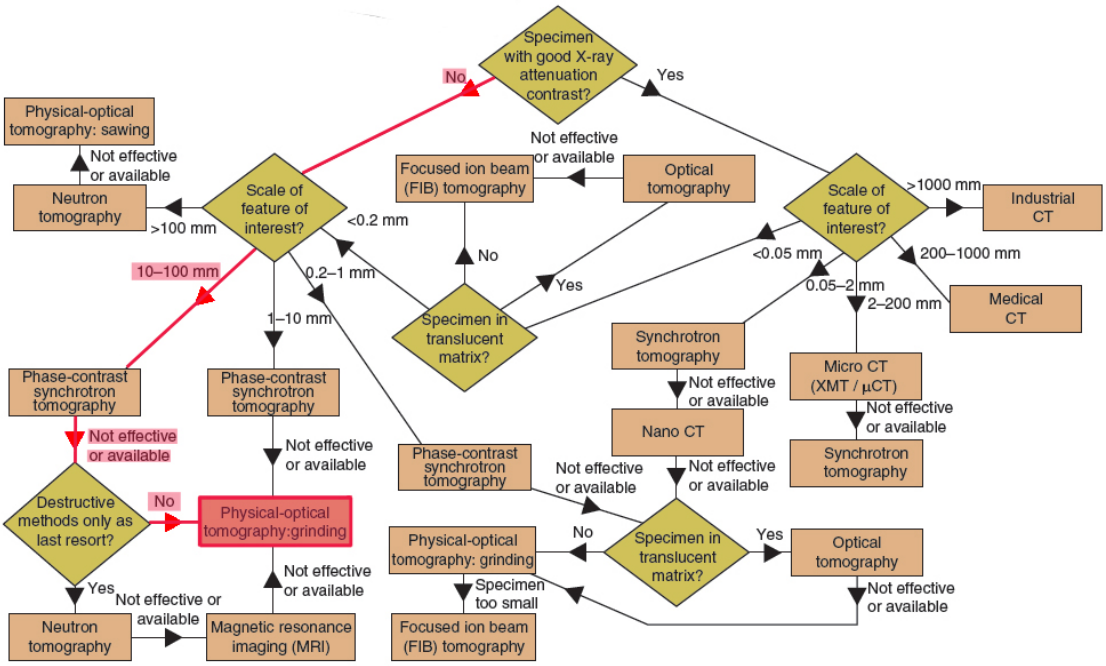

Figure 8. Flow chart with recommendations for tomographic investigations. Green diamond-shaped boxes represent decisions and have multiple exits; brownish rectangular boxes represent recommendations that a particular method should be considered. As one example, the path we followed with our material is highlighted in red (modified after Sutton et al. 2014).

More recently, Longridge et al. (2009) focused on Jurassic ammonites; Hoffmann and Zachow (2011) produced micro-CT scans of a recent *Nautilus* specimen to investigate its buoyancy. The authors hoped to transfer this method to ammonoid material, but several attempts failed, mainly because of insufficient density contrast between the fossil and the surrounding matrix (e.g. Sutton 2008; Hoffmann and Zachow 2011; Hoffmann et al. 2013).

Kruta et al. (2011) examined the delicate buccal mass apparatus of the Mesozoic heteromorph ammonite Baculites using synchrotron X-ray microtomography. Based on the 3D-model of the radula and jaws with contained prey items, they drew conclusions on the position of ammonoids in Cretaceous marine foodwebs.

Concerning Palaeozoic specimens, Kruta et al. (2014) also segmented tomography image stacks of Mississipian ammonoids. There are still further important articles in virtual reconstructions of ammonoids but it is not the aim to exhaustively revise those here.

As examples for the application of serial-grinding method in our lab, Tajika et al. (2015a) worked on buoyancy reconstruction of the Jurassic ammonite *Normannites* and on growth in nautilids (Tajika et al. 2015b). Lukeneder et al. (2014) analysed the external shell morphology and orientations of Mesozoic ammonoids through 3-D tomography. Lemanis et al. (2016) presented a study on ontogenetic changes in surface area to volume ratios in the phragmocone chambers of several phylogenetically only distantly related ammonoids and extant cephalopods. Lately, Hoffmann et al. (2018) published a palaeobiological study combining traditional 2D-analyses with high-resolution CT-scans of the Jurassic ammonoid *Kosmoceras*.

A number of ground-breaking methods of virtual palaeontology are now increasingly employed to improve our knowledge of ammonoid palaeobiology including palaeoecology, evolution and development, etc. Yet, compared to Mesozoic specimens, Palaeozoic ammonoids are poorly studied using these innovative methods (see Kruta el al. 2014 or Lemanis et al. 2016 for studies including a few Palaeozoic ammonoids).

The first two chapters of this thesis are dedicated to Palaeozoic ammonoid reconstructions. These articles present pioneer work in virtual palaeontonlogy of Palaeozoic ammonoids. They address questions related to growth and ontogenetic trajectories extracted from 3D-models (Chapter I) as well as buoyancy and hydrostatics of representatives of some major Palaeozoic ammonoid clades (Chapter II).

CHAPTER I

Growth trajectories of some major ammonoid sub-clades revealed by serial grinding tomography data

Published in *Lethaia*, vol. 48 (2015)

Lethaia
AN INTERNATIONAL JOURNAL OF PALAEONTOLOGY AND STRATIGRAPHY

Growth trajectories of some major ammonoid sub-clades revealed by serial grinding tomography data

CAROLE NAGLIK, CLAUDE MONNET, STEFAN GOETZ, CHRISTIAN KOLB, KENNETH DE BAETS, AMANE TAJIKA AND CHRISTIAN KLUG

LETHAIA

Naglik, C., Monnet, C., Goetz, S., Kolb, C., De Baets, K., Tajika, A. & Klug, C. 2015: Growth trajectories of some major ammonoid sub-clades revealed by serial grinding tomography data. *Lethaia*, Vol. 48, pp. 29–46.

Molluscs such as ammonoids record their growth in their accretionary shells, making them ideal for the study of evolutionary changes in ontogeny through time. Standard methods usually focus on two-dimensional data and do not quantify empirical changes in shell and chamber volumes through ontogeny, which can possibly be important to disentangle phylogeny, interspecific variation and palaeobiology of these extinct cephalopods. Tomographic and computational methods offer the opportunity to empirically study volumetric changes in shell and chamber volumes through ontogeny of major ammonoid sub-clades in three dimensions (3-D). Here, we document (1) the growth of chamber and septal volumes through ontogeny and (2) differences in ontogenetic changes between species from each of three major sub-clades of Palaeozoic ammonoids throughout their early phylogeny. The data used are three-dimensional reconstructions of specimens that have been subjected to grinding tomography. The following species were studied: the agoniatitid *Fidelites clariondi* and anarcestid *Diallagites lenticulifer* (Middle Devonian) and the Early Carboniferous goniatitid *Goniatites multiliratus*. Chamber and septum volumes were plotted against the septum number and the shell diameter (proxies for growth) in the three species; although differences are small, the trajectories are more similar among the most derived *Diallagites* and *Goniatites* compared with the more widely umbilicate *Fidelites*. Our comparisons show a good correlation between the 3-D and the 2-D measurements. In all three species, both volumes follow exponential trends with deviations in very early ontogeny (resolution artefacts) and near maturity (mature modifications in shell growth). Additionally, we analyse the intraspecific differences in the volume data between two specimens of *Normannites* (Middle Jurassic). ☐ *3-D reconstruction, allometry, ammonoidea, ontogeny, palaeozoic, tomography, volumes.*

Carole Naglik [carole.naglik@pim.uzh.ch], Christian Kolb [christian.kolb@pim.uzh.ch], Amane Tajika [amane.tajika@pim.uzh.ch], Christian Klug [chklug@pim.uzh.ch], Paläontologisches Institut und Museum, Universität Zürich, Karl-Schmid-Strasse 4, Zürich 8006, Switzerland; Claude Monnet [claude.monnet@univ-lille1.fr], Géosystèmes – UMR 8217, Université de Lille 1, UFR Sciences de la Terre (SN5), Avenue Paul Langevin, Villeneuve d'Ascq 59655 cedex, France; Stefan Goetz (in memoriam); Kenneth De Baets [kenneth.debaets@fau.de], GeoZentrum Nordbayern Fachgruppe PalâoUmwelt Friedrich-Alexander-Universität Erlangen-Nürnberg, Loewenichstraße, 28 Erlangen 91054, Germany; *manuscript received on 13/08/2013; manuscript accepted on 23/04/2014.*

Knowing how form changes during growth is crucial when studying biological function, as well as intraspecific and interspecific variation and evolution, because evolutionary change in adult form is affected through the evolution of ontogeny (Miller & Foote 2007). Molluscs conserve a record of growth in their accretionary shell, which is frequently preserved in the fossil record, making them ideal tools to study ontogenetic change in an evolutionary context. In particular, ammonoids, an extinct group of marine, externally shelled cephalopods, have been widely used to study evolution (Trueman 1922; Kennedy 1977; Landman 1988; Gerber *et al.* 2007; Monnet *et al.* 2011; Korn 2012 and references therein) for the following reasons: (1) they have a wide distribution in space and time, occurring from the Early Devonian to the end of the Cretaceous (House 1989), which represents a time range of about 320 million years; (2) they had high evolutionary rates (reflected in phenotypical changes), which is a condition needed for index fossils; and (3) their entire ontogeny is recorded in their shells, which is a fundamental prerequisite for studying evolution in the context of development (Erben 1962, 1964, 1965, 1966; Klug 2001; Monnet *et al.* 2011 and references therein; De Baets *et al.* 2012, 2013). The shells of ammonoids superficially resemble *Nautilus* and *Allonautilus,* the only remaining extant ectocochleate cephalopod genera, but they are now known to be phylogenetically closer to coleoids than to nautilids (Jacobs & Landman 1993; Kröger *et al.* 2011). In summary, ammonoids offer the rare possibility to study evolutionary

DOI 10.1111/let.12085

phenomena of a rapidly evolving clade with a great taxonomic diversity and morphological disparity; in the words of Seilacher (1988), 'ammonoids are for palaeontologists what *Drosophila* is in genetics'.

Nevertheless, some aspects of ammonoid palaeobiology have never been studied or only poorly, especially in early ammonoids. Many studies on (fossil) mollusc development still rely on the measurements of two-dimensional (2-D) data (see references in Monnet *et al.* 2009), which, in the case of ammonoids, are septum spacing (e.g. Bucher *et al.* 1996; Bucher 1997; Kraft *et al.* 2008; Korn 2012) or simple morphometric shell parameters and ratios (e.g. Kant 1973a,b; Kant & Kullmann 1988; Bucher *et al.* 1996; Klug 2001; Korn & Klug 2001; Korn 2010, 2012). Important changes in growth and growth rhythms have been documented in early ammonoids in such 2-D studies (e.g. Kullmann & Scheuch 1970, 1972; Kant 1973a,b; Kant & Kullmann 1988; Bucher & Guex 1990; Klofak *et al.* 1999, 2007; Klug 2001). Our study represents not only the first empirical quantification of the ontogenetic changes in ammonoid chamber and septum volumes, but also the first time that novel computational methods were applied to determine these values in early ammonoids. Previous studies mainly focused on optical-physical tomography of Mesozoic ammonoids (e.g. Lukeneder 2012; Tajika *et al.* 2014).

The first attempt to examine internal structures of ammonoids using non-destructive methods has been performed by Lehmann (1932) using X-ray photographs. A recent study published by Hoffmann & Zachow (2011) produced micro-computed tomographies (CT scans) of a recent *Nautilus* specimen. Attempts to produce CT scans of ammonoids, which reveal internal structures such as septa and siphuncle, usually suffer from a low signal to noise ratio in the CT images, or a lack of contrast or detail, particularly in non-hollow, infilled and/or partially recrystallized shells, which consequently hinder a proper segmentation of the region of interest (Hoffmann & Zachow 2011; Hoffmann *et al.* 2013). This is largely related to the similar absorption properties due to similar chemical composition [calcium carbonate ($CaCO_3$)] and thus density of the ammonoid shell and the surrounding sedimentary matrix or the diagenetic mineral chamber filling (compare Kruta *et al.* 2011 for a successful three-dimensional tomography and reconstruction of a differently preserved buccal mass within the shell and external morphology of the shell in derived Mesozoic ammonoids; Lukeneder 2012 and Lukeneder *et al.* 2014 analysed the external shell morphology and orientations of Mesozoic ammonoids with 3-D tomography, respectively). We therefore resorted to serial grinding (a worthy alternative to CT scanning for particular cases: Sutton *et al.* 2014).

Our study focuses on early ammonoids, namely from the Devonian and Carboniferous periods (419–299 Ma). It comprises three specimens, each from a different major sub-clade of Palaeozoic ammonoids (Fig. 1). The results will be further used for empirical tests of ammonoid buoyancy, but in this study, we focus on volumetry and ontogeny in early ammonoids, addressing the following questions:

1 Which volumetric parameters changed allometrically or isometrically?
2 Do these parameters correlate with other classical shell parameters? In other words, can some classical shell parameters and ratios be used as proxies for certain volumetric parameters?
3 Are there growth changes, which are recorded in volumetric changes only? Or do volumetric changes correlate with growth changes, which have been already documented with simple shell parameters and ratios?
4 Are there specific quantifiable patterns in volumetric growth, which are characteristic for certain clades?

Material and methods

Material

CT scans of our material yielded very poor results (for the reasons mentioned in the introduction),

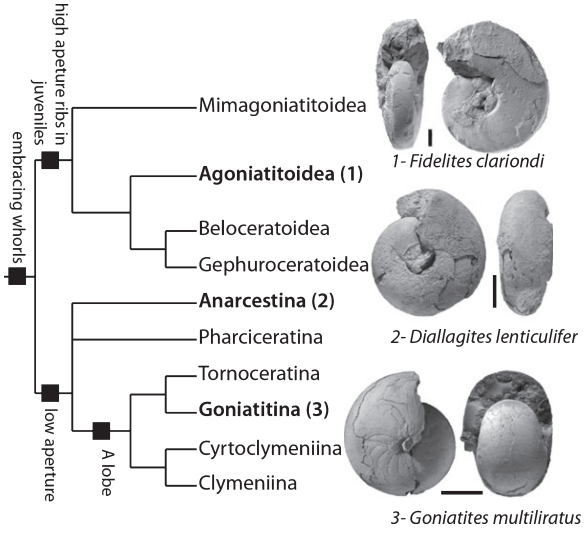

Fig. 1. Simplified cladogram of early ammonoids with some important autapomorphies (modified after Klug & Korn 2004) and the studied specimens before grinding tomography. Scale bar: 1 cm.

which did not allow us to assess volumetric changes. Therefore, an alternative approach was sought to obtain 2-D slices through our ammonoids; the serial grinding method (Garwood *et al.* 2010) has been opted as the best choice. Serial grinding has a long history in palaeontology. One of the pioneers was Sollas (1904), but only recently, computational visualization software is used more commonly to create 3-D models from image stacks (Sutton *et al.* 2001, 2014; Mallison 2011). Although this method is completely destructive and time-consuming, it generates detailed, high-resolution images (around 2000 dpi) of polished sections, which consequently allow a good visualization at a reasonable scale (Sutton *et al.* 2001; Sutton 2008; Garwood *et al.* 2010; Pascual-Cebrian *et al.* 2013). Additionally, these images are in colour, a potentially valuable source of information.

Therefore, the crucial criteria for the selection of fossils were to find: (1) specimens preserving complete shells of; (2) preferably adult specimens with; (3) the complete body chamber and (4) complete phragmocone with, if possible, most septa preserved. The phragmocones of the specimens were broken in half prior to sectioning to ensure that the inner parts were not entirely recrystallized; that is, that the protoconch (initial chamber) and the septa were visible. This method was selected as the best method because it causes a negligible loss of material, while sawing the specimen would have caused a loss of parts of the specimen. The fragments of the specimens (usually two to three large ones with an excellent fit) were subsequently reassembled and glued prior grinding.

The studied materials comprise the Middle Devonian (Eifelian) agoniatitid *Fidelites clariondi* Petter (1959), the Middle Devonian (Eifelian) anarcestid *Diallagites lenticulifer* Klug (2002) (both belong to the Agoniatitida), and the Early Carboniferous goniatitid *Goniatites multiliratus* Gordon (1962) (Fig. 1; Table 1). Due to grinding tomography, all the specimens are now lost. Both Agoniatitida specimens come from the Moroccan Tafilalt region (Anti-Atlas). *Fidelites clariondi* has been found in Early Eifelian condensed limestones of the Jebel Ouaoufilal section (Klug 2002). *Diallagites lenticulifer* was collected from Late Eifelian condensed and slightly dolomitized limestones of the red cliff at Hamar Laghdad (Klug 2002; Klug *et al.* 2010). *Goniatites multiliratus* (Fig. 1) represents the most derived ammonoid of the three specimens in this study. It is probably more closely related to *Diallagites lenticulifer* (Fig. 1). The sectioned specimen was extracted from a large nodule in claystones of the Jackfork Creek, south of Ada, Oklahoma (USA).

Table 1. Maximum conch diameters and resolutions of each sample.

Specimen	*Fidelites clariondi*	*Diallagites lenticulifer*	*Goniatites multiliratus*
Maximum diameter (dm_1)	76.3 mm	41.51 mm	46.97 mm
Calculated increment (μm)	60	48	49
Resolution (dpi)	1600	1200	1200
Voxel size (*X*, *Y*, *Z* in mm)	0.028, 0.028, 0.240	0.017, 0.017, 0.192	0.013, 0.013, 0.20
Number of slices per image stack	114	84	107

All the studied specimens are three-dimensionally preserved. The aragonite of the original shell has been replaced by calcite in *Fidelites clariondi* and *Diallagites lenticulifer*. In *Goniatites multiliratus*, the septa may have been replaced by various minerals, as shown by the differences in their appearance when exposed to ultraviolet light, and also by the fact that some of the septa can be identified in CT images (suggesting that they are preserved in a material that is different in density to the rest of the sample). It is possible that diagenetic processes, such as mineral replacement and recrystallization, might have slightly altered the shell volumes post-mortem. Nevertheless, fine structures on the shell surface are quite well preserved. Additionally, the sediment usually becomes lithified prior to recrystallization, limiting any volumetric changes during the gradual replacement of aragonite by calcite. In contrast to Longridge *et al.* (2009), we thus assume that diagenetic changes in volume were not sufficiently strong that they could significantly alter the results of our study.

Fidelites clariondi (Table 2) was the largest of the examined species with a phragmocone diameter of 49.47 mm; it contained 69 chambers. Among the studied specimens, it was the one with the lowest number of chambers. *Diallagites lenticulifer* (Table 3) follows as the second largest species with a phragmocone diameter of 32.08 mm and with 81 chambers. *Goniatites multiliratus* (Table 4) was the smallest specimen. It lacked the body chamber and had a phragmocone diameter of 29.36 mm, albeit it had the highest amount of chambers: 89. To address the question of intraspecific variability, we also used two specimens belonging to *Normannites mitis* (Westermann 1954) from the Bathonian (Middle Jurassic; Türlen, Argovy, Switzerland).

Due to grinding tomography, all the original specimens are now lost, but digital versions are now available. Therefore, no repository numbers are

Table 2. Measurements of *Fidelites clariondi.*

Fidelites clariondi

	Classical parameters				Volumes			Classical parameters				Volumes	
Chamber	dm_1 (mm)	ah (mm)	WER	Septal distance (°)	Chamber (mm^3)	Septum (mm^3)	Chamber	dm_1 (mm)	ah (mm)	WER	Septal distance (°)	Chamber (mm^3)	Septum (mm^3)
1	1.38	0.64	3.48		0.485	0.015	36	6.62	2.1	2.15	18.7	6.57	0.69
2	1.38	0.52	2.57	53	0.065	0.015	37	6.98	2.26	2.19	24.1	7.34	0.735
3	1.54	0.54	2.37	36.8	0.09	0.015	38	7.44	2.4	2.18	21	9.165	0.74
4	1.67	0.51	2.07	32.3	0.11	0.015	39	7.66	2.46	2.17	22.4	11.11	0.925
5	1.8	0.57	2.14	30.5	0.08	0.015	40	8.25	2.71	2.22	27.8	14.345	1.155
6	1.87	0.59	2.13	46	0.11	0.02	41	8.73	2.94	2.27	32.3	16.955	1.165
7	2.02	0.69	2.31	36.2	0.15	0.02	42	9.22	3.12	2.28	20.7	22.645	1.76
8	2.25	0.76	2.28	22.7	0.19	0.025	43	9.69	3.25	2.26	24.5	23.125	1.975
9	2.28	0.79	2.34	30.8	0.15	0.055	44	10.42	3.45	2.23	28.4	30.055	2.875
10	2.35	0.77	2.21	23.2	0.145	0.055	45	11.12	3.67	2.23	19.8	34.415	2.82
11	2.45	0.81	2.23	20.4	0.195	0.055	46	11.76	3.96	2.27	33.6	41.41	3.03
12	2.48	0.78	2.13	17.7	0.265	0.055	47	12.46	4.17	2.26	27.5	49.53	3.415
13	2.57	0.8	2.11	16	0.215	0.055	48	13.25	4.48	2.28	27.8	53.415	4.29
14	2.65	0.84	2.14	16.1	0.24	0.085	49	14.4	4.93	2.31	26.9	79.635	5.245
15	2.76	0.9	2.20	16.3	0.28	0.085	50	15.2	5.19	2.31	25.6	98.7	7.06
16	2.89	0.94	2.20	13.6	0.405	0.055	51	16.3	5.54	2.29	28.9	112.92	7.95
17	3.04	0.92	2.06	20.9	0.35	0.06	52	17.43	5.94	2.30	26	138.88	9.485
18	3.18	0.95	2.03	18.1	0.515	0.075	53	18.55	6.33	2.30	28.7	169.91	10.82
19	3.24	0.98	2.06	17.6	0.455	0.085	54	19.62	6.72	2.31	27.5	199.04	12.96
20	3.35	1.05	2.12	19.6	0.53	0.09	55	20.7	7.09	2.31	24.3	224.95	13.2
21	3.58	1.15	2.17	24.9	0.755	0.1	56	22.01	7.55	2.32	25.8	273.105	14.405
22	3.75	1.19	2.15	25.8	0.96	0.17	57	23.54	8.24	2.37	23.8	329.085	17.23
23	3.91	1.24	2.14	17.6	0.76	0.165	58	25.31	8.87	2.37	24.7	370.675	19.185
24	4.01	1.27	2.14	22.2	1.1	0.095	59	26.92	9.46	2.38	28.4	469.24	19.845
25	4.18	1.26	2.05	22.7	1.18	0.11	60	29.16	10.45	2.43	27.5	547.82	21.735
26	4.29	1.29	2.04	18.2	1.19	0.145	61	31.03	11.24	2.46	24.6	619.55	21.93
27	4.44	1.34	2.05	21	1.545	0.155	62	33.52	12.35	2.51	23.3	716.99	23.83
28	4.64	1.44	2.10	20.8	1.715	0.185	63	34.85	12.84	2.51	23.3	846.325	23.635
29	4.81	1.48	2.09	17.5	2.09	0.245	64	37.03	13.48	2.47	20.2	936.325	30.24
30	5.09	1.58	2.10	21.4	2.59	0.24	65	39.35	13.36	2.29	27.5	1191.62	42.18
31	5.31	1.64	2.09	21.4	3.43	0.275	66	41.86	15.49	2.52	22.4	1449.32	42.59
32	5.52	1.69	2.08	20	3.21	0.395	67	44.34	16.38	2.51	23.7	1714.36	46.14
33	5.71	1.77	2.10	27.9	3.79	0.395	68	46.59	17.14	2.50	19.7	2136.16	60.01
34	5.93	1.81	2.07	20.2	4.405	0.495	69	49.47	18.32	2.52	21.7	2281.69	67.92
35	6.39	1.99	2.11	32	5.69	0.535							

Abbreviation: ah, aperture heights; dm_1, largest diameter; WER, whorl expansion rate.

Table 3. Measurements of *Diallagites lenticulifer*.

Diallagites lenticulifer

Chamber	Classical parameters				Volumes		Chamber	Classical parameters				Volumes	
	dm_1 (mm)	ah (mm)	WER	Septal distance (°)	Chamber (mm^3)	Septum (mm^3)		dm_1 (mm)	ah (mm)	WER	Septal distance (°)	Chamber (mm^3)	Septum (mm^3)
1	1.5	0.48	2.16		0.39	0.01	42	8.32	1.36	1.43	30.2	10.11	0.28
2	1.67	0.45	1.87	41.1	0.16	0.01	43	8.59	1.45	1.45	37.5	11.785	0.31
3	1.82	0.5	1.90	34	0.22	0.01	44	8.93	1.62	1.49	24	13.165	0.35
4	1.92	0.57	2.02	73.7	0.18	0.01	45	9.2	1.62	1.47	33.2	14.625	0.38
5	2.02	0.56	1.91	58.3	0.2	0.01	46	9.55	1.69	1.48	35.3	15.815	0.43
6	2.18	0.62	1.95	43.5	0.22	0.01	47	9.77	1.7	1.47	27.4	17.595	0.435
7	2.29	0.59	1.81	52.8	0.23	0.015	48	9.98	1.67	1.44	30.3	18.345	0.445
8	2.39	0.57	1.72	38.1	0.29	0.01	49	10.45	1.78	1.45	33.5	19.605	0.465
9	2.59	0.63	1.75	32.5	0.41	0.015	50	10.83	1.9	1.47	30.6	22.33	0.56
10	2.77	0.64	1.69	34.1	0.64	0.02	51	11.35	2.1	1.51	40.5	27.185	0.61
11	2.87	0.63	1.64	47.8	0.55	0.02	52	11.7	2.13	1.49	27.1	31.895	0.67
12	2.92	0.64	1.64	27.5	0.51	0.02	53	11.92	2.17	1.49	33.1	34.23	0.74
13	3.08	0.65	1.61	45.8	0.52	0.025	54	12.54	2.37	1.52	28.4	38.41	0.79
14	3.22	0.69	1.62	53.1	0.56	0.025	55	12.97	2.42	1.51	34.8	42.365	0.895
15	3.34	0.7	1.60	41.9	0.67	0.03	56	13.44	2.51	1.51	33.5	47.02	1.005
16	3.55	0.78	1.64	50.5	0.77	0.04	57	14.02	2.64	1.52	29	47.19	1.14
17	3.68	0.79	1.62	26.4	1.02	0.04	58	14.62	2.93	1.56	33.4	52.53	1.51
18	3.83	0.78	1.58	33.1	0.81	0.05	59	15.15	3.12	1.59	32.6	57.83	1.615
19	4.05	0.79	1.54	39.5	1.85	0.05	60	15.66	3.22	1.58	27.7	59.38	1.79
20	4.21	0.78	1.51	33.6	1.34	0.065	61	16.22	3.34	1.59	32.7	60.51	1.755
21	4.29	0.78	1.49	37.7	1.23	0.065	62	16.67	3.46	1.59	21.2	67.35	2.06
22	4.54	0.85	1.51	44.2	1.675	0.08	63	17.4	3.51	1.57	38.9	99.385	2.495
23	4.63	0.83	1.48	30.7	1.02	0.07	64	18.07	3.66	1.57	31.9	123.795	2.545
24	4.74	0.86	1.49	37.4	1.38	0.105	65	18.67	3.67	1.55	23.4	116.555	2.815
25	4.93	0.85	1.46	39	2.565	0.08	66	19.42	3.85	1.56	29.2	114.4	3.08
26	5.1	0.9	1.47	48.4	2.445	0.085	67	20.17	4	1.56	33.2	153.125	3.35
27	5.41	0.91	1.45	46.6	3.41	0.095	68	20.75	4.07	1.55	24.1	157.995	3.725
28	5.54	0.94	1.45	33.7	3.32	0.095	69	21.78	4.37	1.57	31.7	165.785	3.965
29	5.71	0.92	1.42	32.8	2.64	0.1	70	22.51	4.66	1.59	30.3	166.51	4.27
30	5.8	0.94	1.42	30.2	2.7	0.105	71	23.52	4.86	1.59	37.5	212.945	4.885
31	6	1.04	1.46	27.2	3.54	0.115	72	24.31	5.1	1.60	23.1	189.645	5.29
32	6.16	1.02	1.44	23.6	4.05	0.135	73	25.15	5.33	1.61	25.9	226.65	5.8
33	6.43	1.08	1.44	31.4	4.455	0.155	74	25.8	5.39	1.60	27.9	246.12	5.68
34	6.66	1.18	1.48	40.4	4.71	0.145	75	26.82	5.68	1.61	23.9	246.79	6.095
35	6.74	1.08	1.42	24.6	5.615	0.155	76	27.68	5.82	1.60	23.3	311.98	6.945
36	7.01	1.18	1.45	40.1	5.16	0.17	77	28.73	5.92	1.59	22.3	341.725	7.34
37	7.19	1.2	1.44	33.1	6.18	0.175	78	29.64	6.11	1.59	32.3	382.05	7.8
38	7.35	1.2	1.43	19.3	6.055	0.19	79	30.55	6.35	1.59	27.3	373.255	7.59
39	7.58	1.19	1.41	37.5	8.44	0.205	80	31.52	6.66	1.61	22.1	333.395	7.8
40	7.86	1.25	1.41	27.7	7.385	0.245	81	32.08	6.83	1.61	12.2	252.96	7.65
41	8.02	1.34	1.44	22.7	9.535	0.27							

Abbreviation: ah, aperture heights; dm_1, largest diameter; WER, whorl expansion rate.

Table 4. Measurements of *Goniatites multiliratus*.

Goniatites multiliratus

	Classical parameters				Volumes			Classical parameters				Volumes	
Chamber	dm_1 (mm)	ah (mm)	WER	Septal distance (°)	Chamber (mm^3)	Septum (mm^3)	Chamber	dm_1 (mm)	ah (mm)	WER	Septal distance (°)	Chamber (mm^3)	Septum (mm^3)
1	0.94	0.24	1.80		0.09	0.005	46	5.34	1.45	1.88	25.1	7.165	0.49
2	0.92	0.23	1.78	23	0.02	0.01	47	5.7	1.57	1.90	13.1	5.69	0.53
3	0.95	0.23	1.74	34.1	0.04	0.01	48	5.8	1.63	1.93	23.3	7.96	0.58
4	1.12	0.26	1.70	31.7	0.045	0.01	49	6	1.7	1.95	26.4	10.99	0.575
5	1.18	0.24	1.58	32.3	0.04	0.01	50	6.35	1.78	1.93	18.4	10.06	0.66
6	1.25	0.25	1.56	28	0.045	0.01	51	6.56	1.83	1.92	32	11.78	0.66
7	1.25	0.27	1.63	23.7	0.05	0.01	52	6.83	1.88	1.90	22.7	14.35	0.69
8	1.22	0.26	1.62	28.5	0.04	0.01	53	7.12	1.92	1.87	25.7	16.03	0.775
9	1.22	0.22	1.49	23.7	0.045	0.01	54	7.54	2.01	1.86	23.2	13.84	0.81
10	1.28	0.24	1.51	26.6	0.05	0.01	55	7.89	2.05	1.83	24.1	18.29	0.89
11	1.34	0.18	1.33	26.8	0.085	0.01	56	8.32	2.27	1.89	28.1	20.57	0.92
12	1.42	0.18	1.31	22.5	0.075	0.02	57	8.65	2.35	1.89	24.3	25.92	1.125
13	1.49	0.19	1.31	32.3	0.11	0.02	58	9.01	2.46	1.89	24.5	28.83	1.17
14	1.57	0.26	1.44	28	0.115	0.02	59	9.38	2.59	1.91	17.8	39.235	1.445
15	1.56	0.25	1.42	18.9	0.08	0.02	60	9.68	2.66	1.90	29.9	42.93	1.655
16	1.59	0.32	1.57	20.2	0.075	0.02	61	10.12	2.79	1.91	26.6	46.74	1.76
17	1.65	0.34	1.59	16.4	0.07	0.02	62	10.61	2.83	1.86	27.5	58.14	1.805
18	1.66	0.36	1.63	18.6	0.09	0.02	63	11.13	2.88	1.82	22.9	72.17	2.085
19	1.74	0.38	1.64	20	0.09	0.02	64	11.61	3.01	1.82	27	75.315	2.255
20	1.74	0.31	1.48	19	0.08	0.02	65	12.05	3.03	1.78	33.4	79.38	2.255
21	1.78	0.3	1.45	18.3	0.09	0.02	66	12.72	3.27	1.81	30.9	81.355	2.385
22	1.84	0.27	1.37	16.2	0.345	0.02	67	13.29	3.38	1.80	25.1	88.85	2.375
23	1.91	0.31	1.43	31.9	0.46	0.025	68	13.98	3.48	1.77	23.2	93.055	2.75
24	1.99	0.36	1.49	36.7	0.325	0.03	69	14.43	3.58	1.77	25.4	116	2.71
25	2.14	0.45	1.60	19.7	0.205	0.035	70	15.17	3.78	1.77	27.1	122.205	2.905
26	2.25	0.5	1.65	20.2	0.225	0.035	71	15.69	3.92	1.78	30.2	144.515	3.29
27	2.33	0.52	1.66	21.8	0.23	0.03	72	16.48	4.11	1.77	25.9	160.775	3.755
28	2.37	0.56	1.71	23.1	0.365	0.05	73	17.03	4.13	1.74	24.5	177.95	4.09
29	2.47	0.63	1.80	24.1	0.69	0.07	74	17.51	4.16	1.72	18	205.47	4.555
30	2.56	0.63	1.76	42.2	0.65	0.065	75	18.17	4.31	1.72	22	219.94	5.32
31	2.74	0.65	1.72	17.9	0.605	0.08	76	18.77	4.37	1.70	19.4	216.36	5.77
32	2.81	0.69	1.76	31.7	0.675	0.085	77	19.95	4.68	1.71	19.7	218.72	6.475
33	2.95	0.72	1.75	22.5	0.845	0.105	78	20.61	4.86	1.71	19.3	270.105	6.575
34	3.16	0.74	1.71	23.7	1.105	0.125	79	21.53	5.14	1.73	28.4	293.925	6.655
35	3.35	0.84	1.78	21	1.425	0.15	80	22.17	5.12	1.69	24.1	315.725	6.555
36	3.43	0.87	1.80	29.5	1.325	0.15	81	22.98	5.47	1.72	26.3	338.025	8.325
37	3.64	0.95	1.83	13.1	1.495	0.16	82	23.75	5.6	1.71	22.5	358.94	8.59
38	3.7	0.97	1.84	20.8	1.785	0.17	83	24.57	5.85	1.72	18.2	356.74	8.82
39	3.92	1.08	1.91	23.4	2.055	0.2	84	25.48	5.91	1.70	21	388.02	9.335
40	4.11	1.13	1.90	14.8	2.255	0.22	85	26.3	6	1.68	20.7	403.205	9.98
41	4.19	1.12	1.86	19.8	2.805	0.24	86	27.04	6.26	1.69	20.7	425.8	10.655

(continued)

Table 4. (Continued)

Goniatites multiliratus

	Classical parameters				Volumes			Classical parameters				Volumes	
Chamber	dm_1 (mm)	ah (mm)	WER	Septal distance (°)	Chamber (mm^3)	Septum (mm^3)	Chamber	dm_1 (mm)	ah (mm)	WER	Septal distance (°)	Chamber (mm^3)	Septum (mm^3)
42	4.38	1.17	1.86	29.2	3.105	0.215	87	27.59	6.21	1.67	19.6	436.425	12.2
43	4.53	1.19	1.84	26.7	3.695	0.26	88	28.47	6.43	1.67	25	566.905	14.01
44	4.77	1.23	1.82	34.5	4.84	0.395	89	29.36	6.65	1.67	18.3	545.55	12.96
45	5.08	1.38	1.9	22.3	6.295	0.435							

Abbreviations: ah, aperture heights; dm_1, largest diameter; WER, whorl expansion rate.

given, but we provide pictures of the specimens before grinding (Fig. 1) and the original stacks are available upon request to C. Naglik or C. Klug.

Methods

The serial grinding and data acquisition have been achieved in the Heidelberg tomography laboratory (Germany) and roughly followed the workflow described in Pascual-Cebrian *et al.* (2013) and Tajika *et al.* (2014). The specimens were first embedded in coloured epoxy resin, which contained limestone fragments to reduce the amount of resin required. The block surface was then polished with a G&N MPS 2 – R300 precision surface grinding machine. The thickness of the ground increments varies between 60 μm for *Fidelites clariondi*, 49 μm for *Goniatites clariondi* and 48 μm for *Diallagites lenticulifer* (Table 1 – calculated increments). After each grinding phase, the freshly exposed surface was scanned in a water quench using a modified high-end flatbed scanner EPSON V750pro. The horizontal resolution was limited by the scanner resolution, with a maximum of almost 2000 dpi (features >0.01 mm visible; Table 1 – resolution).

The resulting 2-D slice scans were processed as follows: every fourth slice was imported into a software for vector image edition (Adobe® Illustrator) and manually traced. The segmentation of the different elements was performed manually because the application of an automatic threshold function did not yield results sufficient to calculate volumes from the reconstructions due to three main reasons: (1) the automatic threshold approach in VG Studio Max 2.1 (Volume Graphics GmbH, Heidelberg, Germany) could not be used because of recrystallization mainly of the inner whorls, which had partially destroyed the septa. Shell and septa are sometimes difficult to tell apart in these inner whorls and therefore needed manual reconstruction. By manually reconstructing the septa, we obtained a complete data set; (2) the automatic reconstruction of the siphuncle was also impossible, because the connecting ring is not preserved. However, we can virtually retrace it by following the septal necks, which yielded information about connecting ring thickness (Fig. 2); and (3) similarly, the outer shell needed reconstruction because the shells are never perfectly preserved and locally, shell parts were missing. This manual tracing step in the process made a complete virtual reconstruction possible including the differentiation of the various structures of the shell in colour. Different colours were assigned to the shell wall in 180° segments, to each septum, the siphuncle, as well as each chamber for the volume calculations

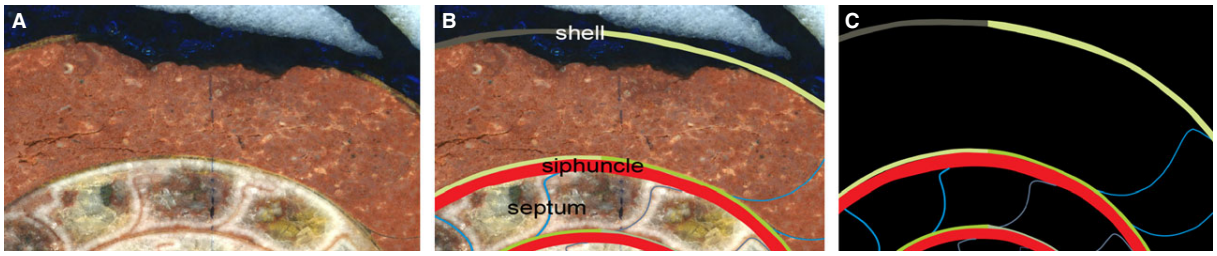

Fig. 2. Part or the 160th 2-D slice of *Diallagites lenticulifer*. A, before tracing. Note the broken shell and the shape of the septal necks, where the siphuncle was inserted. B, retraced part or the shell. Different colours were used for the different structures such as the outer shell, the siphuncle and the septa. C, representation of the final traced slice before being processed.

(Figs 2C, 3B–F). The virtual image stacks of these traced images were processed in VG Studio Max 2.1 (Fig. 3A) entering their respective voxel sizes (Table 1) and thus enabling direct volume calculations of the different retraced parts (Fig. 3B–F) by counts of similar colour voxels in VG Studio Max 2.1. The voxel sizes correspond to the pixel 3-D resolution of the retraced pictures (for x and y dimensions). It was then multiplied by four because only each fourth slice was traced. By doing so, the increment between two slices was calculated to obtain the z dimension (Table 1).

Data set

2-D and 3-D parameters have been measured in detail for each specimen through ontogeny. Concerning the 3-D parameters, we measured all septum and chamber volumes of the phragmocones from the reconstructions. From the classical parameters (Korn 2010), we measured the conch diameters (dm_1 and dm_2, where dm_1 is the largest diameter in cross-section, and dm_2 is the diameter taken half a whorl before, i.e. away from the aperture) and the septal distances (in angles; Arai & Wani 2012). Apertural heights can be calculated by ah = dm_1–dm_2 (Fig. 3). The diameters have been measured as proxy for growth and age to compare those to the volumetric data. These diameters enable the calculation of whorl expansion rate (WER). Statistic tests of correlation have been performed using PAST (Hammer *et al.* 2001).

For this study, we stopped the measurement at the last septum (i.e. the body chamber volumes were not measured) except for the WER (Raup 1966) and the chamber volume expansion rate. Concerning the WER, we did not use Raup & Chamberlain's equation (1967), because it uses radii referring to a coiling axis, which is difficult to locate and which changes its position through ontogeny in real shells (compare Urdy *et al.* 2010a,b). Instead, we used the equation introduced by Korn (2000): WER = $(dm_1/dm_2)^2$. The WER gives information on the aperture shape variation during ontogeny. Thereby, it can indirectly provide information on palaeobiological aspects such as the *syn vivo* orientation of the shells of ammonoids through ontogeny (Saunders & Shapiro 1986; Klug 2001). In accordance with the WER calculation method, we measured the chamber volume expansion rate (CVER) at each half whorl (Table 5) as follows:

We calculated the chamber volume at a certain diameter (dm1), which we divided by the chamber volume at exactly a whorl earlier (chamber corresponding to dm_2);

$$\mathrm{CVER} = V_\alpha / V_{\alpha-w},$$

where V is the volume, α represents a certain chamber, and $\alpha-w$ represents the corresponding chamber of the preceding whorl, 360° behind the first chamber. Septum and chamber volumes were plotted together to find out how they vary during ontogeny. These volumetric data were also plotted versus the classical parameters to see how far they correlate with each other.

Results

Volume changes through ontogeny

Here, we present the first empirical volume data generated for ammonoids from tomographic data. To assess volume changes through ontogeny, we first plotted chamber and septum volumes versus chamber numbers (Fig. 4). It was no surprise that all the curves show exponential increases in volumes during most of the ontogeny because the increase in whorl cross-section largely follows a logarithmic spiral. The coefficients of determination r^2, which represent how well the regression fits the original data points, the best being 1 for these charts, are very high (>0.98, Fig. 4). Nevertheless, in all the curves, some discontinuities occur, which might have their origin in either minor errors in the reconstructions or in

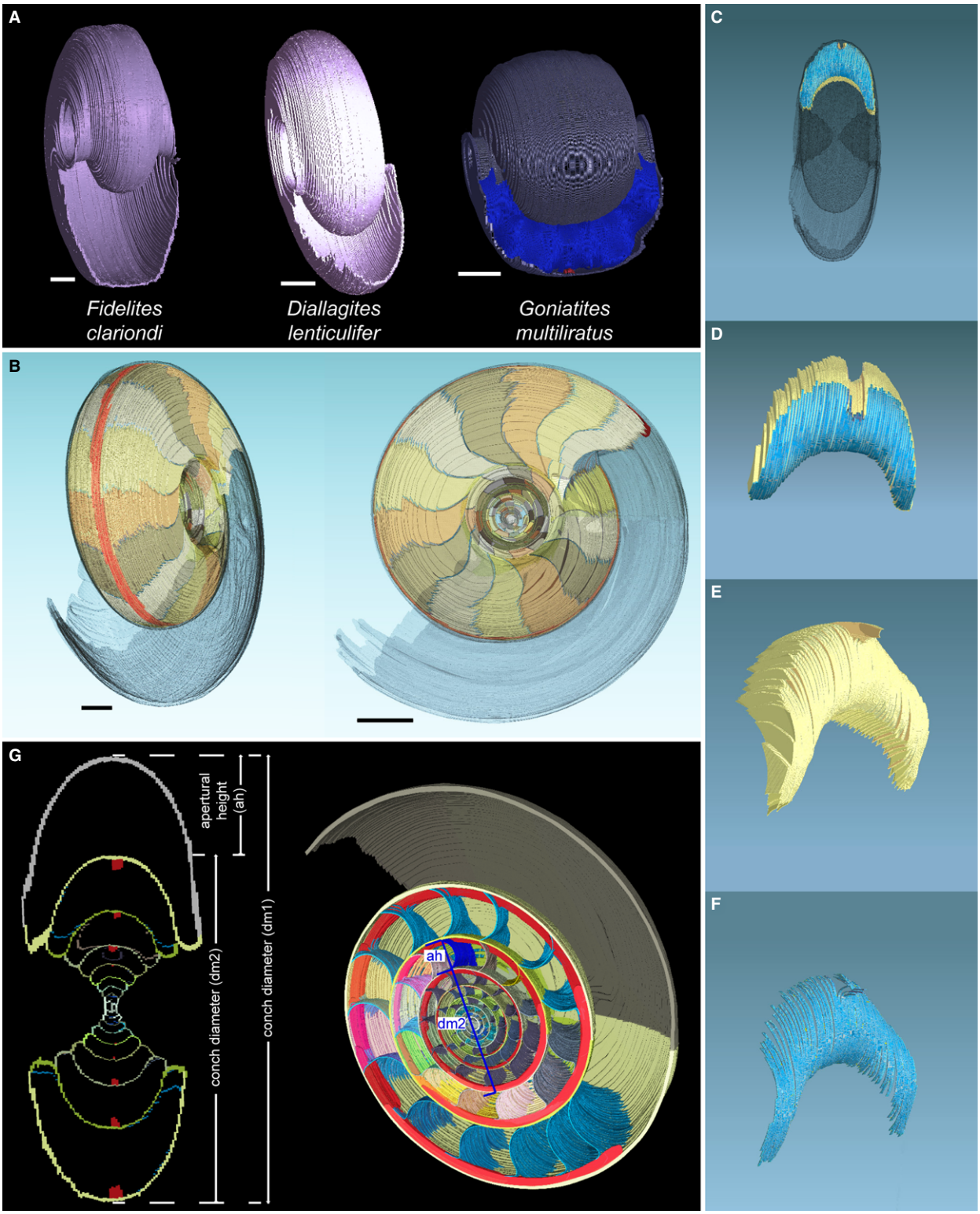

Fig. 3. 3-D reconstructions of the studied specimens. A, apertural oblique views of the generated 3-D empirical models of the specimens using VG Studio Max 2.1. The last septum is visible in *Goniatites multiliratus* because the body chamber is not preserved in this specimen. Scale bar: 0.5 cm. B, coloured inner elements of *Diallagites lenticulifer* (chambers, septa, siphuncle) with transparent shell. Scale bar: 0.6 cm. C, complex chamber/septum within the *D. lenticulifer* shell. D, detail of the complex shown in C. E, isolated chamber volume. F, isolated septum volume. G, classical one-dimensional parameters used in this study (illustrated with *D. lenticulifer*) in cross-section (descriptive terms from Korn 2010) and in the 3-D clipped view showing an example of how the measurements have been taken: corresponding diameters dm_2 and ah for the dark blue septum. These measurements have been taken for each septum.

Table 5. Measurements of the CVER.

Fidelites clariondi CVER Chambers	Value	*Diallagites lenticulifer* CVER Chambers	Value	*Goniatites multiliratus* CVER Chambers	Value
19/4	4.14	9/2	2.56	16/2	3.75
25/8	6.21	11/3	2.50	22/6	7.67
28/10	11.83	13/5	2.60	25/10	4.10
32/14	13.38	16/7	3.35	29/13	6.27
36/19	14.44	18/9	1.98	32/16	9.00
41/25	14.37	20/11	2.44	36/22	3.84
44/28	17.52	22/13	3.22	40/25	11.00
47/32	15.43	25/16	3.33	44/29	7.01
50/36	15.02	27/18	4.21	47/32	8.43
54/41	11.74	30/20	2.01	52/36	10.83
57/44	10.95	33/22	2.66	55/40	8.11
61/47	12.51	36/25	2.01	59/44	8.11
64/50	9.49	39/27	2.48	62/47	10.22
69/54	11.46	42/30	3.74	66/52	5.67
		44/33	2.96	69/55	6.34
		47/36	3.41	73/59	4.54
		50/39	2.65	76/62	3.72
		53/42	3.39	81/66	4.15
		55/44	3.22	85/69	3.48
		58/47	2.99	89/73	3.07
		61/50	2.71		
		65/53	3.41		
		67/55	3.61		
		70/58	3.17		
		73/61	3.75		
		77/65	2.93		
		80/67	2.18		

Abbreviation: CVER, chamber volume expansion rate.

irregular growth phases due to adverse ecological conditions or sub-lethal injuries (compare Kraft *et al.* 2008). This aspect will be addressed below.

The values measured in *Diallagites lenticulifer* and *Goniatites multiliratus* are more similar to each other than to those of *Fidelites clariondi*. At the beginning of ontogeny, the volumes of the three species increase only slightly and steadily. A change in the slope of the trajectories occurred in each specimen around the 19th to 21st chamber. Those changes appeared at chamber volumes between 0.9 mm^3 and 1.23 mm^3 (for corresponding conch diameters between 1.74 mm and 4.29 mm). The slopes become steeper then. In *Diallagites lenticulifer*, a reduction in the volumes of the last formed chambers and septa is visible from the 78th chamber onward. As for *Goniatites multiliratus*, a decrease in chamber volumes is also evident but only in the penultimate chamber. The fourth change in growth of Klug (2001), which corresponds to the deceleration of growth close to maturity, appears to be the origin of this decrease. We deal with this hypothesis in depth later in the discussion.

Fidelites clariondi does not show a terminal decrease in growth, which is as strong as in the other two specimens, albeit the last measured chamber volume does not follow the exponential trend. It shows a slight slowdown in chamber volume increase and a decrease in chamber volume similar to the other two specimens might have occurred, if the ammonoid had continued to grow (Fig. 4).

Chamber versus septum volumes through ontogeny

Septum volumes were plotted versus chamber volumes (Fig. 5) to assess volume growth trajectories. With the exception of some discontinuities and scattered values in the inner whorls, a general linear regression was obtained in each of the three specimens. The linear regression equations are well supported, and the data show a good correlation: r^2 is greater than 0.97 (Fig. 5), as well as $P(\text{uncorr}) \ll 0.001$, thus indicating that this linear regression is statistically significant.

In the case of *Fidelites clariondi* and *Diallagites lenticulifer*, the trends show a slight undulation in the upper parts of the respective curves (Fig. 5). The data of chamber and septum volumes (Fig. 5) correlate well with each other, producing a relatively straight line. Moreover, the r^2 values increase from the oldest (*Fidelites clariondi*) to the youngest examined specimen (*Goniatites multiliratus*). The more derived the species is, the better the linear regression appears to be.

Comparison of the volume data with classical shell parameters

Chamber and septum volumes plotted versus some classical parameters such as the apertural height (ah) and the conch diameter (dm_1, Fig. 6). The power trend lines appear to be the most suitable regressions for these graphs (Fig. 6). The volume changes show a significant correlation of the other parameters with a $P(\text{uncorr}) \ll 0.01$ (in log-transformed variables) and an excellent correlation of the exponential trend (high r^2 values). The typical equation for these power trends is $y = bx^{\alpha}$, where y represents the volumes (ordinate axis), x represents a distance (abscissa axis), and b as well as α are constants. The values of α are all positives and lie between 2.07 and 3.07.

In two of these graphs, *Diallagites lenticulifer* and, less clearly, *Goniatites multiliratus* show a terminal decrease in growth in their supposedly mature stages (compare Fig. 4). The septum volumes plotted versus the conch diameter (dm_1) are the variables, which discriminate the three examined specimens the best.

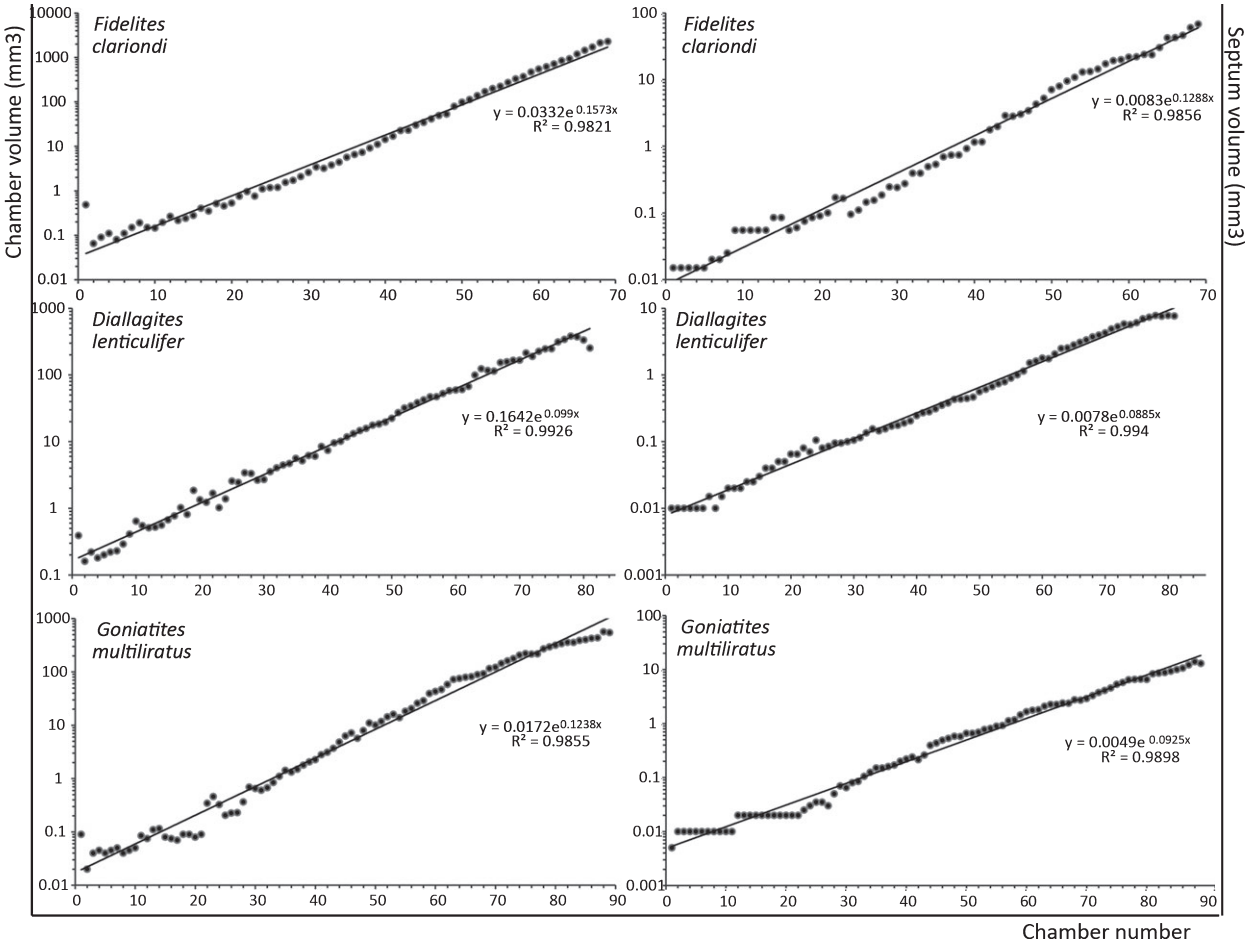

Fig. 4. Volumetric data plotted versus chamber numbers. In the left column, the volumes of the chambers are represented and show an exponential trend for each specimen. The exponential regression equations as well as their r^2 values are displayed on the graphs. Concerning the last chambers, a decrease in volumes is visible in *Diallagites lenticulifer* corresponding to the mature stage. In the right column, similar trends are seen in the evolution of the septum volumes through ontogeny. Generally, values are more similar between *D. lenticulifer* and *G. multiliratus* compared with *F. clariondi*.

Chamber volumes versus septal distances

Septal distances are plotted through chamber volumes in Figure 7. They have been measured in angle from the median section from the original picture stacks. Therefore, the irregular distribution of the data points is caused by the slight obliquity of the cutting planes, which are not perfectly parallel to the plane of symmetry. Because of these artefacts, little can be concluded from the graph of *Goniatites multiliratus* because the artefact contorted the original signal. Indeed, a bi- or tri-phasic trend is evident in *Fidelites clariondi* and *Diallagites lenticulifer*. The decreasing septal distances in the first part of the curve represent the neanic stage (Westermann 1996; Klug 2001). The transition to the juvenile stage, characterized by more widely spaced septa at its beginning (Bucher *et al.* 1996), occurs around a chamber volume of 0.5 mm^3 in *Fidelites clariondi* (around the 17th septum) and around 0.9–1 mm^3 (16th septum) in *Diallagites lenticulifer*. The strongly scattered values of *Goniatites clariondi* do not permit to identify these growth-stage transitions as clearly as in the other two species. The transition between the juvenile and the adult stage remains unclear. *Fidelites clariondi* shows a slight and steady decrease in septal distances from near the 45th chamber, but there are no further distinct changes at the neanic/juvenile transition.

Analysis of some classical shell parameters

Classical shell parameters include the diameter, whorl width, whorl height, aperture height and umbilical width (e.g. Raup & Chamberlain 1967). Diameters of consecutive whorls or any diameter with its apertural height can be used to calculate the WER (see Methods chapter). In Figure 8A, the diameter is used as a proxy for ontogeny and the WER as a proxy for growth. As documented by Klug

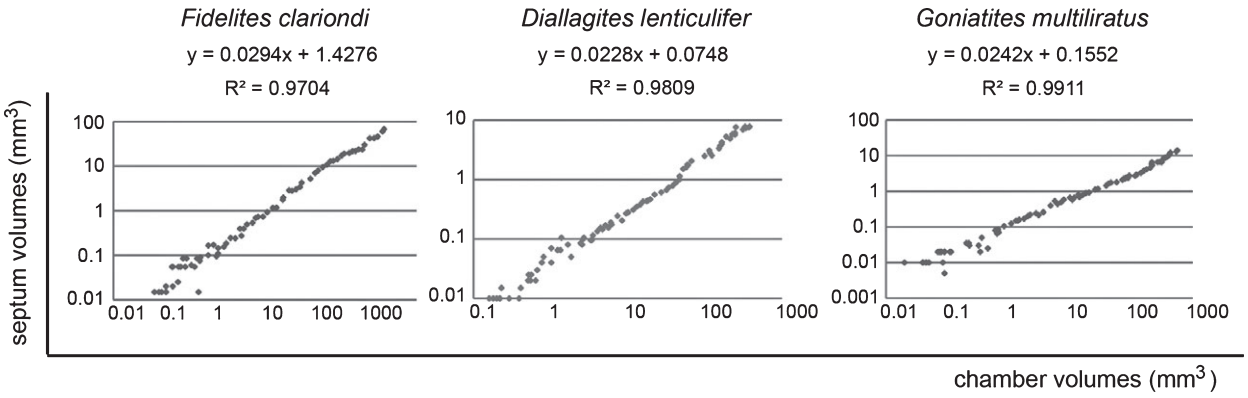

Fig. 5. Chamber volumes plotted versus septum volumes in logarithmic scale. Linear trends are given for each specimen and the linear regression equations with the corresponding r^2 values are displayed above the charts. Note that the lowest values (early ontogeny) are slightly scattered. It is caused by the resolution limits, probably in combination with the increase in the measuring error. In the case of *Fidelites clariondi* and *Diallagites lenticulifer*, the trends show a slight undulation in their upper parts.

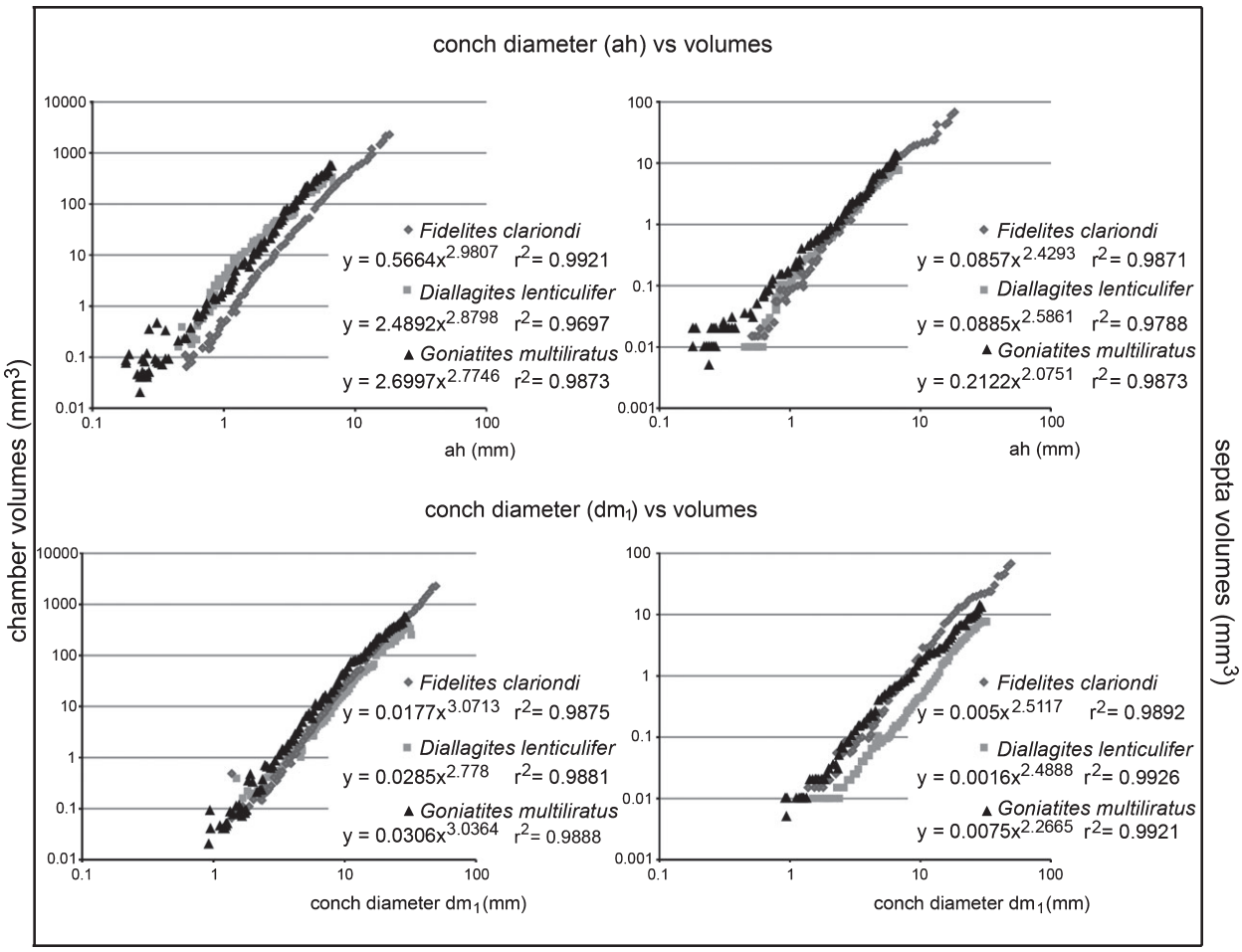

Fig. 6. Top – Aperture heights (ah) versus chamber volumes on the left, and septa volumes on the right in logarithmic scale. Bottom – conch diameters (dm_1) versus chamber volumes on the left and septa volumes on the right (in logarithmic scale). Power trend lines as well as their respective r^2 values are displayed in the charts. These power trends typically show a positive nonlinear correlation between volumetric data and conch parameters. The trends show more similarities between *Fidelites clariondi* and *Diallagites lenticulifer*, perhaps resulting from conch geometry. These two species have more discoidal shells in contrast to the pachyconic shell of *Goniatites multiliratus*. Also, the terminal volume decrease in the mature stage is visible for *D. lenticulifer* and *G. multiliratus*.

(2001), the WER follows two fundamentally different trends in many Palaeozoic ammonoids. Accordingly, anarcestids such as *Diallagites lenticulifer* and goniatitids such as *Goniatites multiliratus* show an initial decrease in WER, followed by a long phase with low WER values and a more or less pronounced

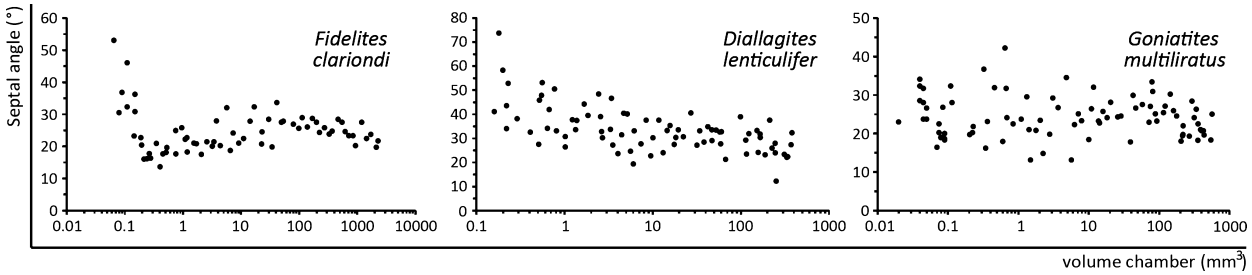

Fig. 7. Septal angles plotted versus chamber volumes for the three specimens. Trends are more clearly visible and described in the text for *Fidelites clariondi* and *Diallagites lenticulifer* compared with the more scattered distribution of the values of *Goniatites multiliratus*. In all cases, an initial decrease in both values appears to be followed by a plateau with rather continuous angle values.

terminal increase in WER. By contrast, in agoniatitids such as *Fidelites clariondi*, the WER decreases initially, but increases more or less strongly throughout the neanic and premature phases and ultimately decreases at maturity.

Chamber volume expansion rate (CVER)

Like the classical WER using diameters (e.g. Korn 2010), chamber volumes of consecutive whorls are used to calculate the CVER (see Data set chapter). Our aim here was to compare how this new parameter evolves in contrast to the WER throughout ontogeny (using the diameter as a proxy for growth). The results are displayed in Figure 8B. As we measured only each half whorl along the shell diameter, we have a lower number of data points than for the WER (Fig. 8A), which has been measured for each chamber. The ontogenetic trends in CVER and WER show more similarities between *Fidelites clariondi* and *Goniaties multiliratus*.

Discussion

Volumetric data

Although some premature volume changes can be correctly interpreted as responses to environmental constraints or injuries resulting from septal crowding caused by various factors (see Kraft *et al.* 2008 and references therein), we suggest that the major trends in chamber volumes have a different driver in the three studied specimens. Our specimens do not show distinct injuries and do not appear to be pathological (which was one criterion to select them). Based on this, the volume changes seen in all of them therefore reflect rather changes in growth during the different growth stages (Fig. 4) than septal crowding due to external perturbations (e.g. Hölder 1956; Kraft *et al.* 2008). The volumes of the three species increase only slightly and steadily, and the first main growth phase can be interpreted as the embryonal and perhaps the neanic growth stages (Westermann 1996; Klug 2001). A change in the slope of the trajectories occurred in each specimen around the 19th to 21st chamber. This change appeared at chamber volumes between 0.9 mm^3 and 1.23 mm^3 (equalling conch diameters between 1.74 mm and 4.29 mm). The slopes of the curves become steeper then. This growth change might reflect the transition from the first post-embryonic stage, that is, the neanic-stage *sensu* Westermann (1958, 1996), to the juvenile stage as outlined by Klug (2001) or to the juvenile stage *sensu* Bucher *et al.* (1996). This abrupt change is consistent with an interval of widely spaced septa occurring at this stage (Bucher *et al.* 1996). Accordingly, the terminal decrease or reduced incremental rate in chamber volumes seen especially in *Diallagites lenticulifer* is most likely linked to the decrease in growth occurring at the mature stage, which was dubbed 'terminal countdown' by Seilacher & Gunji (1993), Bucher *et al.* (1996), Klug (2001), and Klug & Korn (2004). The greater degree of similarity between *Diallagites lenticulifer* and *Goniatites multiliratus* may be related to the fact that they share a low WER, that they are more involute, and/or that they are more closely related to each other than to *Fidelites clariondi.* This mature growth decrease is also supported by the roughly adult size of our specimens, which is known from further material, which is at our disposal.

The disparity in the lowest values of all specimens is likely a result of the limited optical/physical resolution of the scanned images, which introduced some errors, increased by the third dimension during the voxel generations. Therefore, possible biological and/or ecological origins of variations cannot be inferred with certainty because the lower parts of the curve suffer from this inaccuracy. Further investigations on juvenile forms with better preserved materials at higher resolutions may improve the quality of

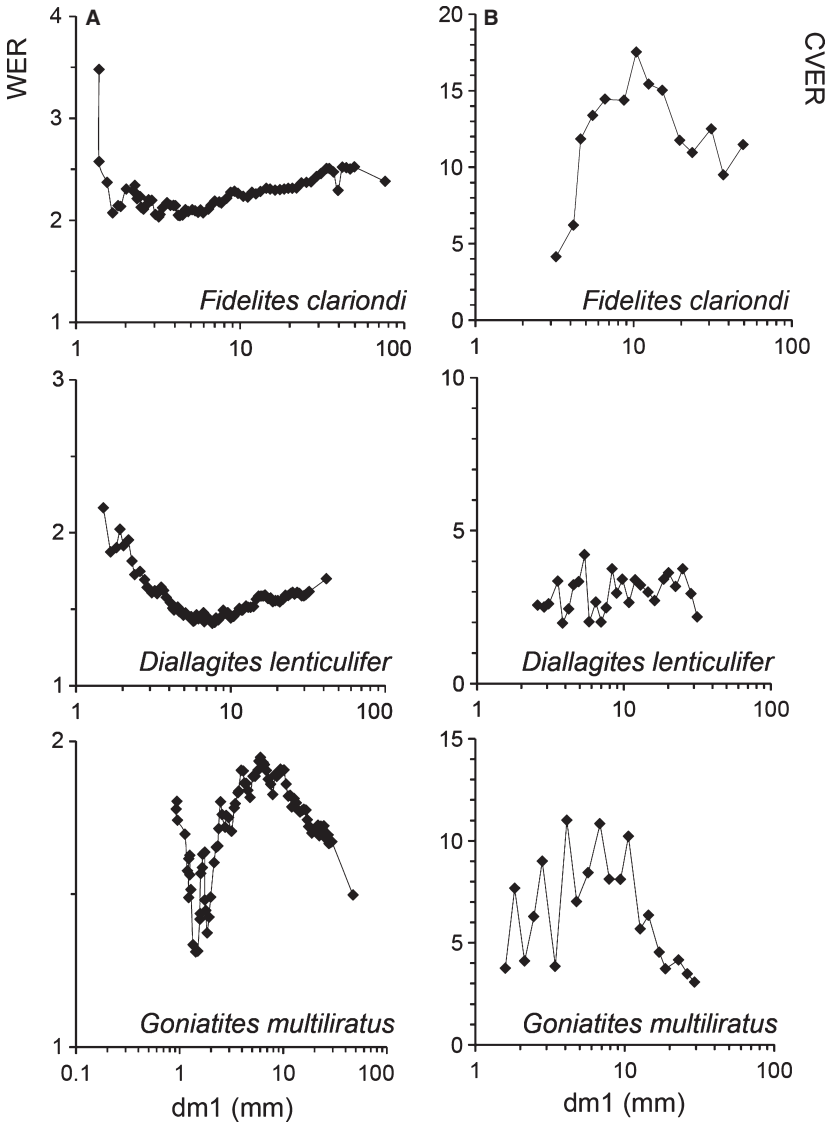

Fig. 8. Allometric growth reflected in the whorl expansion rate (WER) (A) and the chamber volume rate (B) measured virtually from the 3-D reconstructions. The diameter is used as a proxy for ontogeny and the WER as a proxy for growth. A, trends show nonlinear polyphasic allometries described in detail in the text, characterizing the different growth stages in ammonoid ontogeny. B, nonlinear polyphasic allometries are also observed with the chamber volume expansion rate (CVER) and detailed in the text. The sinuosity in B is probably caused by a slight obliquity of the grinding planes relatives to the plane of symmetry.

the data of the embryonic and neanic shells and might enable us to detect whether there are any biologically meaningful variations or not.

In the case of *Fidelites clariondi* and *Diallagites lenticulifer*, the trends show a slight undulation in the upper parts of the respective curves (Fig. 5). It is likely that these undulations represent an artefact of oblique grinding. Nevertheless, other ontogenetic changes may have occurred near adulthood. For example, a thickening of the final septum was found in extant nautilids at the end of ontogeny, which has been interpreted to reflect maturity (Collins & Ward 2010). However, there is currently no support for the shell secretion variations hypothesis in our material.

Many articles have documented allometric growth in ammonoids (e.g. Gould 1966; Bucher *et al.* 1996; Klug 2001; Korn 2012). It has to be taken into account that these authors employed 2-D parameters in their studies of 3-D study objects. Hoffmann & Zachow (2011) illustrated a high-quality 3-D model of a Recent *Nautilus* shell based on CT scans, which appears promising for further comparisons and other investigations, focused on the buoyancy system.

The more derived the species is, the better the linear regression appears to be between septa and chamber volumes (Fig. 5). This linear regression indicates that the allometries in both parameters

show almost identical timings in the three examined taxa. Although our data set is very small in terms of the number of species and should be viewed rather as a test, our results suggest an increase in the correlation of the two volume parameters throughout the evolution of Palaeozoic ammonoids. Naturally, further studies and a larger sample of taxa are necessary to adequately test this hypothesis. The increasing correlation throughout evolution might be related to the progressive tighter shell coiling, yielding a more continuous growth, or this could be an artefact of resolution: the largest and stratigraphically oldest specimen (*Fidelites clariondi*) was examined with a larger slice spacing; its values therefore may be slightly less accurate and this could potentially also contribute to the lower r^2 value of its linear regression.

When it comes to volumetric data plotted versus linear distances (aperture height and diameter, Fig. 6), the relationship between the two parameters reflects allometric growth of these volumes and distances. Allometry was defined by Huxley & Teissier (1936) as follows: '*The elementary law of relative growth* or *law of simple allometry* can be expressed by a formula of the type:

$$y = bx^{\alpha},$$

where y is the part, x the standard or whole, and b and α are constants'.

When both parameters (x and y) are of the same dimension, the constant α represents the deviation from isometry ($\alpha = 1$), and if $\alpha > 1$, parameters show a *positive allometry* (Huxley & Teissier 1936; Gould 1966; Korn 2012). Nevertheless, our case deals with parameters with different dimensions (volumes and lengths). According to Gould (1966), because y is a volume [L^3] and x is a length [L], $\alpha = 3$ indicates isometry. Therefore, it appears that chamber volumes globally grew roughly isometrically with the aperture height and the diameter, because the α values lie between 2.77 and 3.07 (Fig. 6, left column graphs). The degree of isometry of volume chambers appears to be greater with the conch diameter than the aperture height (α values closer to 3). With $2.07 < \alpha < 2.58$ in the graphs of the right column in Fig. 6, the results clearly show a negative allometry ($\alpha < 3$). This means that the y/x ratios decrease with the increasing absolute magnitude of x (see Gould 1966). With regard to the volumetric data plotted versus aperture heights, *Fidelites clariondi* and *Diallagites lenticulifer* show more similarities to each other than to *Goniatites multiliratus*. This might result from differences in conch geometry, which is more discoidal (Korn 2010) in the former two taxa in contrast to the pachyconic shell of *Goniatites multiliratus*. However, this trend is not evident in the volumetric data plotted versus conch diameters (Fig. 6). In that case, *Diallagites lenticulifer* shows slightly different trajectories especially for the septum volumes. The allometry of volumes is more strongly developed in septum volumes compared with the diameter than in the other correlations, as reflected in the α values below 3. In conclusion, it appears that conch diameter seems to be the best candidate to use as y proxy for the volume chambers.

WER and CVER

In accordance with the results of Klug (2001), our sectioned specimen of *Fidelites clariondi* displays the adult phase (the last decreasing phase), which was also described by Korn (2012). The variations in the aperture shape through ontogeny probably reflect changes in the mode of life, because the change in WER is directly linked to the orientation of the shell during the ammonoid's life (Saunders & Shapiro 1986; Klug 2001). In turn, the orientation of the shell impacts the swimming capabilities of the ammonoid, and therefore, these changes probably do have an ecological meaning (Jacobs & Chamberlain 1996; Klug & Korn 2004).

The CVER values can be assimilated to a kind of close-up of the growth curve in the neanic and premature stages (Fig. 8). Surprisingly, the trends show more similarities between *Fidelites clariondi* and *Goniaties multiliratus*. They show a phase of CVER increase until a diameter of 10 mm before decreasing. This is linked to variations in aperture shape within the neanic growth stage. For *Diallagites lenticulifer*, the trend is less variable. This can be due to the fact that its shell is more evolute than the other specimens; the less overlapping whorls possibly resulted in a more stable volume expansion rate through ontogeny.

Intraspecific differences in volume data

So far, hardly any volumetric data are available for several specimens from one species; therefore, not much is known about intraspecific variability in chamber volumes. Yet, we performed a small analysis of volumes from corresponding chambers in two specimens of *Normannites sp*. (Fig. 9). Of course, the statistical power of a little sample size is low, and the intraspecific variability of volumetric data requires much more work. Although we have measured only one chamber volume per whorl, the results (Fig. 9B) show that in terms of volumes,

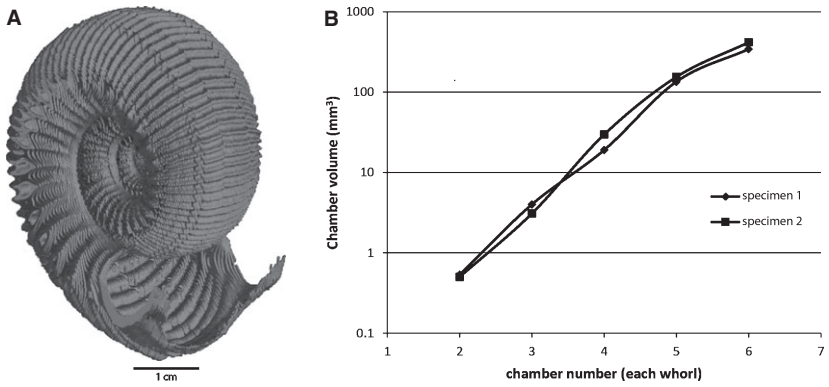

Fig. 9. Intraspecific differences in volume data for *Normannites mitis*. A, 3-D reconstruction of *Normannites mitis*. B, chamber volume comparisons for each whorl in two specimens showing the highly similar trends and values, indicating a low degree of intraspecific variability in the chamber volumes.

there are practically no differences (at least) between these two specimens, which come from the same locality and horizon and are interpreted to belong to the same species. There is just a slight variation, but otherwise, the measured volumes follow exactly the same trends. More data are needed to further test this hypothesis, but our data suggest that the intraspecific variability probably does not affect volumetric changes throughout ontogeny much.

Conclusions and perspectives

For the first time, we generated empirical volume models of ammonoid shells of three species belonging to one important sub-clade of Palaeozoic Ammonoidea each, employing a combination of traditional grinding tomography and novel computational analytical methods. Although our methodology has proven to be time-consuming, our study provides a valuable new source of high-quality data, namely empirical data of chamber and septum volumes. Further improvements in palaeontological micro-CT scanning and Synchrotron X-ray tomography might facilitate and accelerate the production of 2-D slices (and would avoid the loss of specimens) in the future, particularly in recrystallized and infilled Palaeozoic specimens. Based on the measurements taken from our tomographed specimens, we can now answer the questions presented in the introduction:

1 We measured septum and chamber volumes throughout ontogeny and compared them with the classical parameters. They grow exponentially, and chamber volumes show isometry when compared to the aperture height and the diameter with α values near 3. Contrarily, negative allometry ($\alpha < 3$) has been found between septum volumes and linear parameters such as diameter and aperture height. However, the volume values do not strictly follow these exponential trends. In late ontogeny, mature modifications left their traces: the curves become shallower or the trend of an exponential increase even becomes inverted. Due to optical/physical resolution and recrystallization phenomena, volumetric data of the septa of the first whorls lack accuracy, yielding more scattered data points of the first chambers in the graphs.
2 The relationship between classical parameters such as the diameter or the apertural height does show a correlation with the chamber and septum volumes. The line of correlation follows exponential trends. Therefore, it appears like such parameters can indeed be used to estimate changes in chamber and septum volume.
3 As mentioned in (1), some of the growth changes, which had been documented by numerous authors earlier on, can indeed be traced in the volume changes as well. These changes are so far an overall exponential volume increase and the slowdown in volume growth near maturity. We did not find growth changes in the chamber and septum volumes data in addition to the ones previously known from the traditional parameters.
4 *Diallagites lenticulifer* and *Goniatites multiliratus* show slightly more similar growth trajectories in volumes compared with *Fidelites clariondi*. Because of the low number of examined specimens and species, more data are needed to test the hypothesis that these trajectories are more similar within than between different clades. Based on our data, we hypothesize that within more closely related clades, these trajectories would resemble each other more strongly. This is

also supported by the classical shell parameters (e.g. Korn & Klug 2001).

This shows that the examination of the ontogenetic change in chamber and septum volumes can yield information, which may be useful to test phylogenetic and other palaeobiological hypotheses in the future; our preliminary study on intraspecific variability leads to the hypothesis that this aspect does not seem to affect volumetric data much. Naturally, representatives of other sub-clades are needed to see how ontogenetic changes in chamber and septum volumes differ in other major sub-clades.

Last but not least, these data have a great potential and enable us now to investigate the buoyancy system of ammonoids with empirical data. Up to now, only Tajika *et al.* (2014) succeeded to test the buoyancy of a Mesozoic specimen of *Normannites*. Previously, only theoretical mathematical models had been produced by various researchers (Trueman 1940; Saunders & Shapiro 1986; Jacobs 1996; Jacobs & Chamberlain 1996).

Acknowledgements. – We thank the staff of the grinding tomography laboratory in Heidelberg, namely Dominik Hennhöfer and Enric Pascual Cebrian for their thorough work. They kept up the good work after the tragic loss of our co-author Stefan Götz, whom we dearly miss. Field work and expenses involved with the tomography were funded by the Swiss National Science Foundation (Project Numbers 200021-113956/1, 200020-25029 and 200020-132870). We also thank the Moroccan colleagues of the Ministère de l'Energie et des Mines (Rabat and Midelt) for providing permits for field work and sample export. We greatly appreciate the support of Royal Mapes, who organized fieldwork in Oklahoma and Texas for us and who showed us the localities. Stephan Lautenschlager and Imran Rahman kindly commented earlier drafts of this manuscript, Dieter Korn helped us to improve the quality of our manuscript. Iwan Jerjen and Philip Schütz from the Empa (Dübendorf) tried to obtain CT data of our ammonoid materials for volumetry using various machines and software. The equally careful and helpful review by Rene Hoffmann is gratefully acknowledged.

References

Arai, K. & Wani, R. 2012: Variable growth modes in late cretaceous ammonoids: implications for diverse early life histories. *Journal of Paleontology 86*, 258–267.

Bucher, H. 1997: Caractères périodiques et modes de croissances des ammonites : comparaison avec les gastéropodes. *Geobios Mémoire spécial 20*, 85–99.

Bucher, H. & Guex, J. 1990: Rythmes de croissance chez les ammonites triasiques. *Bulletin de la Société vaudoise des sciences naturelles 80*, 191–209.

Bucher, H., Landman, N.H., Klofak, S.M. & Guex, J. 1996. Mode and rate of growth in ammonoids. *In* Landman, N.H., Tanabe, K. & Davis, R.A. (eds): *Ammonoid Paleobiology. Topics in Geology 13*, 408–461. Plenum Press, New York.

Collins, D. & Ward, P. 2010: Adolescent growth and maturity in *Nautilus*. *In* Saunders, W.B. & Landman, N. (eds): *Nautilus*, 421–432. Springer, the Netherlands.

De Baets, K., Klug, C., Korn, D. & Landman, N.H. 2012: Early evolutionary trends in ammonoid embryonic development. *Evolution 66*, 1788–1806.

De Baets, K., Klug, C. & Monnet, C. 2013: Intraspecific variability through ontogeny in early ammonoids. *Paleobiology 39*, 75–94.

Erben, H.K. 1962: Über die ‚forme elliptique' der primitiven Ammonoidea. *Paläontologische Zeitschrift, H. Schmidt-Festband*, *36*, 38–44.

Erben, H.K. 1964: Die Evolution der ältesten Ammonoidea (Lieferung I). *Neues Jahrbuch für Geologie und Paläontologie, Abhandlungen 120*, 107–212.

Erben, H.K. 1965: Die Evolution der ältesten Ammonoidea. II. *Neues Jahrbuch für Geologie und Paläontologie, Abhandlungen 122*, 275–312.

Erben, H.K. 1966: Über den Ursprung der Ammonoidea. *Biological reviews of the Cambridge Philosophical Society 41*, 641–658.

Garwood, R.J., Rahman, I.A. & Sutton, M.D. 2010: From clergymen to computers – the advent of virtual palaeontology. *Geology Today 26*, 96–100.

Gerber, S., Neige, P. & Eble, G.J. 2007: Combining ontogenetic and evolutionary scales of morphological disparity: a study of early Jurassic ammonites. *Evolution & Development 9*, 472–482.

Gordon, M. 1962: Species of Goniatites in the Caney Shale of Oklahoma. *Journal of Paleontology 36*, 355–357.

Gould, S.J. 1966: Allometry and size in ontogeny and phylogeny. *Biological Reviews 41*, 587–640.

Hammer, O., Harper, D.A.T. & Ryan, P.D. 2001: PAST: Paleontological Statistics Software Package for education and data analysis. *Palaeontologia Electronica 4*, 9.

Hoffmann, R. & Zachow, S. 2011. *Non-invasive approach to shed new light on the buoyancy business of chambered cephalopods (Mollusca)*. IAMG Salzburg, 1–11.

Hoffman, R., Schultz, J.A., Schellhorn, R., Rybacki, E., Keupp, H., Gerden, S.R., Lemanis, R. & Zachow, S. 2013: Non-invasive imaging methods applied to neo- and paleontological cephalopod research. *Biogeosciences Discussions 10*, 18803–18851.

Hölder, H. 1956: Über Anomalien an jurassischen Ammoniten. *Paläontologische Zeitschrift 30*, 95–107.

House, M.R. 1989: Ammonoid extinction events. *Philosophical Transactions of the Royal Society of London. Series B, Biological Sciences 325*, 307–326.

Huxley, J.S. & Teissier, G. 1936: Terminology of relative growth. *Nature 137*, 780–781.

Jacobs, D. 1996: Chambered cephalopod shells, buoyancy, structure and decoupling: history and red herrings. *Palaios 11*, 610–614.

Jacobs, D.K. & Chamberlain, J.A. 1996. Buoyancy and hydrodynamics in ammonoids. *In* Landman, N., Tanabe, K. & Davis, R.A. (eds): *Ammonoid Paleobiology. Topics in Geobiology 13*, 169–223. Plenum Press, New York.

Jacobs, D.K. & Landman, N.H. 1993: *Nautilus* – a poor model for the function and behavior of ammonoids? *Lethaia 26*, 101–111.

Kant, R. 1973a: Allometrisches Wachstum paläozoischer Ammonoideen: Variabilität und Korrelation einiger Markmale. *Neues Jahrbuch für Geologie und Paläontologie, Abhandlungen 143*, 153–192.

Kant, R. 1973b: Untersuchungen des allometrischen Gehäusewachstums paläozoischer Ammonoideen unter besonder Berücksichtigung einzelner, Populationen'. *Neues Jahrbuch für Geologie und Paläontologie, Abhandlungen 144*, 206–251.

Kant, R. & Kullmann, J. 1988: Changes in the conch form in the Paleozoic Ammonoids. *In* Wiedmann, J. & Kullmann, J. (eds): *Cephalopods – Present and Past*, 43–50. Schweizerbart, Stuttgart.

Kennedy, W.J. 1977: Ammonite evolution. *In* Hallam, A. (ed): *Patterns of Evolution as Illustrated in the Fossil Record*, 251–304. Elsevier, Amsterdam.

Klofak, S.M., Landman, N.H. & Mapes, R.H. 1999: Embryonic development of primitive ammonoids and the monophyly of the ammonoidea. *In* Oloriz F. & Rodriguez-Tovar F.J. (eds): *Advancing Research on Living and Fossil Cephalopods*, 23–45. Plenum Press, New York.

Klofak, S., Landman, N.H. & Mapes, R.H. 2007: Patterns of embryonic development in early to middle Devonian

Ammonoids. *In* Landman N.H., Mapes R.H. & Davis R.A. (eds): *Cephalopods – Present and Past: New Insights and Fresh Perspectives* 1, 15–56. Springer, Dordrecht.

Klug, C. 2001: Life-cycles of some Devonian ammonoids. *Lethaia 34*, 215–233.

Klug, C. 2002: Quantitative stratigraphy and taxonomy of late Emsian and Eifelian ammonoids of the Anti-Atlas (Morocco). *Courier. Forschungsinstitut Senckenberg 238*, 1–109.

Klug, C. & Korn, D. 2004: The origin of ammonoid locomotion. *Acta Palaeontologica Polonica 49*, 235–242.

Klug, C., Kröger, B., Kiessling, W., Mullins, G.L., Servais, T., Frýda, J., Korn, D. & Turner, S. 2010: The Devonian nekton revolution. *Lethaia 43*, 465–477.

Korn, D. 2000: Morphospace occupation of ammonoids at the Devonian-Carboniferous Boundary. *Paläontologische Zeitschrift 74*, 247–259.

Korn, D. 2010: A key for the description of Palaeozoic ammonoids. *Fossil Record 13*, 5–12.

Korn, D. 2012: Quantification of ontogenetic allometry in ammonoids. *Evolution and Development 14*, 501–514.

Korn, D. & Klug, C. 2001: Biometric analyses of some Palaeozoic ammonoid conchs. *Berliner geowissenschaftliche Abhandlungen 36*, 173–187.

Kraft, S., Korn, D. & Klug, C. 2008: Patterns of ontogenetic septal spacing in Carboniferous ammonoids. *Neues Jahrbuch für Geologie und Paläontologie, Abhandlungen 250*, 31–44.

Kröger, B., Vinther, J. & Fuchs, D. 2011: Cephalopod origin and evolution: a congruent picture emerging from fossils, development and molecules. *BioEssays 33*, 602–613.

Kruta, I., Landman, N., Rouget, I., Cecca, F. & Tafforeau, P. 2011: The role of ammonites in the Mesozoic marine food web revealed by jaw preservation. *Science 331*, 70–72.

Kullmann, J. & Scheuch, J. 1970: Wachstums-änderungen in der Ontogenese paläozoischer Ammonoideen. *Lethaia 3*, 397–412.

Kullmann, J. & Scheuch, J. 1972: Absolutes und relatives Wachstum bei Ammonoideen. *Lethaia 5*, 129–146.

Landman, N.H. 1988: Heterochrony in ammonites. *In* McKinney, M.L. (ed): *Heterochrony in Evolution*, 159–182. Plenum Press, New York.

Lehmann, W.M. 1932: Stereo-Röntgenaufnahmen als Hilfsmittel bei der Untersuchung von Versteinerungen. *Natur und Museum 62*, 323–330.

Longridge, L.M., Smith, P.L., Rawlings, G. & Klaptocz, V. 2009: The impact of asymmetries in the elements of the phragmocone of Early Jurassic ammonites. *Palaeontologia Electronica 12*, 1–15.

Lukeneder, A. 2012: Computed 3D visualization of an extinct cephalopod using computer tomographs. *Computers & Geosciences 45*, 68–74.

Lukeneder, S., Lukeneder, A. & Weber, G.W. 2014: Computed reconstruction of spatial ammonoid-shell orientation captured from digitized grinding and landmark data. *Computers & Geosciences 64*, 104–114.

Mallison, H. 2011: Digitizing methods for paleontology: applications, benefits and limitations. *In* Elewa, A.M.T. (ed): *Computational Paleontology*, 7–43. Springer-Verlag, Heidelberg.

Miller, A.I. & Foote, M. 2007: *Principles of Paleontology*, 354 pp. Freeman and Company, New York.

Monnet, C., Zollikofer, C., Bucher, H. & Goudemand, N. 2009: Three-dimensional morphometric ontogeny of mollusc shells by micro-computed tomography and geometric analysis. *Palaeontologia Electronica 12*, 1–13.

Monnet, C., De Baets, K. & Klug, C. 2011: Parallel evolution controlled by adaptation and covariation in ammonoid cephalopods. *BMC Evolutionary Biology 11*, 115.

Pascual-Cebrian, E., Hennhöfer, D. & Götz, S. 2013: 3D morphometry of polyconitid rudist bivalves based on grinding tomography. *Facies 59*, 347–358.

Petter, G. 1959: Goniatites dévoniennes du Sahara. *Publications du Service de la Carte Géologique de l'Algérie, Nouvelle Série, Paléontologie 2*, 1–313.

Raup, D.M. 1966: Geometric analysis of shell coiling: general problems. *Journal of Paleontology 40*, 43–65.

Raup, D.M. & Chamberlain, J.A. 1967: Equations for volume and center of gravity in ammonoid shells. *Journal of Paleontology 41*, 566–574.

Saunders, W.B. & Shapiro, E.A. 1986: Calculation and simulation of ammonoid hydrostatics. *Paleobiology 12*, 64–79.

Seilacher, A. 1988: Why are nautiloid and ammonoid sutures so different? *Neues Jahrbuch für Geologie und Paläontologie Abhandlungen 177*, 41–69.

Seilacher, A. & Gunji, Y.-P. 1993: Morphogenetic countdown in heteromorph shells: limits of programmability. *Neues Jahrbuch für Geologie und Paläontologie Abhandlungen 190*, 237–265.

Sollas, W.J. 1904: A method for the investigation of fossils by serial section. *Philosophical Transactions of the Royal Society of London 196*, 259–265.

Sutton, M.D. 2008: Tomographic techniques for the study of exceptionally preserved fossils. *Proceedings of the Royal Society B 275*, 1587–1593.

Sutton, M.D., Briggs, D.E.G., Siveter, D.J. & Siveter, D.J. 2001: Methodologies for the visualization and reconstruction of three-dimensional fossils from the Silurian Herefordshire Lagerstätte. *Palaeontologia Electronica 4*, 17.

Sutton, M., Rahman, I. & Garwood, R. 2014: *Techniques for Virtual Palaeontology*, 208 pp. Wiley-Blackwell, Chichester.

Tajika, A., Naglik, C., Morimoto, N., Pascual-Cebrian, E., Hennhöfer, D. & Klug, C. 2014: Empirical 3D model of the conch of the Middle Jurassic ammonite microconch *Normannites*: its buoyancy, the physical effects of its mature modifications and speculations on their function. *Historical Biology: An International Journal of Paleobiology*, 1–11, doi: 10.1080/08912963.2013.872097.

Trueman, A.E. 1922: Aspects of ontogeny in the study of ammonite evolution. *Journal of Geology*, *30*, 140–143.

Trueman, A.E. 1940: The ammnonite body chamber, with special reference to the buoyancy and mode of life of the living ammonite. *Quarterly Journal Geological Society, London 96*, 339–383.

Urdy, S., Goudemand, N., Bucher, H. & Chirat, R. 2010a: Allometries and the morphogenesis of the molluscan shell: a quantitative and theoretical model. *Journal of Experimental Zoology Part B: Molecular and Developmental Evolution 314B*, 1–23.

Urdy, S., Goudemand, N., Bucher, H. & Chirat, R. 2010b: Growth-dependent phenotypic variation of molluscan shells: implications for allometric data interpretation. *Journal of Experimental Zoology Part B: Molecular and Developmental Evolution 314B*, 1–24.

Westermann, G.E.G. 1954: Monographie des Otoitidae (Ammonoidea), Otoites, Trilobiticeras, Itinsaites, Epalxites, Germanites, Masckeites, Normannites. *Beihefte zum Geologischen Jahrbuch 15*, 1–364.

Westermann, G.E.G. 1958: The significance of septa and sutures in Jurassic ammonite systematics. *Geological Magazine 95*, 441–455.

Westermann, G.E.G. 1996: Ammonoid life and habitat. *In* Landman, N.H., Tanabe, K. & Davis, R.A. (eds): *Ammonoid Paleobiology*. *Topics in Geology 13*: 607–707. Plenum Press, New York.

CHAPTER II

Buoyancy of some Palaeozoic ammonoids and their hydrostatic properties based on empirical 3D-models

Published in *Lethaia*, vol. 49 (2016)

Lethaia
AN INTERNATIONAL JOURNAL OF PALAEONTOLOGY AND STRATIGRAPHY

Buoyancy of some Palaeozoic ammonoids and their hydrostatic properties based on empirical 3D-models

CAROLE NAGLIK, FARHAD RIKHTEGAR AND CHRISTIAN KLUG

LETHAIA

Naglik, C., Rikhtegar, F. & Klug, C. 2016: Buoyancy of some Palaeozoic ammonoids and their hydrostatic properties based on empirical 3D-models. *Lethaia*, Vol. 49, pp. 3–12.

The interpretation of the function of the ammonoid phragmocone as a buoyancy device is now widely accepted among ammonoid researchers. During the 20th century, several theoretical models were proposed for the role of the chambered shell (phragmocone); accordingly, the phragmocone had hydrostatic properties, which enabled it to attain neutral buoyancy, presuming it was partially filled with gas. With new three-dimensional reconstructions of ammonoid shells, we are now able to test these hypothetical models using empirical volume data of actual ammonoid shells. We investigated three Palaeozoic ammonoids (Devonian and Carboniferous), namely *Fidelites clariondi*, *Diallagites lenticulifer* and *Goniatites multiliratus*, to reconstruct their hydrostatic properties, their *syn vivo* shell orientation and their buoyancy. According to our models, measurements and calculations, these specimens had aperture orientations of 19°, 64° and 125° during their lives. Although none of our results coincide with the aperture orientation of the living *Nautilus*, they do verify the predictions for shell orientations based on published theoretical models. Our calculations also show that the shorter the body chamber, the poorer was the hydrodynamic stability of the animal. This finding corroborates the results of theoretical models from the 1990s. With these results, which are based on actual specimens, we favour the rejection of hypotheses suggesting a purely benthonic mode of life of ammonoids. Additionally, it is now possible to assess hydrodynamic properties of the shells through ontogeny and phylogeny, leading to insights to validate theoretical modes of life and habitat through the animal's life. ☐ *Ammonoidea, buoyancy, grinding tomography, palaeozoic, shell orientation, virtual palaeontology.*

Carole Naglik [carole.naglik@pim.uzh.ch], and Christian Klug [chklug@pim.uzh.ch], Paläontologisches Institut und Museum, Universität Zürich, Karl-Schmid-Strasse 4, Zürich 8006, Switzerland; Farhad Rikhtegar [farhadr@eth.ch], Laboratory of Thermodynamics in Emerging Technologies, Department of Mechanical and Process Engineering, ETH Zürich, Zürich, Switzerland; *manuscript received on 27/05/2014; manuscript accepted on 30/10/2014.*

The function of ammonoid shells as buoyancy devices has been an intriguing topic for naturalists for several centuries (e.g. Derham 1726; Owen 1832; Vrolik 1843; Meigen 1870; Willey 1902). In the past seven decades, the buoyancy of ammonoids has been theoretically and experimentally studied and documented, starting with the notable pioneer work of Trueman (1940). Subsequently, numerous authors have dealt with this topic (e.g. Raup & Chamberlain 1967; Saunders & Shapiro 1986; Shigeta 1993; Kröger 2002; Klug & Korn 2004; Longridge *et al.* 2009; Tajika *et al.* 2014). Especially the important research on buoyancy regulation in Recent Nautilida (e.g. Denton 1962, 1974; Denton & Gilpin-Brown 1966; Ward & Martin 1978; Ward 1979, 1980, 1982, 1986, 1987; Collins *et al.* 1980; Greenwald *et al.* 1980; Kanie *et al.* 1980; Ward *et al.* 1981; Chamberlain & Moore 1982; Greenwald & Ward 1982; Mangum & Towle 1982; Chamberlain 1987; Greenwald & Ward 1987; Shapiro & Saunders 1987; Crick 1988; Dunstan *et al.* 2011; Tsujino & Shigeta 2012) has promoted an understanding of the mode of life both of nautilids and ammonoids.

As far as ammonoids are concerned, however, most of the investigations have been carried out on Mesozoic material (predominantly Jurassic and Cretaceous; Trueman 1940; Raup & Chamberlain 1967; Kröger 2002; Longridge *et al.* 2009; Tajika *et al.* 2014; Hoffmann *et al.* 2015). Few studies have assessed the buoyancy of Palaeozoic ammonoids, those that have commonly focusing on Carboniferous material (Saunders & Shapiro 1986; Swan & Saunders 1987; Saunders & Work 1996). Even fewer authors tried to reconstruct buoyancy and locomotion for Devonian forms on theoretical grounds (Klug 2001; Klug & Korn 2004; Saunders *et al.* 2004). Globally, the palaeobiology of early ammonoids has been much less studied compared to younger representatives of this clade. One of the possible reasons for this difference is the often poorer preservation (e.g. no nacre preservation in the Devonian) and the lesser abundance of Palaeozoic outcrops and

DOI 10.1111/let.12125

thus the lower availability of suitable material compared with the Mesozoic.

Nowadays, rapid technological progresses in physics and computer sciences have provided benefit to an increasing number of palaeontologists, and since the last decade, methods of 'virtual palaeontology' have been further developed and widely used (e.g. Sutton *et al.* 2001; Garwood *et al.* 2010; Sutton *et al.* 2014; Longridge *et al.* 2009). So far, only a few cases of the application of virtual palaeontological methods to ammonoids have been published (e.g. Longridge *et al.* 2009; Kruta *et al.* 2011; Lukeneder 2012; Hoffmann & Zachow 2011; Hoffmann *et al.* 2014; Hoffmann *et al.* 2015; Tajika *et al.* 2014; Naglik *et al.* 2015a). Hoffmann *et al.* (2014) published a discussion paper on the non-invasive methods applied in cephalopod research, where they reviewed the wealth of research possibilities these new methods are able to offer.

Our present study focuses on the buoyancy of three empirical three-dimensional models of three Palaeozoic ammonoid species. Because of the common lack of density contrast between ammonoid shell material and surrounding sediments, our specimens could not be investigated with a non-invasive approach (Garwood *et al.* 2010; Tajika *et al.* 2014; Lukeneder *et al.* 2014; Naglik *et al.* 2015a). This problem was resolved by employing the serial sectioning/grinding tomography method (Sollas 1904; Garwood *et al.* 2010), which is indeed a destructive method, but which on the other hand usually delivers sufficiently highly resolved image stacks containing colour information. Such image data can be evaluated in order to acquire volumetric data. This grinding tomography method has been applied to three specimens, two of Devonian and one of Carboniferous age.

The aims of this study were: (1) to determine the masses of the various shell parts and the soft tissues as well as other masses affecting the buoyancy of some Palaeozoic ammonoids; (2) to determine the buoyancy of the shells of these ammonoids and thereby answer the question whether they could possibly achieve neutral buoyancy by means of their phragmocones; (3) to reconstruct their *syn vivo* shell orientation; and (4) to use this information to discuss their swimming capabilities.

Material and methods

The empirical datasets used here are the same as those recently published by Naglik *et al.* (2015a). Three specimens of Palaeozoic ammonoids were serially ground and virtually reconstructed. These three specimens were the Middle Devonian (Eifelian) agoniatitid *Fidelites clariondi* Petter 1959 and the anarcestid *Diallagites lenticulifer* Klug 2002 (both belonging to the order Agoniatitida), and the Early Carboniferous (Visean or Serpukhovian) goniatitid *Goniatites multiliratus* Gordon 1962. Both agoniatitids come from the Anti-Atlas region of Morocco, and the goniatitid comes from Oklahoma in the USA (details of the bearing lithologies in Naglik *et al.* 2015a).

All specimens have been automatically ground into slices of a thickness of ~0.05 mm per increment. Each ground surface (slice) has been scanned and each fourth scan of the obtained image stack has been virtually retraced using Adobe Illustrator and Photoshop before being computed in VGstudiomax2.1 (Volume Graphics GmbH, Heidelberg, Germany). Technical details are available in Naglik *et al.* (2015a). Due to the destructive quality of the method, no repository numbers of the specimens are given; pictures taken of the specimens prior to grinding are provided in Naglik *et al.* (2015a) and the original stacks are available upon request to C. Naglik or C. Klug.

Labelling of shell parts

In each fourth slice, the various parts of the shell with a specific density, i.e. the siphuncle, the chambers and the body chamber (segments), were labelled with a different colour. A STL file (STereoLithography ASCII) consisting of a mesh of triangles has been created of each segment of the models using VGstudiomax 2.1. As the polygon-rendering step generated some artifacts in the mesh such as small holes or overlapping triangles, the meshes have then been processed in Geomagic Studio (Geomagic, Inc., Morrisville, NC, USA) in order to smooth and repair them (using built-in functions in the software). Once this step was completed, the obtained volumes (Table 1) were measured directly in the software, and the centres of mass of each segment could be directly computed (see Fig. 1 for the centre of mass of each segment, for each specimen).

Approximations for calculations

Knowing the volumes of all segments, their masses could be determined using some density approximations from the known densities of equivalent materials, which occur in Recent *Nautilus*. Today's nautilids are the most commonly used actualistic analogues for studying buoyancy of ammonoids (e.g. Trueman 1940; Saunders & Shapiro 1986; Jacobs & Chamberlain 1996; Westermann 1998,

Table 1. Volume, density and mass of each segment constituting each specimen.

Segment	Volume (cm^3)	Density (g/cm^3)	Mass (g)
Fidelites clariondi			
Shell + septa	4.548	2.62	11.916
Living chamber	33.712	1.055	35.57
Siphuncle	0.124	1.055	0.131
Phragmocone	12.821	0	0
Total	51.205	–	47.617
Diallagites lenticulifer			
Shell + septa	1.309	2.62	3.429
Living chamber	6.582	1.055	6.944
Siphuncle	0.081	1.055	0.086
Phragmocone	3.421	0	0
Total	11.393	–	10.459
Goniatites multiliratus			
Shell + septa	0.620	2.62	1.624
Living chamber	6.053	1.055	6.386
Siphuncle	0.019	1.055	0.020
Phragmocone	1.643	0	0
Total	8.335	–	8.030

2013; Klug 2001; Kröger 2002; Kruta *et al.* 2014; Tajika *et al.* 2014). Accordingly, we attributed a density of 1.055 g/cm^3 to the soft body (following Saunders & Shapiro 1986). Concerning the soft body, we follow the hypothesis assuming that the soft body volume corresponds to the volume of the body chamber minus the volume of the mantle cavity, which was filled with water (e.g. Shapiro & Saunders 1987; Kröger 2002).

In the cases of *Diallagites* and *Goniatites*, the body chambers were incompletely preserved. Therefore, we examined more complete specimens from the same localities (e.g. Klug 2002) and used literature data in order to reconstruct their body chamber length (Klug 2001; Saunders *et al.* 2004). Depending on the discrepancy between the preserved body chamber length and those either reported in the literature and/or known from other specimens at our disposal, we removed the last five septa of *Diallagites lenticulifer* and the last 16 septa of *Goniatites multiliratus* in order to obtain a presumed complete reconstruction of their body chambers.

All three specimens were more or less mature (Naglik *et al.* 2015a). Using a value for the body chamber length that is as accurate as possible is of utmost importance, since one of the most important factors involved in the control of the stability in *Nautilus* (and, by analogy, in ammonoids) is the body chamber length (Shapiro & Saunders 1987). Following Longridge *et al.* (2009), we assumed a density of 1.055 g/cm^3 for the siphuncle. We could not apply the method suggested in Tajika *et al.* (2014), because the connecting rings of the siphuncle could not be reconstructed in all our specimens. Concerning the shell and septa, there are several different published density values ranging from 2.61 to 2.69 g/cm^3 (e.g. Reyment 1958; Kröger 2002; Longridge *et al.* 2009; Hoffmann *et al.* 2015). Reyment (1958) explained that, although the *Nautilus* shell has a density of around 2.61–2.62 g/cm^3, its septa contain less organic material and thus have densities of 2.93–2.94 g/cm^3, corresponding to the specific density of aragonite in its pure state. Therefore, we compared the centre of mass positions using 2.62 g/cm^3 and using mean values obtained for each single model (calculated mean 'shell + septa' densities between 2.64 and 2.66 g/cm^3). This difference turned out to only insignificantly alter our results; therefore, we decided to keep the commonly used 2.62 g/cm^3 value (Reyment 1958; Saunders & Shapiro 1986; Shapiro & Saunders 1987; Kröger 2002; Tajika *et al.* 2014).

Centres of mass and buoyancy

The centre of mass has been calculated using a simple barycentre equation, determining the respective mass for each coordinate of every segment. The coordinates of the centre of mass (*X;Y;Z*) follows this barycentre equation:

$$X = (m_{\text{shell+septa}} * X_{\text{shell+septa}} + m_{\text{soft part}} * X_{\text{soft part}} + m_{\text{phragmocone}} * X_{\text{phragmocone}} + m_{\text{siphuncle}} * X_{\text{siphuncle}})/m_{\text{shell+septa}} + m_{\text{soft part}} + m_{\text{phragmocone}} + m_{\text{siphuncle}};$$

$$Y = (m_{\text{shell+septa}} * Y_{\text{shell+septa}} + m_{\text{soft part}} * Y_{\text{soft part}} + m_{\text{phragmocone}} * Y_{\text{phragmocone}} + m_{\text{siphuncle}} * Y_{\text{siphuncle}})/m_{\text{shell+septa}} + m_{\text{soft part}} + m_{\text{phragmocone}} + m_{\text{siphuncle}};$$

$$Z = (m_{\text{shell+septa}} * Z_{\text{shell+septa}} + m_{\text{soft part}} * Z_{\text{soft part}} + m_{\text{phragmocone}} * Z_{\text{phragmocone}} + m_{\text{siphuncle}} * Z_{\text{siphuncle}})/m_{\text{shell+septa}} + m_{\text{soft part}} + m_{\text{phragmocone}} + m_{\text{siphuncle}};$$

where $m_{(\alpha)}$ is the mass of each segment α, and X_α; Y_α; Z_α, the coordinates of the centre of each segment.

Then, the resulting coordinates have been computed in the models using Geomagic Studio and XOS (Fig. 2). The centre of buoyancy was directly computed in Geomagic XOS (Fig. 2). The centre of buoyancy is corresponding to the centre of mass of the sea water volume displaced by the animal (Trueman 1940; Raup & Chamberlain 1967; Saunders & Shapiro 1986; Kröger 2002). We take the same assumption as in Tajika *et al.* (2014) for these calculations, namely that the phragmocone chambers were filled with gas.

Shell parameters and ratios

Additionally, we measured the body chamber length (BCL; in degrees), the orientation of the aperture

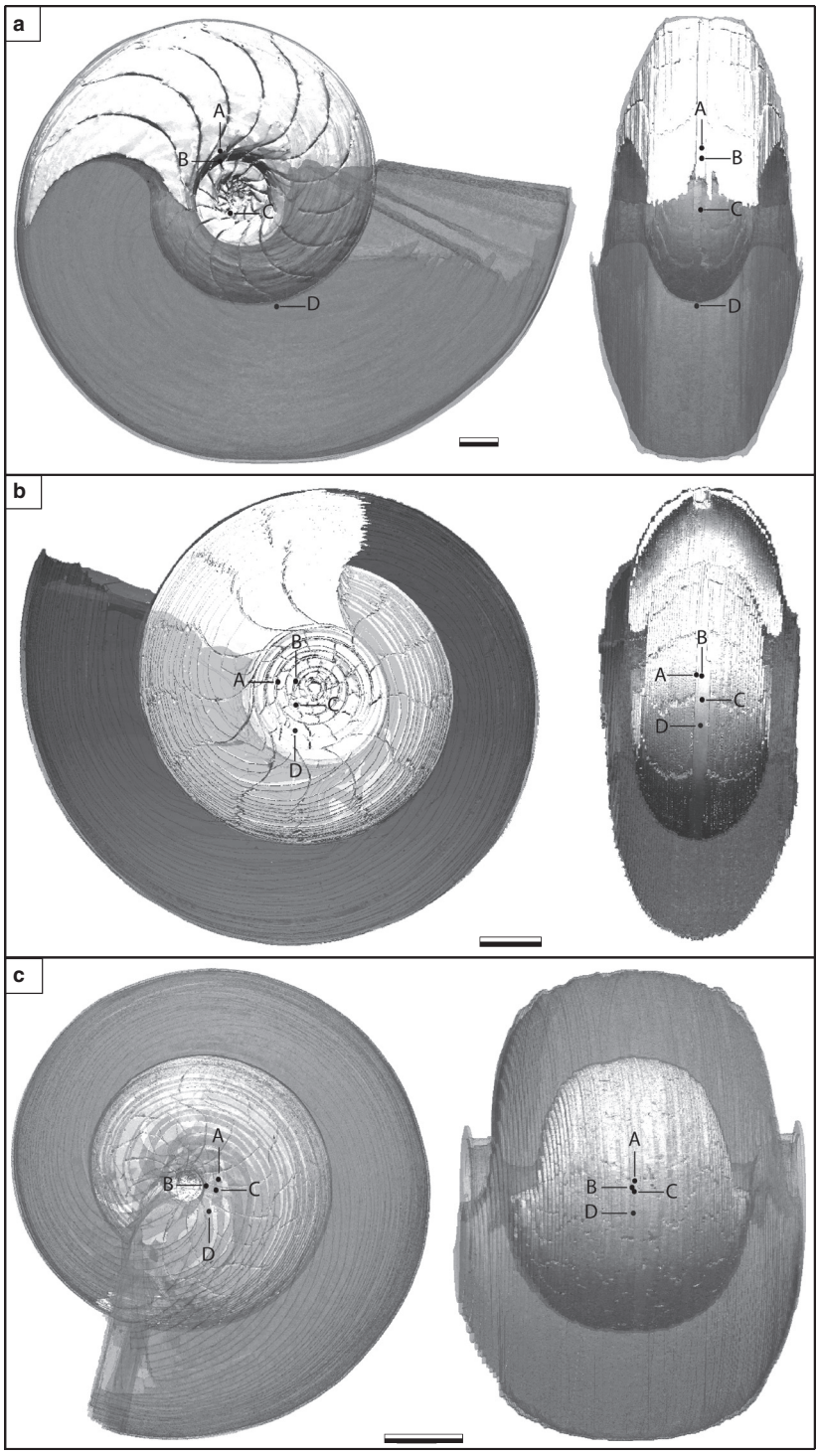

Fig. 1. Model showing centres of mass for each element of animal, from lateral view (left) and posterior view (right). (a), *Fidelites clarindi*; (b), *Diallagites lenticulifer*; (c), *Goniatites multiliratus*. Black dots represent: (A), siphuncle; (B), phragmocone; (C), shell + septa; (D), body chamber. Scale bar: 0.5 cm. 'Letter codes: (A) siphuncle; ' etc

(OR; in degrees from vertical) and the relative stability (ST; Shapiro & Saunders 1987). The relative stability (ST) is calculated as follows (Shapiro & Saunders 1987):

$$ST = f/dm_1$$

where f is the distance between the centre of buoyancy for each species and that of mass and dm_1 is the conch diameter (Fig. 3).

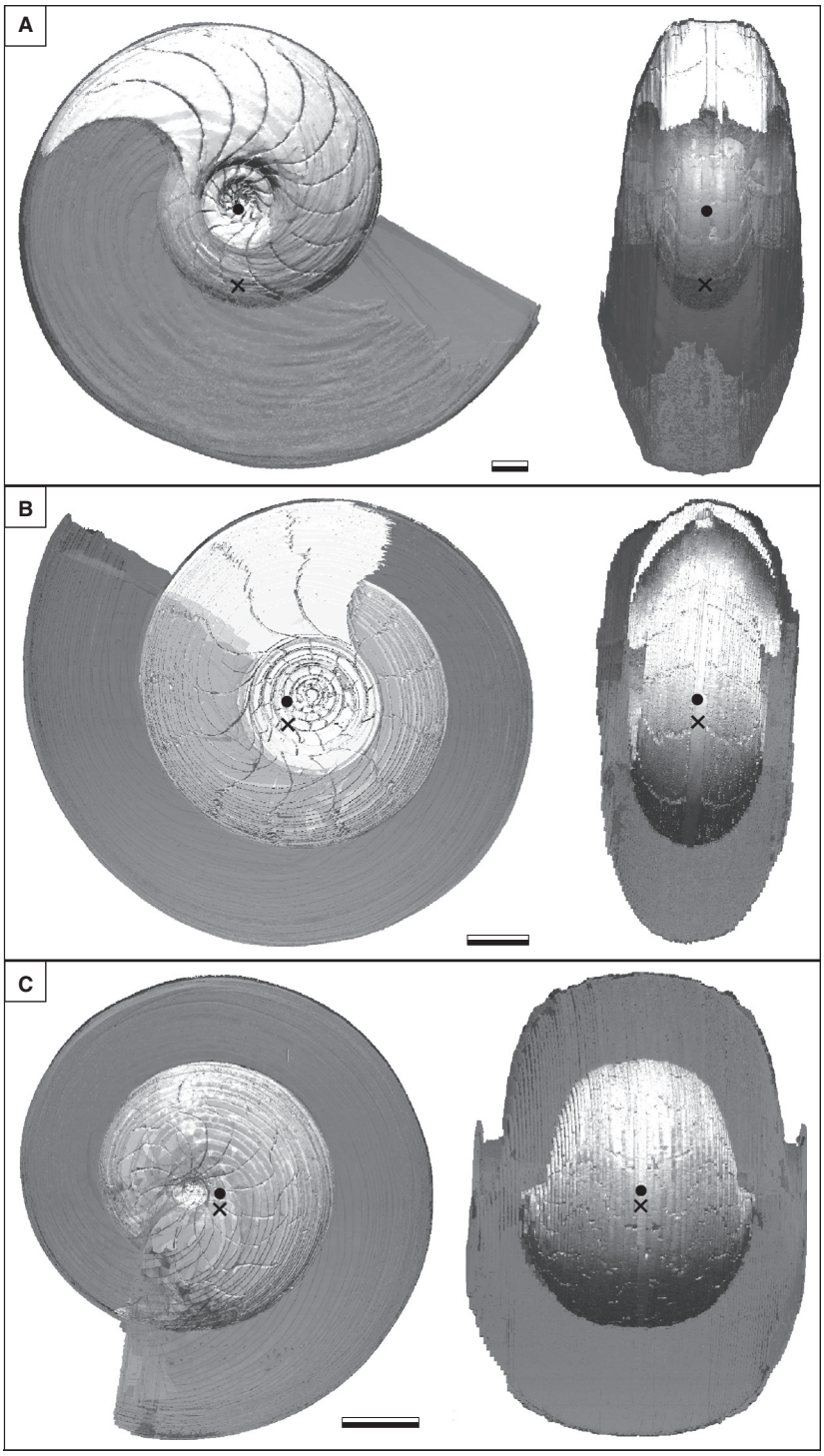

Fig. 2. Positions of the centres of mass (black cross) and buoyancy (black dot) of each reconstructed ammonoid shell model. (A), *Fidelites clariondi*. (B), *Diallagites lenticulifer*. (C), *Goniatites multiliratus*. Scale bar: 0.5 cm.

Results

Shell hydrostatics

The respective positions of the centres of mass and buoyancy for each specimen are shown in Figure 2 and the corresponding coordinates are displayed in Table 2. The coordinate (0; 0; 0) represents the centre of the models (as explained for instance in Longridge *et al.* 2009). If the models were perfectly symmetrical, the Z values would have been 0. A slight discrepancy occurs in our models with absolute Z-values varying from 0 with a range between

0.014 mm and 0.136 mm. This deviation can have several origins, such as an imperfectly symmetrical shell, a slight asymmetry of the siphuncle, but it can also result from minor errors during tracing. Whatever the origin of this difference, even if it results from a small error, this does not compromise the relative positions of the centres of mass and buoyancy, and the reconstruction of the *syn vivo* shell orientation in water.

The orientations of the shells shown in Figure 2 represent the resting position, with the living orientation (i.e., the static orientation of the shell in water, assuming buoyancy as the main function of the shell following Shapiro & Saunders 1987). The values of body chamber lengths (BCL), the orientation of the apertures (OR), the distance between the centres of mass and buoyancy (f) as well as the relative stability (ST) of each specimen are also given in Table 2. The body chamber length varies from 201° (*Fidelites clariondi*) to 354° (*Goniatites multiliratus*) with a length of 282° for *Diallagites lenticulifer*. Using these values, we reconstructed shell orientations, where the aperture is at 69° from the vertical direction in *F. clariondi*, at 125° in *D. lenticulifer* and 19° in *G. multiliratus*. The former two values appear reasonable and roughly coincide with those modelled by Saunders & Shapiro (1986) for similar forms and those modelled by Klug (2001) as well as Klug & Korn (2004) for Devonian taxa.

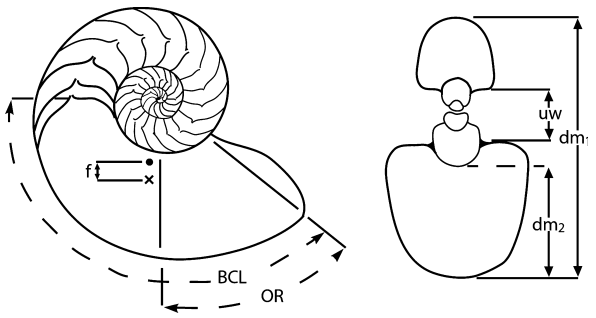

Fig. 3. Parameters used to establish variables and the relative hydrodynamic stability (ST). BCL, body chamber length (in degrees); OR, orientation (in degrees from vertical); f, distance between the mass (cross) and the buoyancy (dot) centres; dm_1, conch diameter; dm_2, conch diameter without the aperture height (modified from Shapiro & Saunders 1987; with classical parameter labels from Korn 2010).

As far as the hydrodynamic stability is concerned, the distance between the centres of mass and buoyancy (*f*) varies from 10.193 mm to 0.962 mm in the three ammonoids (Table 2). The direct consequence of this proximity of the two points is a rather low relative hydrodynamic stability. *F. clariondi*, which has a shorter body chamber, possessed a better hydrodynamic stability with its higher distance f (10.193 mm) and its higher relative stability value of 0.13, although this value is still low. *D. lenticulifer* has a slightly longer body chamber length and an even lower stability value of 0.04 with a distance f of 1.776. With a hydrodynamic stability value of 0.03, *G. multiliratus* has both the longest body chamber and the lowest stability value. As suggested by Saunders & Shapiro (1986), a correlation between body chamber length and hydrodynamic stability is apparent, although more data is needed to support this (*F. clariondi*: BCL = 201°, ST = 0.13, *D. lenticulifer*: BCL = 282°, ST = 0.04; *G. multiliratus*: BCL = 354°, ST = 0.03; Tajika *et al.* 2014; *Normannites mitis*: BCL = 269°, ST = 0.05). In other words, the longer the body chamber, the poorer the stability. Nevertheless, this variation in hydrodynamic stability of the shells probably reflects differences in the respective modes of life (Saunders & Shapiro 1986) including more actively horizontally swimming forms (moderately long body chamber, relatively high ST-value) and other forms, which were most likely vertical migrants (very long or very short body chambers and very low ST-values; Trueman 1940; Westermann 1996).

Buoyancy reconstruction

The virtual reconstructions of these three specimens allowed us to calculate their masses and buoyancies. The volumes, densities and masses of each segment of each specimen are listed in Table 1. With these data, we calculated the total mass of the animal including all segments and compare this mass with the total mass of the displaced seawater. We assume a seawater density of 1.026 g/cm^3 (Trueman 1940; Raup & Chamberlain 1967; Saunders & Shapiro 1986; Kröger 2002; Tajika *et al.* 2014).

Table 2. Mass and buoyancy coordinates of each specimen, as well as their corresponding measured body chamber length (BCL), orientation (OR) and their calculated distance between the two centres (*f*) and their relative stability (ST).

	Mass coordinates (mm)			Buoyancy coordinates (mm)						
	X	*Y*	*Z*	*X*	*Y*	*Z*	BCL (°)	OR (°)	*f* (mm)	ST
Fidelites clariondi	−2.879	−4.981	0.014	−6.971	4.355	0.039	201	69	10.193	0.13
Diallagites lenticulifer	0.534	−2.169	−0.326	0.839	−0.428	−0.149	282	125	1.776	0.04
Goniatites multiliratus	−1.156	−0.116	−0.035	−0.864	0.800	−0.053	354	19	0.962	0.03

The total mass of *Fidelites clariondi* is 47.613 g then lower than the 52.536 g of displaced water. The difference of these two masses is 4.919 g. Similarly, the total mass of *Diallagites lenticulifer* is 10.459 g and the corresponding mass of displaced water amounts to 11.689 g, creating a mass difference of 1.23 g. Finally, the results for *Goniatites multiliratus* are congruent with the previous ones, since the total mass of the animal is 8.030 g compared to 8.552 g for the corresponding displaced water mass. In the last case, the mass difference is very low with only 0.522 g.

These results show that, under the assumption that the phragmocones were filled with only gas, the three specimens would have been strongly positively buoyant, thus causing the animal to stick to the water surface, which is unlikely. These mass differences represent the maximal theoretical buoyancy of these ammonoids (Kröger 2002). Hypothesizing that ammonoids were nearly neutrally buoyant, the difference between calculated and neutral buoyancy represents the fill fraction (*sensu* Kröger 2002) and probably equals the mass of chamber liquid (e.g. Kröger 2002; Tajika *et al.* 2014). Assuming a density of 1.013 g/cm^3 for the cameral liquid (Tajika *et al.* 2014), we determined the fill fraction of the cameral liquid needed by the animals to reach neutral buoyancy. Accordingly, *F. clariondi* would have had 38% of the phragmocone filled by cameral liquid, 36% in *D. lenticulifer* and 31% in *G. multiliratus*. These results have to be viewed with some reservation since we do not know the precise composition of cameral liquid and thus its density, especially if this liquid differed in composition from the ambient sea water. Sea water salinity varies with factors such as depth, temperature, distance from fresh water input (brackish waters, etc.) and we do not know in detail the precise environmental conditions of habitats of the examined species. Nevertheless, these values around 30% of cameral liquid are in agreement with what has been predicted by Heptonstall (1970), Mutvei & Reyment (1973) as well as Reyment (1973) and with what has been found by Tajika *et al.* (2014) for the Jurassic ammonite *Normannites mitis*.

Errors and biases

Hydrostatic properties and buoyancy have been reconstructed using virtual models of three Palaeozoic ammonoid species. Some aspects concerning the accuracy of such models need to be discussed. The study of Tajika *et al.* (2014) had the advantage that *Normannites mitis* has already been used for a buoyancy study earlier, although Trueman (1940) used evident simplifications in his calculations. The results are congruent with what has been predicted based on theoretical models before, taking into account some earlier mistakes such as the shell density value, which was wrong in Trueman (1940), for instance. On the one hand, this supports the validity of the method used to reconstruct these models, and on the other hand, it shows the minor to negligible effect of the resolution limit on the results (Naglik *et al.* 2015a).

Moreover, some simplifications, generalizations and approximations have to be discussed here since all volumetric models of ammonoids will include simplifications. This implies that it is not possible to obtain absolutely accurate volume data, weight values and thus buoyancy models of ammonoids. All the hydrostatic and buoyancy calculations in the literature referring to Raup & Chamberlain's (1967) equations are based on assumptions, which were known to be slightly wrong or not perfectly appropriate for *Nautilus* (Shapiro & Saunders 1987), such as the circular generating curve and the non-inclusion of the weight of the shell in the calculation of the centre of mass. Still, empirical experiments have shown results corresponding well with the ones of Raup & Chamberlain (1967). Therefore, we maintain the hypothesis according to which the soft-tissues are completely included in the body chamber, as well as the commonly used density of 1.055 g/cm^3 for the soft body and 2.62 g/cm^3 for the shell (we tested our models with densities up to 2.66 g/cm^3 without noticeable differences in the results).

The estimate of the cameral liquid density is more critical, since we cannot determine its composition and thus density with certainty; moreover the composition probably could have differed between ammonoid taxa, depending on their respective habitats, physiology and the corresponding physical and chemical environmental conditions. We hence evaluated the effect of the cameral liquid density on the fill fraction in percentage of the phragmocone volume (Fig. 4). This figure shows that the change of the fill fraction is minor to negligible regarding the fact that we assume density values for the cameral liquid with the same as seawater (1.026 g/cm^3). In all cases, a difference of <1% is observed. We tested some other densities and the theoretical minimum density of cameral liquid to reach neutral buoyancy with more than 90% of phragmocone filling in each case, would be a cameral liquid density of 0.4 g/cm^3, which appears unlikely. On the other hand, with a higher -similarly unlikely- density of 2 g/cm^3, a liquid filling between only 16% (*Goniatites multiliratus*) and 19% (*Fidelites clariondi*) would be necessary for the ammonoid animals to reach neutral

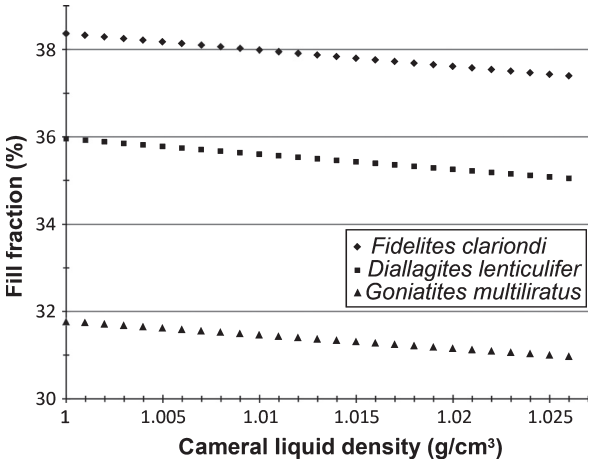

Fig. 4. Effect of the cameral liquid density on the fill fraction percentages of the phragmocone.

buoyancy. Therefore, using a value of 1.013 g/cm^3 appears reasonable.

Concerning the deviation of the *Z* values in mass and buoyancy coordinates, it may have several origins. Three of these are discussed here:

- The specimens are not perfectly symmetrical. This may have occurred *syn vivo* or post-mortem (e.g. by diagenetic compaction or tectonic deformation). A diagenetic or tectonic origin of the asymmetry appears unlikely because we chose these specimens because of their good three-dimensional preservation (Naglik *et al.* 2015a).
- An asymmetry of some elements, especially of the siphuncle, as described in Longridge *et al.* (2009) might account for this asymmetry since the position of the siphuncle has been noticed as to be not completely symmetrical, which has probably been intensified by the moderately low resolution we chose (see methods in Naglik *et al.* 2015a); indeed the smaller the element, the bigger the relative effect of the error caused by resolution, and the siphuncle is the smallest segment with the smallest volume.
- Especially in the case of *Diallagites lenticulifer*, some imprecision in the interpretation of the slices occurred while tracing and labelling them; this means that occasionally, more shell material on one side of the body chamber was drawn erroneously, thus creating a slight disequilibrium (a variant of the partial volume effect; Naglik *et al.* 2015a; Hoffmann *et al.* 2015). We can therefore expect (with further correction) a more symmetrical and thus upright position than that depicted in Figure 2B (right, posterior view).

Mode of life of ammonoids

Taking the results presented above into account as well as the data from literature, we can now confidently state that most, if not all planispiral ammonoids were able to attain neutral buoyancy, because we have examined such remotely related forms as the Devonian *Fidelites clariondi* and the Jurassic *Normannites mitis* (Tajika *et al.* 2014). Since forms with average body chamber lengths of 200° to 300° had accordingly more or less upwardly oriented apertures, a fully benthonic mode of life can be considered as highly unlikely for most groups. Still, the strong variation in orientation of the aperture and in hydrodynamic stability between such forms as *Fidelites* and *Goniatites* are suggestive of a more or less strong ecological differentiation. Ammonoids with short body chambers (body chamber lower than ¾ whorl in length) had moderately good to good hydrodynamic stability values and probably good swimming abilities in a horizontal direction. By contrast, long body chamber forms (body chamber higher than ¾ whorl in length) had a low aperture and low hydrodynamic stability values, suggesting predominantly vertical movements, i.e. most likely planktonic to nektoplanktonic mode of life (Westermann 1996; Lukeneder 2015), possibly including vertical migration (compare Westermann 1996; Ritterbush *et al.* 2014). The low hydrodynamic stability corroborates the conclusions of Jacobs & Chamberlain (1996); (see also Naglik *et al.* 2015b) that most ammonoids were poor to maximally moderately good swimmers in horizontal direction. A high-speed swimming predatory mode of life can thus be excluded.

Conclusions

Using the method of serial grinding combined with a virtual 3D-reconstruction, this present work accomplished empirical calculations of volumes of each segment of the ammonoid shell. We were able to determine the masses of the entire shell, the single shell parts and the entire animal of three taxa, namely of two Devonian agoniatitids (the agoniatid *Fidelites clariondi* and the anarcestid *Diallagites lenticulifer*) and one Carboniferous goniatitid (*Goniatites multiliratus*). Using these data, we showed that Palaeozoic ammonoids could well achieve neutral buoyancy by means of their phragmocones with a proportion of cameral liquid varying from 31% in *G. multiliratus* via 36% in *D. lenticulifer* to 38% in *F. clariondi*. The localization of the centres of mass and buoyancy have been computed for the agoniatid, the anarcestid and the goniatitid. These centres

allowed the reconstruction of the *syn vivo* shell orientations with aperture angles (OR) varying from the probably erroneously low value of 19° in *G. multiliratus* via 69° for *F. clariondi* to 125° in *D. lenticulifer*. These values differ from *Nautilus* (~42°, Shapiro & Saunders 1987), *Normannites mitis* (90–100°, Tajika *et al.* 2014), and from other Palaeozoic ammonoid morphologies investigated by Saunders & Shapiro (1986), although they principally coincide with the discoveries of the latter authors, which were based on theoretical models. Nevertheless, the orientations of the shells of *D. lenticulifer* and *F. clariondi* are roughly concordant with the results of Klug (2001). The low angle of *G. multiliratus* is still reasonably congruent with the low angle of 20° to 30° found for the goniatitid morphs in Saunders & Shapiro (1986).

As far as body chamber lengths compared to relative hydrodynamic stabilities of ammonoids are concerned, it appears as if specimens with shorter body chambers had a higher stability value (*F. clariondi*) than the ones with longer body chambers (*D. lenticulifer*, *G. multiliratus*). Our results thus confirm the suggestion of a negative correlation between the body chamber length and stability (Saunders & Shapiro 1986). In other words, the longer the body chamber, the poorer the hydrodynamic stability. This variation in shell orientation and hydrodynamic stability probably reflects differences in the mode of life. Long body chamber forms with low apertures and low stability values might have been rather vertical migrants while short body chamber forms with high stability values and horizontal apertures were the better swimmers, although high speed swimming can be ruled out for planispiral ammonoids (albeit this statement can probably be inferred to heteromorphs as well).

Acknowledgements. – This work was financially supported by the Swiss National Science Foundation SNF (project numbers 200021-113956/1, 200020-25029, and 200020-132870). The grinding tomography was carried by Stefan Götz (in memoriam), Enric Pascual-Cebrian and Dominik Hennhöfer (Heidelberg). We thank the Laboratory of Thermodynamics in Emerging Technologies of ETH Zürich for giving the initiation of the use of Geomagic STUDIO software for mesh repairs. We especially want to thank Alik Huseynov from the Anthropological Institute and Museum of the University of Zürich who kindly let us use the facilities and allowed us to achieve our work with the software Geomagic XOS for measurements. We thank Alexander Lukeneder as well as one anonymous reviewer who helped to improve the quality of this article.

References

Chamberlain, J.A. Jr 1987: Locomotion of *Nautilus*. *In* Saunders, W.B. & Landman, N.H. (eds): *Nautilus – The Biology and Paleobiology of a Living Fossil*, 489–525. Springer, Dordrecht.

Chamberlain, J.A. Jr & Moore, W.A. Jr 1982: Rupture strength and flow rate of *Nautilus* siphuncular tube. *Paleobiology 8*, 408–425.

Collins, D.H., Ward, P.D. & Westermann, G.E.G. 1980: Function of cameral water in *Nautilus*. *Paleobiology 6*, 168–172.

Crick, R.E. 1988: Buoyancy regulation and macroevolution in nautiloid cephalopods. *Senckenbergiana Lethaea 69*, 13–42.

Denton, E.J. 1962: Some recently discovered buoyancy mechanisms in marine animals. *Proceedings of the Royal Society of London B 265*, 366–370.

Denton, E.J. 1974: On buoyancy and the lives of modern and fossil cephalopods. *Proceedings of the Royal Society of London B 185*, 273–299.

Denton, E.J. & Gilpin-Brown, J.B. 1966: On the buoyancy of the pearly *Nautilus*. *Journal of the Marine Biological Association UK 46*, 723–759.

Derham, W. 1726: *Philosophical Experiments and Observations of the late Eminent Dr. Robert Hooke*, Derham, London.

Dunstan, A.J., Ward, P.D. & Marshall, N.J. 2011: Vertical distribution and migration patterns of *Nautilus pompilius*. *PLoS ONE 6*, e16311 1–10.

Garwood, R.J., Rahman, I.A. & Sutton, M.D. 2010: From clergymen to computers–the advent of virtual palaeontology. *Geology Today 26*, 96–100.

Gordon, M. 1962: Species of *Goniatites* in the Caney Shale of Oklahoma. *Journal of Paleontology 36*, 355–357.

Greenwald, L. & Ward, P.D. 1982: On the source of cameral liquid in the chambered *Nautilus*. *Veliger 25*, 169–170.

Greenwald, L. & Ward, P.D. 1987: Buoyancy in *Nautilus*. *In* Saunders, B.W. & Landman, N.H. (eds): *Nautilus – The Biology and Paleobiology of a Living Fossil*, 547–560. Springer Verlag, Dordrecht.

Greenwald, L., Ward, P.D. & Greenwald, O.E. 1980: Cameral liquid transport and buoyancy control in the chambered nautilus (*Nautilus macromphalus*). *Nature 286*, 55–56.

Heptonstall, W.B. 1970: Buoyancy control in ammonoids. *Lethaia 3*, 317–328.

Hoffmann, R., Schultz, J.A., Schellhorn, R., Rybacki, E., Keupp, H., Gerden, S.R., Lemanis, R. & Zachow, S. 2014: Non-invasive imaging methods applied to neo- and paleontological cephalopod research. *Biogeosciences 11*, 2721–2739.

Hoffmann, R. & Zachow, S. 2011: Non-invasive approach to shed new light on the buoyancy business of chambered cephalopods (Mollusca). *IAMG*, 506–516. doi: 10.5242/iamg.2011.0163

Hoffmann, R., Lemanis, R., Naglik, C. & Klug, C. 2015: Ammonoid buoyancy. *In* Klug, C., Korn, D., De Baets, K., Kruta, I. & Mapes, R.H. (eds): *Ammonoid Paleobiology: Volume 1*, From Anatomy to Ecology. *Topics in Geobiology* 43.

Jacobs, D.K. & Chamberlain, J.A. 1996: Buoyancy and hydrodynamics in ammonoids. *In* Landman, N., Tanabe, K. & Davis, R.A. (eds): *Ammonoid Paleobiology. Topics in Geobiology*, *13*, 169–223. Plenum Press, New York.

Kanie, Y., Fukuda, Y., Nakahara, K., Seki, K. & Hattori, H. 1980: Implosion of living *Nautilus* under increased pressure. *Paleobiology 6*, 44–47.

Klug, C. 2001: Life-cycles of Emsian and Eifelian ammonoids (Devonian). *Lethaia 34*, 215–233.

Klug, C. 2002: Quantitative stratigraphy and taxonomy of late Emsian and Eifelian ammonoids of the Anti-Atlas (Morocco). *Courier Forschungsinstitut Senckenberg 238*, 1–109.

Klug, C. & Korn, D. 2004: The origin of ammonoid locomotion. *Acta Palaeontologica Polonica 49*, 235–242.

Korn, D. 2010: A key for the description of Palaeozoic ammonoids. *Fossil Record 13*, 5–12.

Kröger, B. 2002: On the efficiency of the buoyancy apparatus in ammonoids: evidences from sublethal shell injuries. *Lethaia 35*, 61–70.

Kruta, I., Landman, N.H., Rouget, I., Cecca, F. & Tafforeau, P. 2011: The role of ammonites in the Mesozoic marine food web revealed by jaw preservation. *Science 331*, 70–72.

Kruta, I., Landman, N.H. & Cochran, J.K. 2014: A new approach for the determination of ammonite and nautilid habitats. *PLoS ONE 9*, e87479 1–7.

Longridge, L.M., Smith, P.L., Rawlings, G. & Klaptocz, V. 2009: The impact of asymmetries in the elements of the phragmocone of Early Jurassic ammonites. *Palaeontologia Electronica 12*, 1–15.

Lukeneder, A. 2012: Computed 3D visualisation of an extinct cephalopod using computer tomographs. *Computers and Geosciences 45*, 68–74.

Lukeneder, A. 2015: Ammonoid habitats and life history. *In* Klug, C., Korn, D., De Baets, K., Kruta, I. & Mapes, R.H. (eds): *Ammonoid Paleobiology, volume 1,* From Anatomy to Ecology. Springer, Dordrecht.

Lukeneder, S., Lukeneder, A. & Weber, G.W. 2014: Computed reconstruction of spatial ammonoid-shell orientation captured from digitized grinding and landmark data. *Computers and Geosciences 64*, 104–114.

Mangum, C.P. & Towle, D.W. 1982: The *Nautilus* siphuncle as an ion pump. *Pacific. Science. 36*, 273–282.

Meigen, W. 1870: Über den hydrostatischen Apparat bei *Nautilus pompilius*. *Archiv für Naturgeschichte 36*, 1–36.

Mutvei, H. & Reyment, R. 1973: Buoyancy control and siphuncle function in ammonites. *Palaeontology 6*, 623–636.

Naglik, C., Monnet, C., Götz, S., Kolb, C., De Baets, K. & Klug, C. 2015a: Growth trajectories in chamber and septum volumes in major subclades of Palaeozoic ammonoids. *Lethaia*, *48*, 29–46.

Naglik, C., Tajika, A., Chamberlain, J. & Klug, C. 2015b: Ammonoid locomotion. *In* Klug, C., Korn, D., De Baets, K., Kruta, I. & Mapes, R.H. (eds): *Ammonoid Paleobiology, volume 1,* From Anatomy to Ecology. Springer, Dordrecht.

Owen, R. 1832: *Memoir of the Pearly Nautilus (*Nautilus Pompilius, *Linn.)*. 1–68, Royal College of Surgeons, London.

Petter, G. 1959: Goniatites dévoniennes du Sahara. *Publications du Service de la Carte Géologique de l'Algérie, Nouvelle Série, Paléontologie 2*, 1–313.

Raup, D.M. & Chamberlain, J.A. 1967: Equations for volume and centre of gravity in ammonoid shells. *Journal of Paleontology 41*, 566–574.

Reyment, R.A. 1958: Some factors in the distribution of fossil Cephalopods. Acta Universitatis Stockholmiensis — Stockholm Contribitions in. *Geology 1*, 97–184.

Reyment, R.A. 1973: Factors in the distribution of fossil cephalopods. Part 3: experiments with exact models of certain shell types. *Bulletin of the Geological Institution of the University of Uppsala New Series*. *4*, 7–41.

Ritterbush, K., Hoffmann, R., Lukeneder, A. & De Baets, K. 2014: Pelagic palaeoecology: the importance of recent constraints on ammonoid palaeobiology and life history. *Journal of Zoology 292*, 229–241.

Saunders, W.B. & Shapiro, E.A. 1986: Calculation and simulation of ammonoid hydrostatics. *Paleobiology 12*, 64–79.

Saunders, W.B. & Work, D.M. 1996: Shell morphology and suture complexity in upper carboniferous ammonoids. *Paleobiology 22*, 189–218.

Saunders, W.B., Work, D.M. & Nikolaeva, S.V. 2004: The evolutionary history of shell geometry in Paleozoic ammonoids. *Paleobiology 30*, 19–43.

Shapiro, E.A. & Saunders, W.B. 1987: *Nautilus* Shell Hydrostatics. *In* Saunders, W.B. & Landman, N.H. (eds): *Nautilus: The Biology and Paleobiology of a Living Fossil*, *33*, 527–545. Plenum Press, New York.

Shigeta, Y. 1993: Post-hatching early life history of Cretaceous Ammonoidea. *Lethaia 26*, 133–146.

Sollas, W.J. 1904: A method for the investigation of fossils by serial section. *Philosophical Transactions of the Royal Society of London 196*, 259–265.

Sutton, M.D., Briggs, D.E.G., Siveter, D.J. & Siveter, D.J. 2001: Methodologies for the visualization and reconstruction of three-dimensional fossils from the Silurian Herefordshire Lagerstätte. *Palaeontologia Electronica 4*, 1–17.

Sutton, M.D., Rahman, I.A. & Garwood, R.J. 2014: *Techniques for Virtual Palaeontology*. Wiley, New York. doi:10.1002/9781118591192.

Swan, A.R.H. & Saunders, W.B. 1987: Function and shape in late Paleozoic (mid-Carboniferous) ammonoids. *Paleobiology 13*, 297–311.

Tajika, A., Naglik, C., Morimoto, N., Pascual-Cebrian, E., Hennhöfer, D. & Klug, C. 2014: Empirical 3D-model of the conch of the Middle Jurassic ammonite microconch *Normannites*: its buoyancy, the physical effects of its mature modifications and speculations on their function. *Historical Biology: An International Journal of Paleobiology*, 1–11, doi: 10.1080/08912963.2013.872097

Trueman, A.E. 1940: The ammonite body chamber, with special reference to the buoyancy and mode of life of the living ammonite. *Quarterly Journal of the Geological Society, London 96*, 339–383.

Tsujino, Y. & Shigeta, Y. 2012: Biological response to experimental damage of the phragmocone and siphuncle in *Nautilus pompilius* Linnaeus. *Lethaia 45*, 443–449.

Vrolik, W. 1843: On the anatomy of the pearly *Nautilus*. *Annals and Magazine of Natural History 12*, 173–175.

Ward, P.D. 1979: Cameral liquid in *Nautilus* and ammonites. *Paleobiology 5*, 40–49.

Ward, P.D. 1980: Restructuring the chambered *Nautilus*. *Paleobiology 6*, 247–249.

Ward, P.D. 1982: The relationship of siphuncle size to emptying rates in chambered cephalopods: implications for cephalopod paleobiology. *Paleobiology 8*, 426–433.

Ward, P.D. 1986: Rates and processes of compensatory buoyancy change in *Nautilus macromphalus*. *Veliger 28*, 356–368.

Ward, P.D. 1987: *The Natural History of Nautilus*. Allen & Unwin, Boston.

Ward, P.D. & Martin, A.W. 1978: On the buoyancy of the Pearly *Nautilus*. *Journal of Experimental Zoology 205*, 5–12.

Ward, P.D., Greenwald, L. & Magnier, Y. 1981: The chamber formation cycle in *Nautilus macromphalus*. *Paleobiology 7*, 481–493.

Westermann, G.E.G. 1996: Ammonoid life and habitat, *In* Landman, N.H., Tanabe, K. & Davis, R.A. (eds): *Ammonoid Paleobiology. Topics in Geobiology*, 13, 607–707. Plenum Press, New York.

Westermann, G.E.G. 1998: Life habits of ammonoids. *In* Savazzi, E. (ed.): *Functional Morphology of the Invertebrate Skeleton*, 263–298. John Wiley & Sons, Chichester.

Westermann, G.E.G. 2013: Hydrostatics, propulsion and life-habits of the Cretaceous ammonoid *Baculites*. *Revue de Paléobiologie 32*, 249–265.

Willey, A. 1902: Contributions to the natural history of the pearly Nautilus *: Zoological results based on material from New Britain, New Guinea, Loyalty Islands and elsewhere, collected during the years 1895, 1896 and 1897, volume 6*, University Press, Cambridge, England. 691–830.

CHAPTER III

Ammonoid Locomotion

Published in *Ammonoid Paleobiology, Volume I: from anatomy to ecology. Topics in Geobiology* (2015)

Chapter 17
Ammonoid Locomotion

Carole Naglik, Amane Tajika, John Chamberlain and Christian Klug

17.1 Introduction

The locomotor capacity of ammonoids is still a matter of much debate. This question is intimately linked with questions concerning ammonoid habitat and buoyancy (Ritterbush et al. 2014). Aspects of buoyancy were reviewed by Hoffmann et al. (2015). Based on theoretical models of ammonoid buoyancy (e.g., Trueman 1941; Saunders and Shapiro 1986) in combination with the latest empirical studies on volume models of ammonoids (Tajika et al. 2015; Naglik et al. 2015), we can now confidently reject the hypothesis of an obligatorily benthic mode of life for most ammonoids advocated by Ebel 1983 (see also Westermann 1993, 1996; Kröger 2001 or Jacobs and Chamberlain 1996 for views contrasting Ebel's ideas). The function of the phragmocone as a buoyancy device has been corroborated by a great number of studies (see Hoffmann et al. 2015 and references therein) including the latest volume models of ammonoid shells and the linked buoyancy calculations (Tajika et al. 2015; Naglik et al. 2015), most mathematical models of buoyancy (Hoffmann et al. 2015), the convergent evolution of an upward orientation of the aperture in many

C. Naglik (✉) · A. Tajika · C. Klug
Paläontologisches Institut und Museum, University of Zurich, Karl Schmid-Strasse 6,
8006 Zurich, Switzerland
e-mail: carole.naglik@pim.uzh.ch

A. Tajika
e-mail: amane.tajika@pim.uzh.ch

C. Klug
e-mail: chklug@pim.uzh.ch

J. Chamberlain
Department of Earth and Environmental Sciences,
Brooklyn College of CUNY, Brooklyn, NY 11210, USA

Doctoral Programs in Biology and Earth and Environmental Sciences,
CUNY Graduate Center, New York, NY 10016, USA
e-mail: JohnC@brooklyn.cuny.edu

C. Klug et al. (eds.), *Ammonoid Paleobiology: From Anatomy to Ecology,*
Topics in Geobiology 43, DOI 10.1007/978-94-017-9630-9_17

major ammonoid lineages (e.g., Raup and Chamberlain 1967; Bayer and McGhee 1984; Saunders and Shapiro 1986; Klug 2001; Korn and Klug 2003; Monnet et al. 2011) and the increase of phragmocone complexity through ammonoid evolution (Saunders 1995; Saunders and Work 1996, 1997; Daniel et al. 1997; Saunders et al. 1999). This is significant because *syn vivo* shell orientation can be used as an indicator of locomotion and habitat preference, although there are great limits for the accuracy of such conclusions.

Several authors have sought information on habitat depth and swimming speed in the physical properties of ammonoid shells. For example, shell implosion depths suggest limits for maximum diving depths (e.g., Westermann 1973, 1996; Saunders and Wehman 1977; Jacobs 1992a; Hewitt 1996; Batt 2007). Inferences on diving depth and ammonoid behavior have also been drawn based on siphuncle properties (e.g., Westermann 1971, 1996; Mutvei and Reyment 1973; Mutvei 1975; Chamberlain and Moore 1982; Ward 1982; Hewitt 1996). Oxygen isotopes have also been used to approximate diving/living depths of ammonoids (Moriya et al. 2003; Lukeneder et al. 2010, Lukeneder 2015; Moriya 2015).

Similarly, streamlining and drag have been quantified for a wide range of shell shapes (Kummel and Lloyd 1955; Westermann 1971, 1996; Reyment 1973; Chamberlain 1976, 1981; Chamberlain and Westermann 1976; Jacobs 1992b, Jacobs et al. 1994; Monnet et al. 2011; Ritterbush and Bottjer 2012; Ritterbush et al. 2014), and the results related to mode of life. Mutvei and Reyment (1973) as well as Mutvei (1975) argued that muscle attachment was too small and weak to allow ammonoids to swim well. However, there is some indication suggesting that ammonoids may have powered their locomotion with a muscular mantle not firmly attached to the shell (Jacobs and Landman 1993; Jacobs and Chamberlain 1996). Muscle attachment is discussed in detail in Doguzhaeva and Mapes (2015).

Sedimentary facies in which ammonoids are preserved may provide some information about lifestyle and habitat (Wang and Westermann 1993; Westermann 1996; Tsujita and Westermann 1998; Westermann and Tsujita 1999), although post mortem transport can complicate the picture (e.g., Kennedy and Cobban 1976; Tanabe 1979: Westermann 1996 and references therein). Nevertheless, the broad range of facies types in which ammonoid remains occur in combination with the great disparity in shell morphology supports a wide variety of life habitats and habits for these animals that in principle relate to differing locomotor capabilities as exemplified by Jacobs et al (1994).

Another line of evidence comes from sublethal injuries. It was especially Keupp (review in Keupp and Hoffmann 2015), who, in a series of articles (Keupp 1984, 1985, 1992, 1996, 1997, 2000, 2006, 2008, 2012), proposed that several types of injuries commonly recorded in ammonoid shells were inflicted by benthic crustaceans. If that is correct, this would support at least a temporarily demersal habitat for ammonoids showing such injuries; other injuries related to nektic predators, however, corroborate a nektic mode of life for at least some ammonoid groups (compare Ritterbush et al. 2014; Keupp and Hoffmann 2015).

Finally, *syn vivo* epizoans also provide some information on swimming direction and orientation of the shell (Keupp et al. 1999). However, such cases of epizoans

that can be interpreted in that respect are rare (Seilacher 1960, 1982a, b; Keupp et al. 1999; Seilacher and Keupp 2000; Hauschke et al. 2011). De Baets et al. (2015b) review information obtained from epizoans attached to ammonoids as a function of orientation (e.g., Seilacher 1960). Their results support the swimming orientations discussed herein.

Because ammonoids apparently did not produce unequivocal trace fossils of their movements *syn vivo*, no evidence from this source is available to help interpret ammonoid locomotion.

17.2 Limits of Research on Ammonoid Locomotion

Because ammonoids are extinct, we cannot provide direct, observational evidence on their swimming ability from study of the living creatures. There is no direct way to measure such parameters as maximal swimming speed, maneuverability, or the efficiency of the musculature in extinct animals like ammonoids. Thus, in this paper we attempt to reconstruct ammonoid swimming ability and maneuverability using indirect evidence that can be gleaned from the fossil record; from analogy to the performance of modern relatives; and from awareness of the uncertainties inherent in such an effort.

There are only a few aspects of ammonoid locomotion, which at the outset appear highly plausible to us:

1. Ammonoids generally were able to produce neutral buoyancy by means of their buoyancy apparatus.
2. Most ammonoids were not fully benthic since they did not leave any traces in the sediment, had often upward pointing apertures and were preyed upon by nektic organisms or only from below by benthic organisms.
3. Most ammonoids were probably capable of swimming movement powered by jet propulsion, arm beating, or other mode of propulsion.
4. Locomotor capabilities were not uniform across all ammonoid taxa since they had sometimes quite large differences in shell orientation, hyponomic sinus, body size or shell shape.

17.3 Shell Orientation

17.3.1 Mathematical Models

With his pioneering work on ammonoid shell geometry and buoyancy, Trueman (1941) initiated a line of investigation that continues down to the present day, in which palaeontologists utilize mathematical modeling techniques to gain insight on ammonoid buoyancy and shell orientation. These models usually employ the parameters used by Raup and Chamberlain (1967), namely W (expansion rate), K

(area of last generating curve) and R (distance from the coiling axis). However, such models are predicated on a number of simplifications (e.g., Trueman 1941; Raup (1967); Raup and Chamberlain (1967); Ebel 1983; Saunders and Shapiro 1986; Shapiro and Saunders 1987; Okamoto 1988, 1996; Klug 2001; Korn and Klug 2003). Commonly, these models include the assumption of self-similar (gnomonic), logarithmic shell growth, uniform shell thickness independent of position on the whorl section and the presence of a stable coiling axis. None of these simplifying assumptions necessarily coincide with actual ammonoid shells, i.e., shell growth in ammonoids was not perfectly logarithmic (e.g., Okamoto 1996; Klug 2001; Korn 2012; Tajika et al. 2015; Naglik et al. 2015), shell thickness varies and the coiling axis can permanently change its position throughout ontogeny (e.g., Urdy et al. 2010a, b).

Most authors, who produced mathematical models of shell geometry (Trueman 1941; Raup 1967; Raup and Chamberlain 1967; Saunders and Shapiro 1986; Okamoto 1988, 1996), tested their models, usually with data from Recent nautilids (Packard et al. 1980; Chamberlain 1987; Ward 1987; Jacobs and Landman 1993), and found reasonably good agreement between their results and the modeled attributes of the living animal. According to these models, the orientation of the aperture largely depended on the whorl expansion rate and ranged between about 30° and 110° from the vertical direction in normally coiled ammonoids with planispiral shells (Saunders and Shapiro 1986). In straight bactritoids (Fig. 17.1) and other heteromorph ammonoids, the aperture may have faced more or less downward, for example in more or less orthoconic forms (without counterbalancing options) such as baculitids or in some early ammonoids with very loosely coiled shells such as *Metabactrites* (e.g. Klug and Korn 2004), or in subadult *Anisoceras*, turrilitids and other heteromorphs. As shown in Fig. 17.1, shell orientation may have varied quite strongly throughout ontogeny.

As shown by Westermann (1996), the majority of Mesozoic ammonoids had body chamber lengths between 200° and 300° (Fig. 17.2). According to him and the model by Saunders and Shapiro (1986), this would coincide with an apertural orientation of about 80° to 100°, i.e. with the aperture oriented more or less horizontally. Only forms with extremely high or extremely low whorl expansion rates and body chambers shorter than half a whorl or exceeding one whorl in length would have had an aperture oriented below 50° from vertical.

17.3.2 Mechanical Models

In addition to mathematical modeling, some authors have employed mechanical, i.e. physical, models to help reconstruct shell orientation in ammonoids. Among the first to use such models were Mutvei and Reyment (1973), who built metal-coated, plastic shell models, vacuum molded from real ammonoid and *Nautilus* shells, to investigate the buoyancy and floating position of the animals thus modeled. These authors were later followed in using physical models by, e.g., Elmi (1991, 1993), Seki et al. (2000), Klug and Korn (2004), Westermann (2013) as well as Parent et al. (2014).

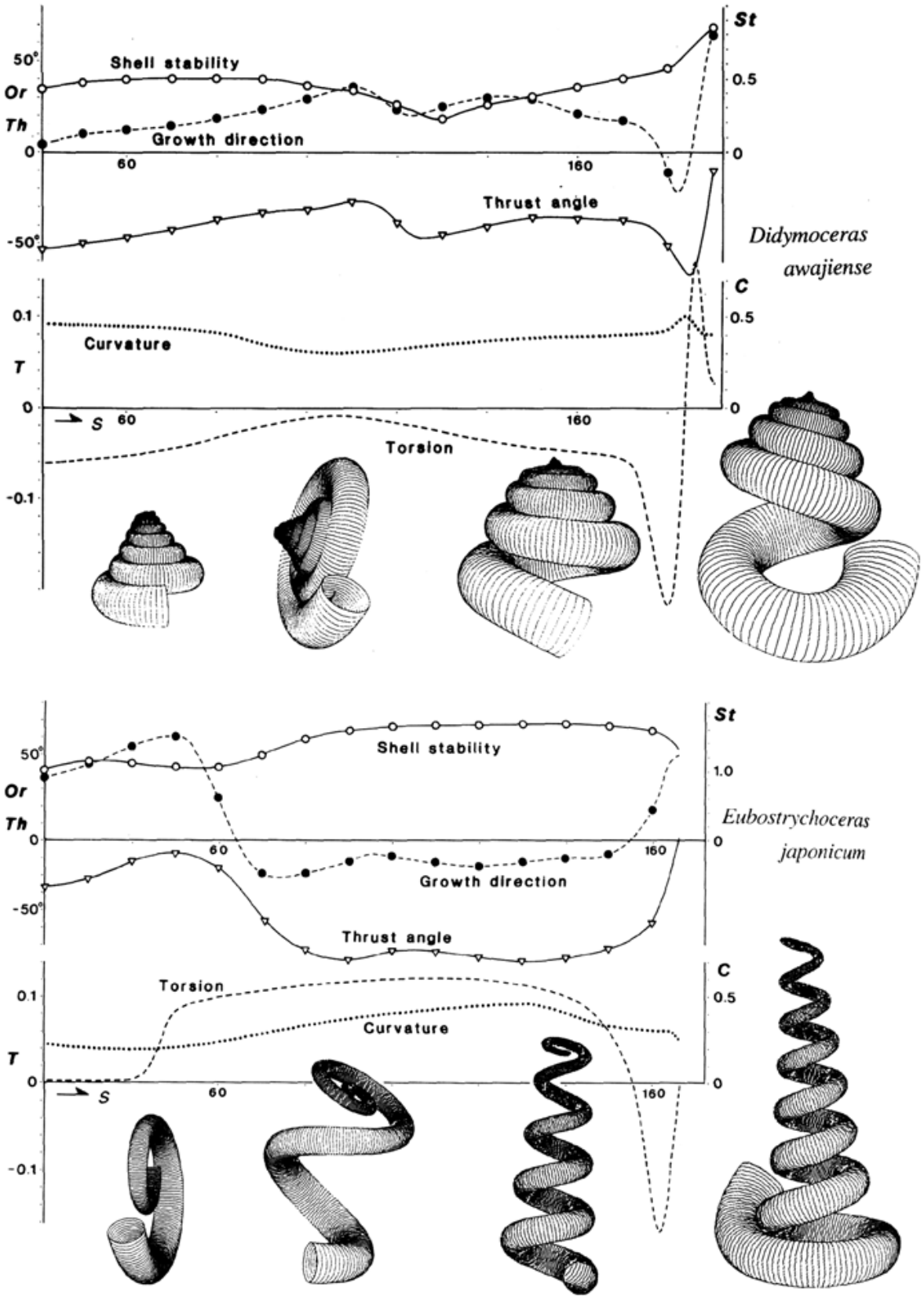

Fig. 17.1 Shell curvature, torsion, growth direction as well as hydrodynamic characters such as hydrodynamic stability, orientation of the aperture and hyponome jet thrust angle. (Source: Okamoto 1996)

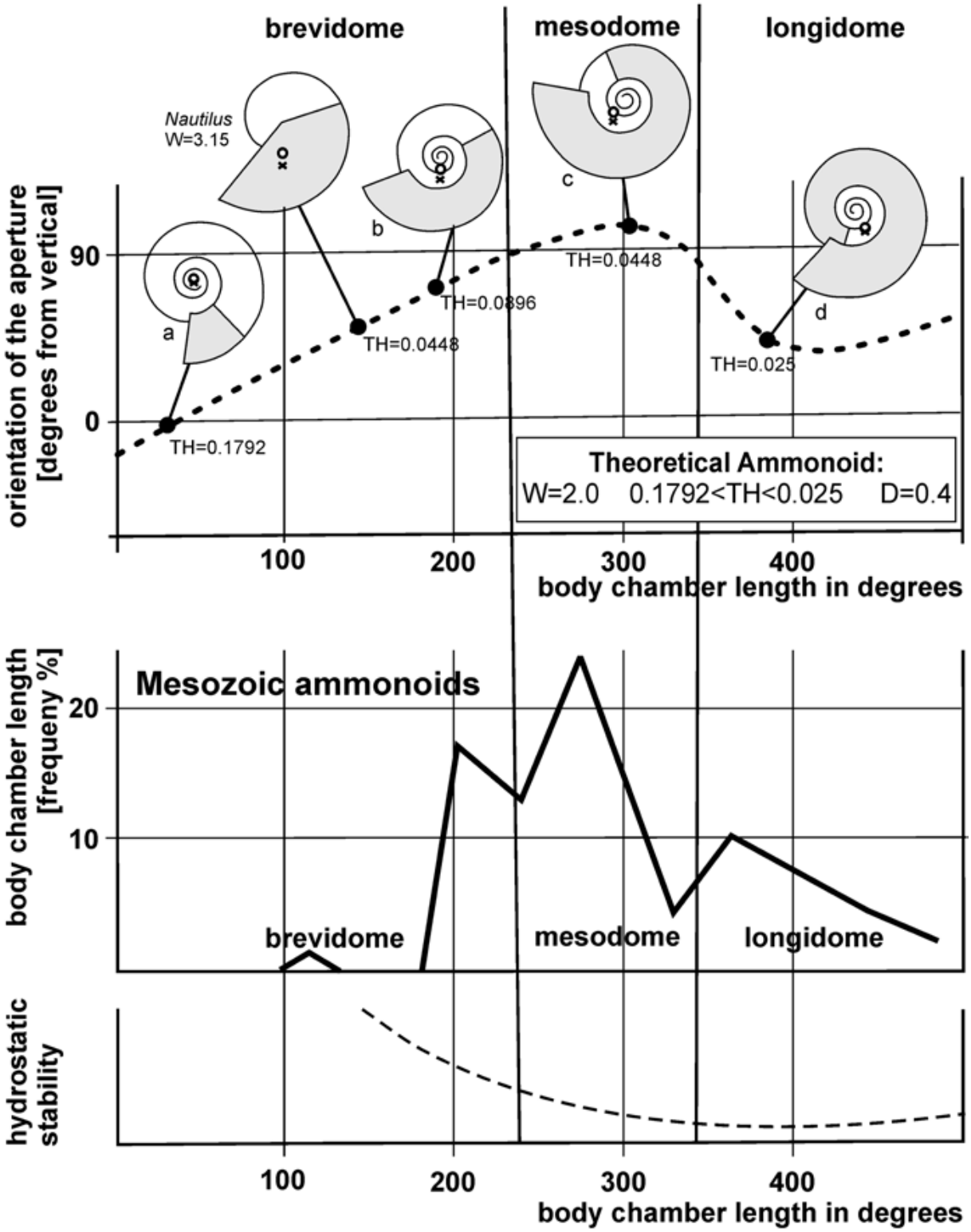

Fig. 17.2 Relationships between shell coiling, body chamber length, orientation of the aperture and hydrostatic stability of Mesozoic ammonoids. *W* whorl expansion rate, *TH* relative shell thickness, *D* relative distance between coiling axis and generating curve. Note the three peaks in body chamber length abundance and that these peaks coincide with a commonly sub-horizontal apertural margin and thus upward facing aperture. (Modified after Westermann (1996) incorporating a graph of Saunders and Shapiro (1986))

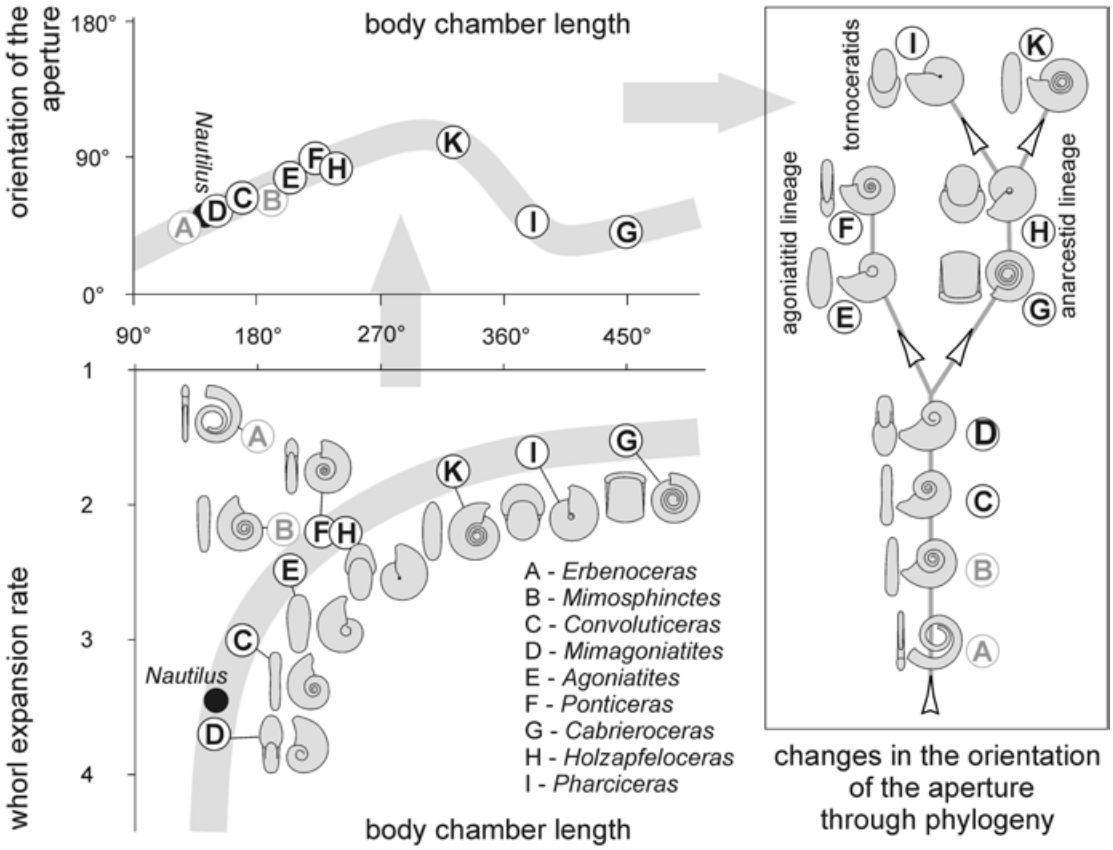

Fig. 17.3 Relationships between shell coiling, body chamber length, orientation of the aperture throughout the evolution of Devonian ammonoids. Note that three of the most important clades more or less independently evolved horizontal apertures early in the evolution of ammonoids. (Source: Klug and Korn 2004)

Klug and Korn (2004) showed, how shell orientation changed from facing downward in Orthocerida and Bactritida with orthoconic shells to oblique downward in Ammonoidea with loosely coiled shells, to oblique upward in less loosely coiled forms, to more or less horizontally upward in fully coiled shells (Fig. 17.3, 17.4). A progression of this type in aperture orientation is associated with iterative evolutionary trends (Fig. 17.3) in the major Devonian ammonoid clades (Mimosphinctoidea, Mimagoniatitoidea, Agoniatitoidea; Korn and Klug 2003) and even in parallel in two Devonian clades (Auguritidae and Pinacitidae; Monnet et al. 2011).

The question of whether ectocochleate cephalopods with orthoconic shells were capable of bringing their shell and body into a horizontal position is of long interest (e.g., Schmidt 1930; Ward 1976). Using physical models, Westermann (2013) demonstrated that a horizontal position in baculitid ammonoids could have been achieved by accumulating liquid in the most apical chambers. Such a horizontal position of cephalopods with orthoconic shells may also have been achieved with apical intracameral or intrasiphuncular deposits (e.g., Actinocerida, Endocerida) or chamber liquid (Westermann 1977, 2013; House 1981). For baculitids, Westermann (2013) suggested a vertical orientation of the shells of juveniles and a nearly horizontal orientation of subadults and adults because he assumed that juveniles had

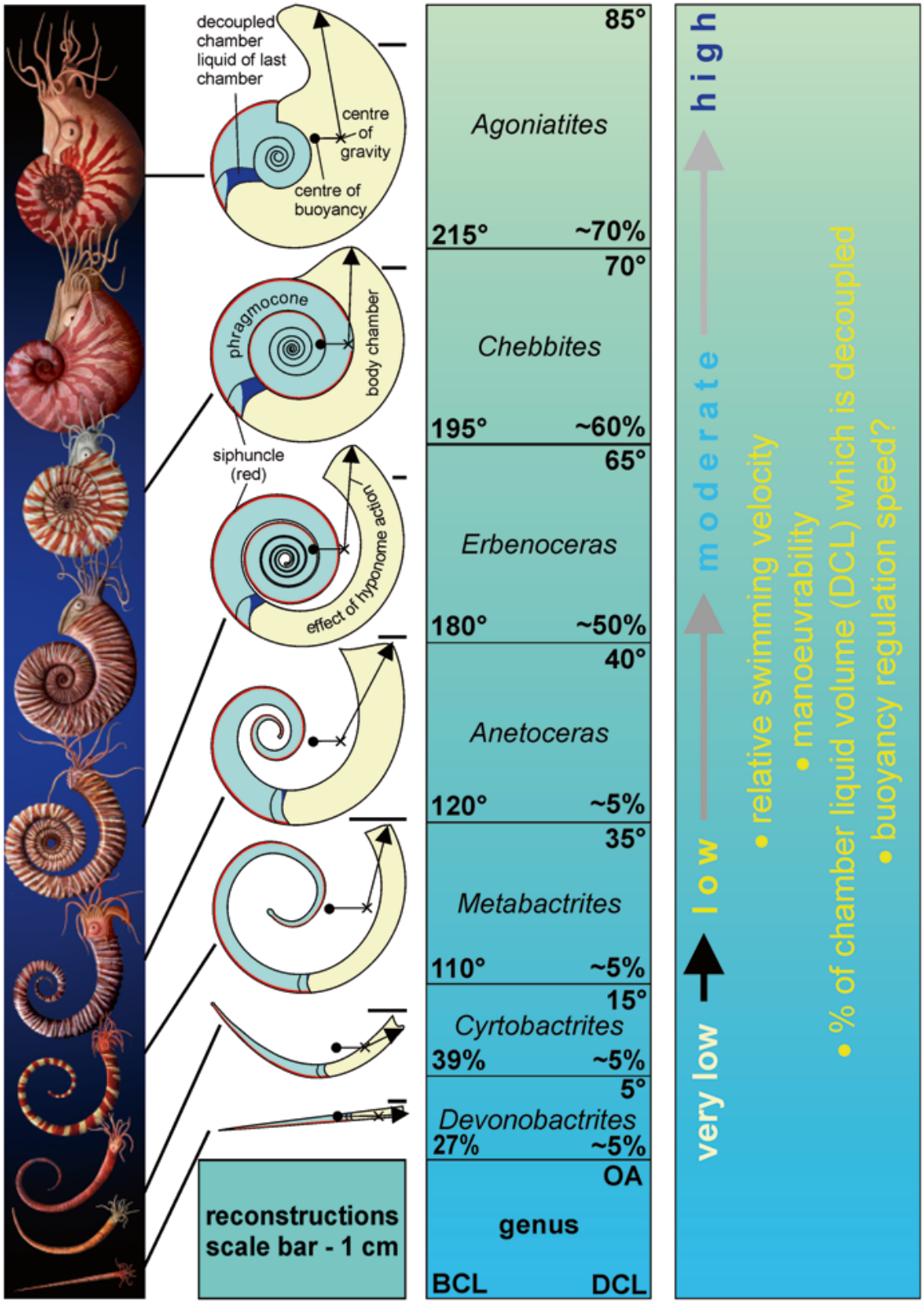

Fig. 17.4 Evolution of coiled ammonoid shells from straight bactritid shells and the consequences for body chamber length, aperture orientation, thrust angle of the hyponome jet, hydrodynamic stability and interpretations for swimming capabilities throughout evolution. (Modified after Klug and Korn 2004 as well as Klug et al. 2008). *BCL* body chamber length, *OA* orientation of the aperture, *DCL* decoupled chamber liquid.

phragmocones with more or less uniformly distributed liquid while in adults, the chamber liquid accumulated apically as a counterweight. The spatial distribution of chamber liquid might have also played a role in other ammonoids (Ward 1979, 1982; Kaplan 2002; Klug et al. 2008), although quantitative evidence on liquid distribution in ammonoid phragmocones has not yet been obtained.

Parent et al. (2014) experimented with a physical model comprised of weights and levers to assess the possible effect of the position of aptychi in aptychophoran ammonites on shell orientation. They concluded that in cases where the aptychus contains a sufficient mass and density relative to the animal's soft tissue and shell, the forward and backward movement of the buccal mass would have affected the orientation of the shell. Ammonites, such as some aspidoceratids, could have altered shell orientation in such a way that the aperture was lowered to $<25°$ from the vertical position.

Earlier physical models suggested capability of certain heteromorph ammonites (particularly the so-called "*shaft and hook shaped body chamber*" ammonoids; Kaplan 2002) to change their shell orientation (Kakabadzé and Sharikadzé 1993; Monks and Young 1998) by displacement of fluid and gas in the phragmocone (Kakabadzé and Sharikadzé 1993), or by moving the soft body of the animal within the living chamber, assuming that the animal was much smaller than its body chamber (Monks and Young 1998).

17.3.3 Empirical Models

We use the term "*empirical models*" to mean three-dimensional physical models of ammonoid shells constructed from stacks of cross-sections cut through a real shell. A similar approach was first employed by Chamberlain (1969), who built Plexiglas shell models from computer-produced topographic cross-sections of hypothetical ammonoid shells, which he then used for hydrodynamic experimentation (Chamberlain 1976, 1980, 1981). More recently, tomographic techniques have been developed, which greatly advance our skill to more confidently reconstruct *syn vivo* shell orientation(e.g., Longridge et al. 2009; Hoffmann and Zachow 2011; Hoffmann et al. 2013; Tajika et al. 2015; Naglik et al. 2015).These models are based on image stacks produced by different tomographic methods. Attempts to obtain image stacks by computer tomography often failed due to the lack of density contrast. This is probably the reason for the relatively late appearance of tomographic images of the interior of ammonoids in the scientific literature. Accordingly, tomographic data were sometimes obtained by serial sectioning (Tajika et al. 2015; Naglik et al. 2015). The latter method has the advantage that the images provide colour information and lack certain artifacts occurring in CT-data such as ring artifacts (see Hoffmann et al. 2013). In any case, these empirical models (Fig. 17.5) largely corroborate the results of mathematical modeling: forms with body chambers $<100°$ or $>360°$ have low apertures while the majority of shell forms with body chambers of 200° to 300° have more or less horizontally arranged apertures facing upward (Tajika et al. 2015; Naglik et al. in press).

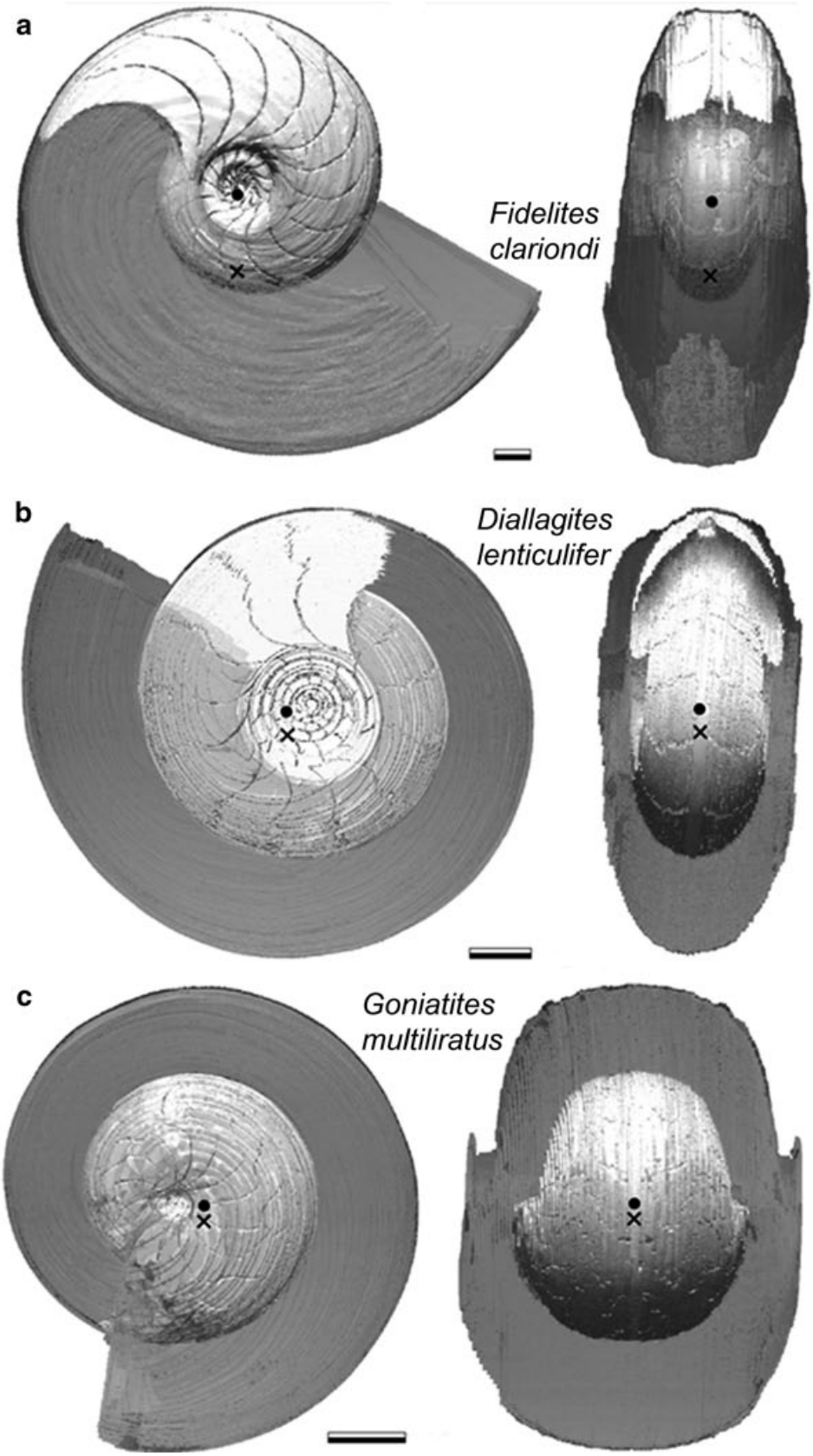

Fig. 17.5 Three Paleozoic ammonoids that have been subjected to grinding tomography in order to produce virtual 3D-reconstructions. Based on the image stacks, centers of mass (x) and buoyancy (o) were established based on these empirical models. (From Naglik et al. 2015). Scale bar: 0.5 cm

17.4 Muscles, Drag and Power

Because we cannot directly observe live ammonoids swimming, testing hypotheses on ammonoid swimming speed and swimming behavior presents obvious challenges to researchers interested in such matters. A wide variety of approaches to these issues are possible, but so far interest has centered primarily on muscles used to generate propulsion, drag, and power.

17.4.1 Muscles

Muscle attachment structures are reviewed by Doguzhaeva and Mapes (2015). According to them, jet-powered swimming could have been possible for forms with a body chamber length of one whorl or less and muscle attachments that would permit some muscles to extend straight across the body chamber and attach to the head and to the funnel.

A basic question here is the following: which of the extant cephalopods, if any, have a propulsive muscular system and mode of locomotion similar to that of ammonoids? The following kinds of muscular systems characterize modern cephalopods:

1. *Nautilus*-like: Because Recent nautilids are the only extant ectocochleate cephalopods, they have commonly been used as paradigms to understand the paleobiology of ammonoids. In modern nautilids, the large cephalic retractor muscles, which are attached to the inner shell wall of the body chamber, pull the head complex back into the body chamber, thus compressing the mantle cavity and expelling a propulsive jet of water out of the hyponome (Packard et al. 1980; Chamberlain 1981, 1987). The occurrence of apparent retractor muscle attachment scars in some ammonoids, as pointed out in Doguzhaeva and Mapes (2015), suggests that such ammonoids may have powered themselves by a "piston-pump" system not unlike what is seen in *Nautilus*.
2. Squid-like: Taking cephalopod phylogeny into account, ammonoids are more closely related to coleoids than to nautilids (Jacobs and Landman 1993; Kröger et al. 2011), and perhaps one may thus expect some similarities in coleoid and ammonoid propulsion systems. Modern squids use their muscular mantle (Bone et al. 1981) to pressurize mantle cavity water, which is then ejected through the funnel. However, the mantle in squids is not surrounded by shell as in *Nautilus*, or ammonoids, and does not function in shell secretion. It is generally considered that ammonoids also used their mantle to secrete the shell, as do ectocochleate cephalopods in general. Whether this necessarily implies that the ammonoid mantle was attached to the inner shell surface, and was secretory rather than muscular and incapable of compressing the mantle cavity is open to debate. In this regard, Jacobs and Landman (1993) as well as Jacobs and Chamberlain (1996) have suggested that the absence of large lateral muscle scars in some ammonoids

may mean that such animals used a squid-like system of propulsion involving the mantle. It has even been suggested that some ammonoids may actually have internalized shells (Doguzhaeva and Mutvei 1991, 1993), but in such cases, the mantle cavity was still located inside the body chamber of the shell. The *Nautilus* hyponome is also muscular and can direct and further compress the propulsive flow, but unlike the tubular funnel in coleoids, the *Nautilus* hyponome is a flap of tissue with folded, overlapping edges. Westermann (2013) proposed that some ammonoids may have had a powerful, coleoid-like tubular hyponome that was the main source of propulsive power. Nevertheless, the fins (probably not present in ammonoids) sometimes also play a role in squid locomotion (Packard 1972; Well 1995; Boyle and Rodhouse 2005)

3. *Argonauta*-like: Females of the octobrachian *Argonauta* produce an egg-case that is used both to shelter the eggs and to pick up air at the water surface in order to regulate buoyancy (Finn and Norman 2010). The shell differs from ammonoid shells in the absence of chambers and the fact that the *Argonauta* shell is secreted by two modified arms; other characters also differ (compare Hewitt and Westermann 2003). The mantle is not firmly attached to the shell and propulsion is carried out by means of the mantle as in other octobrachians (Young 1960; Finn and Norman 2010; Rosa and Seibel (2010).It is highly unlikely that ammonoids propelled themselves in a way analogous to that of a female *Argonauta*.
4. *Vampyroteuthis/Octopus*-like: *Vampyroteuthis* and several octobrachians can swim by contracting their arms with the velar skins, thus expelling water (Boyle and Rodhouse 2005). Since hardly anything is known about ammonoid arms (Klug and Lehmann 2015), it is currently impossible to conclude if such a mode of locomotion occurred in ammonoids.

In our view, it is likely, but not proven, that many ammonoids used longitudinal muscles to power jet propulsion. Evidence for the use of arms, velar webs, fins and mantle muscles in ammonoid locomotion is still poor or lacking. The possible efficiency, energy requirements and energy consumption associated with ammonoid propulsion are discussed in Chap. 17.4.3 below.

17.4.2 Drag

Drag is a physical term, which describes the forces that counteract the motion of an object moving through a fluid, namely seawater in the case of ammonoids. Drag is the product of the inertial and viscous forces acting on such an object, and thus depends on size, shape, and speed of the object, and on the density and viscosity of the fluid. Drag is one of the physical aspects of ammonoids that can be measured directly, even on fossil specimens (Schmidt 1930; Kummel and Lloyd 1955; Chamberlain 1976, 1980, 1981; Chamberlain and Westermann 1976; Jacobs 1992b; Jacobs et al. 1994; Jacobs and Chamberlain 1996). Drag force is usually measured directly, as was done in the studies noted immediately above. In situations where separated flow occurs, as would normally be the case for medium-sized and large

ammonoids moving relatively fast, drag can also be calculated from the following equation.

$$F_D = \tfrac{1}{2} \rho \, v^2 \, C_d A$$

F_D—drag force; ρ—density of the medium (seawater); v—velocity of the object (ammonoid); C_d—drag coefficient of the object (a dimensionless number which can be thought as representing the shape of the moving object); A—an area representative of the size of the moving object.

For objects, such as ammonoids, which have complex shapes, and thus complex flow interactions, shell volume raised to the two-thirds power ($V^{2/3}$) is generally the areal parameter of choice (Chamberlain 1976; Vogel 1981). It is important to understand that C_d is not a constant; it is a coefficient that varies widely for a given object depending on flow conditions. Flow state around an object, like an ammonoid, is described in terms of the Reynolds number.

$$Re = dm \, v / \upsilon \quad \text{with} \quad \upsilon = \gamma / \rho$$

Re—Reynolds number; dm—specimen shell diameter in the direction of motion; v—velocity of the object; υ—kinematic viscosity of seawater (viscosity [γ] divided by seawater density [ρ]). When Re is low (Re < 1000 approximately), flow is attached to the object (this is often referred to as Stokes Flow); drag is due entirely to surface friction; C_d is very high, often more than 100, and varies directly with velocity and Re. Spherical objects generate the least drag because they have the smallest surface area, and hence least frictional drag per unit volume. For ammonoids, these conditions would hold for small ammonoids swimming slowly. When Re exceeds approximately 10,000, flow is separated to some degree from the object (this is often referred to as separated or non-Stokes flow); drag is due to a combination of friction and an adverse pressure gradient created by the separation; and C_d is low and often constant, or nearly so, as Re and velocity change, fusiform objects generate the least drag because they have the smallest possible pressure drag component (fusiform shapes minimize the extent and magnitude of separation and the posterior low pressures that derive from separation). For many objects operating in separated flow, a large reduction in C_d occurs when the character of the fluid boundary layer lying on the surface of the object converts from laminar to turbulent conditions. For ammonoids, separated flow would hold for large ammonoids swimming quickly. At intermediate values of Re (1000 > Re < 10,000 approximately), flow is unstable and can vary from a separated to attached state depending on such factors as object shape and surface features. This would apply to ammonoids of intermediate size moving at intermediate speeds.

Several authors examined drag using ammonoid models (Schmidt 1930; Kummel and Lloyd 1955; Chamberlain 1976; Jacobs 1992b; Jacobs and Chamberlain 1996). Modeling focused on the shell only (Kummel and Lloyd 1955; Chamberlain 1976); the shell and attached prostheses imitating extruding soft parts (Chamberlain 1980); or shell and artificial surface sculpture (Chamberlain 1981). For models

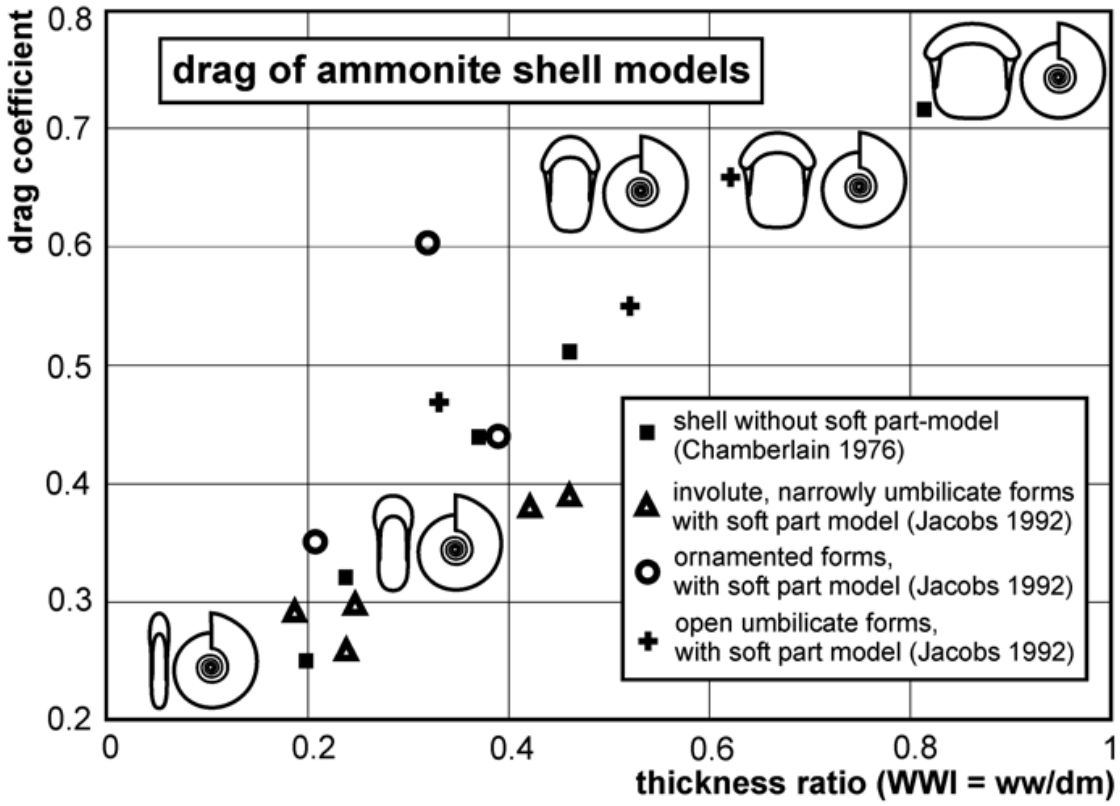

Fig. 17.6 Relationship between the thickness ratio and the drag coefficient, depending to a lesser degree on other factors such as umbilical width and ornament strength. These data (Chamberlain 1976; Jacobs 1992b) were obtained from models in a water tank (modified after Jacobs and Chamberlain 1996)

with representative values of Raup's W and D values (Raup 1966, 1967; Raup and Chamberlain 1967), Chamberlain (1976) determined drag coefficients in separated flow (i.e. for higher velocities and larger shells) where pressure drag is the key hydrodynamic factor. These experiments on models revealed that narrower shells had lower drag values. It appears to be mainly shell thickness and umbilical width, which play important role in generating drag in such flow conditions (Fig. 17.6).

In a later study, Jacobs (1992b) focused on drag for ammonoids of small size and low velocity (Re below about 25000), where frictional drag is the key hydrodynamic factor (see also Jacobs and Chamberlain 1996). Some results of Jacobs (1992b) are reproduced in Fig. 17.7. Note that in each graph in Fig. 17.7, the curves for wide and narrow forms cross at a point between Reynolds numbers of 5000 and 10,000. At Re less than the crossing value, the wider shells have lower drag coefficients (less frictional drag in Stokes flow) than the narrow shells, but at Re greater than the crossing value, the narrow shells have lower drag coefficients (less pressure drag in separated flow). This implies that different shell morphologies are more efficient at different sizes and swimming speeds (Table 17.1). Narrow forms produce less drag than wide forms at higher Reynolds numbers (faster speeds, larger size), while wide shells generate less drag at low Reynolds numbers (slower speeds, smaller size) than do narrow shells. This situation implies that the com-

Table 17.1 Possible swimming behavior of ammonoids in dependence of their shell shape. (Modified after Jacobs and Chamberlain 1996). For *Baculites*, we used the interpretation of Westermann (2013). Additional information comes from Klinger (1981) and Seki et al. (2000)

Shell shape	Slow, continuous swimming	Fast, continuous swimming	Acceleration	Vertical
Compressed involute				
Oxyconic (e.g., *Sphenodiscus*)	Poor	Good	Excellent	Moderate
Platyconic with rounded venter (e.g., *Oppelia*)	Moderate	Excellent	Good	Moderate
Platyconic with tabulate venter (e.g., *Anahoplites*)	Good?	Good	Moderate	Moderate
Moderately compressed				
Platyconic, moderately evolute (e.g., *Mesobeloceras*)	Moderate	Good	Moderate	Moderate
Involute juvenile (e.g., *Scaphites*)		Moderate	Moderate	Moderate
Evolute, rounded whorls (e.g., *Lytoceras*)	Moderate	Moderate	Poor	Moderate
Compressed evolute	Good	Moderate	Moderate	Good
Depressed				
Sphaeroconic involute (e.g., *Goniatites*)	Moderate	Poor	Poor	Moderate
Cadiconic, evolute (e.g., *Cabrieroceras*, *Gabbioceras*)	Moderate	Poor	Poor	Moderate
Heteromorphic				
Orthoconic (e.g., *Baculites*)	Moderate	Moderate	Excellent?	Moderate
Torticonic (e.g., *Turrilites*)	Poor	Poor	Poor	Good
Loosely coiled in three dimensions (e.g., *Nipponites, Didymoceras*)	Poor	Poor	Poor	Good

mon ammonoid ontogenetic change in shell morphology from depressed juvenile whorls to more compressed whorl shape near maturity could be linked with this flow state dependent change in drag coefficient (Jacobs and Chamberlain 1996). The latter authors also suggested that morphologic change related to hydrodynamic factors operating in the evolution of ammonoid clades should be linked with different host facies. This link was examined by various authors (e.g., Ziegler 1967; Batt 1989; Bayer and McGhee 1984; Marchand 1992; Courville and Thierry 1993;

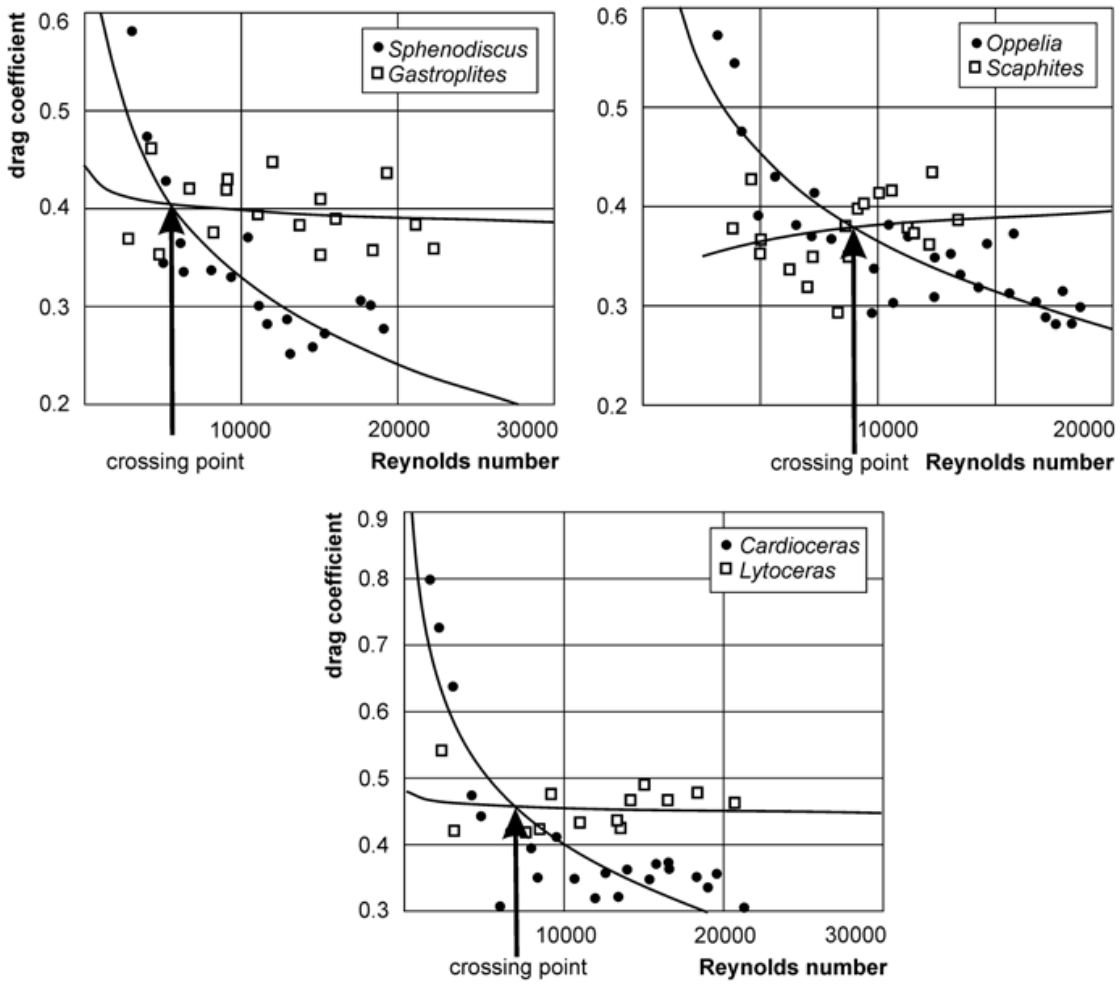

Fig. 17.7 Relationships between drag coefficients and Reynolds number (Re) of three different pairs of Jurassic and Cretaceous ammonoids. In each pair, one form has a narrow shell (*dots*), and one has a wide shell (*open squares*). Note that in each graph the curves for the two forms cross at a point between Reynolds numbers of 5000 and 10000. At Re less than the crossing value, the wider shells have lower drag coefficients (less frictional drag in Stokes flow) than the narrow shells, but at Re greater than the crossing value, the narrow shells have lower drag coefficients (less pressure drag in separated flow)

Jacobs et al. 1994; Klug 2002; Kawabe 2003). Such studies are hampered by the possibility that ammonoid shells were transported post mortem and the imperfect knowledge of habitat depth, because the sedimentary context in which ammonoids are preserved mainly informs about the energy in the water column and the volume of sediment that is delivered in combination with accommodation space. It is possible that ammonoids could have lived in more quiet waters near the sea-floor or in more agitated waters near the surface uncharacteristic of the sedimentary context of the rock itself. Additional factors, such as time-averaging might also complicate straight forward interpretations (compare De Baets et al. 2015a).

In any case, the measurable disparity of ammonoids throughout ontogeny and evolution as well as the recurrent ontogenetic change in shell shape indicate that minimizing drag played an important role in ammonoid evolution. It also indicates

that different forms were possibly specialized for different modes of life with correspondingly different swimming abilities.

17.4.3 Power

The use and availability of power for swimming in ammonoids cannot be measured directly and thus has to be addressed based on actualistic comparisons with living organisms (e.g., Trueman and Packard 1968).

The physical term, power, simply describes the ratio between the work, W, expended in a time interval, t:

$$P = \Delta W / \Delta t$$

Assuming constant velocity during the time interval in question, this can be modified to the following equation using drag force F_D and velocity v:

$$P = F_D \; v$$

Power consumption during swimming thus depends directly on drag coefficient and can be estimated from the relationship between drag coefficient and Reynolds number, and thus with respect to size and velocity (Jacobs 1992b; Jacobs and Chamberlain 1996). In order to assess the differences in power consumption as a function of shell form, size and velocity, Jacobs (1992b) produced drag data for the thick genus *Gastroplites* (ww/dm = 0.42) and the thin genus *Sphenodiscus* (ww/dm = 0.19). His results are reproduced here in Fig. 17.8. According to Fig. 17.8, *Gastroplites* would require less power at sizes below 10 cm and velocities below 50 cm/s. At a shell size of 10–100 cm and speeds below 15 cm/s, the two shell shapes would require about the same power. At higher speeds and sizes exceeding 10 cm, *Sphenodiscus* would need less power and swim more economically. Whether these ammonoids could actually produce the power necessary to swim at these speeds cannot be inferred from such data, however.

Knowledge of swimming speed in fossil ammonoids requires knowledge of the power output generated by live ammonoids. The power produced by live ammonoids is unknown. However, one can gain useful insight into this matter by applying to this question data on power output of modern swimmers, particularly modern cephalopods. Of primary interest is the power output of modern analogues in sustained swimming (powered by aerobic muscle contraction), and in burst swimming (powered by anaerobic muscle contraction). Also of interest is metabolic scope, i.e., the difference between the power requirements during inactivity and periods of maximum activity. Unsurprisingly, power output and metabolic scope differ strongly between living cephalopods such as *Nautilus* with very low metabolic rates and the active squid *Illex* with a high metabolic scope (O'Dor 1982, 1988a, b; Chamberlain 1987; O'Dor and Wells 1990; O'Dor et al. 1990, 1993; O'Dor and Webber 1991). Even among squids, metabolic rates can vary strongly depending on

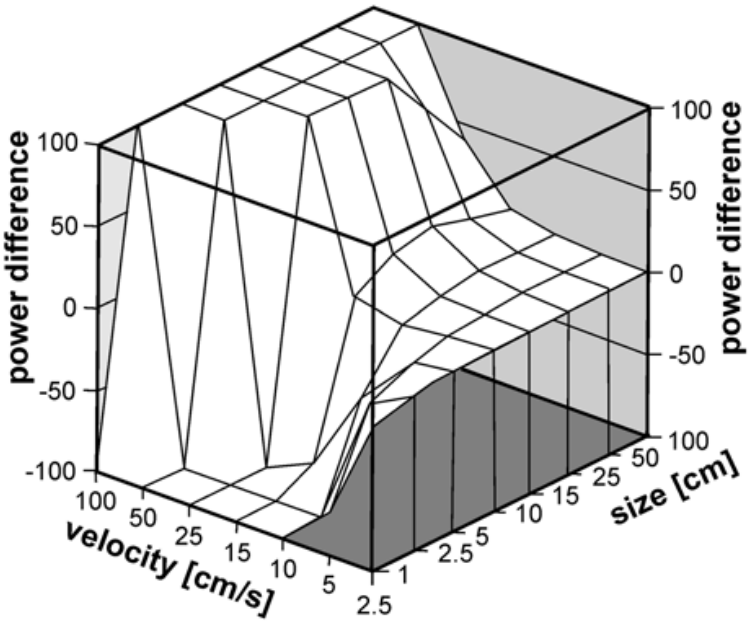

Fig. 17.8 Differences in power consumption (in ergs/s/cm^3) in a broad, depressed form (*Gastroplites*) and in a narrow, laterally compressed form (*Sphenodiscus*). Power difference was calculated by subtracting the power required per unit volume in *Sphenodiscus* from that of *Gastroplites*. Depending on this ratio, one obtains positive or negative values: when the values of power difference are negative, *Gastroplites* requires less power. The greatest power difference is seen at low sizes and high velocities. Jacobs and Chamberlain (1996) considered these differences as so profound that they appear to be biologically significant. Power differences > 100 ergs/s/cm^3 are not shown (modified after Jacobs and Chamberlain 1996)

their habitats (Seibel et al. 1997). For instance, the deep-sea squid *Vampyroteuthis infernalis* has a metabolic rate a hundred times lower than the shallow water *Gonatus onyx* (Seibel et al. 1997).

Estimates of power production in ammonoids depend on whether Recent nautilids are considered the better model organisms with their similarly constructed external shell or whether coleoids should rather be used as paradigms because they are more closely related to ammonoids. Several authors (e.g., Trueman 1941; Swan and Saunders 1987; Jacobs and Landman 1993; Kröger et al. 2011) have argued in favor of coleoids rather than nautilids on the basis of shell form and phylogeny. In order to estimate sustainable swimming speeds in ammonoids, Jacobs (1992b) argued that a metabolic rate of 200 ml of oxygen per kilogram per hour, which is close to that of *Sepia* (O'Dor and Webber 1991), probably represents a reasonable figure for most ammonoids. He also advocated that for ammonoids, sepiids represent the most meaningful model organisms among coleoids because like ammonoids, they have a large chambered phragmocone, which greatly limits the relative proportion of propulsive muscle (and soft tissue generally) to total volume of the animal (see also Chamberlain 1981, 1990, 1992, 1993). By comparison, squids like *Illex*, pack their bodies much more fully with propulsive muscle. O'Dor and Webber (1991) found that the metabolic scope of the highly active *Illex* was four times larger than in *Sepia* and additionally, the efficiency of their muscles exceeds that of sepiids. In

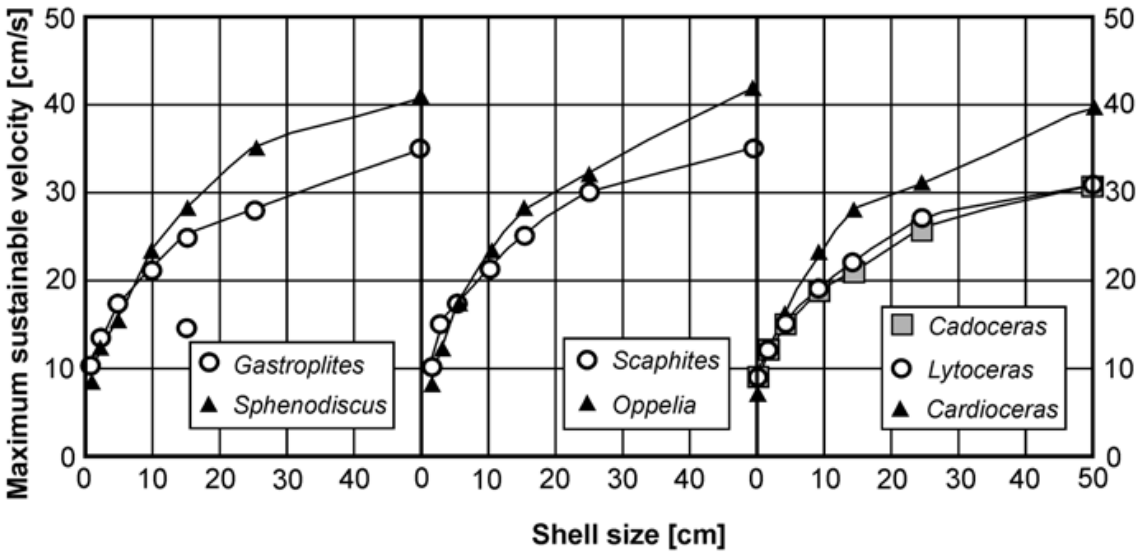

Fig. 17.9 Maximum sustainable swimming velocities in seven ammonoid genera. These are arranged in groups of two or three, always comprising a genus with a more compressed and one with a more depressed shell form. The velocity values are based on the assumption that the maximum power availability was 400 ergs/s/cm^3. Overall, the curves resemble each other and in the curve pairs, they cross each other at a size of 5 to 10 cm (modified after Jacobs (1992b) as well as Jacobs and Chamberlain (1996))

consequence, power output is ten times higher in *Illex*, thus making *Sepia* the better actualistic model organism for ammonoids (Jacobs and Chamberlain 1996).

O'Dor and Webber (1991) observed swimming speeds of maximally 65 cm/s (2.3 km/h), which required a power output of 1000 µJ/s/cm^3. Jacobs (1992b) as well as Jacobs and Chamberlain (1996) concluded that in ammonoids, this figure would probably not have exceeded 600 µJ/s/cm^3 because only about 40 % of the organism's volume is occupied by soft parts. The maximum swimming speeds of some ammonoid species, which are based on these assumptions, are depicted in Fig. 17.9. Maximum swimming speeds of large ammonoids like *Sphenodiscus* with a shell diameter of 25 cm would not have exceeded 100 cm/s (3.6 km/h). *Gastroplites* of the same size would have a speed of about 70 cm/s (2.5 km/h). The latter velocity corresponds to the maximum in *Sepia* (Jacobs and Chamberlain 1996). As a lower limit of energy availability, *Nautilus* can be used as model. Nautilus can activate up to 100 µJ/s/cm^3, i.e. a tenth of that of *Sepia*. Using this figure, a 25 cm *Gastroplites* could reach 40 cm/s (0.54 km/h) and *Sphenodiscus* would have been able to swim 55 cm/s (1.98 km/h). These results are similar to swimming velocity estimates based primarily on drag considerations made by Chamberlain (1981, Fig. 17.8).

In summary, Jacobs (1992b) as well as Jacobs and Chamberlain (1996) found that swimming speed of ammonoids likely depended on various factors including shell shape (e.g. Table 17.1), body chamber angle, size, energy availability and power consumption. For large size, ammonoids with compressed shell form (low ww/dm ratio) could swim faster than those with depressed shells (high ww/dm ratio); while at small size this relationship is reversed.

17.4.4 Acceleration

Accelerating an object in a fluid involves accelerating fluid entrained in the object's wake and also fluid in direct contact with the surface of the object, i.e. in the boundary layer. In the case of swimming organisms, this also applies and in order to estimate swimming speeds and energy requirements, this added mass has to be taken into account (Chamberlain 1987; Jacobs 1992b; Jacobs and Chamberlain 1996). The force required to accelerate this added mass can be quantified by the following equation, which was introduced by Daniel (1984):

$$G = -ar\,V\left(du/dt\right)$$

G—acceleration reaction force; a—added mass coefficient (a function of thickness ratio ww/dm); r—density of the fluid; V—volume of the object/ammonoid; du/dt—acceleration.

The acceleration reaction force occurs both in acceleration and deceleration (Daniel 1984; Chamberlain 1987; Jacobs 1992b; Jacobs and Chamberlain 1996). For ammonoids, the symmetry of the shell in swimming direction, shell shape, differences in acceleration and deceleration processes as well as the formation of vortices in the wake play a role.

In cephalopods, acceleration is produced by a series of water expulsions from the hyponome with interim phases of water intake into the mantle cavity. The animal accelerates when the propulsive muscles contract forcing water from the mantle cavity and decelerates during the recovery phase of the propulsive cycle when water is taken into the mantle cavity in preparation for the next mantle cavity contraction. When an organism starts swimming, energy is mainly invested in acceleration while at higher speeds when velocity is more constant, the energetic cost of drag rises. Acceleration force also depends on the width of the ammonoid shell (ww/dm ratio; Fig. 17.10) and it roughly doubles from ww/dm = 0.2 to a value of 0.4 (Jacobs and Chamberlain 1996). According to Daniel (1984, 1985), the ratio of energetic costs of drag to that of acceleration varies from 48 % in a small squid accelerating from 0 to 2000 cm/s^2 to 62 % in a medusa accelerating to 700 cm/s^2 to 92 % in a salp accelerating to 23 cm/s^2. These values show that the faster an organism accelerates to a higher velocity, the lower the relative energy investment into added mass and the higher the investment into overcoming drag.

This relationship points to a potentially multiple functions of shell shape in ammonoids. While some shell morphologies reduced drag, other shell morphologies, such as oxycones with a small umbilicus, would have reduced the energetic cost invested in added mass (Jacobs 1992b; Jacobs and Chamberlain 1996). In that respect, ammonoids with narrow oxyconic shells would resemble ambush predators among fish (e.g. pike, barracuda) whose body geometry is too elongate to be purely adapted to reduce drag. Instead, their long and narrow shape strongly reduces acceleration reaction force and enables them to accelerate strongly from a standing start. While there is no corroboratory evidence for an ambush predator strategy

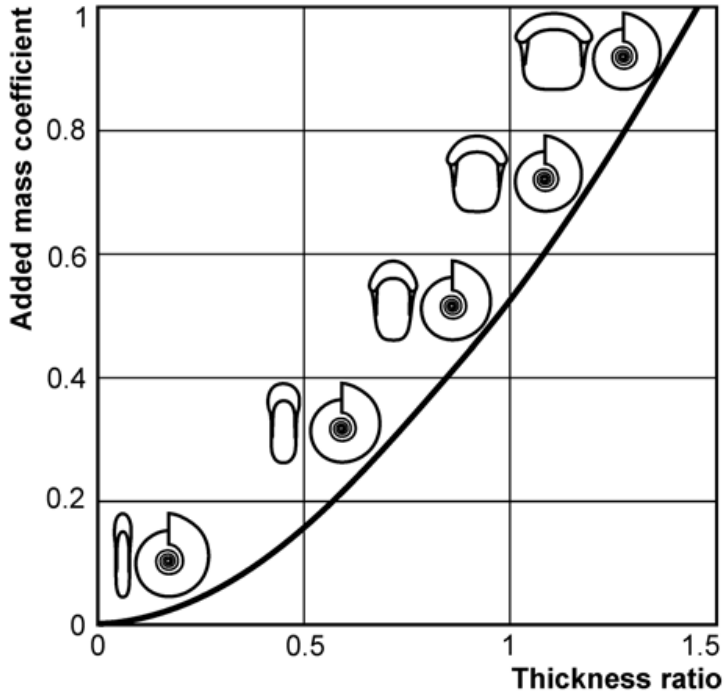

Fig. 17.10 Depending on shell shape and ornament, differing amounts of added mass of water accelerated with the ammonoid in the boundary layer and the wake can be expected. The acceleration reaction is a linear function velocity change (acceleration) and a function of the added mass coefficient, which -in turn- depends on shell shape and orientation relative to the direction of acceleration. According to these relationships, ammonoids with laterally compressed shells had substantially less added mass than ammonoids with depressed shells (modified after Jacobs (1992b) as well as Jacobs and Chamberlain (1996))

in oxyconic ammonoids, the fact that oxyconic shell form evolved many times iteratively and sometimes even in parallel (e.g., Bayer and McGhee 1984; Klug and Korn 2002; Monnet et al. 2011) shows that this shell shape may indeed have had a positive adaptive benefit for ammonoids.

17.4.5 Cost of Transportation

The cost of transportation (COT) is a metric that describes the energetic cost of locomotion. COT has been defined in a variety of ways. For example, in his comparison of the energy cost of different styles of animal locomotion Schmidt-Nielsen (1972) defined COT as (metabolic rate/(body weight and speed). O'Dor (1988a) and O'Dor and Webber (1991) in their study of squid locomotion, and Chamberlain (1990) in his study of *Nautilus* locomotion, determined COT by calculating metabolic output from oxygen consumption data for swimming animals. In all such approaches the aim has been to express COT in terms of the propulsive power produced by a swimming animal relative to some measure of its size, speed, and distance travelled. COT is thus simply stated in terms of propulsive power per unit of animal size per unit of speed or distance traveled where animal size is represented by weight or volume.

The power produced by a swimming ammonoid can be expressed as follows:

$$P = W/t = (F\ d)/t = F\ v$$

where P is the metabolic output (power) used to produce locomotion; W is the work needed for locomotion; t is the time interval over which the locomotion occurs; F is the force or thrust developed by the swimming ammonoid and is assumed to be constant over the interval t; d is the distance traveled; and v is the animal's velocity, also assumed to be constant.

Jacobs (1992b) and Jacobs and Chamberlain (1996) used the power-required data and the efficiency assumptions of Jacobs (1992b) to evaluate COT for a few representative ammonoids. Following Jacobs (1962b), they calculated COT as propulsive power per unit of total shell volume per unit of distance traveled. Their results are diagrammed in Fig. 17.11. The upper panel in this figure indicates that, assuming *Sepia* metabolic output, *Gastroplites* COT depends on size. Larger animals have lower COTs for a given velocity than smaller ones. This is largely the result of larger animals operating in separated flow where drag coefficients are smaller while small animals operate in Stokes flow where drag coefficient is much higher for objects of the same shape. The upper panel also indicates that if we assume *Gastroplites* had a lower metabolic output equivalent to that of *Nautilus*, its COT would also be lower. Perhaps the most interesting observation to be made from Fig. 17.11 is that for each curve there is a specific velocity for which COT is minimal. If energy conservation in swimming ammonoids mirrors that of flying animals, where flight speed usually reflects minimal COT, and there is no reason why it should not, this may mean that this minimal COT speed represents the usual swimming speed for the ammonoid to which the curve applies. The steepness of the curve on either side of the minimum COT speed implies that there would be considerable gain in cost to the animal in moving away from this optimum speed. The lower panel in Fig. 17.11 shows that the modern swimmers plotted here, both coleoids and fish, have COT-velocity curves much less steeply inclined as velocity increases above the minimum COT speed. This means that these modern animals are not nearly so constrained in terms of COT in varying their swimming speed than is the case for the ammonoids plotted here as well. Swimming over a range of velocities does not greatly influence their COT. It would appear that these modern swimmers have a much more flexible swimming repertoire than did fossil ammonoids.

Jacobs (1992b) as well as Jacobs and Chamberlain (1996) suggested that due to their neutral buoyancy, ammonoids, like *Nautilus*, may have had a low use of energy at rest and that the cost of transportation in ammonoids was accordingly low at low velocities. Alternatively, if ammonoids were closer to sepiids in their metabolic rates, the cost of transportation would have been lower at higher swimming speeds depending on their size (Fig. 17.11). Jacobs and Chamberlain (1996, p. 210) summarized this idea as follows: "*ammonoids may not have been pursuit predators, comparable to tuna or some squids, that spend long periods of time chasing down prey at high speed. This would deny the utility of the neutrally buoyant shell in limiting energetic expenditure. However, life styles that require only intermittent bursts*

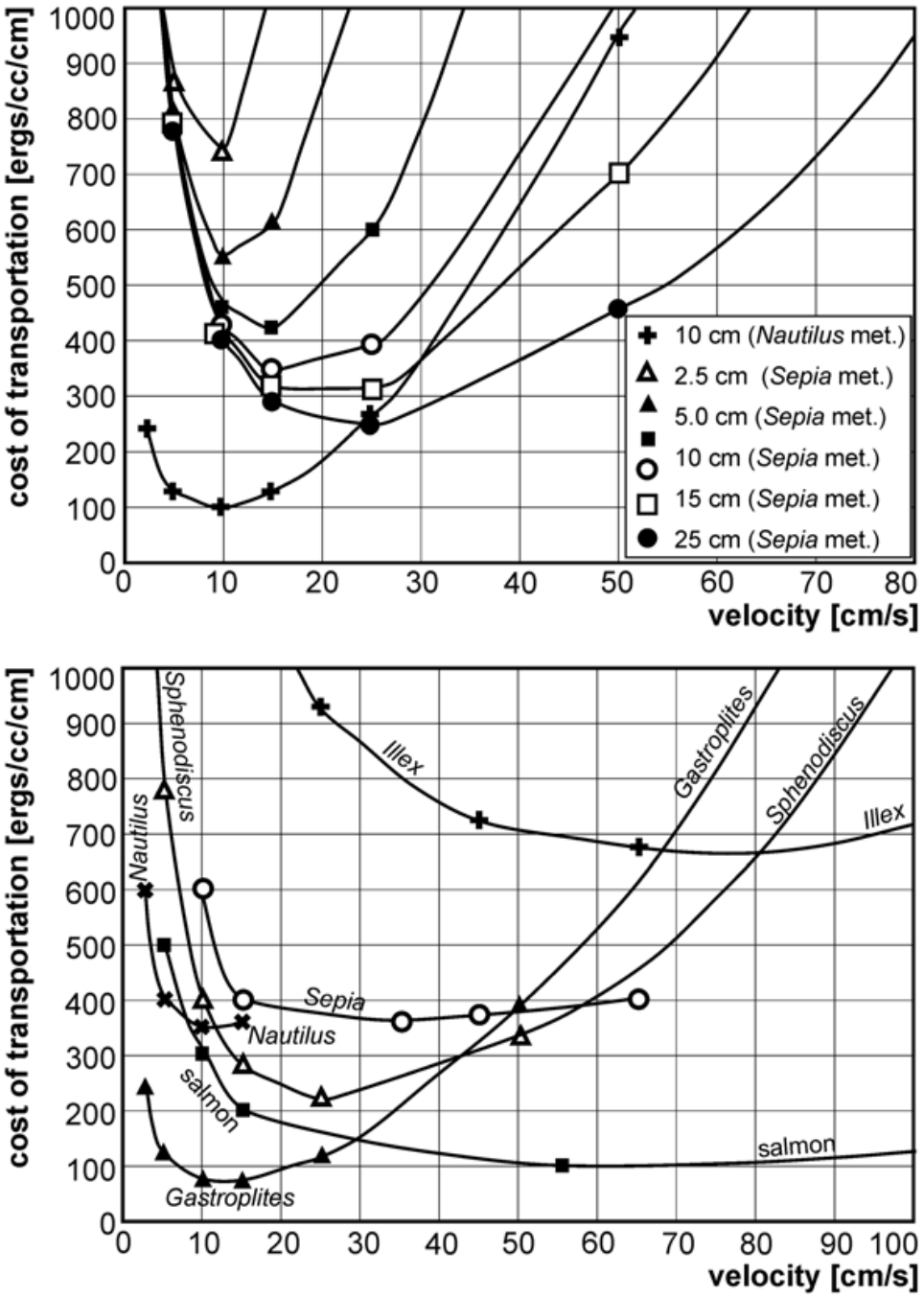

Fig. 17.11 Cost of transportation (*COT*) in relation to velocity depends on shell size and metabolic rate (upper diagram) and differs between modern animal groups (lower diagram). Modified after Jacobs (1992b) as well as Jacobs and Chamberlain (1996). The efficiency of energy conversion into propulsion force is estimated to be 10 %. The upper diagram shows the COT for various sizes of *Gastroplites*, assuming metabolic rates (O'Dor and Webber 1991) of *Sepia* (3900 ergs/s/cm^3) and in one case of *Nautilus* (1/7th of *Sepia*). With increasing size, less energy is required for locomotion. The lower diagram shows the COT of *Sphenodiscus* and *Gastroplites* in comparison to various recent cephalopods and a fish (O'Dor and Webber 1991). Resting metabolic rates were estimated for *Sphenodiscus* to resemble that of *Sepia* and for *Gastroplites* to resemble that of *Nautilus*. At higher velocities, the costs rise much faster in the shelled swimmers than in fishes and squids. However, the ammonoid curves are based on a series of estimates for the metabolic rates, added mass and other modes of locomotion (fins in *Sepia*)

of energy, such as ambush predation, seem possible, and oxyconic shell shape […] *may have been conducive to such a mode of life*." It should be remembered that high speed is not required for successful predation. A predator must only move faster than its prey. If its prey is slow, a predator can be slow also. Oxycones would not need the fast burst speed of *Illex* or *Sphyraena* (barracuda) to prey on slower moving ammonoids.

Jacobs (1992b) and Jacobs and Chamberlain (1996) also pointed out that energy used for transport is energy that cannot be used in other ways; there is a trade-off between these costs and the energetic cost of other life functions. Nautilids have a low metabolism and can fast over lengthy time spans. In such a case, slow swimming speeds (O'Dor et al. 1990) are advantageous in promoting prolonged food searches (Wells 1987; Chamberlain 1990; Jacobs and Chamberlain 1996), as is the case for *Nautilus* (Ward and Wicksten 1980). Wells and O'Dor (1991) thought that other ectocochleates such as ammonoids may have pursued a similar low energy mode of life. They supported this hypothesis by pointing out that increasing numbers of fish occupied high energy nektonic habitats (for these macroecological changes, see Signor and Brett 1984; Bambach 1999; Kröger 2005; Klug et al. 2010) and would have competitively excluded most ammonoids from these habitats. The problem with this hypothesis is twofold: (1) As Jacobs and Chamberlain (1996) pointed out, ammonoids are more closely related to coleoids (some of which use considerable energy in relation to body size and also swim at high velocities) than they are to low energy nautilids (Jacobs and Landman 1993; Kröger et al. 2011). (2) The radiation of gnathostome fish in the Silurian and Devonian, a major event in the evolution and history of diversification of fishes, was also a time in which ammonoids originated and rapidly diversified (Klug et al. 2010). The diversification of teleostean fish in the Mesozoic also appears to be largely independent of ammonoid diversity changes (Jacobs and Chamberlain 1996), although the Cretaceous diversification of deep-bodied acanthopterygians may have been a factor influencing ammonoid diversity late in their history (Chamberlain 1993). Some heteromorphs might have been slower swimmers than nautilids in horizontal direction, although this requires further research (e.g., Ward 1979; Westermann 1996).

17.4.6 The Role of Ornament

As in sharks (Reif 1982; Oefner and Lauder 2012) and golf balls, a fine regular surface ornament can reduce drag by forcing conversion of the boundary layer around an ammonoid shell from laminar to turbulent flow at lower Reynolds numbers than would normally be the case. Boundary layer conversion reduces the scale of the turbulent wake and the pressure drag that results from it. Chamberlain and Westermann (1976) and Chamberlain (1981) examined this phenomenon and concluded that it could have a positive effect for some ammonoids by bringing lower drag and more efficient swimming into the velocity range of some ammonoids. Nevertheless, the lowering of the coefficient of drag would have been significant at Reynolds numbers exceeding 40,000, a figure that could potentially only be achieved in large ammonoids moving at relatively high velocities (Chamberlain 1981).

Jacobs and Chamberlain (1996) speculated that in cadicones, the coarse ribs or nodes as in *Cabrieroceras*, *Gastrioceras* or *Teloceras* might have caused the formation of vortices covering the entire umbilicus. Similarly, they suggested that, in forms with tabulate venter (or with ventral band as in Devonian forms such as *Gyroceratites*, *Armatites* or *Kosmoclymenia*), the water might have been divided into two fields, thus maintaining flow attachment and reducing turbulence in their wake, at least at certain velocities and sizes. They also reasoned that ribs tend to be the largest near the aperture and to be oriented in swimming direction, thus stabilizing the shell orientation during backward swimming in forms, which are more or less involute and carry moderately strong ribs such as *Cardioceras*. Westermann (1966) even speculated that this might be a driving force behind Buckman's law of covariation, although this law can be conveniently explained by morphogenetic processes (Monnet et al. 2015) without an adaptive interpretation (compare Hewitt 1996 for an alternative functional explanation). In contrast, strong ornament significantly increased drag (Chamberlain 1976; Jacobs 1992b; Hewitt 1996; Jacobs and Chamberlain 1996), thus supporting indirectly its possibly defensive function shell sculpture (e.g., Ward 1981).

17.4.7 Hydrodynamics Through Ammonoid Development

As discussed in Hoffmann et al. (2015), the flow regime in which ammonoid swimming took place changed through ontogeny as ammonoids grew in body size and shell diameter. Ontogenetic size increase covered two orders of magnitude or more in most ammonoid taxa. While embryonic shells (Landman et al. 1983; De Baets et al. 2012) vary about one order in magnitude in size between the earliest forms (>5 mm) and several derived Mesozoic forms (ca. 0.5 mm), the adult shells vary from less than 1 cm to over 2 m. Because small individuals have less power in relation to drag, adult ammonoids could probably swim one to two orders of magnitude faster than hatchlings (Jacobs and Chamberlain 1996).

In hatchlings, much of the energy invested in locomotion will be absorbed by skin friction drag. Jacobs and Chamberlain (1996) guessed that a hatchling of 1 mm diameter might have attained a swimming speed of 1 cm/s, which corresponds to a Reynolds number near 10. Accordingly, shells with a high whorl width index would have been favorable. In that light, the common decrease in whorl width index, which occurs at that size, appears less surprising (Fig. 17.12). Jacobs and Chamberlain (1996) assumed that added mass and acceleration was more important for small than for large individuals. Consequently, early ontogenetic stages would have profited more from compressed shell shapes, which would have reduced the energetic cost of the acceleration reaction. Taking limited energy resources into account, it becomes clear that hatchlings and early juveniles were limited in most cases to a rather passive, probably planktonic mode of life. Residence of early ontogenetic stages in the water column is evidenced by ammonitellae and early ontogenetic stages of ammonoids in black shale deposits (e.g., Landman 1988; Mapes and Nützel 2008) and other lines of evidence (Landman et al. 1996; Ritterbush et al. 2014; De Baets et al. 2015c).

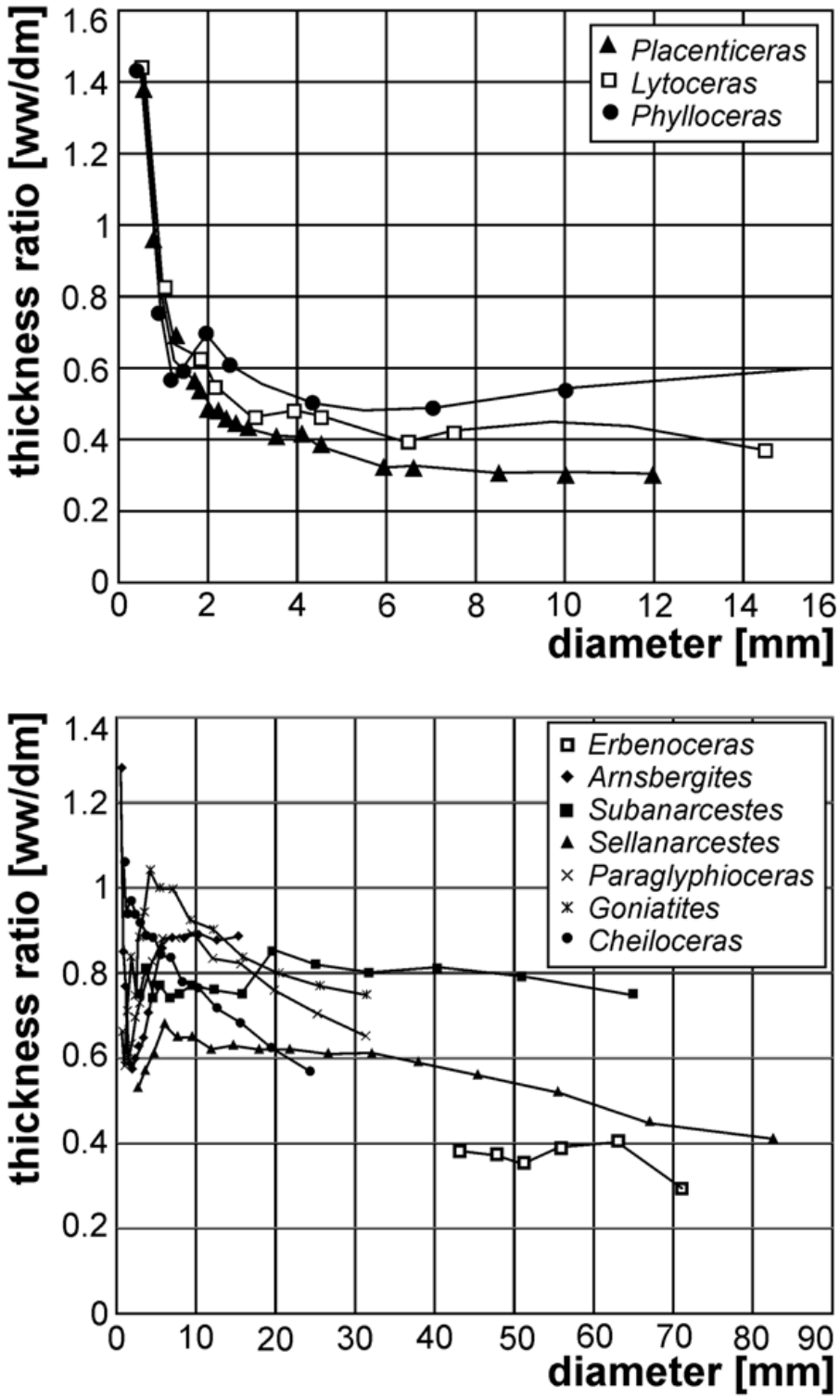

Fig. 17.12 Thickness ratio and shell size in Mesozoic (*top*) and Paleozoic ammonoids (*bottom*) through ontogeny. Modified after Jacobs (1992b) as well as Jacobs and Chamberlain (1996) with new data first reported here. Between hatching (dm < 5mm) and the end of the neanic stage (ca. 10 mm), ammonoids moved only slowly and had wide shells and thus swam at low Reynolds numbers. In all ammonoids, whorl width is reduced after the neanic stage, in Mesozoic forms to values between 0.3 and 0.6 and in Paleozoic forms to values between 0.3 and 0.8. These observations suggest that the ontogenetic late neanic change in shell shape may be an adaptation reflecting the change in hydrodynamic flow conditions

Such accumulations of early ontogenetic stages have often, although not exclusively, been found from the Devonian to the Cretaceous in strata, where benthic life was strongly limited (compare De Baets et al. 2015c). Jacobs (1992b) suggested that the serpenticonic shell shape commonly found in ammonoids (Raup 1967) permitted ammonoids to optimize shell shape for swimming as Reynolds number increased during growth. In contrast, most nautilids (except the aturiids) avoided the smallest size-range for their juveniles, which would have forced the juveniles into a passive planktonic mode of life and similarly, serpenticonic shell shapes are absent in post-Paleozoic Nautilida. Because of these poor locomotory capabilities of ammonoid hatchlings, Jacobs and Chamberlain (1996) considered the possibility of brood care in ammonoids, which finds some support in the occasionally extreme size-dimorphism among ammonoids (e.g., in scaphitids; compare De Baets et al. 2012; 2015c). Walton et al. (2010) speculated on brood care in the Late Devonian genus *Prolobites* based on the extremely low body chamber and terminal aperture, but in this case perhaps outside of the shell of the brooding adult.

Independent of the presence or absence of brood care in ammonoids, the profound morphologic changes that occur around hatching, at the end of the neanic stage, and at maturity (e.g., Westermann 1996; Klug 2001; Korn and Klug 2003) likely had effects on the physical framework for locomotion. It is also striking that commonly, morphologic changes occur at shell diameters between 1 and 2 cm, i.e., when active swimming became feasible for the young ammonoids.

17.5 Information from Epizoans

Some sessile organisms are known to attach themselves in an oriented way depending on the prevailing current direction. Ammonoid shells are well-known to have been inhabited by numerous different invertebrates *syn vivo* (Seilacher 1960; Davis et al. 1999). Some of these epizoans have accordingly been used to interpret the predominant swimming direction of ammonoids. For example, Seilacher (1960) showed bivalve overgrowth on *Buchiceras*, which supported an oblique upward orientation of the aperture of this Cretaceous ammonite.

Keupp et al. (1999) Seilacher and Keupp (2000) as well as Keupp (2012) described a Tithonian aspidocerid inhabited by numerous cirripeds. These epizoans likely attached themselves to the shell of the living ammonite because its aptychi are still in the body chamber and the cirripeds are well articulated. The feeding appendages point in the direction of the aperture, thus suggesting forward swimming, i.e. not backward, as it is usually done by modern cephalopods. This is consistent with the interpretations of Parent et al. (2014) regarding the effect of the aptychi in this genus on swimming speed and swimming direction. Forward swimming would have the advantage that the low hydrodynamic stability of many ammonoids would not have played a big role, because the ammonite shell would have followed the propellent.

Hauschke et al. (2011) described the oriented attachment of a cirripede (goose neck barnacle) on a baculitid. Their findings support forward swimming, but there is also some indication for an approximately horizontal shell orientation during

swimming of this orthoconic ammonite. Westermann (2013) contradicts this interpretation, arguing that these cirripedes might actually have colonized shells without a clear preference of orientation and because he thinks that the apical parts of the phragmocones were largely free of chamber water at such early ontogenetic stages. In addition with the rather long body chambers, it would have made young baculitids swim with their shells in a more or less vertical position.

17.6 Facies of the Host Rock and Habitats

It is one of the classical arguments in cephalopod paleobiology as to whether the host rock facies of a cephalopod fossil can be considered as an indicator of habitat in the live animal. The main reason for doubting the usefulness of studies on the rocks that contain ammonoids is the likelihood of post mortem transport (e.g., Kennedy and Cobban 1976; Tanabe 1979; Marchand 1984). Post mortem transport of nautilids over thousands of kilometers has been shown by various authors (Iredale 1944; Hamada 1964; Stenzel 1964; Toriyama et al. 1965; House 1973, 1987; Chirat 2000). In contrast, Chamberlain et al. (1981) argued that the strong pressure gradient between phragmocone chambers and ambient pressure in modern *Nautilus* leads to rapid post mortem waterlogging of the shell in animals dying within the normal depth range of the live animals (100–300 m). This would rapidly produce negative buoyancy and cause the empty shell to sink, thus precluding significant post-mortem drift (Maeda and Seilacher 1996). Animals dying at shallow depths would have a much greater chance of reaching the ocean surface and drifting significantly from their original habitat. Independent of the correctness of the preceding opinion, some recurring patterns have been found where the same taxa have been discovered in different regions in similar facies (Fig. 17.13 and 17.14; e.g., Westermann 1996). In such cases, one could argue that the same ammonoid taxa may have lived in the same part of a transgression or regression, which thus produced fossils in similar rock types. Especially when ammonoids are found in small basins with restricted connections to the oceans, the probability of extended distances of drift is lower. Naturally, even within small basins, a great range of habitats existed.

Ammonoids were probably not capable of long distance high speed swimming like some modern decabrachian squids or certain pelagic fishes such as tuna. For that reason, Jacobs and Chamberlain (1996) suggested that ammonoids either lived in conditions with slow currents or currents like ocean gyres or in a demersal habitat in regions with slow or absent bottom currents. In one way or the other, ammonoids had to be able to remain in a habitat with favorable conditions, i.e., sufficient food, oxygen, and also mating partners. In turn, it can be expected to find ammonoid remains more commonly in sediments typical for moderate to low water currents (Jacobs 1992b; Jacobs et al. 1994), although not in the deep sea as their shells would have imploded there, or dissolved if below the carbonate compensation depth.

There are several studies, which examined relationships between ammonoid shell shapes and sedimentary facies. For example, Batt (1989, 1993) used shell morpholo-

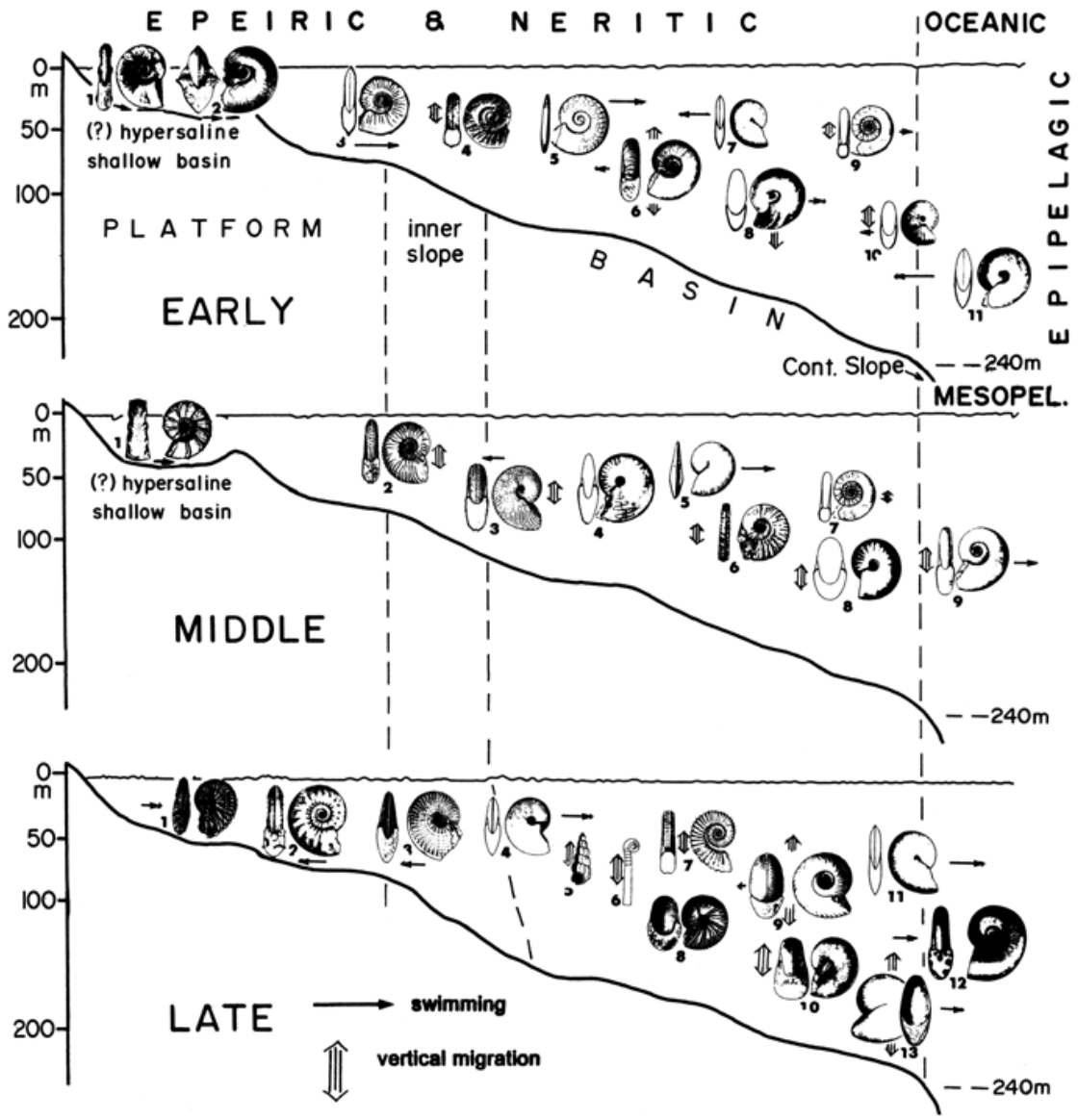

Fig. 17.13 Triassic ammonoid habitats from Wang and Westermann (1993) and Westermann (1996). Early Triassic: *1 Tirolites*, *2 Otoceras*, *3 Inyoites*, *4 Hellenites*, *5 Gyronites*, *6 Anasibirites*, *7 Hedenstroemia*, *8 Isculitoides*, *9 Leiophyllites*, *10 Paranannites*, *11 Procarnites*. Middle Triassic: *1 Ceratites*, *2 Anolcites*, *3 Trachyceras*, *4 Beyrichites*, *5 Longobardites*, *6 Balatonites*, *7 Leiophyllites*, *8 Ptychites*, *9 Monophyllites*. Late Triassic: *1 Tibetites*, *2 Distichites*, *3 Acanthinites*, *4 Discotropites*, *5 Cochloceras*, *6 Rhabdoceras*, *7 Choristoceras*, *8 Juvavites*, *9 Tropites*, *10 Cladiscites*, *11 Pinacoceras*, *12 Rhacophyllites*, *13 Arcestes*

gies to interpret oxygen availability near the sea-floor. In his opinion, heteromorphs like baculitids and loosely coiled forms lived in the water column, while the more tightly coiled heteromorphs and the normally coiled ammonoids occupied a more demersal habitat. Therefore, if the latter group is missing, this might be an indicator of hypoxic to anoxic conditions near the sea-floor (e.g., Monnet and Bucher 2007). Bayer and McGhee (1984) as well as McGhee et al. (1991) employed a more evolutionary approach. They documented how, in the parts of Middle Jurassic transgressive-regres-

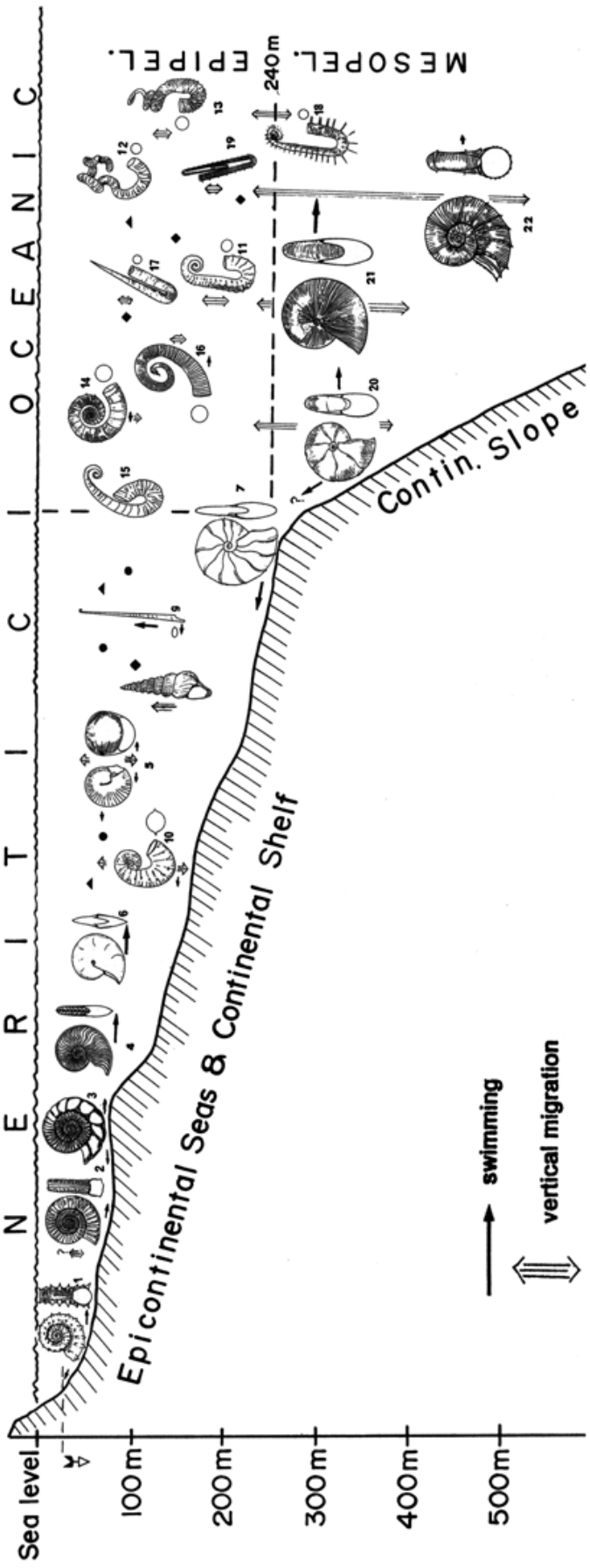

Fig. 17.14 Jurassic and Cretaceous ammonoid habitats from Westermann (1990) and Westermann (1996): *1 Peltoceras*, *2 Arietites*, *3 Perisphinctes*, *4 Harpoceras*, *5 Sphaeroceras*, *6 Oxycerites*, *7 Barremites*, *8 Turrilites*, *9 Baculites*, *10 Scaphites*, *11 Ancyloceras*, *12 Nipponites*, *13 Didymoceras*, *14 Crioceratites*, *15 Labeceras*, *16 Glyptoxoceras*, *17 Hamulina*, *18 Anisoceras 19 Pseudoxybeloceras*, *20 Holcophylloceras*, *21 Phylloceras*, *22 Lytoceras*

sive "Klüpfel cycles" with higher water energy, more involute and compressed shell forms evolved in the Leioceratinae and Graphoceratinae iteratively. Landman and Waage (1993) found that the lineages of the genera *Hoploscaphites* and *Jeletzkytes* both evolved more compressed representatives while the facies changed from the deeper water Pierre Shale to the shallower water sandy Fox Hills Formation. Jacobs et al. (1994) found that more compressed, lower drag shell morphs of *Scaphites whitfieldi* are associated with sandy facies in the Cretaceous Carlisle Shale of the American Western Interior while thicker higher drag shell morphs of the same species occur in finer grain facies. A similar pattern was reported by Courville and Thierry (1993) from *Thomasites* but inverse patterns are sometimes also found in strongly ornamented taxa such as *Schloenbachia* (Wilmsen and Mosavinia 2011), which can complicate interpretations (Ritterbush et al. 2014; De Baets et al. 2015a). Westermann (1996) listed a great number of examples for several marine basins, where he assigned certain ammonoid groups to distinct habitats (Fig. 17.13, 17.14). Klug (2002) suggested that Early and Middle Devonian anarcestids and agoniatitids, which mainly differ in whorl expansion rate and umbilical width, had different ecological preferences since he found them in more clayey or more limey facies, respectively. However, this study used low specimen numbers, thus leading to a low statistical power.

In the Early and Middle Devonian, two such lineages evolved in parallel as shown by Monnet et al. (2011). In the Auguritidae and Pinacitidae, oxyconic shell forms with closed umbilicus evolved independently, and in both lineages, the most derived forms occurred in carbonates that were probably deposited under shallower water conditions than those associated with the ancestral forms. Most of the studies listed in the preceding paragraphs appear to coincide with the interpretations of Jacobs (1992b) as well as Jacobs and Chamberlain (1996), but there are not many such studies, their statistical power tends to be low, and the causality between habit, habitat and shell morphology is difficult to establish with certainty; this can only be achieved by combining multiple lines of evidence including analysis of shell shape, facies and geographic distribution, isotope analysis, etc. (e.g., Tsujita and Westermann 1998; Ritterbush et al. 2014).

A different approach to identify habitat depth is discussed in detail in Chaps. 17.1 and 2. In these studies, stable isotopes of oxygen have been used to assess the habitat depth of various Cretaceous ammonoids (Moriya et al. 2003; Lukeneder et al. 2010). Unfortunately, the error sources of such studies are often large and the number of these studies is still too low. Examination of oxygen isotopes in ammonoid shells is still one of the most promising methods to reveal new information on ammonoid habitats.

17.7 Swimming Modes

Taking the uncertain knowledge of ammonoid soft parts into account, most interpretations of the 'ammonoid power plant' are based on actualistic comparisons. Packard et al. (1980) examined the swimming modes in Recent nautilids (see also

Crick 1898; Chamberlain 1987, 1990, 1992). In *Nautilus*, very slow movement can be produced by the water expelled through the hyponome during aeration of the gills. Normal swimming speeds are produced by mantle cavity water expelled by contraction of the cephalic retractor muscles and funnel muscles. The animal moves forward, backward, up, or down, depending on the orientation of the highly flexible hyponome (Johanson et al. 1972; Ward et al. 1977; Packard et al. 1980; Chamberlain 1981; 1987; Wells and Wells 1985; Webber and O'Dor 1986; Wells and O'Dor 1991).

Many squids including *Sepia* have lateral fins, which function in thrust production and in turning in some squid locomotor behaviors. Octobrachians and some decabrachians use their arms, sometimes connected with velar skins, to swim by expelling water entrained within their arm crowns with rhythmic beating of their arms, in the style of medusoid cnidarian bells. These two modes of locomotion appear unlikely to have been present in ammonoids, or at least, there is no evidence at all yet to support their occurrence among ammonoids.

The most likely mode of swimming is by contracting the mantle cavity, although it is not clear, which muscles were responsible for this task in ammonoids. There are several alternatives, namely the mantle musculature (as in coleoids), the cephalic retractors (as in nautilids) or potentially also other longitudinal muscles (not realized in Recent forms) in combination with the hyponome musculature. It appears also likely that the water was expelled through a hyponome, since hyponomic sinuses are present in many ammonoids. Hyponomes have not yet been found fossilized in ammonoids. Thus, another open question is the flexibility of the ammonoid hyponome. Was it long and flexible enough to point backwards and allow forward swimming?

Recently, Westermann (2013) revived a hypothesis earlier introduced by Schmidt (1930). This "*Twin nozzle-Hypothesis*" roots in the fact that many Mesozoic ammonoids have a more or less long ventral projection (e.g., in *Amaltheus*) combined with a probably more or less horizontal aperture. This would be an adverse combination of character states for straight backwards swimming, because the mentioned ventral apertural projection would have interfered with movement of the hyponome. Therefore, these authors suggested that the hyponome had evolved two openings, one on each side of the ventral projection. Both hyponome parts could be moved independently according to them. This is an interesting idea but so far, it is not supported by fossil evidence.

Monnet et al. (2011) discussed the peculiar way, in which the umbilicus was closed in some Devonian Auguritidae and Pinacitidae. The most derived representatives of both families have largely covered the umbilicus with a projection of the lateral shell over the umbilicus. This projection formed umbilical sinuses, which might have been horizontally aligned with the hyponome sinus. It would have allowed these species to take in water from the swimming direction into the mantle cavity (in *Nautilus*, water is taken in at the same place according to Packard et al. 1980), accelerating the water by compressing the mantle cavity, and expelling it out of the hyponome. This means that these forms potentially sucked water into the mantle cavity after completion of a hyponome jet.

Acknowledgements We greatly appreciate the financial support by the Swiss National Science foundation (project numbers 200021-113956/1, 200020-25029, -132870, and -149120). We greatly appreciate the effort the reviewers Kenneth De Baets (Erlangen) and Benjamin J. Linzmeier (University of Wisconsin-Madison) have put into their reviews, thereby helping us to improve our manuscript.

References

Bambach RK (1999) Energetics in the global marine fauna: a connection between terrestrial diversification and change in the marine biosphere. Geobios 32:131–144

Batt RJ (1989) Ammonite shell morphospace distribution in the Western Interior Greenhorn Sea and some paleoecological implications. Palaios 4:32–43

Batt RJ (1993) Ammonite shell morphotypes as indicators of oxygenation in a Cretaceous epicontinental sea. Lethaia 26:49–63

Batt RJ (2007) Sutural amplitude of ammonite shells as a paleoenvironmental indicator. Lethaia 24:219–225

Bayer U, McGhee GR Jr (1984) Iterative evolution of Middle Jurassic ammonite faunas. Lethaia 17:1–16

Bone Q, Pulsford A, Chubb AD (1981) Squid mantle muscle. J Mar Biol Assoc UK 61:327–342

Boyle P, Rodhouse P (2005) Cephalopods: ecology and fisheries. Wiley, Oxford

Chamberlain JA Jr (1969) Technique for scale modeling of cephalopod shells. Palaeontology 12:48–55

Chamberlain JA Jr (1976) Flow patterns and drag coefficients of cephalopod shells. Palaeontology 19:539–563

Chamberlain JA Jr (1980) The role of body extension in cephalopod locomotion. Palaeontology 23:445–461

Chamberlain JA Jr (1981) Hydromechanical design of fossil cephalopods. In: House MR, Senior JR (eds) The Ammonoidea. Syst Assoc Spec, vol 18. Academic, London

Chamberlain JA Jr (1987) Locomotion of *Nautilus*. In: Saunders WB, Landman NH (eds) *Nautilus*-The biology and paleobiology of a living fossil. Plenum, New York

Chamberlain JA Jr (1990) Jet propulsion of *Nautilus*: a surviving example of early Paleozoic locomotor design. Can J Zool 68:806–814

Chamberlain JA Jr (1992) Cephalopod locomotor design and evolution: the constraints of jet propulsion. In: Rayner MV, Wootton RJ (eds) Biomechanics and evolution. Cambridge University Press, Cambridge

Chamberlain JA Jr (1993) Locomotion in ancient seas: constraint and opportunity in cephalopod adaptive design. Geobios Spec Mem 15:49–61

Chamberlain JA Jr, Moore WA (1982) Rupture strength and flow rate of *Nautilus* siphuncular tube. Paleobiology 8:408–425

Chamberlain JA Jr, Westermann GEG (1976) Hydrodynamic properties of cephalopod shell ornament. Paleobiology 2:316–331

Chamberlain JA Jr, Ward PD, Weaver JS (1981) Post-mortem ascent of Nautilus shells: implications for cephalopod paleobiogeography. Paleobiology 7:494–509

Chirat R (2000) The so-called 'cosmopolitan palaeobiogeographic distribution' of tertiary Nautilida of the genus *Aturia* Bronn 1838: the result of post-mortem transport by oceanic palaeocurrents. Palaeogeogr Palaeoclim Palaeoecol 157:59–77

Courville P, Thierry J (1993) Nouvelles données biostratigraphiques sur les dépôts cénomanoturoniens du Nord-Est du fossé de ia Bénoué (Nigeria). Cretaceous Research 14(4–5):385–396

Crick GS (1898) On the muscular attachment of the animal to the shell in some fossil Cephalopoda (Ammonoidea). Trans Linn Soc NY 7:71–113

Daniel TL (1984) The unsteady aspects of locomotion. Am Zool 24:121–134

Daniel TL (1985) Cost of locomotion: unsteady medusan swimming. J Exp Biol 119:149–164
Daniel TL, Helmuth BS, Saunders WB, Ward PD (1997) Septal complexity in ammonoid cephalopods increased mechanical risk and limited depth. Paleobiology 23:470–481
Davis RA, Mapes RH, Klofak SM (1999) Epizoa on externally shelled cephalopods. In: Rozanov AY, Shevyrev AA (eds) Fossil cephalopods: recent advances in their study. Russian Academy of Sciences, Palaeontological Institute. Moskva
De Baets K, Klug C, Korn D, Landman NH (2012) Evolutionary trends in ammonoid embryonal development. Evolution 66:1788–1806
De Baets K, Bert D, Hofmann R, Monnet C, Yacobucci MM, Klug C (2015a) Ammonoid intraspecific variation. This volume
De Baets K, Keupp H, Klug C (2015b) Parasitism in ammonoids. This volume
De Baets K, Landman NH, Tanabe K (2015c) Ammonoid embryonic development. This volume
Doguzhaeva LA, Mapes RH (2015) Muscle scars in ammonoid shells. This volume
Doguzhaeva LA, Mutvei H (1991) Organization of the soft body in *Aconeceras*(Ammonitina), interpreted on the basis of shell morphology and muscle scars. Palaeontogr A 218:17–33
Doguzhaeva LA, Mutvei H (1993) Structural features in Cretaceous ammonoids indicative of semi-internal or internal shells. In: House MR (ed) The Ammonoidea: environment, ecology, and evolutionary change. Syst Assoc Spec, vol 47. Clarendon Press, Oxford
Ebel K (1983) Berechnungen zur Schwebefähigkeit von Ammoniten. N Jb Geol Paläont Mh 1983:614–640
Elmi S (1991) Données expérimentales sur l'architecture fonctionelle de la coquille des ammonodes Jurassiques. Géobios, Mémoire Spécial 13:155–160
Elmi S (1993) Loi des aires, couche-limite et morphologie fonctionnelle de la coquille des Céphalopodes (Ammonoides). Geobios 26(Suppl 1):121–138
Finn JK, Norman MD (2010) The argonaut shell: gas-mediated buoyancy control in a pelagic octopus. Proc Ro Soc B 277(1696):2967–2971. doi:10.1098/rspb.2010.0155
Gaillard C (1977) Cannelures d'érosion et figures d'impact dues à des coquilles d'ammonites à épines (Oxfordien supérieur du Jura français). Eclogae Geol. Helvetiae 70:701–715
Hamada T (1964) Notes on drifted *Nautilus* in Thailand. Sci Pap Coll Gen Educ Univ Tokyo 14:255–277
Hauschke N, Schöllmann L, Keupp H (2011) Oriented attachment of a stalked cirripede on an orthoconic heteromorph ammonite—implications for the swimming position of the latter. N Jahrb Geol Paläont Abh 202:199–212
Hewitt RA (1996) Architecture and strength of the ammonite shell. In: Landman NH, Tanabe K, Davis RA (eds) Ammonoid paleobiology. Plenum, New York
Hewitt RA, Westermann GEG (2003) Recurrences of hypotheses about ammonites and *Argonauta*. J Paleontol 77:792–795
Hoffmann R, Zachow S 2011 Non-invasive approach to shed new light on the buoyancy business of chambered cephalopods (Mollusca). Extended Abstract IAMG Salzburg 2011:1–9
Hoffmann R, Schultz JA, Schellhorn R, Rybacki E, Keupp H, Gerden SR, Lemanis R, Zachow S (2013) Non-invasive imaging methods applied to neo- and paleontological cephalopod research. Biogeosciences Discuss 10:18803–18851:2013. doi:10.5194/bgd-10-18803-2013
Hoffmann R, Lemanis R, Naglik C, Klug C (2015) Ammonoid buoyancy. This volume
House MR (1973) An analysis of Devonian goniatite distributions. In: Hughes NF (ed) Organisms and continents through time. Spec Pap Palaeont 12:305–317
House MR (1981) On the origin, classification and evolution of the early Ammonoidea. In: House MR, Senior JR (eds) The Ammonoidea: the evolution, classification, mode of life and geological usefulness of a major fossil group. Academic, London
House MR (1987) Geographic distribution of *Nautilus* shells. In: Saunders WB, Landman NH (eds) *Nautilus*. The biology and paleobiology of a living fossil. Plenum, New York
Iredale T (1944) Australian pearly *Nautilus*. Austr. Zool 10:294–298
Jacobs DK (1992a) The support of hydrostatic load in cephalopod shells-adaptive and ontogenetic explanations of shell form and evolution from Hooke 1695 to the present. In: Hecht MK, Wallace B, Macintyre RJ (eds) Evolutionary biology, vol 26. Plenum, New York

Jacobs DK (1992b) Shape, drag, and power in ammonoid swimming. Paleobiology 18:203–220
Jacobs DK, Chamberlain JA (1996) Buoyancy and hydrodynamics in ammonoids. In: Landman NH, Tanabe K, Davis RA (eds) Ammonoid paleobiology. Topics in geobiology13. Plenum, New York
Jacobs DK, Landman NH (1993) Is *Nautilus* a good model for the function and behavior of ammonoids? Lethaia 26:101–110
Jacobs DK, Landman NH, Chamberlain JA Jr (1994) Ammonite shell shape covaries with facies and hydrodynamics: iterative evolution as a response to changes in basinal environment. Geology 22:905–908
Johansen W, Soden PD, Trueman ER (1972) A study in jet propulsion: an analysis of the motion of the squid, *Loligo vulgaris*. J Exp Biol 56:155–156
Kakabadzé MV, Sharikadzé MZ (1993) On the mode of life of heteromorph ammonites (heterocone, ancylocone, ptychocone). Geobios 26(Suppl 1):209–215
Kaplan P (2002) Biomechanics as a test of functional plausibility: testing the adaptive value of terminal-countdown heteromorphy in Cretaceous ammonoids. Abh Geol B-A 57:181–197
Kawabe F (2003) Relationship between mid-Cretaceous (upper Albian–Cenomanian) ammonoid facies and lithofacies in the Yezo forearc basin, Hokkaido, Japan. Cret Res 24:751–763
Kennedy WJ, Cobban WA (1976) Aspects of ammonite biology, biogeography, and biostratigraphy. Spec Pap Palaeontol 17:1–94
Keupp H (1984) Pathologische Ammoniten—Kuriositäten oder paläobiologische Dokumente? (Teil 1). Fossilien 1(6):258–262, 267–275
Keupp H (1985) Pathologische Ammoniten—Kuriositäten oder paläobiologische Dokumente? (Teil 2). Fossilien 2(1):23–35
Keupp H (1992) Rippenscheitel bei Ammoniten-Gehäusen. Fossilien 5:283–290
Keupp H (1996) Paläopathologische Analyse einer Ammoniten-Vergesellschaftung aus der Mittleren Volga-Stufe des subpolaren Urals. Fossilien 1:45–54
Keupp H (1997) Paläopathologische Analyse einer "Population" von *Dactylioceras athleticum* (Simpson) aus dem Unter-Toarcium von Schlaifhausen/Oberfranken. Berliner geowiss Abh E 25:243–267
Keupp H (2000) Ammoniten—paläobiologische Erfolgsspiralen. Thorbecke, Stuttgart
Keupp H (2006) Sublethal punctures in body chambers of Mesozoic ammonites (forma aegra fenestra n.f.), a tool to interpret synecological relationships, particularly predator-prey interactions. Paläontol Z 80:112–123
Keupp H (2008) Wer hat hier zugebissen? Ammoniten-Prädation. Fossilien 2008(2):109–112
Keupp H (2012) Atlas zur Paläopathologie der Cephalopoden. Berliner geowiss Abh E 12:1–390
Keupp H, Hoffmann R (2015) Ammonoid paleopathology. This volume
Keupp H, Röper M, Seilacher A (1999) Paläobiologische Aspekte von syn vivo- besiedelten Ammonoideen im Plattenkalk des Ober-Kimmeridgiums von Brunn in Ostbayern. Berliner geowiss Abh E 30:121–145
Klinger HC (1981) Speculation on buoyancy control and ecology in some heteromorph ammonites. In: House MR, Senior JR (eds) The Ammonoidea. Syst Assoc, Spec, vol 18. Academic, London
Klug C (2001) Life-cycles of Emsian and Eifelian ammonoids (Devonian). Lethaia 34:215–233
Klug C (2002) Quantitative stratigraphy and taxonomy of late Emsian and Eifelian ammonoids of the eastern Anti-Atlas (Morocco). Cour Forschungsinst Senck 238:1–109
Klug C, Korn D (2002) Occluded umbilicus in the Pinacitinae (Devonian) and its palaeoecological implications. Palaeontology 45:917–931
Klug C, Korn D (2004) The origin of ammonoid locomotion. Acta Palaeont Pol 49:235–242
Klug C, Lehmann J (2015) Soft-part anatomy of ammonoids: reconstructing the animal based on exceptionally preserved specimens and actualistic comparisons. This volume
Klug C, Meyer E, Richter U, Korn D (2008) Soft-tissue imprints in fossil and Recent cephalopod septa and septum formation. Lethaia 41:477–492
Klug C, Kröger B, Kiessling W, Mullins GL, Servais T, Frýda J, Korn D, Turner S (2010) The Devonian nekton revolution. Lethaia 43:465–477

Korn D (2012) Quantification of ontogenetic allometry in ammonoids. Evol Dev 14:501–514. doi:10.1111/ede.12003

Korn D, Klug C (2003) Morphological pathways in the evolution of Early and Middle Devonian ammonoids. Paleobiology 29:329–348

Kröger B (2001) Comments on Ebel's benthic-crawler hypothesis for ammonoids and extinct nautiloids. Paläontol Z 75:123–125

Kröger B (2005) Adaptive evolution in Paleozoic coiled cephalopods. Paleobiology 31:253–268

Kröger B, Vinther J, Fuchs D (2011) Cephalopod origin and evolution: a congruent picture emerging from fossils, development and molecules. Bioessays 12. doi:10.1002/bies.201100001

Kummel B, Lloyd RM (1955) Experiments on the relative streamlining of coiled cephalopod shells. J Paleontol 29:159–170

Landman NH (1988) Early ontogeny of Mesozoic ammonites and nautilids. In: Wiedmann J, Kullmann J (eds) Cephalopods-present and past. Schweizerbart, Stuttgart

Landman NH, Cobban WA (2007) Ammonite touch marks in Upper Cretaceous (Cenomanian-Santonian) deposits of the Western Interior Sea. In: Landman NH, Davis RA, Mapes RH (eds) Cephalopods present and past: new insights and fresh perspectives. Springer, Dordrecht

Landman NH, Waage KM (1993) Scaphitid ammonites of the Upper Cretaceous (Maastrichtian) fox hills formation in South Dakota and Wyoming. Bull Am Mus Nat Hist 215:1–257

Landman NH, Rye DM, Shelton KL (1983) Early ontogeny of *Eutrephoceras* compared to recent *Nautilus*and Mesozoic ammonites: evidence from shell morphology and light stable isotopes. Paleobiology 9:269–279

Landman NH, Tanabe K, Shigeta Y (1996) Ammonoid Embryonic Development. In: (Eds) Landman, N.H., Tanabe, K., Davis, R.A. *Ammonoid Paleobiology. Vol. 13, Topics in Geobiology.* 343–405. Plenum Press, New York

Longridge LM, Smith PL, Rawlings G, Klaptocz V (2009) The impact of asymmetries in the elements of the phragmocone of early Jurassic ammonites. Palaeontol Electron 12(1A):1–15

Lukeneder A (2015) Ammonoid habitats and life history. This volume

Lukeneder A, Harzhauser M, Müllegger S, Piller WE (2010) Ontogeny and habitat change in Mesozoic cephalopods revealed by stable isotopes (delta^{18}O, delta^{13}C). Earth and Planetary Science Letters 296:103–111. doi:10.1016/j.epsl.2010.04.053

Maeda H, Seilacher A (1996) Ammonoid taphonomy. In: Landman NH, Tanabe K, Davis RA (eds) Ammonoid paleobiology. Plenum, New York

Mapes RH, Nützel A (2008) Late Palaeozoic mollusc reproduction: cephalopod egg-laying behavior and gastropod larval palaeobiology. Lethaia 42:341–356

Marchand D (1984) Ammonites et paléoenvironnements; une nouvelle approche. Geobios Mém. spécial 8:101–107

Marchand D (1992) Ammonites et paléoprofondeur: les faits, les interprétations. Paleovox 1:49–68

McGhee GC, Bayer U, Seilacher A (1991) Biological and evolutionary responses to transgressive-regressive cycles. In: Einsele G, Ricken W, Seilacher A (eds) Cycles and events in stratigraphy. Springer, Berlin

Monks N, Young JR (1998) Body position and the functional morphology of Cretaceous heteromorph ammonites. Palaeontol Electron 1:15

Monnet C, Bucher H (2007) European ammonoid diversity questions the spreading of anoxia as primary cause for the Cenomanian/Turonian (Late Cretaceous) mass extinction. Swiss J Geosci 100:137–144

Monnet C, Klug C, De Baets K (2011) Parallel evolution controlled by adaptation and covariation in ammonoid cephalopods. BMC Evol Bio 11(115):1–21

Monnet C, De Baets K, Yacobucci MM (2015) Buckman's rules of covariation. In Klug C, Korn D, De Baets K, Kruta I, Mapes RH (eds): Ammonoid Paleobiology, Vol.2: From macroevolution to biogeography. Springer, Dordrecht

Moriya K (2015) Isotope signature of ammonoid shells. This volume

Moriya K, Nishi H, Kawahata H, Tanabe K, Takayanagi Y (2003) Demersal habitat of Late Cretaceous ammonoids: evidence from oxygen isotopes for the Campanian (Late Cretaceous) northwestern Pacific thermal structure. Geology 31:167–170

Mutvei H (1975) The mode of life in ammonoids. Paläontol Z 49:196–206
Mutvei H, Reyment RA (1973) Buoyancy control and siphuncle function in ammonoids. Palaeontology 16:623–636
Naglik C, Monnet C, Götz S, Kolb C, De Baets K, Klug C (2015) Growth trajectories in chamber and septum volumes in major subclades of Paleozoic ammonoids. Lethaia 48(1):29–46
Naglik C, Rikhtegar F, Klug C (in press) Buoyancy of some Palaeozoic ammonoids and their hydrostatic properties based on empirical 3D-models. Lethaia 10pp. DOI 10.1111/let.12125
O'Dor RK (1982) Respiratory metabolism and swimming performance of the squid, *Loligo opalescens*. Can J Fish Aquat Sci 39:580–587
O'Dor RK (1988a) The energetic limits on squid distributions. Malacologia 29:113–119
O'Dor RK (1988b) The forces acting on swimming squid. J Exp Biol 137:421–442
O'Dor RK, Webber DM (1991) Invertebrate athletes: trade-offs between transport efficiency and power density in cephalopod evolution. J Exp Biol 160:93–112
O'Dor RK, Wells MJ (1990) Performance limits of "antique" and "state-of-the-art" cephalopods, *Nautilus* and squid. Am Malacol Union Prog Abstr. 56th Ann Meeting, 52
O'Dor RK, Wells MJ, Wells J (1990) Speed jet pressure and oxygen consumption relationships in free-swimming *Nautilus*. J Exp Biol 154:383–396
O'Dor RK, Forsythe J, Webber DM, Wells J, Wells MJ (1993) Activity levels of *Nautilus* in the wild. Nature 362:626–627
Oeffner J, Lauder GV (2012) The hydrodynamic function of shark skin and two biomimetic applications. J Exp Biol 215:785–795
Okamoto T (1988) Analysis of heteromorph ammonoids by differential geometry. Palaeontology 31:35–52
Okamoto T (1996) Theoretical modeling of ammonoid morphology. In: Landman NH, Tanabe K, Davis RA (eds) Ammonoid paleobiology. Topics in geobiology 13. Plenum, New York
Packard A (1972) Cephalopods and fish: the limits of convergence. Biol Rev 47:241–307
Packard A, Bone Q, Hignette M (1980) Breathing and swimming movements in a captive *Nautilus*. J Mar Biol Assoc UK 60:313–327
Parent H, Westermann GEG, Chamberlain JA Jr (2014) Ammonite aptychi: functions and role in propulsion. Geobios 47:45–55
Raup DM (1966) Geometric analysis of shell coiling: general problems. J Paleont 40:1178–1190
Raup DM (1967) Geometric analysis of shell coiling: coiling in ammonoids. J Paleontol 41:43–65
Raup DM, Chamberlain JA Jr (1967) Equations for volume and center of gravity in ammonoid shells. J Paleontol 41:566–574
Reif WE (1982) Morphogenesis and function of the squamation in sharks. 1. Comparative functional morphology of shark scales, and ecology of scales. N Jahrb Geol Paläont Abh 164:172–183
Reyment RA (1973) Factors in the distribution of fossil cephalopods. Part 3: experiments with exact models of certain shell types. Bull Geol lnst Univ Uppsala N S 4:7–41
Ritterbush K, Bottjer DJ (2012) Westermann Morphospace displays ammonoid shell shape and hypothetical paleoecology. Paleobiology 38:424–446. doi:10.1666/10027.1
Ritterbush K, De Baets K, Hoffmann R, Lukeneder A (2014) Pelagic Palaeoecology: the importance of recent constraints on ammonoid palaeobiology and life history. J Zool. doi:10.1111/jzo.12118
Rosa R, Seibel BA (2010) Voyage of the argonauts in the pelagic realm: physiological and behavioural ecology of the rare paper nautilus, *Argonauta nouryi*. ICES J Mar Sci J du Conseil 67:1494–1500
Rothpletz A (1909) Über die Einbettung der Ammoniten in die Solnhofener Schichten. Abh math-phys Kl der königl Bayr Akad der Wiss München 24(2):313–337
Saunders WB (1995) The ammonoid suture problem: relationship between shell and septal thickness and sutural complexity in Paleozoic ammonoids. Paleobiology 21:343–355
Saunders WB, Shapiro EA (1986) Calculation and simulation of ammonoid hydrostatics. Paleobiology 12:64–79

Saunders WB, Wehman DA (1977) Shell strength of *Nautilus* as a depth limiting factor. Paleobiology 3:83–89

Saunders WB, Work DM (1996) Shell morphology and suture complexity in Upper Carboniferous ammonoids. Paleobiology 22:189–218

Saunders WB, Work DM (1997) Evolution of shell morphology and suture complexity in Paleozoic prolecanitids, the rootstock of Mesozoic ammonoids. Paleobiology 23:301–325

Saunders WB, Work DM, Nikolaeva SV (1999) Evolution of complexity in Paleozoic ammonoids. Science 286:760–763

Schmidt H (1930) Ueber die Bewegungsweise der Schalencephalopoden. Paläontol Z 12:194–208

Schmidt-Nielsen K (1972) Locomotion: energy cost of swimming, flying and running. Science 177:222–228

Seibel BA (2007) On the depth and scale of metabolic rate variation: scaling of oxygen consumption rates and enzymatic activity in the class Cephalopoda (Mollusca). J Exp Biol 210:1–11

Seibel BA, Thuesen EV, Childress JJ, Gorodezky LA (1997) Decline in pelagic Cephalopod metabolism with habitat depth reflects differences in locomotory efficiency. Biol Bull 192:262–278

Seilacher A (1960) Epizoans as a key to ammonoid ecology. J Paleont 34:189–193

Seilacher A (1963) Umlagerung und Rolltransport von Cephalopodengehäusen. N Jahrb Geol Paläont Mh 11:593–615

Seilacher A (1982a) Ammonite shells as habitats in the Posidonia shales of Holzmaden—floats or benthic islands? N Jahrb Geol Paläont Mh 1982:98–114

Seilacher A (1982b) Ammonite shells as habitats—floats or benthic islands? In Einsele G, Seilacher A (eds) Cyclic and event in stratification. Springer, Berlin. doi:10.1007/978–3-642-75829-4_38

Seilacher A, Keupp H (2000) Wie sind Ammoniten geschwommen? Fossilien 5:310–313

Seki K, Tanabe K, Landman NH, Jacobs DK (2000) Hydrodynamic analysis of Late Cretaceous desmoceratine ammonites. Rev Paléobiol Vol spéc 8:141–155

Shapiro EA, Saunders WB (1987) *Nautilus* shell hydrostatics. In: Saunders WB, Landman NH (eds) *Nautilus*—The biology and paleobiology of a living fossil. Plenum, New York

Signor PW III, Brett CE (1984) The mid-Paleozoic precursor to the Mesozoic marine revolution. Paleobiology 10:229–245

Stenzel HB (1964) Living *Nautilu*s. In: Moore RC (ed) Treatise on invertebrate paleontology part K (Mollusca 3). Geological Society of America and University of Kansas Press, Lawrence, pp. K59–K93

Summesberger H, Jurkivsek B, Kolar-Jurkovsek T (1999) Rollmarks of soft parts and a possible crop content of Late Cretaceous ammonites from the Slovenian karst. In: Olóriz F, Rodríguez-Tovar FJ (eds) Advancing research on living and fossil Cephalopods. Kluwer Academic/Plenum, New York

Swan RTH, Saunders, WB (1987) Function and shape in late Paleozoic (mid-carboniferous) ammonoids. Paleobiology 13:297–311

Tajika A, Naglik C, Morimoto N, Pascual-Cebrian E, Hennhöfer DK, Klug C (2015) Empirical 3D-model of the conch of the Middle Jurassic ammonite microconch *Normannites*, its buoyancy, the physical effects of its mature modifications and speculations on their function. Historical Biology: An International Journal of Paleobiology, 27(2):181–191. DOI: 10.1080/08912963.2013.872097

Tanabe K (1979) Palaeoecological analysis of ammonoid assemblages in the Turonian *Scaphites* facies of Hokkaido, Japan. Palaeontology 22:609–630

Toriyama R, Sato T, Hamada T, Komalarjun P (1965) *Nautilus pompilius* drifts on the west coast of Thailand. Jpn J Geol Geog. 36:149–161

Trammer J, Niechwedowicz M (2007) Hydrodynamically controlled anagenetic evolution of Famennian goniatites from Poland. Acta Palaeont Pol 52:63–75

Trueman AE (1941) The ammonite body chamber, with special reference to the buoyancy and mode of life of the living ammonite. Q J Geol So. 96:339–383

Trueman ER, Packard A (1968) Motor performances of some cephalopods. J Exp Biol 49:495–507
Tsujita CJ, Westermann GEG (1998) Ammonoid habitats and habits in the Western Interior Seaway: a case study from the Upper Cretaceous Bearpaw Formation of southern Alberta, Canada. Palaeogeogr Palaeoclim Palaeoecol 144:135–160
Urdy S, Goudemand N, Bucher H, Chirat R (2010a) Allometries and the morphogenesis of the molluscan shell: a quantitative and theoretical model. J Exp Biol B 314:280–302
Urdy S, Goudemand N, Bucher H, Chirat R (2010b) Growth-dependent phenotypic variation of molluscan shells: implications for allometric data interpretation. J Exp Biol B 314:303–26
Vogel S (1981) Life in moving fluids: the physical biology of flow. Princeton University Press, Princeton
Walton S, Korn D, Klug C (2010) Size distribution of the Late Devonian ammonoid *Prolobites*: indication for possible mass spawning events. Swiss J of Geosci 103:475–494
Wang Y, Westermann GEG (1993) Paleoecology of triassic ammonoids. Geobios Mem Spec 15:373–392
Ward PD (1976) Stratigraphy, paleoecology and functional morphology of heteromorph ammonites of the Upper Cretaceous Nanaimo Group, British Columbia and Washington. PhD thesis McMaster University Library, Thesis QE788134 (39005047235555), Hamilton, Canada
Ward P (1979) Functional morphology of Cretaceous helically-coiled ammonite shells. Paleobiology 5:415–422
Ward PD (1981) Shell sculpture as a defensive adaptation in ammonoids. Paleobiology 7:96–100
Ward PD (1982) The relationship of siphuncle size to emptying rates in chambered cephalopods: implications for cephalopod paleobiology. Paleobiology 8:426–433
Ward PD (1987) The natural history of *Nautilus*. Allen and Unwin, Winchester
Ward PD, Wicksten MK (1980) Food sources and feeding behavior of *Nautilus macromphalus*. Veliger 23:119–124
Ward PD, Stone R, Westermann GEG, Martin A (1977) Notes on animal weight, cameral fluids, swimming speed, and colour polymorphism of the cephalopod, *Nautilus pompilius*, in the Fiji Islands. Paleobiology 3:377–388
Webber DM, O'Dor RK (1986) Monitoring the metabolic rate and activity of free-swimming squid with telemetered jet pressure. J Exp Biol 126:205–224
Wells MJ (1987) Ventilation and oxygen extraction by *Nautilus*. In: Saunders WB, Landman NH (eds) *Nautilus*-The biology and paleobiology of a living fossil. Plenum, New York
Wells MJ (1995) The evolution of a racing snail. Mar Freshw Behav Physiol 25:1–12
Wells MJ, O'Dor RK (1991) Jet propulsion and the evolution of Cephalopods. Bull Mar Sci 49:419–432
Wells MJ, Wells J (1985) Ventilation and oxygen uptake by *Nautilus*. J Exp Biol 118:297–312
Westermann GEG (1966) Covariation and taxonomy of the Jurassic ammonite *Sonninia adicra* Waagen. N Jb Geol Paläont Abh 124:289–312
Westermann GEG (1971) Form, structure and function of shell and siphuncle in coiled Mesozoic ammonoids. Life Sci Contrib R Ont Mus 78:1–39
Westermann GEG (1973) Strength of concave septa and depth limits of fossil cephalopods. Lethaia 6:383–403
Westermann GEG (1977) Form and Function of orthocone cephalopod shells with concave septa. Paleobiology 3:300–321
Westermann GEG (1990) New developments in ecology of Jurassic-Cretaceous ammonoids. In: Pallini G, Cecca F, Cresta S, Santantonio M (eds) Fossili, evoluzione, ambiente. Atti II Conv Int Pergola 1987. Tecnostampa, Ostra Vetere
Westermann GEG (1993) On alleged negative buoyancy of ammonoids. Lethaia 26:246. doi:10.1111/j.1502–3931.1993.tb01526.x
Westermann GEG (1996) Ammonoid life and habitat. In: Landman NH, Tanabe K, Davis RA (eds) Ammonoid paleobiology. Plenum, New York
Westermann GEG (2013) Hydrostatics, propulsion and life-habits of the Cretaceous ammonoid *Baculites*. Rev Paléobiol 32:249–265

Westermann GEG, Tsujita CJ (1999) Life habits of ammonoids. In: Savazzi E (ed) Functional morphology of the invertebrate skeleton. Wiley, Hoboken

Wilmsen M, Mosavinia A (2011) Phenotypic plasticity and taxonomy of *Schloenbachia varians* (J. Sowerby, 1817) (Cretaceous Ammonoidea). Paläontol Z 85:169–184

Young JZ (1960) Observations on *Argonauta* and especially its method of feeding. Proc Zool Soc London 133:471–479

Ziegler B (1967) Ammonitenökologie am Beispiel des Oberjura. Geol Rundsch 56:439–446

CHAPTER IV

From a carbonate platform to pelagic sedimentation during the early Devonian and the regional advent of ammonoid faunas in the Zeravshan (Uzbekistan)

To be submitted in *Bulletin of Geoscience*

From a carbonate platform to pelagic sedimentation during the early Devonian and the regional advent of ammonoid faunas in the Zeravshan (Uzbekistan)

Carole Naglik, Kenneth de Baets & Christian Klug

In the Zeravshan Mountains of Uzbekistan, thick Early Devonian carbonatic sedimentary successions are exposed, which display a transition from a reefal to a pelagic facies. This allows us to document and analyze the history of sedimentation and faunal variations of this region. The Late Pragian of the Bursykhirman Mountain is documented with the transition from platform carbonates to pelagic sediments. Lithology and microfacies through the early Emsian sedimentary sequence of two ammonoid-bearing localities were investigated with a focus on the Dzhaus Beds. In addition to this sedimentological analysis, we discuss the palaeobiogeographically peculiar situation of Uzbekistan. Many species found in the Kitab State Geological Reserve are endemic and at least restricted to the South Tien Shan. We suggest a moderately close relationship to southern Chinese and Vietnamese faunas, even though more palaeontological data from these regions is needed for testing. We also revise the cephalopod fauna from the Geological Reserve and introduce the following new taxa: *Beckeroceras* gen. nov., *Uzbekisphinctes* gen. nov., *Ivoites meshchankinae* sp. nov. *Kitabobactrites salimovae* gen. et sp. nov., *Metabactrites rakhmonovi* sp. nov. • Key words: Pragian, Emsian, carbonate microfacies, endemism, Ammonoidea, palaeogeography.

(To be submitted in *Bulletin of Geoscience*)

Carole Naglik & Christian Klug, Palaeontological Institute and Museum, University of Zurich, Karl Schmid-Strasse 4, CH-8006 Zurich, Switzerland; carole.meier@hotmail.com; chklug@pim.uzh.ch • Kenneth de Baets, GeoZentrum Nordbayern. Fachgruppe PaläoUmwelt. Universität Erlangen, Loewenichstr. 28, DE-91054 Erlangen, Germany; kenneth.debaets@fau.de

In Central Asia, Uzbekistan offers the rare opportunity to study the palaeontology in exposures of Cambrian to Recent sediments (Kim et al. 2007). Concerning the Palaeozoic sedimentary records, the Zeravshan-Gissar Mountains located both in Uzbekistan and Tajikistan are particularly important (Bardashev et al. 2005). There, the palaeontological record of the Palaeozoic sequence is both diverse and well preserved. In an area covering a 56 km^2 located about 170 km South-Southeast of Samarkand, Ordovician to Carboniferous sediments are well exposed in a mountainous area. This area is protected since 1979 by the Uzbek government. It is known as the Kitab State Natural Reserve (Fig. 1A) and a research station (Zapovednik village) has been created in order to encourage scientific research in this region (Yolkin et al. 1997). In 2004, Uzbekistan even edited stamps depicting the outcrop of the early Emsian in the Khodzha Kurgan Gorge and the early Emsian ammonoid "*Mimosphinctes*" *rudicostatus* (Ernst & Klug 2011).

The Kitab area is famous for more or less continuous successions ranging from the Middle Ordovician to the Early Carboniferous, with shallow water to terrigenous-siliceous carbonates in the Devonian part and only moderate tectonic disturbance according to Yolkin et al. (2008). Moreover, this area is of great importance for researchers focusing on the Early Devonian due to the presence of the Pragian-Emsian Global Boundary Stratotype Section and Point (Yolkin et al. 1997) as well as the rich cephalopod successions in much of the Emsian. The Pragian-Emsian GSSP was defined here because of the excellent conodont record in the Zinzilban Gorge. The current Pragian-Emsian

GSSP marks the level where the conodont *Polygnathus kitabicus* appeared first (Yolkin et al. 1997), although it is currently being revised (Carls et al. 2008, Kim et al. 2012, Izokh et al. 2011). The current boundary is very close to the lithological boundary between the reefal and the pelagic facies (Kim et al. 2012). The origin of this sedimentological and palaeoecological transition is one of the topics of this article as well as the changes in the ammonoid fauna during the Lower Emsian.

Rich faunas are present in this area such as reefal asssociations of the Lochkovian and Pragian (Madmon Fm.) with tabulate corals, stromatoporoids, rugose corals, and crinoids, brachiopod associations in the latest Pragian (Zinzilban Beds, Norbonak Beds), and pelagic associations of the Emsian (Dzhaus and Obisafit Beds) with tentaculites, ammonoids, bactritids, and occasional brachiopods, orthocerids, oncocerids, trilobites, tabulate corals and bryozoans (Kim et al. 2007 and references therein).

Here, we focus on two palaeontogical aspects, namely the transition from the reefal to the pelagic associations and the pelagic facies of the Dzhaus Beds with its peculiar and highly diverse cephalopod fauna. Although the cephalopod association is overall characteristic for the early Emsian and resembles contemporary associations in, e.g., Bohemia (Chlupáč 1976, Chlupáč & Turek 1977, 1983), China (e.g., Ruan 1981), France (Erben 1960, Lardeux et al. 1979), Germany (e.g., De Baets et al. 2009, 2013b), Morocco (Klug 2001, 2017, De Baets et al. 2010, Klug 2017), or Russia (Bogoslovsky 1963, 1969), it contains a number of endemic taxa (some are newly described here). These cephalopods are interesting, because they comprise some of the oldest ammonoids, which occur in well-dated rocks together with bactritids, dacryoconarids and conodonts. These forms add new details to the understanding of the evolution of bactritids and early ammonoids.

The aims of this study are (1) to document the facies transition from the reefal facies of the Pragian to the pelagic facies of the early Emsian, (2) to achieve an interpretation of the events that led to these changes, (3) to document the Emsian sections of the Kitab region and their ammonoid associations including a correlation, (4) to describe new ammonoid taxa from this region and (5) to discuss the palaeogeographic relationships of the Uzbek cephalopod associations of the Emsian with other regions.

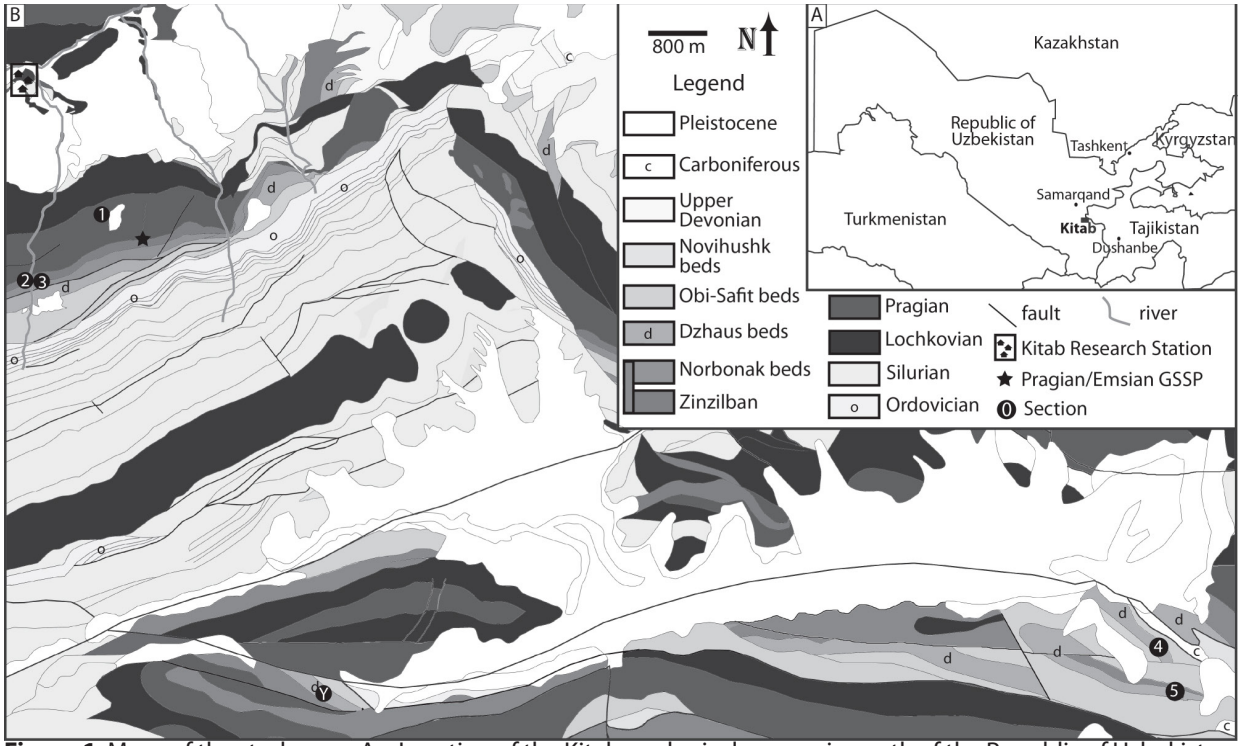

Figure 1. Maps of the study area. A – Location of the Kitab geological reserve in south of the Republic of Uzbekistan. B – Geological map of the investigated area with the studied sections: 1. Bursykhirman; 2. Khodzha Kurgan Gorge West of river; 3. Khodzha Kurgan Gorge; 4. Shirdag North; 5. Shirdag South; Y. Yusupkul.

Geological setting

The Zeravshan-Gissar Mountains of Uzbekistan and Tajikistan are part of the southern Tien Shan. The Tien Shan is an important orogenic system in Central Asia, which formed following the collision of the Indian and Asian plates, which began about 55-50 Ma ago (Pickering et al. 2008 and references therein). Tectonic features that had developed during the Hercynian orogeny occurred predominantly in zones with transitions between different facies and thus sediment types (Bardashev et al. 2005). The Palaeozoic and Mesozoic tectonic history of this region is highly complex. It is characterized by accretionary events of microcontinents, terranes and island arc complexes (Filippova et al. 2001, Windley et al. 2007, Brunet et al. 2017).

In this region, Devonian deposits crop out in a large area. In the Zeravshan Range (Khodzhakurgan and Akbasai Formations), the sedimentary sequence consists of pelagic to hemipelagic deep water carbonates and fine siliciclastics. Units with abundant conodonts and tentaculitids occur with cherts and volcaniclastics (Kim et al. 2007). The first outcrop we investigated is located on the Bursykhirman Mountain, which mostly consists of sediments of the Madmon formation (Late Pragian – section 1 in Fig.1B) and the exposed sediments belong largely to the Khukar regional Stage. It is located in the southern limb of the Dzhindzy-Darya Anticline displaying Silurian dolomites in its core and Devonian on its flanks (Yolkin et al. 2008).

In the same area, still on the southern limb of this anticline, the Kitab regional Stage crops out. It corresponds to the Emsian, which comprises the regional stratigraphic units named (from the oldest to the youngest): Zinzilban, Norbonak, Dzhaus and Obisafit Beds. There, mainly the Dzhaus Beds of two sections have been sampled and studied including the rich ammonoid occurences (sections 2 and 3 – Fig. 1B). These beds mainly consist of mostly thin-bedded limestones with some chert nodules.

The Shirdag sections (sections 4 and 5 – Fig. 1B) are located in an anticline located south-west of the Sumsar syncline, bordered by many faults, and mainly consisting of the Dzhaus beds. Additionally, we examined a section named Yusupkul (section Y – Fig. 1B), which is still in the Shirdag area. It was studied only rarely but appears worth mentioning because of its well preserved ammonoids (Bogoslovsky 1984).

Material and methods

We studied, measured, and sampled seven sections during two field seasons in the Kitab State Geological Reserve. Depending on the section, the quality of the outcrop exposure varied from poor to excellent. Field photos of the four main outcrops are shown in Figure 2. Bursykhirman section starts near the top of the Madmon Formation, i.e. near the top of the Pragian carbonate platform sediments near the summit of the mountain Bursykhirman; this locality lies very close to the Pragian-Emsian GSSP in Zinzilban Gorge (Fig. 1). All the other sections have been sampled only for Emsian fossils and facies. Sections have been measured and sampled for palaeoenvironmental reconstructions using thin sections. 86 thin sections were produced to investigate microfacies: 27 from the Bursykhirman section, 29 from the Khodzha Kurgan section and 30 from the Shirdag section.

We applied the Unitary Association (UA) method (Guex & Davaud 1984, Guex 1991, Monnet et al. 2011a) to our ammonoid dataset using the freely available software PAST® (Hammer et al. 2001). This method produces the most robust stratigraphic schemes by relying on co-occurrences of species only.

Here, we use local lithostratigraphic names. These names are used in the sense of previous authors (compare, e.g., Yolkin et al. 1997, 2008, Kim et al. 2007, Carls et al. 2008).

All fossil specimens and the thin sections are stored at the Palaeontological Institute and Museum at the University of Zurich (PIMUZ numbers).

Results

Bursykhirman Section (1 – Fig. 1B)

This section (N39.173055°, E67.261225°) comprises 210 m of late Lochkovian and Pragian

Figure 2. Parts of the main outcrops of the studied localities. 1. Bursykhirman, lower part of the section; 2. Khodzha Kurgan Gorge; 3. Shirdag; 4. Yusupkul, mostly covered by the vegetation, showing bad exposure to measure a section with confidence compared to the two other zones (Khodzha Kurgan Gorge and Shirdag).

sediments and is shown in Fig. 3. We started measuring the section near the summit of Bursykhirman Mountain and proceeded towards the south. The section consists predominantly of massive peloidal grainstones, floatstones and rudstones, which overlie the reef carbonates of the Madmon-Formation (Lochkovian to Pragian). This section represents older layers compared to the other studied sections and starts in the upper Lochkovian (Sangitovarian regional stage, *pesavis* conodont zone). The first 100 m consist mainly of massive limestones with brachiopods, some rugose and tabulate corals (mainly favositids) and bryozoans (Fig.3 – 1, 2, peloidal float-grainstones). At about 75 m, a more pelagic facies rich in tentaculites (*Paranowakia intermedia*) was found (Fig. 3 – 3) close to the Lochkovian/ Pragian boundary. From about 90 to 100 m, the amount of silica in the limestones and silicified reef debris increased (Fig. 3 – 4). After 110 m, reef debris still occur but become less abundant; this part of the section is dominated by wackestones still belongs to the Pragian (Khukarian regional stage, *sulcatus* zone). On the other hand, the silica content continues to increase slightly. Small phosphoritic concretions occur at about 150m (Fig. 3 – 5) in a coarser microfacies, consisting predominantly of grainstones and rudstones. The top of this section consists mainly of laminated siliceous limestones rich in styliolinids (*Nowakia acuaria*) and some silicified reef debris (such as tabulate corals, Fig. 3 – 6). Towards the top of this section, we found a growing amount of tectonic structures (faults, striations). The last bed included in this section is brecciated. The overlying sediments are covered by vegetation. These sediments likely consist of a more pelagic and more fine-grained facies. It is unclear if the top of this section is already in the pireneae conodont Zone.

Khodzha Kurgan Gorge West of river Section (2 – Fig. 1B)

This section (N39.166019°, E67.248822°)

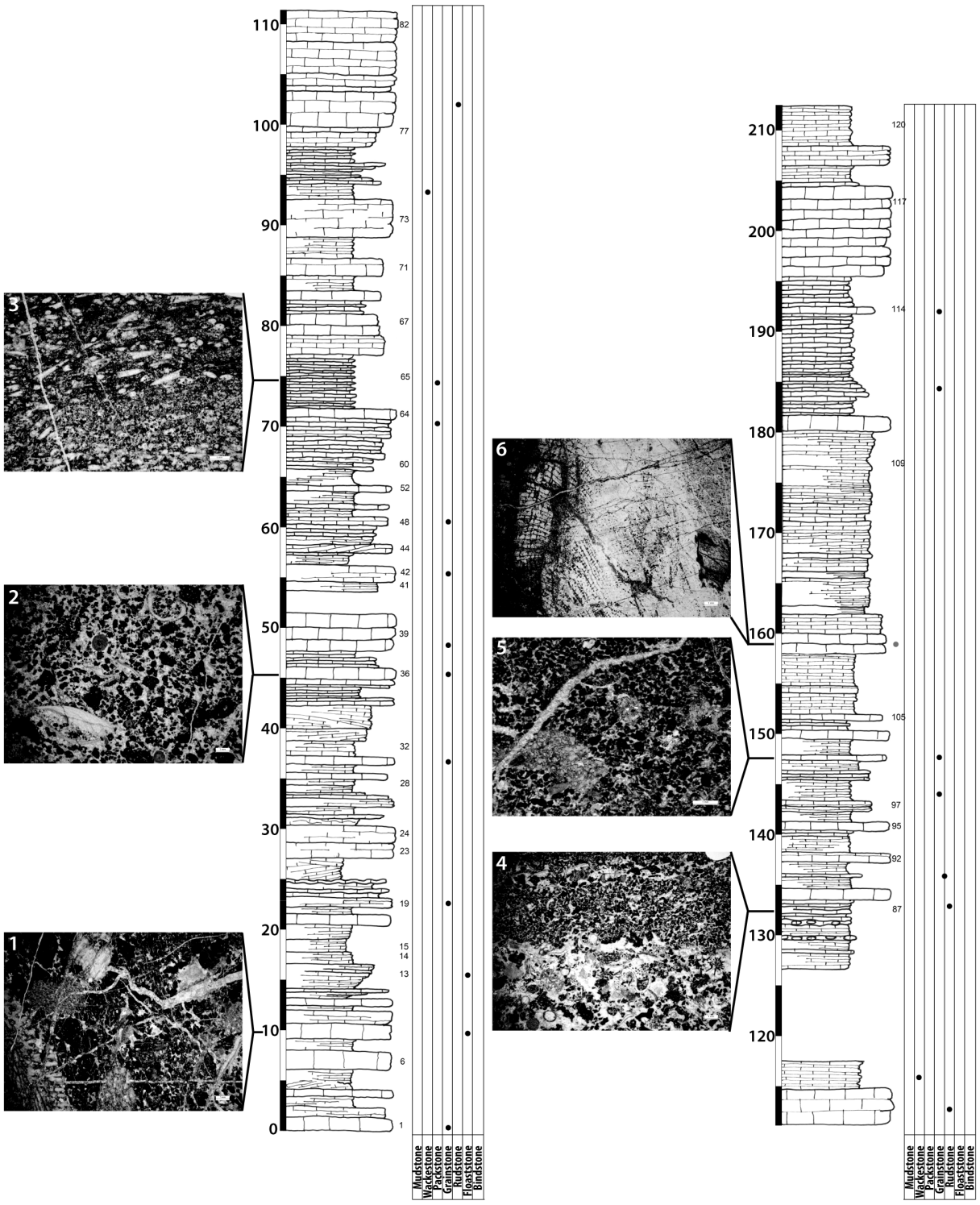

Figure 3. Bursykhirman section with indications of microfacies according to the modified Dunham classification (Dunham 1962; Embry & Klovan 1971). Pictures illustrate the main microfacies. 1 – Peloidal floatstone with reef debris such as bryozoans and tabulate corals. 2 – Peloidal grainstone rich in brachiopods and echinoderm debris. 3 – Peloidal grainstone rich in tentaculites. 4 – Rudstone rich in gastropods, echinoderm debris, undetermined shell debris, and probably several dasycladacean green algae. 5 – Grainstone rich in detritic grains and some phosphoritic concretions. 6 – Silicified reef debris, tabulate coral.

measures 30 m (Fig. 4) and its base corresponds to bed "15.20m" of the Khodza Kurgan Gorge section from the Field Excursion Guidebook (Yolkin et al. 2008; see also Becker et al. 2010). Therefore, the entire section consists of the Dzhaus beds (Kitabian regional stage, *inversus* conodont Zone). It is mainly composed of massive limestone beds (ca. 30-60 cm thick) alternating with thin-bedded limestones. These limestones are overall moderately rich in fauna including brachiopods, crinoids, rugose and tabulate corals. Stromatoporoids were found only once around the sixth meter from the base of the section. Ammonoids start to occur at 7.2 m from the base with *Erbenoceras kimi* contained in a moderately thick-bedded limestone. *Erbenoceras kimi* is found throughout this section and often is associated with Gyroceratites laevis, Kimoceras lentiforme, and less frequently with *Convoluticeras flexuosum*. *Erbenoceras advolvens* is found only once at 11 m, co-occurring with *E. kimi*, *C. flexuosum* and *K. lentiforme*. We did not sample this section for microfacies.

Khodzha Kurgan Gorge Section (3 – Fig. 1B)

This section crops out on the east side of the river; we began measuring at N39.166865°, E67.249827°. It was divided into two parts, because of poor outcrop conditions between the 66th and 78th meter. Its global thickness measures about 123 m (Fig. 4). It starts about 29 m above the base of Dzhaus beds (Kitabian, *inversus* conodont Zone = Stop 16 of Yolkin et al. 2008). This is probably the best section to study the sequence of early Emsian ammonoids in its stratigraphic context in Uzbekistan. The base of this section consists mainly of alternating dark limestone beds with abundant tentaculites. At about 9 m, current-aligned tentaculites appear aligned in a thin massive packstone bed. This succession of alternating massive and thin limestone beds including black laminations goes on until about 25 m. After 16 m, we found the first *Erbenoceras kimi*. Near the base of the section, the microfacies is dominated by wackestones except for a floatstone at 6 m from the base. The following wackestones contain parallel, sometimes slightly wavy, thin brownish laminations.

From about 23-24 m, orthocones occur together with *Gyroceratites laevis* and *Erbenoceras kimi*. Just after the 25th meter, flattened specimens of specimens probably *Convoluticeras flexuosum* are present. The thickness of the following massive limestone beds slightly decreases to the 35th meter. At about 30 m, flattened ammonoids occur abundantly in a grainstone. This grainstone contains a lot of detritic material including some questionable worm tubes. Additionally, *Kitabobactrites salimovae* nov. sp. is there associated with *Gyroceratites laevis*. Then, a sequence of thin-bedded laminated wackestones follows, containing thick limestone lenses with a lateral extent of several meters; it is unclear to us whether these structures are of diagenetic or tectonical origin.

At 38 m, 3-dimensionally preserved, but often fragmented ammonoids such as *Uzbekisphinctes rudicostatus* and *Mimagoniatites fecundus* were extracted from the massive limestones. In this layer, they are accompanied by orthocones, bivalves and brachiopods. The following 7 m consist of alternating thin-bedded and massive limestones, which are very poor in fossils. The massive limestone beds consist of grainstones. The next ammonoid occurrence appears around 45 m in a massive 40 cm-thick bed containing flattened *Kitabobactrites salimovae*, *Gyroceratites laevis* and the last occurrence of *Convoluticeras flexuosum*. Concerning the microfacies, it is again dominated by wackestones. At 49 m, a 70 cm-thick unit of thin cross-bedded limestones contains large orthocones, *Gyroceratites laevis*, and the last *Kitabobactrites salimovae* of this section. This unit also marks the first appearance of *Ivoites meshchankinae* in this section. After a 2 m-thick interval of alternating thin and thick limestone layers with a low fossil content (no ammonoids), a thick and highly fossiliferous interval follows, which yielded ammonoids: Between the meters 51 to 64, many different fossils including tabulate and rugose corals, brachiopods, dacryoconarids (probably *Nowakia elegans*), crinoids, and ammonoids occur. At the base, this unit contains *Erbenoceras kimi*, which is the last occurrence of this species in this section. Otherwise, ammonoids of the genera *Mimosphinctes*, *Mimagoniatites*, *Gyroceratites* and *Ivoites* were extracted from this interval.

The last bed of this interval consists of a

massive reef-debris rudstone. Above this interval, 12.20 m could not be investigated because of the very poor outcrop. At around 78 m, the strata are well exposed again. From there to meter 90, an alternation of thin-bedded and massive limestones occurs with an increasing number of cherts and carbonatic nodules. Simultaneously, the fossil content decreases in abundance and diversity. These strata still contain echinoderm debris and dacryoconarids (*Nowakia cancellata*) are also present. In the lower part of this interval, *Uzbekisphinctes rudicostatus* was found in association with *Ivoites meshchankinae*.

From meter 90 to 103, alternating massive and thin limestones occur with irregular surfaces, which might be interpreted as slumps or as turbidites. This interval also contains some nodular layers. At meter 103 m, a slight facies change is discernible. The colour of sediments turns into a darker grey and the fine-bedded intercalations become even thinner. These thin, alternating beds contain fewer fossils and accordingly no ammonoids have been found in this interval until meter 115. There, the last fossiliferous interval was found; this layer contains crinoids, bivalves, brachiopods, and the last ammonoids of the early Emsian in this section, namely *Gyroceratites laevis*, *Uzbekisphinctes rudicostatus* and *Mimagoniates fecundus*. The last two meters of the section correspond to the base of the Obisafit Beds and consist of a massive 2 m-thick limestone.

Yusupkul Section (Y – Fig. 1B)

Although this area has been investigated and about 60 m of section have been measured (N39.128883°, E67.328448°), we do not present the section here because of the poor outcrop quality (more or less dense vegetation) and tectonic overprint that hampered the lateral correlation of beds (Fig. 2 – 4). Nevertheless, this locality is worth mentioning as an interesting ammonoid locality; particularly *Erbenoceras kimi* and *Gyroceratites laevis* are common. They occur at around 20 m above the base of the section. *Erbenoceras kimi* is found first, followed by *Gyroceratites laevis*. Additionally, we found specimens of *Gaurites sperandus*. Towards the top of the section, *Ivoites* sp. is found associated with *Erbenoceras kimi* and *Gyroceratites laevis*. One of the strata was extremely rich in hatchlings of ammonoids and orthocones. As for the other sections, the facies consists mostly of alternating thin and massive thicker beds of limestones containing occasionally silicified fauna such as rugose and tabulate corals, crinoids and brachiopods.

ShirdagSection NORTH (4 – Fig. 1B)

The Shirdag area is located at about 12 km east of the Yusupkul area. The section Shirdag North (N39.136960, E67.441107°) measures 66 m (Fig. 4) and starts at the top of the Norbonak Beds and mainly encompasses the Dzhaus Beds. Although most of the Norbonak Beds lie in the *excavatus* and *nothoperbonus* conodont Zones, the uppermost part belong already to the *inversus* conodont Zone (Yolkin et al. 2008). Therefore, the entire section presented here belongs to the *inversus* conodont Zone, since the first two recorded beds of our section corresponds to the very top of the Norbonak Beds. The section starts with massive limestones with silicified reef-fauna including stromatoporoids, rugose and tabulate corals, brachiopods and chert-nodules. These are overlain by alternating massive dark cherty limestones and thin-bedded limestones until meter 4. 2.5 m above the base, dacryoconarids and ammonoids were found with the association of *Erbenoceras kimi* and *Ivoites meshchankinae*.

Directly above, *Erbenoceras advolvens* co-occurs with these ammonoid species. In this unit, the thickness of the beds considerably varies laterally. Massive alternating limestones and cherty layers occur until meter 16 with the repeated appearance of *Gyroceratites laevis* between meter 10 m and 16. This last occurrence coincides with the first appearance of *Mimagoniatites fecundus* at the base of a 6 m thick interval of alternating thin-bedded limestones with massive cross-bedded limestones. This interval is also marked by current-aligned dacryoconarids. *Ivoites meshchankinae* nov. sp. disappears just before meter 20.

From meter 21 to 35, reef debris becomes more abundant again with brachiopods (spiriferids), bivalves, rugose and tabulate corals. The dacryoconarid *Nowakia barrandei* also occurs in this interval. Crinoids and stromatoporoids are found near the top of this interval, which also

corresponds to the last occurrence of *Erbenoceras advolvens*. *Erbenoceras kimi* is the next species to disappear at meter 40. Approximatively between meter 37 and 51, the outcrop conditions are very poor and most is covered by scree (excavation is difficult because of the steepness of the slope). Still, at meter 48, the last occurrence of *Mimagoniatites fecundus* was found in association with the first appearance of *Kimoceras lentiforme*, which ranges through to the top of the studied section (meter 66). In contrast to its longer range and moderate abundance in the Khodza Kurgan area, *Uzbekisphinctes rudicostatus* was found here in a short range of the section between meter 50 to 53.

The last eight meters of this section consist of fine-grained cross-bedded limestones near the base, which then grade into more massive and coarse-grained limestones rich in rugose and tabulate corals, and crinoids, associated with a few brachiopods.

Shirdag section SOUTH (5 – Fig. 1B)

Shirdag SOUTH section is located about 730 m south from the NORTH section (39.130778, 67.443500). We studied 156 m of outcropping section there (Fig. 4). This section represents the longest interval of this study, it starts at the top of Norbonak beds, and then the entire Dzhaus beds are recorded. The base of Obisafit beds is also included in there, at the top of the section. The 5-6 first meters correspond to wackestones/crinoid Packstones rich in brachiopods, the limestones are often quite nodular and a reef fauna is observed. This interval corresponds to the top of the Norbonak beds. Then there is an interval of thinner and laminated limestones containing stromatoporoids which mark the base of the Dzhaus beds. These laminated limestones go on until 20 m where they become more massive, and the last unit is a thick bed with ondulating surfaces, similar to a slump deposit. This last unit contains silicified fauna such as brachiopods, rugose and tabulate corals. After this unit the outcrop conditions get bad and there is a gap in the section estimated to be of 7.50 m thick. From 27 m thicker units alternating with thin layers are cropping out consisting more in Rudstone and Grainstone facies with abundant reef fauna fossils: Brachiopods, crinoids, tabulate corals, and dacryoconarids are also found. The first occurrence of ammonoid, namely *Erbenoceras kimi* is found at 40 m from the base of the section, corresponding to about 35 m from the base of Dzhaus beds. *Erbenoceras advolvens* is the second taxa found at 45 m from the base, followed by *Gyroceratites laevis* at 50 m. From 50 to 62 m the thin-bedded limestones alternate with thicker massive beds than previously, and the dominating microfacies consists in Rudstone with brachiopods, dacryoconarids, favositids and bivalves, and stromatoporoids at the top of this unit. In this interval at 56 m, *Erbenoceras advolvens* is found for the last time co-occuring with the first appearance of *Ivoites meshchankinae*. The following 10 meters contain brachiopods, tabulate corals and gastropods. The base of this unit contains laminations, siliceous thin beds and some thin beds consist of mudstones without any fossils seen. At the top of this unit, wavy surfaces are pointed out, probably erosive surfaces as well. It also seems there that some coal debris or small driftwood pieces are found. At 67 m, still in this unit, the only occurrences of both *Mimagoniatites* sp. and *Teicherticeras* cf. *planum* are found together with the first appearance of *Kimoceras lentiforme*. Then from 72 to 88 m, massive limestones with parallel laminations and thin chert layers alternate, with dominant microfacies getting a transition from Rudstones to Grainstones then Wackestones. This interval is less diverse in fauna, mainly with crinoids and dacryoconarids. *Erbenoceras kimi* is although found concerning ammonoids, and tabulate corals are found towards the top. At 88-90 m, although there is not a clear change in the lithology, there is a change in ammonoid diversity. Indeed in this 2 meter-thick interval, the last occurences of the following species occur: *Ivoites meshchankinae*, *Erbenoceras kimi* and *Kimoceras lentiforme*. It is important to mention that in this interval three species appear only there, which are namely *Kitabobactrites salimovae*, *Metabactrites rakhmonovi* and *Beckeroceras khanakasuensis*. In the end, only *Gyroceratites laevis* crosses this interval and is still found later in the section, until the 111th meter, which marks the last ammonoid occurrence for this section. At 94 m an interval of about 2.2 meters cropped out badly so it could

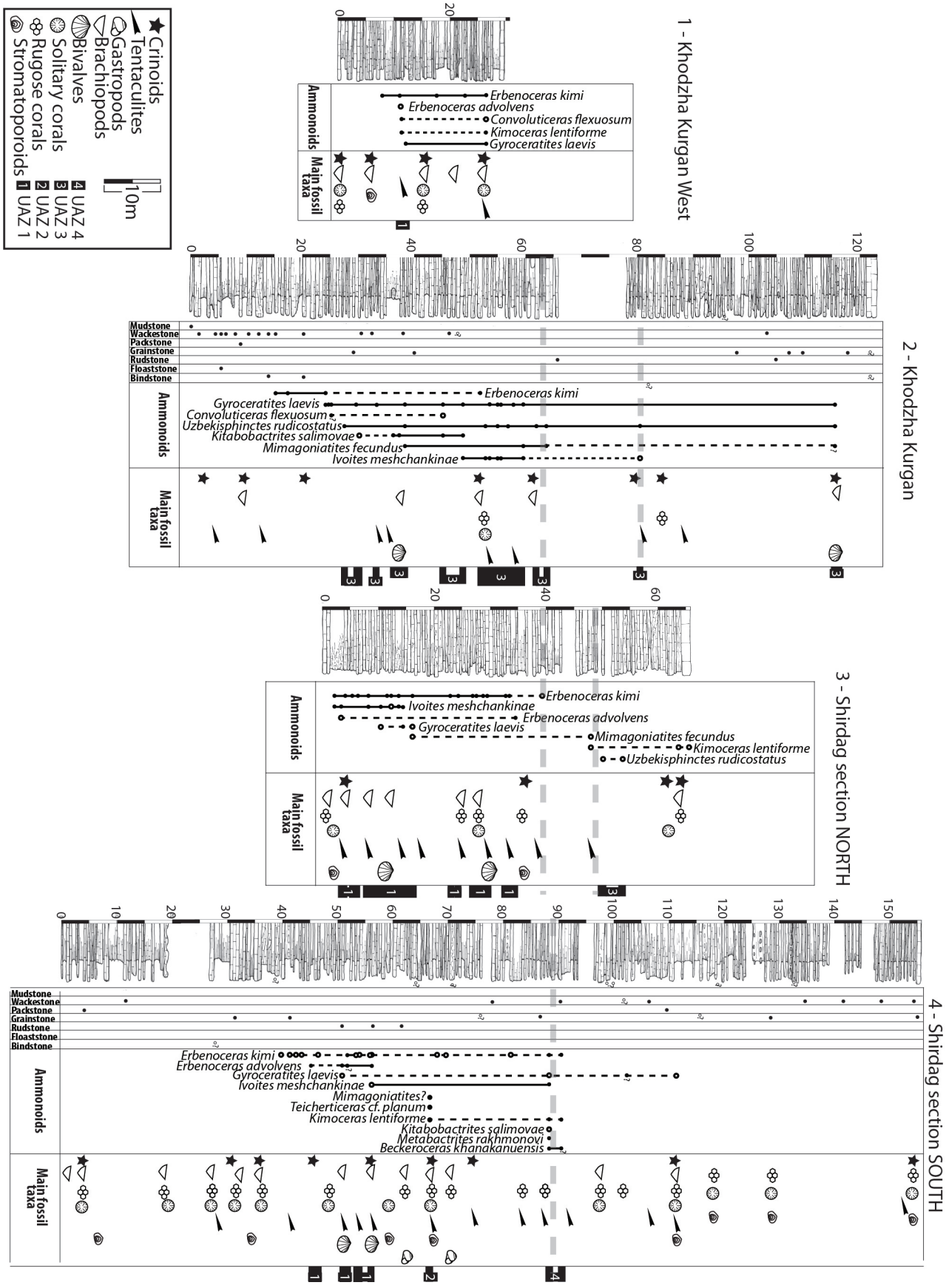

Figure 4. Studied sections with the accompanying fauna (main groups), the ammonoid succession, and the microfacies (Dunham classification), modified after Embry & Klovan (1971). The UA zones are labelled on the right side and suggestions for placing the Daleje Event are marked with the grey dashed line.

not be properly investigated. From about 96.5 m to 111 m, the lithology is dominated by massive limestone beds quite rich in reef fauna such as tabulate corals, brachiopods, stromatoporoids and crinoids. The following unit goes until 128 m and mainly consist on thick (>1m) thin-bedded layer intervals with silicified binds alternating with 30-50cm-thick massive limestones. The top of this unit is once more marked by abundant reef fauna debris From 128 m to the end, the thin-bedded intervals decrease in thickness but the lithology still consists of alternating thin-bedded/massive layers with occasionally nodular limestone layers. Laminated Wackestones are the most representative microfacies for this last part of this section. The last bed of 70cm in thickness is a massive reefal Grainstone, which probably belong to the Obisafit beds.

Systematic palaeontology

We follow the classification scheme and terminology of Korn and Klug (2002) slightly modified by De Baets et al. (2013b). We use the absolute rib index or ARIxx (= ribs counted within a circle centered on the venter with the specified diameter xx in mm) introduced by De Baets et al. (2013b).

In Figure 5, we show some brachiopods that were found in situ. Figure 6 displays some rare findings of trilobites, dacryoconarids and gastropods. Some ammonoids mentioned in the stratigraphic paragraphs above but not described in the systematic section are shown in Figure 7 and 8.

Class Cephalopoda Cuvier, 1797
Order Bactritida Shimansky, 1951
Family Bactritidae Hyatt, 1884

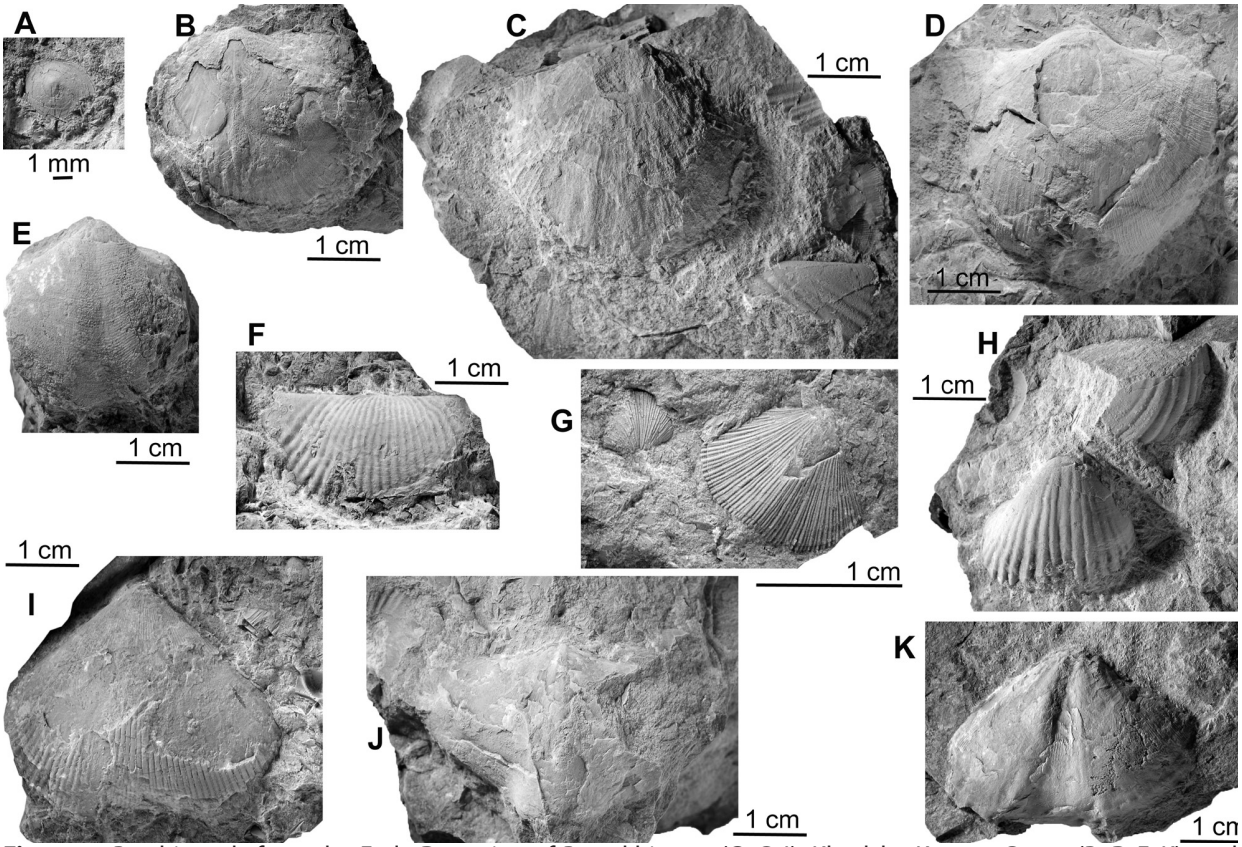

Figure 5. Brachiopods from the Early Devonian of Bursykhirman (C, G-J), Khodzha Kurgan Gorge (B, D-F, K), and Shirdag (A). • A - discinid inarticulate, PIMUZ 31326, Dzhaus Beds, SHK3A. • B-D - *Gorgostrophia neutra*, ventral valves, Emsian. • B - PIMUZ 31327, Dzhaus Beds, KKG 45. • C - PIMUZ 31328, Beds, BH79. • D - PIMUZ 31329, Dzhaus Beds, KKG 237. • E - athyridid indet., PIMUZ 31330, ventral valve, Dzhaus Beds, KKG 49. • F - cf. *Leviconchidiella gyrifera*, PIMUZ 31331, dorsal valve, Dzhaus Beds, KKG 49. • G - *Aulacella eifeliensis*, PIMUZ 31332, dorsal valve, Dzhaus Beds, KKG 49. • H - cf. *Leviconchidiella gyrifera*, PIMUZ 31333, dorsal valve, Norbonak Beds, BH79. • I – *Punctatrypa sibirica*, PIMUZ 31334, Dzhaus Beds, KKG 49. • J, K – *Havlicekia secans*, Beds, BH79. • J – PIMUZ 31335, ventral valve. • K – PIMUZ 31336, dorsal valve.

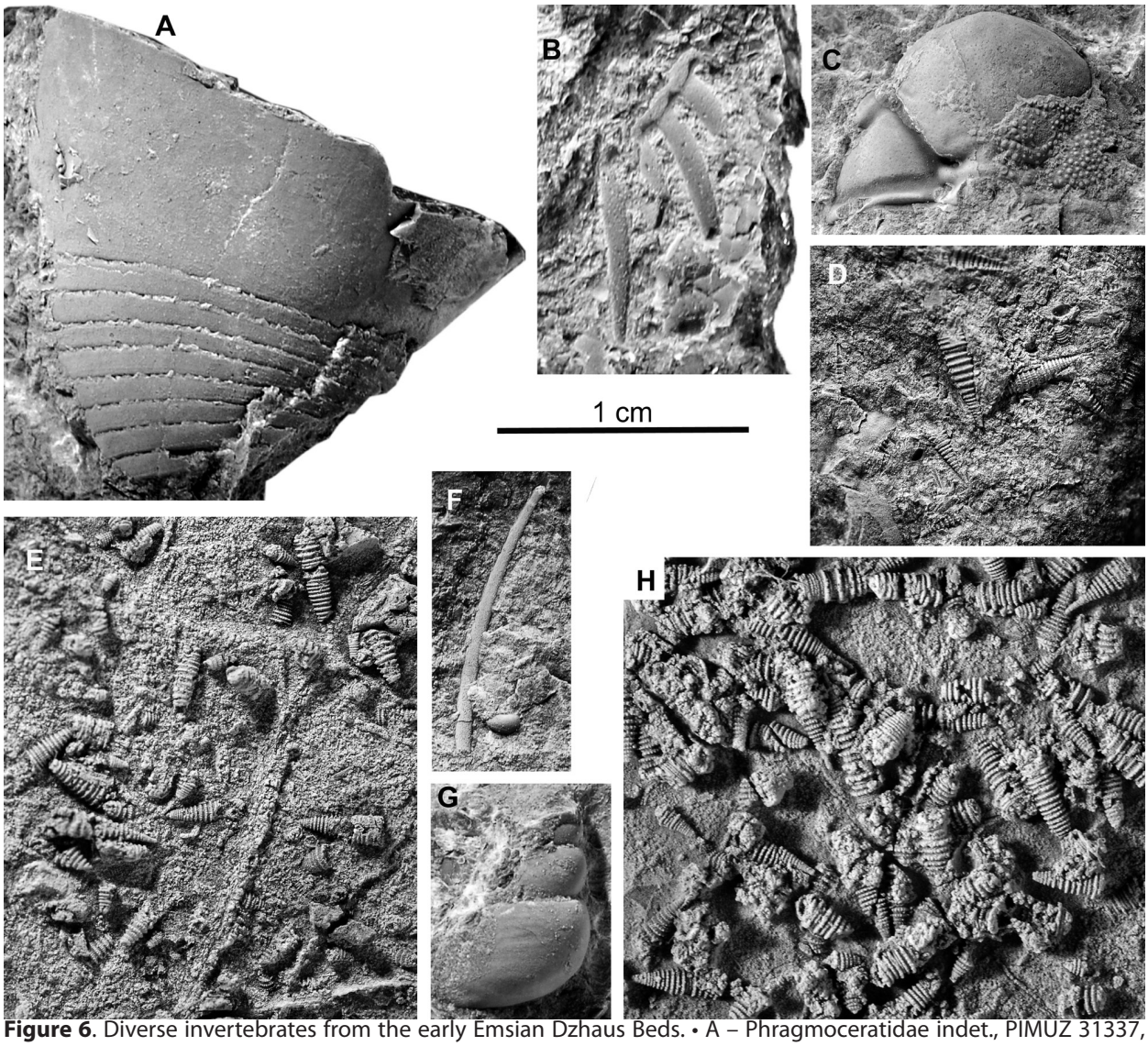

Figure 6. Diverse invertebrates from the early Emsian Dzhaus Beds. • A – Phragmoceratidae indet., PIMUZ 31337, Dzhaus Beds, Khodzha Kurgan Gorge, KKG 69m. • B – *Exastipyx* sp., PIMUZ 28869, fragmentary pygidium, Dzhaus Beds, Yusupkul, YUS01KDB. • C – *Plagiolaria kitabi* Crônier & Tsmeyrek, 2010, PIMUZ 31338, Dzhaus Beds, Yusupkul, YUS 01. • D, E, H – *Nowakia elegans* (Barrande, 1867). • D – PIMUZ 31339, Dzhaus Beds, Shirdag, SHK313. • E, H – PIMUZ 31340, silicified, Dzhaus Beds, from scree, Shirdag. • E – PIMUZ 31340. • H – PIMUZ 31341. • F – PIMUZ 31342, trilobite genal or pygidial spine? Dzhaus Beds, Shirdag, SHK 3A. • G – Gastropoda indet., PIMUZ 31343, Dzhaus Beds, Khodzha Kurgan Gorge.

Genus *Kitabobactrites* gen. nov.

Type species. – *Kitabobactrites salimovae* sp. nov.

Etymology. – After Kitab, a town in Uzbekistan, which is close to the Kitab State Geological Reserve, where the material was found.

Diagnosis. – A bactritid with a gently coiled conch. Initial shaft more strongly curved, terminal part nearly straight. Weak sculpture. Distinct ventrolateral spiral rib and ventrolateral furrow. Sutures simple with broad and moderately deep lateral lobe.

Remarks. – Becker et al. (2010) already recognized this taxon as undescribed. A main problem is that we did not manage to find a specimen that is not deformed. However, the mix of characters is so different from all other cephalopod taxa from this time interval that we confidently erect this new genus and species. As far as conch shape is concerned, the genera *Cyrtobactrites*, *Metabactrites*, *Ivoites* and *Kokenia* are the closest. *Kokenia* is Eifelian in age and thus much younger; also, it has distinct ribs. *Kitabobactrites* lacks such ribs, which are well developed in Ivoites and *Metabactrites.* These three genera occur in the same or slightly

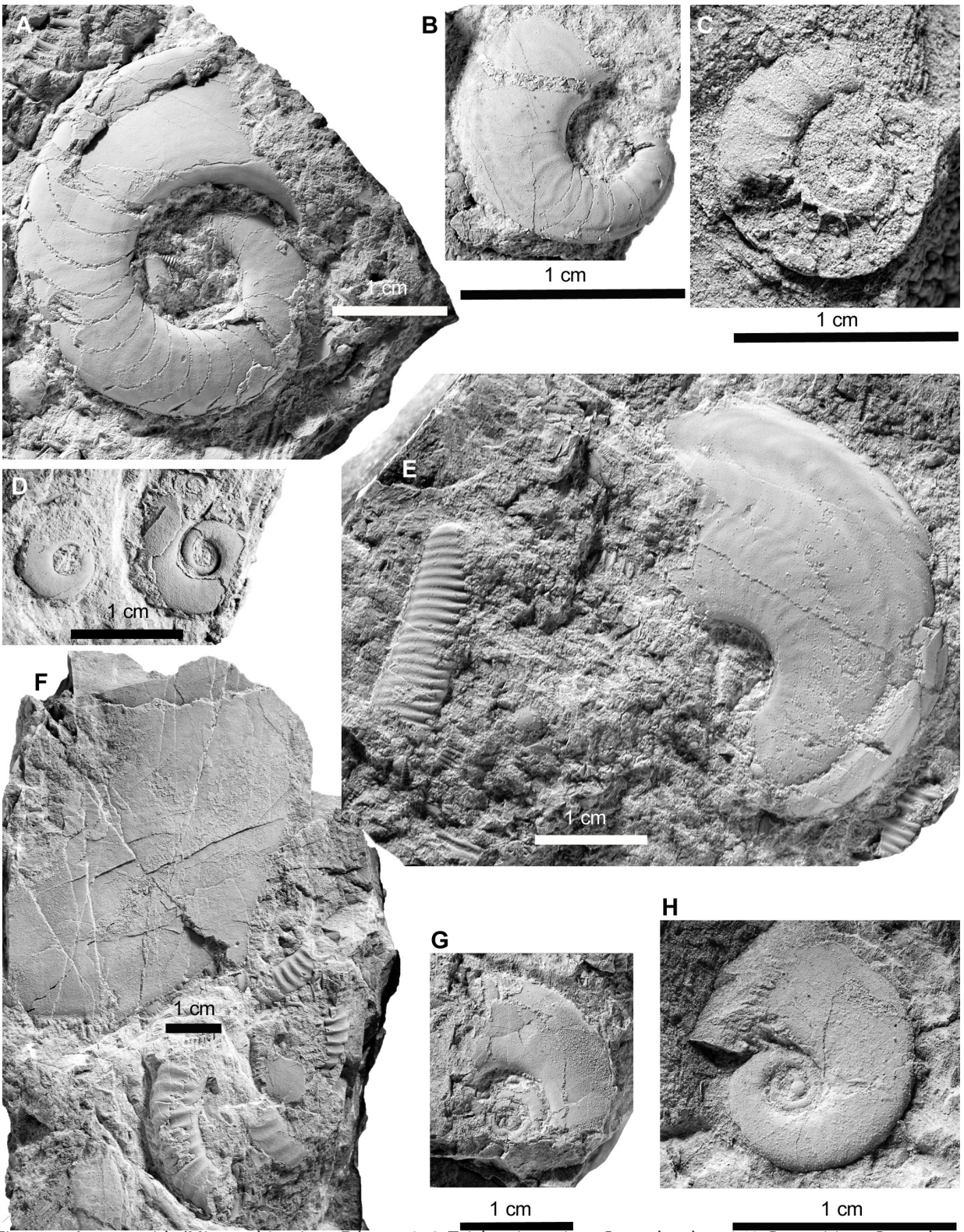

Figure 7. Ammonoids (Mimosphinctinae Erben, 1953, Teicherticeratinae Bogoslovsky, 1969, Parentitinae Bogoslovsky, 1980 and Auguritinae Bogoslovsky, 1961) from the early Emsian Dzhaus Beds. • A – *Teicherticeras* cf. *planum* Bogoslovsky, 1980, PIMUZ 31367, note the faint sculpture, the missing whorl overlap and the spiral lines, Shirdag, Kim's section, KS 121. • B – *Kimoceras lentiforme* Bogoslovsky, 1980, PIMUZ 31368, juvenile specimen, Shirdag, SHK 3A. • C – *Convoluticeras flexuosum* Bogoslovsky, 1984, PIMUZ 31369, slightly silicified specimen, Shirdag, SHK 50. • D – *Gaurites sperandus* Bogoslovsky, 1984, PIMUZ 31370, two juvenile specimens, Yusupkul, YUS02CK. • E – body chamber of *Kimoceras lentiforme* Bogoslovsky, 1980 with subterminal shell fragment of *Metabactrites rakhmonovi* sp. nov. (holotype) and pygidium of *Exastipyx* sp. (not visible here, see Fig. 10), PIMUZ 28869, Shirdag, SHK 3A (specimen refigured from Monnet et al. 2011b). • F-H – *Gaurites sperandus* Bogoslovsky, 1984. • F – PIMUZ 31371, body chamber of nearly adult specimen, Yusupkul, YUS02CK. • G – PIMUZ 31372, premature specimen, Khodzha Kurgan Gorge, KKG 67. • H – PIMUZ 31373, premature specimen showing the protoconch, Yusupkul, YUS02CK.

younger strata. The new genus shares the strong ventrolateral projection of *Cyrtobactrites*, but the latter genus has no ventrolateral furrow and rib. The coiling is actually intermediate between *Cyrtobactrites* and *Metabactrites*. It is included in the Bactritidae because it did probably not form a complete whorl and because it combines character states of growth line course and coiling mode that are unknown from ammonoids but have been documented from bactritids, namely in *Cyrtobactrites* (Erben 1960, Klug et al. 2008). This is of interest, because the genus shows characters typical of slightly more derived ammonoids. For example, the growth line course and presence of a ventrolateral furrow is reminiscent of *Gyroceratites* but the coiling (Fig. 9) is reminiscent of a derived bactritids or of one of the first ammonoids.

Included species. – only the type species.

Occurrence. – So far only known from the early Emsian of the Kitab State Geological Reserve (Uzbekistan).

***Kitabobactrites salimovae* gen. et sp. nov.**
Figure 9A, B, E, G, 10B

2010 Gen. aff. *Cyrtobactrites* n. sp. – Becker et al. 2010, p. 21, Figs. 2.3. 2.4

Holotype. – The holotype PIMUZ 31317 is a whorl fragment showing growth lines and remains of an associated *Gyroceratites* as well as small orthocerids.

Type horizon and locality. – *Polygnathus inversus* conodont Zone, early Emsian, Khodzha Kurgan Gorge, Kitab State Geological Reserve (Uzbekistan).

Material. – Eight slabs (PIMUZ 31318 to 31323) with a total of 18 whorl fragments between 6 and 59 mm are available. KDB also examined the material published by Becker et al. (2010).

Etymology. – Honoring the great support of Firuza Salimova (Tashkent) and her ongoing research on Palaeozoic stratigraphy in Uzbekistan.

Diagnosis. – Cross section probably laterally flattened and with ventrolateral edges accompanied by two furrows and a ventral band. Ribs weak or absent;

Description. – Both the embryonic shell and the terminal aperture are unknown. Nevertheless, based on comparisons with probably closely related forms and the distinct decrease in curvature of specimens with a whorl height of 1 to 2 mm (PIMUZ 31318, 31319, 31323) to such with a whorl height of 10 mm (PIMUZ 31318, 31320; whorl height measured in the flattened state), it appears plausible to conclude that the mature conchs did not grow larger than 100 mm in diameter. Based on our material, it is not possible to judge whether the shell completed one whorl or not. Because of the flattened preservation, it is also not possible yet to reconstruct the whorl cross section. The presence of a strong ventrolateral projection of the growth lines in combination with two well-developed ventrolateral furrows and a ventrolateral ridge (PIMUZ 31317; Fig. 9E) suggest that the shell was, at least in middle and late growth stages, suboval and more or less laterally compressed, possibly with a more or less tabular venter. The characteristic ventrolateral ridges and furrows appear probably stronger than in three-dimensional preservation, because *Gyroceratites* from the same strata displays a similarly preserved ventrolateral structure.
Only in some spots, small parts of growth lines or lirae can be seen, allowing the conclusion that a deep lateral sinus, a high and narrow ventrolateral projection and a deep ventral sinus were present. Most of the larger fragments (e.g., PIMUZ 31320, Fig. 9G) show a fine dorsal crenulation. This crenulation displays about 2 folds per millimeter in the larger specimens (wh ca. 10 mm), which fade out from the dorsum to the flanks. It is very irregular and differs in orientation between specimens. Thus, we interpret this feature as being of partially taphonomic origin (compaction), although it likely originated from growth lines or lirae. The holotype PIMUZ 31317 (Fig. 9E), however, shows the ventrolateral salient well and also that the dorsal crenulation leads into structures turning adapically, i.e. into a lateral sinus (wh ca. 9 mm). In some places, a very weak ribbing is

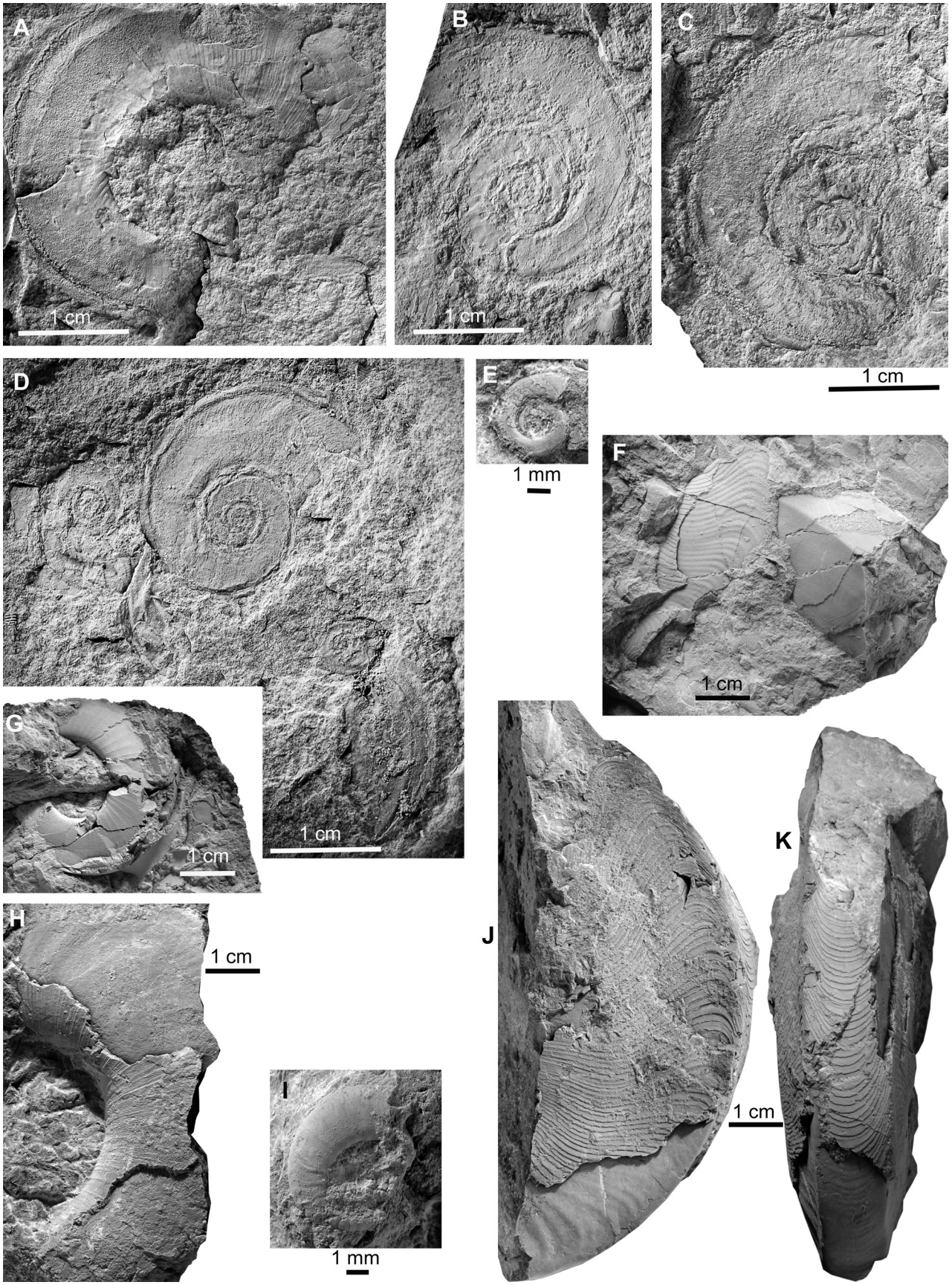
A
1 cm
B
1 cm
C
1 cm
D
1 cm
E
1 mm
F
1 cm
G
1 cm
H
1 cm
I
1 mm
J
1 cm
K

Figure 8. Ammonoids (Mimoceratidae Steinmann, 1890 and Mimagoniatitidae Miller, 1938) from the early Emsian Dzhaus Beds. • A-E – *Gyroceratites laevis* Eichenberg, 1931, mostly flattened specimens, associated with bivalves and bactritids, Khodzha Kurgan Gorge. • A – PIMUZ 31357, large specimen with strong lirae, distinct ventrolateral furrow and external band. The wholes on the flanks might be of diagenetic origin or Housean pits. Note the mature crowding of lirae at the terminal aperture; KKG 43. • B – PIMUZ 31358, shows traces of the septa; KKG 40. • C – PIMUZ 31359, well-preserved aperture. • D – PIMUZ 31360, big, medium and small specimen associated with *Kitabobactrites salimovae* gen. et sp. nov.; KKG 49m. • E – PIMUZ 31361, 3D-preserved juvenile specimen; KKG 23F. • F-K – *Mimagoniatites fecundus* (Barrande, 1865). • F – PIMUZ 31362, two fragments showing lirae (left) and the tabular venter with angular edges (right). • G – PIMUZ 31363, preadult whorl showing lirae. • H – PIMUZ 31364, fragmentary body chamber showing the moderately wide umbilicus. • I – PIMUZ 31365, part of the neanoconch. • J, K – PIMUZ 31366, adult body chamber with strong lirae.

detectable (Fig. 9).
Only very faint traces of the sutures are visible in specimen PIMUZ 31319 (Fig. 9A top right). These traces reveal an asymmetric lateral lobe that has its steeper side dorsally. The presence of a ventral lobe is likely, but it is not visible.

Remarks. – The overall shell geometry of the new genus is intermediate between *Cyrtobactrites* and *Metabactrites*. The very faint ornament is quite untypical for the earliest ammonoids and so is the growth line course and thus the aperture shape of *Kitabobactrites*. In fact, the growth line course is close to that of members of the genus *Gyroceratites*.
This raises the question whether *Gyroceratites* developed from forms like *Kitabobactrites*, thus implying that coiling evolved twice independently at the transition from bactritids to ammonoids. This would not be so surprising because coiling evolved independently many times in the course of cephalopod phylogeny (e.g., Kröger 2005, Kröger et al. 2011). This phylogenetic hypothesis is supported by the presence of "Ritzstreifen" and similar wrinkle layer (see review and references in Korn et al. 2014) in, e.g., *Devonobactrites* and *Gyroceratites*, the growth line course with the strong ventrolateral salient, the presence of a ventral band (Korn 2014 and references therein), and the broad range of umbilical window sizes in *Gyroceratites* (e.g., De Baets et al. 2012a, 2013b). Nevertheless, the alternative hypothesis that *Gyroceratites* is the sistergroup of *Lenzites* and forms a monophylum with *Chebbites* and *Gracilites* is corroborated by, e.g., the rather smooth morphologic transitions with respect to shell shape and the evolution of the particular growth line course (e.g., Korn 2001, Klug et al. 2015, but see Aboussalam et al. 2015).

Occurrence. – Only from the early Emsian of the Kitab State Geological Reserve (Uzbekistan).

Subclass Ammonoidea Zittel 1884
Order Agoniatitida Ruzhencev, 1957
Suborder Agoniatitina Ruzhencev, 1957
Superfamily Mimosphinctoidea Erben, 1953
Family Mimosphinctidae Erben, 1953
Subfamily Anetoceratinae Ruzhencev, 1957

Genus *Ivoites* De Baets, Klug & Korn, 2009

Type species. – Anetoceras hunsrueckianus Erben, 1960.

Ivoites meshchankinae sp. nov.
Figure 11E-G

1976 *Anetoceras* (A.) cf. *Hunsrueckianum* Erben, - Chlupac, p. 304-305. Text-fig. 3b
1983 *Anetoceras* (*Teneroceras*) cf. *hunsrueckianum* Erben, - Chlupac and Turek, p. 19-20, pl. 1, fig. 11, pl. III, figs 3-7
2010 *Ivoites* cf. *hunsrueckianum* Erben. - Becker et al., text-fig. 2,5

Holotype. – The holotype is a well-ornamented demi-whorl (PIMUZ 31348; Fig. 11G). We designate the specimen figured by Becker et al. (2010: fig. 2.5; Münster No. XX), a three-dimensional preserved whorl fragment from Shirdag (PIMUZ 31347; Fig. 11F) and specimens associated on the slab with the holotype (Fig. 11E) as syntypes, which show the changes in coiling and ornamentation throughout ontogeny well.

Type horizon and locality. – *Polygnathus inversus* conodont Zone, early Emsian, Khodzha-

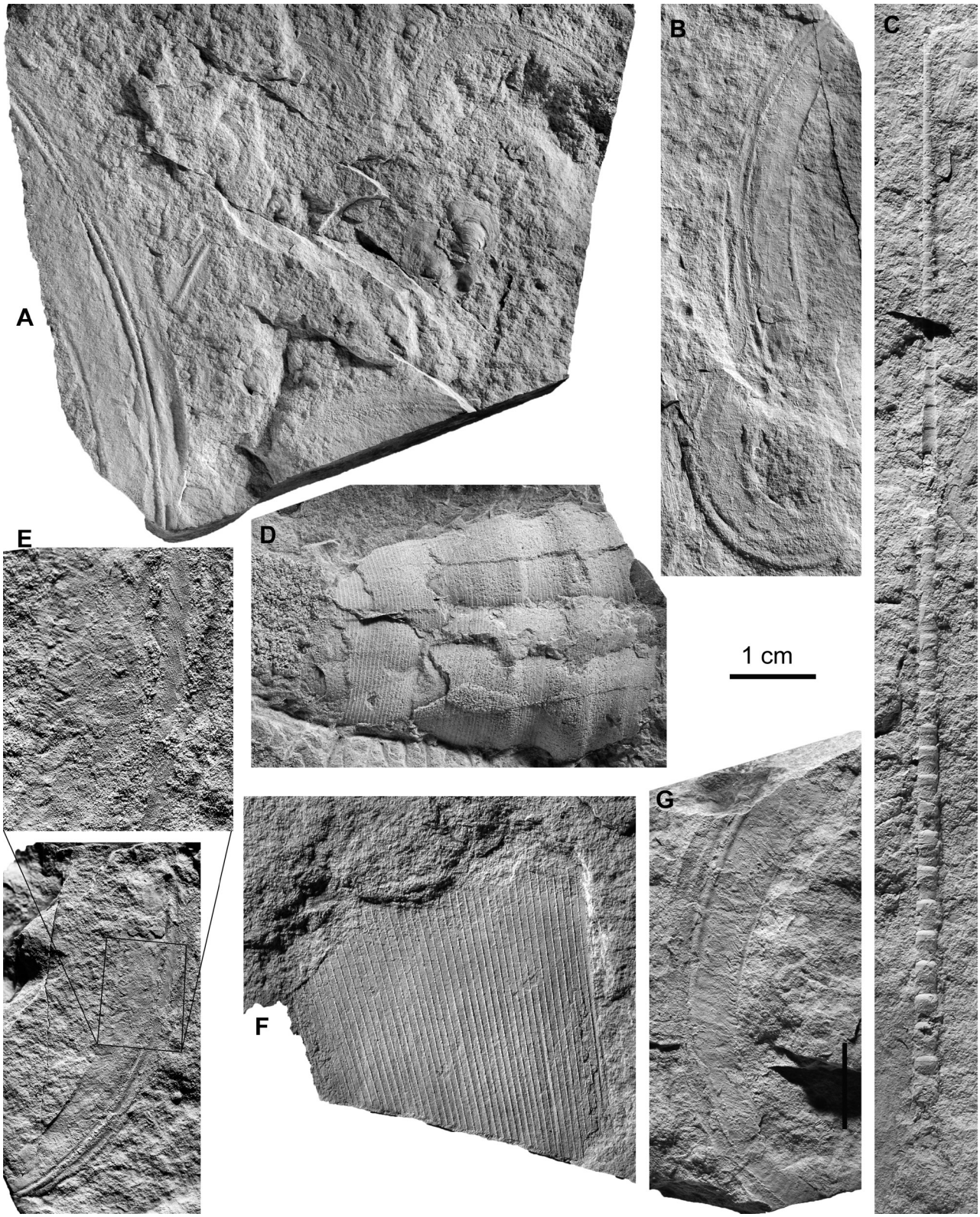

Figure 9. Cephalopods from the early Emsian Dzhaus Beds. • A, B, E, G – *Kitabobactrites salimovae* gen. et sp. nov. • A – PIMUZ 31318, incomplete remains of various growth stages of six *Kitabobactrites salimovae* gen. et sp. nov. Note the more strongly curved early part (top right and left above the center) and the cyrtoconic later part (left and bottom) of the shell. Associated bivalves (probably ligament preserved at burial). Khodzha Kurgan Gorge, KKG 88. • B – *Kitabobactrites salimovae* gen. et sp. nov. (top) associated with *Gyroceratites* cf. *laevis*, PIMUZ 31317, holotype, Khodzha Kurgan Gorge, KKG 88. C – Orthocerida indet., PIMUZ 31345, Khodzha Kurgan Gorge, KKG 33m. D – *Orthocycloceras* sp., PIMUZ 31344, Yusupkul, YUS2CK. E – *Kitabobactrites salimovae* gen. et sp. nov., PIMUZ 31317, holotype, Khodzha Kurgan Gorge, KKG 88. F – Kionoceratidae indet., PIMUZ 31320, Khodzha Kurgan Gorge, KKG 88.

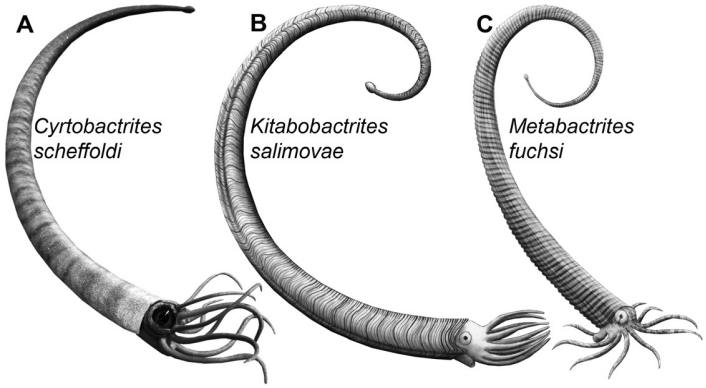

Figure 10. Reconstructions of some coiled bactritids (A, B) and an early ammonoid (C) from the early Emsian. • A – Plastic model made by Beat Scheffold (Zürich) of *Cyrtobactrites scheffoldi* Klug et al., 2008; Tafilalt, Morocco. • B – Reconstruction of *Kitabobactrites salimovae* gen. et sp. nov. (Khodzha Kurgan Gorge, Uzbekistan) based on various whorl fragments including the holotype. The shell completes one whorl, but the aperture and ornamentation resembles other bactritids. • C – Reconstruction of *Metabactrites fuchsi* De Baets et al., 2013b, modified after De Baets et al. (2013), Hunsrück (Germany).

Kurgan gorge, Kitab State Geological Reserve (Uzbekistan).

Material. – In total, 5 whorl fragments from Uzbekistan: Holotype PIMUZ 31348 and two associated syntypes as well as syntype PIMUZ 31347 were collected at Shirdag, syntype Münster No. XX is from Khodzha Kurgan Gorge. Additionally, 31 isolated whorls and fragments flattened in shale as well as an internal mould in limestone from Bohemia (Chlupáč and Turek 1983).

Etymology. – In honour of Natalya Meshchankina (Tashkent), who supported us in the field and for her ongoing research on Palaeozoic stratigraphy in Uzbekistan.

Diagnosis. – small-sized Ivoites (up to 40 mm) with dense ribbing (up to 60 ribs per demi-whorl; ARI10: 33 at wh of 2.1 mm to 17 at 4.1 mm) and uncoiling into the cyrtoconic phase at at diameter around 15 mm; gently curved initial whorl segment and nearly straight terminal shaft; shallow ribs on the juvenile conch and strong, narrowly spaced ribs on the terminal shaft.

Description. – The holotype PIMUZ 31348 has a maximum diameter of about 15.5 mm and a maximum height of 3.6 mm, which becomes less curved towards the aperture. The ribs are rursiradiate and form a gentle dorsal projection and a shallow ventral sinus. There are 58 fine ribs per demi-whorl with ARI10: 30 at the apical end to ARI10: 17 at the apertural end.

Syntypes associated with the holotype are more curved, have a smaller maximum whorl height (wh: 3.3 and 3.4 mm) and a more dense ribbing (ARI10: 29-26) suggesting they represent fragments of specimens, which are yet to uncoil into a straighter shaft.

Syntype PIMUZ 31347 is a 15 mm long three-dimensionally preserved fragment with a maximum height of 4.1 mm, which is less curved than the holotype. It shows a distinct change in curving towards the end, thus suggesting it forms part of the terminal shaft. The whorl cross section is, as far as it is exposed, suboval. The ribs are more densily spaced at the apical end (ARI10: 21 at wh: 3.1 mm) than at the apertural end (ARI10: 17 at wh: 4.1 mm).

Syntype Münster XX comprises a quarter whorl that measures 20 mm across and covers an increase in whorl height from 3.3. to 5.6 mm. Accordingly, this only represents the transition to terminal uncoiling/shaft stage. The rib course is rursiradiate with gently curved lateral portions. The rib spacing decreases from ARI10: 25 to ARI10: 18. Overall, this specimen strongly resembles syntypes associated with the holotype PIMUZ 31347, but it is slightly more strongly curved (i.e., it shows the beginning of the shaft).

Fragments L17716 and L17717 from Bohemia have low maximum whorl height (2,3 and 2,4 mm), are more curved and have a high rib spacing (ARI10: 30 and ARI10: 25) suggesting they represent earlier ontogenetic stages.

Early demi-whorl (negative counterpart; ICh6837) with a maximum wh of about 2,1 mm and maximum diameter of about 12.5 mm is finely ribbed throughout. They initial part with whorl height of about 0,5 mm is still ribbed, but probably starts close to the end of the embryonic shell. The specimen is densily ribbed with about 60 ribs per demi-whorl at 12.5 mm to 59 ribs per demi-whorl or ARI10: 33 ribs at a dm of 10 mm.

Specimen ICh5167 from Bohemia shows the transition from the more coiled part starting with

a wh = 2.1 mm to the shaft ending at a wh = 4.2. It has already 60 ribs at its maximum diameter (which completes less than a half-whorl) and a corresponding ARI10 of 18 (or ARI5 of 9).

Specimen ICh5405 measures about 10 mm across and probably represent a fragment before the uncoiling into the shaft (max. wh: 2,5 mm). It has a ARI10 of 29 ribs which is consistent with this interpretation.

Remarks. – None of the specimens displays the earliest ontogeny (initial chamber missing) or the suture lines. Based on the overall conch morphology and ornamentation, the material can be assigned to Ivoites and it appears plausible to assume that its early ontogeny and suture resembles that of other species.

Our specimens are more tightly coiled and more densily ribbed (about 60 ribs per half whorl at 10 to 15 mm dm) than the type species *I. hunsrueckianus* and most other species of *Ivoites* (*I. medvezhensis*, *I. opitzi*, *I. schindewolfi*, *I. tenuis*) as revised by De Baets et al. (2013b). They are also more densily ribbed than *M. rakhmonovi*. *I. meshchankinae* is most similar in coiling to specimens of *I. tangdingensis* from China, but our specimens are more densily ribbed and the Chinese specimens do not show such a pronounced terminal shaft – although the latter could be a collection artefact.

Occurrence. – The species is known from the the early Emsian of the Kitab State Geological Reserve (Uzbekistan) as well as from Bohemia (previously described as *I.* cf. *hunsrueckianus*). They are most common in the *elegans* Zone, but the species can range from the *barrandei* to the lower part of *cancellata* dacryoconarid Zone in Uzbekistan. In Bohemia, they have so far only been confidently reported from the *elegans* Zone – although a specimen deriving from the Zlichov Limestone could potentially be older (Chlupáč and Turek 1983).

Genus *Metabactrites* Bogoslovsky, 1972

Type species. – *Metabactrites formosus* Bogoslovsky, 1972 by original designation.

Metabactrites rakhmonovi sp. nov.

Figure 11I

2010 ?*Metabactites* n. sp. – Becker et al. 2010, p. 21-22. Fig. 2.6

2011 loosely coiled anetoceratid – Monnet et al. 2011b, Fig. 3E

Holotype. – The holotype is specimen PIMUZ 31350 (Fig. 11I). We designate the specimens figured by Becker et al. (2010: fig. 2.6; Münster No. XX) and well-ornamented whorl fragment (PIMUZ 28869) already published earlier by Monnet et al. (2011b: fig. 3E) as syntypes.

Type horizon and locality. – *Polygnathus inversus* conodont Zone, early Emsian, Shirdag, Kitab State Geological Reserve (Uzbekistan).

Material. – In total 3 whorl fragments: Holotype PIMUZ 31350 and syntype PIMUZ 28869 were collected at Shirdag, syntype Münster No. XX is from Khodzha Kurgan Gorge.

Etymology. – In honour of Utkir J. Rakhmonov (Shahrisabz), who put so much effort into keeping the Kitab State Geological Reserve and the regional research there running, but of course also to show our great appreciation of his warm-hearted hospitality and selfless help during our visits.

Diagnosis. – Metabactrites with gently curved initial whorl segment and nearly straight terminal shaft, shallow, narrowly space ribs setting in on the juvenile conch (ARI5: 9-7) and strong, less narrowly spaced ribs on the terminal shaft (ARI5: 6).

Description. – The holotype PIMUZ 31350 is a 12 mm long and 2.5 mm wide fragment, which is much more distinctly curved than the syntype PIMUZ 28869. The cross section can also be reconstructed as being suboval. The ribs are nearly invisible near the apical end of the fragment (wh ca. 1.6 mm) and become increasingly sharp towards the apertural end of the fragment (ARI5: 7; ARI10: ~ 15).

The syntype PIMUZ 28869 is a 17 mm long and 5.5 mm wide fragment, which is hardly curved (ARI5: 6; ARI10: 10-12). The whorl cross section

is, as far as it is exposed, suboval. The ribs are rursiradiate and form a gentle dorsal projection and a shallow ventral sinus. There are 19 strong ribs distributed over a length of 17 mm.

Syntype Münster XX is half a whorl that measures 10 mm across and covers an increase in whorl height from 1 to 2.5 mm. Accordingly, there is only a very short whorl fragment and the protoconch missing apically. As in the other syntype, the adapical conch part does not reveal ribs (ARI5: 9; ARI10: ~ 21); these develop more or less in the middle of the fragment at a whorl

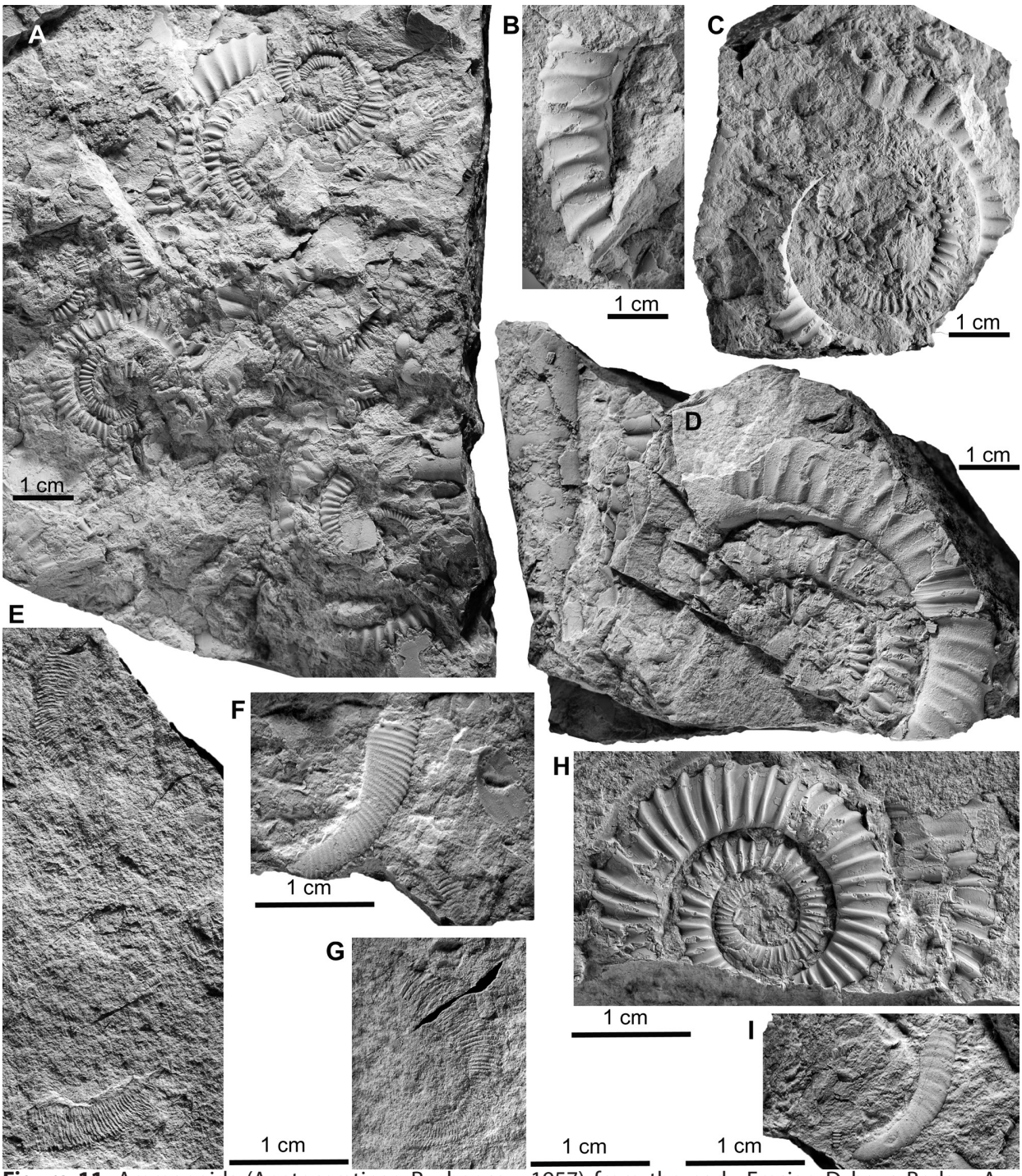

Figure 11. Ammonoids (Anetoceratinae Ruzhencev, 1957) from the early Emsian Dzhaus Beds. • A – *Erbenoceras kimi* Bogoslovsky, 1980, associated with orthocerid remains and gastropods, PIMUZ 31324, Yusupkul, YUS02CK. • B, C – *Erbenoceras advolvens* (Erben, 1960), PIMUZ 31375, Shirdag, Kim's section, KS92. • D – *Erbenoceras kimi* Bogoslovsky, 1980, PIMUZ 31346, Yusupkul, YUS01KDB. • E-G – *Ivoites meshchankinae* (Erben, 1960). • E, G – PIMUZ 31348, Khodzha Kurgan Gorge, KKG 107. • F – PIMUZ 31347, Shirdag, SHK3A. • H – *Erbenoceras kimi* Bogoslovsky, 1980, PIMUZ 31349, Yusupkul, YUS01KDB. • I – *Metabactrites rakhmonovi* sp. nov., PIMUZ 31350, holotype, Shirdag, SHK3A.

height of ca. 1.8 mm. The rib course is rursiradiate with shallow dorsal and ventral sinuses and gently curved lateral portions. Overall, this specimen strongly resembles syntype PIMUZ 31350, but it is more strongly curved and represents the smallest known (probably the youngest) individual.
None of the specimens displays the suture lines. Based on the overall conch morphology and ornamentation, the material can be assigned to Metabactrites and it appears plausible to assume that its suture resembles that of the type species.

Remarks. – Conch geometry, rib course, rib spacing, and ontogenetic changes allow the assignment to the genus *Metabactrites*. The type species *Metabactrites formosus* has less densily spaced ribs while *M. fuchsi* has more densely spaced ribs as measured by the rib index. M. fuchsi appears to have a slight lateral sinus in the ribs, absent in the new species (De Baets et al. 2013b). Also, ribbing begins already at a whorl height below 1 mm, where the conch of *M. rakhmonovi* sp. nov. is still smooth. *M. formosus* does not seem to show a tendency to form a shaft as straight as in the new species.

Occurrence. – Only from the early Emsian of the Kitab State Geological Reserve (Uzbekistan).

Subfamily Mimosphinctinae Erben, 1953

Genus *Beckeroceras* gen. nov.

Type species. – *Erbenoceras khanakasuensis* Yatskov, 1990 by subsequent designation.

Definition. – A mimosphinctin without imprint zone, a low whorl expansion rate (1.6 to 2.1) and a dorsal saddle.

Etymology. – In honor of Ralph Thomas Becker (Münster) and his enormous contribution to research on Devonian stratigraphy worldwide. Also, he suggested to introduce this genus already earlier (Becker et al. 2010) and kindly allowed us to complete this mission.

Included species. – Only the type species.

Remarks. –The genus *Mimosphinctes* used to be characterized by advolute to very evolute shells with bi- or trifurcating rursiradiate ribs. Depending on the absence or presence of an imprint zone, a dorsal lobe developed or not. In the new genus (Fig. 12C, D, F), we include all forms with coarse bi- or trifurcating rursiradiate ribs lacking an imprint zone and a dorsal lobe (compare Becker et al. 2010: p. 20). From a phylogenetic point of view, the now more narrowly defined genus *Mimosphinctes* represents the more derived state due to its tighter coiling and the evolution of a dorsal lobe. This raises the question for the phylogenetic framework. Korn & Klug (2002) included the genera *Chebbites*, *Talenticeras*, and *Mimosphinctes* in the Mimosphinctinae; according to Korn (2001: fig. 8), the Mimosphinctinae would thus be paraphyletic. When looking at the shell geometry, ornamentation and suture lines, great similarities between *Mimosphinctes* and *Erbenoceras kimi* become visible. Notably, *Erbenoceras kimi* is more or less advolute and sometimes, ribs might bifurcate. In this context, one would expect an evolutionary trend towards tighter coiling, but at least the last whorl of *Talenticeras* is less tightly coiled than in *Erbenoceras kimi* or *Beckeroceras*. With our current knowledge, we cannot resolve this contradiction entirely, but we suggest that Talenticeras might be part of a different lineage.

Occurrence. – Dzhaus Beds (Emsian), Zeravshan (Uzbekistan).

Genus *Uzbekisphinctes* gen. nov.

Type species. – *Teicherticeras* (Convoluticeras) *rudicostatum* Bogoslovsky, 1980 by subsequent designation.

Diagnosis. – Mimosphinctin with an imprint zone, a low whorl expansion rate (1.7 to 2.5), a dorsal saddle and a great number of fine secondary ribs.

Etymology. – After Uzbekistan, which hosts the Kitab State Geological Reserve, where the types species was described and figured on a stamp.
Included species. –
discordans: *Convoluticeras discordans* Erben, 1965: p. 300, Daleje Shale, Bohemia (Czech

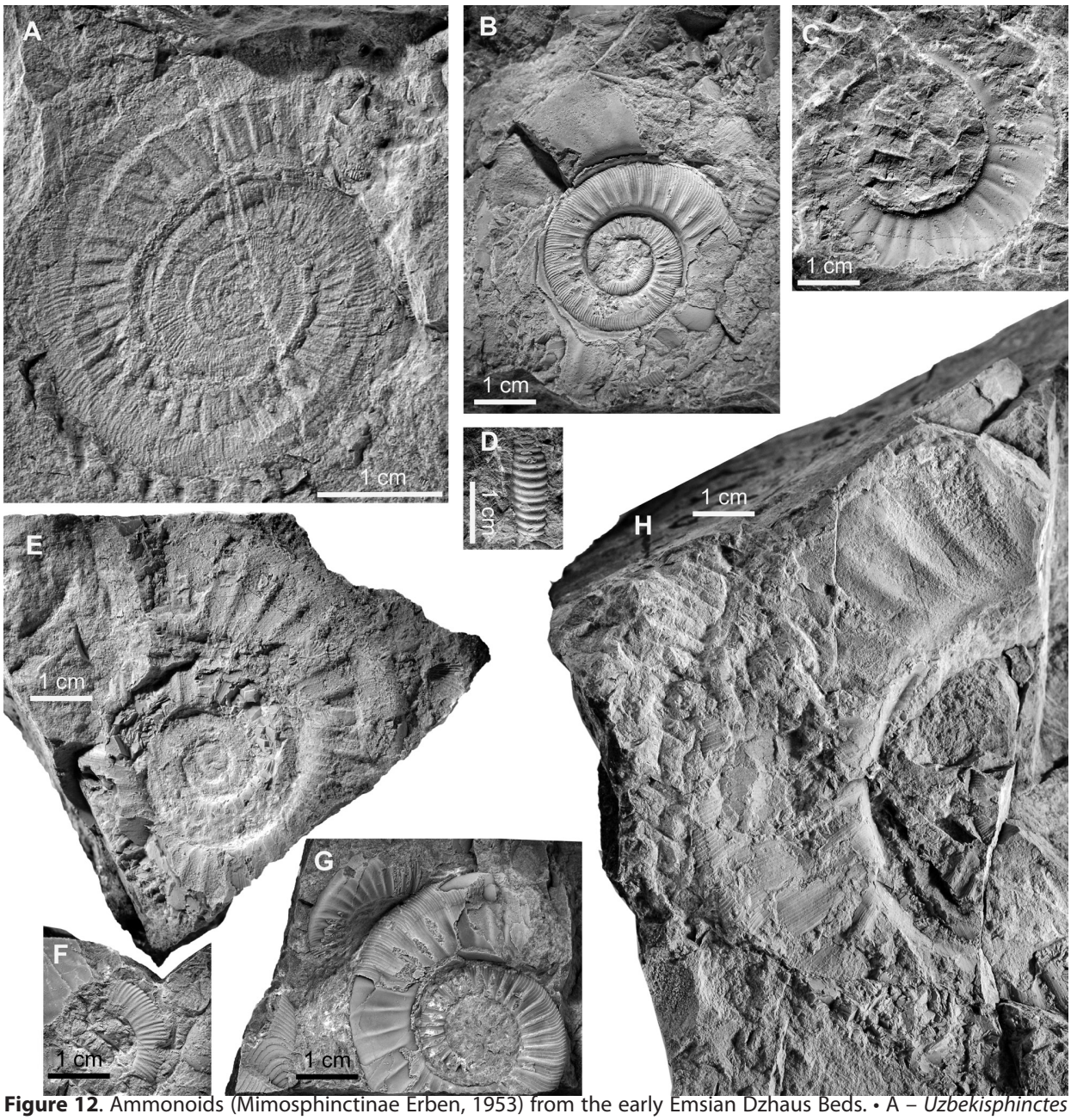

Figure 12. Ammonoids (Mimosphinctinae Erben, 1953) from the early Emsian Dzhaus Beds. • A – *Uzbekisphinctes rudicostatus* gen. nov. Bogoslovsky, 1980, PIMUZ 31351, flattened specimen, associated with large orthocerids, Khodzha Kurgan Gorge, KKG 105. • B – *Uzbekisphinctes rudicostatus* gen. nov. Bogoslovsky, 1980, PIMUZ 28595, specimen with sublethal injury, Khodzha Kurgan Gorge, bed 48, *Polygnathus inversus* Zone, KKG 48 m (reproduced from De Baets et al. 2011). • C – *Beckeroceras khanakasuensis* gen. nov. (Yatskov, 1990), PIMUZ 31352, Shirdag, SHK3A. • D – *Beckeroceras khanakasuensis* gen. nov. (Yatskov, 1990), PIMUZ 31353, fragment showing ventral ribbing, Shirdag, SHK3A. • E – *Uzbekisphinctes rudicostatus* gen. nov. Bogoslovsky, 1980, PIMUZ 31354, slightly deformed specimen, Khodzha Kurgan Gorge, bed 49m, *Polygnathus inversus* Zone. • F – *Beckeroceras khanakasuensis* gen. nov. (Yatskov, 1990), PIMUZ 31355, Shirdag, SHK3A. • G – *Uzbekisphinctes rudicostatus* gen. nov. Bogoslovsky, 1980, PIMUZ 31356, Khodzha Kurgan Gorge, bed 38m, *Polygnathus inversus* Zone. • H – *Uzbekisphinctes rudicostatus* gen. nov. Bogoslovsky, 1980, PIMUZ 31357, very large deformed specimen, Khodzha Kurgan Gorge, *Polygnathus inversus* Zone, KKG 103.

Republic); *rudicostatus*: *Teicherticeras* (*Convoluticeras*) *rudicostatum* Bogoslovsky 1980: p. 58,Dzhaus Beds, Zeravshan (Uzbekistan); primigenitus: *Teicherticeras primigenitum* Erben, 1965: p. 284, Middle Kaub Formation, Hunsrück (Germany).

Remarks. – Typical *Mimosphinctes* (like the type species *M. tripartitus*) with an imprint zone have coarse bi- or trifurcating rursiradiate ribs, while the specimens included in *Uzbekisphinctes* have also an imprint zone, but much finer intercalated ribs and higher degree of coiling (Fig. 12A, B, E, G,

H). The groups have already been individualized by other authors (Becker et al. 2010; De Baets et al. 2013b; Klug 2017). When looking at shell geometry, ornamentation and suture lines, great similarity exist between *U. discordans* and *U. rudiscostatus*. The holotype of "*Mimosphinctes*" *primigenitus* also has finely ribbed secondaries and is very similar in the characters, which are present in this genus (De Baets et al. 2013b). Some specimens attributed to M. erbeni (auct.) from Uzbekistan (Bogoslovsky 1980) and *M. tenuicostatus* from the Northern Urals (Bogoslovsky 1963) also have finer intercalated ribs, but these species are typically more evolute and have a higher primary rib to secondary rib ratio (Klug 2017). From a phylogentic point of view, the now more narrowly defined genus *Uzbekisphinctes* represents the more derived state within Mimosphinctidae due to its tighter coiling, the evolution of a dorsal lobe as well a larger amount of fine secondary ribs. Beckeroceras lacks an imprint zone, has more loosely coiling without an imprint zone and shows differences in ornamentation including coarser primaries and less fine secondaries.

Occurrence. – *U. rudicostatus* is so far only known from Uzbekistan. *U. discordans* has been reported from Bohemia in the Czech Republic, the Rhenish Mountains in Germany and Guangxi in South China (Ruan 1981, 1996; Yu and Ruan 1988). Well-dated specimens derive from the elegans to *cancellata* Zone of China (Yu and Ruan 1988) and Uzbekistan. *U. rudicostatus* can also range into the upper part of the barrandei Zone (Becker et al. 2010). The range of the Hunsrück Slate ammonoid fauna containing M. primigenitus into the barrandei and *elegans* Zone (De Baets et al. 2013b) would also be compatible with known ranges of *Uzbekisphinctes* in other regions.

Discussion

The transition from the 1000 m thick massive platform carbonate of the Madmon Formation (Lochkovian, Pragian; Yolkin et al. 2008) via neritic limestones with brachiopods and reef-debris of the Khukarian (Pragian), Zinzilban and Norbonak Beds (both earliest Emsian in the current GSSP sense; Yolkin et al. 2008) to Emsian pelagic limestones with dacryoconarids and ammonoids (Dzhaus Beds) in a less than 250 meter thick interval suggests a quite rapid change of the palaeoenvironmental settings in this area. We were interested in this transition from a more neritic (late Pragian) to a more pelagic facies (early Emsian), which evolved before the onset of the ammonoid assemblages in this area. In this context, we therefore aimed to better understand the involved regional geological processes. In the following, we discuss the facies changes that occurred during the Pragian and early Emsian and possible interpretations.

Late Pragian – Bursykhirman

The presence of both shallow-water benthic reef-builders and dacryoconarids, a group assumed to have been pelagic (Bouček 1964, Berkyová et al. 2007, Wittmer & Miller 2011), locates the palaeo-position of the studied deposits in the neritic zone of an open-marine-shelf in the fore-reef area (compare Botquelen et al., 2001, Machel and Hunter, 1994). Indeed, the occurrence of these fossil groups with such different living habitats, suggest a connection with the open marine environment. The lower part of this section is dominated by massive peloidal limestones containing fossils of reef-builders such as tabulate corals and brachiopods suggesting a moderately high level of energy in a shallow marine environment. This carbonate factory was likely located on an open-shelf, still above the storm-wave-base (SWB; compare Machel and Hunter 1994 for the Middle to Late Devonian). From meter 75 to about 100, the changing facies documents a change towards deeper water with pelagic conditions as corroborated by the increasing abundance of dacryoconarids. They are not current-aligned and their chaotic orientation suggests still a moderately high level of energy. This would suggest a paleodepth near the SWB. In parallel, the siliciclastic content slightly increased.

In this context, the question arises how the carbonate platform growth came to its end. Classically, such settings where platform carbonates are conformably overlain by pelagic

sediments were interpreted as 'platform drowning' (see table. 1 in Schlager 1981). As convincingly explained by Schlager (1981), it is quite unlikely that subsidence rates exceed the growth rates and sediment accumulation rates of reefs and carbonate platforms. Schlager (1981: p. 208) listed two main causes for platform drowning: (1) "Reduction of benthic growth due to environmental stress" (by salinity drops or rapid drift to higher latitudes) or (2) "rapid pulses of relative sea-level". Alternatively, platform growth might have been inhibited by its emergence due to a regression or tectonic uplift. A subsequent transgression can then bring a sequence of neritic and eventually pelagic platforms, because the main carbonate producers were regionally erased.

Evidence for environmental stress is lacking, since many carbonate-producing benthic faunal elements existed before and after the main facies change; also, evidence for salinity drops or rapid drift to higher latitudes are missing as well. By contrast, a global sea-level rise occurred, e.g., during the Pragian and earliest Emsian (e.g., Haq & Schutter 2008). Whether these transgressive pulses were strong and rapid enough to cause a platform drowning cannot be decided based on our information.

Also, we did not find evidence for a temporal emergence of the Madmon Formation-carbonate platform; a more detailed survey of the transition between the Madmon Formation and the Khodzha Kurgan Formation (i.e. between the Khukarian and the Zinzilban Beds) might shed more light on the involved processes. It is thus unclear whether the transgressions that occurred from the time of deposition of the Khukarian Beds to the Zinzilbanian Beds documented in our section caused the cessation of platform growth or not. Reef-building organisms still occur in the beds between meter 100 and 138, but for some reason not in a sufficient number to resume platform growth. Remarkably, the transition from neritic to pelagic fine-grained sediments with a thin interval containing phosphatic and iron-oxide elements in between suggest a short phase of non-deposition or at least low sediment accumulation rates, killing off of what remained of the reef fauna .

So how do the regional sea-level changes correlate with global transgressive events (e.g., Johnson et al. 1985, Haq & Schutter 2008)? Even though the Pragian to early Emsian transgressions may correlate with a global transgressive event, we are not entirely certain whether it correlates with the Basal Zlichov Event (House 1996) or, as suggested by Carls et al. (2008), the transgression Ia of Johnson et al. (1985); this partially roots in the need of redefinition of the Pragian-Emsian boundary in Uzbekistan. Nevertheless we found maybe tectonic features both around the boundary between the Madmon and the Khodzha Kurgan Formations (Fig. 13) and towards the end of the section (top of the Khukarian Beds); these structures evoke some uncertainty since parts of the section might be missing.

Figure 13. Top of the Bursykhiman section. 1 – the original picture (person at the bottom part of the picture for scale); 2 – Bed limits marked showing a slight variation of dip, and the possible occurrence of a fault. Older beds are marked in green, younger ones are marked in pink and the possible fault is represented in light blue.

Ammonoid succession and the Daleje Event

Correlation of the sections and bathymetric changes during the Early Devonian

The section Khodzha Kurgan West corresponds to unit 15 of the detailed section in Yolkin et al. (2008). In this section, *Erbenoceras kimi* and (?) *Gyroceratites laevis* (or *G. heinricherbeni*) are the most common species. Yolkin et al. (2008) and Becker et al. (2010) also documented occurrences of *Mimosphinctes tripartitus* and *M. erbeni* (auct.), which we did not find. Nevertheless, *Erbenoceras advolvens*, *Convoluticeras flexuosum* and *Kimoceras lentiforme* are found in this unit.

Concerning the second Khodzha Kurgan section, it represents stratigraphically more or less the continuation of the previous one; the last two meters of Khodzha Kurgan West can be roughly correlated with the first two meters of the Khodzha Kurgan section. This section corresponds to unit 16 (Yolkin et al. 2008). In this section, neither *Mimosphinctes tripartitus* nor *M. erbeni* (auct.) have been found during our investigations – but see Becker et al. (2010) for a summary of previous reports.

In Yolkin et al (2008) and Becker et al. (2010), there is a well-defined turnover in ammonoid taxa around bed 47. Indeed, *Erbenoceras kimi* and *Mimosphinctes tripartitus* disappear almost synchronously when *Mimagonitatites fecundus*, *Convoluticeras flexuosum* and *Uzbekisphinctes rudicostatus* appear. In the subsequent layers, *Uzbekisphinctes rudicostatus* co-occurs with *Gyroceratites laevis* and *M. erbeni* (auct.). This turnover coincides with the appearance of the dacryoconarid *Nowakia cancellata*, which marks the global transgressive Daleje Event (sensu House 1985, Chlupáč and Kukal 1986, House 1996). Transposing this information to our studied section, this ammonoid turnover appears less profound. Even though these three genera range into the late Emsian, it is interesting to see we recorded *Uzbekisphinctes rudicostatus* far below the Daleje Event-interval, while *Mimagoniatites* continues until the top of the section. In this respect, our findings differ slightly from those of Yolkin et al. (2008) and Becker et al. (2010).

Another question is linked with the last occurrence of *Ivoites meshchankinae* sp. nov. In all other sections, where this taxon occurs, it disappears before the *cancellata* Zone, i.e. it became extinct before the Daleje Event. In the Khodzha-Kurgan gorge, it is still present in the lower part of the *cancellata* Zone.

As corroborated by the ammonoid occurrences and the increase clay content (covered interval) above meter 60, the Daleje Event in the Khodzha Kurgan section can be placed approximately here. But it is difficult to clearly define a limit at a specific meter rather than an interval, and this statement has two reasons: First, contrarily to some dramatic rapid transgressions, the Daleje transgressive Event is known to be a long-term gradual event (Carls and Valenzuela-Ríos, 2002). Secondly, this difficulty can be explained by being already in a quite distal location from the coast. Compared to a more proximal platform setting on a slope, which would have been strongly affected by sea-level changes and thereby controlling the facies, the sediments do not show a profound difference and they do not become darker like in some other localities (Chlupáč & Kukal 1988). The facies consists of pelagic limestones throughout the section as reflected in the great abundance of dacryoconarids. After 90 meters, beds displaying irregular surfaces suggest that they maybe formed by sediment gravity flows or slumps. Subsequently, the sediments become a bit darker, suggesting possibly lower oxygen levels. Simultaneously, the fossil content decreases as well. The last two meters of the section contain massive limestone layers, which were probably formed in a more proximal setting compared to the the beginning of the section.

The distribution of ammonoids in Shirdag is different compared to Khodzha Kurgan. Presuming it is correct that the North section starts at the limit Norbonak/Dzhaus Beds, it is unusual for this region that the ammonoid occurrences start with an early presence of *Ivoites meshchankinae* sp. nov., appearing simultaneously with *Erbenoceras kimi*, and even before *Gyroceratites laevis*. Moreover, both species disappear quite early within the first 20 meters. The first occurrence of *Mimagoniatites fecundus* coincides more or less with the last occurrence of *Ivoites meshchankinae*. *Erbenoceras kimi* is still present until 40 meters suggesting this layer being still below the Daleje Event.

Uzbekisphinctes rudicostatus appears late in the section, more or less with *Kimoceras lentiforme*, which is also peculiar since *K. lentiforme* appears early in other sections, suggesting this interval is still below the Daleje Event, too. Speaking about this Event, the most likely position to place it would be between 40 m and 48 m regarding ammonoid occurrences. In the field, we found *Nowakia barrandei* in the interval from 21 m to 35 m, which is consistent with this interpretation. This argument goes in favor of placing the Daleje Event in the upper position, supported by finer grained facies, which is more pelagic than in lower layers.

Evidence for slumping might indicate synsedimentary tectonics; it is unclear to what degree these mass movements have been activated by tectonic movements linked with the closure of the Turkestan Ocean (for references see Loury et al. 2018). The range of other fossils as well as ammonoid assemblages suggests that these sections are not condensed. Furthermore, differences in preservation ranging from crushed fossils in shales to three-dimensionally preserved specimens sometimes hamper comparisons. Nevertheless, some taxa are common while others are rare as they have so far been recovered from beds and samples. At first sight, the ammonoid associations therefore appear somewhat chaotic and it is not straightforward to impose a biostratigraphic sequence. Some authors have even suggested that material from nodules could have been transported down the slope (Ruan 1996), but this might just suggest preservation of different faunas. Concerning the last Shirdag section (South), placing the Daleje Event occurring at around 88-90 meters is better supported by index fossils. The three taxa *Kitabobactrites salimovae*, *Metabactrites rakhmonovi* and *Beckeroceras khanakasuensis* appeared before the Daleje Event. We found *K. salimovae* and Becker et al. (2010) also recorded the other two taxa at Khodzha Kurgan below this event. The microfacies and accompanying faunas could suggest a slightly palaeogeographically-sedimentologically more proximal localization for Shirdag and more distal for Khodzha Kurgan. The poor outcrop quality (tectonized and overgrown) of Yusupkul suggests a more pelagic facies with lower carbonate content (Fig. 14). Additionally, the ammonoid and dacryoconarid fauna place most of this section in the lower part of the Dzhaus Beds below the Daleje Event.

Ammonoid zonation

The ammonoids were initially discovered by A. I. Kim in 1957 and jointly examined with H. K. Erben. Some of these taxa were figured in 1978 as nomina nuda in the Field Guide to the 1978 SDS Meeting by Kim et al. (1978), which also listed their stratigraphic position of

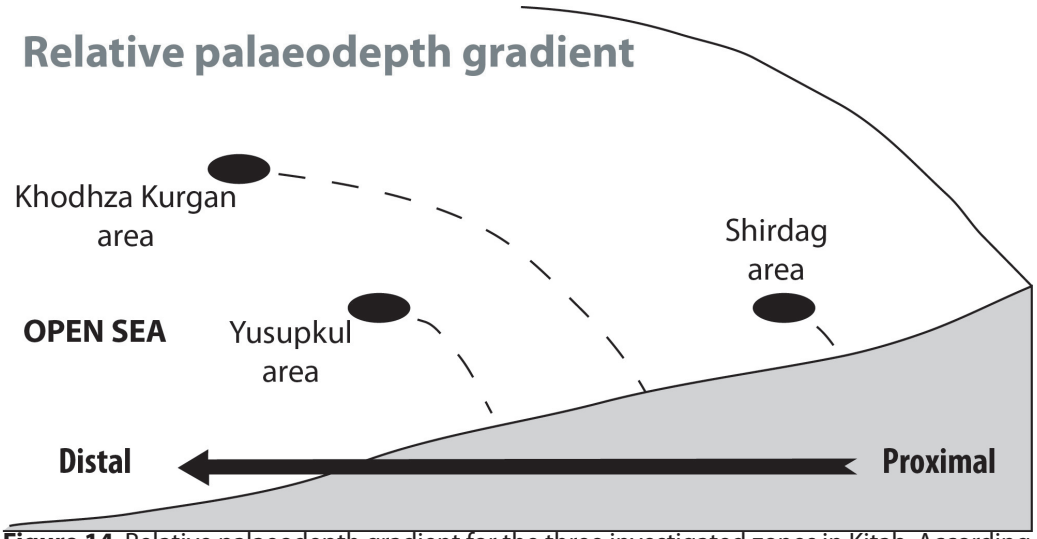

Figure 14. Relative palaeodepth gradient for the three investigated zones in Kitab. According to our data and results, we think that Shirdag had a more proximal position compared to Khodza Kurgan and Yusupkul in a more distal environment.

these samples. These were described in detail by Bogoslovsky (1980, 1984). Some of this material was revised by Yatskov (1990) and Becker et al. (2010) reported some new material discovered and supplemented some of the ranges tabulated in Yolkin et al. (2008). Here, we describe additional material not only from the Khodzha-Kurgan gorge, but from additional sections that we collected during several field trips. In total, 13 taxa have been found in the field. Since Gaurites sperandus has been found only in the Yusupkul section, which is not presented in the synthetic figure (Fig. 4), this taxon has been excluded from the Unitary Association analysis, because it provided one UA itself which was anyway not found in other sections and therefore not useful for correlations.

The ammonoid occurrences of the other 12 taxa have been evaluated employing the Unitary Association method. We found four main Unitary Associations (UAs) in the sampled interval. The taxa included in each UAZ are summarized in Table 1.

The first UA-zone (UAZ 1 – Table 1 and Fig. 4) contains 7 taxa: *Convoluticeras flexuosum, Erbenoceras advolvens*, *Erbenoceras kimi*, *Gyroceratites laevis*, *Ivoites meshchankinae*, *Kimoceras lentiforme*, and *Mimagoniatites fecundus*. *E. advolvens* is the only species characteristic for this UA. This UA is found in all sections except the Khodzha-Kurgan, which is explained by the fact that *E. advolvens* has not been found in this section yet. Nevertheless, it is most likely that the assemblage at the base of the section (ammonoid occurrences of the first 25 meters) belongs to this first UA. Concerning the section Khodzha-Kurgan West, it is likely that the entire ammonoid record is dominated by this UAZ 1, because when correlating this section with the Khodzha-Kurgan section across the stream (less than 100 m apart), it is mostly this lower part that is exposed.

UAZ 2 – Table 1 and Fig. 4 list 7 taxa for this zone as well. It basically consists of the same taxa as UAZ 1 with one exception. *Teicherticeras* cf. *planum* is present and *Erbenoceras advolvens* is absent. As *T.* cf. *planum* has been found in only one bed and in one section, this UA occurs therefore only once throught the sections, and is strictly restricted to the section Shirdag South, around the 67th meter.

UAZ 3 (Table 1 and Fig. 4) comprises 8 taxa including: *Gyroceratites laevis*, *Erbenoceras kimi*, *Convoluticeras flexuosum*, *Mimagoniatites fecundus*, *Ivoites meshchankinae* nov. sp., *Uzbekisphinctes rudicostatus* nov. gen., and *Kitabobactrites salimovae* nov. gen. and sp. *U. rudicostatus* is the index species of this assemblage. UAZ 3 was found in Khodzha Kurgan and Shirdag North sections only. *U. rudicostatus* has not been found in the Shirdag South section. Therefore, the middle part of the section cannot be correlated using this method to any other section.

UAZ 4 (Table 1 and Fig. 4) is the last of the UAZs and was only found in the Shirdag South section. It consists of *Beckeroceras khanakasuensis*, *Erbenoceras kimi*, *Gyroceratites laevis*, *Ivoites hunsrueckianus*, *Kimoceras lentiforme*, *Kitabobactrites salimovae*, and *Metabactrites rakhmonovi*. Thus, this UAZ is not informative for the correlation of our sections. We suspect that this zone is also present in the upper part of the Khodzha-Kurgan gorge as Becker et al. (2010) did recover both *B. khanakasuensis* and *M. rakhmonovi* in their Unit 16 – 28-29 m in the Khodzha-Korgan gorge.

UA	Nspecies	*G. laevis*	*E. kimi*	*E. advolvens*	*C. flexuosum*	*M. fecundus*	*I. meshchankinae*	*K. lentiforme*	*T. planum*	*U. rudicostatus*	*K. salimovae*	*M. khanakasuensis*	*M. rakhmonovi*
4	7	■	■				■	■			■	■	■
3	8	■	■		■	■	■	■		■	■		
2	7	■	■		■	■	■	■	■				
1	7	■	■	■	■	■	■	■					

Table 01. Unitary Associations of the studied sections. Black squares represents the occurrence of the species in the assemblage.

With the available ammonoid-data, this method does not help much with the correlation. It is not entirely clear, whether the low resolution of the correlation could be related to some sampling bias or another cause such as a facies control and synsedimentary tectonics that disturbed the primary order of appearances of ammonoids or the overall stability of ammonoid occurrences in this region or a combination of both that account for this low number of UAZ and the low stratigraphic resolution achieved by ammonoid stratigraphy.

Ammonoid succession and the definition of the Daleje ammonoid turnover

To better understand the ammonoid succession, focusing on the Khodzha-Kurgan gorge makes the most sense as it is provides the most complete Emsian ammonoid record of Uzbekistan (Becker et al. 2010). Comphrehensive sampling of the thick monotonous sequences of Khodzha-Kurgan gorge is a challenge because of fluctuations in fossil abundance, fossil preservation, sedimentary facies and locally unclear tectonic structures. Nevertheless, if we combine our biostratigraphic data from the Khodzha-Kurgan gorge with previous studies and correlate it with the existing dacryoconarid zonation, the picture becomes clearer.

The oldest ammonoids (*Erbenoceras* sp., *Gyroceratites* sp.) in the Khodzha-Kurgan gorge were previously reported from the upper part of the Norbonak beds (Unit 11; Kim et al. 1978); they co-occur with Nowakia zlichovensis and predate the base of the Now. barrandei dacryoconarid Zone (Yolkin et al. 2008, Kim et al. 2012). It might concern *Erbenoceras advolvens* or *E. kimi* and *Gyroceratites* cf. *heinricherbeni*, but given their poor preservation and lack of newly discovered material, it is currently not possible to be sure about their taxonomic assignments.

In other sections, *Erbenoceras kimi*, *Erbenoceras advolvens* and *Gyroceratites heinricherbeni* belong to the oldest ammonoids. Sometimes, they might already be associated with *Ivoites meshchankinae*. Note that previous unfigured reports of *E. kimi* (s.l.) cannot always be taken at face value because two taxa were described as *E. kimi*, which are now assigned to two different genera (*E. kimi*, *Beckeroceras khanakasuensis*) and because some poorly preserved fragments previously attributed to *Erbenoceras kimi* might actually belong to *E. advolvens* – herein reported for the first time from Uzbekistan. *E. advolvens* was occasionally reported as *E.* cf. *solitarium* from the southern Tien Shan (Nikolaeva et al. 2017) and is also known from the Urals (Bogoslovsky 1963, 1969, De Baets et al. 2013b).

In the Zeravshan, the most diverse ammonoid assemblages are known from the Dzhaus beds, mostly covering the *Nowakia barrandei* to the lowermost parts of the *N. cancellata* Zone (Becker et al. 2010, Kim et al. 2012). These provide a unique opportunity to study changes in ammonoid assemblages in layers rich in ammonoids across the Zlichov and Daleje transgressions. House (1985) defined the beginning of the Daleje transgression by the disappearance of auguritids and some mimosphinctids, but regarding biostratigraphic data from Morocco and various other regions (including the type region), these changes might be more gradual (Ferrova et al. 2012, Klug 2017). This is of interest for the definition of the subdivision of the Emsian with proposals ranging for the placement between the *barrandei* and *elegans* Zones (Ferrova et al. 2012, Tonarová et al. 2017, which would correspond to the Zlichov Event according to Aboussalam et al. 2015), to its placement between the *elegans* and *cancellata* Zones (at the traditional Daleje Event: Chlupáč & Kukal 1986, House 1985).

Traditionally, the boundary was linked with the disappearance of the *Anetoceras* fauna (sensu Chlupáč 1976), although the *Ivoites* fauna might be more appropriate as it is probably the only genus which is distributed throughout the entire early Emsian. *Anetoceras*, as revised by De Baets et al. (2009, 2013b), currently comprises coarsely ribbed, gyroconical forms. Finely ribbed, more loosely coiled forms completing fewer whorls are now described as *Ivoites*. Difficulties arise when one tries to verify older unfigured reports of *Anetoceras* as it could concern both finely ribbed *Ivoites* or coarsely ribbed, more tightly coiled *Erbenoceras*. If the disappeareance of the "*Anetoceras* fauna", particularly of representatives of the Anetoceratinae (*Erbenoceras*, *Ivoites*) and Auguritidae (*Celaeceras*, *Kimoceras*), remains an important marker for the subdivision of the

Emsian, the transition from the *elegans* Zone to the *cancellata* Zone is the most important change at least when considering changes in the in ammonoid fauna in the Zeravshan of Uzbekistan. Still, ammonoid taxa traditionally used to date this turnover disappear before this event in the Zeravshan, while other taxa persist into the basalmost *cancellata* Zone (*Ivoites* in the Khodzha-Kurgan Gorge) where *Nowakia elegans* is still reported (Becker et al. 2010).

Peculiarly, there are no marked changes in ammonoid assemblages across the barrandei to *elegans* Zone in the Khodzha-Kurgan gorge. Many taxa cross this boundary including *Mimosphinctes bipartitus*, *M. erbeni* (auct.), and *Uzbekisphinctes rudicostatus*. *Erbenoceras kimi* is the most common taxon while its counterpart *Beckeroceras khanakasuensis* could only be found higher up the sections – above the first occurrence of true *E. kimi* in the *elegans* Zone. *E. kimi* is not restricted to Uzbekistan, but has also been reported from other localities in the South Tien Shan (Bardashev et al. 2005, Nikolaeva et al. 2017). We did not find the association *Kimoceras lentiforme* and *B. khanakasuensis* during our field work in the Khodzha-Kurgan gorge, but it was previously reported from Unit 16 in Becker et al. (2010) allowing to correlate our new in-situ finds in Shirdag with the Khodzha-Kurgan gorge. Both *E. kim*i and *B. khanakasuensis* as well as *K. lentiforme* disappear slightly below the first appearance of *Nowakia cancellata*. In most localities, *Ivoites* and/ or auguritids (*Gaurites sperandus*, *K. lentiforme*) disappear in the basalmost *cancellata* Zone (where there is still an overlap with *N. elegans*), if our correlations with previous dacryoconarid studies are correct in Khodzha-Kurgan (Yolkin et al. 2008, Kim 2011). *Ivoites* might still occur there slightly above the last occurrence of *Nowakia elegans* but disappears before the end of the *cancellata* Zone. *Gyroceratites laevis*, *Uzbekisphinctes rudicostatus* and *Mimagoniatites fecundus* disappear only shortly below the base of the Obisafit beds, but they are still present in the *cancellata* Zone. Ammonoids re-appear above the base of the *richteri* Zone with specimens assigned to *Crispoceras* cf. *crispi* and *Mimagoniatites* cf. *bohemicus* in Unit 31 as well as "*Latanarcestes*" sp. in bed 32 (Kim et al. 1978, Yolkin et al. 2008). The largest drop in diversity therefore corresponds to the transition from the *elegans* to *Nowakia cancellata* Zone in Uzbekistan, which does not correspond to marked changes in facies.

If we project previous findings in our section (KKG with uncertainties) and additional finds from other sections (all sections with uncertainties), this pattern changes very slightly (Fig. 15). Yolkin et al. (2008) reported the last occurrences of coarsely ribbed *Mimosphinctes tripartitus* in the *elegans* Zone, while *M. erbeni* (auct.) is potentially still present lowermost *cancellata* Zone too. A new species has to be erected of the latter as the holotype is probably not conspecific with the Uzbek material (Becker et al. 2010, Klug 2017), but as we did not find additional material we refrained from erecting a new species. A similar pattern is

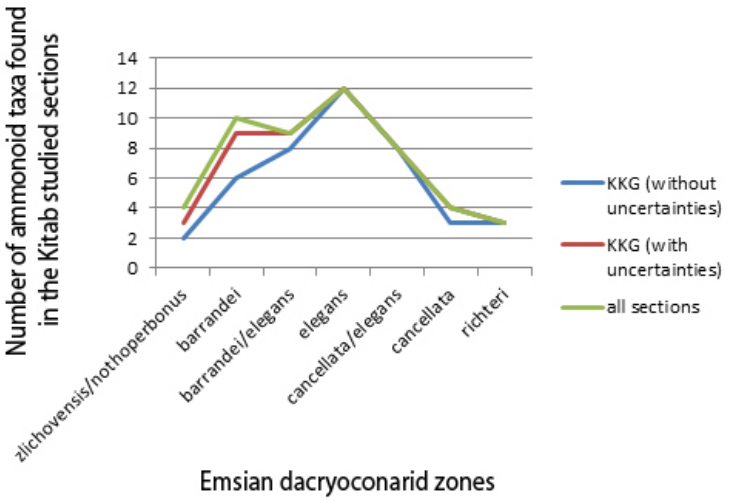

Figure 15. Number of ammonoid taxa in each dacryoconarid zonation (in the Kitab geological reserve).

obtained when we compile previously reported occurrences described from other localities with respect to dacryoconarid zonation. According to an unpublished report and own findings, *Gaurites* co-occurs with *Nowakia barrandei* and disappears before the *elegans* Zone in Yusupkul area and Khodzha-Kurgan. *Erbenoceras kimi* as well as *Beckeroceras khanakasuensis* might be potentially better index species, which disappear before the *cancellata* Zone, while *Ivoites meshchankinae* seemingly only disappears at its base. A stratigraphically very low report by Yolkin et al. 2008 (their Bed 15 – 5m) of *E. kimi*, *M. erbeni* (auct.), *M. tripartitus* and *U. rudicostatus* could not be reproduced. It might correspond to the provenance of the assemblage containing *Teicherticeras planum* (Bogoslovsky 1980), which we did not find during our fieldwork in Khodzha-Kurgan Gorge. We did find specimens of *Teicherticeras* cf. *planum* in Shirdag, which are associated with *G. laevis*, *E. kimi*, *C. flexuosum*, *M. fecundus*, *I. meshchankinae* and *K. lentiforme* and fall into the *barrandei* zone.

The assignments of the ammonoid which are not refigured/restudied are hard to verify as multiple taxa have been confused with one another. For example, some of the specimens previously attributed to *Gyroceratites laevis* might actually represent *G. heinricherbeni* which is more loosely coiled and has a large umbilical window than *G. laevis* (De Baets et al. 2013b), although their separation is hard in poorly preserved specimens when their early ontogeny (and thus the size of the umbilical window) is not preserved. Another issue is the potential confusion of *Beckeroceras khanakasuensis* with *Erbenoceras kimi* (to which some of its type material was previously assigned) or superficial resemblance of poorly preserved specimens of *Mimosphinctes erbeni* (auct.), *Uzbekisphinctes rudicostatus* or *M. tripartitus*.

Some taxa disappear before the last occurrence of *Nowakia elegans*. All in all, major changes and many genera typical for the Zlichovian disappear at the end of the *elegans* to beginning of the *cancellata* Zone in Uzbekistan and beyond. *Gaurites* appears to have a limited stratigraphic range, but *Kimoceras* is more widely distributed and only disappears in the basal part of the *cancellata* Zone in the Khodzha-Kurgan gorge. In other regions, derived auguritids (*Celaeceras*) are still present in the *elegans* Zone in Spain (Montesinos and Garcia-Alcalde 1996) and potentially also in the Barrandian (Chlupáč and Turek 1983). *Gaurites mirandus* might potentially even be present in the basal *cancellata* Zone in the Urals. I*voites meshchankinae* is reported from the *barrandei* Zone to the basalmost *cancellata* Zone. Similarly, small *Ivoites* are thought to be restricted to the *elegans* Zone in China (Ruan 1996) and Bohemia (Chlupáč et al. 1979, Chlupáč & Lukeš 1999).

For the time being, it appears therefore reasonable to keep the Daleje Event (s. str.) as the primary marker for a early/ late Emsian substage boundary, not much lower levels, such as the base of the *nothoperbonus* Zone or the level of the Upper Zlíchov Event, including the base of the *Nowakia elegans* Zone. If the ammonoid turnover remains an important target for its definition, it should be preferentially studied in regions where there is a continuous and diverse ammonoid record without marked facies changes across these events like in South China or Uzbekistan. The Moroccan Anti-Atlas and more traditional regions like the Rhenish Massif or Bohemia are somewhat less informative as the ammonoid faunas are not that informative or of lower diversity across this transition and might also underly certain sampling and preservational biases (Klug 2017). The Uzbek ammonoid assemblages are particularly reminiscent of diverse monotonous early ammonoid faunas reported from South China (Xian et al. 1980, Ruan 1981, Yu & Ruan 1988) interpreted to be mainly deposited on the middle to lower "slope" (Ruan 1996). However, their stratigraphic provenance and taxonomy is poorly documented and in need of revision. As they also contain various anetoceratids, mimosphinctids and oxyconic forms, these might be of great interest for a detailed correlation with Uzbekistan and disentangling changes in ammonoid diversity throughout the Emsian.

The youngest auguritids mostly disappear within the *elegans* Zone; they are quite rare, which might indicate facies controls on their distribution. As these forms are widely distributed palaeogeographically, these might represent more pelagic forms. Anetoceratinae

probably disappeared globally between the end of the *elegans* Zone (e.g., *Erbenoceras*) and the beginning of the *cancellata* Zone (e.g., *Ivoites*). More studies need to be carried out as this genus and various other gyroconically coiled ammonoids have often been overlooked or confused to establish if the disappearance happened more or less synchronously around the globe. Even in Bohemia, the ammonoid occurrences are strongly facies-controlled; they mostly occur in calcareous shales with some exceptions, the lowest diversity appears to fall in the *cancellata* Zone.

Palaeogeography and ammonoid endemism

Presuming that the palaeogeographic map of Scotese (2001) is accurate, the region of today's Zeravshan and other South Tien Shan localities (Sangibaland Mountain in Kyrgyzstan) were separated by large distances from other early Emsian ammonoid occurrences (Fig. 16) in southern China (Guangxi: Shen 1975, Ruan 1981) and Vietnam in the southeast (Mansuy 1921), the Kolyma Basin in the northwest, the North Urals in the west (Bogoslovsky 1963), , and the northern Caucasus in the south (Nikolaeva 2007).

It is striking that many of the ammonoid species described from Uzbekistan (Bogoslovsky 1969, 1972, 1984, Yatskov 1990, Bardashev et al. 2005, Kim et al. 2007, Becker et al. 2010) have only been described from this region. Meanwhile, *Erbenoceras kimi* has also been described from other South Tien Shan localities outside Uzbekistan including Sangibaland Mountain in Kyrgyzstan (Nikolaeva et al. 2017) and potentially also in the Altai Mountains in Turkestan (Kiselev 1987), which were close to each other in the Early Devonian facing the passive margin of the Turkestan or South Tien Shan Ocean (Filippova et al. 2011, Windley et al. 2007, Nikolaeva et al. 2017).

Out of the fourteen species listed in Table 2, nine species (60%) have not been recorded from other regions (i.e. outside the South Tien Shan

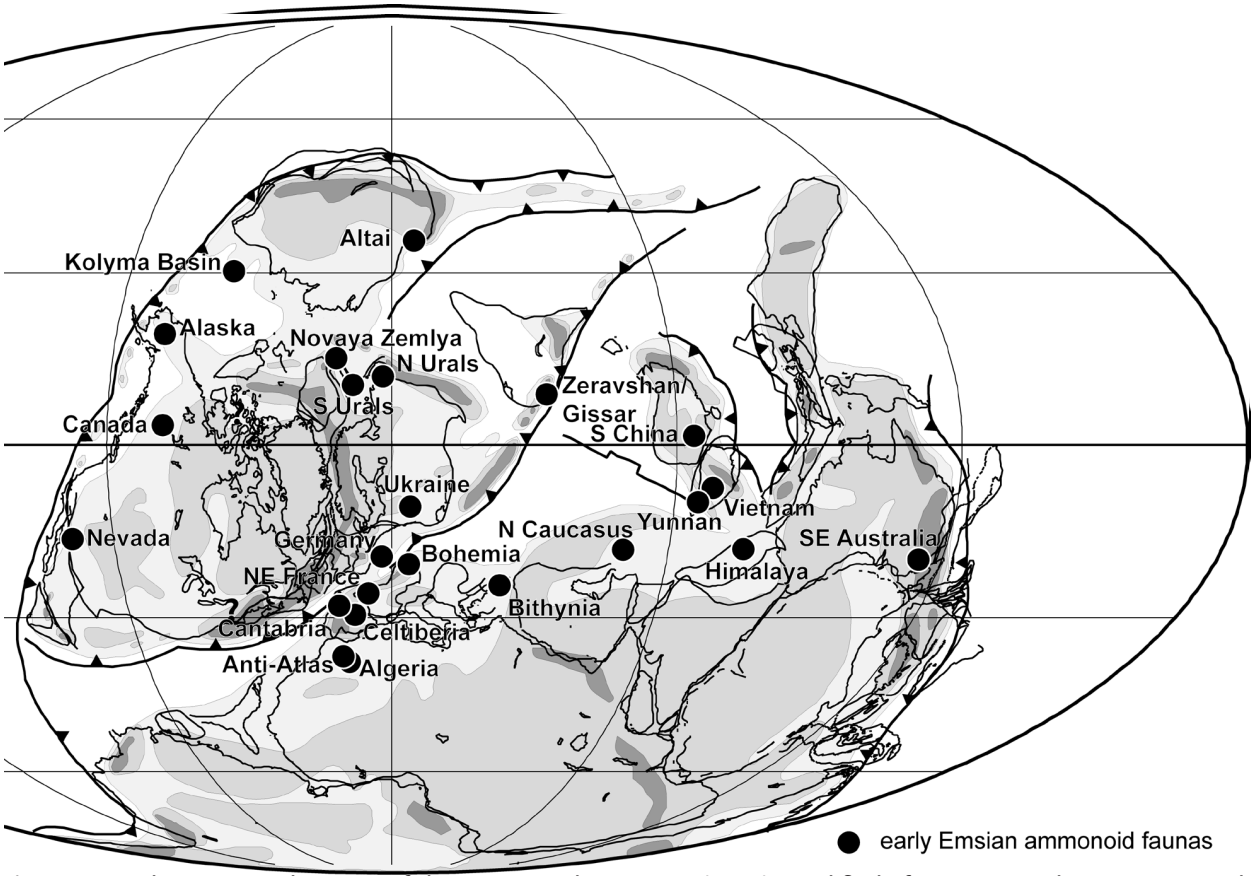

Figure 16. Palaeogeographic map of the Devonian by Scotese (2001), modified after a version by De Baets et al. (2009). Note the rather isolated position of the Uzbek ammonoid occurrences.

Species	Endemic or not	Germany	France	Anti-Atlas	N Caucasus	Spain	Vietnam	S China	Bohemia	Algeria	Bithynia	Northern Urals
Metabactrites rakhmonovi	yes											
Ivoites meshchankinae	no							?	•			
Erbenoceras advolvens	no	•	•	•	•	•	•	•	•		?	•
Erbenoceras kimi	yes*							?				
Uzbekisphinctes rudicostatus	yes											
Beckeroceras khanakasuensis	yes											
Mimosphinctes tripartitus	no	•				•						
Mimosphinctes erbeni (auct.)	yes											
Gyroceratites laevis	no	•	•	•				•	•			
Mimagoniatites fecundus	no	•	•	•	•			•	•	•	•	
Teicherticeras planum	yes											
Kimoceras lentiforme	yes											
Gaurites sperandus	yes											
Convoluticeras flexuosum	yes											
Number of shared species		**4**	**3**	**3**	**2**	**2**	**1**	**3**	**4**	**1**	**1**	**1**

Table 02. Early Emsian ammonoids occurring in Uzbekistan (including other Tien Shan localities) and geographic occurrences of these taxa in other regions (data from the databases GONIAT (Kullmann 2011) and AMMON (Korn & Ilg 2007). Some own records have been added.

Mountains) and thus appear to be endemic. This pattern is observed when just focusing on species reported from the *barrandei* and *elegans* Zones, while endemicity seems less pronounced (about 30%) in the *zlichovensis* and *cancellata* Zones.

In terms of the number of shared species, four species have also been reported from Germany (e.g., Erben 1960, Göddertz 1987, De Baets et al. 2009, 2013a, b) and the Czech Republic (Barrande 1865-1877, Erben 1962, Chlupáč 1976), three each from China (Shen 1975, Ruan 1981, 1996), France (e.g., Erben 1960, Feist 1970), and Morocco (e.g., Petter 1959, Becker & House 1994, Klug 2001, De Baets et al. 2010), two each from Spain (Montesinos & Truyols-Massoni 1987, Montesinos & Sanz Lopez 1999, Truyols-Massoni 1999) and the Caucasus (Nikolaeva 2007) and only one each from Algeria (e.g., Göddertz 1989), Turkey (e.g., Göddertz 1987), the Urals (Bogoslovsky 1963, 1969), and Vietnam (Mansuy 1921). This pattern seemingly suggests closer palaeobiogeographic relationships of the Zeravshan to regions like the Rhenish Massif or Bohemia. However, we suggest that this is an effect of the more intense research and sampling in Europe compared to, e.g., some regions in Asia. According to our own field observations in Guangxi (China; e.g., Shen 1975, Ruan 1981), the Hunsrück (Germany; e.g., De Baets et al. 2009, 2013a, b), Bohemia (Czech Republic; e.g., Barrande 1865-1877, Chlupáč 1976, Chlupáč & Turek 1977, 1983), and northern Africa (e.g., Göddertz 1987, Becker & House 1994, Klug 2001), we predict that additional sampling would reveal closer faunal relationships of the South Tien Shan to Guangxi, Yunnan, and Vietnam than to what today belongs to Europe and northern Africa. This is supported by the absence of large *Erbenoceras* from the Guangxi, Yunnan, and Vietnam and its presence in central Europe and northern Africa as well as by the abundance of small advolute *Erbenoceras* (*E. elegantulum*, *E. kimi*), small *Ivoites* (*I. luofense*, *I. meshchankinae*) and diverse mimosphinctids (*Beckeroceras khanakasuensis*, *Mimosphinctes bipartitus*, *M. erbeni* (auct.), *M. rotatile*, *Uzbekisphinctes discordans*, *U. rudicostatus*) in central and southeast Asia. Of course, there are some almost cosmopolitan species such as *Erbenoceras advolvens* (Klug 2001; Korn & Klug 2012; De Baets et al. 2013a, b), *Gyroceratites laevis* and particularly *Mimagoniatites fecundus* (which

should probably encompass several additional species since it is overly lumped in our opinion).

It is remarkable that the oxyconic forms *Kimoceras* and *Gaurites* are both endemic. *Gaurites* was previously only reported from a restricted stratigraphic interval in one locality (one bed in the *barrandei* Zone), but could now be recovered also from the Khodzha-Kurgan gorge and multiple beds in Yusupkul area. *Kimoceras lentiforme* is known from both Khodzha-Kurgan and Shirdag and has a larger stratigraphic range (Becker et al. 2010).

The family Auguritidae with its close relatives is rather small and contains only a few genera (*Gaurites*, *Celaeceras*, *Weyeroceras*), which are known from regions that were moderately close to each other in the Emsian (Moroccan Anti-Atlas, Spain, Bohemia, North Urals; Barrande 1865-1877, Bogoslovsky 1969, Montesinos & Garcia-Alcalde 1996, Klug 2001, Korn & Klug 2002, Kim et al. 2007, De Baets et al. 2010, Monnet et al. 2011b, Klug et al. 2015). Their absence in other regions might also relate to their rarity related with potential facies or sampling controls on their distribution. Furthermore, oxyconic forms (e.g., *Daxinoceras*) have also been reported from South China (Xian et al. 1980), but are in need of revision.

Acknowledgements

We cordially thank Utkir J. Rakhmonov (Shahrisabz) for his great hospitality and his important support in organizing our visits. Firuza Salimova and Natalya Meshchankina (Tashkent) both were of greatest help during the preparation of our visits; as far as our visits to the Kitab State Geological Reserve are concerned, the entire work would have been impossible without them. The field work and other project related work was supported by the Swiss National Science Foundation (Project numbers 200020_132870 and 200020_149120); we greatly appreciate this support. We thank Catherine Crônier (Lille I) for providing maps, and Sebastien Clausen (Lille I) for helping with making thin sections. Furthermore, we thank Franziska Blattman (Zürich) for helping in the lab, and Maximiliano Meier (Bulle), David Ware (Berlin) and Nicolas Goudemand (Lyon) for helpful discussions about UA method.

References

Aboussalam, Z. S., Becker, R. T., & Bultynck, P. 2015. Emsian (Lower Devonian) conodont stratigraphy and correlation of the Anti-Atlas (Southern Morocco), *Bulletin of Geosciences* 90, 893-980.

Bardashev, I.A., Bardasheva, N.P., Weddige, K. & Ziegler, W. 2005. Stratigraphy and facies of the Middle Paleozoic of parts of southern Tien-Shan in Tajikistan and Uzbekistan. – *Palaeobiodiversity and Palaeoenvironments* 85, 319–364.

Barrande, J. 1865-1877. *Systême Silurien du centre de la Bohême, I. Partie*, Vol. II: Céphalopodes. – Published by the author, Prague/Paris, pls 1-107 (1965), Text, xxxvi + 712 pp. (1867), pls 461-544 (1877).

Becker, R.T., De Baets, K. & Nikolaeva, S. 2010. New ammonoids records from the lower Emsian of the Kitab Reserve (Uzbekistan) – preliminary results. – *SDS Newsletter* 25, 20-28.

Becker, R.T. & House, M.R. 1994. International Devonian goniatite zonation, Emsian to Givetian, with new records from Morocco. – *Courier Forschungsinstitut Senckenberg*, Willi Ziegler Festschrift II 169, 79–135.

Berkyová, S., Fryda, J., and Lukes, P. 2007. Unsuccessful predation on Middle Paleozoic plankton: Shell injury and anomalies in Devonian dacryoconarid tentaculites, *Acta Palaeontologica Polonica* 52, 407.

Bogoslovsky, B. I. 1961. Eyfelskie ammonoidei Urale i voprosy klassi:fi:katsii agoniatitov. *Paleontologicheskiy Zhurnal* 4, 60–70. [in Russian]

Bogoslovsky, B.I. 1963. Oldest Devonian Ammonoids of the Urals. – *Paleontologicheskii Zhurnal* 2, 26-37. [in Russian]

Bogoslovsky, B.I. 1969. Devonian ammonoids: I. Agoniatitids. – 124, 341 pp., 109 pls. [in Russian]

Bogoslovsky, B. I. (1972). Novye rannedevonskie golovonogie Novoy Zemli. *Paleontologicheskiy Zhurnal* 4, 44–51. [in Russian]

Bogoslovsky, B.I. 1980. Early Devonian ammonoids of the Zeravshan Range. – *Paleontologicheskii Zhurnal* 4, 51-66. [in Russian]

Bogoslovsky, B.I. 1984. A new genus of the family Auguritidae and the ammonoids accompanying it from the Lower Devonian of the Zeravshan Range. – *Paleontologicheskii Zhurnal* 1, 30-36. [in Russian]

Botquelen, A., Gourvennec, R., Loib, A. & Le

Menn, J. 2001 : Relations entre les variations des assemblages benthiques emsiens et l'eustatisme dans la coupe de Seillou (Massif armoricain, France). – *Comptes Rendus Académie des Sciences Paris, Sciences de la Terre et des planètes / Earth and Planetary Sciences*, 332, 45–50.

Bouček, B. 1964. *The tentaculites from Bohemia. Their morphology, taxonomy, ecology, phylogeny and biostratigraphy*. 215 pp. Publishing House of the Czechoslovak Academy of Sciences, Prague.

Brunet, M.-F., McCann, T. & Sobel, E.R. 2017. Geological Evolution of Central Asian Basins and the Western Tien Shan Range. – *Geological Society, London, Special Publications* 427, https://doi.org/10.1144/SP427.17

Carls and Valenzuela-Ríos, 2002: Devonian-Carboniferous rocks from the Iberian Cordillera. *Cuadernos des Museol Geominero* 1, 299-414, Madrid.

Carls, P., Slavík, L. & Valenzuela-Ríos, J.I. 2008. Comments on the GSSP for the basal Emsian stage boundary: the need for its redefinition. – *Bulletin of Geosciences* 83, 383-390.

Chlupáč, I. 1976. The oldest goniatite faunas and their stratigraphic significance. – *Lethaia* 9, 303-315.

Chlupáč, I., Lukeš, P., and Zikmundova, J. 1979. The Lower/Middle Devonian boundary beds in the Barrandian area, Czechoslovakia, *Geologica et Palaeontologica* 13, 125-156.

Chlupáč, I. & Kukal, Z. 1986. Reflection of possible global Devonian events in the Barrandian area, C.S.S.R, 169-179. In Walliser, O. H. (ed.) *Global Bio-Events, Lecture Notes in Earth Sciences 8*.

Chlupáč, I., & Kukal, Z. 1988. Possible global events and the stratigraphy of the Palaeozoic of the Barrandian (Cambrian–Middle Devonian, Czechoslovakia). – *Sborník geologických věd, Geologie* 43, 83–146.

Chlupáč, I. & Lukeš, P. 1999. Pragian/Zlíchovian and Zlíchovian/Dalejan boundary sections in the Lower Devonian of the Barrandian area, Czech Republic, *Newsleter on Stratigraphy*, 75-100.

Chlupáč, I. & Turek, V. 1977. New cephalopods (Ammonoidea, Bactritoidea) from the Devonian of the Barrandian area, Czechoslovakia. – *Vestnik Ustředního ústavu geologického* 52, 303-306.

Chlupáč, I. & Turek, V. 1983. Devonian goniatites from the Barrandian area. Czechoslovakia. – *Rozpravy Ustředního ústavu geologického* 46, 1-159.

Crônier, C. & Tsmeyrek, H. S. First Record of the Devonian Phacopid Trilobite 'Plagiolaria' from Uzbekistan [online]. *Memoirs of the Association of Australasian Palaeontologists*,. 39, 43-50.

Cuvier, G. 1797. *Tableau élémentaire de l'histoire naturelle des animaux*. 710 pp. Baudouin, Paris.

De Baets, K., Klug, C. & Korn, D. 2009. Anetoceratinae (Ammonoidea, Early Devonian) from the Eifel and Harz Mountains (Germany), with a revision of their genera. – *Neues Jahrbuch für Geologie und Paläontologie*, Abhandlungen 252, 361-376.

De Baets, K., Klug, C. & Plusquellec, Y. 2010. Zlíchovian faunas with early ammonoids from Morocco and their use for the correlation between the eastern Anti-Atlas and the western Dra Valley. *Bulletin of Geosciences* 85(2), 317–352. DOI 10.3140/bull.geosci.1172

De Baets, K., Goolaerts, S., Rietbergen, T. & Klug, C. 2013a. The first record of Early Devonian ammonoids from Belgium and their significance. – *Geologica Belgica* 16, 148-156.

De Baets, K., Klug, C. & Korn, D. 2011. Devonian pearls and ammonoid-endoparasite coevolution. – *Acta Palaeontologica Polonica* 56, 159–180.

De Baets, K., Klug, C. Korn, D. Bartels, C. & Poschmann, M. 2013b. Emsian Ammonoidea and the age of the Hunsrück Slate (Rhenish Mountains, Western Germany). – *Palaeontographica A* 299, 1-114.

De Baets, K., Klug, C., Korn, D. & Landman, N.H. 2012a. Early evolutionary trends in ammonoid embryonic development. – *Evolution* 66, 1788-1806. DOI: 10.1111/j.1558-5646.2011.01567.x

Dunham, R.J. 1962. Classification of carbonate rocks according to depositional texture. – In Ham, W.E. (Ed.), *Classification of Carbonate Rocks. American Association of Petroleum Geologists Mem*., 1, 108–121.

Eichenberg, W. 1931. Die Schichtenfolge des Herzberg-Andreasberger Sattelzuges. *Neues Jahrbuch für Mineralogie, Geologie und Paläontologie*, Beilage-Band B, 65, 141–196.

Embry, A.F. & Klovan, J.E. 1971. A late Devonian reef tract on northeastern Banks Island, N.W.T. – *Bulletin of Canadian Petroleum Geology*, 19, 730–781.

Erben, H.K. 1953. Goniatitacea (Ceph.) aus dem Unterdevon und Unteren Mitteldevon. – *Neues Jahrbuch für Geologie und Paläontologie*, Abhandlungen 98, 175-225.

Erben, H.K. 1960. Primitive Ammonoidea aus dem Unterdevon Frankreichs und Deutschlands. – *Neues Jahrbuch für Geologie und Paläontologie*, Abhandlungen 110, 1-128.

Erben, H.K. 1962. Über böhmische und türkische Vertreter von Anetoceras (Ammon., Unterdevon). – *Paläontologische Zeitschrift* 36, 14-27.

Erben, H.K. 1965. Die Evolution der ältesten Ammonoidea. II. – *Neues Jahrbuch für Geologie und Paläontologie*, Abhandlungen 122, 275-312.

Ernst, H. U. & Klug, C. 2011. *Perlboote und Ammonshörner Weltweit. Nautilids and Ammonites Worldwide*. Pfeil, München, 224pp.

Feist, R. 1970. Présence d'*Anetoceras* (*Erbenoceras*) mattei n.sp. (Ammonoidée primitive) dans le Dévonien inférieur de la Montagne Noire. – *Comptes Rendus Hebdomadaires des Séances de l'Academie des Sciences, Serie D: Sciences Naturelles* 270, 290-293.

Ferrová, L., Frýda, J., and Lukeš, P. 2012. High-resolution tentaculite biostratigraphy and facies development across the Early Devonian Daleje Event in the Barrandian (Bohemia): implications for global Emsian stratigraphy, *Bulletin of Geosciences* 87, 587-624.

Filippova, I., Bush, V., and Didenko, A. 2001. Middle Paleozoic subduction belts: the leading factor in the formation of the Central Asian fold-and-thrust belt, *Russian Journal of Earth Sciences* 3, 405-426.

Göddertz, B. 1987. Devonische Goniatiten aus SW-Algerien und ihre stratigraphische Einordnung in die Conodonten-Abfolge. – *Palaeontographica A* 197, 127-220.

Göddertz, B. 1989. Unterdevonische hercynische Goniatiten aus Deutschland, Frankreich und der Türkei. – *Palaeontographica A* 208, 61-89.

Guex, J. & Davaud, E. 1984. Unitary associations method: use of graph theory and computer algorithm. – *Computers and Geosciences* 10, 69–96.

Guex, J. 1991. *Biochronological Correlations*, 252 pp. Springer Verlag, Berlin.

Hammer, Ø., Harper, D.A.T. & Ryan, P.D. 2001: PAST: paleontological statistics software package for education and data analysis. – *Palaeontologia Electronica* 4, 9.

Haq, B.U. & Schutter, S.R. 2008: A chronology of Paleozoic sealevel changes. – *Science* 322, 64–68.

House, M.R. 1996. Juvenile goniatite survival strategies following Devonian extinction Events. In Hart, W. (ed). Biotic recovery from Mass Extinction Events. – *Geological Society Special Publication* 102, 163-186.

Hyatt, A. 1883-1884. Genera of fossil cephalopods. – *Proceedings of the Boston Society of Natural History* 22, 253-338.

Izokh, N., Yolkin, E., Weddige, K., Erina, M., & Valenzuela-Ríos, J. 2011. Late Pragian and Early Emsian conodont polygnathid species from the Kitab state geological reserve sequences (Zeravshan–Gissar mountainous area, Uzbekistan), *Geologiya i Geofizika* 15, 49-63.

Johnson, J.G., Klapper, G. & Sandberg, C.A. 1985. Devonian eustatic fluctuations in Euramerica. *Geological Society of America* Bulletin 96, 567–587.

Kim, A.I., Yolkin, E.A., Erina, M.V. & Gratsianova, R.T. 1978. Type sections of the Lower and Middle Devonian boundary sediments in Middle Asia. *A Guide to Field Excursions, Field Session of the International Subcommission on the Devonian Stratigraphy, Samarkand*. 48 pp., 78 pls. (Tashkent)

Kim, A.I., Salimova, I.A., Kim, N.A. & Meshchankina, N.A. 2007. *Palaeontological Atlas of Phanerozoic Faunas and Floras of Uzbekistan, Volume I: Palaeozoic (Cambrian, Ordovician, Silurian, Devonian, Carboniferous, Permian)*. – Republic of Uzbekistan State Committee on Geology and Mineral Resources, Tashkent, 261 pp.

Kim, A. I., Erina, M. V., Kim, I. A., Salimova, F. A., Meshchankina, N. A., & Rakhmonov, U. D. 2012. The Pragian–Emsian event and subdivision of the Emsian in the Zinzilban and Khodzha–Kurgan sections, *SDS Newsletter* 27, 38-41.

Kiselev, G., and Starshinin, D. 1987. Golovonogie mollyuski srednego Paleozoya yuzhnogo Tyan-Shanya (Isucennost, taksonomicheskiy sostav, stratigraficheskoe rasprostranenie), Vestnik Sankt Petersburgskogo Universiteta, Seriya 7, *Geologiya, Geografiya* 3, 84-88.

Klug, C. 2001. Early Emsian ammonoids from the eastern Anti-Atlas (Morocco). – *Paläontologische Zeitschrift* 74, 479-515.

Klug, C. 2017. First description of the Early Devonian ammonoid Mimosphinctes from Gondwana and stratigraphical implications. – *Swiss Journal of Palaeontology* 136, 345-358.

Klug, C. Kröger, B., B., Rücklin, M., Korn, D., Schemm-Gregory, M., De Baets, K. & Mapes, R. H. 2008. Ecological change during the early Emsian (Devonian) in the Tafilalt (Morocco), the origin of the Ammonoidea, and the first African pyrgocystid edrioasteroids, machaerids and phyllocarids. – *Palaeontographica A* 283, 1-94.

Klug, C. Kröger, B., Vinther, J., Fuchs, D. & De Baets, K. 2015. Ancestry, origin and early evolution of ammonoids. – In Klug, C., Korn, D., De Baets, K., Kruta, I. & Mapes, R.H. (eds.): *Ammonoid paleobiology, Volume II: from macroevolution to paleogeography. Topics in Geobiology* 44, 20 pp., Springer, Dordrecht.

Korn, D. 2001. Morphometric evolution and phylogeny of Palaeozoic ammonoids. Early and Middle Devonian. – *Acta Geologica Polonica* 51, 193–215.

Korn, D. 2014. *Armatites kaufmanni* n. sp., the first Late Devonian goniatite with ventral spines. – *Neues Jahrbuch für Geologie und Paläontologie* Abhandlungen 271, 349–352.

Korn, D. & Ilg, A. 2007. AMMON, www.wahre-staerke.com/ammon/

Korn, D. & Klug, C. 2002. *Ammoneae Devonicae*. – *Fossilium Catalogus I: Animalia*, 138. – Backhuys Publishers, Leiden, 375 pp.

Korn, D. & Klug, C. 2012. Palaeozoic ammonoids – diversity and development of conch morphology. – In: Talent, J. (ed.), *Extinction intervals and biogeographic perturbations through time: Earth and Life (International Year of Planet Earth)*. 491-534, (Springer) Netherlands.

Korn, D., Mapes, R.H. & Klug, C. 2014. The massive wrinkle layer of an Early Carboniferous ammonoid from Morocco. – *Palaeontology* 57, 771-781.

Kröger, B. 2005. Adaptive evolution in Paleozoic coiled Cephalopods. – *Paleobiology* 31, 253-268.

Kröger, B., Vinther, J. & Fuchs, D. 2011. Cephalopod origin and evolution: A congruent picture emerging from fossils, development and molecules. – *BioEssays* 33, 602-613.

Kullmann, J. 2011. GONIAT, http://www.goniat.org/

Lardeux, H., Morzadec, P., Bultynck, P., and Walliser, O. H. 1979. La Grange Limestone, Massif Armoricain, *Field Excursion Guidebook*, 5-7.

Loury, C., Rolland, Y., Guillot, S., Lanari, P., Ganino, C., Melis, R., Jourdon, A., Petit, C., Beyssac, O., Gallet, S. & Moni, P. 2018. Tectonometamorphic evolution of the Atbashi high-P units (Kyrgyz CAOB, Tien Shan): Implications for the closure of the Turkestan Ocean and continental subduction–exhumation of the South Kazakh continental margin. – *Journal of Metamorphic Geology*, 1–27. DOI: 10.1111/jmg.12423

Machel, H.G. & Hunter, I.G. 1994. Facies Models for Middle to Late Devonian Shallow-marine Carbonates, with Comparisons to Modern Reefs: a Guide for Facies Analysis. – *Facies* 30, 155-176.

Mansuy, H. 1921. Description de fossiles des terrains Paléozoïques et Mésozoïques du Tonkin septentrional (feuilles de Cao-Bang, de Ha-Lang, de That-Khe et de Lang-Son). – *Mémoires du Service Géologique de l'Indochine* 8 (1), 11-27.

Miller, A. K. 1938. Devonian ammonoids of America. *Geological Society of America, Special papers*, 14, 1–262.

Monnet, C., Klug, C., Goudemand, N., De Baets, K. & Bucher, H. 2011a. Quantitative biochronology of Devonian ammonoids from Morocco and proposals for a refined unitary association method. – *Lethaia* 44, 469–489.

Monnet, C., Klug, C. & De Baets, K. 2011b. Parallel evolution controlled by adaptation and covariation in ammonoid cephalopods. – *BMC Evolutionary Biology* 11, 1-21.

Montesinos, J.R. & Garcia-Alcalde, J.L. 1996. An occurrence of the auguritid ammonoid Celaeceras in the Lower Devonian of northern Spain. – *Palaeontology* 39, 149–155.

Montesinos, J.R. & Sanz López, J. 1999. Ammonoideos del Devónico Inferior y Medio en el Pirineo Oriental y Central. Antecedentes históricos y nuevos hallazgos. – *Revista Española Paleontología*, Nº extr. Homenaje Prof. J.Truyols, 97-108.

Montesinos, J.R. & Truyols-Massoni, M. 1987. La Fauna de Anetoceras y el límite Zlichoviense-Dalejense en el Dominio Palentino (NO. de España). – *Cuaderno Laboratorio Xeolóxico de Coruña* 11, 191-208.

Nikolaeva, S. 2007. Discovery of Emsian Ammonoids in the Northern Caucasus. – *Paleontologicheskii Zhurnal* 5, 34-39. [In Russian]

Nikolaeva, S., Kim, A., and Erina, M. 2017. An early Emsian (Zlichovian) ammonoid assemblage from Sangibaland Mountain (Shakhimardan River Basin) (South Tien Shan, Kyrgyzstan), *Palaeobiodiversity and Palaeoenvironments*, 10.1007/s12549-017-0291-2.

Petter, G. 1959. Goniatites Dévoniennes du Sahara. – *Publications du Service de la Carte Géologique de l'Algérie, Nouvelle Série, Paléontologie* 2, 1-313.

Pickering, K.T., Koren, T.N., Lytochkin, V.N. & Siveter, D.J. 2008. Silurian Devonian active-margin deep-marine systems and palaeogeography, Alai Range, Southern Tien Shan, Central Asia. – *Journal of the Geological Society* 165, 189-210.

Ruan, Y.-P. 1981. Devonian and earliest Carboniferous Ammonoids from Guangxi and Guizhou. – *Memoirs of the Nanjing Institute of Geology & Paleontology* 15, 1-152. [in Chinese]

Ruan, Y. P. 1996. Zonation and distribution of the early Devonian primitive ammonoids in South China, in: *Centennial Memorial Volume of Prof. Sun Yunzhen: Paleontology and Stratigraphy*, edited by: Wang, H.-Z., and Wang, X.-L., China University of Geosciences Press, Wuhan, 104-112.

Ruzhencev, V. E. (1957). Filogeneticheskaya sistema paleozoyskikh ammonoidey. *Byulleten' Moskovskogo obshchestva ispytately prirody, novaya seriya, otdel geologicheskiy*, 31(2), 49–64.

Schlager, W. 1981, The paradox of drowned reefs and carbonate platforms. – *Geological Society of America*, Bulletin 92, 197-211.

Scotese, C.R. 2001. Digital Paleogeographic Map Archive on CD-Rom, Paleomap Project. Arlington, Texas.

Shen, Y.T. 1975. Discovery of primitive ammonoids from Nandan of Guangxi and its stratigraphic significance. – *Professional Papers in Stratigraphy and Paleontology* 1, 86-104. [In Chinese]

Shimansky, V.N. 1951. K voprosu ob evoliutsii verkynepaleozoishikh pyramkh golovonikh. – *Akademia Nauk SSSR Doklady* 79, 867-870. [In Russian]

Steinmann, G. & Döderlein, L. 1890. *Elemente der Paläontologie*. 848pp; Leipzig (Engelmann).

Tonarová, P., Vodrážková, S., Ferrová, L., de la Puente, G.S., Hints, O., Frýda, J. & Kubajko, M. 2017. Palynology, microfacies and biostratigraphy across the Daleje Event (Lower Devonian, lower to upper Emsian. new insights from the offshore facies of the Prague Basin, Czech Republic. – *Palaeobiodiversity and Palaeoenvironments* 97, 419-438

Truyols-Massoni, M. 1999. La Edad de las Capas con Mimosphinctes en el Devónico de la Cordillera Cantábrica (NW de España). – *Trabajos de Geología* 21, 377-384.

Windley, B. F., Alexeiev, D., Xiao, W., Kröner, A., and Badarch, G. 2007. Tectonic models for accretion of the Central Asian Orogenic Belt, *Journal of the Geological Society*, 164, 31-47, 10.1144/0016-76492006-022.

Wittmer, J. M., and Miller, A. I. 2011. Dissecting the global diversity trajectory of an enigmatic group: The paleogeographic history of tentaculitoids, *Palaeogeography, Palaeoclimatology, Palaeoecology* 312, 54-65,

Xian, S., Wang, S., Zhou, X., Xiong, J., and Zhou, T. 1980. Nandan typical stratigraphy and paleontology of Devonian in South China. *Guizhou People's Publishing House (Guyang)*.

Yatskov, S.V. 1990. The oldest ammonoid family, the Anetoceratidae. – *Paleontologicheskii Zhurnal* 1990, 25-32. [in Russian]

Yolkin, E.A., Kim, A.I. & Talent, J.A. Eds., 2008. *Devonian Sequences of the Kitab Reserve area. – Field Excursion Guidebook, Internat. Conf. "Global Alignments of Lower Devonian Carbonate and Clastic Sequences"* (SDS/IGCP 499 Project joint field meeting), 97 pp. (Publishing House of SB Ras, Novosibirsk).

Yolkin, E.A., Kim, A.I.,Weddige, K.,Talent, J.A. & House, M.R. 1997. Definition of the Pragian/ Emsian State boundary. – *Episodes 20* (4), 235–240.

Yu, C. M., and Ruan, Y. P. 1988. Proposal and comment on the definition of the Emsian, Dévonian of The World, Vol. III: Paleoecology And biostratigraphy. *Canadian Society of Petroleum Geologists Memoir* 14, 179-191.

Zittel, K.A. von 1881-1885. *Handbuch der Palæontologie. I. Abtheilung. Palæozoologie. II. Band. Mollusca und Arthropoda*. – 1-893; München, Leipzig (Oldenbourg).

CONCLUSIONS AND PERSPECTIVES

CONCLUSIONS AND PERSPECTIVES

VOLUMETRIC ANALYSES AND MODES OF LIFE (chapters I, II and III)

Virtual palaeontology has become the new tool of the trade in palaeontology. This development reached cephalopod research and I was able to apply these methods to ammonoids in order to address questions related to hydrostatic properties of their conchs, their ontogeny and their mode of life. Combining the use of optical-physical method (in this case, serial grinding) with computational analytical methods, I generated volume models of shells of three ammonoid species which are: the agoniatitid Fidelites clariondi, the anarcestid Diallagites lenticulifer (Middle Devonian) and the goniatitid Goniatites multiliratus (Early Carboniferous).

Although being time-consuming, the state-of-the art methods of virtual palaeontology allowed me to carry out pioneering work in that field for Palaeozoic ammonoids. In Chapter I, I focused on the documentation of growth trajectories. I compiled chamber and septum volumes through ontogeny and compared the resulting trajectories with those obtained from classical 2D-parameters. In Chapter II, I determined the masses of the entire conchs, single parts of the conchs, the soft parts and the entire animals. All these empirical data allowed me to analyse the development of different parameters through ontogeny, and compare the results with those of theoretical studies to test their validity.

Chamber volumes grow isometrically when compared to aperture height and diameter. By contrast, septum volumes show a negative allometry compared to the same 2D-parameters. Volumes grow exponentially through ontogeny, except during late ontogeny. Mature modifications are well recorded while earlier ontogenetic stages are not. This can mainly be explained by the still insufficient optical/ physical resolution (voxel size) and recrystallization of the Palaeozoic materials, which reduced the quality of primary data particularly of the first chambers of the phragmocone.

Exponential correlations between diameters or apertural heights versus chamber and septum volumes were found. My results confirm that 2D-parameters can be used as some kind of proxy to estimate ontogenetic changes in chamber and septum volumes, as it was predicted previously by theoretical models.

Another question was whether Palaeozoic ammonoids could have achieved neutral buoyancy by means of their chambered conchs. In chapter II, I calculated that the proportion of cameral liquid required for neutral buoyancy varies between 31% to 38% in the investigated specimens. Syn-vivo shell orientations have been calculated; the according aperture angles vary from about 20° to 125° from the vertical. These values differ from modern Nautilus but this is not surprising since it actually conforms to mathematical models. My results also confirmed the negative correlation between body chamber length and hydrodynamic stability. These variations in shell orientation and hydrodynamic stability suggest differences in the modes of life of the examined ammonoidgroups. Assessing these Palaeobiological aspects in Palaeozoic ammonoids, I got the chance to contribute a chapter to the new edition of Ammonoid Paleobiology. Together with my colleagues Christian Klug, Amane Tajika and John Chamberlain, I authored a chapter on Ammonoid Locomotion.

Concerning the two volumetric studies (chapters I and II) and the perspectives for future achievements, we found that growth trajectories are more similar between those two species, which are known already to be closer phylogenetically. These data are of course not sufficient to establish a general rule, but with the continuous progress of computer technologies, in the near future, methods to achieve high resolution 3D-models of Palaeozoic ammonoids using rather non-destructive data-acquisition will become easier and faster as well. Further testing will then be facilitated and those worthwhile to compare growth trajectories of further ammonoid taxa and additionally between several specimens within one species (intraspecific variation). Possibly, such

volumetric comparisons could help in resolving open phylogenetic questions. Moreover, empirical volumetric analyses in loosely coiled forms and heteromorphs would be interesting in order to test hypotheses related with their buoyancy, swimming capabilities and potential habitat.

EARLY DEVONIAN AMMONOID FAUNAS IN THE ZERAVSHAN MOUNTAINS OF UZBEKISTAN (Chapter IV)

The Zeravshan-Gissar Mountains are part of the southern Tien Shan orogenic system in central Asia. In Uzbekistan, the Kitab geological reserve is well known among Devonian workers since the Pragian/ Emsian Global Boundary Stratotype Section and Point (GSSP) is located there. In Chapter IV, I present the results of field investigations we carried out in 2012. We documented the sedimentary changes that occurred during the late Pragian transition from a reefal to a pelagic facies (which persisted into the Emsian and Eifelian), with regards to possible causes or events that led to the end such a massive carbonate platform (coral limestones more than 1000 meters in thickness). We could not unequivocally identify the trigger of this important drowning, but we hypothesize that tectonic events occurred with an intense eustatic trangression.. The combination of these two synchronous events represents a plausible explanation why the reef organisms did not manage to keep pace with the sea-level rise. We are not entirely sure, however, whether this transgression correlates with the Basal Zlichov Event or a later one. The redefinition of the Pragian-Emsian boundary in Uzbekistan is currently under revision. Consequently, the question for the correlation of this transgressive event should be answered soon.

Two Uzbek localities in particular bear numerous ammonoid taxa, namely the Khodzha Kurgan Gorge and the Shirdag valley. Stratigraphically, we focused on the Dzhaus Beds (Late Emsian, inversus zone) where ammonoids were first documented in the 1950s. In this stratigraphic interval, the Daleje transgression occurred. In Uzbekistan, the onset of this Event is not represented by a sharp change from a shallower to a more pelagic facies as in many other regions worldwide. The highly diverse ammonoid assemblages in Uzbekistan recorded a turnover in ammonoid fauna, which is consistent with the base of the cancellata dacryoconarid Zone used to define the base of the Daleje Event sensu stricto. Accordingly, my co-authors and I suggest an interval it probably correlated with in the Khodzha Kurgan and Shirdag areas.

Even though this Event is not always easy to spot, it is of stratigraphical and palaeoecological relevenace. Thus, we support the use of this Event for the subdivision of the Emsian into two substages. Fourteen ammonoid species have been discovered and reported from the studied area. 60% of these species occurring in the barrandei and elegans dacryoconarid Zones appear to be endemic. In the zlichovensis and cancellata dacryoconarid Zones, this percentage drops to 30% of endemism. Interestingly, Uzbek cephalopod faunas appear to share more species with European localities than with palaeogeographically closer regions such as South China, Vietnam or Northern Urals. Nevertheless, we suspect that this seeming similarity roots in a sampling bias, because European outcrops have been sampled much more intensely and for a longer time than these Asian regions. In the future, regions such as Vietnam, Northern Urals and especially South China should be re-visited and investigated more carefully in order to enhance the database of Emsian faunas. Because of the great similarity of some Uzbek with some southeast Asian species, we suspect that such studies will change the picture and will perhaps reveal closer relationships between these regions than between Uzbekistan and Europe.

We revised the cephalopod fauna from the Geological Reserve and introduced several new taxa: Beckeroceras gen. nov., Uzbekisphinctes gen. nov., Ivoites meshchankinae sp. nov., Kitabobactrites salimovae gen. et sp. nov., and Metabactrites rakhmonovi sp. nov.

In the future, more Emsian ammonoid localities should be investigated especially from the

surrounding regions in order to improve our knowledge of the origination of the ammonoid clade and to better understand their rapid evolution. We visited Devonian localities in South China (Guangxi Province) in 2011. These localities bear a great potential for improving the knowledge of the palaeogeographic relations between South China and Uzbekistan but also to answer questions linked to the origin for the ammonoid clade.

REFERENCES

REFERENCES

Algeo, T.J. and Scheckler, S.E 1998. Terrestrial-marine teleconnections in the Devonian: links between the evolution of land plants, weathering processes, and marine anoxic events. *Philosophical Transactions of the Royal Society B: Biological Sciences*. 353, 113–130.

Algeo, T. J., Scheckler, S. E. & Maynard, J. B. 2001. Effects of the Middle to Late Devonian spread of vascular land plants on weathering regimes, marine biota, and global climate. 213–236. In Gensel, P.G. & Edwards, D. (eds*.). Plants Invade the Land: Evolutionary and Environmental Approaches*. Columbia University Press, New York, 512 pp.

Alroy, J., Aberhan, M., Bottjer, D. J., Foote, M., Fürsich, F. T., Harries, P. J., Hendy, A. J. W., Holland, S. M., Ivany, L. C., Kiessling, W., Kosnik, M. A., Marshall, C. R., McGowan, A. J., Miller, A. I., Olszewski, T. D., Patzkowsky, M. E., Peters, S. E., Villier, L., Wagner, P. J., Bonuso, N., Borkow, P. S., Brenneis, B., Clapham, M. E., Fall, L. M., Ferguson, C. A., Hanson, V. L., Krug, A. Z., Layou, K. M., Leckey, E. H., Nürnberg, S., Powers, C. M., Sessa, J. A., Simpson, C., Tomašových, A. and Visaggi, C. C. 2008. Phanerozoic Trends in the Global Diversity of Marine Invertebrates. *Science* 321: 97–100.

Barash, M.S. 2016. Causes of the great mass extinction of marine organisms in the Late Devonian. *Oceanology*, 56: 863–875.Bardashev, I. A., Bardasheva, N. P., Weddige, K. and Ziegler, W. 2005. Stratigraphy and facies of the Middle Paleozoic of parts of southern Tien-Shan in Tajikistan and Uzbekistan. *Palaeobiodiversity and Palaeoenvironments*, 85:319–364.

Barnosky, A.D., Matzke, N., Tomiya, S., Wogan, G.O.U., Swartz, B., Quental, T.B., Marshall, C., McGuire, J.L., Lindsey, E.L., Maguire, K.C., Mersey, B. and Ferrer, E.A. 2011. Has the Earth's sixth mass extinction already arrived? *Nature* 471: 51–57 doi:10.1038/nature09678.

Barrande ‚J. 1865. *Systême Silurien du centre de la Bohême, I. Partie, Vol.II: Céphalopodes* – pls.1-107; Praha & Paris.

Barrande ‚J. 1877. *Systême Silurien du centre de la Bohême, I. Partie,Vol.II: Céphalopodes* .– pls. 461-544; Praha & Paris.

Becker, R. T. and House, M. R. 1994. International Devonian goniatite zonation, Emsian to Givetian, with new records from Morocco. *Courier Forschungsinstitut Senckenberg*, 169: 79–135.

Becker, R. T., De Baets, K. and Nikolaeva, S. 2010. New ammonoids records from the lower Emsian of the Kitab Reserve (Uzbekistan) – preliminary results. *SDS Newsletter*, 25: 20–28.

Benton, M. J. 2005. *Vertebrate Paleontology*, Third Edition. Blackwell Publishing, Oxford, 455 pp.

Berner, R.A., Beerling, D.J., Dudley, R., Robinson, J.M. and Wildman, R.A. Jr. 2003. Phanerozoic atmospheric oxygen. *Annu. Rev. Earth Planet. Sci.*, 31: 105–134.

Bogoslovsky, B. I. 1969. Bogoslovsky, B. I. 1969. Devonian ammonoids: I. Agoniatitids. *Trudy Paleontologicheskogo Instituta Akademii Nauk SSSR* 124, 341 [in Russian]

Bogoslovsky, B. I. 1972. New Early Devonian cephalopods of Novaya Zemlya. *Paleontologicheskii Zhurnal* 4:44–51. [in Russian]

Bogoslovsky, B. I. 1980. Early Devonian ammonoids of the Zeravshan Range. *Paleontologicheskii Zhurnal*, 4:51–66. [in Russian]

Bogoslovsky, B. I. 1984. A new genus of the family Auguritidae and the ammonoids accompanying it from the Lower Devonian of the Zeravshan Range. *Paleontologicheskii Zhurnal*, 1:30–36. [in Russian]

Bosscher, H. and Schlager, W. 1993. Accumulation Rates of Carbonate Platforms. *The Journal of Geology*, 101/3 345-355.

Breyn, J.P. 1732. Dissertatio Physica de Polythalamiis, nova Testa¬ceorum classe, cui quædam præmittuntur de Methodo Testacea in Classes et Genera distribuendi. Huic adiictur Commen¬tatiuncula de Belemnitis Prussicis; tan¬dem¬que Schediasma de Echinis metho¬dice disponendis. Cum figuris. – 1-64, pl.1-7; Gedani (Cornelium a Beughem).

Carls, P. 1999. El Devónico de Celtiberia y sus fósiles. *Jornadas Aragonesas de Paleontología*, 6:101–164.

Chlupáč, I. 1976. The oldest goniatite faunas and their stratigraphic significance. *Lethaia* 9: 303–315.

Cohen, K.M., Finney, S.C., Gibbard, P.L. and Fan, J.-X. 2013; updated. The ICS International Chronostratigraphic Chart. *Episodes* 36: 199-204.

De Baets, K., Klug, C. and Korn, D., 2011. Devonian pearls and ammonoid-endoparasite coevolution. *Acta Palaeontologica Polonica* 56:159–180.

De Baets, K., Klug, C. & Monnet, C. 2013. Intraspecific variability through ontogeny in early ammonoids. *Paleobiology* 39:75–94.

Donoghue, P.C.J., Bengtson, S., Dong, X.-P., Gostling, N.J, Huldtgren, T., Cunningham, J.A., Yin, C., Yue, Z., Peng, F. & Stampanoni, M. 2006. Synchrotron X-ray tomographic microscopy of fossil embryos. Nature 442: 680-683.Dzik, J. 1981. Origin of the Cephalopoda. Acta Paleontologica. Polonica 26(2): 161-191.

Erben, H.K. 1954. Goniatitaceae (Cephalopoda) aus dem Unterdevon und dem Unteren Mitteldevon. – *Neues Jahrbuch für Geologie und Paläontologie*, 98:175-225.

Erben, H.K. 1960. Primitive Ammonoidea aus dem Unterdevon Frankreichs und Deutschlands. – *Neues Jahrbuch für Geologie und Paläontologie*, 110:1-128.

Erben, H.K. 1962. Über die ‚forme elliptique' der primitiven Ammonoidea. *Paläontologische Zeitschrift*, H. Schmidt-Festband, 36, 38–44.

Erben, H.K. 1964. Die Evolution der ältesten Ammonoidea (Lieferung I). *Neues Jahrbuch für Geologie und Paläontologie*, 120:107–212.

Erben, H.K. 1965. Die Evolution der ältesten Ammonoidea. II. *Neues Jahrbuch für Geologie und Paläontologie*, 122:275–312.

Erben, H.K. 1966. Über den Ursprung der Ammonoidea. *Biological reviews of the Cambridge Philosophical Society* 41:641–658.

Ernst, H. U. and Klug, C. 2011. *Perlboote und Ammonshörner Weltweit. Nautilids and Ammonites Worldwide*. Pfeil, München.

Feist, R. 1970. Présence d'*Anetoceras* (*Erbenoceras*) *mattei* sp. n. (Ammonoidée primitive) dans le Dévonien inférieur de la Montagne Noire. *Comptes Rendus Hebdomadaire des Séances de l'Académie des Sciences, Série D: Sciences Naturelles* 270:290–293.

Frey, L., Naglik, C., Hofmann, R., Schemm-Gregory, M., Frýda, J., Kröger, B., Taylor, P. D.., Wilson, M. A. and Klug, C. 2014. Diversity and palaeoecology of invertebrate associations of the Early

Devonian in the Tafilalt (Morocco, Anti-Atlas). *Bulletin of Geoscience* 89(1): 75-112, Czech Geological Survey, Praha. http://www.geology.cz/bulletin/contents/art1459.

Garwood, R.J., Rahman, I.A. & Sutton, M.D. 2010: From clergymen to computers – the advent of virtual palaeontology. *Geology Today* 26: 96–100.

Göddertz, B. 1987. Devonische Goniatiten aus SW-Algerien und ihre stratigraphische Einordnung in die Conodonten-Abfolge. *Palaeontographica A*, 197:127–220.

Göddertz, B. 1989. Unterdevonische hercynische Goniatiten aus Deutschland, Frankreich und der Türkei. *Palaeontographica A*, 208:61–89.

Goldring, W. 1927. The oldest known petrified forest. Sci. Mon., 24, 514–529.

Goswami, A., Milne, N. and Wroe, S. 2011. Biting through constraints: cranial morphology, disparity and convergence across living and fossil carnivorous mammals. *Proceedings of the Royal Society of London B: Biological Sciences*, 278(1713):1831-1839.

Goudemand, N., Orchard, M.J., Urdy, S., Bucher, H. and Tafforeau, P. 2011. Synchrotron-aided reconstruction of the conodont feeding apparatus and implications for the mouth of the first vertebrates. *Proceedings of the National Academy of Sciences of the United States of America*, 108(21): 8720–8724. https://doi.org/10.1073/pnas.1101754108

Haq, B.U. and Schutter, S.R. 2008. A chronology of Paleozoic sea-level changes. *Science*, 322: 64-68.

Hoffmann, R. and Zachow, S. 2011. Non-invasive approach to shed new light on the buoyancy business of chambered cephalopods (Mollusca). *IAMG* Salzburg, 1–11.

Hoffmann, R., Lemanis, R., Naglik, C. and Klug, C. 2015. Ammonoid buoyancy. – In: Klug, C., Korn, D., De Baets, K., Kruta, I. & Mapes, R. H. (eds.): *Ammonoid paleobiology, Volume I: from anatomy to ecology*. Topics in Geobiology, 43: 621-656, Springer, Dordrecht.

Hoffmann, R., Lemanis, R., Falkenberg, J., Schneider, S., Wesendonk, H. and Zachow, S. 2018. Integrating 2D and 3D shell morphology to disentangle the palaeobiology of ammonoids: a virtual approach. *Palaeontology*, 61(1) 89–104.

House, M.R. 1989: Ammonoid extinction events. *Philosophical Transactions of the Royal Society of London. Series B, Biological Sciences* 325:307–326.

House, M. R. 1996. Juvenile goniatite survival strategies following Devonian extinction Events. In Hart, W. (ed). *Biotic recovery from Mass Extinction Events*. – Geological Society Special Publication, 102:163-186

House, M. R. 2002. Strength, timing, setting and cause of mid-Palaeozoic extinctions. *Palaeogeography, Palaeoclimatology, Palaeoecology* 181: 5–25.

House, M. R. and Pedder, A. E. H. 1963. Devonian goniatites and stratigraphic correlations in Western Canada. *Palaeontology* 6:491–539.

House, M. R. and Senior, J. R. 1981. The Ammonoidea. *Systematic Association Special Volume* 18: 1-593. London, Academic Press.

Hutchinson, J. R., Ng-Thow-Hing, V. and Anderson, F.C. 2007. A 3D interactive method for estimating body segmental parameters in animals: application to the turning and running performance of Tyrannosaurus rex. *Journal of Theoretical Biology*, 246(4):660-680.

Jacobs, D. K., and Landman, N. H. 1993. Nautilus— a poor model for the function and behaviour of ammonoids? *Lethaia* 26(2):101-111.

Kaufmann, B. 2006. Calibrating the Devonian Time Scale: A synthesis ofU–Pb ID–TIMS ages and conodont stratigraphy. *Earth-Science Reviews* 76 175–190.

Keupp, H. 2000. *Ammoniten. Paläobiologische Erfolgsspiralen*. Thorbecke, Sigmaringen 165 pp

Klug, C. 2001a. Life-cycles of some Devonian ammonoids. *Lethaia* 34:215–233.

Klug, C. 2001b. Early Emsian ammonoids from the eastern Anti-Atlas (Morocco). *Paläontologische Zeitschrift*, 74 479–515.

Klug, C., Kröger, B., Kiessling, W., Mullins, G.L., Servais, T., Frýda, J., Korn, D. and Turner, S. 2010. The Devonian nekton revolution. *Lethaia*, 43: 465–477.

Klug, C., De Baets, K., Naglik, C. and Waters, J. 2014. New species of *Tiaracrinus* from the latest Emsian of Morocco. *Acta Palaeontologica Polonica* 59(1): 135-145, Warszawa.

Klug, C., Korn, D., Landman, N. H., Tanabe, K., De Baets, K. and NAGLIK, C. 2015. Describing ammonoid conchs. – In: Klug, C., Korn, D., De Baets, K. Kruta, I. and Mapes, R. H. (eds.): *Ammonoid paleobiology, Volume I: from anatomy to ecology*. Topics in Geobiology, 43: 3-24, Springer, Dordrecht.

Knauth, L. Paul; Kennedy, Martin J. 2009. The late Precambrian greening of the Earth. *Nature*. 460: 728–732.

Kravchinsky, V.A., Konstantinov, K.M., Courtillot, V., Savrasov, J.I., Valet, J-P., Cherniy, S.D., Mishenin, S.G. and Parasotka, B.S. 2002: Palaeomagnetism of East Siberian traps and kimberlites: two new poles and palaeogeographic reconstructions at about 360 and 250 Ma. *Geophysical Journal International*, 148(1): 1–33.

Kröger, B., Vinther, J. and Fuchs, D. 2011. Cephalopod origin and evolution: a congruent picture emerging from fossils, development and molecules. *Bioessays* 33(8):602-613.

Kruta, I., Landman, N., Rouget, I., Cecca, F. & Tafforeau, P. 2011. The role of ammonites in the Mesozoic marine food web revealed by jaw preservation. *Science*, 331, 70–72.

Kruta, I., Landman, N.H., Mapes, R. and Pradel, A. 2014. New insights into the buccal apparatus of the Goniatitina; palaeobiological and phylogenetic implications. *Lethaia*, 47:38–48.

Lehmann, W.M. 1932. Stereo-Röntgenaufnahmen als Hilfsmittel bei der Untersuchung von Versteinerungen. *Natur und Museum*, 62:323–330.

Lemanis R, Korn D, Zachow S, Rybacki E and Hoffmann, R. 2016. The Evolution and Development of Cephalopod Chambers and Their Shape. *PLoS ONE*, 11(3): e0151404. doi:10.1371/journal.pone.0151404

Loza, C.M., Latimer, A.E., Sanchez-Villagra, M.R. and Carlini, A.A. 2017. Sensory anatomy of the most aquatic of carnivorans: the Antarctic Ross seal, and convergences with other mammals. *Biology Letters*. 13:20170489.http://dx.doi.org/10.1098/rsbl.2017.0489

Lukeneder, A. 2012: Computed 3D visualization of an extinct cephalopod using computer tomographs. *Computers & Geosciences*, 45, 68–74.

Lukeneder, S., Lukeneder, A. and Weber, G.W. (2014): Computed reconstruction of spatial ammonoid-shell orientation captured from digitized grinding and landmark data. *Computers & Geosciences* 64, 104–114.

McGhee, G.R. Jr 1996. *The Late Devonian mass extinction*. Columbia University Press, New York.

McGhee, G. R. Jr 2005. Paleozoic/Devonian. 194-200.

McGhee, G.R. Jr., Clapham, M.E., Sheehan, P.M., Bottjer, D.J. and Droser, M.L. 2013. A new ecological-severity ranking of major Phanerozoic biodiversity crises. *Palaeogeography, Palaeoclimatology, Palaeoecology,* 370: 260–270

Meyer-Berthaud, B., Scheckler, S. E. and Wendt, J. 1999. Archaeopteris is the earliest known modern tree. *Nature*, 398, 700–701.

Miller, A. K., Furnish, W. M. and Schindewolf, O. H. 1957. Paleozoic Ammonoidea. – 5011-5079. In Moore, R. C. (ed.). *Treatise on Invertebrate Paleontology, Part L, Mollusca*. 14. Cephalopoda, Ammonoidea. – University of Kansas Press, Lawrence, 490 pp.

Montesinos, J. R. and Truyols-Massoni, M. 1987. La Fauna de *Anetoceras* y el límite Zlichoviense-Dalejense en el Dominio Palentino (NO. de España). *Cuaderno Laboratorio Xeolóxico de Coruña*, 11: 191–208.

Montesinos, J. R. and García-Alcalde, J. L. 1996. An occurrence of the auguritid ammonoid *Celaeceras* in the Lower Devonian of northern Spain. *Palaeontology*, 39:149–155.

Morris, S. C. 1989. Burgess Shale Faunas and the Cambrian Explosion. *Science*, 246: 339-346. DOI: 10.1126/science.246.4928.339

Mutvei, H., Zhang, Y-B. and Dunca, H. 2007. Late Cambrian plectonocerid nautiloids and their role in cephalopod evolution. *Palaeontology*, 50 (6): 1327-1333.

Neenan, J.M. and Scheyer, T. M. 2012. The Braincase and Inner Ear of *Placodus gigas* (Sauropterygia, Placodontia)—A New Reconstruction Based on Micro-Computed Tomographic Data. *Journal of Vertebrate Paleontology*, 32(6):1350-1357.

Nikolaeva, S. 2007. Discovery of Emsian Ammonoids in the Northern Caucasus. *Paleontologicheskii Zhurnal*, 34–39. [In Russian]

Racki, G., Rakociński, M., Marynowski, L. and Wignall, P.B. 2018. Mercury enrichments and the Frasnian-Famennian biotic crisis: A volcanic trigger proved? *Geology*, DOI: 10.1130/G40233.1

Raup, D.M. and Sepkoski, J.J., Jr. 1982. Mass extinctions in the marine fossil record. *Science*, 215: 1501–1503.

Ricci, J., Quidelleur, X., Pavlov, V., Orlov, S., Shatsilloc, A. and Courtillot, V. 2013. New 40Ar/39Ar and K–Ar ages of the Viluy traps (Eastern Siberia): Further evidence for a relationship with the Frasnian–Famennian mass extinction. *Palaeogeography, Palaeoclimatology, Palaeoecology*, 386: 531-540.

Ruan, Y.-P. 1996. Zonation and distribution of the early Devonian primitive ammonoids in South China. 104-112. In Wang, H.-Z. and Wang, X.-L. (eds). *Centennial Memorial Volume of Prof. Sun Yunzhu: Palaeontology and Stratigraphy.* China University of Geosciences Press, Wuhan, 186 p.

Rye, R. and Holland, H.D. 1998. Paleosols and the evolution of atmospheric oxygen: a critical review. *American Journal of Science* 298: 621–672.

Saunders, W. B., and Landman, N. 2009. *Nautilus: The Biology and Paleobiology of a Living Fossil*, Reprint with Additions. Springer Science & Business Media.

Scheckler, S. E. 2001. Afforestation - the first forest. 67-71. In Briggs, D. E. G. & Crowther, P. (eds.): *Palaeobiology II*. Blackwell Science, Oxford, 583 pp.

Scotese, C. R. 2001. *Atlas of Earth History*. PALEOMAP Project, Arlington, 52 pp.

Seilacher, A. 1988. Why are nautiloid and ammonoid sutures so different? *Neues Jahrbuch für Geologie und Paläontologi*e. 177:41–69.

Servais, T., Harper, D. A.T., Li, J., Munnecke, A., Owen, A.W. and. Sheehan, P. 2009. Understanding the Great Ordovician Biodiversification Event (GOBE): Influences of paleogeography, paleoclimate, or paleoecology? *GSA Today*, 19, no. 4/5, doi: 10.1130/GSATG37A.1.

Sheehan, P.M. 1996. A new look at Ecological Evolutionary Units (EEUs). *Palaeogeography, Palaeoclimatology, Palaeoecology*, 127:21–32, doi: 10.1016/S0031-0182(96)00086-7.

Shen,Y. T. 1975. Discovery of primitive ammonoids from Nandan of Guangxi and its stratigraphical significance. *Professional Papers in Stratigraphy and Paleontology* 1: 86-104. [In Chinese]

Sollas, W.J. 1903. A method for the investigation of fossils by serial sections. *Philosophical Transactions of the Royal Society of London, B*, 196 (214–224), 259–265.

Sowerby, J. 1812–1814. *Mineral Conchology of Great Britain*, I. 234 pp.

Stein, W.E., Berry, C.M., VanAller Hernick, L. and Mannolini, F. 2012. Surprisingly complex community discovered in the mid-Devonian fossil forest at Gilboa. *Nature*, 483: 78-81.

Sutton, M.D., Briggs, D.E.G., Siveter, D.J. & Siveter, D.J. 2001. Methodologies for the visualization and reconstruction of three-dimensional fossils from the Silurian Herefordshire Lagerstätte. *Palaeontologia Electronica* 4, 17.

Sutton, M., Rahman, I. and Garwood, R. 2014: *Techniques for Virtual Palaeontology*, 208 pp. Wiley-Blackwell, Chichester.

Tajika, A., Naglik, C., Morimoto, N., Pascual-Cebrian, E., Hennhöfer, D. K. and Klug, C. 2015a. Empirical 3D-model of the conch of the Middle Jurassic ammonite microconch *Normannites*, its buoyancy, the physical effects of its mature modifications and speculations on their function. – *Historical Biology* 27(2): 181-191, London.

Tajika, A., Morimoto, N., Wani, R., Naglik, C. and Klug, C. 2015b. Intraspecific variation of phragmocone chamber volumes throughout ontogeny in modern *Nautilus* and the Jurassic ammonite *Normannites*. – PeerJ, 3:e1306: 28 pp.; San Francisco, London. DOI 10.7717/peerj.1306.

Tessitore, L., Schemm-Gregory, M., Korn, D., Wild, F. R. W. P., Naglik, C. and Klug, C. 2013. Taphonomy and palaeoecology of the green pentamerid brachiopods from the Devonian of Aferdou el Mrakib, eastern Anti-Atlas, Morocco. *Swiss Journal of Palaeontology*, 132 (1): 23-44.

Tessitore, L., Naglik, C., De Baets, K., Galfetti, T. and Klug, C. 2016. Neptunian dykes in the Devonian carbonate buildup Aferdou El Mrakib (eastern Anti-Atlas, Morocco) and implications for its origin. *Neues Jahrbuch für Geologie und Paläontologie, Abhandlungen*, 281 (3): 247-266; Stuttgart.

Walliser, O.H. 1996. *Global Events and Event Stratigraphy in the Phanerozoic*. Springer Verlag, Berlin, 333 pp.

Ward P.D. 1987. *The natural history of Nautilus*. Boston: Allen and Unwin.

Ward, P. D., and Bandel, K. 1987. Life history strategies in fossil cephalopods. In Boyle, P.R. (ed.). *Cephalopod life cycles*, 2: 329-350. Academic Press, London, 329–350.

Webby, B.D., Droser, M.L., Paris, F., and Percival, I. 2004. *The Great Ordovician Biodiversification Event*. New York, Columbia University Press, 484 pp.

Wellman, C.H., Osterloff, P.L. and Mohiuddin, U. 2003. Fragments of the earliest land plants. *Nature*. 425: 282–285.

Yatskov, S. V. 1990. The oldest ammonoid family, the Anetoceratidae. *Paleontologicheskii Zhurnal*, 25–32. [in Russian]

Yolkin, E. A., Bakharev, N. K., Alekseenko, A. A., Izokh, N. G., Klets, A. G., Mezentseva, O. P., Rodina, O. A. abd Udodov, Y. V. 2000. Emsian (Lower Devonian) ammonoids and tentaculites from the Kuvash reference section of the Gorny Altai (southern West Siberia). *News of Paleontology and Stratigraphy* 2-3:189–194. [in Russian with English abs.]

APPENDIX I-A

Describing ammonoid conchs

Published in *Ammonoid Paleobiology, Volume I: from anatomy to ecology. Topics in Geobiology* (2015)

Chapter 1
Describing Ammonoid Conchs

Christian Klug, Dieter Korn, Neil H. Landman, Kazushige Tanabe, Kenneth De Baets and Carole Naglik

1.1 Introduction

Because ammonoid jaws are rare (Tanabe et al. 2015) and preserved soft parts as well as radulae (Klug and Lehmann 2015; Kruta et al. 2015) are even rarer, most paleontologists are limited in the available morphological information to the conch when describing ammonoids. Taking the great diversity and disparity as well as the over 300 Ma of the clade's existence into account, it becomes obvious that the different ammonoid clades have divergent sets of characters requiring descriptive procedures adapted to the requirements. For example, in the earliest ammonoids, details

C. Klug (✉) · C. Naglik
Paläontologisches Institut und Museum, University of Zurich, Karl Schmid-Strasse 6, 8006 Zurich, Switzerland
e-mail: chklug@pim.uzh.ch

C. Naglik
e-mail: carole.naglik@pim.uzh.ch

D. Korn
Museum für Naturkunde, Leibniz-Institut für Evolutions- und Biodiversitätsforschung, Invalidenstraße 43, 10115 Berlin, Germany
e-mail: dieter.korn@mfn-berlin.de

N. H. Landman
Division of Paleontology (Invertebrates), American Museum of Natural History, Central Park West at 79th St., New York 10024-5192, NY, USA
e-mail: landman@amnh.org

K. Tanabe
Department of Historical Geology and Paleontology, The University Museum, The University of Tokyo, Hongo 7-3-1, Tokyo 113-0033, Japan
e-mail: tanabe@um.u-tokyo.ac.jp

K. De Baets
GeoZentrum Nordbayern, Fachgruppe PaläoUmwelt, Universität Erlangen, Loewenichstr. 28, 91054 Erlangen, Germany
e-mail: kenneth.debaets@fau.de

C. Klug et al. (eds.), *Ammonoid Paleobiology: From Anatomy to Ecology*, Topics in Geobiology 43, DOI 10.1007/978-94-017-9630-9_1

of the suture line and the ornamentation are often less important while conch geometry yields important information. By contrast, ornamentation and sutures can be essential for the systematics of Late Paleozoic and Mesozoic ammonoid groups, while conch shape might play a lesser role. Additionally, intraspecific variability differs strongly between ammonoid clades and thus, small differences between some forms might justify the introduction of a new species whereas in other clades, such a small difference could fall within the broad range of intraspecific variability (De Baets et al. 2015).

Nevertheless, we will try to give a guideline on the optimal features that systematic descriptions of ammonoid species should take into consideration offering some suggestions which certainly go beyond the normal framework of descriptions, but which would give them a special above average quality. At the same time we are well aware that some of our suggestions would lead to some kind of 'de luxe' description, presuming all our suggestions are fully implemented.

Naturally, this is not the first attempt to produce a guideline for a more uniform and intelligible mode of ammonoid description. Many pioneers, however, did not explicitly state their strategies in describing ammonoids in their monographs, although these authors commonly followed certain rules.

Miller et al. (1957) and Arkell (1957) summarized the available morphological terms in the Treatise for Invertebrate Paleontology for Paleozoic and Mesozoic ammonoids, respectively. As far as Paleozoic ammonoids are concerned, it was Ruzhencev (1960) who set the standards for the description of Paleozoic ammonoids. His descriptions are not only well-structured but also provide the same set of information in a uniform order, accompanied by photographs of lateral and ventral views as well as suture lines and often cross sectional drawings. His introduction to conch shape and terminology in the Osnovy Paleontologii (Ruzhencev 1962, 1974) belongs to the best that have been printed.

Branco (1879–1880) described general characteristics of the early internal conch features of some ammonoids. Subsequent works with SEM (Tanabe et al. 1979; Drushchits and Doguzhaeva 1982) have demonstrated that the study of ontogenetic development of internal structures is as important as that of suture, shape and sculpture of conchs to construct an adequate scheme of major taxonomy and systematics of Ammonoidea (Kulicki et al. 2015).

In his famous books, Lehmann (1976, 1981, 1990) presented important descriptive terms with simple line drawings. However, his main focus was on paleobiological aspects of ammonoids.

Landman et al. (1996) and Westermann (1996) also defined morphological terms in a qualitative way. They distinguished various types of conch shapes for 'normal', planispirally coiled, ammonoids (with touching or overlapping whorls): cadiconic, discoconic, elliptospheroconic, planorbiconic, platyconic, serpenticonic, spheroconic. They also use specific terms to refer to "heteromorph" ammonoids, which are not planispirally coiled and/or have successive whorls in contact with one another: ancyloconic, breviconic, gyroconic, hamitoconic, orthoconic, scaphitoconic, torticonic and vermiconic. For relative terms, they use 'evolute' for more loosely coiled conchs, 'involute' was used to refer to tightly coiled conchs with a large whorl overlap and 'advolute' was used to refer to whorls, which are touching but not overlapping.

Landman et al. (1996) and Westermann (1996) also used the terms 'brevidomic', 'mesodomic' and 'longidomic' to describe body chamber lengths of approximately one-half whorl, three-fourth whorl, and a whorl or more in length, respectively. Body chamber length is usually expressed as the Body chamber angle (BCA) or the

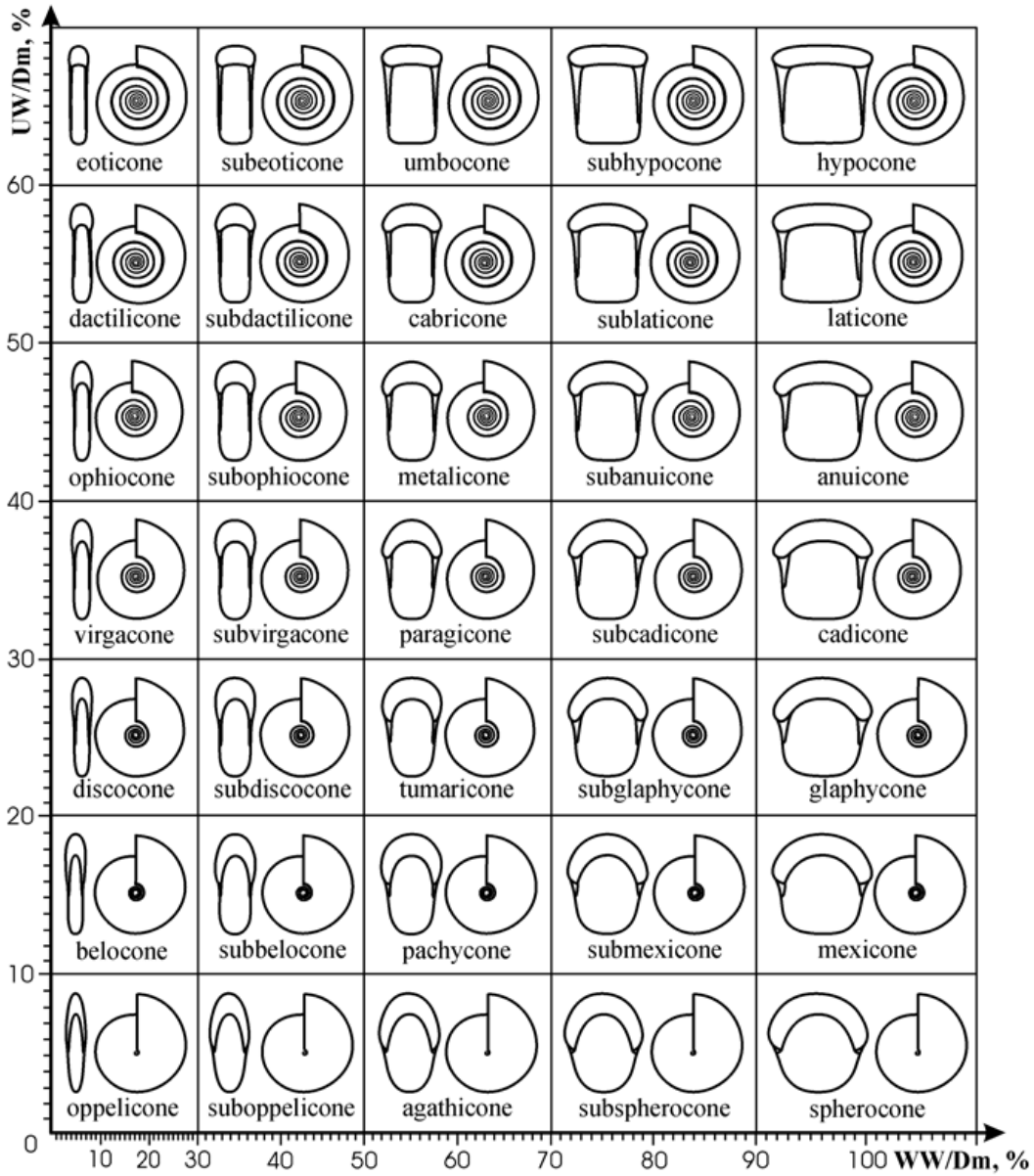

Fig. 1.1 Description of conch shapes as suggested by Kutygin (with permission, from Kutygin 1998) for Permian ammonoids. In the terminology of Arkell (1957), the following terms would be synonymous: oxycone—oppelicone; serpenticone—eoticone/dactilicone; platycone—suboppelicone/subbelocone; sphaerocone—subcadicone via mexicone and agathicone to spherocone

angular length measured from the septal neck (medial saddle of the external lobe) of the ultimate septum to the peristome (apertural edge), excluding lappets or rostra.

In several of his articles and monographs, Korn (e.g., Korn 1997; Korn and Klug 2002, 2003, 2007) quantified terms which he commonly uses to describe morphological aspects of ammonoid conchs. In order to make this more broadly known, he published "*A key for the description of Palaeozoic ammonoids*" (Korn 2010), where he listed terms, how to calculate certain ratios, and how to illustrate them properly.

Kutygin (1998) subdivided conch shapes of normally coiled ammonoids according to their umbilical width/conch diameter ratio versus whorl width/conch diameter ratio (Fig. 1.1). He outlined a theoretical morphospace of ammonoid conch-shapes, which he used to illustrate morphological change through ontogeny (Kutygin 2006).

Other examples for comprehensive definitions of terms are the monographs of Schlegelmilch (1976, 1985, 1994). He produced drawings of ribbing types, whorl cross sections, conch shapes, keels, shapes of apertures, and other conch parts.

Here, we provide an introduction to the terminology and methodology needed and/or recommended to describe ammonoids in general. There is such a wealth of terms, definitions and methods that we include only the most widely used ones.

1.2 Geometry

1.2.1 Classical Conch Parameters

Possibly, Moseley (1838) and Guido Sandberger (1851, 1953a, 1953b, 1857) were the first who described the coiling of ammonoid conchs mathematically. More recently, with the works of Trueman (1941) and Raup (Raup and Michelson 1965; Raup 1967), the quantification of ammonoid conch morphology has reached the 'high table' of ammonoid workers. Raup (1961, 1966) mainly used the following parameters:

S Shape of the generating curve;
W Whorl expansion rate;
D Position of the generating curve relative to the coiling axis;
T Rate of whorl translation. T equals zero in planispiral conchs and thus is of lesser interest in ammonoid research.

Instead of radii, which refer to the coiling axis, Korn (1997, 2010) began to use diameters to calculate whorl expansion rates. Diameters are much easier to measure and the coiling axis usually varies in its position through ontogeny. Accordingly, the main conch parameters (Fig. 1.2; Tab. 1.1) are:

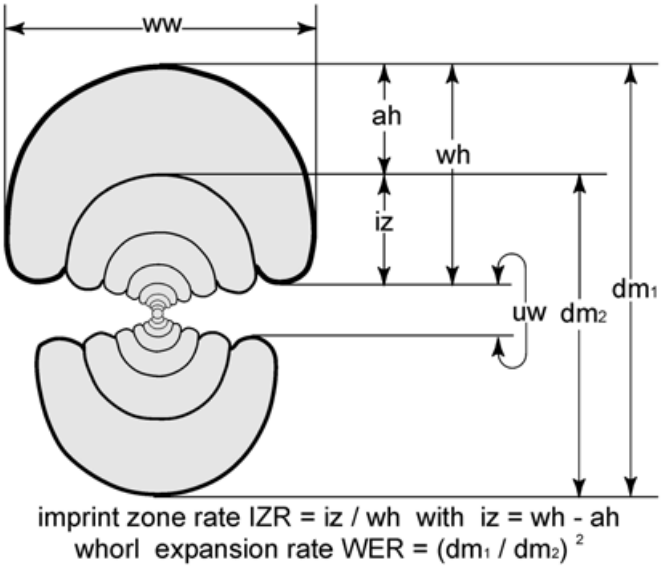

Fig. 1.2 Overview over the main conch parameters and ratios, exemplified on a cross section of the Middle Devonian ammonoid *Subanarcestes*

Table 1.1 Classification of the maximum conch diameters of individual specimens, the conch shape (ww/dm), the whorl width index (ww/wh), the umbilical width index (uw/dm), the whorl expansion rate (WER), and the whorl overlap or imprint zone rate (IZR). All values taken from Korn (2010)

Parameter	Descriptive term	Equation	Value
Max. conch diameter	Very small	dm	<25 mm
Max. conch diameter	Small	dm	25–50 mm
Max. conch diameter	Moderate	dm	50–100 mm
Max. conch diameter	Large	dm	100–200 mm
Max. conch diameter	Very large	dm	>200 mm
Conch shape	Extremely discoidal	ww/dm	<0.35
Conch shape	Discoidal	ww/dm	0.35–0.60
Conch shape	Pachyconic	ww/dm	0.60–0.85
Conch shape	Globular	ww/dm	0.85–1.10
Conch shape	Spindle-shaped	ww/dm	>1.10
Whorl width index WWI	Strongly compressed	ww/wh	<0.50
Whorl width index WWI	Weakly compressed	ww/wh	0.50–1.00
Whorl width index WWI	Weakly depressed	ww/wh	1.00–1.50
Whorl width index WWI	Moderately depressed	ww/wh	1.50–2.00
Whorl width index WWI	Strongly depressed	ww/wh	2.00–2.50
Whorl width index WWI	Very strongly depressed	ww/wh	2.50–3.00
Whorl width index WWI	Extremely depressed	ww/wh	>3.00
Umbilical width index UWI	Very narrow (involute)	uw/wh	<0.15
Umbilical width index UWI	Narrow (subinvolute)	uw/wh	0.15–0.30
Umbilical width index UWI	Moderate (subevolute)	uw/wh	0.30–0.45
Umbilical width index UWI	Wide (evolute)	uw/wh	0.45–0.60
Umbilical width index UWI	Very wide (very evolute)	uw/wh	>0.60
Whorl expansion rate WER	Very low	$[dm/(dm-ah)]^2$	<1.50
Whorl expansion rate WER	Low	$[dm/(dm-ah)]^2$	1.50–1.75
Whorl expansion rate WER	Moderate	$[dm/(dm-ah)]^2$	1.75–2.00
Whorl expansion rate WER	High	$[dm/(dm-ah)]^2$	2.00–2.25
Whorl expansion rate WER	Very high	$[dm/(dm-ah)]^2$	2.25–2.50
Whorl expansion rate WER	Extremely high	$[dm/(dm-ah)]^2$	>2.50
Imprint zone rate IZR	Weakly embracing	(wh−ah)/wh	<0.15
Imprint zone rate IZR	Moderately embracing	(wh−ah)/wh	0.15–0.30
Imprint zone rate IZR	Strongly embracing	(wh−ah)/wh	0.30–0.45
Imprint zone rate IZR	Very strongly embracing	(wh−ah)/wh	>0.45

- conch diameter: The maximum diameter is abbreviated as dm (or dm_1). In order to determine the whorl expansion rate, a second diameter value is needed, namely the diameter measured half a whorl earlier (180° behind the aperture or dm_1, respectively; dm_2). The conch diameter has often been used as proxy for size

(and relative age). However, other properties like body chamber volume might be more suitable as a proxy for size because it better reflects the volume of the soft body than the conch diameter, especially when comparing forms with very different conch geometries (e.g., Bucher et al. 1996; Dommergues et al. 2002; De Baets et al. 2012, 2013a, 2015). In extant coleoids (Nixon and Young 2003; Boyle and Rodhouse 2005), mostly the (dorsal) mantle length (which would correspond with the body chamber length in ammonoids) is used as a measure of size. Other measures are also used such as weight (which would correspond to the weight of the soft tissue with or without the conch) or the total length (with arms as they can form a major part of the coleoid). Nevertheless, the diameter will always be an important parameter in ammonoids as it is easy to obtain and has been widely used and available in the literature (Bucher et al. 1996).

- whorl width: It is measured perpendicular to the plane of symmetry and abbreviated as ww. In ornamented forms, this parameter is commonly measured between the ornament, so it represents a kind of minimal value. If this measurement is taken from older ontogenetic stages (e.g., from cross sections) in half a whorl distance (each 180 degrees), the values are labeled accordingly ww_1, ww_2, ww_3. This can also be done with the following parameters.
- whorl height: This parameter, abbreviated as wh, is measured parallel to the plane of symmetry from the umbilical seam or umbilical wall to the middle of the venter.
- umbilical width: Being a secondary parameter, it can be measured from umbilical wall to umbilical wall or it can be calculated as follows:
  $uw = dm_1 - wh_1 - wh_2$
- aperture height: This value is measured from the dorsum of the preceding whorl to the dorsum of the whorl under consideration. It can also be calculated:
  $ah = dm_1 - dm_2$
- imprint zone width: This parameter describes the degree of whorl overlap and is measured from the umbilical seam of the whorl under consideration to the dorsum of the preceding whorl. It may be calculated using the following equation:
  $iz = wh_1 - ah = wh_1 - (dm_1 - dm_2)$

1.2.2 Cross Section and Ratios

An easy way to assemble a lot of morphometric data from ammonoids is to produce cross sections perpendicular to the plane of symmetry and through the initial chamber. This allows quantification of ontogenetic change in the parameters listed above and also makes changes in shell thickness and in whorl cross section visible. A peculiar aspect of conch shape, made visible by cross sections, is the umbilical lid (a continuation of the lateral conch wall partially covering the umbilicus) of the Early Devonian auguritids and the Middle Devonian pinacitids (Klug and Korn 2002; Monnet et al. 2011) as well as in Middle Devonian pharciceratids (Bockwinkel et al. 2009). In the Auguritidae and Pinacitidae, the lateral wall begins to extend over the umbilicus starting in the juvenile whorls. Although this is just an example,

such cross sections can also reveal shell thickenings at the umbilicus, keels and other morphological details (e.g., Tozer 1972).

The greatest advantage of cross sections is the access to comprehensive morphometric data throughout ontogeny. In order to assure accuracy of the cross sections, the section should optimally run through the maximum diameter of the initial chamber (protoconch) and should be perpendicular to the plane of symmetry (Fig. 1.3). The values measured on complete specimens or sections can then be used to calculate the following simple ratios (Korn 2010):

- conch width index: CWI = ww/dm
- whorl width index: WWI = ww/wh
- umbilical width index: UWI = uw/dm = $(dm_1 - wh_1 - wh_2)/dm_1$

Based on the conch width index and the umbilical width index, the conch shapes and cross sections can be classified as (Fig. 1.4):

- discoidal (CWI < 0.60)
- pachyconic (0.60 ≤ CWI < 0.85)
- globular (0.85 ≤ CWI < 1.10)
- spindle-shaped (CWI ≥ 1.10)

According to the umbilical width, ammonoid conchs can be termed as

- involute (UWI < 0.15)
- subinvolute (0.15 ≤ UWI < 0.30)
- subevolute (0.30 ≤ UWI < 0.45)
- evolute (0.45 ≤ UWI < 0.60)
- very evolute to advolute (UWI ≥ 0.60)
- advolute: whorls touch but do not overlap
- heteromorphic/criocone: whorls do not touch

Cross sections also better reveal details of the conch morphology such as the vaulting of lateral or ventral walls. They help to describe the whorl cross section more correctly.

1.2.3 Expansion Rates

Due to their nearly logarithmic conch growth, most conch parameters also increase at differing rates. Caused by allometric growth, the change in certain parameters through ontogeny is not necessarily perfectly linear in a loglog-space (Kant 1973; Kant and Kullmann 1980; Klug 2001; Korn and Klug 2003; Urdy et al. 2010a, 2010b; Korn 2012; Urdy 2015). In order to quantify these changes, parameters taken from transverse cross sections or values measured in the plane of symmetry can be used.

Longitudinal (median) sections should optimally be in the plane of symmetry, i.e. the siphuncle or the siphuncular perforations should be visible completely. These sections offer the opportunity to measure parameters such as apertural height

Fig. 1.3 Example of **cross sections** of various ammonoids: **a** *Sellanarcestes* cf. *tenuior*, late Emsian, Devonian, Filon 12, Tafilalt, Morocco; protoconch is visible, almost perpendicular to the

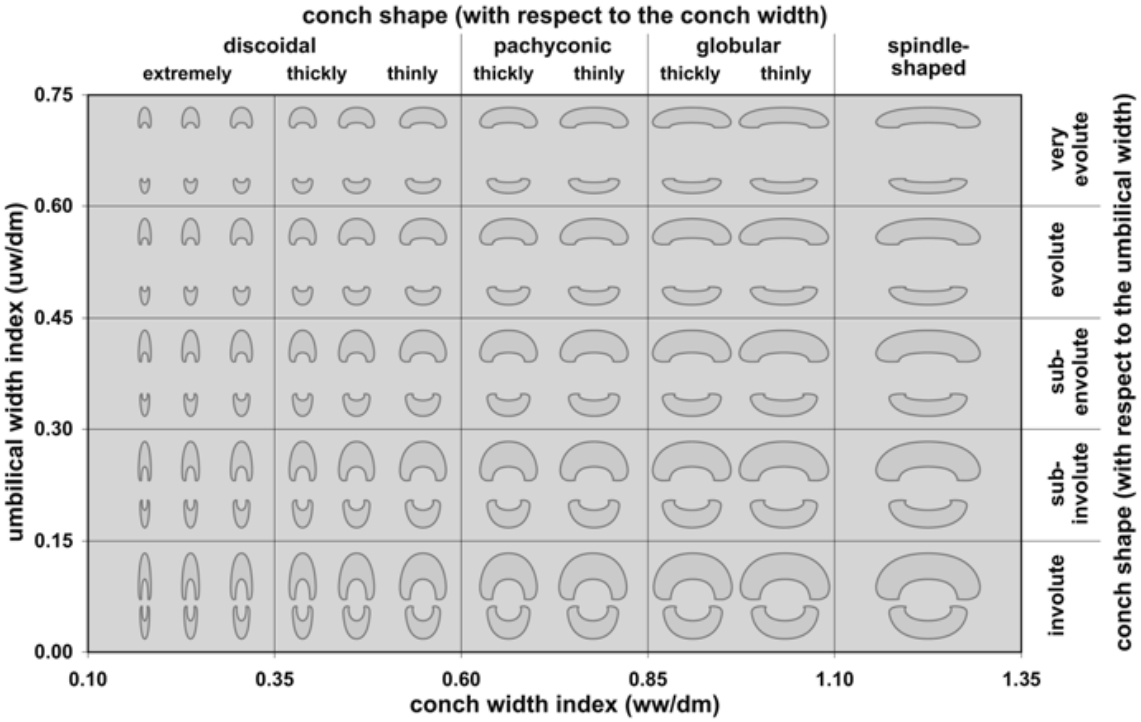

Fig. 1.4 Bivariate plot illustrating the terminology of the conch width index (ww/dm) on the x-axis and umbilical width index (uw/dm) on the y-axis (from Korn 2010)

and diameter in small increments, while whorl width, umbilical width, imprint zone width, and whorl height cannot be measured. Additionally, the angle between septa becomes measurable (Bucher et al. 1996; Kraft et al. 2008).

plane of symmetry (note the septa). **b** *Subanarcestes macrocephalus*, middle Eifelian, Filon 12, Tafilalt, Morocco; note the siphuncle. **c** *Goniatites multiliratus*, Visean, Elm Creek, Oklahoma, USA; note the symmetry in the septa, indicating a plane perpendicular to the plane of symmetry. **d, e** *Macrocephalites* sp., PIMUZ 19078, Callovian, Jurassic, Anwil, Switzerland; note the approximately symmetrically cut septa. **Orientation of ornament:** *F, Parkinsonia parkinsoni,* Bajocian, Port-en-Bessin, France, dm 124 mm, Staatliches Museum für Naturkunde Stuttgart. G, *Lytoceras fimbriatum,* Pliensbachian, Jurassic, Fresney-le-Puceux near Caen, France, dm 209 mm, Staatliches Museum für Naturkunde Stuttgart. H. *Erbenoceras advolvens,* GPIT 1849-2002, early Emsian, Devonian, northern Tafilalt, Morocco, dm 156 mm. (all images: W. Gerber, Tübingen; A, B reproduced from Ernst and Klug 2010). **Spiral ornamentation.** I to K: Lateral structures. I, *Maxigoniatites saourensis,* Visean, Carboniferous, near Merzouga, Tafilalt, Morocco, dm 72 mm. J. *Amaltheus margaritatus,* PIMUZ 13468, Pliensbachian, Reichenbach near Aalen, Germany. K, *Douvilleiceras mammillatum,* Albian, Cretaceous, Courcelles near Troyes, France, dm 10.8 cm, image: A. E. Richter, Augsburg. L to N: ventral structures. L, *Arietites* sp., Sinemurian, Jurassic, Mögglingen, Germany, dm 70 mm, Staatliches Museum für Naturkunde Stuttgart. (image: W. Gerber, Tübingen). M, *Euhoplites proboscideus,* PIMUZ 23108, Lower Gault, Albian, Cretaceous, Folkestone, Kent, UK, dm 40 mm. N, *Venezoliceras karsteni,* J 17830, Albian, NNE of Barbacoa, Venezuela, dm 110 mm, Naturhistorisches Museum Basel. **Ribbing patterns.** O, *Virgatisphinctes* sp., PIMUZ 16975, Unterhausen near Neuburg/Donau, Germany, dm 110 mm. P, *Pavlovia pallasioides,* Kimmeridgian, Jurassic, Kimmeridge Bay, Dorset, UK, dm 140 mm.

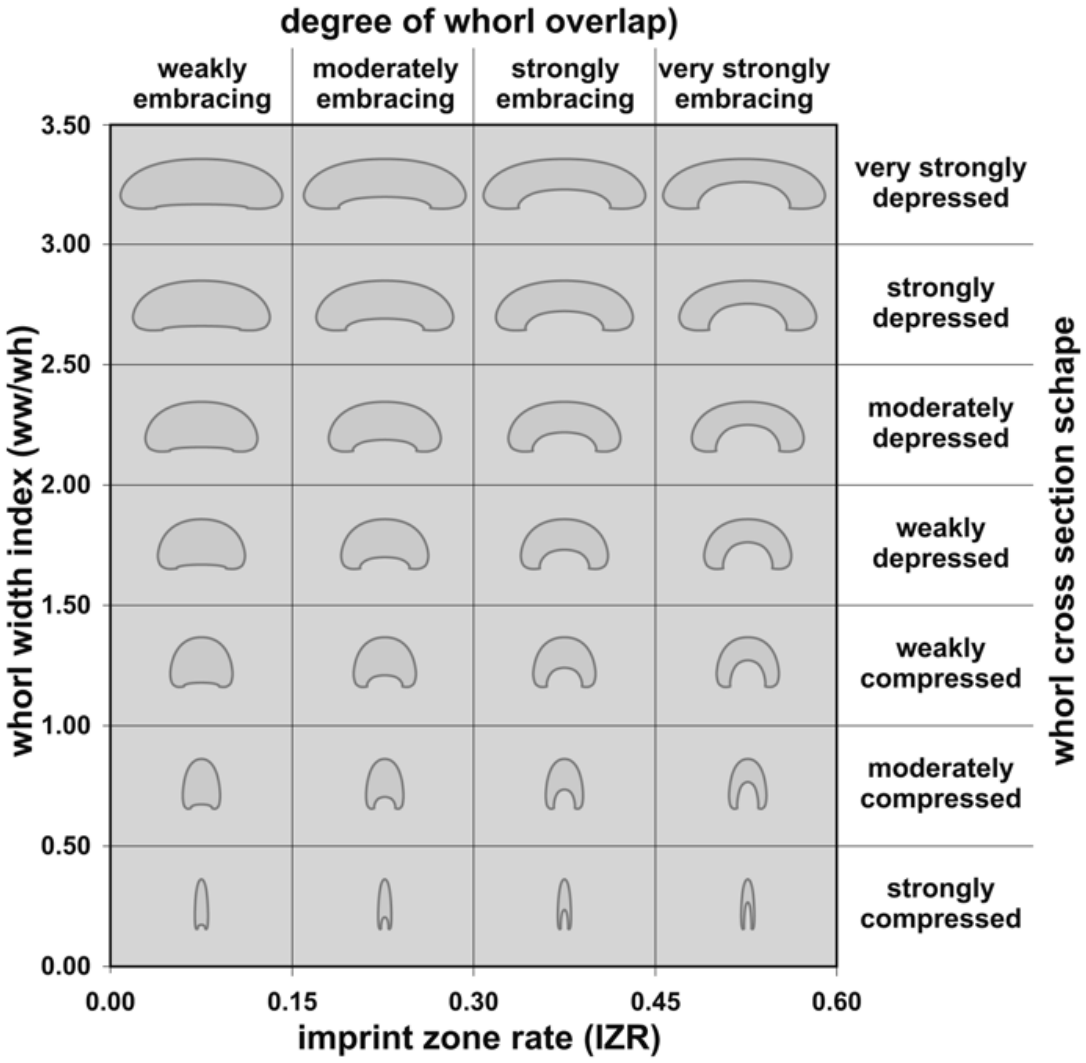

Fig. 1.5 Bivariate plot illustrating the terminology of the imprint zone rate (IZR) on the x-axis and whorl width index (ww/wh) on the y-axis (from Korn 2010)

Parameters measured through ontogeny on either kind of cross sections can be utilized to calculate the following expansion rates:

- whorl expansion rate:
  $WER_1 = (dm_1/dm_2)^2 = [dm_1/(dm_1 - ah_1)]^2$
- imprint zone rate:
  $IZR_1 = wh_1 - ah1/wh_1 = -[wh_1 \cdot (dm - dm_2)]/wh_1$

See Fig. 1.5 and Tab. 1.1 for subdivisions of whorl expansion rates and imprint zone rates.

Korn and Klug (2002) introduced a slightly different formula for the Whorl Expansion Rate (WER) than the one used by Raup (1967), which better reflects the growth of the soft-body during ontogeny (in loosely coiled forms) and which is easier and more precisely applicable than the classical equation proposed by Raup and Michelson (1965).

Parent et al. (2010, 2011) also independently arrived at a similar formula for planispirally coiled Mesozoic forms. They slightly modified the Raup-model to also include planispirally coiled forms with non-touching whorls.

1.3 Ornamentation

1.3.1 Radial Elements

All ammonoids bear fine or coarse radial elements on the conch. The finest structures are commonly the growth lines (Bucher et al. 1996), which are formed during conch growth. They form when shell is secreted discontinuously at the aperture and may be spaced at distances of around 0.1 mm (Vermeij 1993; Bucher et al. 1996). Characteristically, they are interrupted and cannot be traced around the entire whorl. To examine them, well preserved original or replacement shell is needed.

Lirae are usually much stronger; they are also formed more or less regularly with distances sometimes exceeding 1 mm. Normally, lirae can be traced around the ammonoid's circumference, but the limits between growth lines and lirae are not clearly defined. Both are simply fine and coarse traces of former apertures, recording their shape through growth.

Ribs represent even larger undulations in the conch wall and are not present in all ammonoid taxa. Their shape, arrangement, strength, etc. varies broadly and significant changes during ontogeny may be observed. Rather often, ribs continue into nodes or spines. They still carry valuable taxonomic information, although the strength of the ribs often covaries with the whorl cross section (Checa et al. 1996). Their strength, spacing and orientation may be quantified for taxonomic purposes (e.g., De Baets et al. 2013a, 2013b).

Constrictions are less frequent than the previously mentioned radial elements; they usually occur in a lower number than ribs (often between one and five per whorl) and commonly are produced at growth halts (megastriae; see Bucher et al. 1996; Urdy 2015). At least on the internal mould (steinkern), constrictions are visible as furrows. Often, constrictions are internal shell thickenings which may have made interim apertures more resistant against mechanical damage by any cause during growth halts. In some cases, the shell thickening equalized the inward bent shell surface in such a way, that it is barely visible from the outside. Since they represented growth halts, the orientation of younger radial elements tend to display an orientation differing from that of the preceding ones. In some cases, these interim apertures carried collars, spines or nodes, which can be diagnostic for certain taxa.

The orientation of the radial elements (Fig. 1.3, 1.6) can be described as rectiradiate (radial orientation), proradiate or prorsiradiate (turning toward the aperture in the ventral direction) and rursiradiate (turning away from the aperture in the ventral direction). Depending on their curvature, the ribs can be concave (vaulted away from the aperture) or convex (vaulted towards the aperture); these two terms can

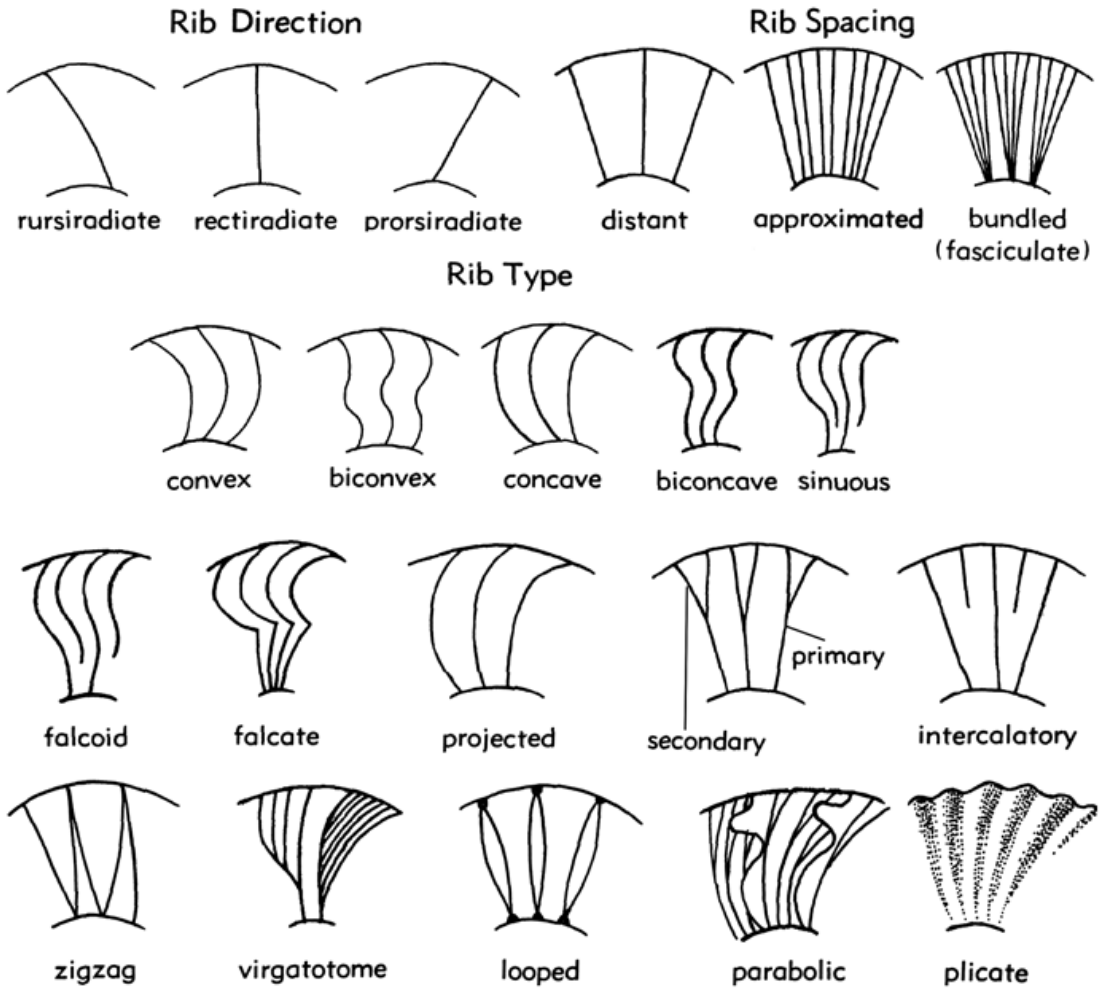

Fig. 1.6 Rib shape, spacing and course (modified from Arkell 1957)

be combined with the prefix pro- when they are inclined anteriorly (ventrad) and retro- when they are inclined posteriorly (ventrad). If the rib is partially concave and partially convex, it is called sinusoidal (sigmoid, sinusoid) and if the dorsal part of the rib is straight it is termed falcate. Ribs can split in various ways (Fig. 1.3, 1.6):

- simple (not branching)
- monoschizotomous (branching once): primary splits into two (bipartite, biplicate, dichotomous), three (tripartite) or four (quadripartite) secondary ribs
- dischizotomous (branching twice): primary splits into three (polygyrate) or four (bidichotomous) branches
- polyschizotomous (branching more than twice): branching only on one side of the primary rib (virgatipartite, virgatotomous) or branching on both sides of the primary (diversipartite)
- fibulate: ribs split and fuse again, forming a narrow ellipsis

In several Devonian and Carboniferous ammonoid species, subadult to adult specimens display the wrinkle layer (Korn et al. 2013). In all cases, these wrinkles are irregular and form a kind of fingerprint pattern on the dorsal shell. The elevation

of the wrinkles varies between a fraction of a millimetre and a few millimetres. In contrast to the wrinkle layer, Ritzstreifen extend over the entire conch and occur only in the Devonian (Sandberger and Sandberger 1850; Korn et al. 2013; compare Kulicki et al. 2015).

The spacing of radial elements is usually measured per half-whorl or demi-whorl (e.g., RDW or ribs per demi-whorl = the amount of ribs counted on a half-whorl). Other parameters such a rib-indexes have also been used to quantify rib spacing more locally (or on fragments: compare Yacobucci 2004; De Baets et al. 2013a).

1.3.2 Spiral Elements

Spiral ornament can be subdivided according to position, i.e. ventral, lateral, or dorsal. Many ammonoids display spiral ornament such as spiral lines, which are usually rather weak compared to many radial structures (Fig. 1.3). Spiral lines are particularly common in Paleozoic ammonoids, where they sometimes form reticulate patterns when they occur in combination with radial lirae or ribs. Another common phenomenon is spiral rows of spines or tubercles (Fig. 1.3), which may occur laterally and ventrally.

In the Early Jurassic Amaltheidae, the dorsal conch commonly displays spiral wrinkles comparable to the radial wrinkles of the wrinkle layer known from Paleozoic ammonoids (Fig. 1.3). As far as ventral structures are concerned, keels have to be mentioned. These may be sharp or rounded, they can be connected to the flanks with a smooth transition or they can be clearly set off, they may be accompanied by a pair of furrows or a set of several parallel keels can occur (e.g. in Frasnian Beloceratidae). Families such as the Parkinsoniidae or the Hoplitidae have a midventral furrow.

1.3.3 Spines, Nodes, Tubercles

There are several kinds of ornamentation, which are neither truly radial nor spiral in orientation. Spines are pointed and elongate, while tubercles and nodes are knob-shaped. The term node is sometimes used for bigger structures, although the use is not uniform and some might consider nodes and tubercles synonymous terms. All these structures can be arranged radially and/or spirally, for example in *Douvilleiceras* (Fig. 1.3).

Some Paleozoic forms have developed deep ventral sinuses in their aperture (ventral band). At the edge of this sinus, collar-like projections developed in some genera, which formed long ventral ‘median spines’ in genera such as *Armatites* or *Kosmoclymenia* (e.g., Korn 1979, 2014).

1.4 Septa

1.4.1 Suture Line

The suture line is the line, where the septal mantle first attached the organic septal membrane and later the septum is formed by mineralization of the membrane. Its importance in systematics and taxonomy varies, depending on the researcher and also on the taxon under consideration. In Early and some Middle Devonian forms, differences in the suture line are sometimes so subtle that other conch characters are of greater use (e.g., Chlupáč and Turek 1983).

Nevertheless, the suture line yields valuable information on systematics and ultimately also phylogeny. In order to produce good drawings of suture lines, growth lines or constrictions, various techniques can be used.

1. A very simple procedure that can be applied to sutures, which lack microscopic detail, is the following: A sharp pencil is used to trace the suture line directly on the specimen. Afterwards, a strip of thin transparent duct tape is used to cover the entire suture line under consideration. After rubbing the surface of the tape, where the suture was colored before, the tape can be removed and attached to a sheet of paper. Next steps are scanning and tracing the suture line formerly copied on tape with any vector graphic software.
2. The classical method is to mount the specimen with modeling clay under a binocular microscope and then use a drawing mirror (camera lucida) or a grid within an ocular in order to transfer the suture on paper. In order to depict the entire suture, the specimen needs to be turned and mounted again in a new position on the modeling clay. The raw drawing can then also be scanned and traced with vector graphic software.

The convention is that the saddles (Klug and Hoffmann 2015) point with their convex sides towards the top (aperture). The plane of symmetry (the center of the E-lobe) is marked by an arrow, the umbilical shoulder (if present) can be indicated by a dotted line, the umbilical seam by a curve segment and the dorsal intersection with the plane of symmetry is indicated by either two straight dashes or two straight lines. If possible, mostly the right side of the suture is depicted, at least until the umbilicus and, if visible, the internal suture is also added.

In the case of suture lines, it is also very helpful, when more than one ontogenetic stage is depicted, because the change in complexity through ontogeny can be extreme, especially in Mesozoic species. It is also important to illustrate an adult suture, because usually, the adult sutures display the peak complexity.

1.4.2 The Septum in Space

In many publications, the third dimension of the septum is neglected. This is somewhat justified because normally, the septum displays the strongest folding at the suture line. The way in which the septum is folded, however, might yield additional

information for the discrimination of taxa or for the reconstruction of phylogenetic relationships. Accordingly, it can be rewarding to pay special attention to the morphology of the entire septum, also because it might display soft-tissue imprints (Klug et al. 2008).

To some extent, septum shape depends on the whorl cross section. For example, in strongly compressed as well as in extremely depressed forms, there are often high numbers of sutural elements (Ruzhencev 1949). Corresponding pairs of sutural elements are often linked by bulges in the septum, namely in the case of compressed forms symmetrically arranged in lateral direction, in the case of depressed forms arranged in approximately dorsoventral direction. Depending on the orientation of this bulging (see Klug and Hoffmann 2015 for illustrations), the terms central fluting (bulges are radially arranged relative to the initial chamber), lateral fluting (bulges are perpendicular to the plane of symmetry) or radial fluting (bulges are arranged radially around the center of the septum) were introduced. Additionally, ammonoid septa may be synclastically (concave toward the aperture) or anticlastically folded (partially concave and partially convex toward the aperture).

1.5 Discriminating New Species

Naturally, the requirements for the introduction of a new species are not uniform across all taxonomic and stratigraphic boundaries. Nevertheless, some common rules apply to most groups of ammonoids. In the following, we will highlight some important aspects that can be taken into account, when new species are described. We are well aware that not all material yields all the information to perform all the studies listed below.

1.5.1 Ontogeny

A common problem with many taxa that have been introduced in the nineteenth century is that hardly anything is known about ontogenetic changes in these taxa. However, some parts of ammonoid conchs grow allometrically (Klug 2001; Korn 2012) and in the course of their growth, variability was not uniform (Ropolo 1995; De Baets et al. 2013a). This has been more generally shown for mollusk conchs by Urdy et al. (2010a, 2010b). Variability is often the lowest in the early and the latest whorls, i.e. these are the most characteristic, but still variable (De Baets et al. 2015).

If the material permits, as many of the major ontogenetic stages (embryonic conch, neanoconch, juvenile conch, preadult conch, adult conch; Westermann 1996; Klug 2001) as possible, especially of the last three stages, should be displayed and described in order to avoid that future researchers ascribe different ontogenetic stages of the same species to a different taxon.

1.5.2 Intraspecific Variability and the Quality of Characters

Discrete characters such as the absence or presence of certain structures or significant differences in numbers of lobes can be very helpful to identify species and also to justify the introduction of new species. In the case of characters, where transitions in character states between the supposedly new species and closely related species are known, intraspecific variability can be examined based on some tens of specimens of one size class in order to use such a character to explain the separation of a new species (De Baets et al. 2013a, 2015). The obvious disadvantage of the quantitative evaluation of intraspecific variability and its description as well as illustration is that they cost a lot of time and that they require a lot of printed space. Therefore, compromises are usually unavoidable and intraspecific variability cannot be examined for every single species. Nevertheless, it is a good idea to attempt to understand the intraspecific variability of the group one has to deal with, because then, the meaning of differences in any character between specimens can be more confidently interpreted with respect to its meaning, be it variation within a species or a difference in taxon.

When differences between supposedly new species in ratios such as UWI, CWI or WWI and in expansion rates such as WER and IZR (see Chap. 1.2) are evaluated, awareness of the respective intraspecific variability of the character under consideration can be of great help to both justify species separation and to avoid mistakes (e.g. by overestimating the character's meaning); however, intraspecific variability is roughly known only for a few species and genera, hampering such studies. This implies that, if time, the material, and thus the morphometric data permit, tests could be carried out to understand how the various character states are distributed through ontogeny. Are they normally distributed within a size class? Are one or several maxima present? Optimally, there should be two or more clearly separate peaks in the curve in order to make a quantitative character useful for species separation. An example, how such data can be represented, is given in Fig. 1.7. In any case, intraspecific variability of ammonoids is so poorly studied that it yields a wide array of possibilities for future studies (De Baets et al. 2015).

As stated above, intraspecific variability changes through ontogeny; it is usually the highest in middle whorls. This is partially reflected in some studies on covariation, Buckman's laws as well as in some other articles on variability (Hohenegger and Tatzreiter 1992; Dagys and Weitschat 1993; Checa et al. 1996; Korn and Klug 2007; De Baets et al. 2013a). If possible, we recommend basing descriptions on several specimens displaying several ontogenetic stages only. Furthermore, it is very helpful to include information on adult specimens, because adult conch modifications can show important diagnostic characters.

Sexual dimorphism (Klug et al. 2015) also contributes to intraspecific variability, especially in Mesozoic forms (Makowski 1962; Callomon 1963; Westermann 1964). Since dimorphism mostly applies to the last part of ontogeny, aspects of variability linked to dimorphism can be discriminated from variability within one sex.

Another poorly studied topic is differences in variability between regions; one of the inherent problems is the difficulty to reconstruct whether regional morpho-

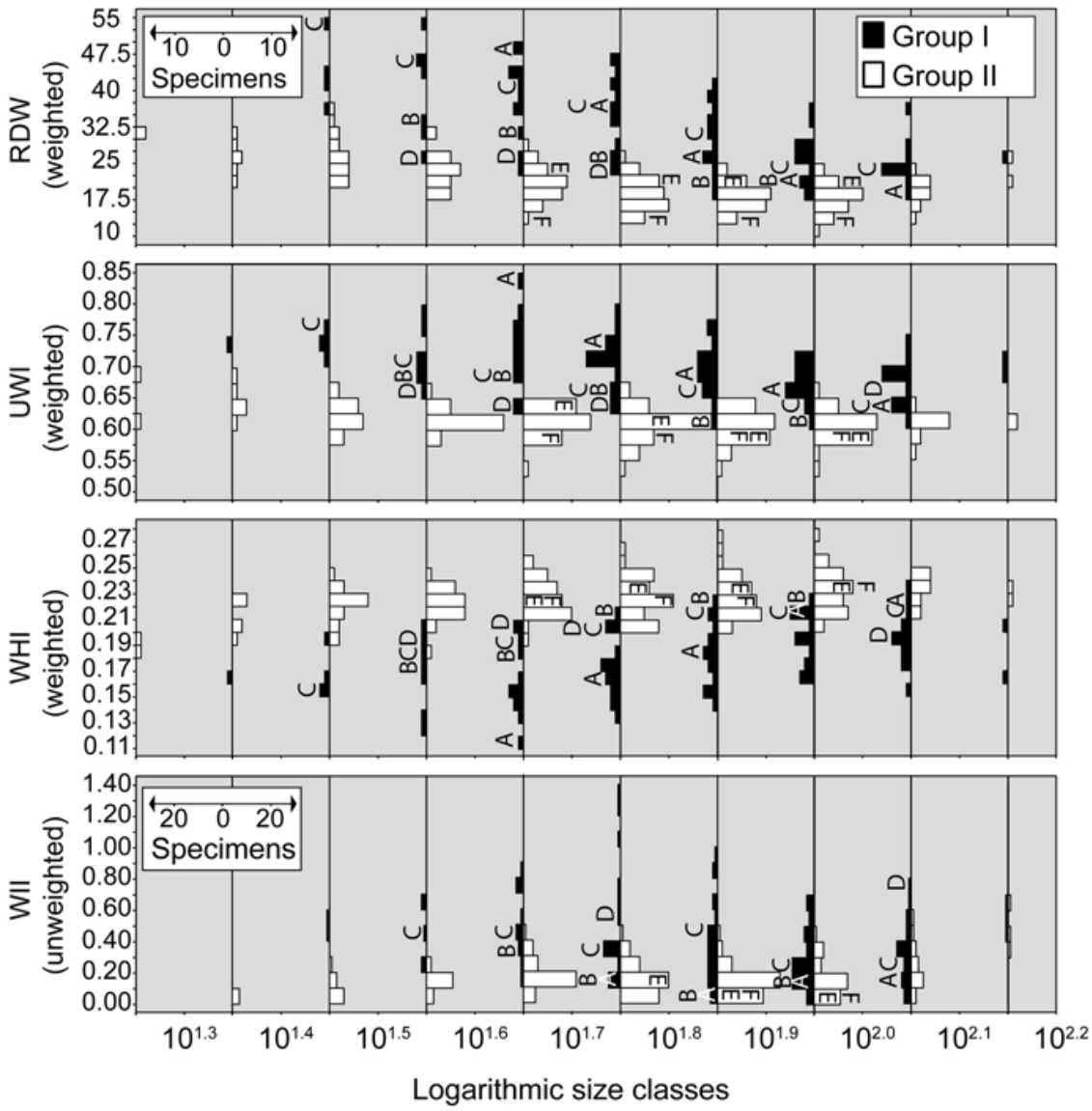

Fig. 1.7 Diagrams from De Baets et al. (2013a). Back-to-back histograms of Group I (*black*) and Group II (*white*) for ribs per half-whorl, RDW (weighted); umbilical width index, UWI (weighted); whorl height index, WHI (weighted); and whorl interspace index, WII (nonweighted)

logical differences originate in the facts that they are different species or whether these differences were caused by phenotypic plasticity or variation (Jacobs et al. 1994; Wilmsen and Mosavinia 2011). Body size may have varied geographically; intraspecific variability has certainly differed between regions, too (De Baets et al. 2015).

Although the study of intraspecific variability might appear as a nuisance, partially because it is time-consuming and partially because it is difficult to understand and describe in detail, it is actually an interesting topic for research since variation is essential for evolution, particularly heritable phenotypic variation (Hunt 2004, 2007). Furthermore, research on links between ecology and variability can also be rewarding (Jacobs et al. 1994; De Baets et al. 2015).

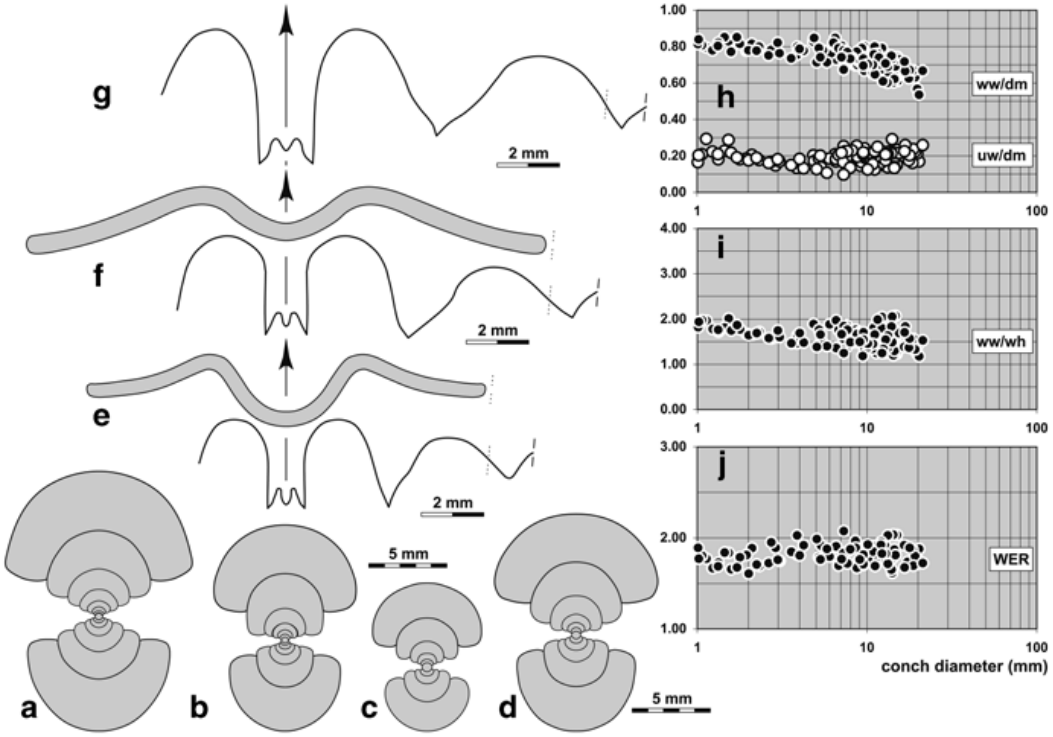

Fig. 1.8 An example of how to organise an illustration when a new species is described (Korn et al. 2010): *Eurites permutus* from the early Late Tournaisian of Oued Temertasset (Mouydir, Algeria). **a** Cross section, MB.C.18849.1. **b** Cross section, MB.C.19040.3. **c** Cross section, MB.C.19040.4. **d** Cross section, MB.C.19040.5. **e** Suture line and constriction, MB.C.18835.1, at 11.0 mm dm, 7.9 mm ww, 5.3 mm wh. **f** Suture line and constriction, MB.C.18978.1, at 14.0 mm dm, 10.4 mm ww, 7.0 mm wh. **g** Suture line, MB.C.19040.1, at 19.0 mm dm, 12.5 mm ww, 9.0 mm wh. **h–j** Ontogenetic development of the conch width index (ww/dm), umbilical width index (uw/dm), whorl width index (ww/wh), and whorl expansion rate (WER) of all specimens

1.5.3 Number of Specimens and Figures

As ammonoids may show great intraspecific variability and since many taxa display allometric growth in their conch, it is advantageous when more than one specimen is available when a new species is described. If possible, these specimens should show the major growth stages, especially the juvenile, the preadult, and the adult stage. Similarly, it is helpful when the main allometric changes, as well as a large part of the intraspecific variability of one growth stage can be illustrated.

As far as the number of figures is concerned, we recommend producing some graphs illustrating the ontogenetic change of morphometric aspects of the ornamentation (rib spacing, ornament strength, ornament orientation etc.), UWI, WWI and WER through ontogeny of several specimens. This yields an idea of intraspecific variability and allometry. Optimally, one specimen of each growth phase should be illustrated, with the adult growth phase being possibly the most important. If dimorphism is strongly expressed, a dimorphic pair can be illustrated. Furthermore, a cross section (photograph or drawing after a photograph) may yield valuable ontogenetic information and drawings of the suture as well as of growth lines, the aperture, constrictions, etc. Some of these illustrations may be meaningfully combined (see Fig. 1.8).

1.6 Organizing A Species Description

Classically, a diagnosis is given first, usually combined with information on synonymies, origin of the name, type material, its provenance, other materials used and the repository. Although slightly dated, Matthews (1973) and Bengtson (1988) are still some of the best references for how best to use synonymy lists and open nomenclature, respectively. The diagnosis should be concise and contain the major characters of the taxon. It should list the main aspects of conch morphology and ontogeny, ornament, and suture line (Korn 2010).

In the detailed description, the same topics should be addressed in the same order, but in greater detail. The task and strength of such a descriptive text is to highlight important parameters and character states. Comparisons can be listed in the "comparisons" or "remarks" paragraph.

As most ammonoids underwent more or less profound changes in morphology throughout their ontogeny, it is advantageous to provide a reasonable amount of information on these ontogenetic trajectories, at least as far as such data can be obtained. Some examples for representations of ontogenetic changes can be found in the following articles: Korn (1997); Klug (2001); Monnet et al. (2012).

Although Korn et al. (2010) replaced the descriptive paragraphs in the systematic section by tables with the main morphological information, many might want to list the characters and their states in descriptions. One can order the descriptions according to

- specimen
- ontogeny (initial chamber, ammonitella, juvenile/neanic, preadult, adult/mature/gerontic)
- character (conch shape, ornamentation, suture line)

It is the easiest for the reader, when one of these orders is chosen and adhered to throughout the entire manuscript. Naturally, several aspects will vary according to the individual style.

Acknowledgments Some of the insights grew in the course of the research projects with the numbers 200021-113956/1, 200020-25029, and 200020-132870 funded by the Swiss National Science Foundation SNF (CK, CN, KDB). We greatly appreciate the constructive reviews of Ottilia Szives (Budapest) and Christian Meister (Geneva).

References

Arkell WJ (1957) Introduction to Mesozoic Ammonoidea. In: Moore RC (ed) Treatise on Invertebrate Paleontology. Part L, Mollusca 4, Cephalopoda-Ammonoidea. GSA and University of Kansas Press, L80–L100

Bengtson P (1988) Open nomenclature. Palaeontology 31:223–227

Bockwinkel J, Becker RT, Ebbighausen V (2009) Upper Givetian ammonoids from Dar Kaoua (Tafilalt, SE Anti-Atlas, Morocco). Berl Paläobiol Abh 10:61–128

Boyle P, Rodhouse P (2005) Cephalopods: ecology and fisheries. Blackwell Publishing, Singapore

Branco W (1879–1880) Beiträge zur Entwicklungsgeschichte der fossilen Cephalopoden. Palaeontogr 26(1879):15–50 (27(1880):17–81)
Bucher H, Landman NH, Klofak, SM, Guex J (1996) Mode and rate of shell growth. In: Landman NH, Tanabe K, Davis RA (eds) Ammonoid paleobiology. Plenum, New York
Callomon JH (1963) Sexual dimorphism in Jurassic ammonites. Trans Leic Lit Philos Soc 57:21–56
Checa A, Company M, Sandoval J, Weitschat W (1996) Covariation of morphological characters in the Triassic ammonoid *Czekanowskites rieberi*. Lethaia 29:225–235
Chlupáč I, Turek V (1983) Devonian goniatites from the Barrandian area. Rozpr Ustred Ust Geol 46:1–159
Dagys AS, Weitschat W (1993) Extensive intraspecific variation in a Triassic ammonoid from Siberia. Lethaia 26:113–121
De Baets K Klug C Korn D Landman NH (2012) Early evolutionary trends in ammonoid embryonic development. Evolution 66:1788–1806
De Baets K Klug C Monnet C (2013a) Intraspecific variability through ontogeny in early ammonoids. Paleobiology 39(1):75–94
De Baets K Klug C Korn D Bartels C Poschmann M (2013b) Emsian Ammonoidea and the age of the Hunsrück Slate (Rhenish Mountains, Western Germany). Palaeontogr A 299(1–6):1–113
De Baets K, Bert D, Hofmann R, Monnet C, Yacobucci MM, Klug C (2015) Ammonoid intraspecific variability (this volume)
Dommergues J-L, Montuire S, Neige P (2002) Size patterns through time: the case of the Early Jurassic ammonite radiation. Paleobiology 28:423–434
Drushchits VV, Doguzhaeva LA (1982) Ammonites under the electron microscope. Moscow University Press, Moscow (in Russian)
Ernst HU, Klug C (2011) Perlboote und Ammonshörner weltweit. Nautilids and Ammonites worldwide. Pfeil Verlag, München
Hohenegger J, Tatzreiter F (1992) Morphometric methods in determination of ammonite species, exemplified through *Balatonites* shells (Middle Triassic). J Paleont 66:801–816.
Hunt G (2004) Phenotypic variation in fossil samples: modeling the consequences of time-averaging. Paleobiology 30:426–443
Hunt G (2007) Variation and early evolution. Science 317:459–460
Jacobs DK, Landman NH, Chamberlain JA (1994) Ammonite shell shape covaries with facies and hydrodynamics: iterative evolution as a response to changes in basinal environment. Geology 22:905–908
Kant R (1973) Allometrisches Wachstum paläozoischer Ammonoideen: Variabilität und Korrelation einiger Merkmale. Neues Jahrb Geol Paläontol Abh 143(2):153–192
Kant R, Kullmann J (1980) Umstellungen im Gehäusebau jungpaläozoischer Ammonoideen. Neues Jahrb Geol Paläontol Mh 1980(11):673–685
Klug C (2001) Life-cycles of Emsian and Eifelian ammonoids (Devonian). Lethaia 34:215–233
Klug C, Hoffmann R (2015) Ammonoid septa and sutures. (this volume)
Klug C, Korn D (2002) Occluded umbilicus in the Pinacitinae (Devonian) and its palaeoecological implications. Palaeontology 45:917–931
Klug C, Lehmann J (2015) Soft-part anatomy of ammonoids: reconstructing the animal based on exceptionally preserved specimens and actualistic comparisons. (this volume)
Klug C, Meyer E, Richter U, Korn D (2008) Soft-tissue imprints in fossil and recent cephalopod septa and septum formation. Lethaia 41:477–492
Klug C, Zatoń M, Parent H, Hostettler B, Tajika A (2015) Mature modifications and sexual dimorphism. (this volume)
Korn D (1979) Mediandornen bei *Kosmoclymenia* Schindewolf (Ammonoidea, Cephalopoda). N Jahrb Geol Paläont Mh 7:399–405
Korn D (1997) The Palaeozoic ammonoids of the South Portuguese Zone. Memórias do Instituto Geológico e Mineiro 33:1–131
Korn D (2010) A key for the description of Palaeozoic ammonoids. Foss Rec 13:5–12
Korn D (2012) Quantification of ontogenetic allometry in ammonoids. Evol Dev 14(6):501–514
Korn D (2014) *Armatites kaufmanni* n. sp., the first Late Devonian goniatite with ventral spines. Neues Jahrb Geol Paläontol Abh 271:349–352

Korn D, Klug C (2002) Ammoneae Devonicae. In: Riegraf W (ed) Fossilium catalogus. Backhuys, Leiden
Korn D, Klug C (2003) Morphological pathways in the evolution of Early and Middle Devonian ammonoids. Paleobiology 29:329–348
Korn D, Klug C (2007) Conch form analysis, variability, morphological disparity, and mode of life of the Frasnian (Late Devonian) Ammonoid *Manticoceras* from Coumiac (Montagne Noire, France). In: Landman NH, Davis RA, Mapes RH (eds) Cephalopods present and past: New insights and fresh perspectives. Springer, Dordrecht
Korn D, Klug C (2012) Palaeozoic ammonoids—diversity and development of conch morphology. In: Talent J (ed) Extinction intervals and biogeographic perturbations through time: earth and Life (International year of planet earth). Springer, Netherlands
Korn D, Ebbighausen V, Bockwinkel J, Klug C (2003) On the A-mode sutural ontogeny in prolecanitid ammonoids. Palaeontology 46:1123–1132
Korn D, Bockwinkel J, Ebbighausen V (2010) The ammonoids from the Argiles de Teguentour of Oued Temertasset (early Late Tournaisian; Mouydir, Algeria). Foss Rec 13:35–152
Korn D, Mapes RH, Klug C (2013) The coarse wrinkle layer of Palaeozoic ammonoids: new evidence from the Early Carboniferous of Morocco. Palaeontology 57:771–781. doi:10.1111/pala.12087
Kraft S, Korn D, Klug C (2008) Ontogenetic patterns of septal spacing in Carboniferous ammonoids. Neues Jahrb Geol Paläontol Abh 250:31–44
Kruta I, Landman NH, Tanabe K (2015) Ammonoid radulae. (this volume)
Kulicki C, Tanabe K, Landman NH, Kaim A (2015) Ammonoid shell microstructure. (this volume)
Kutygin RV (1998) Shell shapes of Permian ammonoids from northeastern Russia. Paleont Zh 1998 (1):20–31
Kutygin RV (2006) Methods for studying ammonoid shell shape (example of Permian Goniatitida from northeastern Asia). Russiskaja Akademija Nauk Paleontologiczeskij Institut, pp 96–98 [in Russian]
Landman NH, Tanabe K, Davis RA (eds) (1996) Ammonoid paleobiology. Plenum, New York
Lehmann U (1976) Ammoniten. Ihr Leben und ihre Umwelt. Enke, Stuttgart, p 171
Lehmann U (1981) The ammonites: their life and their world. Cambridge University Press, New York
Lehmann U (1990) Ammonoideen. Enke, Stuttgart
Makowski H (1962) Problem of sexual dimorphism in ammonites. Palaeontol Pol 12:1–92
Matthews SC (1973) Notes on open nomenclature and synonymy lists. Palaeontology 16:713–719
Miller AK, Furnish WM, Schindewolf OH (1957) Paleozoic Ammonoidea. In: Moore RC (ed) Treatise on Invertebrate Paleontology, Part L, Mollusca 4, Cephalopoda-Ammonoidea. GSA and University of Kansas Press, L11–L20
Monnet C, Klug C, De Baets K (2011) Parallel evolution controlled by adaptation and covariation in ammonoid cephalopods. BMC Evol Biol 11(115):1–21
Monnet C, Bucher H, Guex J, Wasmer M (2012) Large-scale evolutionary trends of Acrochordiceratidae Arthaber, 1911 (Ammonoidea, Middle Triassic) and Cope's rule. Palaeontology 55:87–107
Moseley H (1838) On the geometrical forms of turbinated and discoid shells. R Soc Lond Phil Trans 138:351–370
Nixon M, Young JZ (2003) The brains and lives of cephalopods. Oxford University Press, Oxford
Parent H, Greco AF, Bejas M (2010) Size-Shape relationships in the Mesozoic Planispiral Ammonites. Acta Palaeont Pol 55, 85–98
Parent H, Bejas M, Greco A, Hammer O (2011) Relationships between dimensionless models of ammonoid shell morphology. Acta Palaeont Pol 57:445–447
Raup DM (1961) The geometry of coiling in gastropods. Proc Natl Acad. Sci U S A 47:602–609
Raup DM (1966) Geometric analysis of shell coiling: general problems. J Paleontol 40(5):1178–1190
Raup DM (1967) Geometric analysis of shell coiling: coiling in ammonoids. J Paleontol 41(1):43–65
Raup DM, Michelson A (1965) Theoretical morphology of the coiled shell. Science 147:1294–1295

Ropolo P (1995) Implications of variation in coiling in some Hauterivian (Lower Cretaceous) heteromorph ammonites from the Vocontian basin, France. Mem Descr della Carta Geol Ital 51:137–165.

Ruzhencev VE (1949) Biostratigrafiya verkhnego karbona (Upper Carboniferous biostratigraphy). Dokl Akad Nauk SSSR 67(3):529–532

Ruzhencev VE (1960) Printsipy sistematiki, sistema i filogeniya paleozoyskikh ammonoidey (Principles of systematics, the system and phylogeny of Paleozoic ammonoids). Trudy Paleontol Inst Akad Nauk SSSR 133:1–331 [in Russian]

Ruzhencev VE (1962) Nadotryad Ammonoidea. Ammonoidei. Obshchaya chast' (Superorder Ammonoidea. Ammonoidei. General section). In: Orlov YA, Ruzhencev VE (eds) Osnovy Paleontologii, 5, Mollyuski: Golovonogie 1. Akademiya Nauk SSSR, Moskva

Ruzhencev VE (1974) Superorder Ammonoidea. General section. In: Orlov YA, Ruzhencev VE (eds) Fundamentals of paleontology. V. Mollusca: Cephalopoda I, Jerusalem.

Sandberger G (1851) Beobachtungen über mehrere schwierige Puncte der Organisation der Goniatiten. Jahrb Ver Nat Herzogthum Nassau 7:292–304

Sandberger G (1853a) Einige Beobachtungen über Clymenien; mit besonderer Rücksicht auf die westphälischen Arten. Verh Naturhist Ver Preuss Rheinl Westph 10:171–216

Sandberger G (1853b) Über Clymenien. Neues Jahrb Miner Geogn Geol Petrefakten-K 1853:513–523

Sandberger G (1857) Paläontologische Kleinigkeiten aus den Rheinlanden. Verh Naturhist Ver Preuss Rheinl Westph 14:140–142

Sandberger G, Sandberger F (1850–1856) Die Versteinerungen des rheinischen Schichtensystems in Nassau. Mit einer kurzgefassten Geognosie dieses Gebietes und mit steter Berücksichtigung analoger Schichten anderer Länder I-XIV, vol 1850, pp 1–72

Schlegelmilch R (1976) Die Ammoniten des süddeutschen Lias. Fischer, Stuttgart

Schlegelmilch R (1985) Die Ammoniten des süddeutschen Doggers. Fischer, Stuttgart

Schlegelmilch R (1994) Die Ammoniten des süddeutschen Malms. Fischer, Stuttgart.

Tanabe K, Kruta I, Landman NH (2015) Ammonoid buccal mass and jaw apparatus. (this volume)

Tanabe K, Obata I, Fukuda Y, Futakami M (1979) Early shell growth in some Upper Cretaceous ammonites and its implications to major taxonomy. Bull Nat Sci Mus (Tokyo) C 5:155–176

Tozer ET (1972) Observations on the shell structure of Triassic ammonoids. Palaeontology 15:637–654

Trueman AE (1941) The ammonite body chamber, with special reference to the buoyancy and mode of life of the living ammonite. Quart J Geol Soc Lond 96:339–383

Urdy S (2015) Theoretical modelling of the molluscan shell: what has been learnt from the comparison among molluscan taxa? (this volume)

Urdy S, Goudemand N, Bucher H, Chirat R (2010a) Allometries and the morphogenesis of the molluscan shell: a quantitative and theoretical model. J Exp Zool B 314:280–302

Urdy S, Goudemand N, Bucher H, Chirat R (2010b) Growth dependent phenotypic variation of molluscan shell shape: implications for allometric data interpretation. J Exp Zool B 314:303–326

Vermeij GJ (1993) A natural history of shells. Princeton University Press, Princeton

Westermann GEG (1964) Sexual-Dimorphismus bei Ammonoideen und seine Bedeutung für Taxonomie der Otoitidae (einschliesslich Sphaeroceratinae; Ammonitina, M. Jura). Palaeontogr A 124:1–3, 33–73

Westermann GEG (1996) Ammonoid life and habit. In: Landman NH, Tanabe K, Davis RA (eds) Ammonoid paleobiology. Plenum, New York

Wilmsen M, Mosavinia A (2011) Phenotypic plasticity and taxonomy of *Schloenbachia* varians (J. Sowerby, 1817) (Cretaceous Ammonoidea). Paläontol Z 85:169–184

Yacobucci MM (2004) Buckman's Paradox: variability and constraints on ammonoid ornament and shell shape. Lethaia 37:57–69

APPENDIX I-B

Ammonoid Buoyancy

Published in *Ammonoid Paleobiology, Volume I: from anatomy to ecology. Topics in Geobiology* (2015)

Chapter 16
Ammonoid Buoyancy

René Hoffmann, Robert Lemanis, Carole Naglik and Christian Klug

16.1 Introduction

In this chapter we summarize the current knowledge on the buoyancy apparatus of ammonoids. We also discuss the ability of ammonoids to use their phragmocone to obtain neutral buoyancy. A major line of reasoning is the actualistic comparison with living nautilids (e.g., Ward 1979, 1982, 1986, 1987) and other phragmocone-bearing cephalopods (e.g., Ward and Boletzky 1984; Warnke et al. 2010). The upward acting buoyant force is a product of the volume and density of the displaced liquid (in this case seawater, since all cephalopods are marine) which is equivalent to the volume of the submerged object, its magnitude is equal to the weight of the displaced fluid (Archimedes principle, see, e.g., Heath 1897).

The buoyant force acts through a definable point called the centre of buoyancy which is the centre of mass of the displaced fluid (e.g., Trueman 1941). The magnitude of the buoyant force depends only on the volume of the submerged object. Two objects of equivalent volume will experience the same buoyant force regardless of their respective masses. The net buoyancy which predicts whether an object will rise, sink, or stabilize in a column of water, is the difference between the weight of the submerged object and the buoyant force. Some animals evolved mechanisms to

R. Hoffmann (✉) · R. Lemanis
Department of Earth Sciences, Institute of Geology, Mineralogy, and Geophysics,
Ruhr-Universität Bochum, Universitätsstraße 150, 44801 Bochum, Germany
e-mail: rene.hoffmann@rub.de

R. Lemanis
e-mail: robert.lemanis@rub.de

C. Naglik · C. Klug
Paläontologisches Institut und Museum, University of Zurich,
Karl Schmid-Strasse 6, CH-8006 Zurich, Switzerland
e-mail: carole.naglik@pim.uzh.ch

C. Klug
e-mail: chklug@pim.uzh.ch

C. Klug et al. (eds.), *Ammonoid Paleobiology: From anatomy to ecology*,
Topics in Geobiology 43, DOI 10.1007/978-94-017-9630-9_16

change their effective weight while retaining their volume (e.g., *Argonauta* see Finn and Norman 2010).

Changing the spatial distribution of mass causes a simultaneous shift of the respective centre of mass (coincident with the centre of gravity). Mineralized hard parts and muscle tissue of active marine animals are denser than seawater and have negative buoyancy when separated from the rest of the organism. Macroscopic animals spending large parts of their lifetime in the free water column evolved two general solutions to this problem that can be broadly divided into active and passive methods. Active methods are characterized by propelling a volume of water in the direction opposite to the direction of motion (i.e. swimming). Certain animals, such as the flatfish, tuna and some sharks, depend on the force generated through swimming to counteract their sinking due to negative buoyancy. Passive methods are seen in organisms that have evolved gas floats or incorporate low density tissue or fluids in their bodies in order to negate the need to expend energy to counteract sinking. These gas floats, tissues and fluids have a density below the density of water and provided the animal with a total density equal or very close to that of water, a condition referred to as neutral buoyancy (this can also be expressed as the point in which the total weight of the animal is equal in magnitude to the buoyant force).

The ammonia-containing tissues of some squids (Denton et al. 1969) or the swim bladder of some fish (Denton 1962) are examples of tissues and organs which reduce weight and thereby enable the entire organism to reach neutral buoyancy. Similar to the swim bladder, cephalopods evolved a chambered shell (the phragmocone) which acts as a gas float for buoyancy control. It is well known that cephalopods with chambered shells use their phragmocone to regulate their actual weight which also causes a shift of the centre of gravity, to become neutrally buoyant (Ward 1987).

Buoyancy control is applied very regularly by cephalopods with chambered shells such as *Nautilus, Sepia* and *Spirula*, for example in order to facilitate their vertical migrations in *Nautilus* (Crick 1988; Clarke 1969; Denton and Gilpin-Brown 1961b; Dunstan et al. 2011). Changes between negatively, neutrally and positively buoyant animals were observed by Bidder (1962) for aquarium reared *Nautilus* suggesting that liquid can move into and out of the phragmocone chambers.

In addition to the extinct ammonoids and some coleoids, a number of extinct Paleozoic taxa and the Mesozoic and Cenozoic nautilid clade have such chambered shells (Fig. 16.1). The actual weight of an ammonoid is the sum of the shell (conch, septa), soft parts (soft body in the body chamber, siphuncle and pellicle in the phragmocone), liquids and gas in the chambers—the latter being negligible. It was demonstrated that in modern cephalopods with chambered shells the newly built chamber was initially filled with liquid (Ward 1987). The liquid was subsequently pumped out of the chambers by the siphuncle rendering the shell less dense than sea water. Thereby the shell compensates the actual weight of the animal resulting in neutral buoyancy. This mechanism allows for flotation without expending muscular energy just to stay in the water column.

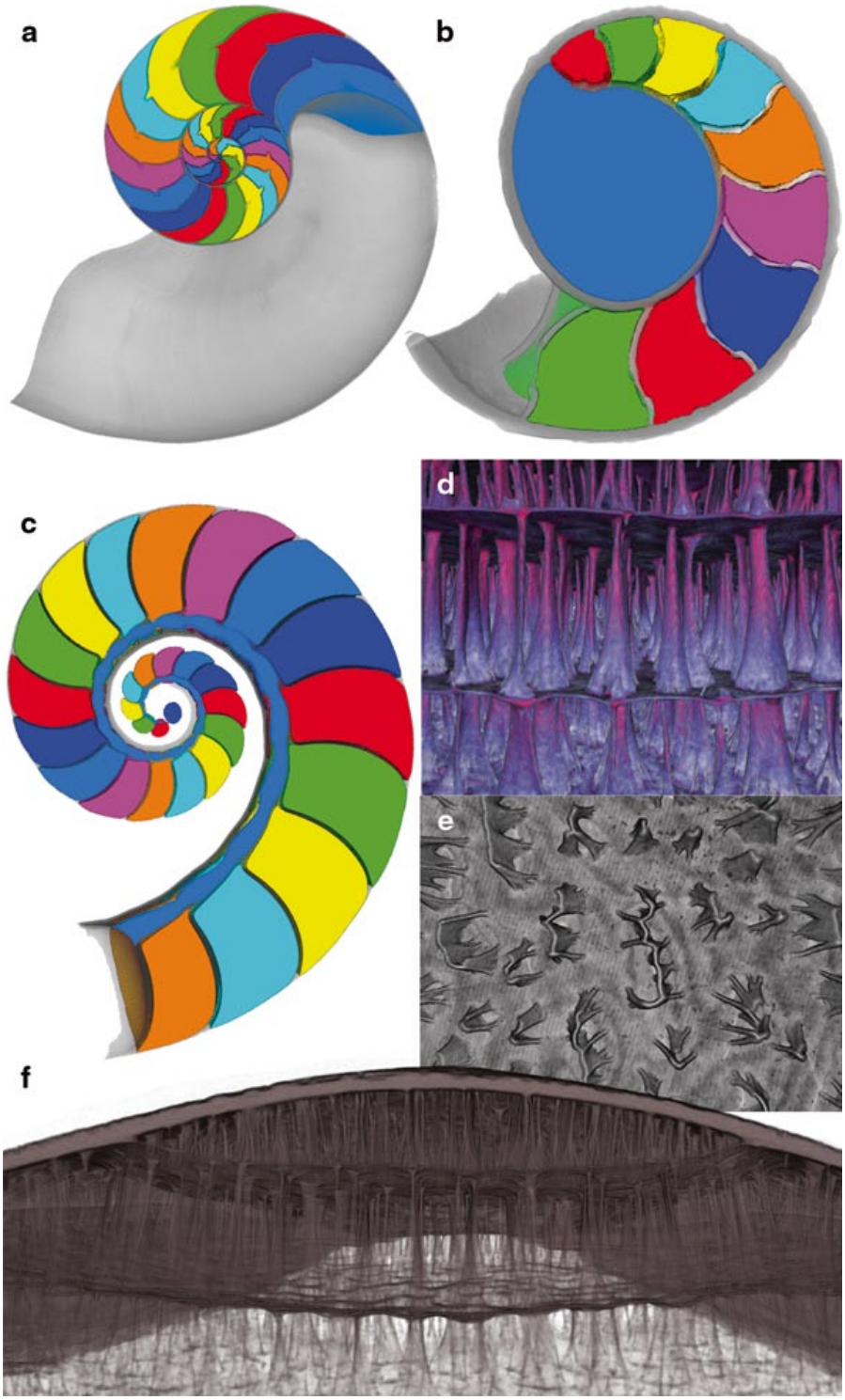

Fig. 16.1 **a–f** section through the shells of chambered cephalopods. **a** *Nautilus pompilius* with the body chamber in grey and the phragmocone chambers coloured, note the slight septal crowding between the last and the penultimate septum. **b** juvenile *Cadoceras* sp. with its protoconch (in *blue*) and the earliest chambers of the phragmocone in different colours. **c** *Spirula spirula* with the siphuncle (*blue*) running through the complete shell. **d–f** *Sepia officinalis*. **d** a close up of f showing the perpendicular pillars between the chamber walls of the phragmocone. **e** a top view of the same pillars showing the complex structure that is reminiscent of ammonoid septa but do not subdivide the chamber. **f** cross section through the cuttlebone of a juvenile *Sepia officinalis* with the thick dorsal shield on top and three subsequent chambers and pillars

16.2 History

Derham (1726) was the first to suggest that the *Nautilus* shell was a buoyancy compensation apparatus and suggested the possible role of gas pressure in expelling water from the shell (*fide* Derham 1726). However, the understanding of the function of the nautilid phragmocone remained unclear until the early 1960s. A simple test to prove Hooke's suggestion, puncturing the shell while immersed in water, was suggested by Owen (1832, 1878). Owen (1832), who was well familiar with the vascularisation necessary for pressurised gas generation in fish swim bladders, recognized the lack of those structures in *Nautilus* and therefore doubted the idea of pressurized gas suggested by Hooke (1695). Only Buckland (1836), Pfaff (1911), Spath (1919), and Westermann (1956) accepted the non-elevated gas-pressure in chambered cephalopods but did not develop new ideas about the chamber emptying process. Arkell (1957), the preeminent ammonitologist of his time, attacked Westermann's (1956) objections and supported the gas pressure theory. Surprisingly, the simple experiment suggested by Owen (1832, 1878) was performed about 130 years later in the framework of functional and anatomical studies in the 1960–1970s by Denton (1962, 1971, 1974), Denton and Gilpin-Brown (1961a, b, c, 1966, 1971, 1973), as well as Denton et al. (1961, 1967). They demonstrated that the nautilid shell does not contain an elevated gas pressure. By these experiments, it became clear that the cephalopod shell does support the hydrostatic load resulting from the overlying column of water at atmospheric pressures in the chambers. They also demonstrated that the siphuncle was the organ responsible for osmotically emptying the cameral liquid and that the pressure within the shell is at one atmosphere or below. Approximately neutral buoyancy in extant chambered cephalopods (*Nautilus*, *Sepia* and *Spirula*) is achieved by changing the ratio of gas and liquid in the phragmocone chambers by osmotic pressure in the siphuncular cells. The hypothesis of pre-septal gas as a buoyancy mechanism invented by Hooke (1695) was rejected by Bidder (1962). For a detailed historical review, the reader is referred to Jacobs (1992) as well as Jacobs and Chamberlain (1996).

First extensive trials for quantitative calculations of the buoyancy of chambered cephalopods were made by means of mathematical models. Such models were published by Moseley (1838), Trueman (1941), and later by Currie (1957); the latter two models were corrected by Heptonstall (1970), Reyment (1958, 1973), Mutvei and Reyment (1973), Westermann (1977), Saunders and Shapiro (1986), Tsujita and Westermann (1998), Westermann (1998b), Kröger (2000) and the latest much more complex calculations were done by Kröger (2002), Hammer and Bucher (2006) and Longridge et al. (2009).

Recently, empirical data have been employed by some authors in order to reconstruct the buoyancy of ammonoids (Tajika et al. 2014; Naglik et al. 2014). These empirical data were produced by both technically intricate, energetically expensive and time-consuming methods such as grinding tomography, computer tomography and synchrotron tomography (for overviews see Sutton et al. 2001; Hoffmann and Zachow 2011; Hoffmann et al. 2014; Sutton et al. 2014).

16.3 Ammonoid Life Habits

One of the oldest and still lasting debates among ammonoid researchers is related with the life habits of ammonoids including whether they could actively swim or not (Naglik et al. 2015). Several attempts were made (e.g., Trueman 1941; Heptonstall 1970) to calculate the buoyancy of fossil cephalopods in order to reconstruct their mode of life. Already Trueman (1941) faced the difficulties of mathematical calculation of masses and volumes of extinct animals by applying geometrical approximations (see below). Since no perfect mathematical method is available and the results of buoyancy calculations seem to support either positive, occasionally neutral or sometimes negative buoyancy for ammonoids, this debate seemed to never end. By contrast, new empirical studies will put an end to these debates, hopefully.

In general, the discussion is twofold. On the one hand, ammonoid life habit is compared to benthic gastropods and thus, this idea is dubbed the "benthic crawler" hypothesis. That all ammonoids were gastropod-like benthic crawlers was repeatedly stressed by Ebel (1983, 1985, 1990, 1992, 1993, 1999) and Rein (1999) for ceratitid ammonoids. These authors even included the shape of the soft body in this hypothesis and reconstructed the head-foot-complex of ammonoids with a gastropod-like foot. Similarly, *Nipponites* was, for a long time, the single known example of an ectocochleate cephalopod referred to a sessile, benthonic habit (Diener 1912; Schmidt 1930; Moore et al. 1952; Tasch 1973). This hypothesis was later rejected by Ward and Westermann (1977) based on new buoyancy calculations in favour for a planktic mode of life. Ebel's (1983) theory was criticized by Westermann (1993, 1996, 1998a), Engeser (1996), Jacobs and Chamberlain (1996), and Kröger (2001) and most other ammonoid researchers. Shigeta (1993) reported on positively buoyant hatchlings becoming markedly negatively buoyant at 2.0–2.5 mm diameter (see Jacobs and Chamberlain 1996, p. 185 for further explanations).

These other researchers including Denton and Gilpin-Brown (1961a, 1973), Ward and Martin (1978) and many more now favour a swimming mode of life of extinct ammonoids similar to their extant relatives and assume that ammonoids were well capable of attaining neutral buoyancy. Neutral buoyancy was suggested by Westermann (1990) and Kröger (2000, 2001) for Jurassic and Cretaceous ammonoids and for Late Paleozoic ammonoids by Swan and Saunders (1987). Heptonstall (1970) calculated a density for ammonites well below that of seawater. A planktic mode of life for heteromorphic ammonoids with a U-shaped body chamber has been considered by Schmidt (1925), Berry (1928), Donovan (1964), Packard (1972), Klinger (1981), and Westermann (1996). Furthermore, Crick (1988), exemplified for nautiloids, outlined the problem of cephalopods not as a problem of increasing buoyancy but as a problem of reducing it. This point of view was supported by the calculations of Westermann (1998a) for earliest plectronocerid cephalopods. Endosiphonal or endocameral deposits in orthoconic cephalopods point in a similar direction (e.g. Westermann 2013). These precipitations act as ballast in the apical part of the phragmocone to offset the strong buoyancy of the phragmocone and to

control the attitude of the shell (Kröger 2001). Denton and Gilpin-Brown (1971) reported for *Spirula* that the earliest 1–5 chambers of the phragmocone were filled with liquid. Liquid ballast also occurs in the cuttlebone of extant *Sepia* (Denton and Gilpin-Brown 1961a) as a solution (without carbonate precipitation) to maintain neutral buoyancy and/or a horizontal swimming position. Recently, Westermann (2013) could successfully demonstrate for the orthoconic *Baculites* that the apical part of the phragmocone must have been filled with liquid if a horizontal swimming position is accepted. Seilacher (1960) described an ammonoid (*Buchiceras*) that was not only able to control its buoyancy to some extend but could also compensate a significant change of density that had occurred due to encrustations by oysters during lifetime. The same phenomenon was demonstrated by Klug et al. (2004) for Triassic *Ceratites* which reacted on *syn vivo Placunopsis*-overgrowth by shortening the body chamber. Seilacher's (1960) example was used by Heptonstall (1970) to demonstrate that this *Buchiceras* must have had about 25 % of its phragmocone volume filled with liquid as removable ballast (which is more or less the case in Recent nautilids and was demonstrated by Tajika et al. 2014 for a Jurassic ammonite). Similarly heavy *syn vivo* encrustations by oysters and Cirripedia were shown by Keupp et al. (1999). Other indicators not directly related with buoyancy calculations point to a swimming habit of ammonoids as well. These are the presence of ammonites in black shale deposits representing oceanic anoxic events with oxygen depleted bottom water and the lack of trace fossils. A bottom crawling habit of ammonites with a strong muscular foot comparable to gastropods would favour the preservation of these soft parts in Konservat-Lagerstätten like La Voulte (France; Charbonnier 2009) or Herefordshire (UK; Sutton et al. 2006). However, not a single report about ammonoid trace fossils or massively phosphatized soft body is known to the authors (only poorly carbonized parts; Klug et al. 2012; Klug and Lehmann 2014).

During the last two decades, a more differentiated approach for ammonoid life habits based on shell shape (Westermann 1996, 1998b; Ritterbush and Bottjer 2012), analyses of stable isotopes (Moriya et al. 2003; Lukeneder et al. 2010; Kruta et al. 2014) and sedimentological data (Reboulet et al. 2005) became available.

Universal ammonoid behaviour was challenged by recent observations of depth distribution of *Nautilus pompilius*. Dunstan et al. (2011) document a continuous nightly movement between 130–700 m water depth and a daytime behaviour of either stasis in relatively shallow 160–225 m depth or active foraging in depths between 489–700 m. Additionally, Dunstan et al. (2011) demonstrated the same depth distribution for juveniles and daytime feeding behaviour. These data document a more complex vertical migration pattern dictated by optimal feeding, avoidance of daytime predators, requirements for resting periods at around 200 m to regain nearly neutral buoyancy, upper temperature limits of 25 °C and implosion depths of 800 m. These are important facts that should be considered in future discussions about ammonoid distribution and behaviour.

16.4 Pumping Mechanism

In order to understand buoyancy control and the mode of life of fossil cephalopods, it is most important to understand the ecology and functional morphology of their close living relatives with functional phragmocones, i.e. *Nautilus*, *Spirula* and *Sepia*.

Bruun (1943), who worked on *Spirula*, was the first to mention an osmotic mechanism in cephalopods acting to remove the cameral liquid. However, the osmotic difference between fresh and salt water produces an osmotic pressure of about 25 atmospheres. This value is achieved in 240 m water depth. At greater depths, the hydrostatic pressure will exceed osmotic pressure and chambers would be re-filled with liquid causing negative buoyancy. Due to the occurrence of *Spirula* far below 240 m, Bruun (1943, 1950) rejected the osmotic pump hypothesis. Further observations by Clarke (1970) on the depth distribution confirmed Bruun's (1943) earlier report. Clarke (1970) found high concentrations of juvenile *Spirula* in depths between 1000–1750 m and larger specimens between 600–700 m. Depth distribution during ontogeny is fortunately also recorded in the stable oxygen isotopes of these cephalopod shells. Based on the shells of two live caught specimens of *Spirula*, Warnke et al. (2010) documented ontogenetic changes in terms of depth distribution. Juveniles hatch at around 800 m water depth and subsequently migrate upwards to around 350–400 m; as adults, they sink again down to about 550–600 m (Warnke et al. 2010).

Similar discrepancies between the actual depth distribution (Dunstan et al. 2011) and limitation by the osmotic mechanisms were observed for *Nautilus*. Ward and Martin (1978) demonstrated that below 250 m water depths the osmotic pressure gradient between the siphuncle tissue and phragmocone chambers of *Nautilus* causes an influx of liquid into the chambers, resulting in negative buoyancy. Furthermore, it is possible for *Nautilus* to empty its chambers and regain neutral buoyancy only at depths less than 250 m. Again, the limitation of a simple osmotic mechanism is contradicted by the observation of juvenile *Nautilus pompilius* at 703 m depth reported by Dunstan et al. (2011). After migrating below a water depth of 250 m, a resting and re-equilibration period at around 200 m becomes necessary which has been documented by Dunstan et al. (2011). Note that diving depth of *Nautilus* is limited by temperature, chamber re-filling and shell implosion with the greatest depth being around 800 m (Kanie et al. 1980; Ward et al. 1980a).

After Bruun's (1943, 1950) scepticism, the mechanisms of buoyancy control of extant chambered cephalopods (*Nautilus*, *Sepia* and *Spirula*) have been clarified by the work of Denton and Gilpin-Brown (1961a, b, c, 1966, 1971) and Denton et al. (1961, 1967). Denton and Gilpin-Brown (1961a, b, c) as well as Denton et al. (1961) were not aware of the experiment suggested by Owen (1832), so they started their extensive survey to explore the buoyancy mechanism in cephalopods with the cuttlebone of the cuttlefish *Sepia*. According to the old theory of Hooke (1695), they expected to find pressurized gas within the chambers of freshly caught specimens.

Surprisingly, gas did not emanate from the live caught cuttlefish as a consequence of the sudden ascent and decompression. Gas was also not detected in the tissue surrounding the cuttlebone. When punctured under water, fluid flows into the chambers because phragmocone chamber gas pressure is usually around 0.8 atmospheres. It was observed that more fluid enters the recently formed chambers of the cuttlebone than into older ones, thus indicating a continuously increasing gas pressure. Gas within the chambers was composed of primarily nitrogen, much less oxygen (Bert 1867) and more carbon dioxide compared to atmospheric conditions and the fluid was principally a solution of sodium chloride. Gas pressure in older chambers was in equilibrium with the gases in the blood. *Sepia* varies in density as a result from a change in the density of the cuttlebone being negatively buoyant during day time and neutrally or positively buoyant at night. Quick changes of density and thus buoyancy were arranged by changing the amount of liquid and gas volume in the cuttlebone but not under pressurized conditions. Accordingly, Denton and Gilpin-Brown (1961a, b, c) as well as Denton et al. (1961) assumed an osmotic mechanism to pump cameral liquid into or out of the chambers. While the chamber liquid can be hyposmotic to sea water (when caught in greater depths), the cuttlefish blood is almost isosmotic with sea water. Changes of cameral liquid must be carried out by exchanges in salt or water across the siphuncular membrane in order to balance the hydrostatic pressure by an osmotic force. The siphuncular membrane covering the siphuncular wall acts as a barrier; through active transport of ions across that membrane, water follows due to the higher salt concentration compared to the cameral liquid. Contrary, concentration changes of the liquid within each chamber depend on diffusion of salts either towards or away from the region of the siphuncular membrane. When the cameral liquid of a newly built chamber was completely emptied, gas migrated under very low pressure by passive diffusion from the blood of the cuttlefish into that chamber.

Nautilus and *Spirula*, were also studied by Denton and Gilpin-Brown (1966, 1971) as well as Denton et al. (1967). Both taxa share a siphuncular tube which runs through all chambers of the phragmocone, while in *Sepia*, the siphuncle is almost flat (siphuncular field). Only through the permeable siphuncle, exchanges of liquids and substances between chambers and tissues can take place (Denton and Gilpin-Brown 1966; Collins and Minton 1967; Chamberlain and Moore 1982). However, the results they obtained show very great similarities with their findings in *Sepia*. Gas pressure in the chambers of *Spirula* was lowest in newly built chambers but remains below normal atmospheric pressure at sea-level (around 0.8 atmospheres). Concerning the gas pressure, the same holds true for *Nautilus* and consists mainly of nitrogen (Vrolik 1843). Contrary to *Sepia*, the liquid of a newly formed chamber in *Nautilus* was isosmotic with sea water at first. Concentration of salts within the liquid of a new chamber decreases to about one fifth of that of sea water and the animal's blood before water begins to leave and before the first gas bubble enters the chamber. During later ontogenetic stages, the earliest chambers will become refilled with liquid that gradually changes from hyposmotic to isosmotic to sea water (Denton 1971). For *Nautilus* with its external shell, the general physiology was found to be very similar to those of *Spirula* and *Sepia*. One could argue that these

three living genera represent an extant phylogenetic bracket *sensu* Witmer (1995), thus corroborating similar buoyancy regulation in ammonoids. Nevertheless, there are many neutrally buoyant living coleoids that employ different mechanisms. Unlike *Sepia*, both *Nautilus* and *Spirula* are as close to neutral buoyancy as possible.

For *Nautilus*, it has been demonstrated that cameral liquid first closely resembles sea water in its ion content, but with sufficient differences to assume that cameral liquid is a secreted body fluid and not unaltered sea water (Denton and Gilpin-Brown 1966; Greenwald and Ward 1982; Mangum and Towle 1982). Prior to removing the cameral liquid, some NaCl was removed by the siphuncle; subsequently, true emptying including salt and water transport out of the chamber starts (Denton and Gilpin-Brown 1966; Ward 1979). Salt concentration progressively decreases at the beginning after 50 % of the cameral liquid was removed; the remaining liquid lost direct contact with the siphuncle and salt concentration increases (Ward 1979; Ward et al. 1981). At the same time when cameral liquid is removed from the chamber, a vacuum is created into which various blood gases (nitrogen, argon, carbon dioxide, oxygen) diffuse. After about 50 % of the cameral liquid in the final chamber was pumped out, a new chamber formation cycle starts (Ward et al. 1981). The cameral liquid of the newest chamber initially acts as a brace against external hydrostatic pressure (Collins et al. 1980) and as a damper (buffer) to avoid explosion of the siphuncle (not yet calcified) due to blood pressure. Denton and Gilpin-Brown (1966) as well as Ward and Martin (1978) stressed that emptying is a slow and irreversible process in *Nautilus*. Ward and Greenwald (1982) and Greenwald and Ward (1987) managed to demonstrated that emptying, i.e. chamber refilling, can also be reversed.

Finally, Denton (1971, 1974) summarized that the mechanism of pumping salts and water is basically the same in *Sepia*, *Nautilus* and *Spirula*. Later, in the context of fossil cephalopods (nautiloids, ammonoids, and belemnoids), Denton and Gilpin-Brown (1973) assumed a similar mechanism for chambered fossil cephalopods with a siphuncle.

However, even after the osmotic mechanism had been adequately clarified, the same conflict between observed depth distribution of chambered cephalopods and the assumed depth limitations for the osmotic pump remain unclear; the largest difference in osmolarity between chamber liquid and sea water could produce a pressure equalled at 240 m water depth (Denton and Gilpin-Brown 1966; Greenwald et al. 1980, 1984). By contrast, Clarke (1970) has shown that *Spirula* spends only a small fraction of its life at depths with less pressure. Denton (1971) described the observation that dead *Spirula* does not fill with liquid when exposed to high hydrostatic pressures.

16.4.1 Decoupling

One possible explanation for the conflict between osmotic pumping and observed habitat was the decoupling argument (Denton and Gilpin-Brown 1966; Denton

et al. 1967). It was suggested that *Nautilus* and *Spirula* emptied cameral liquid above 250 m water depths and when migration into greater depths takes place, the chamber liquid was decoupled. That means that chamber liquid was not in direct contact with the siphuncle. The decoupling argument has been applied by ammonite workers to explain chamber, septal and suture complexity of ammonoids (e.g., Gottobrio and Saunders 2005).

This assumption is contradicted by the report of Ward et al. (1984) and Dunstan et al. (2011) for *Nautilus* and by Clarke (1970) for *Spirula*. Ward et al. (1984) documented the vertical distribution of one *Nautilus* specimen being tracked for seven days which was commonly below 240 m and Dunstan et al. (2011) recorded the deepest encounters of living *Nautilus pompilius* at 703 m. However, as stressed by Jacobs (1992, 1996) as well as Jacobs and Chamberlain (1996), decoupling would not prevent liquid to flow back into the chambers when hydrostatic pressure exceeds the osmotic pressure. The presence of the pellicle, a wetted organic sheet that covers the septal surface of *Nautilus* chambers with the potential for fluid transport, makes it highly unlikely that fluid can be successfully isolated. The pellicle acts as a wick or blotting paper. As a consequence, decoupling of liquid from the siphuncle was rejected in favour of local osmosis, where organisms can concentrate salts in intracellular structures (Diamond and Bossert 1967). Maybe this rejection was related to a misinterpretation of the idea of Denton and Gilpin-Brown (1966) as well as Denton et al. (1967) and the decoupling model. In his final summary, Denton (1974) already mentioned for *Nautilus* that the chalky tube and the pellicle still allow liquid to be drawn towards the permeable part of the siphuncle after losing direct connection. Pumping is still possible but at a lower rate. Similar cases are reported for *Sepia* and *Spirula*, both with a very small region through which liquids can be exchanged between living tissue and the chambers.

The theory of decoupled liquid was revived by Kröger (2003) and is agreed here in its narrow sense. It was pointed out that the decoupled theory is based on decoupled spaces used by cephalopods like buffer zones while changing their position in the water column. The decoupled spaces thereby protect the animal against liquid flowing back into the phragmocone chambers. The theory was based on the empirically observed phenomenon of decoupled spaces in *Sepia*. It was stressed that any decoupling space that creates a system with different salinity acts like the standing gradient model proposed by Diamond and Bossert (1967). It is more energetically efficient to transport liquid along an osmotic gradient than with no or against an osmotic gradient. Decoupled spaces therefore should be much smaller than the entire chamber, because ion concentration is more rapid and easier to maintain. These kinds of spaces are especially useful in species with an active use of their buoyancy apparatus (Kröger 2003).

16.4.2 Local Osmosis

The second explanation discussed by Denton and Gilpin-Brown (1966) as well as Denton et al. (1967) was that localized high concentrations of solutes could be built

up in a "*pumping*" epithelium by a mechanism similar to that proposed by Diamond and Bossert (1967, 1968) as "*standing gradient model*" and used to extract liquids from the chambers of the shell by simple osmosis.

Later, Denton and Gilpin-Brown (1973) cited a study of hyperosmotic pumping observed for sea birds suggesting a similar system for cephalopods in depths below 250 m. Such a pumping mechanism was described by Greenwald et al. (1982, 1984) for the *Nautilus* siphuncle. The siphuncular epithelium (Fig. 16.2) has microvilli at the site of putative NaCl absorption into the cell as well as elaborate folds of the basement membrane. These folds are located at the site of NaCl extrusion from the cell extending throughout the cytoplasm as a network of blind ending sacs (canaliculi). The canaliculi were lined with numerous mitochondria (Greenwald et al. 1980, 1982, 1984; Ward et al. 1980b; Mangum and Towle 1982; Tanabe et al. 2000). That arrangement is typical for tissues that carry out NaCl solute and water transport against osmotic or hydrostatic pressure (Berridge and Oschman 1972) and was found in a single ammonoid siphuncle of *Akmilleria* so far (Tanabe et al. 2000). This transport system is known as local osmosis system (Diamond and Bossert 1967), in which mitochondria supply ATP (energy) to salt ion pumps (= hyperosmotic pump of Jacobs 1996). The hyperosmotic pump actively transported Na^+ ions across cell membranes into microscopic intracellular channels, while Cl^- ions follow passively to maintain the charge balance. The resulting locally elevated solute concentration causes water to diffuse from the cytoplasm of the cell (local osmosis) into the microscopic channels (Fig. 16.2). In turn, these high pressures in the intracellular channels exceed the hydrostatic pressure and water thus flows into the channels and therefore into the siphuncle. This water leaves the cell through the openings of the folds. In the case of the channels, their geometry plays an important role. Water diffuses readily across the relatively large surface area of the channel, but flow down the channel and into the siphuncular lumen is much more rapid than diffusive processes.

The ultrastructure of the *Nautilus* siphuncle epithelium (Mangum and Towle 1982; Tanabe et al. 2000) and the presence of the sodium transport enzyme Na^+/K^+-ATPase (Bonting 1970) localized at the folds supports the assumption of the presence of a local osmosis system in the siphuncle of *Nautilus*. The salt of the basolateral labyrinth was transported by Na-K-ATPase into the intracellular system of canaliculi. A sufficiently high salt concentration generates a high osmotic concentration that draws liquid out of the chambers against either osmotic or hydrostatic gradients (Greenwald et al. 1984). These canaliculi systems were observed for the twelve most recent chambers but not from the third or fourth oldest chambers. It therefore appears likely that the earliest chambers did not contain living siphuncular tissue. Thus, intracellular channels can transport fluid against very high pressures as long as ions are present to be pumped.

The above described local osmosis model allows for cameral liquid emptying below 240 m water depths and could pump against almost any pressure. Accordingly, the limitation of osmotic pumping is now the concentration of ions that could be maintained in the tube instead of the ion concentration of the ambient sea water (Greenwald et al. 1982). Decoupling in its wider sense becomes needless for the

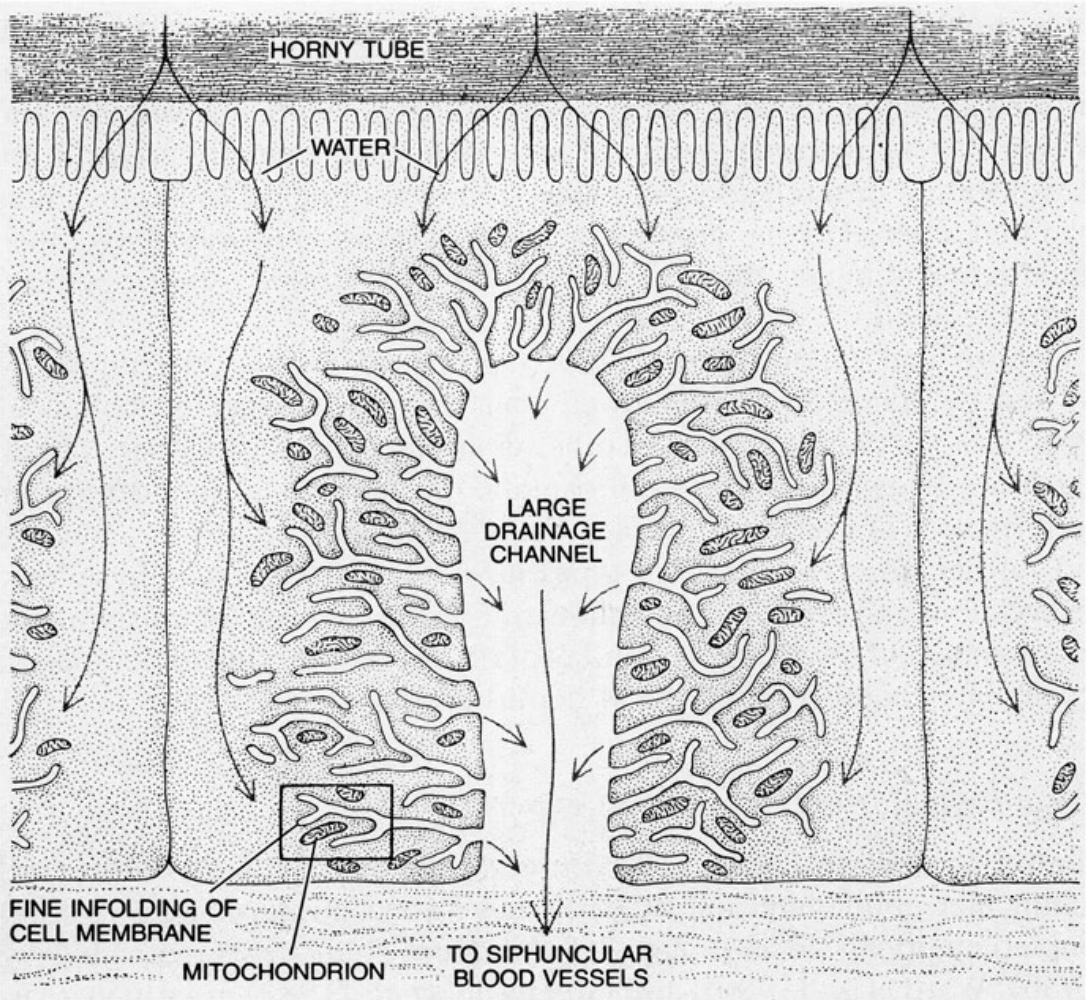

AQ1 **Fig. 16.2** Diagrammatic representation of a single transporting cell of siphuncular epithelium. Water molecules (*arrows*) move from horny tube, across the brush border, and into the cell. Fine infoldings within the cell communicate with a central drainage canal. The water ultimately reaches the siphuncular blood vessels, and is then carried to the body (reproduction from Ward et al. 1980b, by courtesy Peter D. Ward, Adelaide)

explanation of depth distribution in the presence of local osmosis in extant cephalopods. Due to the finding of soft parts in the *Akmilleria* siphuncle with preserved ultrastructure including canaliculi, it is now likely that local osmosis was the active pumping mechanism in ammonoids (Tanabe et al. 2000). However, presence of canaliculi for *Spirula* has not been objectively demonstrated (Chun 1915).

16.4.3 Preseptal Gas

Since Hooke (1695) compared the buoyancy mechanism in *Nautilus* with the fish bladder (Derham 1726), the gas pressure hypothesis became widely accepted without any justification (see Chap. 16.2). Meigen (1870) and Schmidt (1925) supposed

that *Nautilus* used preseptal gas to control its density. The gas pressure hypothesis then was also applied to fossil cephalopods but was rejected by Bidder (1962) for *Nautilus*.

The explanation of an internal pressure-driven buoyancy regulation with the last septum remaining uncalcified and functioning analogue to a fish swim bladder, i.e. the Cartesian diver model (Seilacher and LaBarbera 1995, Seilacher and Gishlick 2015), was rejected by Jacobs (1996), Kröger (2002) and Klug et al. (2008) for various reasons. No fossil indications such as muscle scars were found supporting the proposed muscular diaphragm enclosing a gas bubble and other mechanical implausibilities. Guex (2005) stressed the presence of a preseptal cavity in cephalopods recognized by the Haftband-Struktur, without providing new evidence. That cavity was suggested to allow adult ammonites to continue with growth, even if the phragmocone did not contain any cameral liquid by passive diffusion of gas into the preseptal cavity. In our opinion, this idea is currently lacking any support.

16.4.4 Role of the Siphuncle

The structure and detailed explanation of the function of the ammonoid siphuncle will be given elsewhere (Kulicki 1996; Tanabe and Landman 1996; Tanabe et al. 2000, 2015). Ward (1982) demonstrated the proportional dependence between the siphuncular surface area and the chamber emptying rate in *Nautilus* (see also Kröger 2003). Because siphuncular epithelia of *Nautilus*, *Sepia*, *Spirula* and ammonoids are histologically similar (Denton and Gilpin-Brown 1973; Drushchits and Doguzhaeva 1981; Barskov 1990, 1996, 1999; Tanabe et al. 2000), it was assumed that pumping power and morphology of siphuncular epithelia, the place of osmotic pumping, remained constant during cephalopod evolution (Ward 1982; Kröger 2003). A detailed structural description for the *Nautilus* siphuncle was presented by Ward (1987) as well as Tanabe et al. (2000), for *Virgatites* (Perisphinctidae) by Barskov (1996) and for *Akmilleria* (Prolecanitida) by Tanabe et al. (2000). Besides osmotic or hydrostatic pressures, the osmotic pump mechanism responsible for emptying and refilling of cameral liquid depends on the diameter and ultrastructure of siphuncle and surrounding tissues. Recently, Westermann et al. (2002) localized putative neurotransmitters in the mantle and siphuncle of *Nautilus pompilius* with the assumed function of blood circulation as well as complex secretory mechanisms. The siphuncle diameter itself is limited by strength requirements (Westermann 1971; Ward 1982; Jacobs 1992; Hewitt 1996; Hewitt and Westermann 1997). Depth distribution of chambered cephalopods is further limited by shell- and siphuncular strength. Westermann (1971, 1982) introduced the siphuncular strength index. Concerning the siphuncle, tubes of smaller diameter are stronger but have a smaller active surface for pumping which will lower the emptying rate. According to Westermann (1971, 1982), lytoceratids and phylloceratids have a greater siphuncular strength index, thus indicating that these forms lived at greater depths compared to other ammonites. Ward and Martin (1978) reported on chamber emptying rates of a maximum of 1.0 ml/day/chamber in living *Nautilus*.

By contrast, Ward and Greenwald (1982) reported a maximal refilling rate of 100 µl/h in response to a sudden buoyancy increase in living *Nautilus*. Based on the observed maximum emptying rate of 1 ml/day and maximum refilling rate of 2 ml/day, Ward and Greenwald (1982) concluded that *Nautilus* can only fine tune its buoyancy in order to ensure that the animal is always slightly negatively buoyant (which human scuba-divers also do). But these rates are not rapid enough to serve for the observed diurnal migrations, i.e. daily buoyancy-aided ascents and descents as suggested by Hooke (1695), Willey (1902), and Heptonstall (1970). Consequently, the siphuncle of *Nautilus* is only capable of long term but not of short term or sudden buoyancy regulations.

Due to their large siphuncular surface area relative to chamber volume, only sepiids and potentially some Paleozoic cephalopods such as actinocerids and endoceroids are able to adjust their buoyancy on a daily basis (Ward 1982; Kröger 2003). For ammonoids, Ward (1982) excluded the possibility of diurnal migration (see below).

Based on the calibrated pumping rate of siphuncular tissue, it turned out that the actively pumping siphuncular area is too small relative to the chamber volume. Instead, these cephalopods, including nautilids, may have accommodated vertical movements through active locomotion as observed for extant *Nautilus* (O'Dor et al. 1993).

Jacobs and Chamberlain (1996) argued that structural and energetic reasons prevent the development of large siphuncular tubes in cephalopods allowing for rapid density changes. The structural argument is based on the fact that the siphuncular strength is inversely related to diameter. This limitation was also observed in cuttlefish. Ward and Boletzky (1984) reported that shallow water forms have a flat cuttlebone with a large siphuncular area, while forms from deeper water have a cylindrical cuttlebone with a smaller surface area. Shallow water sepiids apparently can change their density faster compared to deeper forms (which might be linked with physical necessities). Energetic limitations are due to energy costs of pumping and maintaining empty chambers. These costs are proportional to the siphuncular surface area and will increase with water depths (hydrostatic pressure).

By contrast, Bandel and Stinnesbeck (2006) stressed that the permeable zone within the siphuncular tube of *Spirula* is as long as one chamber (Fig. 16.3). As a

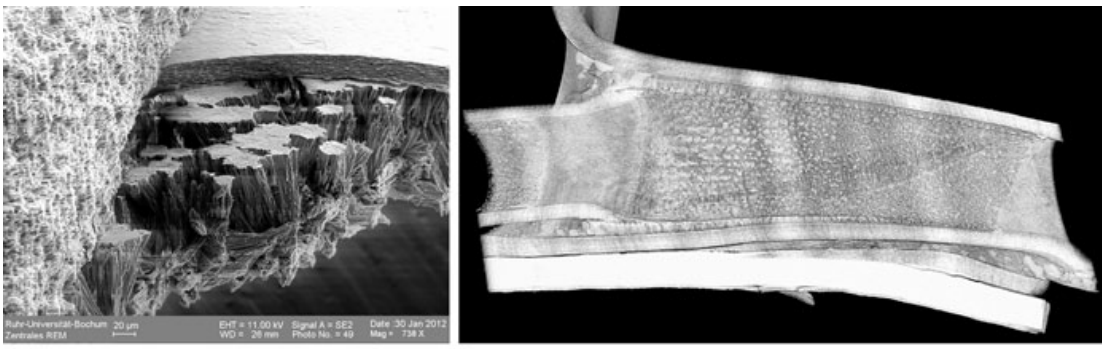

Fig. 16.3 **a** Siphuncle of *Nautilus pompilius*. **b** Siphuncle of *Spirula spirula* with the porous zone all along the inside of the septal neck

consequence, most of the actively pumping siphuncle epithelium is in contact with the cameral liquid and the ratio of pumping area to chamber volume is increased. Due to its small size and the precise buoyancy adjustment with its largest chamber volume of about 2 ml (Denton 1971), buoyancy may change fairly rapidly (Bandel and Boletzky 1979) and is mainly supported by pumping cameral liquid in or out of the chambers.

Following Mutvei and Reyment (1973), Kröger (2003) rejected Ward's (1982) idea that the relation of siphuncular surface area to chamber volume (si = siphuncle surface area index) was too small to support daily buoyancy adjustments in ammonoids. Kröger (2003) compared 250 cephalopods including nautiloids, ammonoids and coleoids. He demonstrated that cephalopods with high but also small si values were capable of rapid buoyancy adjustments. Already Heptonstall (1970) stressed that in ammonoids, the siphuncle with its extreme ventral position has the greatest possible length and hence is in the most efficient position for cameral liquid exchange.

Exceptional with respect to the position of the siphuncle is the group of Late Devonian clymeniids with the siphuncle in a dorsal position. Superficially almost indistinguishable from other ammonoids in terms of shell geometry and sutural complexity, clymeniids differ by their two to three times larger siphuncle diameter and up to 33 % thicker shells. With its dorsal position, the siphuncle surface and volume was decreased by about 50 % compared to narrower ventral siphuncles (Gottobrio and Saunders 2005). The reduction of siphuncular active pumping area was partially or fully compensated by its increased thickness. According to Westermann (1971, 1982), this restricted clymeniids to a shallow marine habitat.

Several authors focused on the refill ability of the siphuncle (Keupp 1997, 2000, 2012; Daniel et al. 1997; Kröger 2002). Based on observations of repaired injuries accompanied by shell loss, these authors speculated on a high rate of liquid refill. That refill had to compensate for the decreased weight by shell loss before the animals reached the surface.

16.4.5 Role of Cameral Liquid

In all three extant cephalopods that built a chambered shell (*Nautilus*, *Spirula*, and *Sepia*), the liquid that fills a newly formed chamber differs in composition from sea water and is recognized as a body fluid (Denton 1974). During ontogeny, the role of liquid for supporting buoyancy adjustment decreases with the growing total volume of the animal. Juvenile *Nautilus* retains about 32 % cameral liquid while adults keep 12 % of liquid compared to the phragmocone volume (Ward 1980, 1987). By perforating a single chamber directly above the hood (i.e. about 270° behind the aperture) of a *Nautilus* of 200 mm diameter, Tsujino and Shigeta (2012) demonstrated that *Nautilus* loses its neutral buoyancy due to water logging. The exact volume of water causing the permanent benthic position of *Nautilus* was not measured (pers. com. Tsujino). Nevertheless, the specimen managed to swim actively by producing

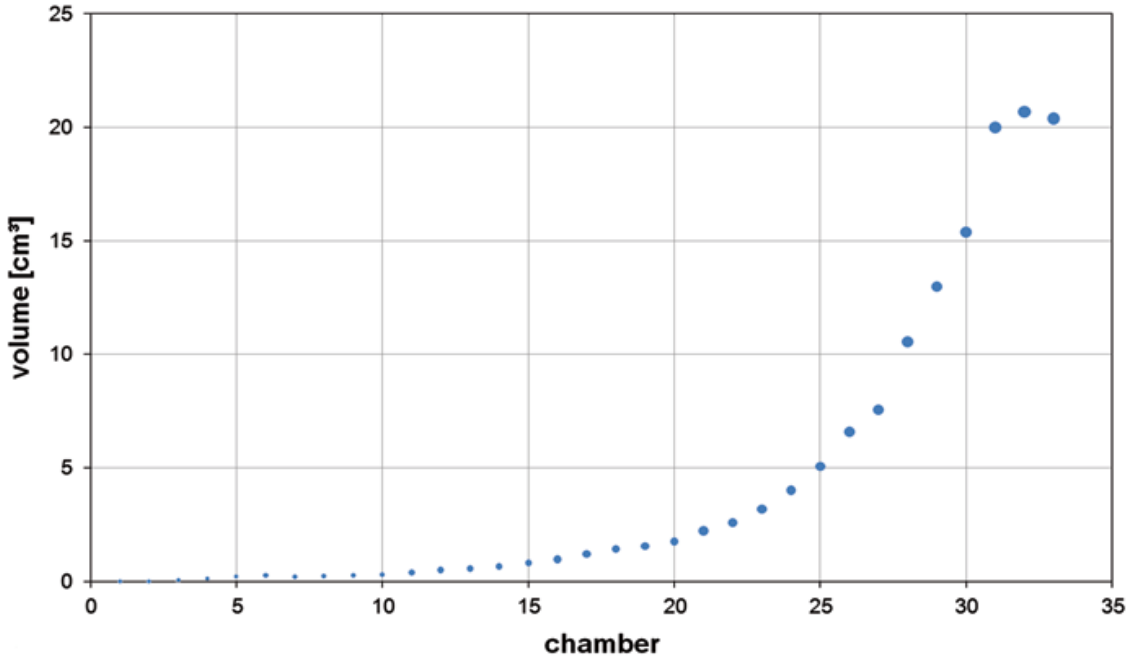

Fig. 16.4 Chamber volume for the 33 chambers of the *Nautilus pompilius* shell shown in Fig. 16.1A. Septal crowding can be recognised by decreased chamber volume

a jet over a short time close to the sediment surface. Furthermore, the siphuncle was cut and afterwards, the adapertural part of the siphuncle decomposed. This demonstrated that perforation of the phragmocone and siphuncle is not necessarily a fatal injury.

Denton et al. (1967) found small amounts of liquid in the last three chambers of a *Spirula* phragmocone made of 30 chambers, followed by 18 completely emptied chambers. In the subsequent chambers, the amount of liquid rises with the five smallest chambers being completely filled with liquid. When the animal grows, the earliest, smallest chambers of an adult animal have only a small fraction of volume of the latest chambers (Fig. 16.4). Kröger (2003) speculated that the high energy cost of emptying these chambers and maintenance is inversely related to their importance of buoyancy regulation. This may be the reason for chamber refill of the earliest, smallest chambers observed in *Spirula* (Denton et al. 1967).

Retained liquid was interpreted as ballast water for buoyancy regulation, e.g., to balance density increase due to shell and tissue growth, epizoa growing on the outer shell, injuries that cause partial water logging and to support vertical migration (Heptonstall 1970; Denton 1974; Keupp et al. 1999). At the time of sexual maturity, when growth ended, most or all cameral liquid was removed in living *Nautilus* (Collins et al. 1980).

The pellicle, the organic sheet covering the inner surface of phragmocone chambers of *Nautilus* (Denton and Gilpin-Brown 1966), *Spirula* (Appellöf 1893; Denton and Gilpin-Brown 1973) and ammonoids (Weitschat and Bandel 1991), transfers the cameral liquid from the more remote parts of the chambers to the siphuncle. As exemplified by Kröger (2003), the relative inner surface of the chambers represents

the potential of liquid refill rate under the assumption that the ammonoid chambers were also covered with the pellicle. For comparison of the ability of cephalopods to compensate slow or rapid buoyancy increase (e.g. due to shell loss by predation), Kröger (2003) introduced the inner chamber area index (*cai*) which is the inner chamber surface against its volume.

16.5 Buoyancy Calculations for Ammonoids

Due to comparable shell architecture and the presence of a siphuncle, the observed pumping mechanisms in extant relatives (*Nautilus*, *Spirula*, and *Sepia*) like osmotic pumping and local osmosis are assumed to act in ammonoids as well. Besides, it remains unclear if and how much liquid was kept in the ammonoid phragmocone (fill fraction in the sense of Kröger 2002), original shell density, ratio of soft body and body chamber volume. Further issues related with the calculation of the buoyancy for extinct animals like the relationship of density and volume and simplifying assumptions are discussed below.

16.5.1 Issues of Buoyancy Calculation

Trueman (1941) conducted the first extensive research to calculate masses and volumes of ammonoid taxa. For extant *Nautilus*, Trueman (1941) calculated the volume of the shell by the displaced amount of water and determined the volume of each chamber by cutting the shell along its median plan and fill the chambers with liquid. For extinct ammonoids, Trueman (1941) measured shell and septal thickness and applied the density of crystal aragonite for the shell. He assumed that the siphuncle contributed about 1 % to the total weight of the shell while the septa contributed 10 % (see his tab. 1, p. 360 ff). Trueman's (1941) and Currie's (1957) data were re-evaluated by Heptonstall (1970) using modern estimates for cephalopod tissue and shell densities. Mainly the equations of Raup and Chamberlain (1967) were applied to buoyancy calculations with additional corrections and extrapolations for different shell parameters such as ribs introduced by Kröger (2002). However, coiling of the shell is not dictated by mathematical parameters and does not follow a perfect logarithmic spiral. Shigeta (1993) could demonstrate that the planispiral whorls show a polyphasic allometric growth pattern (see also Klug 2001 and references therein). Coiling parameters and shapes may also change during ontogeny as is possible for all other morphological features and subsequently derived ratios (see Chap. 9 for intraspecific variability). Therefore, geometrical approximation of actual shapes of structures such as the whorl section as circles or polygons or the complex shape of septa bias the results. Calculations based on the statement that volumes in general are approximated by the visual matching of geometrical triangles, rectangles or trapezes (Ebel 1983) have therefore been rejected (e.g., Jacobs and Chamberlain 1996).

16.5.2 Volumes

Another point is the over- or underestimation of body chamber lengths and the volume of the soft body. Complete body chambers are rarely reported for ammonoids and nautiloids (Klug et al. 2014b). In earlier approaches, body chamber lengths were calculated for a range of ammonoids assuming neutral buoyancy. Therefore, information about volumes and densities of all negatively buoyant structures (shell and soft body) are required. A major error in buoyancy calculations is related with the unknown, and therefore approximated, body chamber length and the resulting soft body volume (Kröger 2002). Additionally, the pellicle and cameral sheets have to be taken into account with approximately 14 % of the chamber volume and a density of 1.055 g/cm³ as assumed by Hewitt and Westermann (1996).

Additional problems arise, because the actual distribution of shell material in the ammonoid phragmocone is not trivial to quantify in detail. Hammer and Bucher (2006) calculated for the ammonoid *Intornites* that the shell material makes up about 18 % (about 11.8 g) of the total mass (65.56 g). In their empirical study, Tajika et al. (2014) found that in *Normannites*, the shell mass is about 15 % (5.9 g) of the entire mass (24.36 g with aptychi). These discrepancies in shell-weight proportion of total weight are related with the fact that shell wall thickness is not constant but increases during ontogeny and wedges out or may strengthen near the adult aperture. Shell wall thickness also varies in different positions such as on the umbilicus, flanks or venter (Kröger 2002). Also, ornamentation like ribs, nodes or clavi contribute to the total shell weight but may increase or decrease in expression and density during ontogeny. In order to take ribs into account, Magnin in Delanoy et al. (1991) introduced a factor of sculpture (F_s) under the assumption of a sinusoidal curvature and was subsequently used by Kröger (2002). However, ribs neither are exactly radial nor represent an ideal sinusoidal curvature and their expression may also vary along the shell surface, becoming more prominent with a stronger curvature of the conch wall (Guex et al. 2003; Hammer and Bucher 2005).

Averaged values for septal thickness do not account for the fact that septal thickness decreases to the shell margin (Westermann 1975; Hewitt 1985; Hewitt and Westermann 1987). For example, estimations for septal thickness were expressed as ratio of the whorl height. Shigeta (1993) applied 2 % of the whorl height as being the septal- and conch wall thickness, while Westermann (1993) found 1.3–1.8 % in several Late Cretaceous ammonite genera and in epicontinental ammonoids, he measured a ratio of 1 % of whorl height. Westermann (1993) states that fluted septa thin out from the centre to the margin at about the same rate as fluting increases area; consequently, fluting does not add extra shell and weight in such way that similar total weights were obtained independent of the degree of fluting, assuming a simple plate of constant thickness equalling that of the centre of the septum. This has never been proven.

Finally, Saunders and Shapiro (1986) employed thickness terms for the shell and septa derived from digitized sections of the specimens that should lead to more reliable results. Nevertheless, the distribution of shell material did not resemble the

three dimensional distribution of shell material. By contrast, a simple circular whorl section was assumed by Saunders and Shapiro (1986). For compressed shells, this assumption is likely to produce an overestimate of shell volume relative to shell mass and an overestimate of body chamber length.

16.5.3 Shell Density

Another problem related with the shell is not only the approximation of its volume but the assumed density of the ammonoid shell material. Trueman (1941) applied the highest value with 2.94 g/cm³ which is the density of the aragonite crystal and was also used by Raup and Chamberlain (1967) as well as Crick (1988). These authors overlooked the values presented as relative density by Schwartz (1894) with 2.68 g/cm³ and Kelly (1901) with 2.688 g/cm³. After Trueman (1941), Reyment (1958) introduced a second lighter value of 2.62 g/cm³ due to the recognized incorporation of high amounts of organic components into the mollusc shell. Kelly (1901) implied 15% organic components within the nacre of *Nautilus* and *Spirula* nacre due to the different densities between crystal and nacre. For the organic components, Kelly (1901) assumed a density of 1.1–1.2 g/cm³. That value (2.62 g/cm³) was used by most of the subsequent worker such as Heptonstall (1970), Reyment (1973), Tanabe (1975), Ward and Westermann (1977), Saunders and Shapiro (1986), Okamoto (1988), Shigeta (1993), Kröger (2002), Hammer and Bucher (2006). Other density values used so far given in chronological order are: 2.6 g/cm³ by Westermann (1977), 2.53 g/cm³ by Collins et al. (1980) and Ebel (1983), 2.67 g/cm³ by Chamberlain et al. (1981) and Longridge et al. (2009), 2.7 g/cm³ for the shell *Nautilus* by Greenwald and Ward (1987), 2.5958 g/cm³ by Ebel (1993), 2,69 g/cm³ by Hewitt and Westermann (1996) and Hewitt et al. (1999) and finally 2.65 g/cm³ by Westermann (2013) for nacre density.

Applied shell densities vary from 2.53–2.94 g/cm³. Variation of shell density within the shell was mentioned by Mutvei (1983) due to incorporation of different amounts of organic matter. For a *Nautilus* shell, collected some thirty years ago, Hoffmann and Zachow (2011) documented different shell densities for the conch wall (2.57 g/cm³) and the septa (2.51 g/cm³). Hewitt and Westermann (1996) reported that the density of the *Nautilus* phragmocone with a value of 2.668 g/cm³ differs from that of the adult body chamber with a reduced density of 2.582 g/cm³. On the contrary, the same density was assumed mostly for the conch wall and septa of ammonoids (e.g. Longridge et al. 2009), thus neglecting the small contribution of 2–6% (Trueman 1941) of the septa documented for Mesozoic ammonoids or 6% of septa and siphuncle (Raup and Chamberlain 1967) to the total shell volume. While Saunders and Shapiro (1986) report values of 5–14.6% for septa and siphuncle of the volume of the entire shell, Kröger (2002) decided to choose a mean value of 5.7%.

16.5.4 Soft Body Density

Imprecise calculations for the shell may cause significant errors in the estimations of the body chamber length and thus the soft body volume and could also lead to wrong assumptions about the paleobiology of ammonoids. Trueman (1941) calculated a soft body density of 1.13 g/cm³ under the assumption that the body chamber was completely filled with the soft body. Later, it was generally accepted that the ammonoid soft body had the same density as that of *Nautilus* (1.06 g/cm³) and that the soft body completely filled the body chamber (e. g. Reyment 1973; Tanabe 1975; Ward and Westermann 1977; Greenwald and Ward 1987; Monks and Young 1998). The latter was criticized by Kröger (2002) as too high. Up to 15 % has to be subtracted from the body chamber volume for the mantle cavity which is used by the animal for respiration and jet propulsion (Chamberlain 1987; Wells 1990). This mantle cavity ratio remains constant throughout ontogeny (Chamberlain 1987). Recently, Westermann (2013) suggested that only two thirds of the body chamber were occupied by the soft body with the remainder being filled with sea water. It can be speculated that ammonoids with long body chambers had similar or higher values.

Other density values for the soft body are given in chronological order with 1.068 g/cm³ applied by Denton and Gilpin-Brown (1961a, b, c, 1966) as well as Heptonstall (1970), 1.067 g/cm³ applied by Raup and Chamberlain (1967), Okamoto (1988) and Shigeta (1993), instead, Ward and Westermann (1977) applied 1.05–1.07 g/cm³, Ward (1986) differentiated the *Nautilus* soft body in coelomic fluid with a density of 1.026 g/cm³ and the tissues with 1.068 g/cm³, 1.0568 g/cm³ was applied by Ebel (1993), while Saunders and Shapiro (1986), Hewitt and Westermann (1996), Hewitt et al. (1999), Hammer and Bucher (2006) as well as Longridge et al. (2009) applied 1.055 g/cm³, Hoffmann and Zachow (2011) applied a mean value of 1.047 g/cm³ based on the two values presented by Ward (1986) and most recently Westermann (2013) applied 1.065 g/cm³ taking the buccal mass including the aptychus into account. Tajika et al. (2014) separately considered soft tissue density and jaw density.

For the buccal mass of the cephalopod head region, including the radula and the chitinous jaw apparatus, an average density of *Nautilus* jaw elements of 1.655 g/ml was reported by Hewitt and Westermann (1993). Both the volume of siphuncle has to be subtracted from chamber volume and the density of soft tissue has to be applied to the siphuncle volume. To be precise, one should include the pellicle, the wettable tissue covering the inner surface of each chamber, in buoyancy calculations, although its contribution in terms of total weight might be low.

For *Nautilus*, Ward et al. (1977) reported a maximum crop content of 76 g (21.7 % of the soft body mass). This crop content was responsible for a mass increase (negative buoyancy) of the animal in sea water of 0.9 g, while the same animal weighed under water with its shell was only 0.3 g. Accordingly, the crop content needs to be considered due to its nontrivial mass.

16.5.5 Sea Water Density

There was a more or less uniform use for the values of sea water density with 1.025 g/cm³ for sea water at the sea surface at room temperature (Greenwald and Ward 1987) or 1.026 g/cm³ used by Raup and Chamberlain (1967), Heptonstall (1970), Ward and Westermann (1977), Saunders and Shapiro (1986), Ebel (1993), Kröger (2002), as well as Hammer and Bucher (2006). Only Tanabe (1975) applied a density of 1.00 g/cm³ for Late Cretaceous sea water. This is of importance for buoyancy calculations to estimate the weight of the sea water volume displaced by the animal's total volume.

16.5.6 Model Approach

In order to avoid mathematical assumptions, approximations or speculations, Mutvei and Reyment (1973), Monks and Young (1998) as well as Westermann (2013) successfully carried out flotation experiments on more or less exact plastic models of key ammonoid morphotypes including three kinds of heteromorphs. The correct specific weight was obtained by electroplating the models internally and externally with metal. The major outcome of the experiments was that ammonoids must have retained much more cameral liquid in the chambers compared to the extant *Nautilus*. Additionally, ammonoids were possibly better adapted for vertical movements with a continuous adjustment to pressure gradients. The latter statement is supported by the wide occurrence of ammonoids like vascoceratids in shallow marine deposits. They possibly did not need larger adjustments of buoyancy which might be reflected in their simplified suture line although this is speculative (compare Klug et al. 2008). By contrast, ammonoids with highly complex suture lines can be speculatively interpreted as actively using their buoyancy apparatus for vertical movement (see also decoupling).

Due to its high density compared to the soft body, it turned out that the exact determination of shell volume was one of the main issues in earlier attempts for buoyancy calculation. Shell thickness must be measured for different ontogenetic stages. Thickness of the conch wall must be distinguished from thickness of the septa due to different densities (Hoffmann and Zachow 2011). Loss of shell volume during diagenesis was stressed by Reyment (1958) and Heptonstall (1970). Longridge et al. (2009) for the reason of diagenesis reduced the volume of their model by 7.6% before they included it in the calculations. It has to be taken into account that this assumption of material loss is based on the suggestion that during diagenesis, such volume changes occurred on a regular basis. We think that this is incorrect, because in most cases, shell replacement occurs after sediment consolidation, thus inhibiting volume alterations. In most cases, the measurable volumes even in calcitic replacement shells will probably be more or less accurate (e.g., Tajika et al. 2014; Naglik et al. 2014). It remains arguable whether limits of error from neutral buoyancy in seawater of +/−10% (Westermann 1993; Kröger 2002) are acceptable or not, especially when volumes are measured empirically using any kind of

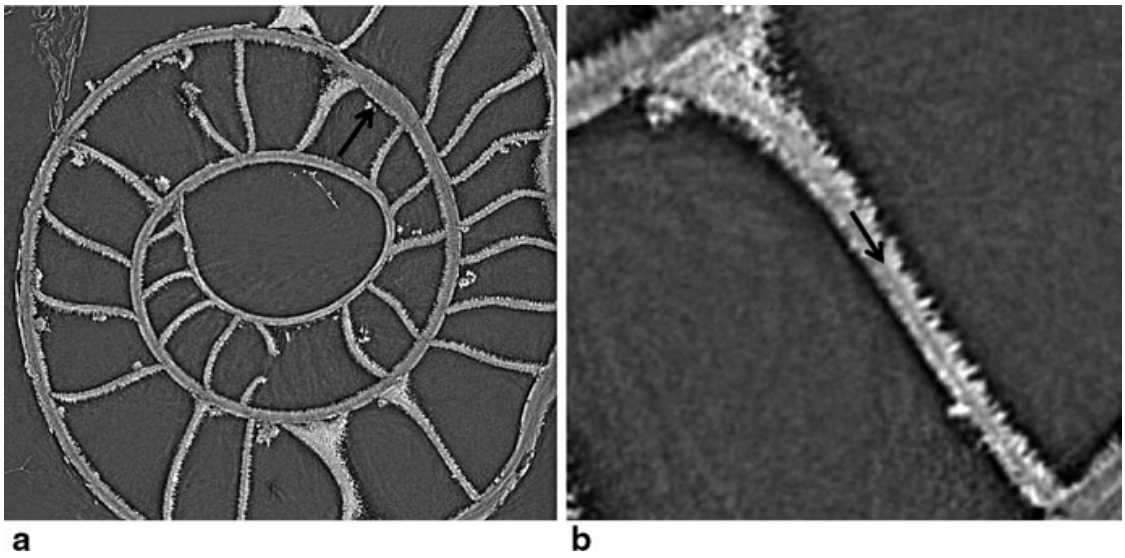

Fig. 16.5 juvenile *Cadoceras* sp. (Callovian of Russia) with secondary calcite crystals covering the inner surface of its chambers. **a** black arrow points to the nepionic constriction. **b** close up of a single septum with crystals growing on both sides and are in total about four to eight times thicker compared to the septa nevertheless this specimen was positively buoyant in fresh water, the specimen was scanned with a spatial resolution of 0.74 µm isotropic voxel size, length of the lower image edge is 1.4 mm

tomography (Fig. 16.5). According to Kröger (2002), an exact estimation of the soft body volume represents a major challenge because a few degrees of change in the length of the body chamber can alter the entire shell weight significantly.

16.6 New Approaches for Improved Buoyancy Calculations

16.6.1 Computer Tomography

Attempts to reconstruct ammonoid buoyancy had largely depended on mathematical modelling as discussed above. These models have not only simplified geometry and aspects of shell ornamentation but have often ignored changes in shell and septa thickness (for example: Trueman 1941, Westermann 1990, Ebel 1992, Kröger 2002) as well as allometric growth etc. Modern technology has provided novel approaches to address the buoyancy of ammonites as well as broader questions of functional morphology in the form of tomography including X-ray (CT), synchrotron and grinding tomography.

CT generates a series of X-ray images of the rotated object that are used to reconstruct a stack of 2D images. These images reveal the internal and external morphology of the object of interest in a non-invasive manner, whereas grinding tomography is destructive (Sutton et al. 2001; Tajika et al. 2014; Naglik et al. 2014). The

details visible in CT images largely depend on (1) how the X-rays interact with the materials in the field of view (i.e. density differences and the absorption properties of the material) and (2) the contrast of material properties between two adjacent materials (Stock 2009). If two adjacent materials possess the same material properties distinction between the different materials may be impossible. CT applications in biological and paleontological sciences often utilize micro-CT and synchrotron micro-CT (e.g., Dumont et al. 2005; Jones et al. 2012; Schmidt et al. 2013) which, compared to common medical CT scanners, produce scans with a much higher-resolution of up to fractions of a micron (for a more detailed review of these methods and their underlying science see Stock 2009 or Sutton et al. 2014).

These methods can be used to reconstruct a 3D model of a scanned specimen from the image stack using a variety of commercial software (e.g., Avizo, Amira, VGstudiomax, Geomagic) and freeware (e.g., S.P.I.E.R.S., YaDIV). Hoffmann (2010) illustrated this method by creating 3D models of two ammonite specimens, namely *Argonauticeras besairiei* and *Gaudryceras* sp. These 3D models, provided the datasets possess sufficient resolution, can be used to perform 3D measurements such as volume and surface area calculations which can then be applied to functional analysis of the buoyancy apparatus of cephalopods as shown in Longridge et al. (2009), Hoffmann and Zachow (2011) and Tajika et al. (2014). The benefit of these empirical 3D models over mathematical models is their ability to accurately maintain the original geometry of the shell and thereby eliminating errors due to oversimplification and the use of average shell properties used by previous methods of buoyancy reconstruction. However, depending on the resolution of the scans and the visibility of fine structures, there still are limitations in accuracy.

The creation of these 3D models from CT data can be a relatively straightforward process in extant animals as the specimens scanned are usually complete (i.e. undamaged), show no post-depositional deformation exhibited by many fossils, and possess no sediment infill that can make the separation of the shell material from sedimentary or diagenetic infill much more difficult and very time-consuming. However, the modelling process for both extant and extinct specimens is principally the same; if preservation and image-quality permits, the shell material can be isolated automatically by the thresholding algorithms of the program from the surrounding medium (i.e. rock or air) in the CT scans and any shelly material not selected can be added or subtracted manually (in the case of fossil specimens, some parts of the surrounding rock may have been included in the threshold; Fig. 16.6). Once the shell material is selected, measurements relevant to reconstruction of the function of the buoyancy apparatus, such as the volume of the chambers and surface area of the siphuncle, become possible; see Hoffmann and Zachow (2011) for an example of volumetric analysis using CT data for *Nautilus pompilius* (Fig. 16.4) and for examples of ammonoids, for which grinding tomography was used, see Tajika et al. (2014) and Naglik et al. (2014) (Fig. 16.7).

It is important to note that tomographic methods have their own sets of complications that can arise. One of the main benefits of this method is the preservation of the original geometry of the shell, but this is only true if the CT scanner used has a sufficient resolution relative to the size of the specimen. If the resolution of the

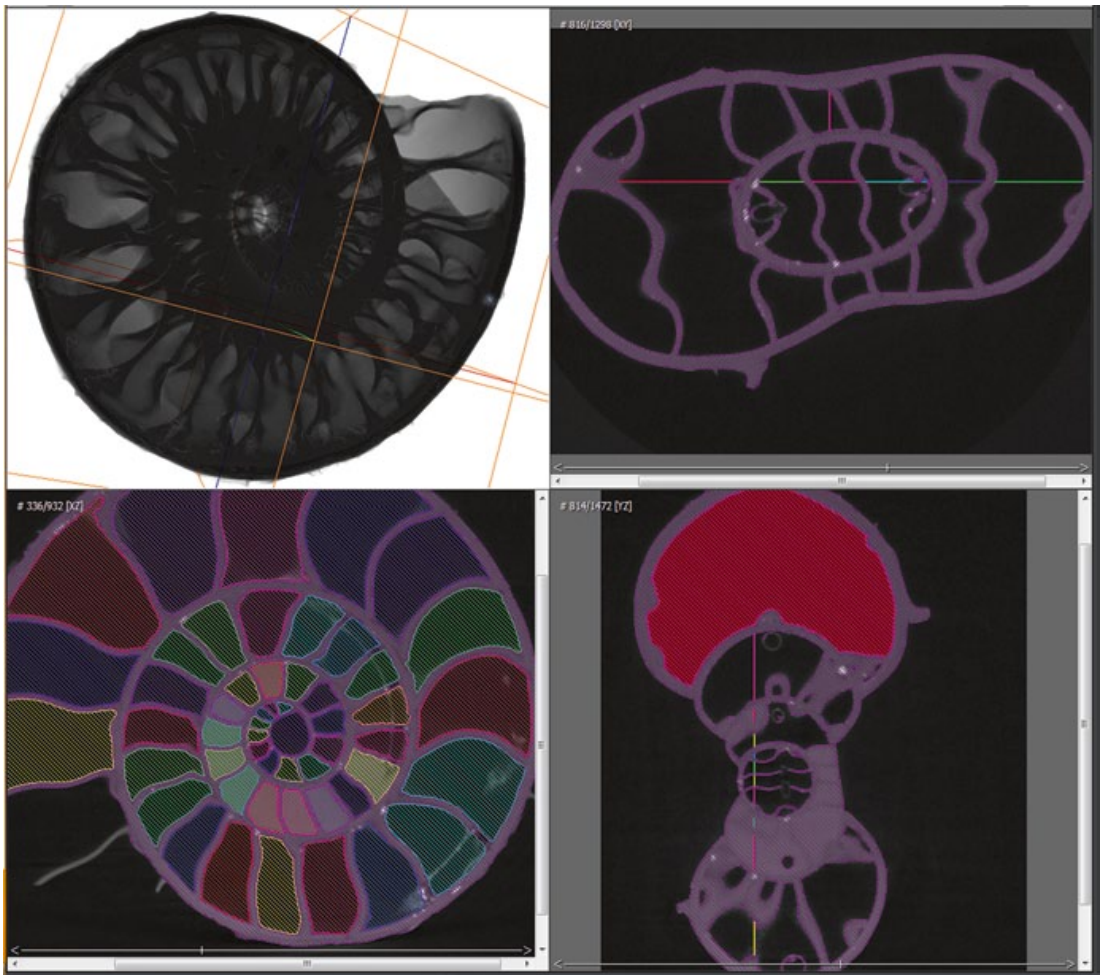

Fig. 16.6 Computer tomographic dataset of a scanned ammonoid visualized with the 3D software Avizo Fire 7.0, the specimen is being segmented, i.e., the selection of different materials of interest such as air, shell, sediment, scan artefacts

scanner is much larger than the structure of interest then some relevant geometric detail will be lost. For instance, if the resolution of the scanner is 1 mm but the width of the septa is only 1 µm, then a reliable reconstruction of the septa will be impossible. If the specimen is filled with material that has the same absorption properties as the specimen, such as a carbonate ammonite shell full of carbonate sediments, then the differentiation of the shell material and the surrounding medium will be possible only with grinding tomography and impossible with conventional CT. Advanced CT techniques such as phase contrast CT which is sensitive to changes in refractive index, can increase the differentiation between materials with similar absorption properties. In depth discussion of such techniques as well as additional experimental CT methods currently being explored that can mitigate this limitation can be found in Sutton et al. (2014).

The extraction of a complete surface from the data can be relatively quick for extant specimens, on the order of one to several days. By contrast, fossil specimens may require a much greater amount of work due to the complications explained above. A single ammonite specimen can take several months to complete depending

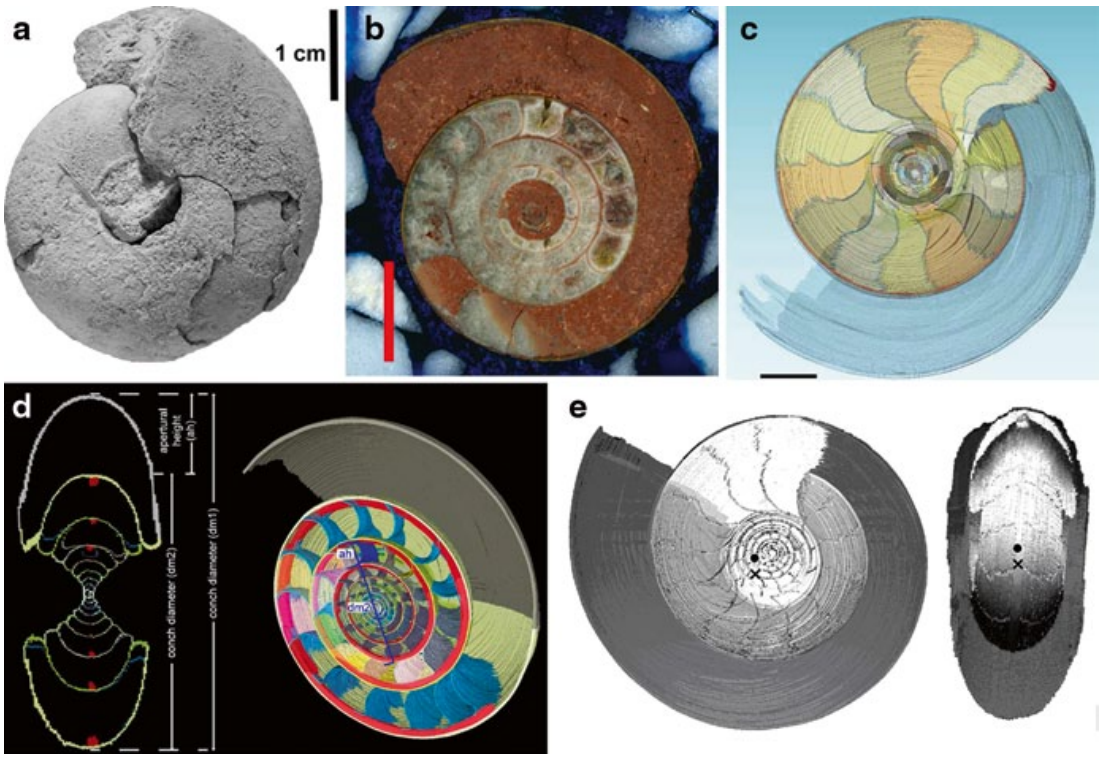

Fig. 16.7 The process from the fossil to the volume model (modified from Naglik et al. 2014, in press.): **a** *Diallagites lenticulifer*, Eifelian, Devonian, Hamar Laghdad (Morocco); the now pulverized specimen. **b** One of the 334 scans of the specimen in A; note that missing parts were manually reconstructed; the colour information is preserved, but the various shell structures are not uniformly well visible. **c** virtual reconstruction of the shell using only every fourth slice; the outer shell is here transparent, to show the color-labelled phragmocone chambers. **d** two different sections showing the labelled shell parts. E, reconstruction of shell orientation using the volume model (x—center of mass; o—center of buoyancy)

on the detail, quality of the images and contrast between shell and internal sediment or mineral filling.

Errors can be introduced by what we refer to as the partial volume effect (PVE). CT data is generated in voxels which can be thought of as 3D pixels. A single value is assigned to each voxel. This value controls the shade (from black to white) of each voxel shown on the CT slice. Because each voxel is represented only by a single value, the shade of a voxel represents an average of the material properties, if two or more materials are neighbouring the same voxel. This means that, when segmenting different materials, you may accidentally include a certain percentage of the surrounding materials due to the difficulty of detecting the exact boundary between adjacent materials. The PVE can be mitigated by scanning an object with similar absorption properties as the material of interest but with a known volume or density that can be used as a standard to accurately segment the specimen. This procedure is called quantitative computed tomography (qCT) in the medical literature, where the standard is referred to as a "phantom" (Kalender et al. 1995). It should be noted that this error is not unique to CT data and is also present in all scanned images represented by pixels.

16.6.2 Grinding Tomography

As already mentioned, X-ray tomography and synchrotron tomography can only display limits of materials in a scanned object, if there is a difference in physical properties of the materials under consideration. In ammonoids, this commonly causes problems, because the shell is carbonatic, even if it is diagenetically modified into calcite, and often, the phragmocone chambers as well as the body chamber are filled by carbonate, too. In such cases, CTs and variations of it will not produce useful image stacks. By contrast, if a colour contrast exists between shell and sediment or cement, this will be well visible in scans of ground surfaces obtained by grinding tomography (Fig. 16.7).

Of course, there is no perfect method and thus, grinding tomography (serial sectioning) has also its disadvantages and errors. For example, depending on image resolution and the spacing of ground surfaces, the partial volume effect will also produce errors. Another problem can occur, when the material is clayey. This may cause mechanical problems in the grinding process and thus bad scans. In contrast to synchrotron tomography, the resolution is lower in all three dimensions. The ammonoids tomographed by Tajika et al. (2014) and Naglik et al. (2014), for example, were ground and scanned each 60 - 48 µm with a scanner resolution of 2000 dpi. Therefore, a much lower resolution is obtained, but colour information is gained. The specimen gets destroyed by this method, so it is reasonable to apply it only to specimens of common taxa. In consequence, the application of this method makes sense for specimens smaller than 30 cm (depending also on the dimensions of the structure of interest that should be at least twice the resolution), where only a moderate resolution is needed to produce moderately well resolved volume models. Depending on the scientific question, this might well make sense and produce stimulating results based on empirical data (Tajika et al. 2014; Naglik et al. 2014; Naglik et al. in press).

16.6.3 Synchrotron and Neutron Tomography

In recent years, the use of synchrotron tomography has become fashionable in paleontology (e.g., Sutton et al. 2014). This method has the great advantage of producing image stacks of incredibly high resolution, thus revealing finest details (e.g., Kruta et al. 2011, Hoffmann et al. 2014 and references therein) and a small partial volume effect. At the same time, the application of this method is energy consuming, it requires enormous apparatuses of very limited access to researchers, it produces data sets of gigantic volume using a lot of computer disc space, data processing requires fast hardware with large RAM and often expensive software, sample size (usually <10 cm) is much more limited than in CT, and no colour information is preserved. In contrast to grinding tomography, however, the specimens are not lost.

Using neutron sources has been tested by us. This has a number of disadvantages such as a low resolution (>0.1 mm), the risk of producing radioactive nuclides in

the sample and the low permeability of materials containing a lot of hydrogen and oxygen. Perhaps, this method might be of use in very special kinds of preservation, where the sample contains low amounts of hydrogen and a lot of iron or else.

16.7 Efficiency of the Ammonoids Hydrostatic Apparatus

Ward (1982) doubted that ammonoids used the buoyancy apparatus to support short term vertical migration comparable to the diurnal migration of the extant *Nautilus*. His interpretation was mainly based on the active siphuncular area available for liquid pumping. If we accept that there are no substantial differences in all known cephalopod siphuncular epithelia (Tanabe et al. 2000), the ratio between chamber volume and siphuncular volume should be a measure of short time buoyancy change ability (see above). On the contrary, Kröger (2002) convincingly demonstrated the efficiency of the ammonoid hydrostatic apparatus. He analyzed the five greatest sublethal injuries found in Mesozoic ammonoids and calculated the loss of shell mass that has occurred. It turned out that the maximum tolerated shell loss was four times larger than in extant *Nautilus*. Furthermore, his findings implied a buoyancy compensation mechanism that includes a rapid liquid refill of the phragmocone chambers. *Nautilus* could compensate for a maximum shell loss requiring a liquid refill of 3 % of the chamber volume (Ward 1987) equaling a shell loss of 5 % of the total shell mass (Ward 1986).

Daily density changes of *Sepia* are maintained by a compensatory liquid exchange of about 6 % of the chamber volume (Denton and Gilpin-Brown 1961b, 1973). Kröger (2002) expected a possibly higher compensatory liquid refill in ammonoids than the 6 % of *Sepia*. He could also demonstrate that the capability of compensation of drastic shell mass loss in ammonoids was significantly higher than in *Nautilus* and exceeds the observed values for normal daily density changes of *Sepia*. Mesozoic ammonites compensated a maximum shell loss requiring a liquid refill of more than 10 % of the chamber volume with an observed maximum of 18 %. If we assume that the shell loss has to be compensated before the animal rose to the sea surface, the compensation mechanism must have acted very rapidly. The above mentioned necessary liquid refill to compensate for shell loss mainly depends on the active siphuncular surface in relationship with the chamber volume. This relationship, the connecting ring surface area in mm²/ chamber volume in ml, is the *si* of Kröger (2003). He calculated the following values: *Lithacoceras*—0.043 (Kröger 2002), adult *Spirula*—0.01, adult *Nautilus*—0.01, *Sepia*—0.1 (Ward 1982). Based on five specimens a mean *si* of 0.028 was presented for Paleozoic ammonoids and Kröger (2003) concluded that the ammonoid buoyancy apparatus was much more involved in active buoyancy regulation than in *Nautilus* and *Spirula*.

Liquid refill into the chambers is the only mechanism to compensate for a sudden increase of buoyancy. While Ward and Greenwald (1982) and Ward (1986) found an upper limit of liquid refill at approximately 3 % of the chamber volume, it was much higher (9–18 %) and therefore efficient in ammonoids (Kröger 2002).

This high ability of refill in ammonoids was explained by the more complex architecture of the phragmocone of the ammonoids with folded septa compared to the simple septa in the *Nautilus* phragmocone. In both groups, the inner surfaces of the chambers are lined with the pellicle (Weitschat and Bandel 1991). The pellicle is hydrophilic and plays an important role in the transportation of liquid out of and into the chambers by the use of capillary forces. The effect or power of the capillary forces for rapid refill of liquid into the chambers were demonstrated by the refloatation experiments of dry *Nautilus pompilius* shells by Hewitt and Westermann (1996). As for the refilling of liquid into the phragmocone, Wani et al. (2005) found through field experiments that waterlogging of the phragmocone in modern nautili does not occur until the mantle tissue detaches from the shell due to decomposition. Kröger (2002) assumed a direct relationship between the volume of capillary tissue (pellicle), ability of capillary fluid transport and of fluid storage (decoupling in its narrow sense). Due to higher capillary forces in the small pockets of complexly folded septa, chamber liquid will be stored in these spaces (Kulicki 1979; Weitschat and Bandel 1991; Checa 1996). A large pellicle volume is related to a large surface lined by the pellicle that is directly linked with the complexity of septa. Therefore, the highest ability of liquid transport can be assumed for ammonoids with the most complex septa such as, e.g., lytoceratids and phylloceratids. Daniel et al. (1997) were the first to consider the refill ability in conjunction with septal complexity. Mesozoic ammonoids survived a significantly higher shell loss than *Nautilus* or Paleozoic ammonoids (Keupp 2012) with much simpler suture lines. It can be assumed that survived shell loss is positively correlated with suture line complexity, although this requires further testing.

16.8 Evolution of the Hydrostatic Apparatus

Possibly, the phragmocone is the most important autapomorphy of the Cephalopoda (for cephalopod ancestry and origin see Klug et al. 2015a; Kröger et al. 2011; Ax 2001). With respect to cephalopod buoyancy, a hypothesis suggested by Dzik (1981) has to be mentioned: According to Pojeta (1980), the siphuncle of the earliest cephalopods, i.e. the Plectronoceridae, might be homologous to the snorkel-like process of monoplacophoran Yochelcionellidae. Dzik (1981) then suggested that stemgroup cephalopods or derived monoplacophorans have produced a hyposaline liquid, stored it in the apex of the shell, thereby reducing their buoyancy and becoming able to swim. This is in accordance with the osmotic process involved in the removal of cameral liquid in ammonoids and other chambered cephalopods. In the opinion of Dzik (1981), the septa then evolved by a repeated change of apical liquid- and carbonate secretion, followed by gas diffusion which was enabled by the growing partial pressures produced by the ionic pump in the chambers.

In the course of cephalopod evolution, the buoyancy apparatus underwent many modifications including thick (endocerid) and thin (orthocerid) siphuncles, simple (actinocerid) and complex (ammonoid) septa, straight (orthocerid) and coiled (am-

monoid) phragmocones. Undoubtedly, the major innovations characterizing most Ammonoidea are the ventral siphuncle, the tightly coiled shell and more or less strongly folded septa. In how far morphological evolutionary innovations represent adaptations to improve its function to regulate buoyancy is nearly impossible to prove. In any case, we do not doubt that buoyancy control was the phragmocone's principal function because it persisted throughout the entire phylogeny and underwent an increase in complexity which was partially reversed only in very few taxa (e.g., Cenomanian *Neolobites*).

Above, we have mentioned the line of reasoning that the increasing sutural frilling might serve to increase the surface of the phragmocone (see Chap. 3). This complexity is largely limited to the part of the septa, where they are in contact with the outer shell (the suture), while much of the septum remains gently folded. This arrangement is not the optimal construction to maximize the pellicle-covered surface of the inside of the chamber. This might indicate a different meaning of the suture frilling which has been suggested by Klug et al. (2008). Accordingly, the complexity increased the length of attachment of the organic preseptum prior to mineralization and might have helped to allow an earlier start of the emptying process in newly formed chambers. In both cases, the increase in sutural frilling is linked with a rise in efficiency of the buoyancy apparatus, thus supporting the likely great importance of buoyancy regulation in ammonoids. In turn, this points at the possibly immense meaning of the control of vertical movements in the life of ammonoids. Taking the implosion depths of ammonoids of perhaps above 300 m into account (e.g., Westermann 1973, 1996), the importance of buoyancy control becomes essential for survival. Phragmocone differentiation could be speculatively explained as a reflection of specializations to certain depths and/ or distinct modes of vertical migration. With the increase in accuracy and number of buoyancy models of ammonoid species, we will hopefully learn more about their habitats and perhaps also behavior in terms of vertical migration.

Acknowledgements CK and CN thank the Swiss National Science Foundation (SNF project numbers 200021-113956⁄ 1, 200020-25029, and 200020-132870) and RH and RL thank the Deutsche Forschungsgemeinschaft (DFG project numbers HO 4674/2-1) for financial support of their research, especially for the grinding tomography. We greatly appreciate the work of the members of the Heidelberg grinding tomography lab, namely Stefan Götz, who died much too young, Enrique Pascual-Cebrian, and Dominik Hennhöfer (all Heidelberg).

References

Appellöf A (1893) Die Schalen von *Sepia*, *Spirula* und *Nautilus*—Studien über den Bau und das Wachstum. Kongl Svenska Vetensk Akad Handl 25:1–106

Arkell WJ (1957) Sutures and septa in Jurassic ammonite systematic. Geol Mag 94:235–248

Ax P (2001) Das System der Metazoa. Fischer, Stuttgart

Bandel K, von Boletzky S (1979) A comparative study of the structure, development and morphological relationships of chambered cephalopod shells. Veliger 21:313–354

Bandel K, Stinnesbeck W (2006) *Naefia* Wetzel 1930 from the Quiriquina Formation (Later Maastrichtian, Chile): relationship to modern *Spirula* and ancient Coleoidea (Cephalopoda). Acta Univ Carol Geol 49:21–32

Barskov IS (1990) Internal structure of siphuncle of the Late Jurassic ammonite *Virgatites virgatus*. Trans Paleontol Inst 243:127–132

Barskov IS (1996) Phosphatized blood vessels in the siphuncle of Jurassic ammonites. Bull Inst Océanogr, (Monaco, special) 14:335–341

Barskov IS (1999) Why ammonoids have complex septa and sutures? In: Rozanov AY, Shevyrev AA (eds) Fossil cephalopods: recent advances in their study. Russian Academy of Science, Moscow

Berridge MJ, Oschman JL (1972) Transporting epithelia. Academic Press, New York

Berry E (1928) Cephalopod adaptations—the record and its interpretations. Q Rev Biol (Baltimore) 3:92–108

Bert P (1867) Mémoire sur la physiologie de la Seiche. Mem Soc Sci Phys Nat Bordeaux 5:114–138

Bidder AM (1962) Use of the tentacles, swimming and buoyancy control in the Pearly *Nautilus*. Nature 196:451–454

Bonting SL (1970) Sodium-potassium activated adenosine triphosphatase and cation transport. In: Bittar I (ed) Membranes and Ion Transport. Wiley, New York

Bruun AF (1943) The biology of *Spirula spirula* (L.). Dana Rep 4:1–46.

Bruun AF (1950) New light on the biology of *Spirula*, a mesopelagic cephalopod (Essays on the natural sciences in honour of Captain Allan Hancock). University of Southern California Press, Los Angeles, pp 61–72

Buckland W (1836) Geology and mineralogy considered with reference to natural theology, vol 1. William Pickering, London

Chamberlain Jr JA (1987) Locomotion of *Nautilus*. In: Saunders WB, Landman NH (eds) *Nautilus*—the biology and paleobiology of a living fossil. Springer, Dordrecht

Chamberlain JA Jr, Moore WA Jr (1982) Rupture strength and flow rate of *Nautilus* siphuncular tube. Paleobiology 8:408–425

Chamberlain JA Jr, Ward PD, Weaver JS (1981) Post-mortem ascent of *Nautilus* shells: implications for cephalopod paleobiogeography. Paleobiology 7:494–509

Charbonnier S (2009) Le Lagerstätte de la Voulte un environment bathyal au Jurassique. Mém Mus Natl Hist Nat 199:1–272

Checa A (1996) Origin of intracameral sheets in ammonoids. Lethaia 29:61–75

Chun C (1915) The Cephalopoda part 1: Oegopsida, part 2: Myopsida, Octopoda—text and atlas. Scientific results of the German deepsea expedition on board the steamship "Valdivia" 1898–1899

Clarke MR (1969) Cephalopoda collected on the Sond Cruise. J Mar Biol Assoc UK 49:961–976

Clarke MR (1970) Growth and development of *Spirula spirula*. J Mar Biol Assoc UK 50:53–64

Collins DH, Minton P (1967) Siphuncular tube of *Nautilus*. Nature 216:916–917

Collins DH, Ward, PD, Westermann GEG (1980) Function of cameral water in *Nautilus*. Paleobiology 6:168–172

Crick RE (1988) Buoyancy regulation and macroevolution in nautiloid cephalopods. Senck Leth 69:13–42

Currie ED (1957) The mode of life of certain goniatites. Trans Geol Soc Glasg 22:169–186

Daniel TL, Helmuth BS, Saunders WB, Ward PD (1997) Septal complexity in ammonoid cephalopods increased mechanical risk and limited depth. Paleobiology 23:470–481

Delanoy G, Magnin A, Sélébran M, Sélébran J (1991) *Moutoniceras nodosum* d'Orbigny, 1850 (Ammonoidea, Ancyloceratina), une très grande ammonite hétéromorphe du Barrémien inférieur. Rev Paléobiol 10:229–245.

Denton EJ (1962) Some recently discovered buoyancy mechanisms in marine animals. Proc R Soc Lond B 265:366–370

Denton EJ (1971) Examples of the use of active transport of salts and water to give buoyancy in the sea. Phil Trans R Soc Lond B 262:277–287

Denton EJ (1974) On buoyancy and the lives of modern and fossil cephalopods. Proc R Soc Lond B 185:273–299
Denton EJ, Gilpin-Brown JB (1961a) The buoyancy of the cuttlefish *Sepia officinalis* (L.). J Mar Biol Assoc UK 41:319–342
Denton EJ, Gilpin-Brown JB (1961b) The effect of light on the buoyancy of the cuttlefish. J Mar Biol Assoc UK 41:343–350
Denton EJ, Gilpin-Brown JB (1961c) The distribution of gas and liquid within the cuttlebone. J Mar Biol Assoc UK 41:365–381
Denton EJ, Gilpin-Brown JB (1966) On the buoyancy of the pearly *Nautilus*. J Mar Biol Assoc UK 46:723–759
Denton EJ, Gilpin-Brown JB (1971) Further observations on the buoyancy of *Spirula*. J Mar Biol Assoc UK 51:363–373
Denton EJ, Gilpin-Brown JB (1973) Floatation mechanisms in modern and fossil cephalopods. Adv Mar Biol 11:197–268
Denton EJ, Gilpin-Brown JB, Howarth JV (1961) The osmotic mechanism of the cuttlebone. J Mar Biol Assoc UK 41:351–364
Denton EJ, Gilpin-Brown JB, Howarth JV (1967) On the buoyancy of *Spirula spirula*. J Mar Biol Assoc UK 47:181–191
Denton EJ, Gilpin-Brown JB, Shaw TI (1969) A buoyancy mechanism found in cranchid squid. Proc R Soc Lond B 174:271–279
Derham W (1726) Philosophical experiments and observations of the late eminent Dr. Robert Hooke, Derham, London
Diamond JM, Bossert WH (1967) Standing gradient osmotic flow—a mechanism for coupling water and solute transport in epithelia. J Gen Physiol 50:2061–2083
Diamond JM, Bossert WH (1968) Functional consequences of ultra-structural geometry in "backwards" fluid-transporting epithelia. J Cell Biol 37:694–702
Diener C (1912) Lebensweise und Verbreitung der Ammoniten. Neues Jahrb Miner Geol Palaontol 2:67–89
Donovan D (1964) Cephalopod phylogeny and classification. Biol Rev 39:259–287
Drushchits VV, Doguzhaeva LA (1981) Ammonites under the electron microscope (internal shell structure and systematics of Mesozoic Phylloceratidae, Lytoceratidae and 6 families of Early Cretaceous Ammonitidae). Moscow University, Moscow
Dumont ER, Piccirillo J, Grosse IR (2005) Finite-element analysis of biting behavior and bone stress in the facial skeletons of bats. Anat Rec 283A:319–330
Dunstan AJ, Ward PD, Marshall NJ (2011) Vertical Distribution and Migration Patterns of *Nautilus pompilius*. PLoS One 6:e16312
Dzik J (1981) Origin of the Cephalopoda. Acta Palaeont Pol 26:161–91
Ebel K (1983) Berechnungen zur Schwebfähigkeit von Ammoniten. Neues Jahrb Geol Paläontol (MMonatshefte) 1983:614–640
Ebel K (1985) Gehäusespirale und Septenform bei Ammoniten unter der Annahme vagil benthischer Lebensweise. Paläontol Z 59:109–123
Ebel K (1990) Swimming abilities of ammonites and limitations. Paläontol Z 64:25–37
Ebel K (1992) Mode of life and soft body shape of heteromorph ammonites. Lethaia 25:179–193
Ebel K (1993) Negative buoyancy of ammonoids—reply. Lethaia 26:260
Ebel K (1999) Hydrostatics of fossil ectocochleate cephalopods and its significance for the reconstruction of their lifestyle. Paläontol Z 73:277–288
Engeser, T (1996) The position of the Ammonoidea within the Cephalopoda. In: Landman NH, Tanabe K, Davis RA (eds) Ammonoid paleobiology. Topics in Geobiology 13. Plenum, New York
Finn, JK, Norman, MD (2010) The argonaut shell: gas-mediated buoyancy controlin a pelagic octopus. Proc R Soc B 277:2967–2971
Gottobrio WE, Saunders WB (2005) The clymeniid dilemma: functional implications of the dorsal siphuncle in clymeniid ammonoids. Paleobiology 31:233–252
Greenwald L, Ward PD (1982) On the source of cameral liquid in the chambered *Nautilus*. Veliger 25:169–170.

Greenwald L, Ward PD (1987) Buoyancy in *Nautilus*. In: Saunders BW, Landman NH (eds) *Nautilus*—the biology and paleobiology of a living fossil. Springer, Dordrecht

Greenwald L, Ward PD, Greenwald OE (1980) Cameral liquid transport and buoyancy control in the chambered nautilus (*Nautilus macromphalus*). Nature 286:55–56

Greenwald L, Cook CB, Ward PD (1982) The structure of the chambered *Nautilus* siphuncle: the siphuncular epithelium. J Morphol 172:5–22

Greenwald L, Verderber G, Singley C (1984) Localization of Na-K ATPase activity in the *Nautilus* siphuncle. J Exp Zool 229:481–484

Guex J (2005) Buoyancy control and growth rates in ammonoids: new preliminary remarks about an old Red Herring. Bull Géol Lausanne 365:1–4

Guex J, Koch A, O'Dogherty L, Bucher H (2003) A morphogenetic explanation of Buckman's law of covariation. Bull Soc Géol Fr 174:603–606

Hammer Ø, Bucher H (2005) Buckman's law of covariation—a case of proportionality. Lethaia 38:67–72

Hammer Ø, Bucher H (2006) Generalized ammonoid hydrostatics modelling, with application to *Intornites* and intraspecific variation in *Amaltheus*. Paleontol Res 10:91–96

Heath TL (1897) The works of Archimedes. Clay and Sons, Cambridge University Press, Warehouse, London

Heptonstall WB (1970) Buoyancy control in ammonoids. Lethaia 3:317–328.

Hewitt RA (1985) Numerical aspects of sutural ontogeny in the Ammonitina and Lytoceratina. Neues Jahrb Geol Palaontol Abh 170:273–290

Hewitt RA (1996) Architecture and strength of the ammonoid shell. In: Landman NH, Tanabe K, Davis RA (eds) Ammonoid paleobiology. Plenum, New York.

Hewitt RA, Westermann GEG (1987) Function of complexly fluted septa in ammonoid shells 2. Septal evolution and conclusions. Neues Jahrb Geol Palaontol Abh 174:135–169

Hewitt RA, Westermann GEG (1993) Growth rates of ammonites estimated from aptychi. Geobios Mem Spec 15:203–208

Hewitt RA, Westermann GEG (1996) Post-mortem behaviour of Early Paleozoic nautiloids and paleobathymetry. Paläontol Z 70:405–424

Hewitt RA, Westermann GEG (1997) Mechanical significance of ammonoid septa with complex sutures. Lethaia 30:205–212

Hewitt RA, Westermann GEG, Judd RL (1999) Buoyancy calculations and ecology of Callovian (Jurassic) cylindroteuthid belemnites. Neues Jahrb Geol Paläont Abh 211:89–112

Hoffmann R (2010) New insights on the phylogeny of the Lytoceratoidea (Ammonitina) from the septal lobe and its functional interpretation. Rev Paléobiol 29:1–156

Hoffmann R, Zachow S (2011) Non-invasive approach to shed new light on the buoyancy business of chambered cephalopods (Mollusca). IAMG 2011 publication, Salzburg. doi:10.5242/iamg.2011.0163:506-516

Hoffmann R, Schultz JA, Schellhorn R, Rybacki E, Keupp H, Gerden SR, Lemanis R, Zachow S (2014) Non-invasive imaging methods applied to neo- and paleontological cephalopod research. Biogeosciences 11: 2721–2739. doi:10.5194/bg-11-2721-2014

Hooke R (1726) Philosophical experiments and observations. In: Derham W (ed) Printers to the Royal Society 8:807–810

Jacobs DK (1992) The support of hydrostatic load in cephalopod shells—adaptive and ontogenetic explanations of shell form and evolution from Hooke 1695 to the present. In: Hecht MK, Wallace B, MacIntyre RJ (eds) Evolutionary biology, 26, Plenum, New York

Jacobs DK (1996) Chambered cephalopod shells, buoyancy, structure and decoupling: history and red herrings. Palaios 11:610–614

Jacobs DK, Chamberlain JA Jr (1996) Buoyancy and hydrodynamics in ammonoids. In: Landman NH, Tanabe K, Davis RA (eds) Ammonoid paleobiology. Topics in geobiology 13. Plenum, New York

Jones D, Evans AR, Siu KWK (2012) The sharpest tool in the box? Quantitative analysis of conodont element functional morphology. Proc R Soc Biol 279:2849–2854

Kalender W, Felsenberg D, Genant HK (1995) The European Spine Phantom—a tool for standardization and quality control in spinal bone mineral measurements by DXA and QCT. Eur J Radiol 20:83–92

Kanie Y, Fukuda Y, Nakahara K, Seki K, Hattori H (1980) Implosion of living *Nautilus* under increased pressure. Paleobiology 6:44–47

Kelly A (1901) Beiträge zur mineralogischen Kenntnis der Kalkausscheidungen im Tierreich. Jenä Z 35:429–494

Keupp H (1997) Paläopathologische Analyse einer "Population" von *Dactylioceras athleticum* (Simpson) aus dem Unter-Toarcium von Schlaifhausen/Oberfranken. Berl Geowiss Abh 25:243–267

Keupp H (2000) Ammoniten—Paläobiologische Erfolgsspiralen. Thorbecke, Stuttgart

Keupp H (2012) Atlas zur Paläopathologie der Cephalopoden. Berl Paläobiol Abh 10:1–390

Keupp H, Röper M, Seilacher A (1999) Paläobiologische Aspekte von syn vivo-besiedelten Ammonoideen im Plattenkalk des Ober-Kimmeridgiums von Brunn in Ostbayern. Berl Geowiss Abh 30:121–145

Klinger HC (1981) Speculations on buoyancy control and ecology in some heteromorph ammonites. Syst Assoc Spec Vol 18:337–355

Klug C (2001) Life-cycles of Emsian and Eifelian ammonoids (Devonian). Lethaia 34:215–233

Klug C, Lehmann J (2015) Soft part anatomy of ammonoids: reconstructing the animal based on exceptionally preserved specimens and actualistic comparisons (this volume)

Klug C, Korn D, Richter U, Urlichs M (2004) The black layer in cephalopods from the German Muschelkalk (Middle Triassic). Palaeontology 47:1407–1425

Klug C, Meyer E, Richter U, Korn D (2008) Soft-tissue imprints in fossil and Recent cephalopod septa and septum formation. Lethaia 41:477–492

Klug C, Riegraf W, Lehmann J (2012) Soft-part preservation in heteromorph ammonites from the Cenomanian-Turonian Boundary Event (OAE 2) in the Teutoburger Wald (Germany). Palaeontology 55:1307–1331

Klug C, Kröger B, Vinther J, Fuchs D, De Baets K (2015a) Ancestry, origin and early evolution of ammonoids. (this volume)

Klug C, Zatoń M, Parent H, Hostettler B, Tajika A (2015b) Mature modifications and sexual dimorphism. (this volume)

Kröger B (2000) Schalenverletzungen an jurassischen Ammoniten—ihre paläobiologische und palökologische Aussagefähigkeit. Berl Geowiss Abh 33:1–97

Kröger B (2001) Discussion—comments on Ebel's benthic-crawler hypothesis for ammonoids and extinct nautiloids. Paläontol Z 75:123–125

Kröger B (2002) On the efficiency of the buoyancy apparatus in ammonoids: evidences from sublethal shell injuries. Lethaia 35:61–70

Kröger B (2003) The size of the siphuncle in cephalopod evolution. Senckenberg Lethaea 83:39–52

Kröger B, Vinther J, Fuchs D (2011) Cephalopod origin and evolution: a congruent picture emerging from fossils, development and molecules. Bioessays 12 pp. doi:10.1002/bies.201100001

Kruta I, Landman NH, Rouget I, Cecca F, Tafforeau P (2011) The role of ammonites in the Mesozoic marine food web revealed by exceptional jaws preservation. Science 331(70):70–72

Kruta I, Landman NH, Cochran JK (2014) A new approach for the determination of ammonite and nautilid habitats. PLoS One 9:e87479 doi:10.1371/journal.pone.0087479

Kulicki C (1979) The ammonite shell, its structure, development and biological significance. Palaeontol Pol 39:97–142

Kulicki C (1996) Ammonoid shell microstructure. In: Tanabe K, Davis RA (eds) Ammonoid Paleobiology. Plenum, New York

Longridge LM, Smith PL, Rawlings G, Klaptocz V (2009) The impact of asymmetries in the elements of the phragmocone of early Jurassic ammonites. Palaeontol Electron 12:1–15

Lukeneder A, Harzhauser M, Müllegger S, Piller WE (2010) Ontogeny and habitat change in Mesozoic cephalopods revealed by stable isotopes (delta^{18}O, delta^{13}C). Earth Planet Sci Lett 296:103–114 doi:10.1016/ j.epsl.2010.04.053

Mangum CP, Towle DW (1982) The *Nautilus* siphuncle as an ion pump. Pac Sci 36:273–282
Meigen W (1870) Über den hydrostatischen Apparat bei *Nautilus pompilius*. Arch Naturgesch 36:1–36
Monks N, Young JR (1998) Body position and the functional morphology of Cretaceous heteromorph ammonites. Palaeontogr Electron, http:/www-odp.tamuedu/paleo/1998_1/toc.htm. Accessed 17 Jan 2015
Moore R, Lalicker C, Fischer A (1952) Invertebrate fossils. McGraw-Hill Co., New York
Moriya K, Nishi H, Kawahata H, Tanabe K, Takayanagi Y (2003) Demersal habitat of Late Cretaceous ammonoids: evidence from oxygen isotopes for the campanian (Late Cretaceous) northwestern Pacific thermal structure. Geology 31:167–170
Moseley H (1838) On the geometrical form of turbinated and discoid shells. Phil Trans R Soc Lond 1838:351–370
Mutvei H (1983) Flexible nacre in the nautiloid *Isorthoceras*, with remarks on the evolution of cephalopod nacre. Lethaia 16:233–240
Mutvei H, Reyment RA (1973) Buoyancy control and siphuncle function in ammonoids. Palaeontology 16:623–636
Naglik C, Monnet C, Götz S, Kolb C, De Baets K, Klug C (2015) Growth trajectories in chamber and septum volumes in major subclades of Paleozoic ammonoids. Lethaia: DOI:10.1111/let.12085. Accessed 17 Jan 2015
Naglik C, Rikhtegar F, Klug C (2014) Buoyancy of some Palaeozoic ammonoids and their hydrostatic properties based on empirical 3D-models. Lethaia: ca. 14 pp.
O'Dor RK, Forsythe J, Webber DM, Wells J, Wells MJ (1993) Activity levels of *Nautilus* in the wild. Nature 362:626–628
Okamoto T (1988) Changes in life orientation during the ontogeny of some heteromorph ammonites. Paleontology 31:281–294
Owen R (1832) Memoir of the Pearly Nautilus (*Nautilus Pompilius*, Linn.). London. pp 1–68
Owen R (1878) On the relative positions to their constructions of the chambered shells of cephalopods. Proc Zool Soc Lond 1878:955–975
Packard A (1972) Cephalopods and fish: the limits of convergence. Biol Rev 47:241–307
Pfaff E (1911) Über Form und Bau der Ammonitensepten und ihre Beziehungen zur Suturlinie. Jahresber Niedersächs Geol Ver (Geol Abt Naturhist Ges Hannover) 4:207–223
Pojeta J Jr (1980) Molluscan phylogeny. Tulane Stud Geol Paleontol 16:55–80
Raup DM, Chamberlain JA Jr (1967) Equations for volume and center of gravity in ammonoids shells. J Paleontol 41:566–574
Reboulet S, Giraud F, Proux O (2005) Ammonoid abundance variations related to changes in trophic conditions across the Oceanic Anoxic Event 1d (Latest Albian, SE France). Palaios 20:121–141
Rein S (1999) On the swimming abilities of *Ceratites* De Haan and *Germanonautilus* Mojsisovics from the Upper Muschelkalk (Middle Triassic). Freiber Forschungsheft C481:39–47
Reyment RA (1958) Some factors in the distribution of fossil Cephalopods. Acta Univ Stockh—Stockh Contrib in Geol 1:97–184
Reyment RA (1973) Factors in the distribution of fossil cephalopods. Part 3: experiments with exact models of certain shell types. Bull Geol Inst Univ Uppsala N. S. 4:7–41
Ritterbush KA, Bottjer DJ (2012) Westermann Morphospace displays ammonoid shell shape and hypothetical paleoecology. Paleobiology 38:424–446
Saunders WB, Shapiro EA (1986) Calculation and simulation of ammonoid hydrostatics. Paleobiology 12:64–79
Schmidt M (1925) Ammonitenstudien. Fortschr Geol Palaeontol 10:75–363
Schmidt H (1930) Über die Bewegungsweise der Schalencephalopoden. Paläontol Z 12:194–208
Schmidt DN, Rayfield ER, Cocking A (2013) Linking evolution and development: synchrotron radiation X-ray tomographic microscopy of planktic foraminifers. Palaeontology 56:741–749
Schwarz EHL (1894) The Aptychus. Geol Mag, N S(Decade IV) 1:454–459
Seilacher A (1960) Epizoans as a key to ammonoid ecology. J Paleontol 34:183–193
Seilacher A, Gishlick AD (2015) Morphodynamics. CRC Press Taylor & Francis Group

Seilacher A, Labarbera M (1995) Ammonites as Cartesian Divers. Palaios 10:493–506
Shigeta Y (1993) Post-hatching early life history of Cretaceous Ammonoidea. Lethaia 26:133–146
Spath LF (1919) Notes on ammonites. Geol Mag 56:26–58, 65–74, 115–122, 170–177, 220–225
Stock SR (2009) MicroComputed tomography: methodology and applications. CRC Press, London
Sutton MD, Briggs DEG, Siveter DJ et al (2001) Methodologies for the Visualization and Reconstruction of Three-dimensional Fossils from the Silurian Herefordshire Lagerstätte. Palaeontol Electron 4:1–17
Sutton MD, Briggs DEG, Siveter DJ, Siveter DJ (2006) Fossilized soft tissues in a Silurian platyceratid gastropod. Proc Royal Soc B 273(1590):1039–1044
Sutton MD, Rahman IA, Garwood RJ (2014) Techniques for virtual palaeontology. Wiley, New York. doi:10.1002/9781118591192
Swan ARH, Saunders WB (1987) Function and shape in late Paleozoic (mid-Carboniferous) ammonoids. Paleobiology 13:297–311
Tajika A, Naglik C, Morimoto N, Pascual-Cebrian E, Hennhöfer DK, Klug C (2014) Empirical 3D-model of the conch of the Middle Jurassic ammonite microconch *Normannites*, its buoyancy, the physical effects of its mature modifications and speculations on their function. Hist Biol, 27:181–191. Accessed 17 Jan 2015
Tanabe K (1975) Functional morphology of *Otoscaphites puerculus* (Jimbo), an Upper Cretaceous ammonite. Trans Proc Palaeont Soc Jpn, N S 99:109–132
Tanabe K, Landman NH (1996) Septal neck—siphuncular complex of ammonoids. In: Landman NH, Tanabe K, Davis RA (eds) Ammonoid paleobiology, Plenum, New York
Tanabe K, Mapes RH, Sasaki T, Landman NH (2000) Soft part anatomy of the siphuncle in Permian prolecanitid ammonoids. Lethaia 3:83–91
Tanabe K, Sasaki T, Mapes RH (2014) Soft-part anatomy of the siphuncle in ammonoids (this volume)
Tasch P (1973) Paleobiology of invertebrates. Wiley, New York.
Trueman AE (1941) The ammonite body chamber with special reference to the buoyancy and mode of life of the living ammonite. Quart J Geol Soc Lond 96:339–383
Tsujino Y, Shigeta Y (2012) Biological response to experimental damage of the phragmocone and siphuncle in *Nautilus pompilius* Linnaeus. Lethaia 45:443–449
Tsujita CJ, Westermann GEG (1998) Ammonoid habitats and habits in the Western Interior Seaway: a case study from the Upper Cretaceous Bearpaw Formation of southern Alberta, Canada. Palaeogeogr Palaeoclim Palaeoecol 144:135–160
Vrolik W (1843) On the Anatomy of the Pearly *Nautilus*. Ann Mag Nat Hist 12:173–175
Wani R, Kase T, Shigeta Y, De Ocampo R (2005) New look at ammonoid taphonomy, based on field experiments with modern chambered nautilus. Geology 33:849–852
Ward PD (1979) Cameral liquid in *Nautilus* and ammonites. Paleobiology 5:40–49
Ward PD (1980) Restructuring the chambered *Nautilus*. Paleobiology 6: 247–249
Ward PD (1982) The relationship of siphuncle size to emptying rates in chambered cephalopods: implications for cephalopod paleobiology. Paleobiology 8:426–433
Ward PD (1986) Rates and processes of compensatory buoyancy change in *Nautilus macromphalus*. Veliger 28:356–368
Ward PD (1987) The Natural History of *Nautilus*. Allen & Unwin, Boston
Ward PD, von Boletzky S (1984) Shell implosion depth and implosion morphologies in three species of *Sepia* (Cephalopoda) from the Mediterranean Sea. J Mar Biol Assoc UK 64:955–966
Ward PD, Greenwald L (1982) Chamber refilling in *Nautilus*. J Mar Biol Assoc UK 62:469–475
Ward PD, Martin AW (1978) On the buoyancy of the Pearly *Nautilus*. J Exp Zool 205:5–12
Ward PD, Westermann GEG (1977) First occurrence, systematics, and functional morphology of *Nipponites* (Cretaceous Lytoceratina) from the Americas. J Paleontol 51:367–372
Ward PD, Stone R, Westermann GEG, Martin A (1977) Notes on animal weight, cameral fluids, swimming speed, and color polymorphism of the Cephalopod *Nautilus pompilius* in the Fiji Islands. Paleobiology 3:377–388
Ward PD, Greenwald L, Rougerie F (1980a) Shell implosion depth for living *Nautilus macromphalus* and shell strength of extinct cephalopods. Lethaia 13:182

Ward PD, Greenwald L, Greenwald OE (1980b) The buoyancy of the chambered *Nautilus*. Sci Am 243:190–203

Ward PD, Greenwald L, Magnier Y (1981) The chamber formation cycle in *Nautilus macromphalus*. Paleobiology 7:481–493

Ward PD, Carlson B, Weekley M, Brumbaugh B (1984) Remote telemetry of daily vertical and horizontal movement by *Nautilus* in Palau. Nature 309:248–250

Warnke KM, Oppelt A, Hoffmann R (2010) Stable isotopes during ontogeny of *Spirula* and derived hatching temperatures. Ferrantia 59:191–201

Weitschat W, Bandel K (1991) Organic components in phragmocones of boreal Triassic ammonoids: implications for ammonoid biology. Paläontol Z 65: 269–303

Wells M (1990) The dilemma of the jet set. New Sci 1704:44–47

Westermann GEG (1956) Phylogenie der Stephanocerataceae und Perisphinctaceae des Dogger. Neues Jahrb Geol Paläont Abh 103:233–279

Westermann GEG (1971) Form, structure and function of shell and siphuncle in coiled mesozoic ammonoids. Life Sci Contrib, R Ont Mus 78:1–39

Westermann GEG (1973) Strength of concave septa and depth limits of fossil cephalopods. Lethaia 6:383–403

Westermann GEG (1975) Model for origin, function and fabrication of fluted cephalopod septa. Paläontol Z 49:235–253

Westermann GEG (1977) Form and function of orthoconic cephalopod shells with concave septa. Paleobiology 3:300–321

Westermann GEG (1982) The connecting rings of *Nautilus* and Mesozoic ammonids: implications for ammonite bathymetry. Lethaia 15:373–384

Westermann GEG (1990) New developments in ecology of Jurassic-Cretaceous ammonoids. In: Pallini G, Cresta S, Santantonio M (eds) Fossili, Evolutione, Ambiente. Atti II Convenio Internationale Pergola 1987

Westermann GEG (1993) On alleged negative buoyancy of ammonoids. Lethaia 26:246

Westermann GEG (1996) Ammonoid life and habitat. In: Landman NH, Tanabe K, Davis RA (eds) Ammonoid paleobiology, Plenum, New York

Westermann GEG (1998a) Life habits of nautiloids. In: Savazzi E (ed) Functional morphology of the invertebrate skeleton. Wiley, Chichester

Westermann GEG (1998b) Life habits of ammonoids. In: Savazzi E (ed) Functional morphology of the invertebrate skeleton. Wiley, Chichester

Westermann GEG (2013) Hydrostatics, propulsion and life-habits of the Cretaceous ammonoid *Baculites*. Rev Paléobiol 32:249–265

Westermann B, Beuerlein K, Hempelmann G, Schipp R (2002) Localization of putative neurotransmitters in the mantle and siphuncle of the mollusc *Nautilus* L. (Cephalopoda). Histochem J 34:435–440

Willey A (1902) Contributions to the natural history of the Pearly Nautilus. In: Wiley A (ed.) Zoological results part 6, Cambridge University Press, Cambridge

Witmer LM (1995) The extant phylogenetic bracket and the importance of reconstructing soft tissues in fossils. In: Thomason JJ (ed) Functional morphology in vertebrate paleontology. Cambridge University Press, Cambridge

APPENDIX I-C

Empirical 3D model of the conch of the Middle Jurassic ammonite microconch *Normannites*: its buoyancy, the physical effects of its mature modifications and speculations on their function

Published in *Historical Biology: An International Journal of Paleobiology, 27:2* (2015)

Historical Biology, 2015
Vol. 27, No. 2, 181–191, http://dx.doi.org/10.1080/08912963.2013.872097

Taylor & Francis
Taylor & Francis Group

Empirical 3D model of the conch of the Middle Jurassic ammonite microconch *Normannites*: its buoyancy, the physical effects of its mature modifications and speculations on their function

Amane Tajika[a]*, Carole Naglik[a1], Naoki Morimoto[b2], Enric Pascual-Cebrian[c3], Dominik Hennhöfer[c4] and Christian Klug[a5]

[a]*Paläontologisches Institut und Museum, Universität Zürich, Karl-Schmid-Strasse 4, Zürich 8006, Switzerland*
[b]*Laboratory of Physical Anthropology, Graduate School of Science, Kyoto University, Kitashirakawa Oiwake-cho, Sakyo-ku, 606-8502 Kyoto, Japan;* [c]*Institut für Geowissenschaften, Universität Heidelberg, Im Neuenheimer Feld 234, Heidelberg 69120, Germany*

(*Received 1 October 2013; accepted 2 December 2013; first published online 21 February 2014*)

A 3D model of the Middle Jurassic ammonoid *Normannites* with an apertural modification from Thürnen, Switzerland, was constructed using physical–optical tomography. It was tested to determine whether the formation of the apertural modification affected shell orientation, to estimate buoyancy regulation and to reconstruct the mode of life of this ammonoid. No drastic postural changes occurred between the 3D models that excluded and included lappets, suggesting that the lappets were not formed to change the *syn vivo* shell orientation and, in turn, locomotion. We speculate that these adult shell modifications served to protect the soft parts during the reproduction period. Buoyancy calculations based on the model assume that ammonoids were positively buoyant when the phragmocone was devoid of liquid. When 31% of the entire phragmocone was filled with liquid, the living animal would have reached neutral buoyancy in contrast to 27% of cameral liquid filling when the weight of the aptychi is included. Provided that smaller ammonoids had more cameral liquid than bigger ammonoids, such as the modern *Nautilus*, *Normannites* examined in this study would have been able to maintain neutral buoyancy and might have had a demersal, nektobenthic or nektonic habitat somewhere in the water column.

Keywords: microconch ammonites; sexual dimorphism; functional morphology; buoyancy; grinding tomography; Jurassic

Introduction

Mollusc shells grow by accretion and thus usually carry information of their entire ontogeny within their shells. In most cases, shell shape changes through ontogeny, enabling the identification of distinct growth stages. This is also true for ammonoid conchs. In ammonoids, several growth phases have been distinguished, namely the protoconch stage, the ammonitella stage, the first post-hatching neanic or juvenile phase, the preadult or late juvenile stage, and the adult or mature stage (Westermann 1996; Klug 2001). Close to maturity, the conch of most ammonoids underwent morphologic modifications that are characteristics for some species. These modifications may comprise the following aspects (see Ward 1987 for adult modifications in Recent nautilids; Davis et al. 1969; Ward 1987; Davis et al. 1996; Klug 2004; Collins and Ward 2009):

- septal crowding and thickening;
- apertural shell thickening;
- black band;
- deepening of the ocular sinuses;
- reduction of whorl height and width (whorl expansion rate decrease);
- changes in colour pattern;
- change in body chamber length;
- crowding and increasing thickness of growth lines and lirae;
- changes in ornamentation;
- changes in umbilical width (often increase); apertural modifications, sometimes including constrictions and/or lappets (a pair of lateral apophyses) and so on.

The process involving all these changes has been dubbed morphogenetic countdown by Seilacher and Gunji (1993), and may have affected the mode of life of adult ammonoids. Particularly in the case of ammonoids, shell allometry and mature modifications are important because ammonoids used their shells as buoyancy devices. Thus, such modifications might have changed the orientation of the shell.

It is known that some ammonoid species have two different adult morphologies, a phenomenon defined as dimorphism (Makowski 1962; Callomon 1963; Davis 1972); the two respective forms are termed antidimorphs. The phenomenon of ammonoid dimorphism was first reported by de Blainville (1840), who suggested that it is linked to the two sexes. Since then, this explanation has become widely accepted (Makowski 1962; Callomon 1963; Lehmann 1981; Davis et al. 1996). Although unequivocal evidence is missing, many researchers agree on the assumption that macroconchs of the antidimorphic pairs are the females and the microconchs are males (Mangold-Wirz 1963; Westermann 1969; Davis et al. 1996). Mature modifications comprise the main characters to differentiate between the two supposed sexes (Davis et al. 1996). Even though a number of ammonoids with

*Corresponding author. Email: amane.tajika@pim.uzh.ch

mature modifications have been reported, the function of these modifications has been debated. Senility, pathology and genetic disorder were given as alternative explanations for mature modifications (Hyatt 1874; Coëmme 1917). However, these are most likely not the reasons taking the uniformity of modifications within respective taxa into account (Davis 1972; Davis et al. 1996). A number of researchers have given separate taxon names for each antidimorph. Pairs of *Morrisiceras morrisi* (macroconch) and *Holzbergia schwandorfense* (microconch; Zatoń 2008), and *Asphinctites tenuiplicatus* (macroconch) and *Polysphinctites secundus* (microconch; Zatoń 2010) are two out of many examples.

Classical and modern approaches

The first paleontologist, who worked on buoyancy and shell orientation was Trueman (1940). He determined the positions of the centres of mass and buoyancy using actual specimens and plaster casts. Later, Raup (1967) attempted to determine the orientation and hydrostatic stability of ammonoids by using coiling equations. Raup and Chamberlain (1967), as well as Saunders and Shapiro (1986), developed the equation into a computational approach, discussing shell orientation, buoyancy and stability. However, as they presumed a steady whorl expansion rate and standardised shell as well as septum thicknesses, their results represent good theoretical models for the location of the centres of mass and buoyancy, despite being based on empirical values of *Nautilus*.

The advent of modern scanning technique has rendered several paleontological examples of 3D models of various fossils. Computer tomography based on a 3D-modelling procedure described in Garwood et al. (2010) has been considered as one of the best solutions, as specimens are not destroyed in the procedure and it takes less time than many other methods (Hounsfield 1973; Haubitz et al. 1988; Kak and Slaney 2001; Garwood et al. 2010; Hoffmann and Zachow 2011). This method was also used to study ammonoids (Lukeneder and Lukeneder 2011) and nautiloids (Hoffmann and Zachow 2011). These attempts demonstrated the limitations of computer tomography to construct detailed 3D models. The main reason is the similar densities which provide tomograms with low contrast and resolution. Kruta et al. (2011) performed several synchrotron scans to identify a calcareous aptychus in the body chamber of an ammonite using both a medical scanner and a μCT scanner only to find that no internal structure can be revealed. PPC-SR-μCT yields extraordinarily high-quality tomographic data (Garwood et al. 2010) as Kruta et al. (2011) showed with their first 3D model of a delicate ammonite radula. However, the limited availability of the facility, its high energy consumption and heavy data load make it difficult for paleontologists to use PPC-SR-μCT for all materials. Additionally, even synchrotron tomography requires density contrasts to reveal internal details of an object. Physical–optical tomography (grinding tomography), which constructs 3D models out of 2D stacks, is a traditional destructive method, which has been used to reconstruct vertebrates and brachiopods (Sollas 1904; Sollas and Sollas 1913; Muir-Wood 1934; Ager 1965; Kermack 1970; Kielan-Jaworowska et al. 1986; Sutton et al. 2001; Bednarz and McIlroy 2009). To obtain 2D images, serial grinding is commonly used, which repeatedly grinds off a thin sheet of defined thickness from a specimen with the newly exposed surface recorded by a high-resolution camera or a flatbed scanner.

One of our aims was to test the shell of a microconch for potential physical effects of the apertural modifications. For this purpose, an empirical 3D model was constructed, which we used to determine masses of various shell parts and to reconstruct shell orientation, as well as buoyancy.

In addition to the 3D reconstruction of the shell of the microconchiate *Normannites*, this study aims to answer the following questions: (1) What was the *syn vivo* shell orientation based on the 3D model? (2) What was the mass of the entire shell and of the apertural modification? (3) Did the apertural modification alter the shell orientation significantly? (4) Was the shell more or less neutrally buoyant, presuming an entirely gas-filled phragmocone? (5) What was the mode of life of *Normannites mitis*?

Material

The examined specimen is a Middle Jurassic ammonite of the species *Normannites mitis* Westermann 1954. It was found in the Middle Bajocian (Middle Jurassic) of Thürnen, Switzerland. Because our aim was to determine whether an adult modification had a physical effect on buoyancy and *syn vivo* shell orientation, an ammonite species with strong adult modifications (well-developed lappets) was selected.

The studied specimen of *Normannites mitis* was considered well suited because the locality is known for its complete specimens with calcitic replacements shells. Much of the recrystallised shell including the protoconch, most septa, the siphuncle and the body chamber with its apertural modifications are preserved and visible in the sections. Although the innermost parts of the siphuncle of this specimen are not preserved, the impact on the volume calculation is assumed to be low as the thickness of the inner part of the siphuncle is much less than 1 mm.

Methods

Physical–optical tomography (Garwood et al. 2010) was chosen to obtain a stack of 2D images for the construction

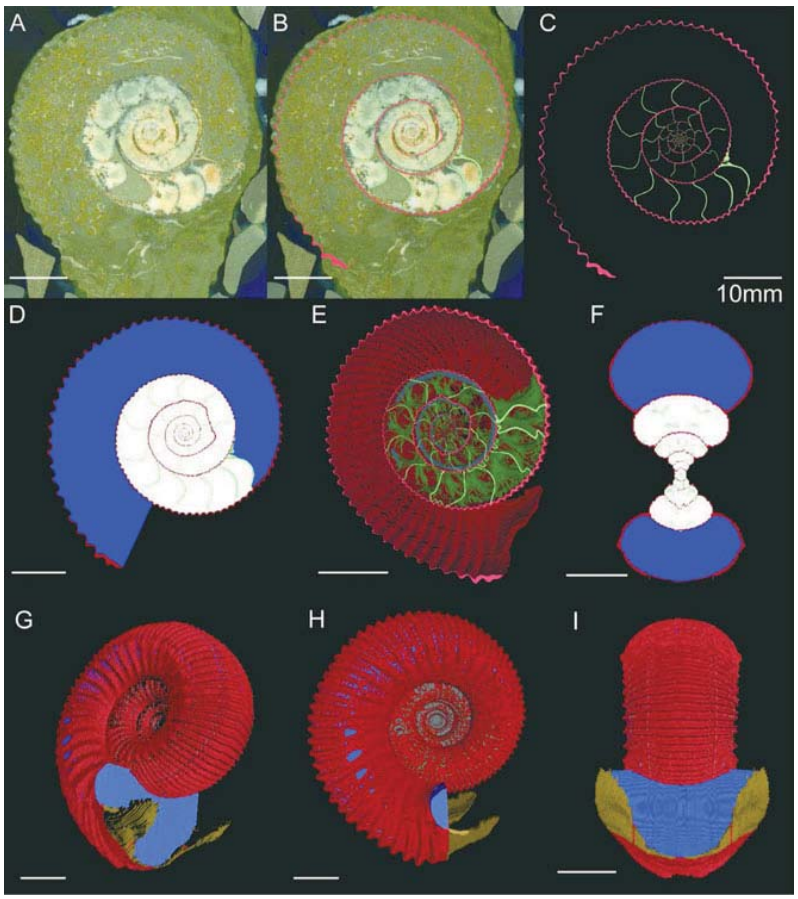

Figure 1. (Colour online) Median sections (the 190th 2D slice) and constructed 3D models of *Normannites mitis*. Assumed soft body, lappets, septa, phragmocone and outer shell are marked in blue, brown, green, white and red, respectively. Scale bars: 1 cm. (A) original scan; (B) marked shell and siphuncle; (C) drawing for 3D reconstruction with a black background; (D) complete drawing for 3D reconstruction; (E) 3D reconstruction of studied specimen *Normannites mitis* from the 418th 2D slice to the 174th without soft body to show the internal structure; (F) cross-sectional view of the 3D model; (G–I) 3D reconstructions of studied specimen *Normannites mitis*.

of a 3D model. Although the method is time-consuming and destructive, real colours and thus also colour contrast of all internal features are provided and, in turn, precise models can be constructed (Götz 2003, 2007; Götz and Stinnesbeck 2003; Garwood et al. 2010; Mallison 2011; Pascual-Cebrian et al. 2013). As the specimen was subjected to this method, the ammonite fossil is completely pulverised.

For the collection of empirical data, we produced serial sections of the specimen in the Heidelberg Grinding Tomography Laboratory (Germany), following the procedure described by Pascual-Cebrian et al. (2013). The specimen was in alternation ground, polished and scanned with a G&N: MPS 2R-300S surface-grinding machine. The distance of two increments is 60 μm. Scanning of the newly exposed surfaces took place in a water quench using a modified high-end flatbed scanner EPSON V750pro with a resolution of 2400 dpi.

From the obtained set of 422 scans, we produced a virtual 3D model of the ammonoid. The resulting 2D scans were imported into Adobe® Illustrator in which every fourth slice was manually traced. The manual tracing started with the 422nd slice, which is the outermost section, to slightly beyond the median section (the 174th slice) in such a manner that the entire siphuncle is fully contained (Figure 1(A)–(C)). The rest of the slices were produced by duplicating and mirroring the counterparts of the other side as ammonoid conchs are nearly bilaterally symmetric. Each component (body chamber, phragmocone, shell and septa) was marked by different colours so that the volumes could be calculated separately. The volume of the soft body was defined as the volume of the body chamber. As far as the siphuncle is concerned, every slice, where the siphuncle is visible, was traced for the volume calculation.

In the fifth whorl, a shell deformation and a planispirally coiled structure are visible. Superficially,

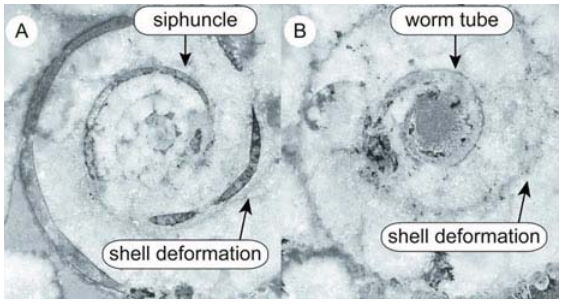

Figure 2. (Colour online) A worm tube observed in a serial section. (A) Siphuncle in the 190th section and (B) a worm tube in the 173rd section.

this structure resembled a dislocated siphuncle segment, because it was not situated in the plane of symmetry. A closer look of a reconstructed cross section in in the VGstudiomax®2.1 software revealed that the structure lies in a plane parallel to the plane of symmetry at the umbilical seam. This position in combination with the excentric coiling of the ammonite shell in this whorl corroborates that this tube is not part of the siphuncle but a worm tube (Figure 2). This epizoan grew on the ammonoid *syn vivo*, i.e. it is a true epizoan *sensu* Davis et al. (1999).

We traced the shell as it was seen with its deformation because the effect of the deformation on the mass distribution of the entire shell and weight should not make any difference. The worm-tube structure was not included in the buoyancy calculation.

We used the software VGstudiomax®2.1 to construct a 3D model out of the 2D stack. Using the voxel size, which corresponds to the pixel resolution of the traced images (x and y dimensions) and the vertical distance between two images (z dimension), the stack was processed in VGstudiomax®2.1 for the direct volume calculations of traced segments (chamber volumes, septum volumes and shell volume; Figure 1(E)–(I)). Taking into account that every fourth slice has been traced, the z dimension of the voxel is four times of the increment between each two successive slices (0.24 mm). The conch diameter and thickness of the 3D model are 5.02 and 2.39 cm, respectively.

Centres of buoyancy and mass

The centre of buoyancy of ammonoids is defined as the centre of gravity of the seawater displaced by the soft body and its shell (Trueman 1940; Raup and Chamberlain 1967; Saunders and Shapiro 1986; Kröger 2002). At rest, the centres of mass of the shell and of the soft parts of the living animal had to lie on a straight vertical line connecting both points. Initially, the centre of mass of the body chamber was calculated on each 2D drawing, and then the centre of mass of each 2D drawing was calculated and thereafter combined into the centre of mass of the whole body chamber. The same procedure was applied to the calculation of the centre of mass of the shell. Subsequently, the two calculated centres of mass of the body chamber and shell are combined into the centre of mass of the specimen, considering assumed densities of 1.055 g/cm^3 for the soft body (average mean of studied *Nautilus* soft parts; Saunders and Shapiro 1986) and 2.62 g/cm^3 for the shell (density of a *Nautilus* shell; Reyment 1958; Saunders and Shapiro 1986; Kröger 2002). The siphuncle is composed of mainly two parts (Tanabe et al. 1982; Ward 1987; Mutvei et al. 2010): the connecting ring, which was composed of glycoprotein fibres with numerous narrow pore canals (presumed density 1.22 g/cm^3: protein density; Fischer et al. 2004) and the inner soft part (presumed density 1.055 g/cm^3: the same density as of the soft body of the animal). We measured the ratio of the connecting ring cross-section area to the cross-section area of the soft part in the scan of the median section, thus calculating the density of the entire siphuncle (1.079 g/cm^3). Moreover, in order to find whether or not the apertural lappets had affected shell orientation, the lappets were excluded from the calculation and the centre of mass without the lappets was determined. It should be noted that the calculation of the two centres was performed based on the assumption that the phragmocone is filled with cameral gas. All calculations were performed in MATLAB 7.1 (MathWorks).

Results and discussion

Volume, mass and shell orientation

The results of the volume measurements are given in Table 1. Figure 3 shows the relative positions of the centres of buoyancy and mass of the reconstructed *Normannites mitis*. The *syn vivo* orientation of the specimen was empirically examined by Trueman (1940) and has been thought that its aperture was turned upward, which is corroborated by our empirical 3D model. In Trueman (1940), the centre of mass was defined as the centre of mass of the body chamber and the centre of buoyancy as the centre of gravity of displaced water by the entire animal. He assumed that the orientation of ammonoids was determined by the body chamber length (= soft tissue) because the other parts of the ammonoids (shell and siphuncle) have a lesser effect on the entire mass.

Hydrodynamic stability of animals in seawater is indicated by the distance between the centres of buoyancy and that of mass: a large distance between the two centres implies a higher hydrodynamic stability like that of *Nautilus* with a shorter body chamber (Trueman 1940; Saunders and Shapiro 1986; Okamoto

Table 1. Results of volume measurements, assumed densities for each segment and calculated mass.

Segment	Volume (cm^3)	Assumed density (g/cm^3)	Mass (g)
Outer shell	1.82	2.62	4.76
Lappets	0.13	2.62	0.35
Septa	0.28	2.62	0.73
Siphuncle	0.054	1.079	0.058
Soft tissue	17.13	1.055	18.07
Phragmocone	5.68	0	0
Aptychi	0.15	2.62	0.39
Total (without aptychi)	25.09		23.97
Water displaced by the entire animal (without aptychi)	25.09	1.026	25.74
Total (with aptychi)	25.24		24.36
Water displaced by the entire animal	25.24	1.026	25.89

1996). Although in our volume measurement, the lappet volume (0.13 cm^3) amounted to merely 0.76% of its body chamber volume (17.13 cm^3; Table 1), a slight change of the orientation and hydrodynamic stability between the two 3D models with and without lappets was discovered. In other words, if *Normannites mitis* had not had lappets on its aperture, it would have been hydrodynamically slightly more stable. The fact that no drastic postural changes occurred between the 3D models with and without lappets suggests that the lappets did not serve the function to change the *syn vivo* shell orientation and, in turn, locomotion. Thus, the negligible postural change indicates that the apertural modification with its lappets did not probably improve the swimming abilities of the mature ammonoid animal. This implies that improvement of mobility was not the key function of the modifications during the time of mating and breeding.

Buoyancy reconstruction

The empirical 3D model of *Normannites mitis* permits the estimation of the buoyancy of this ammonite. The buoyancy estimation is based on a comparison between

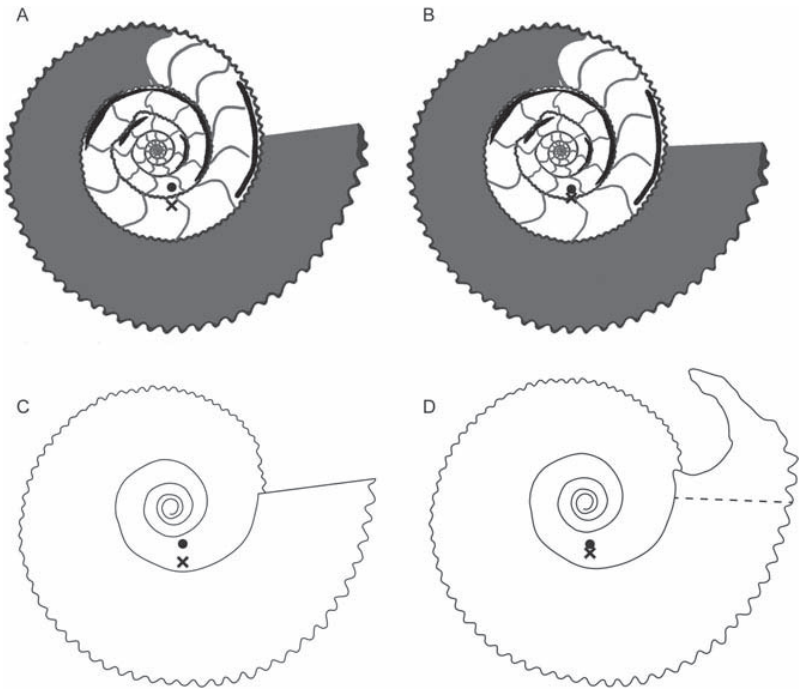

Figure 3. Calculated centres of mass and buoyancy of *Normannites mitis*, with and without lappets. Positions of centres of mass are marked by crosses and positions of centres of buoyancy by black dots. Dashed line represents the estimated boundary between the lappet and body chamber. (A, C) Positions of centres of mass and buoyancy without the lappets (A: median section; C: exterior) and (B, D) positions of centres of mass and buoyancy with the lappets (B: median section; D: exterior).

the mass of the animal and the water displaced by it, which is assumed to be completely submerged in seawater. The mass of the animal was calculated from the volume and densities of each component (shell, siphuncle and body chamber), assuming that the body chamber volume is equivalent to the soft part volume (Figure 1(D)) and the phragmocone is filled with gas. Each volume, density and calculated mass is given in Table 1. The total mass (23.97 g) consists of 18.07 g of soft tissue, 4.76 g of outer shell, 0.73 g of septa, 0.35 g of lappets and 0.058 g of siphuncle, in contrast to 25.74 g of water mass displaced by the animal. The comparison of the results of the mass determinations shows that under conditions, where the phragmocone is completely filled with gas, the animal would have been slightly lighter than the seawater displaced by it. In other words, when the phragmocone was devoid of liquid, the animal had positive buoyancy, especially when the additional mass of the calcareous lower beak (aptychus) is ignored (for the Praestriaptychus of '*Normannites*', see Westermann 1954: figs. 31–94 32; pl. 32). Moreover, it is possible to calculate the volume of cameral liquid required to attain neutral buoyancy. Ward (1979) presented the ratio of cameral liquid volume to cameral liquid salinity in *Nautilus macromphalus* and *Nautilus pompilius*. The data for *Nautilus macromphalus* appear reasonable, considering the epipelagic habitat of many Ammonitina to which *Normannites mitis* belongs (Anderson et al. 1994; Westermann 1996). The data show that the salinity of cameral liquid does not exceed the salinity of seawater, even though the salinity is variable (between 15% and 100% of seawater salinity), depending on the proportion of the liquid. As such, we assume a mean value for the salinity of cameral liquid (1.75%), i.e. between the values of fresh (0%) and seawater (3.5%; Antonov et al. 2009). Assuming that seawater density (1.026 g/cm^3) corresponds to seawater salinity (3.5%) and that freshwater density (1.00 g/cm^3) to fresh water salinity (0%), the mean value of the density is 1.013 g/cm^3. The calculated buoyancy with different cameral liquid fillings is shown in Table 2 and Figure 4. The results demonstrate that 31% of the chamber filling is sufficient to reach neutral buoyancy (Figure 4), when the mass of the aptychi is ignored.

According to Lehmann (1972), *Normannites* had a Praestriaptychus-type lower jaw, the microstructure of which was calcitic lamellar with organic layers (Trauth 1937). In order to calculate the size and weight of the aptychi of our specimen (not preserved), we two-dimensionally measured (1) the ratio between the shell diameter of another *Normannites* specimen and the width of its aptychi in a picture shown in Trauth (1937, pl. 11, fig. 1) and (2) the ratio of the area of the entire ammonoid to the aptychi area on VGstudiomax®2.1 (Figure 5). Thickness of the aptychi was calculated as 0.01% of its width (Trauth 1937). As shown in Figure 5(B), only one side of aptychi is seen in Trauth (1937, pl. 11, fig. 1). Therefore, we measured the aptychus width in the picture and doubled the width (Figure 5(B),(C)). The aptychi density was estimated to be the same as calcite (2.62 g/cm^3) and the organic layer was ignored because of its small contribution to the entire aptychi mass (Trauth 1937). The ratio between shell diameter of the ammonoid and aptychi width (14:1) and the ratio of the area of the entire ammonoid to the aptychi area (27:1) permitted the calculation of values for the aptychi thickness (0.14 cm), the aptychi area (0.54 cm^2) and ultimately the weight of the aptychi of our specimen (0.39 g). The results of the measurements and calculations in combination with the calculated buoyancy with different cameral liquid fillings are summarised in Table 3 and Figure 6, respectively. The results suggest that when 27% of the entire phragmocone was filled with cameral liquid, the animal was neutrally buoyant with the above calculated aptychi mass, compared with 31% of cameral liquid filling when the aptychi mass is ignored. Mutvei and Reyment (1973) as well as Reyment (1973) found that neutrally buoyant adult ammonoids retained more cameral liquid than adult *Nautilus*. The amount of cameral liquid of *Nautilus* is highly variable, depending on the size (ranging from almost 0% to more than 30% of the phragmocone volume; Ward 1979). Heptonstall (1970) calculated the percentage of cameral liquid occupying the phragmocone of ammonoids on the presumption that ammonoids could

Table 2. Assumed cameral liquid weight and total weight of the animal corresponding to each cameral liquid filling with and without aptychi mass.

Proportion of cameral liquid in the entire phragmocone volume of cameral liquid (%)	0	10	20	30	40	50	60	70	80	90	100
Cameral liquid volume (cm^3)		0.57	1.14	1.70	2.27	2.84	3.41	3.98	4.54	5.11	5.68
Cameral liquid weight (g)		0.58	1.15	1.72	2.30	2.88	3.45	4.03	4.60	5.18	5.75
Total weight (without aptychi mass, g)	23.97	24.55	25.12	25.69	26.27	26.85	27.42	28.00	28.57	29.15	29.72
Total weight (with aptychi mass, g)	24.36	24.94	25.51	26.08	26.66	27.24	27.81	28.39	28.96	29.54	30.11

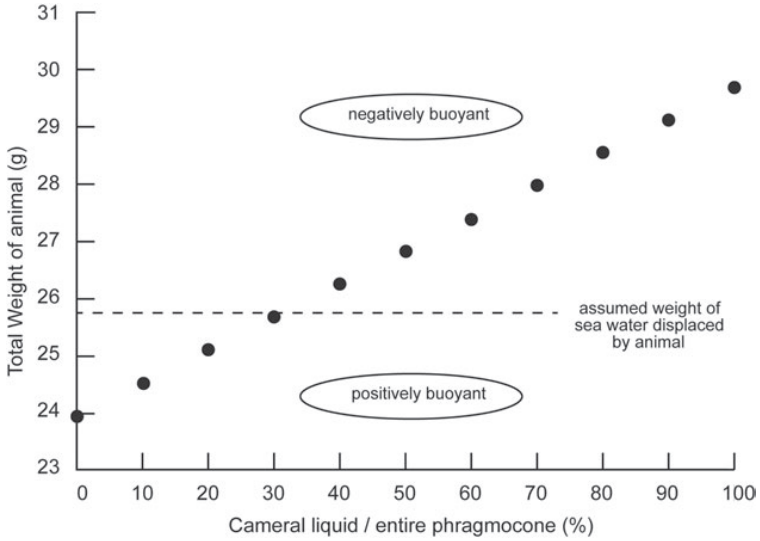

Figure 4. Cameral liquid percentage plotted against total weight of reconstructed *Normannites mitis* (without aptychi mass).

retain neutral buoyancy. He suggested that a large amount of water was required to attain neutral buoyancy (for Ammonitina, the percentages range from 22% to 52%). A proportion of 27% of cameral liquid needed for neutral buoyancy calculated in this study is consistent with Heptonstall's results.

According to Ward (1987), cameral liquid volume and total weight of *Nautilus pompilius* and *Nautilus macromphalus* are negatively correlated. This negative correlation between cameral liquid volume and total weight shows that an animal with a weight of less than 100 g has more than 30% of cameral liquid. If this correlation is applicable to ammonoids, our specimen with a weight of approximately 24 g must have retained much more than 30% cameral liquid volume against the entire phragmocone volume. Considering this, *Normannites mitis* was most likely able to become and remain fairly neutrally buoyant. We cannot conclude whether this ammonite had a demersal (nekto-

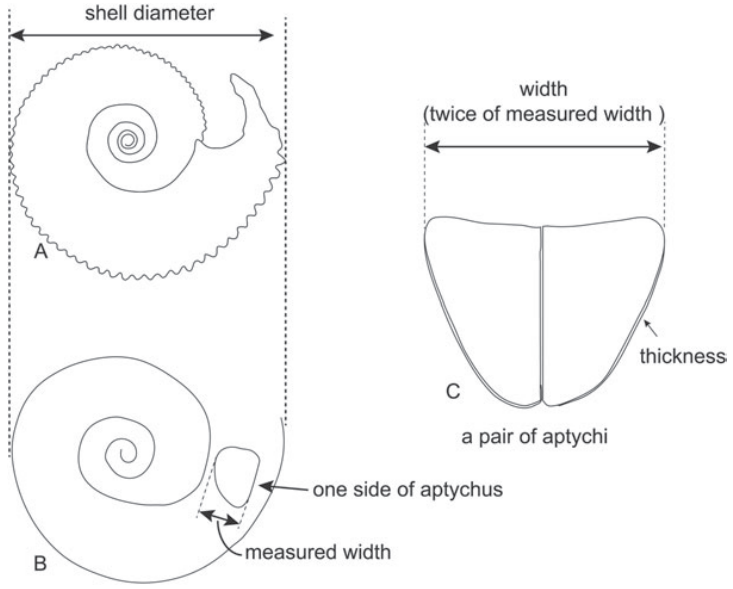

Figure 5. Measurement of shell diameter and aptychi. (A) Illustration of *Normannites mitis* (this study); (B) illustration of an ammonoid preserved with aptychus (simplification of the picture from Trauth 1937, pl. 11, fig. 1) and (C) illustration of a pair of aptychi (simplification of the picture from Trauth 1937, pl. 11, fig. 3).

Table 3. Assumed aptychi size and weight.

	Ratio	Measurement
Shell diameter vs aptychi width (Trauth 1937)	14:1	
The entire shell area vs aptychi area (Trauth 1937)	27:1	
Shell diameter (cm)		49.95
Width of aptychi of our specimen (cm)		14.12
Thickness of aptychi of our specimen (cm)		0.14
Area of the entire shell (median section) of our specimen (cm^3)		14.65
Aptychi area of our specimen (cm^3)		1.08
Aptychi volume of our specimen (cm^3)		0.15
Density (calcite; g/cm^3)		2.62
Aptychi weight of our specimen (g)		0.39

benthic) habitat as suggested by Moriya et al. (2003) or whether it lived somewhat higher in the water column (Lukeneder et al. 2010), but at least it appears plausible to assume that it inhabited the water column and not the sea floor.

Orientation of the shell

With the knowledge of the spatial distribution of mass, the localisation of the centres of mass was identified. Accordingly, the aperture of adult *Normannites mitis* was facing upward at an angle of 90–100° from the vertical (with lappets: 92.8°; without lappets: 97.7°). This is in accordance with moderately good horizontal swimming abilities (Saunders and Shapiro 1986; Westermann 1996; Klug 2001; Korn and Klug 2003; Klug and Korn 2004), shared with many other ammonoid species.

Ammonoids might have been able to modify actively their shell orientation. As pointed out in previous articles (Monks and Young 1998; Landman et al. 2012), if the soft tissues and especially the jaws with the calcified lower jaw (Westermann 1954; Parent and Westermann in press) were stretched out outside the aperture, the orientation might have turned slightly downward by the more or less horizontal shift of an accumulation of a relatively large mass. The life orientation demonstrated in this study could be extended in future studies with the possible positions of aptychi, whose calcitic material would affect the distribution of mass as well as soft body extension and size of the mantle cavity.

Discussion on the function of adult modifications

In the light of the peculiar morphology of the apertural lappets of the microconch studied here, it appears surprising that the mass of the lappets did not affect the orientation of the living animal significantly. Accordingly, we suggest that these lappets might have served a function other than buoyancy and enhancement of mobility. Alternative hypotheses should be more or less linked with reproduction, as these adult conch modifications show a rather stable morphology. The most obvious hypotheses (most of which are actually rather difficult to test) are:

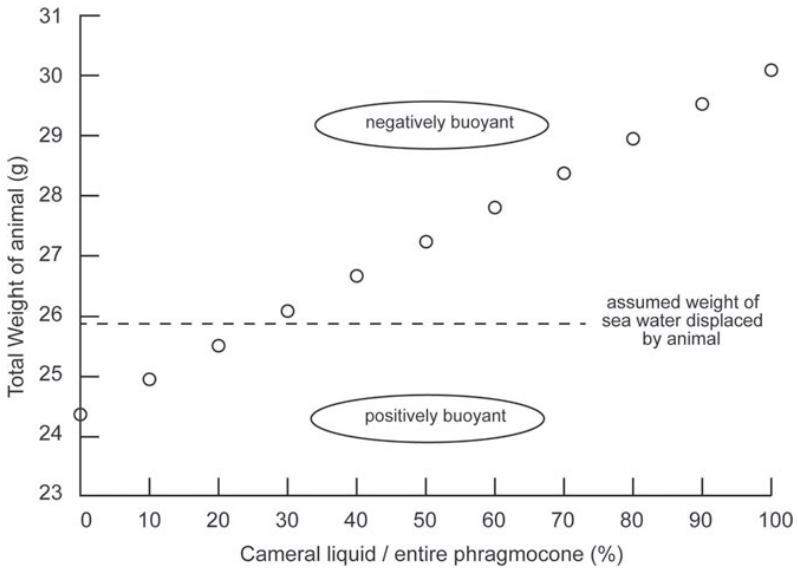

Figure 6. Cameral liquid percentage plotted against total weight of reconstructed *Normannites mitis* (with aptychi mass).

(1) reinforcement of the terminal aperture as protection from predators (Keupp and Riedel 2010);

(2) sexual display (Keupp and Riedel 2010);

(3) attachment of sexual organs (modified arms to transfer spermatophores like in *Argonauta*; Landman et al. 2012);

(4) the sinuses between the lappets provided space for reproductive organs such as modified arms (Landman et al. 2012); and

(5) fabricational noise, which did not bother the ammonoid or alter its reproductive success significantly (Seilacher 1974).

Hypothesis 1: It has been suggested that animals preying on ammonoids often attacked the aperture to reach the soft tissue (Landman and Waage 1986; Keupp and Riedel 2010). By contrast, Klompmaker et al. (2009) reported frequent attacks on Mesozoic ammonites, which left traces on the venter in the posterior part of the body chamber. Nevertheless, predators attacking the soft parts were a likely threat for ammonites, and thus any protection of the aperture, such as the apertural modifications, a hood or modified beaks, would have been useful.

Sexual cannibalism has been reported from *Octopus cyanea* (Hanlon and Forsythe 2008). Although the phylogenetic relationship is remote, a shell thickening and extension of the apertural shell might speculatively have represented structures for protecting their soft tissues at maturity against the sometimes much larger females (Keupp and Riedel 2010) or predators of other taxa. By contrast, Seilacher (1999) did not agree with this speculation because such protections are more urgently needed in females (macroconchs) than in males (microconchs) for their reproductive success and thus evolutionary fitness.

Hypothesis 2: Although sexual display could speculatively have been a function (Keupp and Riedel 2010), no evidence is available to test this hypothesis.

Hypotheses 3 and 4: Landman et al. (2012) points out that a male scaphitid ammonite with the aperture upward would have had difficulties to copulate if it had short and weak arms and that it is probable that they had a modified arm, which transferred spermatophores as in *Argonauta* (Okutani 1990). Provided that *Normannites mitis* possessed such modified arms, the lappets might have functioned as the attachment for them, which served to transfer spermatophores. Nevertheless, corresponding muscle attachments in the lappets or a microconch with soft-tissue preservation need to be found to test hypotheses 3 and 4.

Hypothesis 5: Fabricational noise (Seilacher 1974) as an explanation for apertural modifications appears unlikely, as it is a feature which occurs iteratively in several clades over a long time span.

Conclusions

Buoyancy, orientation of the shell and the effect of large apertural lappets and an apertural shell thickening in an adult specimen of *Normannites mitis* from the Middle Jurassic of Thürnen, Switzerland, were examined based on a detailed virtual 3D model. This model was constructed using a 2D stack obtained by physical–optical tomography (grinding tomography). With the data obtained from this empirical model, we arrived at the following conclusions:

(1) The location of the centres of mass and buoyancy was identified in order to reconstruct the shell orientation. The specimen under consideration thus had a more or less horizontal aperture including the apertural lappets.

(2) In the absence of liquid in the phragmocone chambers, the total mass of the entire animal with a conch diameter of 5.02 cm is 23.97 g. This weight comprises 18.07 g soft tissues, 4.76 g outer shell, 0.73 g septa, 0.35 g apertural lappets and 0.058 g siphuncle, in contrast to 25.74 g of water displaced by the animal. Presuming neutral buoyancy, the animal would have weighed 25.74 g at a diameter of 5.02 g.

(3) Buoyancy calculation from volumes and assumed densities of each segment suggests that when the phragmocone was filled with gas, the ammonite was positively buoyant and 31% of chamber liquid is necessary in order to reach neutral buoyancy (when the calcitic aptychi are not considered) and 27% (when the aptychi are considered).

(4) If ammonoids had the same ontogenetic trend of negative correlation between body mass and cameral liquid volume as extant *Nautilus*, *Normannites mitis* would have been able to attain neutral buoyancy and might have inhabited the water column, either in a demersal (nektobenthic) habitat or somewhere higher in the water column.

(5) Only a minor difference occurs in the orientation of the shell of the living animal when the lappets are present compared with when they are removed from the model. This suggests that the function of the lappets was probably not a consequence of an

adult change in their shell orientation and thus mode of life, especially in their locomotion. We speculate that these adult shell modifications served as protection of soft parts around the time of reproduction against predation attempts.

Acknowledgements

Beat Imhof (Trimbach, Switzerland) donated the two specimens, which were serially sectioned. We are sincerely grateful to Dr. Michał Zatoń and Dr. Dieter Korn for their critical comments on the early draft. We would also like to express our sincere gratitude to Stefan Götz who developed the grinding tomography and passed away in July 2012.

Funding

The Swiss National Science Foundation supported this study (Project numbers 200020-25029, 200020_149120, 200020-132870 and 200021_149119).

Notes

1. Email: carole.naglik@pim.uzh.ch
2. Email: morimoto@aim.uzh.ch
3. Email: enric.pascual@geow.uni-heidelberg.de
4. Email: dominik.hennhoefer@geow.uni-heidelberg.de
5. Email: chklug@pim.uzh.ch

References

Ager DV. 1965. Serial grinding techniques. In: Kummel B, Raup D, editors. Handbook of palaeontological techniques. San Fransisco: H. Freeman and Company. p. 212–224.

Anderson TF, Popp BN, Williams AC, Ho L-Z, Hudson JD. 1994. The stable isotopic record of fossils from the Peterborough Member, Oxford Clay Formation (Jurassic), UK. J Geol Soc. 151:125–138.

Antonov JI, Seidov D, Boyer TP, Locarnini RA, Mishonov AV, Garcia HE, Baranova OK, Zweng MM, Johnson DR. 2009. World Ocean Atlas 2009 Volume 2: Salinity. In: Levitus S, editor. NOAA Atlas NESDIS 69. Washington (DC): National Oceanographic Data Center.

Bednarz M, McIlroy D. 2009. Three-dimensional reconstruction of "Phycosiphoniform" burrows: implications for identification of trace fossils in core. Palaeontol Electron. 12(3):13A.

Callomon JH. 1963. Sexual dimorphism in Jurassic ammonites. Trans Leicester Lit Philos Soc. 57:21–56.

Coëmme S. 1917. Note critique sur le genre Cadomoceras. Bull Soc géol France Sér 4. 17:44–54.

Collins D, Ward PD. 2009. Adolescent growth and maturity in *Nautilus*. In: Saunders WB, Landman NH, editors. The biology and Paleobiology of a living fossil. Topics in geobiology. Vol. 9. Dordrecht: Springer.

Davis RA. 1972. Mature modification and dimorphism in selected Late Paleozoic ammonoids. Bull Am Paleontol. 62(272):23–130.

Davis RA, Furnish WM, Glenister BF. 1969. Mature modification and dimorphism in selected late Paleozoic ammonoids. In: Westerman GEG, editor. Sexual dimorphism in fossil metazoa and taxonomic implications. International Union of Geological Sciences, Series A, Number 1 Stuttgart: E. Schweizerbart'sche Verlagsbuchhandlung. p. 101–110.

Davis RA, Landman NH, Dommergues JL, Marchand D, Bucher H. 1996. Mature modifications and dimorphism in ammonoid cephalopods. In: Landman NH, Tanabe K, Davis RA, editors. Ammonoid paleobiology. New York: Plenum. p. 464–539.

Davis RA, Mapes RH, Klofak SM. 1999. Epizoa on externally shelled cephalopods. In: Rozanov AY, Shevyrev AA, editors. Fossil cephalopods: recent advances in their study. Moscow: Russian Academy of Sciences, Palaeontological Institute. p. 32–51.

de Blainville MHD. 1840. Prodrome d'une monographie des ammonites. In: Supplement du Dictionnaire des Sciences Naturelles. Paris: Bertrand. p. 1–31.

Fischer H, Polikarpov I, Craievich AF. 2004. Average protein density is a molecular-weight-dependent function. Protein Sci. 13 (10):2825–2828.

Garwood RJ, Rahman IA, Sutton MD. 2010. From clergymen to computers – the advent of virtual palaeontology. Geol Today. 26(3):96–100.

Götz S. 2003. Larval settlement and ontogenetic development of Hippuritella vasseuri (DOUVILLÉ) (Hippuritoidea, Bivalvia). Geol Croat. 56(2):123–131.

Götz S. 2007. Inside rudist ecosystems: growth, reproduction and population dynamics. In: Scott RW, editor. Cretaceous rudists and carbonate platforms: environmental feedback. SEPM Special Publication Vol. 87. Tulsa (OK): Society for Sedimentary Geology. p. 97–113.

Götz S, Stinnesbeck W. 2003. Reproductive cycles, larval mortality and population dynamics of a Late Cretaceous hippuritid association: a new approach to the biology of rudists based on quantitative three-dimensional analysis. Terra Nova. 15(6):392–397.

Hanlon RT, Forsythe JW. 2008. Sexual cannibalism by *Octopus cyanea* on a Pacific coral reef. Mar Freshwater Behav Physiol. 41:19–28.

Haubitz B, Prokop M, Dohring W, Ostrom JH, Wellnhofer P. 1988. Computed tomography of Archaeopteryx. Paleobiology. 14 (2):206–213.

Heptonstall WB. 1970. Buoyancy control in ammonoids. Lethaia. 3:317–328.

Hoffmann R, Zachow S. 2011. Non-invasive approach to shed new light on the buoyancy business of chambered cephalopods (Mollusca). Paper presented at: IAMG; September 5–9; Salzburg, Austria.

Hounsfield GN. 1973. Computerized transverse axial scanning tomography. Br J Radiol. 46(552):1016–1022.

Hyatt A. 1874. Abstract of a memoir on the biological relations of the Jurassic ammonites. Proc Boston Soc Nat History. 17:236–241.

Kak AC, Slaney M. 2001. Principles of computerized tomographic imaging. Philadelphia (PA)/New York: Society for Industrial and Applied Mathematics/IEEE Press.

Kermack DM. 1970. True serial-sectioning of fossil material. Biol J Linn Soc. 2:47–53.

Keupp H, Riedel F. 2010. Remarks on the possible function of the apophyses of the Middle Jurassic microconch ammonite *Ebrayiceras sulcatum* (Zieten 1830), with a discussion on the palaeobiology of Aptychophora in general. Neues Jahrb Geol Paläontol Abh. 255(3):301–314.

Kielan-Jaworowska Z, Presley R, Poplin C. 1986. The cranial vascular system in taeniolabidoid multituberculate mammals. Philos Trans Roy Soc B. 313:525–602.

Klompmaker AA, Waljaard NA, Fraaije RHB. 2009. Ventral bite marks in Mesozoic ammonoids. Palaeogeogr Palaeoclimatol Palaeoecol. 280:245–257.

Klug C. 2001. Life-cycles of Emsian and Eifelian ammonoids (Devonian). Lethaia. 34:215–233.

Klug C. 2004. Mature modifications, the black band, the black aperture, the black stripe, and the periostracum in cephalopods from the Upper Muschelkalk (Middle Triassic, Germany). Mitteilungen aus dem Geol-Paläontol Inst Univ Hamburg. 88:63–78.

Klug C, Korn D. 2004. On the origin of ammonoid locomotion. Acta Palaeontol Pol. 49:235–242.

Korn D, Klug C. 2003. Morphological pathways in the evolution of Early and Middle Devonian ammonoids. Paleobiology. 29:329–348.

Kröger B. 2002. On the efficiency of the buoyancy apparatus in ammonoids: evidences from sublethal shell injuries. Lethaia. 35:61–70.

Kruta I, Landman N, Rouget I, Cecca F, Tafforeau P. 2011. The role of ammonites in the Mesozoic marine food web revealed by Jaw Preservation. Science. 331(6013):70–72.

Landman NH, Cobban WA, Larson NL. 2012. Mode of life and habitat of scaphitid ammonites. Geobios. 45:87–98.
Landman NH, Waage KM. 1986. Shell abnormalities in scaphitid ammonites. Lethaia. 19(3):211–224.
Lehmann U. 1972. Aptychen als Kieferelemente der Ammoniten. Paläont Z. 46(1–2):34–48.
Lehmann U. 1981. The Ammonites: their life and their world. New York: Cambridge University Press.
Lukeneder A, Harzhauser M, Müllegger S, Piller WE. 2010. Ontogeny and habitat change in Mesozoic cephalopods revealed by stable isotopes (δ18O, δ13C). Earth Planet Sci Lett. 296:103–114.
Lukeneder S, Lukeneder A. 2011. Methods in 3D modelling of Triassic ammonites from Turkey (Taurus, FWF P22109-B17). Paper presented at: IAMG. September 5–9; Salzburg, Austria.
Makowski H. 1962. Problem of sexual dimorphism in ammonites. Palaeontol Pol. 12:1–92.
Mallison H. 2011. Digitizing methods for paleontology: applications, benefits and limitations. In: Elewa AMT, editor. Computational paleontology. Berlin: Springer. p. 7–43.
Mangold-Wirz K. 1963. Biologie des céphalopodes benthiques et nectoniques de la mer Catalane. Vie Milieu. 13(Suppl.):1–285.
Monks N, Young JR. 1998. Body position and the functional morphology of Cretaceous heteromorph ammonites. Palaeontogr Electron. 1(1):1A.
Moriya K, Nishi H, Kawahata H, Tanabe K, Takayanagi Y. 2003. Demersal habitat of Late Cretaceous ammonoids: evidence from oxygen isotopes for the Campanian (Late Cretaceous) northwestern Pacific thermal structure. Geology. 31:167–170.
Muir-Wood HM. 1934. On the internal structure of some Mesozoic Brachiopoda. Philos Trans Roy Soc B. 505:511–567.
Mutvei H, Reyment R. 1973. Buoyancy control and siphuncle function in ammonites. Palaeontology. 6:623–636.
Mutvei H, Dunca E, Weitschat W. 2010. Siphuncular structure in the Recent *Nautilus*, compared with that in Mesozoic nautilids and ammonoids from Madagascar. GFF. 132:161–166.
Okamoto T. 1996. Theoretical modeling of ammonoid morphology. In: Landman NH, Tanabe K, Davis RA, editors. Ammonoid paleobiology. New York: Plenum. p. 225–251.
Okutani T. 1990. Squids, cuttlefish and octopuses. Marine Freshwater Behav Physiol. 18(1):1–17.
Parent H, Westermann G, Chamberlain Jr A. in press. Ammonite aptychi: Functions and role in propulsion. Geobios. http://www.sciencedirect.com/science/article/pii/S0016699514000023
Pascual-Cebrian E, Hennhöfer DK, Götz S. 2013. 3D morphometry of polyconitid rudist bivalves based on grinding tomography. Facies. 59:347–358. doi:10.1007/s10347-012-0310-8
Raup DM. 1967. Geometric analysis of shell coiling: coiling in ammonoids. J Paleontol. 41(1):43–65.
Raup DM, Chamberlain JA. 1967. Equations for volume and center of gravity in ammonoid shells. J Paleontol. 41(3):566–574.
Reyment RA. 1958. Some factors in the distribution of fossil cephalopods. Stockholm Contrib Geol. 1:97–184.
Reyment RA. 1973. Factors in the distribution of fossil cephalopods. Part 3: Experiments with exact models of certain shell types. Bull Geol Inst Univ Upsala New Ser. 4(2):7–41.
Saunders WB, Shapiro EA. 1986. Calculation and simulation of ammonoid hydrostatics. Paleobiology. 12(1):64–79.
Seilacher A. 1974. Fabricational noise in adaptive morphology. Syst Biol. 22(4):451–465.
Seilacher A. 1999. Oecoptychius-Rätsel. Fossilien. 3:131.
Seilacher A, Gunji YP. 1993. Morphogenetic countdown: another view on heteromorph shells in gastropods and ammonites. Neues Jahrb Geol Paläontol. 190:237–265.
Sollas WJ. 1904. A method for the investigation of fossils by serial section. Philos Trans Roy Soc Lond. 196:259–265.
Sollas IBJ, Sollas WJ. 1913. A study of the skull of a *Dicynodon* by means of serial sections. Philos Trans Roy Soc B. 204:201–225.
Sutton MD, Briggs DEG, Siveter DJ, Siveter DJ. 2001. Methodologies for the visualization and reconstruction of three-dimensional fossils from the Silurian Herefordshire Lagerstätte. Paleontol Electron. 4(1):17.
Tanabe K, Fukuda Y, Obata I. 1982. Formation and function of the siphuncle-septal neck structures in two Mesozoic ammonites. Trans Proc Palaeontol Soc Jpn New Ser. 128:433–443.
Trauth F. 1937. Die Praestriaptychi und Granulaptychi des Oberjura und der Unterkreide. Paläont Z. 19(1–2):134–162.
Trueman AE. 1940. The ammonite body chamber, with special reference to the buoyancy and mode of life of the living ammonite. Quart J Geol Soc. 96:339–383.
Ward PD. 1979. Cameral Liquid in *Nautilus* and Ammonites. Paleobiology. 5(1):40–49.
Ward PD. 1987. The natural history of nautilus. Boston: Allen and Unwin.
Westermann GEG. 1954. Monographie der Otoitidae (Ammonoidea), *Otoites*, *Trilobiticeras*, *Itinsaites*, *Epalxites*, *Germanites*, *Masckeites*, *Normannites*. Geol Jahrb Beihefte. 15:1–364.
Westermann GEG. 1969. Supplement: sexual dimorphism, migration, and segregation in living cephalopods. In: Westermann GEG, editor. Sexual dimorphism in fossil metazoa and taxonomic implications. Stuttgart: International Union of Feological Sciences Series A No. 1. p. 18–20.
Westermann GEG. 1996. Ammonoid life and habitat. In: Landman NH, Tanabe K, Davis RA, editors. Ammonoid paleobiology. New York: Plenum. p. 607–707.
Zatoń M. 2008. Taxonomy and palaeobiology of the Bathonian (Middle Jurassic) tulitid ammonite *Morrisiceras*. Geobios. 41:699–717.
Zatoń M. 2010. Bajocian-Bathonian (Middle Jurassic) ammonites from the Polish Jura. Part 2: Families Stephanoceratidae, Perisphinctidae, Parkinsoniidae, Morphoceratidae and Tulitidae. Palaeontographica A. 292(4–6):115–213.

APPENDIX I-D

Diversity and palaeoecology of Early Devonian invertebrate associations in the Tafilalt (Anti-Atlas, Morocco)

Published in *Bulletin of Geoscience, 89(1)* (2014)

Diversity and palaeoecology of Early Devonian invertebrate associations in the Tafilalt (Anti-Atlas, Morocco)

LINDA FREY, CAROLE NAGLIK, RICHARD HOFMANN, MENA SCHEMM-GREGORY, JIŘÍ FRÝDA, BJÖRN KRÖGER, PAUL D. TAYLOR, MARK A. WILSON & CHRISTIAN KLUG

Quantitative analyses of the taxonomic composition and palaeoecology of five Early Devonian faunules (earliest Lochkovian to early Emsian) collected from the locality Jebel Ouaoufilal in the Tafilalt (Morocco) were conducted. We examined 3376 specimens belonging to 158 species and their stratigraphic distribution. The quantitative data sets were analysed for alpha diversity and ecospace utilization. Macrofossils of every faunule were identified, counted and grouped according to ecological categories of tiering, motility and feeding behaviour. Based on these data, we noted (i) a strong increase in species richness, especially in benthic species, from the lowermost Lochkovian to the Pragian stage and a following subtle decrease in the early Emsian and (ii) a considerable expansion of ecospace use from the earliest Lochkovian to the early Emsian. These general trends are considered to be a result of favourable living conditions due to a growing oxygen content at the sea floor, which correlates with a regional and potentially a global regression from the Lochkovian to the Pragian. A transgression in the early Zlíchovian probably reduced the species richness by decreasing the oxygenation of bottom waters. Additionally, we described and figured three new genera and six new species of the diverse Pragian faunule (86 species): the hederelloid *Filihernodia buccina* gen. et sp. nov., the crinoid *Hexawacrinus claudiakurtae* gen. et sp. nov., the gastropods *Oriomphalus multiornatus* sp. nov., *Eohormotomina restisevoluta* gen. et sp. nov., and the cephalopods *Tenuitheoceras secretum* gen. et sp. nov. and *Arionoceras kennethdebaetsi* sp. nov. We record the first occurrence of *Tiaracrinus moravicus* from Africa. • Key words: Early Devonian, alpha diversity, palaeoecology, Cephalopoda, Gastropoda, Anti-Atlas, Morocco.

FREY, L., NAGLIK, C., HOFMANN, R., SCHEMM-GREGORY, M., FRÝDA, J., KRÖGER, B., TAYLOR, P.D., WILSON, M.A. & KLUG, C. 2014. Diversity and palaeoecology of Early Devonian invertebrate associations in the Tafilalt (Anti-Atlas, Morocco). *Bulletin of Geoscience 89(1)*, 75–112 (12 figures, appendix). Czech Geological Survey, Prague. ISSN 1214-1119. Manuscript received June 13, 2013; accepted in revised form October 29, 2013; published online December 12, 2013; issued January 21, 2014.

Linda Frey, Carole Naglik, Richard Hofmann & Christian Klug, Palaeontological Institute and Museum, University of Zurich, Karl Schmid-Strasse 4, CH-8006 Zurich, Switzerland; linda.frey@uzh.ch; carole.naglik@pim.uzh.ch; richard.hofmann@pim.uzh.ch; chklug@pim.uzh.ch • Mena Schemm-Gregory, in memoriam • Jiří Frýda, Faculty of Environmental Science, Czech University of Life Sciences, Kamýcká 129, 165 21 Praha 6 – Suchdol, Czech Republic; bellerophon@seznam.cz • Björn Kröger, Freie Universität Berlin, Geologische Wissenschaften, Fachrichtung Paläontologie, Malteserstrasse 74-100, D-12249 Berlin, Germany; bjoekroe@gmx.de • Paul D. Taylor, Department of Earth Sciences, Natural History Museum, Cromwell Road, SW7 5BD London, United Kingdom; p.taylor@nhm.ac.uk • Mark A. Wilson, Department of Geology, College of Wooster, Wooster, OH 44691-2363; mwilson@wooster.edu

The eastern Anti-Atlas in Morocco is famous for its highly fossiliferous Palaeozoic rocks. Many palaeontological and stratigraphical studies on the Devonian of the Tafilalt and the Maïder have been carried out during the twentieth and twenty-first century (Clariond 1934a, b; Roch 1934; Termier & Termier 1950; Massa *et al.* 1965; Hollard 1967, 1974, 1981; Alberti 1980, 1981; Becker & House 1994, 2000; Bultynck & Walliser 2000a, b; Klug 2001, 2002; Klug *et al.* 2008a, b; De Baets *et al.* 2010; Franchi *et al.* 2012). Well-exposed sedimentary successions of the Early Devonian age crop out in the Tafilalt, *e.g.* between the Jebel Ouaoufilal and the mine of Filon 12 (Fig. 1). These more or less complete exposures, the local abundance of fossils and their sometimes excellent preservation yield the possibility to study Early Devonian faunal associations in their stratigraphic context in the Tafilalt.

In this study, we describe and figure well-preserved macrofossils of five Early Devonian faunules (earliest Lochkovian to early Emsian, according to Bultynck & Walliser 2000b), which comprise a highly diverse Pragian

DOI 10.3140/bull.geosci.1459

Bulletin of Geosciences • Vol. 89, 1, 2014

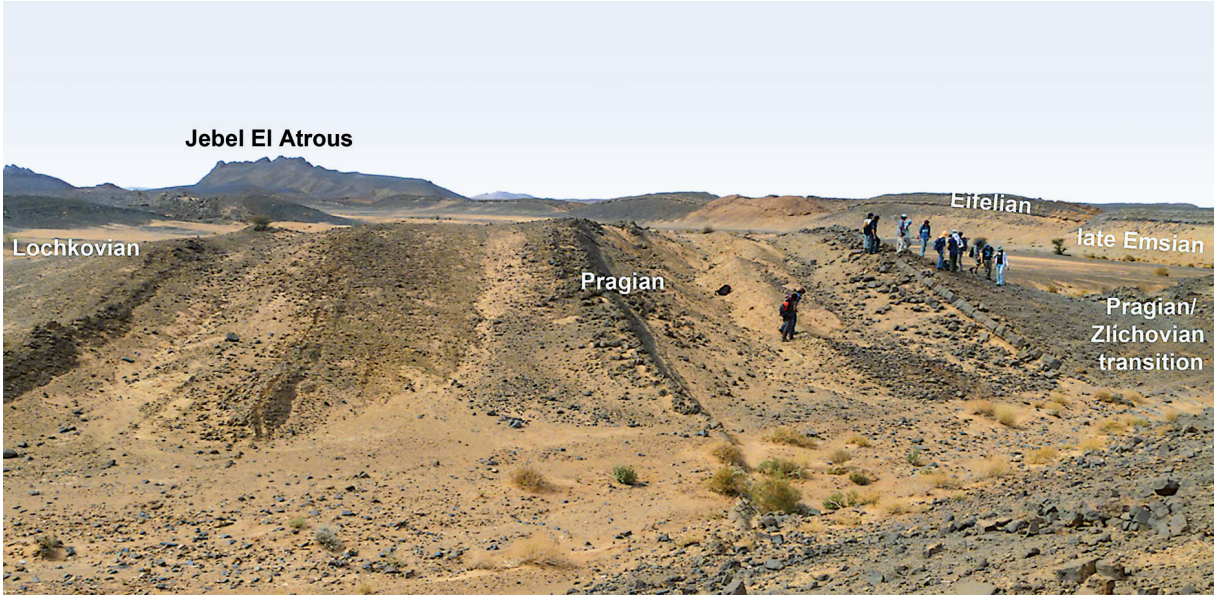

Figure 1. Field photograph of the outcrop near Jebel Ouaoufilal and Filon 12. Image courtesy of Richard Hofmann (Zurich).

fauna of the Jebel Ouaoufilal (Filon 12). We found species of cephalopods, gastropods, anthozoans, brachiopods, trilobites, bivalves, crinoids, hederelloids, rostroconchs, hyolithids and machaerids, the larger representatives of which are sometimes covered by epizoans. Our main focus is on these Early Devonian faunules, which we examined for alpha diversity and palaeoecology. Fluctuations in species richness and palaeoecology during the Early Devonian of Morocco have been noted before by several authors (*e.g.*, Massa *et al.* 1965, Hollard 1974, Belka *et al.* 1999, Klug *et al.* 2008a, Kröger 2008). Belka *et al.* (1999) and Kröger (2008) recognized an increase in diversity, especially in benthic species, over time during the Early Devonian of the Tafilalt and correlated it to a change in oxygen content at the sea floor. This hypothesis was, however, not yet tested by collecting and analysing quantitative data. Kröger (2008) examined species richness and composition of the cephalopod associations at the Filon 12-section, but statistical analyses on the species diversity of all groups of macroscopic invertebrates over the whole Early Devonian interval have not been executed before. A palaeoecological study of the Tafilalt including two Emsian faunules was published by Klug *et al.* (2008a). They observed an ecological change in the early Emsian (Zlíchovian, *sensu* Bultynck & Walliser 2000b) based on two species rich faunules that differ in species composition.

To investigate the changes in species richness and the local palaeoecology from the earliest Lochkovian to the early Emsian in the Tafilalt quantitatively, we analysed the faunules based on alpha diversity and ecospace use. The term alpha diversity was introduced by Whittaker (1960, 1972), who described the species richness within a single habitat or community. The three-dimensional display of ecospace utilisation, developed by Bush *et al.* (2007), consists of multiple ecological parameters, to which each species can be assigned. These parameters are vertical tiering, motility level and feeding mechanism. We employed the same ecological parameters in our analysis. Additionally, the analysis of ecospace utilisation of the Moroccan Early Devonian faunules may reveal local macroecological changes, which were linked with the "Devonian nekton revolution" (Klug *et al.* 2010). The "Devonian nekton revolution" refers to a radiation of marine nektonic animals due to the rapid occupation of the water column in the Devonian and the synchronous decrease in planktonic and demersal taxa.

The aims of our study are (1) to describe and illustrate the well preserved macrofossil material of five successive Early Devonian faunules from the Tafilalt, (2) to describe new taxa of the highly diverse Pragian faunule, (3) to quantitatively analyse changes in alpha diversity and ecospace use through the Early Devonian of the southern Tafilalt, and (4) to discuss possible environmental and evolutionary factors, which might have initiated, controlled or influenced these changes in diversity and ecology.

Material and methods

All the fossil specimens listed, figured and described in this work come from the locality Jebel Ouaoufilal in the Tafilalt

of Morocco (*e.g*. Klug *et al.* 2000, 2013). This locality is sometimes also called Filon 12 (*e.g*., Kröger 2008) after the local mine, which is world-renowned for its excellent vanadinite crystals and associated minerals.

The associations described here are earliest Lochkovian to early Emsian age ("*Scyphocrinites*"/*Camarocrinus* level to *Erbenoceras*/*Anetoceras* level; see Bultynck & Walliser 2000b, Corriga *et al.* 2013). They were collected from the extensive outcrops of Devonian strata between the southwestern flank of Jebel Ouaoufilal, which is composed of Early Carboniferous siliciclastics, and the mentioned mine Filon 12. This area is located 7 km W of Taouz and 40 km S of the town of Rissani. The Early Devonian section can be found approximately at the coordinates N 30°56´ 57˝, W 04°02´ 39˝.

The samples of early to late Lochkovian age were taken bed by bed, whereas the samples of the lowermost Lochkovian, the Pragian and the early Emsian (early Zlíchovian) strata were collected from clayey to marly intervals. These intervals lie between limestone beds that form shallow ridges (as visible in Fig. 1) and so, the transport of material was limited to a few meters. Therefore, the according data do probably contain a slight bias from time-averaging and the sampling method. Some of the fossils, such as the large loboliths of the crinoid *Camarocrinus*, were identified and counted in the field in order to keep the weight of samples reasonably low. The remaining, mostly small, specimens of the faunules were quantitatively sampled and studied in the lab for species identification and subsequent specimen counts (abundance). We defined whole fossils or fossil fragments as single individuals except fin spines of the acanthodian genus *Machaeracanthus*. *Machaeracanthus* possessed four fin spines (Südkamp & Burrow 2007), and in order to account for the possibility that some of the fragments might have been parts of one spine or of several spines of one individual, we divided the total number of spines by two (although this number is admittedly arbitrary). Similarly, we did not include crinoid columnals in the study, because it was impossible to estimate the number of crinoid individuals since the crinoids were never entirely articulated. In the case of the genus *Camarocrinus*, we counted the loboliths, because only one of these buoyancy devices was present in each individual (Haude 1992).

The species counts were plotted as histograms per faunule and per ecological guild per faunule. Abundance and diversity data were rarefied for each faunule with the software package PAST (Hammer *et al*. 2001), in order to reduce the sampling bias and to compare more objectively the species richness of the faunules, which are of different sample sizes (Sanders 1968).

After these investigations, we grouped all taxa according to ecological categories compiled by Bush *et al.* (2007), who classified marine animals with respect to vertical tiering, motility level and feeding mechanism. Vertical tiering is defined by the vertical distribution of animals in or on the sediment as well as in the water column and includes the categories pelagic, erect, surficial, semi-infaunal, shallow infaunal und deep infaunal (Ausich & Bottjer 1982, Bottjer & Ausich 1986, Bush *et al*. 2007).

To the pelagic group, we assigned animals that lived in the water column. This includes the nekton such as fishes and certain cephalopods and the plankton such as the specialized genus *Camarocrinus*, which probably drifted at the water surface with its lobolith functioning as a buoy (Haude 1992). All other crinoid species were stalked and thus were interpreted as erect benthonic animals, which were attached to the seafloor or to objects on the seafloor with their body parts reaching more or less far into the water column. Less highly erected benthonic organisms such as brachiopods, bryozoans, corals, gastropods, hyoliths, hederelloids, phyllocarids, trilobites, and some bivalve species, we allocated to the category surficial. Rostroconchs, pyrgocystid edrioasteroids and some bivalves belonged to semi-infaunal animals (Kříž 2000, Klug *et al*. 2008a). Machaerids, the bivalve *Panenka* and palaeotaxodont bivalves are assigned to the shallow infaunal benthos, whereas only one deep infaunal bivalve species was found (Kříž 2000, Klug *et al*. 2008a).

Motility level refers to the locomotory capabilities of organisms and is subdivided in six categories: freely, fast or slow motile animals, attached or unattached facultatively motile animals and attached or unattached non-motile animals (Bush *et al*. 2007). Freely, fast motile organisms are represented by fishes and some arthropods because of their active locomotion by fins or legs in the water column or on the sea floor. Cephalopods including Actinocerida, Pseudorthocerida, Oncocerida, and Orthocerida were either slow swimming or vertically migrating animals that lived in the water column; they were rather slow swimming compared to many modern decabrachian coleoid cephalopods (*e.g*., Westermann 1999, Westermann & Tsujita 1999). Therefore, we assigned cephalopods together with gastropods and machaerids to the freely moving, slow motile category. According to Kříž (2000), most bivalves included in the study are considered as unattached, facultatively motile animals or, in the case of epibyssate bivalves, to attached, facultatively motile organisms. Corals, crinoids, bryozoans, hederelloids, edrioasteroids and brachiopods belonged to the non-motile/ attached animals (Racheboeuf 1990, Williams *et al*. 2000). The unattached non-motile category includes rostroconchs, hyoliths and a species of brachiopods (?*Dagnachonetes* sp.) (Williams *et al.* 2000).

"Feeding mechanism" categorises the behaviour of organisms to acquire food and is grouped in six subdivisions: suspension feeding, surface deposit feeding, mining, grazing, predatory and other (Bush *et al*. 2007). We consider

Bulletin of Geosciences • Vol. 89, 1, 2014

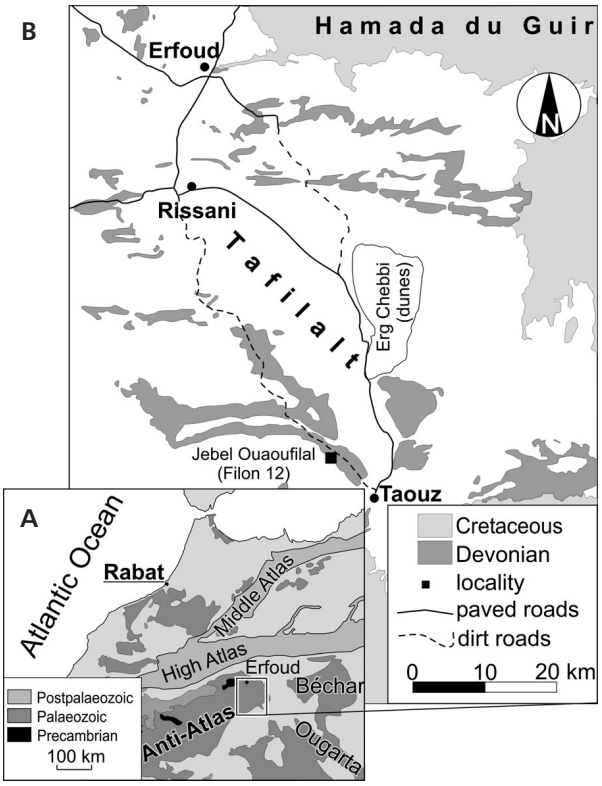

Figure 2. Geological map of Morocco. • A – distribution of Palaeozoic rocks in the Anti-Atlas. • B – map of Devonian outcrops in the Tafilalt.

tabulate corals, brachiopods, rostroconchs, bryozoans, hederelloids, crinoids, edrioasteroids, hyoliths, phyllocarids and epibyssate bivalves as suspension feeders that fed on small planktonic organisms from the water column. The majority of the bivalve species found in our Early Devonian faunules fed on buried nutrition and, therefore, mining was the common feeding mechanism. The predatory category includes fishes, rugose corals, nautiloids and trilobites that were able to catch prey capable of escaping and resisting. The trilobites of the faunules include members of the Orders Phacopida and Corynexochida that were supposedly microphagous predators because of the shape of their cephalon, the way of the attachment of hypostomes and the well-developed sensory fields (Eldredge 1971, Miller 1976, Whittington 1988, Fortey & Owens 1999). We assigned the cephalopod species to microphagous predators as well based on the actualistic knowledge about the diet of modern *Nautilus* species. However, no undisputable cephalopod beaks older than Late Devonian are known. In the crop and stomach contents of recent Nautilida, fragments of small crustaceans and molts of larger crustaceans were found, which were detected by their chemosensory tentacles (Saunders & Ward 1987). Bush *et al*. (2007) grouped all remaining feeding behaviours together as "others". We added the new category "coprophagy". Two coprophagous species in the study belong to a single gastropod Family, the Platyceratidae (Peel 1984; Gahn & Baumiller 2003, 2006; Webster & Donovan 2012; Donovan & Webster 2013).

The classification of taxa according to vertical tiering, motility and feeding mechanism led to different combinations of ecological categories, which represent different modes of life (Bush *et al*. 2007). We evaluated how many species and individuals per mode of life were present in each faunule and how their relative abundances changed through time. Additionally, the trophic nucleus concept was used to reveal which species and modes of life dominate the faunules. The trophic nucleus is defined by those species that contribute to 80% of all individuals of a fauna (Neyman 1967).

The morphometric parameters for the description of cephalopod conchs were adopted from Teichert *et al.* (1964) and Kröger (2008). For the description of crinoids, we used terms and parameters adopted from Ubaghs (1978) and Jell & Jell (1999). The descriptive terms and measurements for the description of gastropods were derived from Cox (1960). Morphometric parameters of hederelloids were adopted from Bassler (1953) and Taylor & Wilson (2008).

All the material used for this study is housed in the Paläontologisches Institut und Museum der Universität Zürich (PIMUZ 30587–30662). A second sample of the newly introduced hederelloid genus *Filihernodia* was deposited in the Department of Earth Science of the National History Museum in London (NHMUK PI BZ 7494).

Geological background

The Moroccan Anti-Atlas is a broad NE-SW oriented Variscan anticlinorium, which makes up a part of the northern margin of the Sahara Craton (Piqué & Michard 1989). Palaeozoic sedimentary rocks can be found along a NE-SW trending axis in the Anti-Atlas and include Devonian outcrops that cover an area of about 20.000 km^2 (Kaufmann 1998; see Fig. 2A). Devonian rocks are exposed along E-W trending synclines in the Tafilalt but parts of these rocks are interrupted by reverse faults with strike-slip components (Toto *et al.* 2008). Especially, the Silurian and Early Devonian claystone successions were deformed and/ or cut by faults, which led to incomplete exposures of the Early Devonian rock succession in the Tafilalt, especially in parts of the southern flanks of the synclines. Some exceptions are probably the southeastern limb of the so-called Amessoui-syncline between the abandoned village El Atrous, the mine of Filon 12, Taouz, and the Jebel Ouaoufilal (Klug *et al.* 2013, see Fig. 2B).

In the Early Devonian, the Anti-Atlas was situated between 40° to 60° south (Scotese 1997). Moderately cool

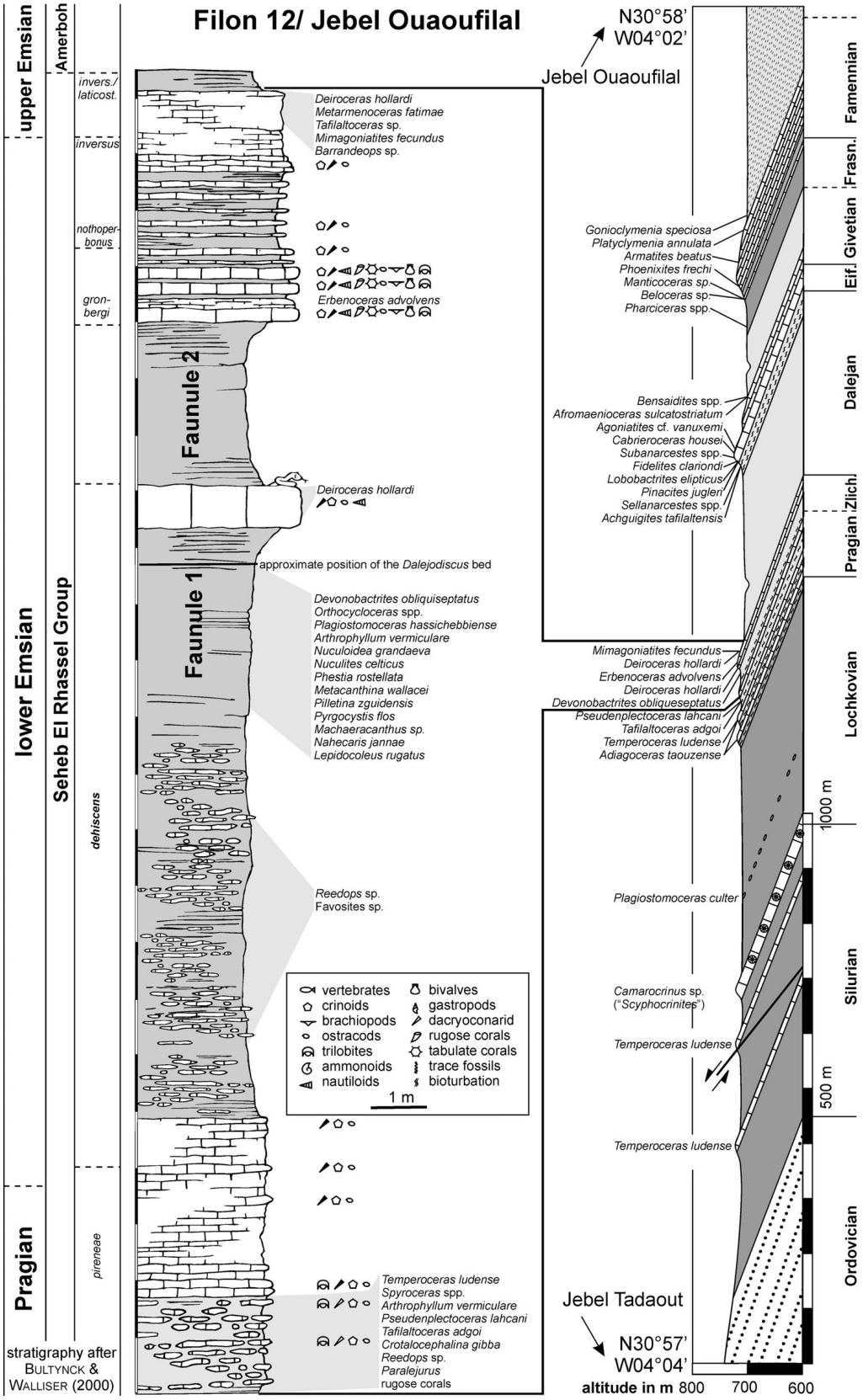

Figure 3. Devonian section at Jebel Ouaoufilal (Filon 12). Modified after Klug *et al.* (2013). The section on the right has the same scale in horizontal and vertical direction (1:10,000).

Bulletin of Geosciences • Vol. 89, 1, 2014

water temperatures on the shelves of western and northern Gondwana have been confirmed by oxygen isotope analyses by van Geldern *et al*. (2006, see also Lubeseder *et al*. 2009). Early Devonian deposits display a rather uniform, mostly clayey to marly facies as well as moderate thickness changes in the eastern Anti-Atlas (Belka *et al*. 1997, Kaufmann 1998).

In the late Silurian and early Lochkovian (Early Devonian) successions, claystones are prevalent (Hollard 1981). These often dark coloured claystones (which are light greyish to pinkish when weathered) contain intercalated marlstone and limestone successions, which were formed by concentrated accumulations of planktonic crinoids (*e.g*. the scyphocrinoid limestone in which scyphocrinoid ossicles occur in rock-forming numbers), few orthoconic cephalopod shells (although some thin limestone interbeds are almost entirely composed of cephalopod shells) and occasionally bivalves as well as platyceratid gastropods (Haude 1992, Brachert *et al*. 1992, Kříž 2000, Lubeseder *et al*. 2009, Corriga *et al*. 2013). The limestones were deposited under low oxygen conditions below the storm wavebase and are characterized by massive beds with a maximum thickness of approximately 1 m near Filon 12 (Kříž 1998, Kröger 2008, see Fig. 3).

In the early Lochkovian, approx. 40 m above the *Scyphocrinites* Beds, marls with nodules dominated by the orthoconic cephalopod *Plagiostomoceras culter* are following near Filon 12 (Kröger 2008, Klug *et al.* 2013). In the late Lochkovian succession of dark claystones, some layers of dark grey to almost black more or less nodular limestones occur, which contain cephalopods, nowakiids, bivalves and a moderately low diversity in benthic species. Despite the presences of some benthic species, the facies of these limestones in combination with the predominance of freely motile cephalopods points at low oxygen conditions in and on the sediment (Klug *et al.* 2013).

In the Pragian and Emsian, the carbonate content of the sediments is clearly higher than in the Lochkovian deposits, which is reflected by the dominance of marls and nodular limestones (Hollard 1981, Lubeseder *et al.* 2009). These limestones are much lighter in colour suggesting a lower content in organic material which points at more oxygenated conditions at the sea floor (Klug *et al.* 2013). In the Filon 12 section, Pragian strata contain four limestone layers, which are alternating with nodular marly limestones with macrofossils (Kröger 2008). Especially in the claystone succession above the limestone "K3" of Kröger (2008), several nodular limestone layers occur, which are very rich in macrofossils such as trilobites, cephalopods, echinoderms, gastropods, tabulate and rugose corals (Klug *et al.* 2008a, Kröger 2008). The last limestone bed is overlain by light greyish marls, which are overlain by greenish claystones with limonitised faunas as well as limonite pseudomorphoses after pyrite. The localisation of the boundary between the Pragian and the Emsian is highly controversial and here, we were following the stratigraphy introduced by Bultynck & Walliser (2000a, b) for the Tafilalt. Accordingly, the Pragian-Emsian boundary is probably located near the base of the greenish claystones in the Tafilalt (Walliser 1984, 1985; Bultynck & Walliser 2000b; Klug *et al*. 2008a; Klug *et al.* 2013; Kröger 2008).

In the greenish claystones, a highly fossiliferous fauna of the early Emsian, "faunule 1" *sensu* Klug *et al*. (2008a) and De Baets *et al*. (2010), occurs. These claystones are followed by the "*Deiroceras* limestone" with abundant large *Deiroceras hollardi* and are overlain by claystones of "faunule 2" described by Klug *et al.* (2008a) in the northern Tafilalt (see also Kröger 2008). The subsequent *Erbenoceras* Limestone consists of fossiliferous wackestones containing dacryoconarids in great abundance as well as subordinate crinoid ossicles, corals, trilobites, ostracods, bivalves, brachiopods, and the early ammonoids *Erbenoceras advolvens* as well as *Anetoceras* sp. (Klug 2001, De Baets *et al.* 2013).

The *Erbenoceras* limestones are overlain by an over 100 m thick claystone sequence. These claystones were deposited during and after the initial Daleje transgression (see, *e.g*., Kröger 2008, Lubeseder *et al.* 2009, Klug *et al.* 2013). During the late Emsian, the carbonate content increased more or less steadily and stayed high during much of the Middle and parts of the Late Devonian succession in the Amessoui Syncline (Döring 2002, Fröhlich 2004). In the late Middle Devonian, a platform and basin topography began to form, driven by early Variscan tectonic movements and differential subsidence (Wendt *et al.* 1984; Wendt 1985, 1988). Four depositional areas developed in the Anti-Atlas: the Maïder Platform, the Maïder Basin, the Tafilalt Platform and the Tafilalt Basin (Wendt 1988, Belka *et al*. 1997, Klug & Korn 2002).

Faunules of the earliest Lochkovian to early Emsian

Faunule 1 (Fig. 4A/ Table 1 in Appendix), earliest Lochkovian

This faunule was found in the basalmost rocks of the section, representing the Silurian-Devonian boundary beds. This is corroborated by the presence of the plate-loboliths ("Platten-Lobolithen") and conodonts (Haude & Walliser 1998, Corriga *et al.* 2013). We found four taxa including species of *Camarocrinus*, orthoconic cephalopods, bivalves and platyceratid gastropods. Ecospace consists of four modes of life (see Fig. 5). The trophic nucleus includes *Camarocrinus* sp. and an orthocerid species, which belong to the unattached pelagic, non-motile suspension feeders and pelagic, slow motile predators.

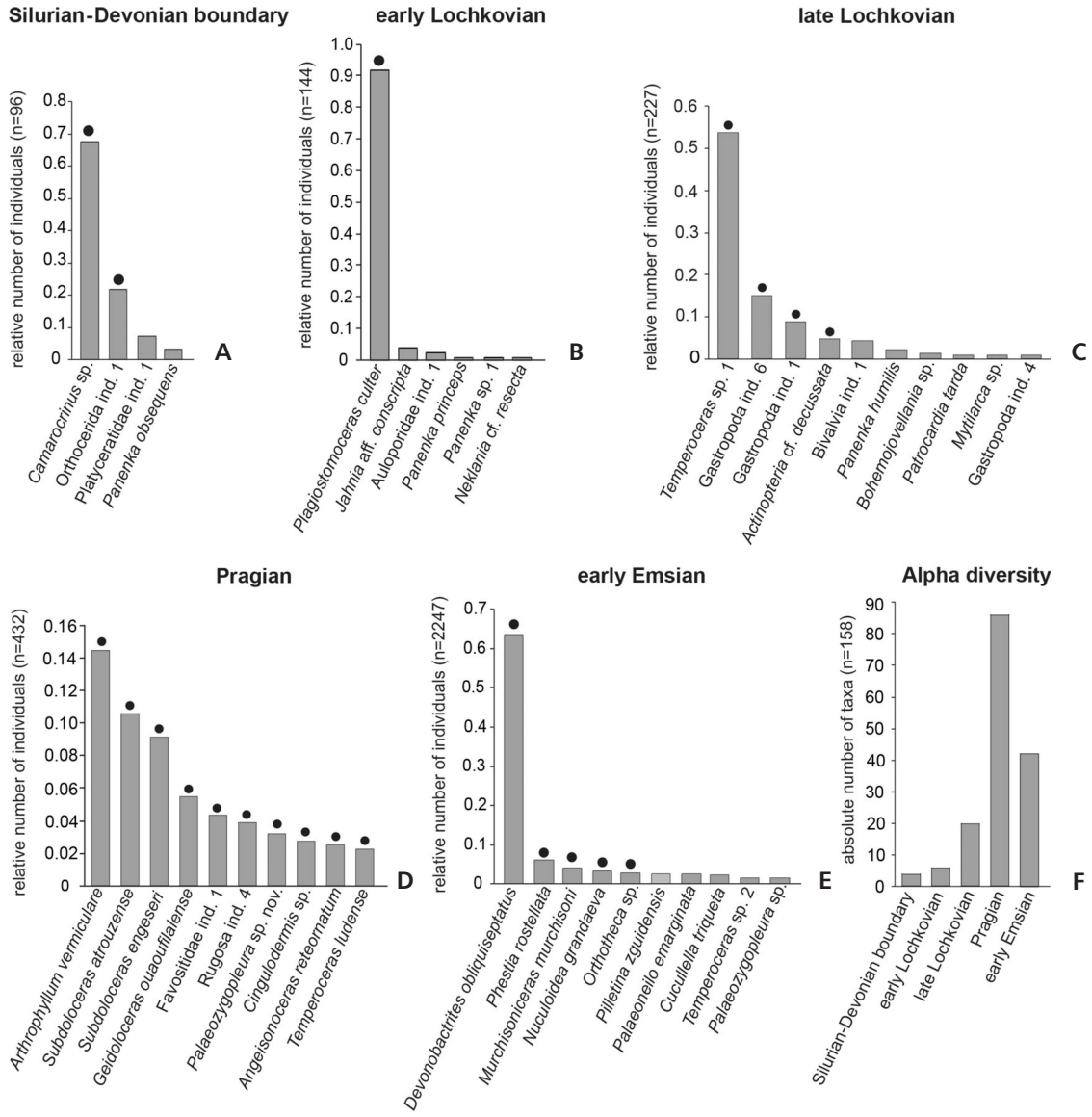

Figure 4. Alpha diversity of the species found in the earliest Lochkovian to early Emsian rocks at the Jebel Ouaoufilal (Filon 12) in the Tafilalt (Morocco); dots above the bars mark the dominant species of the faunules. • A – Silurian-Devonian boundary, all 4 sampled taxa depicted. • B – early Lochkovian, all 6 sampled taxa depicted. • C – late Lochkovian, only 10 taxa out of 20 sampled taxa illustrated. • D – Pragian, only 10 taxa out of 87 sampled taxa illustrated. • E – early Emsian, 10 taxa out of 42 sampled taxa illustrated. • F – overview of the changes in alpha diversity during the Early Devonian of the Taouz area. Additional taxa are listed in the appendix (Table 1).

Faunule 2 (Fig. 4B/ Table 1 in Appendix), early Lochkovian

The second faunule of the section is of early Lochkovian age (Belka *et al.* 1999). Species richness is limited to six taxa that include infaunal bivalves, a species each of cephalopods and of tabulate corals. Ecospace utilization is limited to three modes of life (see Fig. 5). The trophic nucleus contains the orthocerid species *Plagiostomoceras culter,* which is a pelagic, slow motile predator.

Faunule 3 (Fig. 4C/ Table 1 in Appendix), late Lochkovian

This faunule of our Jebel Ouaoufilal section is of late Lochkovian age (Klug *et al.* 2013) and species richness is composed of 20 species, which comprises bivalves, gastropods, orthocerids, rare brachiopods and one bryozoan species. The ecospace utilization includes six modes of life (see Fig. 5). Four species contribute to the trophic nucleus: *Temperoceras* sp. 1, Gastropoda ind. 6, Gastropoda ind. 1 and

Bulletin of Geosciences • Vol. 89, 1, 2014

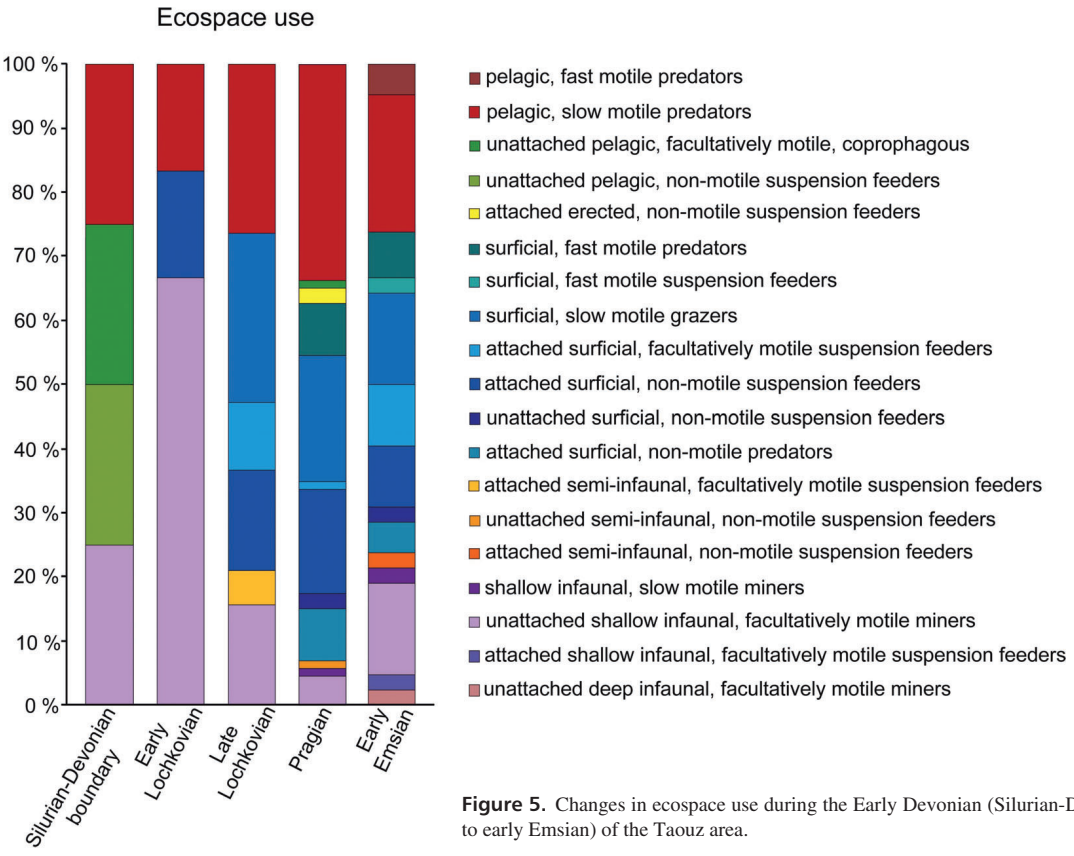

Figure 5. Changes in ecospace use during the Early Devonian (Silurian-Devonian boundary to early Emsian) of the Taouz area.

Actinopteria cf. *decussata*, which had modes of life such as freely pelagic, slow motile predators, freely surficial, slow motile grazers and attached semi-infaunal, facultatively motile suspension feeders.

Faunule 4 (Fig. 4D/ Table 1 in Appendix), Pragian

The faunule was found in the Pragian rocks of the section at the Jebel Ouaufilal (Klug *et al.* 2013). The species richness consists of 86 species and contains many orthocerids, actinocerids, oncocerids, gastropods, brachiopods, bivalves, crinoids, tabulate and rugose corals, arthropods, rostroconchs, hyolithids, machaerids and a new hederelloid genus. 12 modes of life contribute to the ecospace of this faunule (see Fig. 5). The trophic nucleus comprises 27 species and includes nautiloids, tabulate and rugose corals, gastropods, brachiopods, bivalves and trilobites. These species had six different modes of life: freely pelagic, slow motile predators, attached surficial, non-motile suspension feeders, surficial, slow motile grazers, attached surficial, non-motile predators, surficial, fast motile predators, unattached shallow infaunal, facultatively motile miners.

Faunule 5 (Fig. 4E/ Table 1 in Appendix), early Emsian

The faunule belongs to the uppermost sediments of the section and is of early Emsian age ("faunule 1" of Klug *et al.* 2010, 2013). The faunule is composed of 42 species of bivalves, bactritids, orthocerids, actinocerids, oncocerids, gastropods, arthropods, corals, machaerids, fishes, and edrioasteroids. The ecospace consists of 14 modes of life (see Fig. 5). The trophic nucleus contains five species: *Devonobactrites obliquiseptatus, Phestia rostellata, Murchisoniceras murchisoni, Nuculoidea grandaeva, Orthotheca* sp. These species belong to four modes of life such as freely pelagic, slow motile predators, unattached deep-infaunal, facultatively motile miners, unattached shallow-infaunal, facultatively motile miners and unattached surficial, non-motile suspension feeders.

Diversity fluctuations

To investigate changes in alpha diversity and faunal composition during the Early Devonian of the Taouz area, we identified as many of the fossils as possible and counted all taxa of every faunule and compared their abundances. At

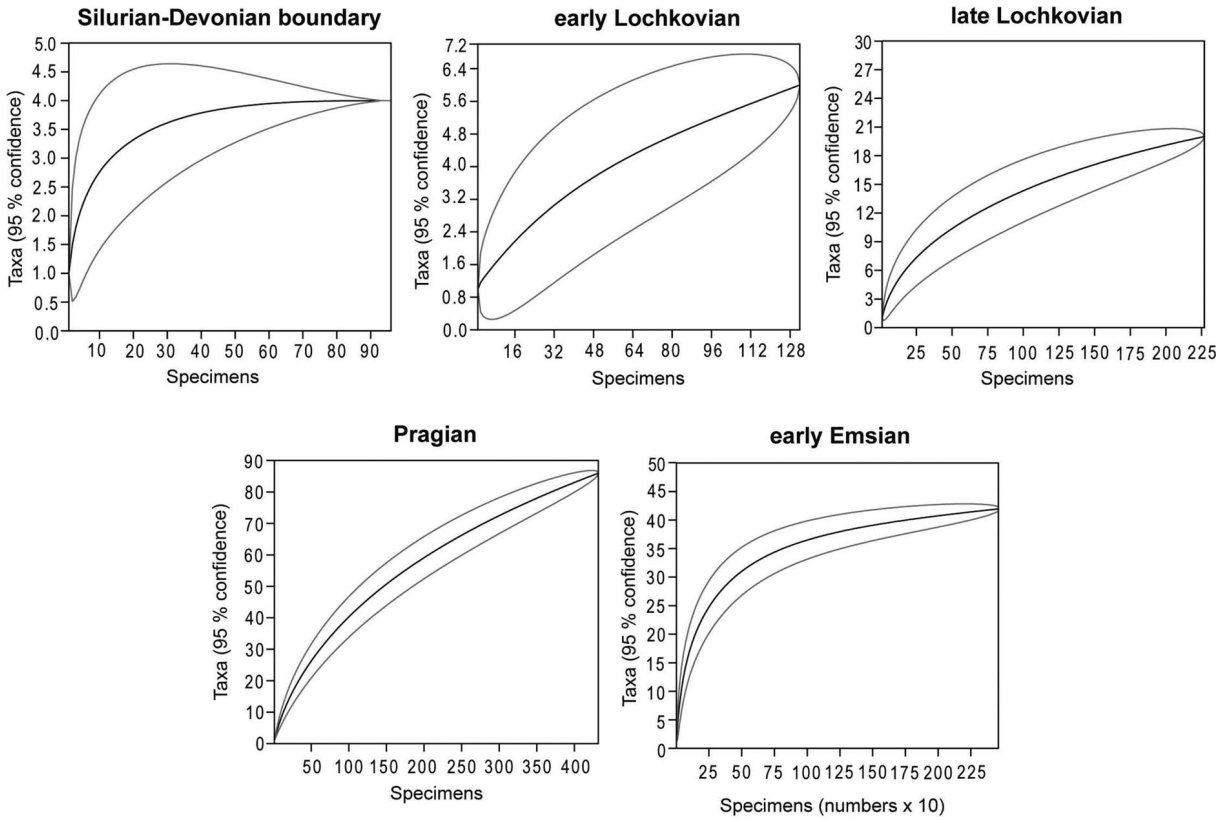

Figure 6. Rarefaction analyses of all Early Devonian faunules (earliest Lochkovian to early Emsian) collected from the Jebel Ouaoufilal (Filon 12).

the Silurian-Devonian boundary, the species richness was low. We found fossils of four species although we have missed some species of orthocerids, which according to Kröger (2008) occur therein. This is due to the fact that some layers are composed of almost only cephalopod shells while others are strongly dominated by *Camarocrinus* remains, *i.e.*, when sampling for cephalopods, the focus is on the cephalopod strata but we focused on the youngest crinoid-layer. Nevertheless, we assume that the diversity would be similarly low in the cephalopod layers and benthos is certainly also rare therein.

The diversity in groups and species increased slowly from the early Lochkovian (6 species) to the late Lochkovian (20 species). During the Pragian, the species diversity reached its Early Devonian maximum (86 species). The early Emsian faunule (42 species) had a lower species diversity than the Pragian faunule.

These findings show that alpha diversity increased significantly from the Silurian-Devonian boundary to the Pragian and decreased somewhat in the early Emsian (Fig. 4F). Rarefaction analyses indicated that in all faunules except in the oldest (earliest Lochkovian) and the youngest faunules (early Emsian) studied here further collecting would increase the number of species in the faunal lists. The Pragian faunule still remains the most diverse among the examined faunules and we probably sampled only a fraction of the actual diversity (Fig. 6). In addition to the species diversity, the taxonomic composition of the examined faunules changed between the faunules and most of the species found in one faunule were not discovered in faunules of a different age. Furthermore, the number of invertebrate taxa of a higher systematic rank increased through time and vertebrate remains appeared in the two youngest faunules.

Ecospace utilisation

Grouping of species according to the categories of tiering, motility and feeding mechanism resulted in different combinations of categories reflecting different modes of life (Bush *et al*. 2007). These categories helped us investigating changes in ecospace occupation during the Early Devonian at our section of the Jebel Ouaoufilal (see Fig. 5).

The ecospace use at the Silurian-Devonian boundary is poor in modes of life. Especially unattached pelagic animals are common which are slow, facultative or non-motile and which fed on feces, small food particles in the

Bulletin of Geosciences • Vol. 89, 1, 2014

water column or small prey. Another mode of life is represented by unattached shallow infaunal, facultatively motile, mining bivalves. This result is, however, not entirely representative because of the relatively poor sampling. Most likely, we missed some species of orthocones and possibly also bivalves.

In the early Lochkovian faunule, three modes of life were present of which only one (unattached shallow infaunal, facultatively motile miners) dominated, reaching 67% relative abundance. This mode of life is represented by bivalves, which show a slight increase in diversity compared to the Silurian-Devonian boundary. Species of freely pelagic, slow motile predators that are represented by orthocones still exist but have a lower relative abundance (17%) than in the faunule of the earliest Lochkovian (25%). With the appearance of tabulate corals, a new mode of life (attached surficial, non-motile suspension feeders) occurred in the sedimentary sequence at Filon 12, while two modes of life from the Silurian-Devonian boundary (unattached pelagic, facultatively motile, coprophagous organisms or non-motile suspension feeders) apparently vanished with the disappearance of the early Lochkovian faunule.

In the late Lochkovian faunule, three additional modes of life appeared: freely surficial, slow motile grazers, attached surficial, facultatively motile suspension feeders and attached semi-infaunal, facultatively motile suspension feeders. These modes were represented by gastropods, brachiopods, epibyssate and semi-infaunal bivalves. A total of six modes of life existed then but none of them is clearly dominant. The highest relative abundances of the Lochkovian faunule are represented by freely pelagic, slow motile predators and freely surficial, slow motile grazers (26% for each).

In the Pragian faunule, six new modes of life appeared and so the number of modes of life had more than doubled. Especially surficial modes of life became more abundant and unattached semi-infaunal, non-motile and attached erect, non-motile suspension feeders were found for the first time. But of these 12 modes of life, the freely pelagic, slow motile predators have the highest relative abundance of almost 34%. A further increase can be documented in "faunule 1" (Klug *et al.* 2008a, De Baets *et al.* 2010) of the early Emsian (14 modes of life). No mode of life is significantly dominant but freely pelagic, slow motile predators have the highest relative abundance (21%). While five new modes of life were present, we did not rediscover two that existed in the Pragian (attached erect and unattached semi-infaunal, non-motile suspension feeders). We found fossils of freely pelagic, fast motile predators that were represented by two fish species and a small increase in semi-infaunal and infaunal modes of life (attached semi-infaunal, non-motile and attached shallow infaunal, facultatively motile suspension feeders, and unattached deep infaunal, facultatively motile miners).

We found evidence that the number of modes of life increased, and thus the ecospace use expanded from the Silurian-Devonian boundary towards the early Emsian. In the Early Devonian of the Taouz area, we found only 19 of the 216 theoretically possible modes of life. The number of modes of life recorded here corresponds well with the results of Bush *et al.* (2007), who found 21 modes of life for the mid Palaeozoic (Late Ordovician to Devonian) and 23 to 25 for the late Cenozoic (Miocene to Pleistocene) of North America and Europe. The specific types of modes of life found in the Early Devonian of the Taouz area mostly correspond to those found in the mid Palaeozoic by Bush *et al.* (2007). Differences between the two studies (the types of modes of life and their number) are influenced by the size of samples and study area, the time span, preservational biases and different palaeoenvironments. For example, Bush *et al.* (2007) described a tropical environment in the Palaeozoic of North-America while North Africa was situated in a more temperate climate (Kaufmann 1998, Scotese & McKerrow 1990).

As we examined all categories of ecospace occupation of Bush *et al.* (2007) separately, we found an increase of ecological categories that were occupied by species over time in the section at the Jebel Ouaoufilal. The greatest change occurred in the Pragian faunule. At this time, the number of surficial species, freely walking or slowly swimming species and predator species had the highest absolute abundances within the classes of tiering, motility and feeding mechanism (see Fig. 7).

Dominance changes in taxic composition and modes of life

We examined changes in dominance based on analyses of the trophic nucleus. The trophic nucleus includes species, whose abundances contribute to 80% of the total number of specimens per fauna (Neyman 1967). Moreover, we analyzed to what modes of life (combination of tiering, motility and feeding mechanism according to Bush *et al.* 2007) the dominant species belonged (see Table 1 in appendix).

At the Silurian-Devonian boundary, the trophic nucleus contained two species and two different modes of life while only one species and a single mode of life were predominant in the early Lochkovian faunule. Compared to this, the late Lochkovian faunule contained more dominant species and modes of life (4 species, 3 modes of life). The distribution of dominance changed profoundly from the Lochkovian to the Pragian. 27 species and six modes of life were contributing to the trophic nucleus of the Pragian faunule. A strong decrease in the number of predominant species occurred in the early Emsian (5 species), whereas the number of modes of life only decreased to four modes of life (see Fig. 4A–E).

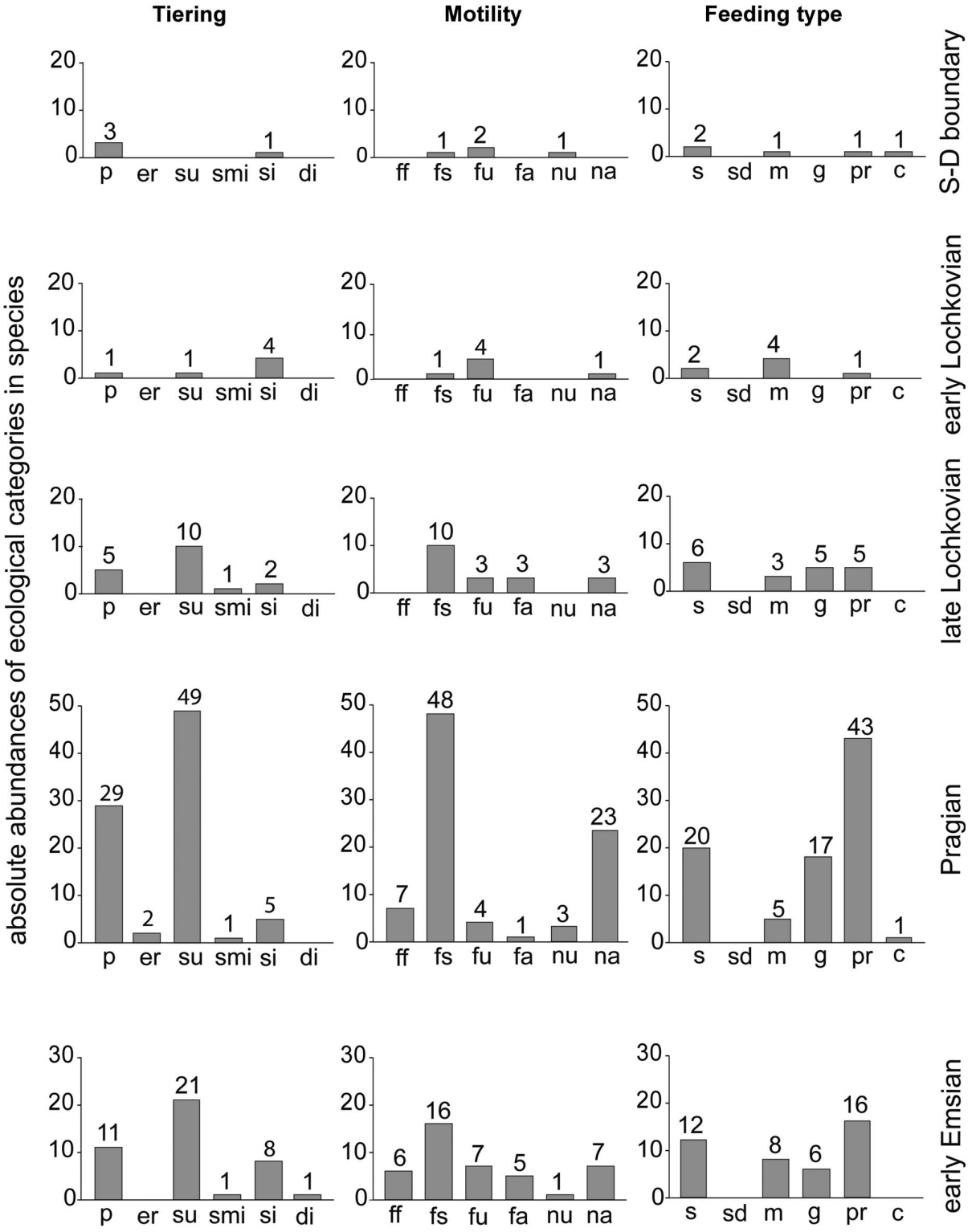

Figure 7. Changes in tiering, motility and feeding behaviour in the Early Devonian of the Taouz area. Ecological categories: Tiering – p: pelagic, er: erect, su: surficial, smi: semi-infaunal, si: shallow infaunal, di: deep infaunal; Motility – ff: freely fast, fs: freely slow, fu: facultatively unattached, fa: facultatively attached, nu: non-motile and unattached, na: non-motile and attached; Feeding type – s: suspension feeder, m: miner, g: grazer, pr: predators, c: coprophagous (Bush *et al*. 2007).

Bulletin of Geosciences • Vol. 89, 1, 2014

The number of dominant species increased through time and the Pragian faunule with the highest species richness also had the highest number of dominant species. The trophic nucleus includes species with pelagic modes of life in the earliest Lochkovian and contains a lot of species of different groups and especially pelagic and surficial modes of life in the Pragian. In the early Emsian, the number of dominant species strongly decreased, and pelagic, infaunal and surficial modes of life are dominating.

Discussion

The alpha diversity increased from the Silurian-Devonian boundary to the Pragian and slightly decreased in the early Emsian of the Tafilalt. We found an expansion of the ecospace use and major changes in dominant species and modes of life in the trophic nuclei of the Early Devonian. Such changes in diversity and ecospace use can be caused by sea level changes, changes in oxygenation of the sediment and water on the sea floor, differences in salinity, or sediment input. A sampling bias might alter the primary data in such way, that a trend can be seen, which does not correspond to the actual original change in ecology. Sampling is affected by, *e.g*., different sample sizes, poor sampling and time-averaging. The sampling bias due to sample size was reduced by rarefying the abundance data of the faunules by the software package PAST (Hammer *et al*. 2001). In how far the dimensions of the sampled intervals produced a bias is difficult to estimate. In our opinion, however, this change in diversity and ecology is real, because even in single beds, many more species and fossil groups can be seen in cross sections and furthermore, the Pragian diversity has been corroborated by others, who examined, *e.g*., Pragian trilobites (*e.g*. Alberti 1969). Time-averaging refers to the accumulation of a local community over time, which does not represent the local community structure at a single moment, because due to their short life spans, communities accumulate faster than sediments (Walker & Bambach 1971). Therefore, short-term events are usually not visible in fossil assemblages. Indeed, the long-term trends as seen in the section at the Jebel Ouaoufilal reflect extreme changes in species richness and composition and the faunules were obviously affected by various environmental factors. Fluctuations in sea level or bottom oxygenation are possibly the reasons for changes in diversity and ecospace utilization. Littoral parts of the sea are mostly low in diversity because of high water currents and perturbations while the environment of the shelves is more stable and therefore has higher species richness (Ziegler 1972). The realms of the deep sea are poor in species because the supply of organic food usually decreases with water depth.

Many facts support the hypothesis that a sea level fall and additional oxygenation of the sea floor occurred during the Early Devonian in the Tafilalt. The faunule of the Silurian-Devonian boundary was poor in species and modes of life. Especially modes of life including pelagic species, such as orthocones, *Camarocrinus* and gastropods attached to *Camarocrinus* were abundant. The faunule was dominated by two species (Orthocerida ind. 1, *Camarocrinus* sp.) with following modes of life: freely pelagic, unattached non-motile suspension feeders and freely pelagic, slow motile predators. The missing benthos (except the infaunal bivalve *Panenka obsequens*) and the dominating pelagic species indicate low oxygen conditions on the sea floor and in the sediment during the earliest Lochkovian. Haude (1992) and Haude & Walliser (1998) reported that the planktonic scyphocrinoids existed from the Late Silurian to the early Lochkovian when the deposition of organic material and therefore of black shales prevailed. This fact in combination with the dominance of other pelagic organisms (nautiloids and graptolites) and the commonly dark sediments rich in pyrite and organic matter, reflect hypoxic to anoxic conditions and thus poor living conditions at the bottom (Haude 1992). Kříž (2000) described a community of large infaunal bivalves ("*Panenka* Community"), which co-occurred with *Scyphocrinites* and cephalopods in the earliest Lochkovian of the Tafilalt. Based on the large size,

Figure 8. Lochkovian bivalves, Pragian trilobites and brachiopods from the Jebel Ouaoufilal in the Tafilalt. • A – *Odontochile* cf. *hausmanni* (Brongniart, 1822); fragment of the pygidium, × 1; PIMUZ 30645. • B–D – *Reedops* cf. *cephalotes hamalagdianus* Alberti, 1983; dorsal view of the cephalon, lateral view of the whole specimen, dorsal view of the thorax, × 1; PIMUZ 30646. • E–G – *Reedops bronni* (Barrande, 1846); lateral view of the whole specimen, dorsal view of thorax and pygidium, × 1; PIMUZ 30647. • H, I – *Cheirurus* (*Crotalocephalus*) sp.; dorsal and lateral view of the cephalon, × 2; PIMUZ 30648. • J–N – *Desquamatia* sp.; lateral, dorsal, posterior, ventral and anterior view of the valves, × 1; PIMUZ 30649. • O–S – ?*Aulacella eifeliensis* (Verneuil, 1850); lateral, dorsal, posterior, ventral and anterior view of the valves, × 2; PIMUZ 30650. • T–X – Brachipoda gen. et. sp. indet.; lateral, dorsal, posterior, ventral and anterior view of the valves, × 2; PIMUZ 30651. • Y–AC – ?*Protathyris* sp.; lateral, dorsal, posterior, ventral and anterior view of the valves, × 2; PIMUZ 30652. • AD–AO – *Cingulodermis* sp.; AD–AH – lateral, dorsal, posterior, ventral and anterior view of the valves, × 2; PIMUZ 30653; AI–AO – lateral, dorsal, posterior, ventral and anterior view of the valves, × 2; PIMUZ 30654. • AP – aff. *Eoglossinotoechia* sp.; ventral view, × 2; PIMUZ 30655. • AQ, AR – *Panenka princeps* Barrande, 1881; dorsal and lateral views, × 1; PIMUZ 30656. • AS – *Panenka humilis* Barrande, 1881; lateral view, × 1; PIMUZ 30657. • AT – *Neklania* cf. *resecta* Barrande, 1881; insight view of the left valve, × 1; PIMUZ 30658. • AU – *Jahnia* aff. *conscripta* (Barrande, 1881); lateral view, × 3; PIUMZ 30659. • AV, AW – *Actinopteria* cf. *decussata* Hall, 1884; AV – lateral view, × 2; PIMUZ 30660; AW – lateral view of two specimens, × 2; PIMUZ 30660. • AX – *Mytilarca* sp.; lateral view, × 1; PIMUZ 30661. • AY – *Patrocardia tarda* (Barrande, 1881); lateral view, × 1; PIMUZ 30662.

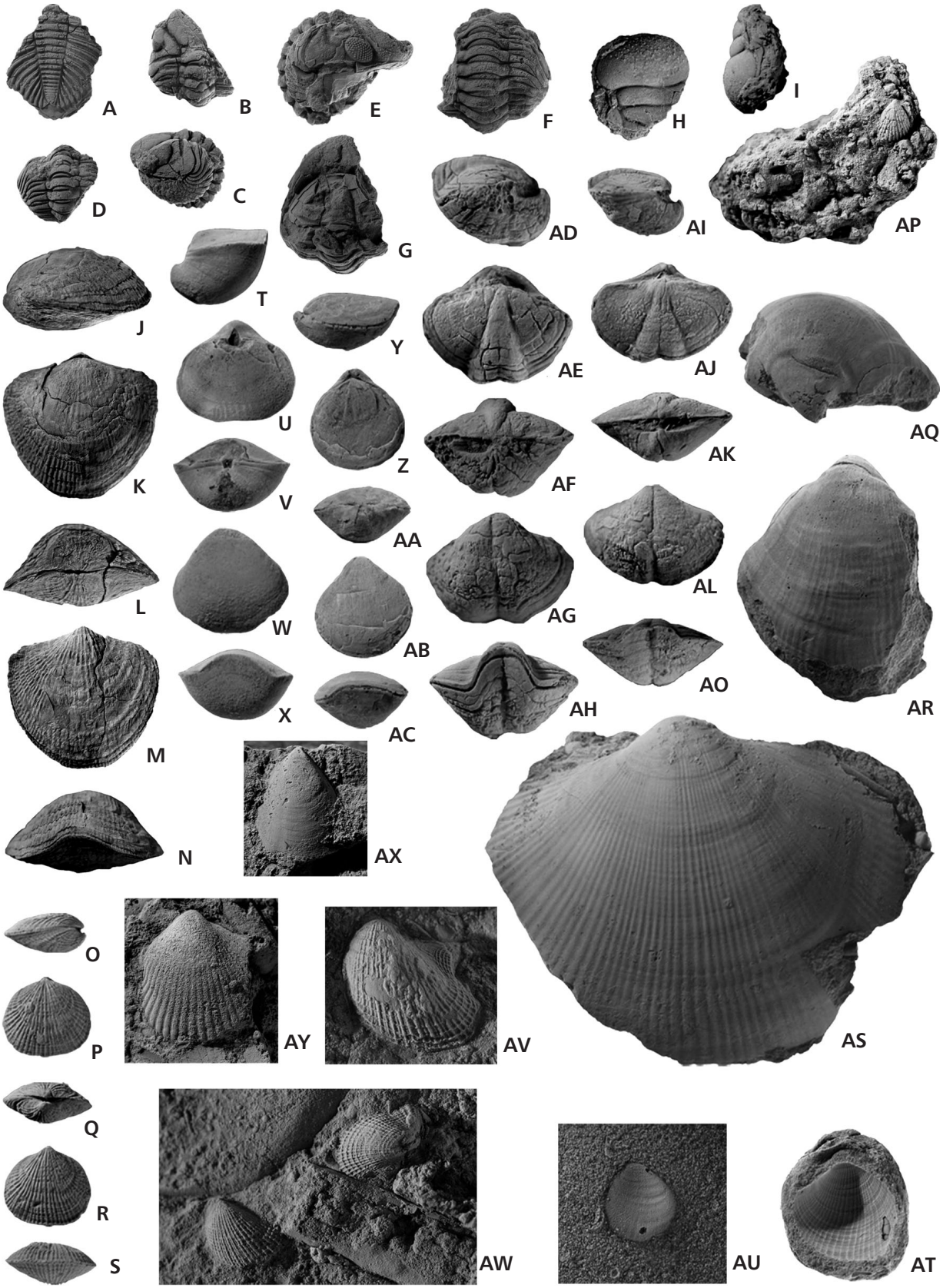
A
B
E
F
H
I
D
C
G
AD
AI
AP
J
T
Y
AE
AJ
AQ
K
U
Z
AF
AK
V
AA
AL
L
W
AB
AG
AO
AR
M
X
AC
AH
N
AX
AS
O
AY
AV
P
Q
R
S
AW
AU
AT

Bulletin of Geosciences • Vol. 89, 1, 2014

the low species diversity (*Panenka obsequens*, *Panenka* aff. *bellula* and *Dualina* sp.) and the preservation of the bivalves, he assumed a soft bottom environment with low oxygen conditions and low water movement at the sea floor. Unfortunately, we found only three individuals of *Panenka obsequens* and we did not find the other two species of the "*Panenka* Community" in our section at the Jebel Ouaoufilal (Filon 12). But the low diversity, the rather large size of the bivalves and the accompanying pelagic fauna indicates similar living conditions at the sea floor as reported by Kříž (2000).

In the early Lochkovian, the species diversity was higher because of the increased diversity in infaunal bivalves (Genera: *Panenka, Neklania, Jahnia*) and the appearance of a tabulate coral species. The ecospace use expanded slightly but the faunule still has a low diversity of modes of life, which include only pelagic and infaunal categories. A cephalopod species, which belonged to freely pelagic, slow motile predators (*Plagiostomoceras culter*), strongly dominated the faunule. These facts all together testify that the bottom water was still similarly low in oxygen as during the Late Silurian and earliest Lochkovian.

In the late Lochkovian, the increase in alpha diversity and the gentle increase in modes of life with the first appearance of surficial gastropods and brachiopods in the section indicated slightly improved living conditions at the sea floor. We noted that the faunule was no longer dominated by pelagic species but also comprised surficial, freely slow moving grazers (two gastropod species) and attached, semi-infaunal, facultatively motile suspension feeders (*Actinopteria* cf. *decussata*), which also reflected changes in the environment. The species composition of the bivalves was similar to the "*Panenka-Jahnia-Neklania* Community" described by Kříž (2000). This community contained a high diversity of infaunal bivalves and also epibyssate bivalves that indicate improved living conditions at the bottom due to higher oxygen content. In our sample, we found infaunal bivalves such as *Panenka humilis*, *Neklania* cf. *obtusa* and *Jahnia* sp., epibyssate bivalves such as *Mytilarca* sp. and *Patrocardia tarda* and the semi-infaunal bivalve *Actinopteria* cf. *decussata* (see Fig. 8). Unfortunately, a lot of taxa of the "*Panenka-Jahnia-Neklania*" community were missing. But higher diversity in infaunal species and appearance of semi-infaunal and epibyssate bivalves reflect a better ventilated sea floor and therefore better living conditions for benthic species in the late Lochkovian.

Subsequently, the extreme increase in alpha diversity from 20 species in the late Lochkovian to 86 in the Pragian, the increase in modes of life including surficial, erect, semi-infaunal and infaunal organisms and a highly diverse trophic nucleus (27 species, especially including pelagic and surficial modes of life) reflect good living conditions for benthonic as well as demersal life. In particular, the drastic increase in benthic species and the colour change of the sediment towards light grey permits the supposition that a steady rise of oxygen content near the seafloor occurred in combination with a sea-level fall. This is in accordance with the Devonian sea level curve of Morocco presented by Kaufmann (1998) and is linked to a conspicuous sediment colour change, which occurs in the entire Tafilalt (Alberti 1981, Belka *et al.* 1999, Bultynck & Walliser 2000b, Kröger 2008). Kröger (2008) correlated the increase in benthic taxa and cephalopods species at the Filon 12 with the "*pesavis* Bioevent" or "Lochkovian-Pragian Boundary Event" (Chlupáč & Kukal 1988, 1996; Schönlaub 1996), which coincides with global changes in sediment colours, benthic diversity and/ or taxonomic composition at the Lochkovian-Pragian boundary (Alberti 1969, Schönlaub 1996, Talent & Yolkin 1987, Talent *et al.* 1993, Kříž 1998, Ferreti *et al*. 1999, Chlupáč *et al.* 2000, García-Alcalde *et al.* 2000). These facts in combination with the Devonian eustatic sea level curves (Johnson *et al.* 1985, 1996) revealed a change of oxygen content of the sea floor caused by a potential global sea level fall.

The early Emsian fauna ("faunule 1" of Klug *et al.* 2008a) is also quite diverse although it contains less taxa (42 species), whereas the number of modes of life increased (from 12 modes of life in the Pragian to 14 in the early Emsian). The high abundance of surficial species led to the assumption that oxygen conditions in and on the sediment were similarly high as during the Pragian. Based on the faunal composition and the facies, Klug *et al.* (2008a) concluded that the environmental conditions of the early Emsian can be considered as favorable and reasonably well oxygenated; however, the commonly limonitic and formerly pyritic preservation of this fauna shows that only the top part of the sediment was oxygenated while deeper layers were probably anoxic. Analysis on the trophic nucleus of the early Emsian faunule shows an elementary change in the number of dominant species. There was an extreme decrease in dominant species (from 27 species in the Pragian to 5 in the early Emsian) and a slight decrease in modes of life (from 5 modes of life in the Pragian to 4 in the early Emsian) contributing to the trophic nucleus. Modes of life including pelagic and infaunal species were dominant in the early Emsian faunule, whereas only one surficial species was prevalent. This fact, in combination with the limonitised macrofossils and the occurrence of greenish claystones reflect a less well-oxygenated bottom than in the Pragian. Additionally, we found a high number of infaunal bivalve taxa belonging to the Palaeotaxodonta in the early Emsian faunule. Recent representatives of this group are known to tolerate moderately low oxygen conditions in the sediment. The decrease in bottom oxygenation could be explained by a transgression during the early Zlíchovian (Kröger 2008, Lubeseder *et al.* 2009). This early Emsian change in sea level possibly correlates to the transgressive cycle Ib *sensu* Johnson *et al.* (1996).

In the present work, the discussed sea level changes mainly represent long-term trends in the Early Devonian of the Taouz area but naturally, many short-term fluctuations in sea level occurred in this time span as well. Alternations of limestones and claystones in our section at the Jebel Ouaufilal and in other sections in the eastern (Belka *et al.* 1999, Kröger 2008) and southwestern Anti-Atlas (Lubeseder *et al.* 2009) indicate numerous regional sea level fluctuations. Comparisons between our results and the sections of previous authors show similar changes in species richness and ecospace use during the Early Devonian in the Tafilalt, but lateral facies changes and diachronicity of boundaries are possible and should be examined in greater detail in the future.

In Early Devonian faunules of the Tafilalt, the ecological turnover of the "Devonian nekton revolution" (Klug *et al.* 2010) is predominantly reflected in the faunal changes at the transition from "faunule 1" to "faunule 2" (Zlíchovian, early Emsian) of Klug *et al.* 2008a, where parts of the abundance of non-ammonoid cephalopods were replaced by rather diverse early ammonoids (Klug *et al.* 2008a). Pelagic predators were already abundant in the Silurian and stayed common until the early Emsian but they mainly consist of slow motile microphagous orthocerids, actinocerids, oncocerids and bactritids. Nektonic predators such as the acanthodian *Machaeracanthus* were found in small numbers in the early Emsian faunule of our section. Demersal and planktonic species stayed dominant in the Pragian and early Emsian faunules in the Taouz area.

Conclusions

We examined five Early Devonian faunules near the Jebel Ouaoufilal in the southern Tafilalt for alpha diversity and ecospace utilization. All 3376 specimens were identified as far as possible and assigned to different modes of life including the ecological groups tiering, motility and feeding mechanism according to the method introduced by Bush *et al*. (2007). These analyses revealed a strong increase in species richness and an extension in ecospace utilisation during the Early Devonian (earliest Lochkovian to early Emsian *sensu* Bultynck & Walliser 2000b) of the Taouz area. The highest number of species has been found in the Pragian and the expansion of ecospace utilization reached its maximum in the early Emsian. Especially taxa with surficial, slow motile or predatory modes of life became most diverse in the Pragian and decreased somewhat in the early Emsian. The number of dominant species contributing to the trophic nucleus increased from the Silurian-Devonian boundary to the Pragian and extremely decreased in the early Emsian. All these changes reflect favorable conditions for life on the sea floor during the Pragian of the Tafilalt. Increasing benthic and demersal diversity in the Pragian coincides with colour changes in sediments and faunal changes in the whole Tafilalt and other parts of the world at the Lochkovian-Pragian boundary (Alberti 1969, 1981; Talent & Yolkin 1987; Talent *et al.* 1993; Kříž 1998; Schönlaub 1996; Ferreti *et al.* 1999; Belka *et al.* 1999; Bultynck & Walliser 2000b; García-Alcalde *et al.* 2000; Chlupáč *et al.* 2000; Kröger 2008). The ecological change correlates with a steady rise of oxygen content near the bottom in combination with a regional if not global regression. This is in accordance with existing Devonian sea level curves of Morocco (Kaufmann 1998) and eustatic sea level curves of Johnson *et al.* (1985; see also Haq & Schutter 2008). In the early Emsian faunule of our section in the Tafilalt, we found a decrease in benthic species with a simultaneous increase in infaunal palaeotaxodont bivalves, which are tolerant to low oxygen conditions. This fact in combination with limonitised fossils and the sediments consisting of greenish claystone documents a less oxygenized sea floor than in the Pragian. This decline in oxygen content at the sea floor could have been triggered by a transgression during the early Zlíchovian (Kröger 2008, Lubeseder *et al.* 2009) that possibly correlates with the transgressive cycle Ib *sensu* Johnson *et al.* (1996).

Our analysis of the earliest Lochkovian to early Emsian faunules (according to Bultynck & Walliser 2000b) of the Taouz area did not show a macroecological change similar to the "Devonian nekton revolution" (Klug *et al.* 2010). Demersal and planktonic species were predominant and were not significantly displaced by nektonic organisms such as acanthodian and ammonoids through time. The geological range and time span studied here limit the comparison of our results with the diversity changes that occurred during the "Devonian nekton revolution" (Klug *et al.* 2010); this is linked with the fact that faunule compositions were examined here on a regional level only and some important changes might have occurred within the Emsian, perhaps between "faunule 1" and "faunule 2" (Zlíchovian, early Emsian) of Klug *et al.* (2008a). However, the "faunule 2" of Klug *et al.* (2008a) in our section did not yield many fossils and it reflects only geographically limited changes in palaeoecology.

Systematic palaeontology

Phylum Mollusca Linnaeus, 1758
Class Amphigastropoda Simroth, 1906
Family Bellerophontidae M'Coy, 1851
Subfamily Cymbulariinae Horný, 1963

New genus aff. *Coelocyclus* Perner, 1903

Remarks. – Horný (1963) established the new Subfamily Cymbulariinae within the Family Bellerophontidae, inclu-

Bulletin of Geosciences • Vol. 89, 1, 2014

ding four genera: *Cymbularia* Koken, 1896, *Ptychosphaera* Perner, 1903, *Prosoptychus* Perner, 1903, and *Coelocyclus* Perner, 1903. However, since his work of 1963, no revision of this widely distributed group has been published.

New genus aff. *Coelocyclus* sp. nov.
Figure 9AC–AE

Material. – One shell (PIMUZ 30604) from the Pragian of Jebel Oaoufilal in the Tafilalt (Morocco), housed in the Paläontologisches Institut und Museum der Universität Zürich.

Remarks. – Only a single shell is available, which resembles species of the genus *Coelocyclus* Perner, 1903. However, its very sharp circumbilical ridge and very low whorl profile differ from the morphological range of *Coelocyclus*. These distinct shell features suggest a position close to *Coelocyclus* but probably in an independent genus.

Occurrence. – Only one specimen from Jebel Ouaoufilal (Filon 12) in the Tafilalt of Morocco is known.

Class Gastropoda Cuvier, 1797

Remarks. – Family-level classification of Bouchet *et al.* (2005) is used in the following sections.

Family ?Oriostomatidae Wenz, 1938

Genus *Oriomphalus* Horný, 1992a

Type species. – *Oriomphalus puellarum* Horný, 1992a; Pragian, Early Devonian; basal part of Loděnice Limestone, Praha Formation, Prague Basin, Czech Republic.

Remarks. – Horný (1992a) placed two Early Devonian species, *Oriomphalus puellarum* Horný, 1992a and *O. supraliratus* (Rohr & Smith 1978), within the new genus *Oriomphalus. O. supraliratus,* was described from the Lochkovian beds of the Canadian Arctic Islands and was originally placed within the genus *Cyclonema* (*Cyclonema*) Hall, 1852 by Rohr & Smith (1978). The type species *Oriomphalus puellarum* Horný, 1992a comes from the basal part of the Loděnice Limestone (Praha Formation, Pragian, middle Early Devonian) of the Prague Basin. Later, Frýda & Manda (1997) reported the occurrence of another species, *O.* aff. *O. puellarum*, from the *Monograptus uniformis* graptolite Biozone (early Lochkovian). The higher systematic position of the genus *Oriomphalus* is still uncertain because of the lack of data on its protoconch morphology. Judging from teleoconch morphology, it probably belongs to the archaeogastropod lineage and close to the genus *Australonema* Tassell, 1980.

***Oriomphalus multiornatus* sp. nov.**
Figure 9A–O

Holotype. – The holotype (PIMUZ 30598) is figured in Fig. 9M–O and is housed in the Paläontologisches Institut und Museum der Universität Zürich.

Type horizon and locality. – Pragian, *pireneae* Zone; Seheb El Rhassel Group, Jebel Ouaoufilal (Filon 12), Tafilalt, Morocco.

Material. – Seven shell fragments (PIMUZ 30587, PIMUZ 30594–30598) from the Jebel Ouaoufilal in the eastern Tafilalt, Morocco.

Etymology. – *Multiornatus*, combination of *multi* (much) and *ornatus* (decorated).

Diagnosis. – The species of *Oriomphalus* is ornamented with several distinct spiral threads crossed by dense collabral threads at early shell whorls and a wide pleural angle.

Description. – Description is based on all specimens (PIMUZ 30587, PIMUZ 30594–30598). Species with a small, turbiniform shell having at least seven whorls; whorl profile slightly shouldered in early whorls and rounded in later whorls; whorl profile between the sutures strongly convexly arched; sutures distinctly impressed; pleural

Figure 9. Pragian gastropods from the Jebel Ouaoufilal in the eastern Tafilalt. • A–O – *Oriomphalus multiornatus* gen. et sp. nov.; A–C – apical, lateral and basal views of the shell, × 2; PIMUZ 30594. D, E – apical and apertural views, × 2; PIMUZ 30595. F–I – apical, apertural, lateral and basal views, × 2; PIMUZ 30596. J, K – apical and apertural views, × 2; PIMUZ 30597. M–O – apical, apertural and lateral views, × 2; PIMUZ 30598. P–U – *Australonema* sp. nov. P, R – apical, apertural and basal views, × 2; PIMUZ 30599. S–U – apical, apertural and basal views, × 2; PIMUZ 30600. V, W – ?*Spirina* sp.; dorsal and lateral view, × 2; PIMUZ 30601. • X, Y – *Palaeozygopleura* sp. nov.: lateral and apertural views, × 1; PIMUZ 30602. • Z–AB – *Orthonychia* sp.; apertural, lateral, dorsal views, × 1; PIMUZ 30603. • AC–AE – new genus aff. *Coelocyclus* sp. nov.; apertural, lateral and dorsal views, × 1; PIMUZ 30604. • AF–AH – aff. *Tychobrahea* Horný, 1992a; apical, lateral and basal views, × 2; PIMUZ 30605. • AI–AN – *Rihamphalus gracilis* (Říha, 1938); AI, AK – apical, lateral and basal views, × 1; PIMUZ 30606; AL–AN – apical, apertural and basal views, × 2; PIMUZ 30607. • AO, AP – *Paraoehlertia* sp.; apical and lateral views, × 3; PIMUZ 30608. • AQ–AT – *Eohormotomina restisevoluta* gen. et sp. nov.; AQ, AR – apical and lateral views, × 3; PIMUZ 30609; AS, AT – apical and lateral views, × 3; PIMUZ 30610. • AU, AV – *Umbotropis* sp.; apical and lateral views, × 1; PIMUZ 30611.

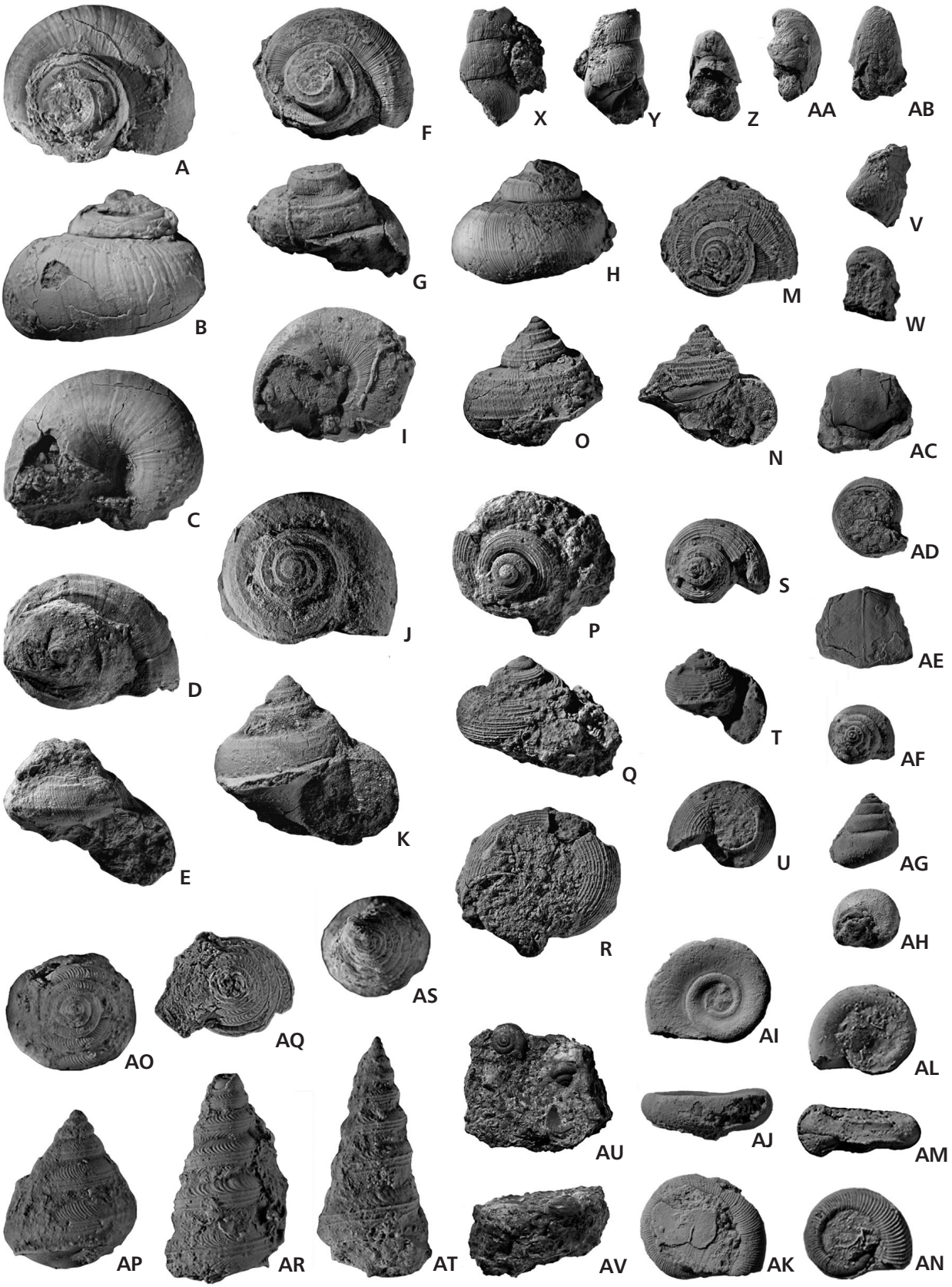
A
B
C
D
E
F
G
H
I
J
K
X
Y
Z
AA
AB
V
M
W
O
N
AC
P
S
AD
AE
Q
T
AF
U
AG
R
AH
AS
AQ
AO
AI
AL
AU
AJ
AM
AP
AR
AT
AV
AK
AN

Bulletin of Geosciences • Vol. 89, 1, 2014

angle is about 90°; early whorls slightly shouldered; adult whorls rounded; shell base narrowly phaneromphalous. Shell ornamentation consists of several distinct spiral threads, only on the upper and median portion of the whorl crossed by collabral threads in early shell whorls. The spiral threads are crossed by more or less regularly spaced, dense, collabral threads, which are always weaker than the stronger spiral threads of young whorls; the spiral threads disappear on more adult whorls; circumbilical thread present on all whorls. The protoconch is unknown.

Remarks. – The shell of *Oriomphalus multiornatus* gen. et sp. nov. differs from all known species of the genus, such as the Pragian *O. puellarum* and the Lochkovian *O. supraliratus* as well as *O.* aff. *puellarum*, by a much wider pleural angle. In addition, it has a more distinct shell ornamentation than *O. puellarum* and *O.* aff. *puellarum*; it is also more shouldered in early whorls (compare with Horný 1992a, pl. I, figs 5–8 as well as Frýda & Manda 1997, pl. 8, figs 6, 7). The Lochkovian *O. supraliratus* has a much higher shell and less prominent collabral threads than *O. multiornatus* gen. et sp. nov.

Occurrence. – The species is only known from the locality Jebel Ouaoufilal in the eastern Tafilalt, Morocco.

Genus *Australonema* Tassel, 1980

Type species. – *Cyclonema australis* Etheridge, 1890; Pragian, Cave Hill Quarries, Lilydale Limestone Formation, Australia.

Remarks. – Tassell (1980) established the new genus *Australonema* for gastropods with numerous, closely spaced spiral elements of ornamentation and placed it within the Subfamily Gyronematinae Knight, 1956 of the Family Holopeidae Wenz, 1938. Tassell (1980) described and transferred six species from Early Silurian to Early Devonian strata of Australia to the genus *Australonema*. He also suggested the replacement of the Wenlockian *Cyclonema carinatum* var. *multicarinatum* Lindström, 1884 to *Australonema.* Later, Gubanov & Yochelson (1994) described an additional new species of *Australonema*, namely *A. varvarae* from the Wenlockian of Siberia. The same authors also questioned the higher taxonomy of *Australonema* and noted a similarity of this genus to *Oriostoma* Munier-Chalmas, 1876. Gubanov & Yochelson (1994) pointed out that the presence of a shallow but distinct umbilicus in *Oriostoma* distinguishes *Australonema* from the latter genus. However, as shown by Tassell (1980), the shells of *Australonema* species including the type species *A. australis* (Etheridge, 1890), also have a well developed umbilicus. Yochelson & Linsley (1972) described and illustrated a specimen of *Cyclonema lilydalensis* Etheridge, 1891 (= *A. lilydalensis*) with an *in situ* paucispiral operculum. A paucispiral operculum was also found in the Wenlockian *A. varvarae* Gubanov & Yochelson, 1994 and by Horný (1998), in the Pragian *A.* cf. *guillieri* (Oehlert, 1881). Recently, two new species were described from the Prague basin: *A. blodgetti* Frýda & Manda, 1997 from the *Monograptus uniformis* graptolite Biozone (early Lochkovian) and *A. havliceki* Frýda & Bandel, 1997, from the uppermost part of the Třebotov Limestone (Daleje-Třebotov Formation, lowermost Eifelian).

***Australonema* sp. nov.**
Figure 9P–U

Material. – Two shells (PIMUZ 30599–30600) from the Pragian of the Jebel Ouaoufilal in the Tafilalt (Morocco), housed in the Paläontologisches Institut und Museum der Universität Zürich.

Remarks. – The specimens of *Australonema* sp. nov. clearly belong to the genus *Australonema*. This species differs from all known Devonian species of *Australonema* by a very low spire. However, the limited material and the preservation do not suffice to introduce a new species.

Occurrence. – Only two specimens have been found which are limited to the southern Tafilalt in Morocco.

Family Eotomariidae Wenz, 1938

Genus *Paraoehlertia* Frýda, 1998a

Type species. – *Paraoehlertia parva* Frýda, 1998a; earliest Eifelian, Middle Devonian; uppermost part of the Třebotov Limestone, Daleje-Třebotov Formation, Prague Basin, Czech Republic.

Remarks. – The genus *Paraoehlertia* differs from the closely related genus *Oehlertia* in its wide periselenizone area, minutely phaneromphalous base, and opisthocline apertural margin below the selenizone. The genus *Paraoehlertia* unites several, hitherto undescribed species from the Lower Devonian of Europe. The archaeogastropod protoconch type (Frýda 1998a) in the type species places this genus within the Subclass Archaeogastropoda.

***Paraoehlertia* sp.**
Figure 9AO, AP

Material. – A single specimen (PIMUZ 30608) with nicely

preserved ornamentation (PIMUZ X) from the Jebel Ouaoufilal in the eastern Tafilalt (Morocco).

Remarks. – Only a single shell is available. However, its well-preserved ornamentation shows all diagnostic characters of the genus *Paraoehlertia*. Ongoing revision of the Early Devonian gastropods from Europe and Australia (by Jiří Frýda) revealed several already described species of *Paraoehlertia* that were placed in different eotomariid genera. Species-level placement of the Moroccan *Paraoehlertia* will be possible after finishing the ongoing revisions.

Family Gosseletinidae Wenz, 1938

Genus *Umbotropis* Perner, 1903

Type species. – *Umbotropis albicans* Perner, 1903; Lower Devonian; Prague Basin, Czech Republic.

Remarks. – The type species *Umbotropis albicans* Perner, 1903 comes from the Lower Devonian of the Prague Basin. Knight (1941) designated the holotype as derived from the specimens shown by Perner (1903) in figs 6, 7 on pl. 42 from the neighbourhood of the village Měňany. The type horizon of this species is not clearly established but it probably comes from limestones of Pragian age. Another Pragian species of the genus *U. rihai* Frýda & Manda, 1997, was described from the Prague basin. Besides these species, the Emsian *U. mesoni* Tassell, 1982 from the "*Receptaculites*" Limestone of Australia is the only further species of this genus.

***Umbotropis* sp.**
Figure 9AU, AV

Material. – Two shells (PIMUZ 30611) from the Jebel Ouaoufilal in the Tafilalt (Morocco).

Remarks. – Both shells from the Jebel Ouaoufilal in the Tafilalt clearly display generic features of the genus *Umbotropis*. The lack of additional shell characters (because of their weathered surface) does not allow their determination on the species level.

Family Murchisonidae Koken, 1896

Genus *Eohormotomina* gen. nov.

Type species. – *Eohormotomina restisevoluta* gen. et sp. nov.; Pragian, Early Devonian; Jebel Ouaoufilal (Filon 12), Tafilalt, Morocco.

Etymology. – *Eohormotomina*, using the combination of *Eos* (= dawn) and the generic name *Hormotomina*.

Diagnosis. – A high-spired murchisoniid with selenizone bearing a medial spiral cord and bordered by two spiral cords. Selenizone situated at midwhorl height; whorl surface above and below selenizone bears prominent collabral, strongly prosocline costae forming a deep sinus.

Remarks. – The genus *Eohormotomina* is very close to the genus *Hormotomina* Grabau & Shimer, 1909, based on *Murchisonia maia* Hall, 1861, from the Columbus Limestone (Eifelian) of Ohio. In contrast to *Hormotomina*, the shell of the Pragian *Eohormotomina restisevoluta* gen. et sp. nov. is ornamented with distinct collabral costae and has a wider pleural angle. The shell of *Eohormotomina* also resembles *Parahormotomina sibertae* Blodgett, Frýda & Racheboeuf, 1999, from the Kersadiou Formation (middle Givetian) in the vicinity of Brest (Brittany, northwestern France). *Eohormotomina* differs from *Parahormotomina* by the absence of two spiral cords, one just above, and the other slightly below the suture. By the absence of a distinct spiral cord below its selenizone and distinct collabral costae, *Parahormotomina* differs from the genus *Bouskaspira* Frýda 1999, which is based on the Pragian species *Aclisina fugitiva* Perner, 1907.

***Eohormotomina restisevoluta* sp. nov.**
Figure 9AQ–AT

Holotype. – Shell fragment (PIMUZ 30609) is figured in Fig. 9AQ, AR. Paläontologisches Institut und Museum der Universität Zürich.

Type horizon and locality. – Pragian, *pireneae* Zone; Seheb El Rhassel Group, Jebel Ouaoufilal (Filon 12), Tafilalt, Morocco.

Material. – The holotype (PIMUZ 30609) and a second shell fragment (PIMUZ 30610) were collected from the Jebel Ouaoufilal in the Tafilalt.

Etymology. – From *restis* (Latin) – rope and *evolutus* (Latin) – enrolled; referring to the superficial resemblance to an enrolled pile of rope.

Diagnosis. – See generic diagnosis.

Description. – Description is based on all specimens (PIMUZ 30609–30610). Specimens with high spired shells with at least nine whorls; spiral angle about 30 degrees. Selenizone raised, forming whorl periphery, situated at midwhorl height, whorl profile above selenizone distinctly

Bulletin of Geosciences • Vol. 89, 1, 2014

convex; selenizone bordered by prominent spiral cords and bearing a prominent median cord; width of selenizone about one third of the distance between sutures; upper spiral cord of selenizone slightly above mid-whorl height; whorl profile below selenizone flat on spiral whorls, gently rounded on final whorl; whorl surface above and below selenizone bears prominent collabral, strongly prosocline costae forming a deep sinus. The initial part of shells is unknown.

Remarks. – Horný (1992b) noted the occurrence of a single shell fragment from the Loděnice Limestone (Pragian) of Bohemia, which shows diagnostic features of *Hormotomina* Grabau & Shimer, 1909 and might represent the oldest evidence for this genus. However, the shell surface of this poorly preserved fragment bears traces of distinct prosocline cords as in *Eohormotomina restisevoluta* gen. et sp. nov. Therefore, it is possible that the shell fragment from the Loděnice Limestone belongs to our newly described genus *Eohormotomina.*

Occurrences. – The species has been found in the Tafilalt (Morocco) and is suspected to occur in the Loděnice Limestone of the Barrandian area (Czech Republic).

Family ?Euomphalidae de Koninck, 1881

Genus *Rihamphalus* Frýda, 1998b

Type species. – *Porcellia gracilis* Říha, 1938; Pragian, Early Devonian; Prague Basin, Czech Republic.

Remarks. – Říha (1938) placed his newly described species within the genus *Porcellia* Léveillé and noted its similarity to the Silurian species *P. sinistrorsa* Perner, 1903. However, *P. sinistrorsa* has a sinistrally coiled shell with a distinct selenizone in contrast to *Rihamphalus gracilis* (Říha, 1938). Frýda (1997) placed *P. sinistrorsa* within the new genus *Pernericirrus* of the Family Porcelliidae, which unites shells with dextral coiling in the early whorls and sinistral or planispiral coiling in the later whorls of the teleoconch (Frýda & Blodgett 1998). The shell of *R. gracilis* (Říha, 1938) bears characteristic features of members of the Family Euomphalidae. Nevertheless, diagnostic features of the Euomphalidae, such as the shape of the protoconch, were not hitherto documented in *Rihamphalus*, and so its higher taxonomic position is uncertain.

***Rihamphalus gracilis* (Říha, 1938)**
Figure 9AI–AN

Material. – Five shell fragments (PIMUZ 30588, PIMUZ 30606–30607) were collected from the Jebel Ouaoufilal in the eastern Tafilalt of Morocco.

Remarks. – All shell features of the shells coming from the locality Jebel Ouaoufilal fit well to those of the type species *Rihamphalus gracilis*. The genus was previously only known from the Prague basin. Ongoing revision of the Early Devonian gastropods of Australia (by Jiří Frýda) revealed another undescribed species of the genus *Rihamphalus*.

Occurrence. – The species is known from the Prague Basin in the Czech Republic and the Tafilalt in Morocco.

Superfamily Loxonematoidea Koken, 1889
Family Palaeozygopleuridae Horný, 1955

Genus *Palaeozygopleura* Horný, 1955

Type species. – *Zygopleura alinae* Perner, 1907; Pragian, Early Devonian; Dvorce-Prokop Limestone, Praha Formation, Prague Basin, Czech Republic.

Remarks. – Devonian species of this genus were recorded from Europe, North America, Australia, and Africa. Blodgett *et al.* (1988, 1990) showed an Old World Realm distribution of *Palaeozygopleura,* which most probably arose in the Rhenish - Bohemian Region of the Old World Realm, where the majority of the Early Devonian species and also the oldest species of this genus occur (Frýda 1993, Frýda & Blodgett 2004, Frýda *et al.* in press). Ongoing revision of the Early Devonian gastropods from Europe and Australia (by Jiří Frýda) revealed about ten hitherto undescribed species of *Palaeozygopleura.*

***Palaeozygopleura* sp. nov.**
Figure 9X, Y

Material. – 14 shell fragments (PIMUZ 30589, PIMUZ 30602) from the Pragian of the Jebel Ouaoufilal in the Tafilalt (Morocco). The specimens are housed in the Paläontologisches Institut und Museum der Universität Zürich.

Remarks. – The fragments found between the Jebel Ouaoufilal and Filon 12 bear distinct shell characters, which allows placing them doubtlessly to the genus *Palaeozygopleura.* Judging from the fragment size, this species is probably the biggest of all *Palaeozygopleura* species and by this character, it resembles a hitherto undescribed species from the Pragian of France. However, the shape of its asymmetric arched costae (Fig. 9X, Y) differs from the species found in France. The Moroccan specimens belong to a new species of *Palaeozygopleura*, but incomplete shells (*i.e.*, fragments formed

only by two whorls) prevent to establish a new species. Beside this new Moroccan species, the only other African species of *Palaeozygopleura* is *P. vaneki* Frýda, Ferrová, Berkyová, and Frýdová, 2008, reported by De Baets *et al.* (2010) from early Emsian strata of Morocco.

Occurrence. – The new species is restricted to the Tafilalt of Morocco.

Class Cephalopoda Cuvier, 1797
Order Pseudorthocerida Barskov, 1963
Family Spyroceratidae Shimizu & Obata, 1935

Genus *Cancellspyroceras* Kröger, 2008

Type species. – *Orthoceras loricatum* Barrande, 1868 by subsequent designation; Pragian Lower Devonian; lower part of the Dvorce-Prokop Limestone, Bohemia, Czech Republic.

***Cancellspyroceras loricatum* (Barrande, 1868)**
Figure 10A, B

Material. – Six fragments of phragmocones (PIMUZ 30590, PIMUZ 30612) from the Jebel Ouaoufilal, Tafilalt, Morocco. PIMUZ 30612 with injury and with overgrowth of *Filihernodia buccina* Taylor & Wilson gen. et sp. nov.

Diagnosis. – See Kröger (2008).

Description. – The maximum observed length of the largest fragment (PIMUZ 30612) is 264 mm. The widest conch diameter is 73.9 mm at the most abapical chamber and the smallest conch diameter is 30.5 mm at the most adapical chamber. Slightly cyrtoconic shell, angle of expansion approx. 11°. Ornamented shell with longitudinal and transverse lirae. Irregular distance between transverse lirae, longitudinal lines and transverse lirae become narrower from the abapical to the adapical part of the fragment. At a diameter of 49.4 mm, the ornamentation is interrupted by a big injury (height: 11.9 mm; width: 42.5 mm).

Occurrence. – *Cancellspyroceras loricatum* has been reported from the Pragian, Czech Republic and Morocco.

Family Pseudorthoceratidae Flower & Caster, 1935

Genus *Geidoloceras* Kröger, 2008

Type species. – *Geidoloceras ouaoufilalense* Kröger, 2008, original designation; Pragian, Early Devonian; Filon 12, Tafilalt, Morocco.

Figure 10. Large fragment of a Pragian nautiloid from the Jebel Ouaoufilal in the Tafilalt. • A, B – *Cancellspyroceras loricatum* (Barrande, 1868); lateral views of phragmocone fragment, × 0.5; PIMUZ 30612.

***Geidoloceras ouaoufilalense* Kröger, 2008**
Figure 11G, H

Holotype. – The specimen MB.C.9627 is housed in the Museum für Naturkunde Berlin.

Type horizon and locality. – Pragian; bed KMO-II, Filon 12 section, Tafilalt, Morocco.

Material. – 24 fragments of phragmocones (PIMUZ 30591, PIMUZ 30616) from Jebel Ouaoufilal, Tafilalt, Morocco.

Diagnosis. – Emended after Kröger (2008): Orthoconic or

Bulletin of Geosciences • Vol. 89, 1, 2014

slightly cyrtoconic shell with almost circular conch cross-section, angle of expansion approx. 10–12°. Shell ornamentation with transverse, narrow ridges. Siphuncle subcentral, expanding within the chambers, cyrtochoanitic septal necks.

Description. – The length of the phragmocone fragment PIMUZ 30616 is 31.5 mm with an orthoconic shell. Maximum observed conch diameter 20.4 mm, minimum observed conch diameter 16.4 mm, angle of expansion approx. 12°. Shell ornamentation with oblique transverse narrow ridges, 6 ridges per 1 mm. Three chambers are fully preserved; septal distance of the three abapical chambers is 5.5 mm and 4.8 mm of the two adapical chambers. Siphuncle subcentral; distance of the third septum (aboral) from the margin of the conch 9.3 mm on the dorsal side and 7.9 mm on the ventral side. Siphuncle tube expands within chambers, largest expansion of the connecting ring measures 3.4 mm. Short septal necks cyrtochoantic, diameter of septal perforation 1.7 mm.

Occurrence. – The species is restricted to the Pragian in the Tafilalt in Morocco.

Genus *Subdoloceras* Kröger, 2008

Type species. – *Subdoloceras tafilaltense* Kröger, 2008; Pragian, Early Devonian; Filon 12, Tafilalt, Morocco.

***Subdoloceras atrouzense* Kröger, 2008**
Figure 11I–L

Holotype. – Specimen MB.C.9595 in the Museum für Naturkunde Berlin.

Type horizon and locality. – Pragian; bed KMO-II, Filon 12 section, Tafilalt, Morocco.

Material. – 46 phragmocones (PIMUZ 30592, PIMUZ 30617–30618) from Jebel Ouaoufilal, Morocco, Pragian.

Diagnosis. – See Kröger (2008).

Description. – The length of the orthocone fragment PIMUZ 30617 is 28.7 mm. Orthoconic conch, conical shape, and circular conch cross-section. Maximum conch diameter is 14.5 mm at the adoral site and minimum diameter is 6.3 mm at the aboral side, angle of expansion approx. 15°. Shell ornamented with 10 fine transverse ridges, straight. Septal distance is 2.0 mm at the most adoral chamber and 1.2 mm at the most aboral chamber. Siphuncle subcentral and thin.

Occurrence. – The species is restricted to the Tafilalt of Morocco.

Order Orthoceratida Kuhn, 1940
Family Orthoceratidae M'Coy, 1844

***Tenuitheoceras* gen. nov.**

Type species. – *Tenuitheoceras secretum* gen. et sp. nov., designated herein; Pragian, Early Devonian; Jebel Ouaoufilal (Filon 12), Tafilalt, Morocco.

Diagnosis. – Slender, orthoconic shell shape with compressed cross-section. Ornamented shell with faint oblique transverse striae. Angle of expansion 6°, narrow septal dis-

Figure 11. Phragmocone fragments of Lochkovian and Pragian nautiloids from the Jebel Ouaoufilal in the Tafilalt. • A, B – *Pseudendoplectoceras lahcani* Kröger, 2008; lateral and septal views, fragments of the phragmocone, × 1; PIMUZ 30613. • C, D – *Endoplectoceras* sp.; lateral views, phragmocone with shell remains, × 2; PIMUZ 30614. • E, F – *Tafilaltoceras adgoi* Kröger, 2008; lateral and septal views, phragmocone incrusted by tabulate coral and crinoids, × 1; PIMUZ 30615. • G, H – *Geidoloceras ouaoufilalense* Kröger, 2008; lateral view and longitudinal section of an incomplete phragmocone, × 1; PIMUZ 30616. • I–M – *Subdoloceras atrouenze* Kröger, 2008; I, J – lateral views of phragmocone fragment with epizoans, × 1.5; PIMUZ 30617; K–M – lateral and septal views of phragmocone with epizoans and machaerid fragment, × 1.5; PIMUZ 30618. • N, O – *Subdoloceras engeseri* Kröger, 2008; lateral views of phragmocone fragment, × 1; PIMUZ 30619. • P – *Spyroceras cyrtopatronus* Kröger, 2008; lateral view of phragmocone fragment, × 1.5; PIMUZ 30620. • Q – *Spyroceras patronus* (Barrande, 1866); lateral view of phragmocone fragment, × 1.5; PIMUZ 30621. • R – *Spyroceras latepatronus* Kröger, 2008; lateral view of phragmocone fragment, × 1.5; NHMUK PI BZ 7494. • S–U – *Arthrophyllum vermiculare* (Termier & Termier, 1950); S – lateral view of phragmocone fragment, × 1.5; PIMUZ 30623; T – lateral view of phragmocone with tabulate coral, × 1.5; PIMUZ 30624; U – longitudinal section of phragmocone, × 1; PIMUZ 30625. • V, W – *Orthocycloceras tafilaltense* Kröger, 2008; lateral and septal views of phragmocone, × 1.5; PIMUZ 30626. • X–Z – *Tenuitheoceras secretum* gen. et sp. nov.; longitudinal section and lateral views of phragmocone, × 1.5; PIMUZ 30627. • AA, AB – *Adiagoceras* sp.; lateral views of phragmocone, × 1; PIMUZ 30628. • AC, AD – *Arionoceras kennethdebaetsi* sp. nov.; longitudinal section and lateral view of phragmocone fragment, ×1; PIMUZ 30629. • AE, AF – *Angeisonoceras reteornatum* Kröger, 2008; lateral and septal view of phragmocone, × 1; PIMUZ 30630. • AG – *Anaspyroceras* sp.; lateral view of phragmocone fragment, × 1.5; PIMUZ 30631. • AH–AJ – *Harrisoceras* sp.; lateral and septal views of phragmocone fragment, × 1.5; PIMUZ 30632. • AK – *Plagiostomoceras culter* (Barrande, 1866); lateral view of the mould of the body chamber and several phragmocone chambers, × 1; PIMUZ 30633. • AL–AM – *Plagiostomoceras* sp.; lateral views of phragmocone fragment, × 1.5; PIMUZ 30634. • AN–AO – *Hemicosmorthoceras* sp.; lateral views of phragmocone fragment, × 1.5; PIMUZ 30635.


A
B
C
D
E
F
G
H
I
J
K
L
M
N
O
P
Q
R
S
T
U
V
W
X
Y
Z
AA
AB
AC
AD
AE
AF
AG
AH
AI
AJ
AK
AL
AM
AN
AO

Bulletin of Geosciences • Vol. 89, 1, 2014

tance approx. 0.3 of the conch cross-section. Siphuncle subcentral, long septal necks approx. 0.3 of the septal distance, orthochoanitic. Diameter of septal perforation approx. 0.1 of conch diameter.

Etymology. – After the similar genus *Theoceras* Kröger, 2008 and *tenuis* (Latin) – narrow, referring to the compressed cross section.

Remarks. – The genus *Tenuitheoceras* is similar to *Theoceras* Kröger, 2008 in having a slender, orthoconic conch and narrow septal distances. It differs in having a compressed conch cross-section, relatively long septal necks and a subcentral siphuncle instead of an eccentric siphuncle as in *Theoceras*. Moreover, the septal necks of the new genus do not form a funnel.

Included species. – Only the type species.

***Tenuitheoceras secretum* sp. nov.**
Figure 11X–Z

Holotype. – The specimen in Fig. 11X–Z, PIMUZ 30627, Paläontologisches Institut und Museum der Universität Zürich.

Type horizon and locality. – Pragian, *pireneae* Zone; Seheb El Rhassel Group, Jebel Ouaoufilal (Filon 12), Tafilalt, Morocco.

Material. – Holotype: phragmocone fragment (PIMUZ 30627) from Jebel Ouaoufilal (Filon 12), Tafilalt, Morocco.

Etymology. – *Secretum* (Latin) – clandestine, secret, lurking: referring to the fact that this species did not reveal its traits superficially.

Diagnosis. – See generic diagnosis.

Description. – The holotype PIMUZ 30627 measures 28.7 mm. Slender and orthoconic shape with compressed conch cross-section with the maximum diameter of 13.3 mm, angle of expansion approx. 6°. Shell ornamented with 4 faint transverse striae per 1 mm. Three chambers are well preserved; the maximum distance between two septa is 4.3 mm in the most adapical chamber and the smallest distance 3.9 mm in the second chamber. Siphuncle subcentral with distances of 5.8 mm dorsal and 4.9 mm ventral from the conch margin. Septal necks are orthochoanitic, relatively long, length of the longest septal neck 1.4 mm in the most adapical chamber. Diameter of septal perforation is 1.1 mm.

Occurrence. – Only the holotype from the Tafilalt of Morocco is known.

Family Arionoceratidae Dzik, 1984

Genus *Arionoceras* Barskov, 1966

Type species. – *Orthoceras canonicum* Meneghini, 1857 by subsequent designation; Wenlock, Silurian; Cea di San Antonio, Fluminimaggiore, Sardinia, Italy.

***Arionoceras kennethdebaetsi* sp. nov.**
Figure 11AC, AD

Holotype. – The phragmocone fragment PIMUZ 30629 (Fig. 11AC, AD), Paläontologisches Institut und Museum der Universität Zürich.

Type horizon and locality. – Pragian, *pireneae* Zone; Seheb El Rhassel Group, Jebel Ouaoufilal (Filon 12), Tafilalt, Morocco.

Material. – Only the holotype (PIMUZ 30629) from the Jebel Ouaoufilal (Filon 12), Tafilalt, Morocco.

Etymology. – Species named after the Kenneth De Baets, honouring his contributions to research on Palaeozoic cephalopods.

Diagnosis. – Orthoconic conchs with circular conch cross-section. Shell ornamentation with transverse striae is forming a deep sinus. Angle of expansion approx. 6°, septal distance approx. 0.34 of the conch diameter. Siphuncle central, short septal necks approx. 0.23 of the septal distance, suborthochoanitic. Diameter of septal perforation approx. 0.1 of conch cross-section, bigger than length of septal necks.

Description. – The maximum fragment length of the holotype (PIMUZ 30629) is 27.5 mm. Orthoconic conch, circular cross-section with the largest diameter 24.8 mm, angle of expansion approx. 6°. Fine transverse striae form a deep sinus, 4 striae per 1 mm, sutures straight. Three chambers are preserved, the highest septal distance measures 8.0 mm in the two most adapical chambers. Siphuncle central, small septal necks, suborthochoanitic, 1.8 mm long, septal perforation 2.2 mm in diameter.

Remarks. – *Arionoceras kennethdebaetsi* sp. nov. resembles *A. capillosum* Barrande, 1867 in having a similar angle of expansion, the same chamber/conch diameter ratio, the same septal perforation/conch diameter ratio and septal

neck morphology. But *A. kennethdebaetsi* sp. nov. differs from *A. capillosum* in having a much deeper sinus. The newly described species has been found in the Pragian stage and is the youngest *Arionoceras* species of Morocco so far.

Occurrence. – Only the holotype from the Tafilalt of Morocco is known.

Family Geisonoceratidae Zhuravleva, 1959

Genus *Angeisonoceras* Kröger, 2008

Type species. – *Orthoceras davidsoni* Barrande, 1870; Upper Silurian; Lochkov, Bohemia, Czech Republic.

***Angeisonoceras reteornatum* Kröger, 2008**
Figure 11AE, AF

Holotype. – The specimen MB.C.9946 is in the Museum für Naturkunde Berlin.

Type horizon and locality. – Pragian; bed KMO-II, Filon 12 section, Tafilalt, Morocco.

Material. – 11 phragmocone fragments (PIMUZ 30593, PIMUZ 30630) from the Pragian, Jebel Ouaoufilal, Tafilalt, Morocco.

Diagnosis. – See Kröger (2008).

Description. – The phragmocone fragment PIMUZ 30630 is 35.0 mm long, orthoconic, slightly acuminate, with a circular conch cross-section. The maximum diameter at the most abapical part of the phragmocone is 19.9 mm; the minimum diameter at the most adapical septum is 17.8 mm, angle of expansion approx. 5°. Ornamented shell with 5 oblique transverse ridges per 1.0 mm, interrupted by smooth longitudinal striae. Five chambers are preserved with a measurable septal distance of 5.7 mm at the most adapical chamber. Siphuncle subcentral, with a siphuncle diameter of 2.0 mm at the adapical part of the fragment.

Occurrence. – The species is only known from the Tafilalt of Morocco.

Order Oncocerida Flower, *in* Flower & Kummel (1950)
Family Nothoceratidae Fischer, 1882

Genus *Tafilaltoceras* Kröger, 2008

Type species. – *Tafilaltoceras adgoi* Kröger, 2008 by original designation; Pragian, Early Devonian; Filon 12, Tafilalt, Morocco.

***Tafilaltoceras adgoi* Kröger, 2008**
Figure 11E, F

Holotype. – Specimen MB.C.9634, Museum für Naturkunde Berlin.

Type horizon and locality. – Pragian; bed KMO-I, Filon 12 section, Tafilalt, Morocco.

Material. – 1 phragmocone fragment (PIMUZ 30615) from Jebel Ouaoufilal, Tafilalt, Morocco.

Diagnosis. – Emended after Kröger (2008): Cyrtoconic shell expanding with slightly depressed conch cross-section; angle of expansion approx. 12 to 14°. Straight septa; slightly concave. Siphuncle marginally, at the convex side of the shell; siphuncular diameter approx. 0.1 of conch cross-section, suborthochoantic septal necks, diameter of septal perforation approx. 0.16 of conch diameter.

Description. – Phragmocone fragment PIMUZ 30615 is 85.0 mm long with cyrtoconic shell and slightly oval conch cross-section. The maximum observed conch diameter measures 39.4 mm and the smallest diameter 19.5 mm, angle of expansion is approx. 14°. Shell ornamentation is not visible, because the specimen is completely encrusted by tabulate corals and a crinoid holdfast (Fig. 11E). 20 chambers are preserved, which display straight sutures; the smallest septal distance at the most adapical chamber is 2.9 mm and the largest septal distance at a diameter of 30.8 mm. Siphuncle on the convex side of the conch, siphuncle diameter 3.0 mm at the aboral side and 4.9 mm at the adoral side.

Remarks. – The shell ornamentation of *Tafilaltoceras adgoi* is still uncertain. The holotype found by Kröger (2008) and our new specimen (PIMUZ 30615) are extremely encrusted by epizoans. The species is emended with regard to the variability of the angle of expansion. In contrast to the holotype (angle of expansion: 12°), the new material reveals an angle of expansion of 14°.

Occurrence. – Pragian, Tafilalt, Morocco.

Phylum Echinodermata Klein, 1734
Class Crinoidea Miller, 1821
Subclass Camerata Wachsmuth & Springer, 1885
Order Monobathrida Moore & Laudon, 1943
Suborder Compsocrinina Ubaghs, 1978

Bulletin of Geosciences • Vol. 89, 1, 2014

Superfamily Hexacrinitacea Wachsmuth & Springer, 1885
Family Hexacrinitidae Wachsmuth & Springer, 1885

***Hexawacrinus* gen. nov.**

Type species. – *Hexawacrinus claudiakurtae* gen. et sp. nov., designated herein; Pragian, Early Devonian, Jebel Ouaoufilal (Filon 12), Tafilalt, Morocco.

Definition of genus. – Monocyclic calyx with conical shape, smooth plates, 3 basals in the first row, 6 plates (5 radials and 1 anal plate?) in the second row. Length of basals approx. 0.6 of radial lengths, hexagonal. The radials are the biggest plates, heptagonal and hexagonal plates are alternating. The following primibrachs are smaller than basals and radials, approx. 0.48 of the size of the radials, hexagonal, higher in width than in length. The branches are connected to the primibrachs, contact point on the primibrachs is weakly developed. Two rows of interprimibrachs, small, second row interprimibrachs are the smallest plates, hexagonal. Sutures between plates are strongly developed.

Remarks. – The new genus differs from *Hexacrinites* Austin & Austin, 1843 in lacking contact points for branches at the anterior parts of the radials. The specimen shows some affinity to *Wacrinus caseyensis* Jell & Jell, 1999. The sequence of the basals, radials, primibrachs and interprimibrachs is the same. Moreover, in both species, the contact points for the branching sclerites are situated at the same position, namely at the anterior parts of the primibrachs. However, the proportions of the plates strongly differ (*e.g.* basals are bigger and reach a higher level) and the plates are more symmetric than in *Wacrinus*. The general calyx shape is rather conical than subspherical.

Included species. – Only the type species.

***Hexawacrinus claudiakurtae* sp. nov.**
Figure 12E–G

Holotype. – The specimen (PIMUZ 30636) is figured in Fig. 12E, F and is housed in the Paläontologisches Institut und Museum der Universität Zürich.

Type horizon and locality. – Pragian, *pireneae* Zone; Seheb El Rhassel Group, Jebel Ouaoufilal (Filon 12), Tafilalt, Morocco.

Material. – The calyx fragment PIMUZ 30636 has been found at the Jebel Ouaoufilal in the eastern Tafilalt of Morocco.

Etymology. – The species is named after the finder Claudia Kurt (Basel), who kindly donated the specimen.

Diagnosis. – As for genus.

Description. – The calyx fragment PIMUZ 30636 is 13.0 mm long and 12.6 mm wide and has a slightly conical shape. All three basal plates are hexagonal and of similar shape and size. Their length is in between 3.6 mm and 3.8 mm and reach approx. 0.6 of the length of the following radial plates. Their maximum width is between 5.9 mm and 6.1 mm. In the second row, just three plates are completely preserved. They are the biggest plates of the calyx with similar size: length: 5.5 to 5.9 mm; width: 5.0 to 5.5 mm; they have an alternating heptagonal or hexagonal shape. All of them might be affiliated to radials. Two primibrachs are visible that are following two different radials. They are 2.4 mm in length and 3.9 mm in width, symmetric and hexagonal. They abut radials and interprimibrachs. One of the primibrachs shows a slight concave depression at the anterior margin and might be a potential contact point for a secundibrach. Two interprimibrachs on the first level are present. They are 2.9 to 3.3 mm long and 2.9 to 3.4 mm wide, hexagonal, slightly smaller than the primibrachs. Their margins abut radials, primibrachs and two interprimibrachs on the second level. Just two second row interprimibrachs are preserved. They are the smallest plates of the fragment, hexagonal and symmetric, 1.8 mm long and 1.9 mm wide.

Occurrence. – A single specimen of Pragian age has been found at the Jebel Ouaoufilal in the eastern Tafilalt of Morocco. Other occurrences are not known.

Figure 12. Hederelloids, crinoids, tabulate and rugose corals from the Pragian of the Jebel Ouaoufilal in the Tafilalt. • A–D – *Filihernodia buccina* gen. et sp. nov. Taylor & Wilson; A – large colony on a nautiloid, × 2; PIMUZ 30612; B–D – detail views of a small colony on a nautiloid, produced by a scanning electron microscope (SEM), B × 20 and C, D × 40; NHMUK PI BZ 7494. • E–G – *Hexawacrinus claudiakurtae* gen. et sp. nov.; lateral and basal views of calyx fragment, × 2; PIMUZ 30636. • H – *Tiaracrinus moravicus* Ubaghs & Bouček, 1962; lateral view of the radial plate of the calyx, × 2; PIMUZ 30637. • I, J – *Cleistopora* cf. *geometrica* Milne-Edwards & Haime, 1851; view on three corallites and bottom, × 1; PIMUZ 30638. • K, L – *Proclevia* sp.; view on corallites and bottom side, × 1; PIMUZ 30639. • M–O – Favositidae Dana, 1846; M – lateral view, × 1; PIMUZ 30640; N, O – top and lateral view, × 1; PIMUZ 30641. • P, Q – unidentified tabulate coral; top and bottom view, × 1; PIMUZ 30642. • R – *Aulopora* sp.; small corallites on a hyolithid, × 2; PIMUZ 30643. • S – unidentified rugose coral; lateral view on a corallite, × 1.5; PIMUZ 30644.

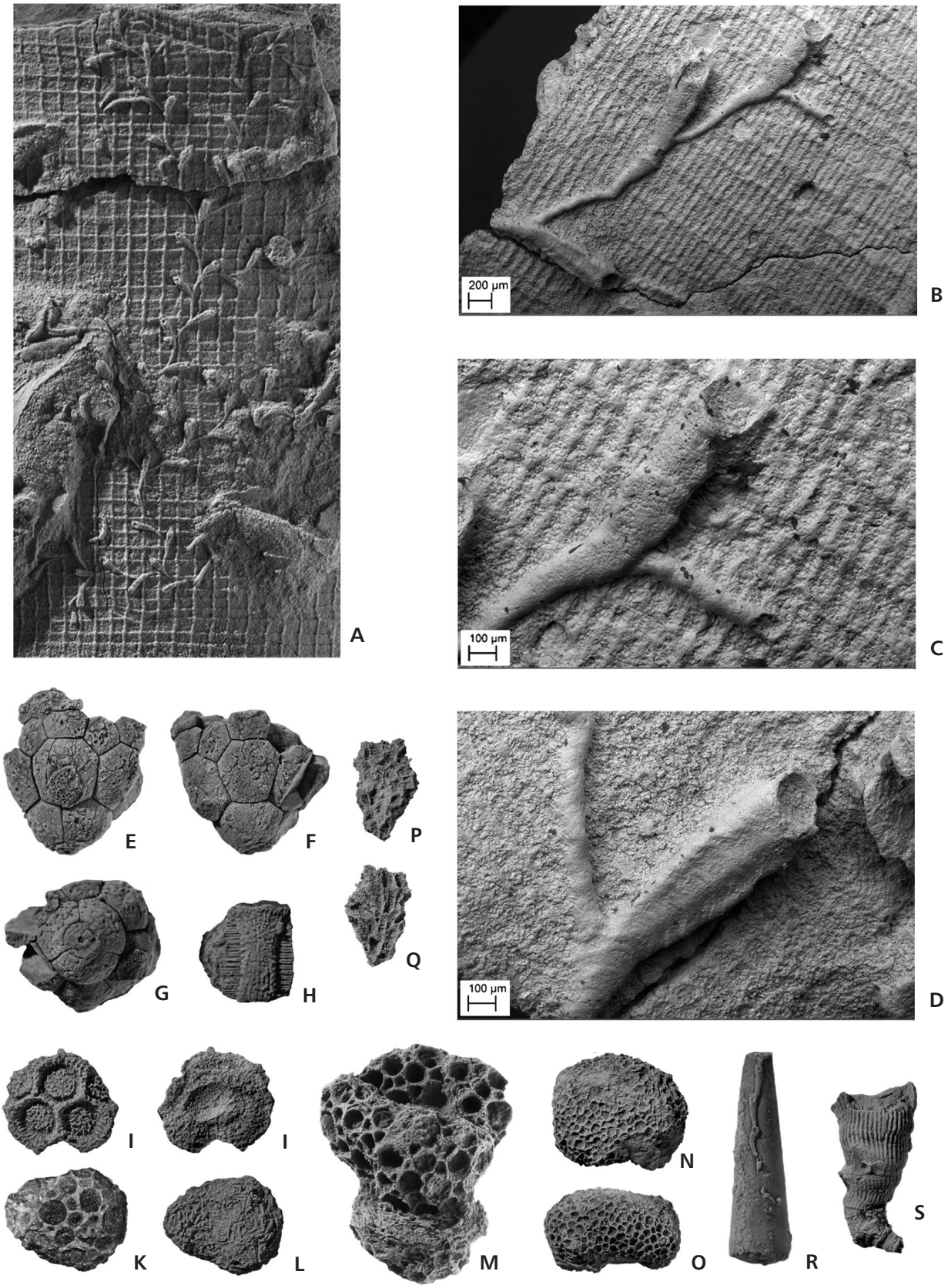
A
200 µm
B
100 µm
C
100 µm
D
E
F
P
G
H
Q
I
I
K
L
M
N
O
R
S

Bulletin of Geosciences • Vol. 89, 1, 2014

Subclass Disparida Moore & Laudon, 1943
Order Cladida Moore & Laudon, 1943
Suborder Compsocrinina Ubaghs, 1978
Superfamily Belemnocrinacea S.A. Miller, 1892
Family Zophocrinidae S.A. Miller, 1892

Genus *Tiaracrinus* Schultze, 1866

Type species. – *Tiaracrinus quadrifrons* Schultze, 1866; Eifelian, Middle Devonian; Freilingen Formation, Nollenbach Member, Eifel, Germany.

***Tiaracrinus moravicus* Ubaghs & Bouček, 1962**
Figure 12H

Holotype. – Specimen BR 362, stored in the National Museum of Prague, Czech Republic.

Type horizon and locality. – Emsian, Lower Devonian; Plumlov, Moravia, Czech Republic.

Material. – A cup fragment (PIMUZ 30637) collected from the Jebel Ouaoufilal, Tafilalt, Morocco.

Diagnosis. – After Hauser (2008): Elongate conical calyx, with reduced, longitudinally oval radial rib field, 4 oval radials with epispiral ridges and grooves and bulging three-part radial ring.

Description. – The maximum length of the fragment PIMUZ 30637 is 7.8 mm and the maximum width is 6.4 mm. The radial is large, has an ornamented surface displaying irregular ridges and bulges; its outline is rectangular to slightly oval in shape, slightly convex with epispiral ridges and grooves at the margins. There are 13 deep and 12 shallow grooves alternating regularly on the right side of the radial. On the left side, 14 deep grooves and 8 smaller grooves are visible. The radial becomes distally wider and displays 4 weak ridges.

Remarks. – In contrast to the type material, the here described new material, which consist of one radial plate, preserves the skeletal material and thus the surface ornamentation. The assignment to *Tiaracrinus moravicus* is based on the shape of the radial with the oval radial rib fields and the broad radial channels. Between the radial rib fields, the sclerite's surface displays an ornamentation of fine ribs, tubercles and nodes. In this respect, it resembles *T. oehlerti*, which has been suggested to be conspecific by Hauser (2008) and as sister species by Klug *et al.* (2013). Since the new Moroccan material displays the morphology of the outside of the radial, it can now be concluded that (1) *T. moravicus* and *T. oehlerti* are not conspecific and should be kept as separate species, (2) the two species are indeed sister species, which (3) is now corroborated by the coeval occurrence of the two species, which are clearly older than four other species of *Tiaracrinus* (*T. rarus*, *T. jeanlemenni*, *T. tetraedra*, *T. quadrifrons*). The here described new specimen represents the first record of *T. moravicus* from Africa.

Occurrence. – An Emsian specimen has been found in Plumlov, Moravia, Czech Republic and a Pragian specimen is here described from the Jebel Ouaoufilal, Tafilalt, Morocco.

Phylum *Incertae sedis*
Suborder Hederelloidea Bassler, 1939

Remarks. – Hederelloids are among the most common encrusting sclerobionts on Devonian hard substrates. Although traditionally considered as cyclostome bryozoans (*e.g.*, Bassler 1953 in the bryozoan *Treatise*), they differ from cyclostomes and bryozoans in several important respects. Notably, hederelloid walls have a prismatic microstructure and the zooids are often larger than those found in any unequivocal bryozoans. Taylor & Wilson (2008) reconsidered the affinities of these colonial animals, noting similarities in zooidal budding pattern to that of the colonial phoronid worm *Phoronis ovalis*. Despite the lack of a mineralized skeleton in recent phoronids, the resemblance led these authors to hypothesize that hederelloids were an extinct (Silurian–Permian) clade of colonial phoronids that evolved calcified skeletons.

Family Reptariidae Simpson, 1897

Genus *Filihernodia* Taylor & Wilson gen. nov.

Type species. – *Filihernodia buccina* gen. et sp. nov. Taylor & Wilson; Pragian, Early Devonian; Jebel Ouaoufilal (Filon 12), Tafilalt, Morocco.

Etymology. – Alluding to its similarity with *Hernodia* Hall, 1881, but having zooids that are very narrow proximally, hence *fili* from *filum* meaning "thread, string, filament, fibre".

Genus definition. – Hederelloid with horn-shaped zooids originating as narrow buds mid-way along the lengths of parent zooids, alternately on the left and right sides, except at branch bifurcations, where a pair of daughter zooids is present, one on each side of the parent; new buds diverge at about 60° from parent zooids and broaden distally.

Remarks. – Five genera of hederelloids are currently recognized (Taylor & Wilson 2008). This new genus most closely resembles *Hernodia* but differs in having zooids that are very narrow proximally and broad distally, whereas the zooids of *Hernodia* have a uniform width. Indeed, the threefold increase in width along the zooids of *Filihernodia* is an unusual attribute among hederelloids as a whole. Furthermore, slender zooids of *Filihernodia* rapidly separate from their parent zooids, giving the colony a more gracile morphology than *Hernodia* in which daughter zooids diverge at low angles and tend to adhere to the sides of their parents for some distance before separating. The longitudinal ridges visible on the surfaces of some zooids of *Filihernodia* are lacking in other hederelloids, where transverse growth bands tend to be better developed.

Included species. – Only the type species.

***Filihernodia buccina* sp. nov. Taylor & Wilson**
Figure 12A–D

Holotype. – The specimen (PIMUZ 30612) is figured in Fig. 12A, and is housed in the Paläontologisches Institut und Museum der Universität Zürich.

Type horizon and locality. – Pragian, *pireneae* Zone; Seheb El Rhassel Group, Jebel Ouaoufilal (Filon 12), Tafilalt, Morocco.

Material. – Holotype: PIMUZ 30612 (large colony in Zurich). Paratype: NHMUK PI BZ 7494 (small specimen scanned at the NHM) in Fig. 12B, C. Both specimens have been found at the Jebel Ouaoufilal (Filon 12) in the Tafilalt of Morocco.

Etymology. – *Buccina*, L. for shepherd's horn, in reference to the shape of the zooids.

Diagnosis. – As for genus.

Description. – Colony (NHMUK PI BZ 7494) encrusting, uniserial, runner-like, comprising slender, gently sinuous, bifurcating branches formed of zooids budded approximately mid-length on the side of a zooid from the preceding generation, alternately to the left and the right and diverging at up to 60°. Branch bifurcation is infrequent, arising from budding of paired daughter zooids on the two opposite sides of a parent zooid, which is straighter than normal, the two branches diverging initially at about 90°. Early astogeny is unknown.

Zooids tubular, horn-shaped, curved through an angle of up to about 45°, narrow proximally, gradually broadening distally towards the terminal aperture. Total zooid length 2.5–3.5 mm, proximal width about 0.12–0.14 mm, distal width 0.38–0.46 mm. Walls non-porous, marked by faint transverse growth lines and up to three, low longitudinal ridges in some zooids. Aperture is subcircular and about 0.26–0.28 mm in diameter.

Remarks. – As noted above, this new genus and species most closely resembles *Hernodia*, which Bassler (1939) distinguished from other hederelloids on the basis of its elongate, club-shaped zooids budding alternately from about the middle of the sides of the preceding zooids. Bassler (1939) described eight species of *Hernodia* from the Silurian-Devonian of the United States, noting two further species from the Silurian and Devonian of Bohemia. One named and one questionable species of *Hernodia* were subsequently described from the Devonian of Germany (Solle 1952, 1968).

Compared to species of *Hernodia*, *F. buccina* has colonies of a more gracile appearance, with long, narrow zooids that diverge from their parent zooids at relatively high angles. Species such as *H. tennesseensis* Bassler, 1935 and *H. concinna* Bassler, 1935, by contrast, have low angles of bud divergence, resulting in the new buds being aligned subparallel and often initially adherent to the parent zooid. In terms of zooid size, *F. buccina* is most similar to *H. davisi* Bassler, 1935 from the Hamilton Group of the Falls of the Ohio, but zooids of this species maintain an almost constant width along their lengths.

Occurrence. – The species is only known from the Pragian of the Jebel Ouaoufilal in the Tafilalt (Morocco).

Acknowledgements

We greatly appreciate the support by the Swiss National Science Foundation (Project No. 200021–113956/1, 200020–25029, and 200020–132870). Jens Koppka (Porrentruy) kindly checked our determinations of the trilobites. Joachim Hauser (Bonn) helped with the determination of the new crinoid species. We thank the students of the University of Zurich who joined the palaeontological fieldwork course 2012 in Morocco and helped to collect the fossil material included in the study. Participation of Jiří Frýda was supported by the Grant Agency of the Czech Republic (P210/12/2018).

References

Alberti, G.K.B. 1969. Trilobiten des jüngeren Siluriums sowie des Unter- und Mitteldevons; I. Mit einigen Beiträgen zur Silur-Devon Stratigraphie einiger Gebiete Marokkos und Oberfrankens. *Abhandlungen der Seckenbergischen naturforschenden Gesellschaft 520*, 1–692.

Alberti, G.K.B. 1980. Neue Daten zur Grenze Unter-/Mittel-

Devon, vornehmlich aufgrund der Tentaculiten und Trilobiten im Tafilalt (Marrokko). *Neues Jahrbuch für Geologie und Paläontologie, Monatshefte 1980*, 581–594.

Alberti, G.K.B. 1981. Daten zur stratigraphischen Verbreitung der Nowakiidae (Dacryoconarida) im Devon von NW-Afrika (Marokko, Algerien). *Senckenbergiana lethaea 62*, 205–216.

Alberti, G.K.B. 1983. Trilobiten des jüngeren Siluriums sowie des Unter- und Mittel-Devons; IV. *Senckenbergiana lethaea 61(1)*, 1–87.

Ausich, W.I. & Bottjer, D.J. 1982. Tiering in suspension-feeding communities on soft substrata throughout the Phanerozoic. *Science New Series 216(4542)*, 173–174.

Austin, T. & Austin, T. Jr. 1843. A Description of several new genera and species of Crinoidea. *Annals and Magazine of Natural History (series 1) 11(69)*, 195–207.

Barrande, J. 1846. *Notice préliminaire sur le système silurien et les trilobites de Bohême.* 86 pp. Hirschfeld, Leipzig. DOI 10.5962/bhl.title.9141, DOI 10.5962/bhl.title.9142

Barrande, J. 1866. *Système silurien du centre de la Bohême, I. Partie, Vol. II: Céphalopodes 2*. Pl. 108–244. Privately published, Prague & Paris.

Barrande, J. 1867. *Système silurien du centre de la Bohême, I. Partie, Vol. II: Céphalopodes 1*. 712 pp. Privately published, Prague & Paris.

Barrande, J. 1868. *Système silurien du centre de la Bohême, I. Partie, Vol. II: Céphalopodes 3.* Pl. 245–350. Privately published, Prague & Paris.

Barrande, J. 1870. *Système silurien du centre de la Bohême, I. Partie, Vol. II: Céphalopodes 4.* Pl. 351–460. Privately published, Prague & Paris.

Barrande, J. 1881. *Système silurien du centre de la Bohême. Classe des Mollusques, ordre des Acéphalés 6.* 342 pp. Privately published, Prague & Paris.

Barskov, I.S. 1963. System and phylogeny of the Pseudorthoceratids. *Byulleten Moskovskogo obshchevestva ispytatelei prirody, Otdel geologicheskii 38(4)*, 149–150.

Barskov, I.S. 1966. *Cephalopods of the Late Ordovician and Silurian of Kazakhstan and Middle Asia. Autoreferat dissertatcii na soiskanie utchenoyi stepeni kandidata geologicheskii mineralogicheskii nauka.* 200 pp. Izdatel'stvo Moskovskogo Universiteta, Moscow.

Bassler, R.S. 1935. Bryozoa (generum et gentyporum index et bibliographia). *Fossilium Catalogus. I: Animalia Pars 67*, 1–229.

Bassler, R.S. 1939. The Hederelloidea, a suborder of Paleozoic cyclostomatous Bryozoa. *Proceedings of the United States National Museum 87*, 25–91. DOI 10.5479/si.00963801.87-3068.25

Bassler, R.S. 1953. Bryozoa, G1–G253. *In* Moore, R.C. (ed.) *Treatise on Invertebrate Paleontology, Part G*. Geological Society of America and University of Kansas Press, Lawrence.

Becker, R.T. & House, M.R. 1994. International Devonian goniatite zonation, Emsian to Givetian, with new records from Morocco. *Courier Forschungsinstitut Senckenberg 169*, 79–135.

Becker, R.T. & House, M.R. 2000. Emsian and Eifelian ammonoid succession at Bou Tchrafine (Tafilalt platform, Anti-Atlas, Morocco), 21–26. *In* El Hassani, A. & Tahiri, A. (eds) *Moroccan meeting of the Subcommision on Devonian Stratigraphy (SDS) – IGCP 421 Excursion Guidebook, Notes et Mémoirs du Service Géologique 399*.

Belka, Z., Kaufmann, B. & Bultynck, P. 1997. Conodont-based quantitative biostratigraphy for the Eifelian of the eastern Anti-Atlas, Morocco. *Geological Society of American Bulletin 109*, 643–651. DOI 10.1130/0016-7606(1997)109<0643.

Belka, Z., Klug, C., Kaufmann, B., Korn, D., Döring, S., Feist, R. & Wendt, J. 1999. Devonian conodont and ammonoid succession of the eastern Tafilalt (Ouidane Chebbi section), Anti-Atlas, Morocco. *Acta Geologica Polonica 49(1)*, 1–23.

Blodgett, R.B., Frýda, J. & Racheboeuf, P.R. 1999. Upper Middle Devonian (Givetian) gastropods from the Kersiadou Formation, Brittany, France. *Journal of Paleontology 73(6)*, 1081–1100.

Blodgett, R.B., Rohr, D.M. & Boucot, A.J. 1988. Lower Devonian gastropod biogeography of the Western Hemisphere, 281–294. *In* McMillan, N.J., Embry, A.F. & Glass, D.J. (eds) *Devonian of the World. Canadian Society of Petroleum Geologists Memoir 14(3)*.

Blodgett, R.B., Rohr, D.M. & Boucot, A.J. 1990. Early and Middle Devonian biogeography, 277–284. *In* McKerrow, W.S. &. Scotese, C.D. (eds) *Palaeozoic Palaeogeography and Biogeography. Geological Society Memoir 12*.

Bottjer, D.J. & Ausich, W.I. 1986. Phanerozoic development of tiering in soft substrata suspension-feeding communities. *Paleobiology 12(4)*, 400–420.

Bouchet, P., Rocroi, J. P., Frýda, J., Hausdorf, B., Ponder, W., Valdes, A. & Warén, A. 2005. Classification and nomenclator of gastropod families. *Malacologia 47*, 1–368.

Brachert, T.C., Buggisch, W., Flügel, E., Hüssner, H., Joachimski, M.M., Tourneur, F. & Walliser, O.H. 1992. Controls of mud mound formation: the Early Devonian Kess-Kess carbonates of the Hamar Laghdad, Anti-Atlas, Morocco. *Geologische Rundschau 81*, 15–44. DOI 10.1007/BF01764537

Brongniart, A. 1822. Les Trilobites, 1–65. *In* Brongniart, A. & Desmarest, A.G. (eds) *Histoire naturelle des crustacés fossiles, sous les rapports zoologiques et géologiques*. F.G. Levrault, Paris & Strasbourg.

Bultynck, P. & Walliser, O.H. 2000a. Emsian to Middle Frasnian sections in the northern Tafilalt, 11–20. *In* El Hassani, A. & Tahiri, A. (eds) *Moroccan meeting of the Subcommision on Devonian Stratigraphy (SDS) – IGCP 421 Excursion Guidebook, Notes et Mémoires du Service Géologique 399.*

Bultynck, P. & Walliser, O.H. 2000b. Devonian boundaries in the Moroccan Anti-Atlas. *Courier Forschungsinstitut Senckenberg 225*, 211–226.

Bush, A.M., Bambach, R.K. & Daley, G.M. 2007. Changes in theoretical ecospace utilization in marine fossil assemblages between the mid-Paleozoic and late Cenozoic. *Paleobiology 33(1)*, 76–97. DOI 10.1666/06013.1

Chlupáč, I., Galle, A., Hladil, J. & Kalvoda, J. 2000. Series and stage boundaries in the Devonian of the Czech Republic. *Courier Forschungsinstitut Senckenberg 225*, 159–172.

Chlupáč, I. & Kukal, Z. 1988. Possible global events and the stratigraphy of the Palaeozoic of the Barrandian (Cambrian-Middle Devonian, Czechoslovakia). *Sborník geologických věd, Geologie 43*, 83–146.

Chlupáč, I. & Kukal, Z. 1996. Reflection of possible global De-

vonian events in the Barrandian area, C.S.S.R, 169–179. *In* Walliser, O.H. (ed.) *Global Bio-events, a critical approach. Lecture Notes on Earth Sciences 8*.

Clariond, L. 1934a. Sur le Dévonien du Tafilalet et du Maroc. *Compte rendu sommaire des séances de la Société Géologique de France 1934*, 5–11.

Clariond, L. 1934b. A propos d'une coupe de la région d'Erfoud. *Compte rendu sommaire des séances de la Société Géologique de France 1934*, 223–224.

Corriga, M.G., Corradini, C., Haude, R. & Walliser, O.H. 2013. Upper Silurian and Lower Devonian conodonts and crinoids from the scyphocrinoid beds of southeastern Morocco, 71–72. *In* Lindskog, A. & Mehlqvist, K. (eds) *Proceedings of the 3rd IGCP 591 Annual Meeting, Lund, Sweden*.

Cox, L.R. 1960. Gastropoda. General characteristics of Gastropoda, I84–I169. *In* Moore, R.C. (ed.) *Treatise on Invertebrate Paleontology, Part I, Mollusca 1*. Geological Society of America & University of Kansas Press, Boulder & Lawrence.

Cuvier, G. 1797. *Tableau élémentaire de l'histoire naturelle des animaux*. 710 pp. Baudouin, Paris.

Dana, J.D. 1846. *Structure and classification of zoophytes: U.S. Exploring Expedition during the years 1838–1842 under the command of Charles Wilkes, U.S.N. 7*. 740 pp. Lea & Blanchard, Philadelphia.

De Baets, K., Klug, C. & Monnet, C. 2013. Intraspecific variability through ontogeny in early ammonoids. *Paleobiology 39(1)*, 75–94. DOI 10.1666/0094-8373-39.1.75

De Baets, K., Klug, C. & Plusquellec, Y. 2010. Zlíchovian faunas with early ammonoids from Morocco and their use for the correlation between the eastern Anti-Atlas and the western Dra Valley. *Bulletin of Geosciences 85(2)*, 317–352. DOI 10.3140/bull.geosci.1172

Donovan, S.K. & Webster, G.D. 2013. Platyceratid gastropod infestations of Neoplatycrinus Wanner (Crinoidea) from the Permian of West Timor: speculations on thecal modifications. *Proceedings of the Geologists' Association*. DOI 10.1016/ j.pgeola.2013.01.004

Döring, A. 2002. *Sedimentological Evolution of the late Emsian to early Givetian carbonate ramp in the Mader (eastern Anti-Atlas, SE-Morocco).* 80 pp. Ph.D. thesis, Eberhard-Karls-Universität, Tübingen, Germany.

Dzik, J. 1984. Phylogeny of the Nautiloidea. *Palaeontologia Polonica 45*, 1–203.

Eldredge, N. 1971. Patterns in cephalic musculature in the Phacopina (Trilobita) and their phylogenetic significance. *Journal of Palaeontology 45*, 52–67.

Etheridge, R. 1890. Descriptions of Upper Silurian fossils from the Lilydale Limestone, Upper Yarra District, Victoria. *Records of the Australian Museum 1(1)*, 60–67. DOI 10.3853/j.0067-1975.1.1890.1227

Etheridge, R. 1891. Further descriptions of the Upper Silurian fossils from the Lilydale Limestone, Upper Yarra District, Victoria. *Records of the Australian Museum 1(7)*, 125–130. DOI 10.3853/j.0067-1975.1.1891.1244

Ferreti, A., Gnoli, M. & Vai, G.B. 1999. Silurian to Lower Devonian communities of Sardinia, 271–281. *In* Boucot, A.J. & Lawson, J.D. (eds) *Paleocommunities – a case study from the Silurian and Lower Devonian*. Cambridge University Press, Cambridge.

Fischer, P. 1882. *Manuel de conchyliologie et de paléontologie conchyliologique ou histoire naturelle des mollusques vivants et fossiles, I. Partie: Synopsis des genres*, 327–418. Savy, Paris.

Flower, R.H. & Caster, K.E. 1935. The cephalopod fauna of the Conewango Series of the Upper Devonian in New York and Pennsylvania. *Bulletins of American Paleontology 22(75)*, 1–74.

Flower, R. H & Kummel, B. 1950. A classification of the Nautiloidea. *Journal of Paleontology 24*, 604–616.

Fortey, R.A. & Owens, R.M. 1999. Feeding habits in trilobites. *Palaeontology 42(3)*, 429–465. DOI 10.1111/1475-4983.00080

Franchi, F., Schemm-Gregory, M. & Klug, C. 2012. A new species of *Ivdelinia* Andronov, 1961 and its palaeoecological and palaeobiogeographical implications (Morocco, Givetian). *Bulletin of Geosciences 87(1)*, 1–11. DOI 10.3140/bull.geosci.1294

Fröhlich, S. 2004. *Evolution of a Devonian carbonate shelf at the northern margin of Gondwana (Jebel Rheris, eastern Anti-Atlas, Morocco)*. 71 pp. Ph.D. thesis, Eberhard-Karls-Universität, Tübingen, Germany.

Frýda, J. 1993. Oldest representative of the family Palaeozygopleuridae (Gastropoda) with notes on its higher taxonomy. *Journal of Paleontology 67*, 822–827.

Frýda, J. 1997. Oldest representatives of the superfamily Cirroidea (Vetigastropoda) with notes on their early phylogeny. *Journal of Paleontology 71(5)*, 839–847.

Frýda, J. 1998a. Some new and better recognized Devonian gastropods from the Prague Basin (Bohemia). *Bulletin of the Czech Geological Survey 73(1)*, 41–49.

Frýda, J. 1998b. Some new and better recognized Devonian gastropods from the Prague Basin (Bohemia): part II. *Bulletin of the Czech Geological Survey 73(4)*, 355–363.

Frýda, J. 1999. Further new gastropods from the Early Devonian Boucotonotus – Palaeozygopleura Community of the Prague Basin. *Journal of the Czech Geological Society 44*, 317–325.

Frýda, J. & Bandel, K. 1997. New Early Devonian gastropods from the Plectonotus (Boucotonotus)-Palaeozygopleura Community in the Prague Basin (Bohemia). *Mitteilungen aus dem Geologisch-Paläontologischen Institut der Universität Hamburg 80*, 1–58.

Frýda, J. & Blodgett, R.B. 1998. Two new cirroidean genera (Vetigastropoda, Archaeogastropoda) from the Emsian (late Early Devonian) of Alaska with notes on the early phylogeny of Cirroidea. *Journal of Paleontology 72*, 265–273.

Frýda, J. & Blodgett, R.B. 2004. New Emsian (late Early Devonian) gastropods from Limestone Mountain, Medfra B-4 quadrangle, west-central Alaska (Farewell terrane), and their paleobiogeographic affinities and evolutionary significance. *Journal of Paleontology 78(1)*, 111–132. DOI 10.1666/0022-3360(2004)078<0111:NELEDG>2.0.CO;2

Frýda, J., Ferrová, L., Berkyová, S. & Frýdová, B. 2008. A new Early Devonian palaeozygopleurid gastropod from the Prague Basin (Bohemia) with notes on the phylogeny of the Loxonematoidea. *Bulletin of Geosciences 83(1)*, 93–100. DOI 10.3140/bull.geosci.2008.01.093

Frýda, J., Ferrová, L. & Frýdová, B. 2013. Review of palaeozygopleurid gastropods (Palaeozygopleuridae, Gastropoda)

from Devonian strata of the Perunica microplate (Bohemia), with a re-evaluation of their stratigraphic distribution, notes on their ontogeny, and descriptions of new taxa. *Zootaxa 3669(4)*, 469–489. DOI 10.11646/zootaxa.3669.4.3

Frýda, J. & Manda, Š. 1997. A gastropod faunule from the Monograptus uniformis graptolite Biozone (Early Lochkovian, Early Devonian) in Bohemia. *Mitteilungen aus dem Geologisch-Paläontologischen Institut der Universität Hamburg 80*, 59–122.

Gahn, F.J. & Baumiller, T.K. 2003. Infestation of Middle Devonian (Givetian) camerate crinoids by platyceratid gastropods and its implications for the nature of their biotic interaction. *Lethaia 36*, 71–82. DOI 10.1080/00241160310003072

Gahn, F.J. & Baumiller, T.K. 2006. Using platyceratid gastropod behaviour to test functional morphology. *Historical Biology 18*, 397–404. DOI 10.1080/08912960600668524

García-Alcade, J., Truyóls-Massoni, M., Pardo-Alonso, M., Bultynck, P. & Carls, P. 2000. Devonian chronostratigraphy of Spain. *Courier Forschungsinstitut Senckenberg 225*, 131–144.

Grabau, A.W. & Shimer, H.W. 1909. *North American index fossils: Invertebrates 1*. 853 pp. New York.

Gubanov, A.P. & Yochelson, E.L. 1994. A Wenlockian (Silurian) gastropod shell and operculum from Siberia. *Journal of Paleontology 68*, 486–481.

Hall, J. 1852. Containing descriptions of the organic remains of the lower middle division of the New York system. *Paleontology of New York 2*, 1–362.

Hall, J. 1861. Descriptions of new species of fossils from the Upper Helderberg, Hamilton and Chemung Groups; with observations upon previously described species. *Fourteenth Annual Report of the Regents of the University of the State of New York on the condition of the State Cabinent of Natural History and the Historical and Antiquarian Collection annexed thereto, Albany*, 99–109.

Hall, J. 1881. Bryozoans of the Upper Helderberg and Hamilton groups. *Transactions of the Albany Institute 10*, 145–197.

Hall, J. 1884. Lamellibranchiata, I. Monomyaria of the Upper Helderberg, Hamilton, Portage and Chemung Groups. *New York Geological Survey, Paleontology 5(1)*, 1–268.

Hammer, Ø., Harper, D.A.T. & Ryan, P.D. 2001. PAST: Palaeontological statistics software package for education and data analysis. *Palaeontologia Electronica 4(1)*, 1–9.

Haq, B.U. & Schutter, S.R. 2008. A Chronology of Paleozoic Sea-Level Changes. *Science 322(5898)*, 64–68. DOI 10.1126/science.1161648

Haude, R. 1992. Scyphocrinoiden, die Bojen-Seelilien im hohen Silur-tiefen Devon. *Palaeontographica, Abteilung A 222*, 141–187.

Haude, R. & Walliser, O.H. 1998. Conodont-based Upper Silurian–Lower Devonian range of scyphocrinoids in SE Morocco, 94–96. *In* Gutiérrez-Marco, J.C. & Rábano, I. (eds) *Proceedings of the sixth international graptolite conference of the GWG (IPA) and the SW Iberia field meeting 1998 of the International Subcommission on Silurian Stratigraphy (ICS-IUGS)*. Instituto Tecnológico Geominero de España, Madrid.

Hauser, J. 2008. Revision von Tiaracrinus (Crinoidea, Cladida) aus dem Paläozoikum der Eifel und dem Sauerland (Rheinische Schiefergebirge), Massive Armoricain (Frankreich), Böhmen (Tschechien) und Nord-Afrika (Algerien). *Crinoiden des Devon*, 1–8. http://www.devon-crinoiden.de/tiaracrinus.pdf

Hollard, H. 1967. Le Dévonien du Maroc et du Sahara nord occidental. *International Symposium on the Devonian System, Calgary 1, Canadian Society of Petroleum Geologists 1*, 203–244.

Hollard, H. 1974. Recherches sur la stratigraphie des formations du Dévonien moyen, de l'Emsien supérieur au Frasnien, dans le Sud du Tafilalt et dans le Ma'der (Anti-Atlas oriental, Maroc). *Notes du Service géologique du Maroc 36(264)*, 7–68.

Hollard, H. 1981.Tableaux de Corrélation du Silurien et Dévonien de l'Anti-Atlas. *Notes du Service géologique du Maroc 42(308)*, 23–46.

Horný, R.J. 1955. Palaeozygopleuridae nov. fam. (Gastropoda) ze středočeského devonu. *Sborník Ústředního ústavu geologického, Oddíl paleontologický 21(1)*, 17–74.

Horný, R.J. 1963. Lower Paleozoic Bellerophontina (Gastropoda) of Bohemia. *Sborník geologických věd, Paleontologie 2*, 57–164.

Horný, R. 1992a. New Lower Devonian gastropod genera of Bohemia (Mollusca). *Časopis Národního muzea, Řada přírodovědná 158(1–4)*, 105–107.

Horný, R. 1992b. *Lytospira* Koken a *Murchisonia* (*Hormotomina*) Grabau et Shimer v českém spodním devonu. [*Lytospira* Koken and *Murchisonia* (*Hormotomina*) Grabau et Shimer in the Lower Devonian of Bohemia.] *Časopis Národního muzea, Řada přírodovědná 160(1–4)*, 55–56.

Horný, R.J. 1998. Two additional, isolated, paucispiral gastropod opercula from the Lower Devonian Koněprusy Limestone (Bohemia, Barrandian area). *Journal of the National Museum (Prague), Natural History Series 167 (1–4)*, 91–94.

Jell, P.A. & Jell, J.S. 1999. Crinoids, a blastoid and a cyclocystoid from the Upper Devonian reef complex of the Canning Basin, Western Australia. *Memoirs of The Queensland Museum 43*, 201–236.

Johnson, J.G., Klapper, G. & Elrick, M. 1996. Devonian transgressive-regressive cycles and biostratigraphy, Northern Antelope Range, Nevada: Establishment of reference horizons for global cycles. *Palaios 11*, 3–14. DOI 10.2307/3515112

Johnson, J.G., Klapper, G. & Sandberg, C.A. 1985. Devonian eustatic fluctuations in Euramerica. *Geological Society of America Bulletin 96*, 567–587. DOI 10.1130/0016-7606(1985)96<567:DEFIE>2.0.CO;2

Kaufmann, B. 1998. Facies analysis, stratigraphy and diagenesis of Middle Devonian reef- and mud-mounds in the Mader (eastern Anti-Atlas, Morocco). *Acta Geologica Polonica 48(1)*, 43–106.

Klein, J.T. 1734. *Naturalis dispositio Echinodermatum: Accesseit Lucubratiuncula de aculeis echinorum marinorum, cum Spicilegio de belemnitis*. Typis Thom. Joh. Schreiberi. DOI 10.5962/bhl.title.65731

Klug, C. 2001. Early Emsian ammonoids from the eastern Anti-Atlas (Morocco) and their succession. *Paläontologische Zeitschrift 74(4)*, 479–515. DOI 10.1007/BF02988158

Klug, C. 2002. Quantitative stratigraphy and taxonomy of late Emsian and Eifelian ammonoids of the eastern Anti-Atlas

(Morocco). *Courier Forschungsinstitut Senckenberg 238*, 1–109.

Klug, C. & Korn, D. 2002. Occluded umbilicus in the Pinacitinae (Devonian) and its palaeoecological implications. *The Palaeontological Association 45(5)*, 917–931.

Klug, C., Korn, D., Naglik, C., Frey, L. & de Baets, K. 2013. The Lochkovian to Eifelian succession of the Amessoui Syncline (southern Tafilalt), 51–60. *In* Becker, R.T., El Hassani, A. & Tahiri, A. (eds) *International Field Symposium "The Devonian and Lower Carboniferous of northern Gondwana", Morocco 2013*.

Klug, C., Korn, D. & Reisdorf, A. 2000. Ammonoid and conodont stratigraphy of the late Emsian to early Eifelian (Devonian) at the Jebel Ouaoufilal (near Taouz, Tafilalt, Morocco), 45–56. *In* Tahiri, A. & El Hassani, A. (eds) *Travaux de l'Institut Scientifique, Série Géologie & Géographie Physique 20. Proceedings of the Subcommission on Devonian Stratigraphy (SDS) – IGCP 421 Morocco Meeting*.

Klug, C., Kröger, B., Kiessling, W., Mullins, G. L., Servais, T., Frýda, J., Korn, D. & Turner, S. 2010. The Devonian nekton revolution. *Lethaia 43*, 465–477. DOI 10.1111/j.1502-3931.2009.00206.x

Klug, C., Kröger, B., Korn, D., Rücklin, M., Schemm-Gregory, M., De Baets, K. & Mapes, R.H. 2008a. Ecological change during the early Emsian (Devonian) in the Tafilalt (Morocco), the origin of the Ammonoidea, and the first African pyrgocystid edrioasteroids, machaerids and phyllocarids. *Palaeontographica, Abteilung A 283(4–6)*, 83–176.

Klug, C., Meyer, E., Richter, U. & Korn, D. 2008b. Soft-tissue imprints in fossil and Recent cephalopod septa and septum formation. *Lethaia 41*, 477–492. DOI 10.1111/j.1502-3931.2008.00100.x

Knight, J.B. 1941. Paleozoic gastropod genotypes. *Geological Society of America, Special Paper 32*, 1–510.

Knight, J.B. 1956. New families of Gastropoda. *Washington Academy of Sciences Journal 46*, 41–42.

Koken, E. 1896. *Die Leitfossilien*. 848 pp. Chr. Herm. Trachnitz, Leipzig.

Koken, E. 1889. Über die Entwicklung der Gastropoden vom Kambrium bis zur Trias. *Neues Jahrbuch für Mineralogie, Geologie und Paläontologie, Beilage Band 6*, 305–484.

Koninick, L.G. de 1881. Faune du calcaire carbonifère de Belgique, Pt. 3, Gastéropodes. *Annales du Musée royal d'Histoire naturelle de Belgique, paleontological series 6*, 1–170.

Kříž, J. 1998. Recurrent Silurian-lowest Devonian cephalopod limestone of Gondwanan Europe and Perunica, 183–198. *In* Landing, E. & Johnson, M.E. (eds) *Silurian cycles; linkages of dynamic stratigraphy with atmospheric, oceanic, and tectonic changes. New York State Museum Bulletin 491*.

Kříž, J. 2000. Lochkovian bivalves of Bohemian type from the eastern Anti-Atlas (Lower Devonian, Morocco). *Senckenbergiana lethaea 80(2)*, 485–523.

Kröger, B. 2008. Nautiloids before and during the origin of ammonoids in Siluro-Devonian section in the Tafilalt, Anti-Atlas, Morocco. *Special Papers in Palaeontology 79*, 1–110.

Kuhn, O. 1940. *Paläozoologie in Tabellen*. 50 pp. Fischer Verlag, Jena.

Leveille, C. 1835. Aperçu géologique de quelques localités très riches en coquilles sur les frontières de France et de Belgique. *Mémoires de la Société géologique de France 2(1)*, 29–40.

Lindström, G. 1884. On the Silurian gastropoda and Pteropoda of Gotland. *Kongliga Svenska Vetenskaps Akademiens Handlingar 19(6)*, 1–250.

Linnaeus, C. 1758. *Systema Naturae per Regna Tria Naturae, secundum Classes, Ordines, Genera, Species, cum Characteribus, Differentiis, Synonymis, Locis*. *Tomus I.* 823 pp. Laurentii Salvii, Holmiae (Stockholm).

Lubeseder, S., Redfern, J. & Boutib, L. 2009. Mixed siliciclastic-carbonate shelf sedimentation-Lower Devonian sequences of the SW Anti-Atlas, Morocco. *Sedimentary Geology 215(1–4)*, 13–32. DOI 10.1016/j.sedgeo.2008.12.005

Massa, D., Combaz, A. & Manderscheid, G. 1965. Observations sur les séries siluro-dévoniennes des confins algéro-marocains du Sud. *Notes et Mémoires, Compagnie Française des Pétroles 8*, 1–188.

M'Coy, F. 1844. *A synopsis of the characters of the Carboniferous Limestone fossils of Ireland*. 274 pp. University Press, Dublin. DOI 10.5962/bhl.title.11559

M'Coy, F. 1851. On some new Silurian Mollusca. *Annals and Magazine of History, including Zoology, Botany, and Geology, 2nd series 7*, 45–63.

Meneghini, G. 1857. Paléontologie de l'Ile Sardaigne, 53–144. *In* La Marmora, A. (ed.) *Voyage en Sardaigne*. Imprimerie Royal, Turin.

Milne-Edwards, H. & Haime, J. 1851. *Monographie des Polypiers fossiles des terrains palaeozoïques, précédée d'un tableau général de la classification des polypes*. 502 pp. Gide et J. Baudry, Paris.

Miller, J.S. 1821. *A natural history of the Crinoidea or lily-shaped animals, with observation on the genera Astria, Euryale, Comatula, and Marsupites*. 150 pp. Bryan & Co., Bristol.

Miller, J. 1976. The sensory fields and life mode of *Phacops rana* (Green, 1832). *Transactions of the Royal Society of Edinburgh 69*, 337–367. DOI 10.1017/S0080456800015350

Miller, S.A. 1892. *North American geology and palaeontology. First appendix*, 665–718. Western Methodist Book Concern, Cincinnati.

Moore, R.C. & Laudon, L.R. 1943. Evolution and classification of Paleozoic crinoids. *Geological Society of America, Special Paper 46*, 1–153. DOI 10.1130/SPE46-p1

Munier-Chalmas, E. 1876. Mollusques nouveaux des terrains paléozoiques des environs de Rennes. *Journal de Conchyliologie, 3e series 16*, 102–109.

Neyman, A.A. 1967. Limits to the application of the 'trophic group' concept in benthic studies. *Oceanology, Academy of Sciences of the USSR 7*, 49–155.

Oehlert, D. 1881. Documents pour servir à l'étude des faunes dévoniennes dans l'ouest de la France. *Mémoires de la Société Géologique de France, 3e série 2*, 1–38.

Peel, J. 1984. Faunal succession and mode of life of Silurian gastropods in the Arisaig Group, Nova Scotia. *Palaeontology 21*, 258–306.

Perner, J. 1903. Gastéropodes, 1–164. *In* Barrande, J. (ed.) *Systême silurien du centre de la Bohême 4(1)*. Prague.

Perner, J. 1907. Gastéropodes, 1–380. *In* Barrande, J. (ed.) *Systême silurien du centre de la Bohême 4(2)*. Prague.

Bulletin of Geosciences • Vol. 89, 1, 2014

Piqué, A. & Michard, A. 1989. Moroccan Hercynides: A synopsis. The Paleozoic sedimentary and tectonic evolution at the northern margin of west Africa. *American Journal of Science 289*, 286–330. DOI 10.2475/ajs.289.3.286

Racheboeuf, P.R. 1990. Les Brachiopodes Chonetacés dans les assemblages benthiques siluriens et dévoniens. *Palaeogeography, Palaeoclimatology, Palaeoecology 81*, 141–171. DOI 10.1016/0031-0182(90)90045-9

Říha, A. 1938. Příspěvek k poznání nových plžů ze středočeského paleozoika. *Věstník Královské České společnosti nauk, Třída matematicko-přírodovědecká*, 1–12.

Roch, E. 1934. Sur des phénomènes remarquables observés dans la région d'Erfoud (confins algéro-marocains du Sud). *Association Études de la Géologie Méditerranéenne Occidentale 5*, 1–10.

Rohr, D.M. & Smith, R.E. 1978. Lower Devonian Gastropoda from the Canadian Arctic Islands. *Canadian Journal of Earth Sciences 15*, 1228–1241. DOI 10.1139/e78-131

Sanders, H.L. 1968. Benthic diversity: A comparative study. *American Society of Naturalists 102(925),* 243–282. DOI 10.1086/282541

Saunders, W.B. & Ward, P.D. 1987. Ecology, distribution and population characteristics of *Nautilus*, 135–162. *In* Saunders, W.B. & Landman, N.H. (eds) *The Biology and Paleobiology of a Living Fossil.* Reprinted with additions (2009). Springer, Berlin.

Schönlaub, H.P. 1996. Significant geological events in the Paleozoic record of the Southern Alps (Austrian part), 163–168. *In* Walliser, O.H. (ed.) *Global events and event stratigraphy in the Phanerozoic*. Springer, Berlin.

Schultze, L. 1866. Monographie der Echinodermen des Eifler-Kalkes. *Denkschrift Königlichen Akademie der Wissenschaften., mathematisch-naturwissenschaftlichen Klasse 26,* 113–230.

Scotese, C.R. 1997. *Paleogeographic Atlas*. 37 pp. PALEOMAP Progress Report 90-0497, Department of Geology, University of Texas at Arlington.

Scotese, C.R. & McKerrow, W.S. 1990. Revised world maps and introduction, 1–21. *In* McKerrow, W.S. & Scotese, C.R. (eds) *Palaeozoic Palaeogeography and Biogeography*. *Geological Society of London Memoirs 12*.

Shimizu, S. & Obata, T. 1935. New genera of Gotlandian and Ordovician nautiloids. *Journal of the Shanghai Science Institute, Section 2*, 1–10.

Simpson, G.B. 1897. A handbook of the genera of the North American Paleozoic Bryozoa. *Fourteenth Annual Report of the State Geologist, New York 1894*, 407–608.

Simroth, H. 1906. Versuch einer neuen Deutung der Bellerophontiden. *Sitzungsberichte der Naturforschenden Gesellschaft zu Leipzig 1905*, 3–8.

Solle, G. 1952. Neue Untergattungen und Arten der Bryozoen-Gattung *Hederella* und eine *Hernodia* im rheinischen Unterdevon. *Notizblatt des Hessischen Landesamtes für Bodenforschung zu Wiesbaden 6(3)*, 35–55.

Solle, G. 1968. Hederelloidea (Cyclostomata) und einige ctenostome Bryozoen aus dem rheinischen Devon. *Abhandlungen des Hessischen Landesamtes für Bodenforschung 54*, 1–40.

Südkamp, W.H. & Burrow, C.J. 2007. The acanthodian *Machaeracanthus* from the Lower Devonian Hunsrück Slate of the Hunsrück region (Germany). Systematic palaeontology. *Paläontologische Zeitschrift 81*, 97–104. DOI 10.1007/BF02988383

Talent, J.A., Mawson, R., Andrew, A.S., Hamilton, J. & Whiteford, D.J. 1993. Middle Palaeozoic extinction events: faunal and isotope data. *Palaeogeography, Palaeoclimatology, Palaeoecology 104*, 139–152. DOI 10.1016/0031-0182(93)90126-4

Talent, J.A. & Yolkin, E.A. 1987. Transgression-regression patterns for the Devonian of Australia and southern West Siberia. *Courier Forschungs-Institut Senckenberg 92*, 235–249.

Tassell, C.B. 1980. Further gastropods from the Early Devonian Lilydale Limestone, Victoria. *Records of the Queen Victoria Museum 69*, 1–27.

Tassell, C.B. 1982. Gastropods from the Early Devonian "Receptaculites" Limestone, Taemas, New South Wales. *Records of the Queen Victoria Museum 77*, 1–59.

Taylor, P.D. & Wilson, M.A. 2008. Morphology and affinities of hederelloid "bryozoans", 301–309. *In* Hageman, S.J., Key, M.M., Jr. & Winston, J.E. (eds) *Bryozoan Studies 2007: Proceedings of the 14th International Bryozoology Conference, Boone, North Carolina, July 1–8, 2007. Virginia Museum of Natural History, Special Publication 15*.

Teichert, C., Kummel, B., Sweet, W.C., Stenzel, H.B., Furnish, W.M., Glenister, B.F., Erben, H.K., Moore, R.C. & Zeller, D.E.N. 1964. Endoceratoidea-Actinoceratoidea-Nautiloidea, K13–K124. *In* Moore, R.C. (ed.) *Treatise on Invertebrate Paleontology, Part K, Mollusca 3, Cephalopoda*. Geological Society of America and University of Kansas Pres, Boulder & Lawrence.

Termier, G. & Termier, H. 1950. Paléontologie Marocaine. II. Invertébrés de l'ére Primaire. Fascicule III. Mollusques. *Notes et Mémoires du Service Géologique, Rabat 78*, 1–246.

Toto, E.A., Kaabouben, F., Zouhri, L., Belarbi, M., Benammi, M., Hafid, M. & Boutib, L. 2008. Geological Evolution and structural style of the Palaeozoic Tafilalt sub-basin, eastern Anti-Atlas (Morocco, North Africa). *Geological Journal 43*, 59–73. DOI 10.1002/gj.1098

Ubaghs, G. 1978. Part T Echinodermata 2, T403–T812. *In* Moore, R.C. (ed.) *Treatise on Invertebrate Paleontology, Part T*. Geological Society of America and University of Kansas Press 2, Lawrence.

Ubaghs, G. & Bouček, B. 1962. Sur la présence du genre *Tiaracrinus* Schultze (Crinoidea) dans le Dévonien inférieur de Moravie (*Tiaracrinus moravicus* n. sp.). *Sborník Ústředního ústavu geologického, Oddíl paleontologický 27*, 41–50.

Van Geldern, R., Joachimski, M.M., Day, J., Jansen, U., Alvarez, F., Yolkin, E.A. & Ma, X.-P. 2006. Carbon, oxygen and strontium isotope records of Devonian brachiopod shell calcite. *Palaeogeography, Palaeoclimatology, Palaeoecology 240*, 47–67. DOI 10.1016/j.palaeo.2006.03.045

Verneuil, N. de 1850. Notes sur les fossiles Dévoniens du district de Sabéro (León). *Bulletin de la Société Géologique de France 7(2)*, 155–186.

Wachsmuth, C. & Springer, F. 1885. Revision of the Paleocrinoidea, Part III: Discussion and classification of the brachiate crinoids, and conclusion of the generic description. *Proceedings of the Academy ofNatural Sciences of Philadelphia*, 223–364.

WALKER, K.R. & BAMBACH, R.K. 1971. The significance of fossil assemblages from fine grained sediments: Time-averaged communities. *Geological Society of America Abstracts with Programs 3*, 783–784.

WALLISER, O.H. 1984. Global events, event-stratigraphy and "chronostratigraphy" within the Phanerozoic, 208. *In* BOGDANOV, N.A. (ed.) *27th International Geological Congress. Abstracts*, *section 1*.

WALLISER, O.H. 1985. Natural boundaries and Commission boundaries in the Devonian. *Courier Forschungsinstitut Senckenberg 75*, 401–408.

WEBSTER, G.D. & DONOVAN, S.K. 2012. Before the extinction – Permian platyceratid gastropods attached to platycrinitid crinoids and an abnormal four-rayed *Platycrinites wachsmuthi* (Wanner) from West Timor. *Palaeoworld 21(3–4)*, 153–159. DOI 10.1016/j.palwor.2012.08.001

WENDT, J. 1985. Disintegration of the continental margin of northwestern Gondwana: Late Devonian of the eastern Anti-Atlas (Morocco). *Geology 13*, 815–818. DOI 10.1130/0091-7613(1985)13<815:DOTCMO>2.0.CO;2

WENDT, J. 1988. Facies pattern and paleogeography of the Middle and Late Devonian in the eastern Anti-Atlas (Morocco), 467–479. *In* MCMILLAN, J., EMBRY, A.F. & GLASS, D.J. (eds) *Devonian of the World, volume I*. Canadian Society of Petroleum Geologists, Calgary.

WENDT, J., AIGNER, T. & NEUGEBAUER, J. 1984. Cephalopod limestone deposition on a shallow pelagic ridge: the Tafilalt Platform (upper Devonian, eastern Anti-Atlas, Morocco). *Sedimentology 31(5)*, 601–625. DOI 10.1111/j.1365-3091.1984.tb01226.x

WENZ, W. 1938. Gastropoda, Teil I. *In* SCHINDEWOLF, O.H. (ed.) *Handbuch der Paläozoologie 6.* 1639 pp. Borntraeger, Berlin.

WESTERMANN, G.E.G. 1999. Life of habits of nautiloids. *In* SAVAZZI, E. (ed.) *Functional Morphology of the Invertebrate Skeleton*. John Wiley & Sons, New York.

WESTERMANN, G.E.G. & TSUJITA, C.J. 1999. Life habits of ammonoids, 299–325. *In* SAVAZZI, E. (ed.) *Functional Morphology of the Invertebrate Skeleton*. John Wiley & Sons, New York.

WHITTAKER, R.H. 1960. Vegetation of the Siskiyou Mountains, Oregon and California. *Ecological Monographs 30*, 279–338. DOI 10.2307/1943563

WHITTAKER, R.H. 1972. Evolution and measurements of species diversity. *Taxon 21(2–3)*, 213–251. DOI 10.2307/1218190

WHITTINGTON, H.B. 1988. Hypostomes of post-Cambrian trilobites. *Memoirs of the New Mexico Bureau of Mines and Mineral Resources 44*, 321–339.

WILLIAMS, A., BRUTON, C.H.C. & CARLSON, S.J. 2000. Brachiopoda (revised), 1–920. *In* KAESLER, R.S. (ed.) *Treatise on Invertebrate Paleontology, Part H (2–3)*. Geological Society of America & University of Kansas Press, Lawrence.

YOCHELSON, E.L. & LINSLEY, R.M. 1972. Opercula of two gasteropods from the Lilydale Limestone (Early Devonian) of Victoria, Australia. *National Museum of Victoria, Memoir 33*, 1–14.

ZHURAVLEVA, F.A. 1959. On the family Michelinoceratidae. *Materialy k Osnovam paleontologii 3,* 47–48.

ZIEGLER, B. 1972. *Allgemeine Paläontologie: Einführung in die Paläontologie, Teil 1*. 181 pp. Schweizerbart'sche Verlagsbuchhandlung, Stuttgart.

Bulletin of Geosciences • Vol. 89, 1, 2014

Appendix

Table 1. Absolute abundances of the species found in the earliest Lochkovian to early Emsian rocks at the Jebel Ouaoufilal in the eastern Tafilalt of Morocco, and their ecological classification after Bush *et al.* (2007). Ecological categories: Tiering – p: pelagic, er: erect, su: surficial, smi: semi-infaunal, si: shallow infaunal, di: deep infaunal; Motility – ff: freely fast, fs: freely slow, fu: facultative unattached, fa: facultative attached, nu: non-motile and unattached, na: non-motile and attached; Feeding mechanism – s: suspension feeder, m: miner, g: grazer, pr: predators, c: coprophagous.

Class	Species	S-D boundary	early Lochkovian	late Lochkovian	Pragian	early Emsian	Mode of life
?Class	*Filihernodia buccina* gen. et sp. nov.	0	0	0	2	0	su, na, s
Stenolaemata	*Treptosomes* or *Cytoporates*	0	0	1	0	0	su, na, s
Crinoidea	*Hexawacrinus claudiakurtae* gen. et sp. nov.	0	0	0	1	0	er, na, s
	Tiaracrinus cf. *moravicus*	0	0	0	1	0	er, na, s
	Camarocrinus sp.	65	0	0	0	0	p, nu, s
Edrioasteroidea	*Rhenopyrgus flos*	0	0	0	0	11	smi, na, s
Anthozoa	Favositidae 1	0	0	0	19	2	su, na, s
	Cleistopora cf. *geometrica*	0	0	0	4	0	su, na, s
	Proclevia sp.	0	0	0	1	0	su, na, s
	Tabulata 1	0	0	0	3	0	su, na, s
	Tabulata 2	0	0	0	2	0	su, na, s
	aff. *Striatopora* sp.	0	0	0	7	0	su, na, s
	Auloporidae 1	0	3	0	0	0	su, na, s
	Aulopora sp.	0	0	0	1	0	su, na, s
	Rugosa 1	0	0	0	1	0	su, na, pr
	Rugosa 2	0	0	0	3	0	su, na, pr
	Rugosa 3	0	0	0	2	4	su, na, pr
	Rugosa 4	0	0	0	17	22	su, na, pr
	Rugosa 5	0	0	0	6	0	su, na, pr
	Rugosa 6	0	0	0	3	0	su, na, pr
	Rugosa 7	0	0	0	1	0	su, na, pr
Trilobita	*Reedops bronni*	0	0	0	1	0	su, ff, pr
	Reedops cf. *cephalotes hamalagdadianus*	0	0	0	7	0	su, ff, pr
	Pseudocryphaeus sp.	0	0	0	1	0	su, ff, pr
	Pilletina zguidensis	0	0	0	0	60	su, ff, pr
	Metacanthina wallacei	0	0	0	0	3	su, ff, pr
	Odontochile cf. *hausmanni*	0	0	0	1	0	su, ff, pr
	Cheirurus (*Crotalocephalus*) sp.	0	0	0	2	0	su, ff, pr
	Hollardops sp.	0	0	0	1	0	su, ff, pr
	Paralejurus elayounensis	0	0	0	2	0	su, ff, pr
	Paralejurus campanifer	0	0	0	0	1	su, ff, pr
Malacostraca	*Nahecaris jannae*	0	0	0	0	5	su, ff, s
Rhynchonellata	*Desquamatia* sp.	0	0	0	4	0	su, na, s
	?*Aulacella eifeliensis*	0	0	0	1	0	su, na, s
	aff. *Eoglossinotoechia* sp.	0	0	0	1	0	su, na, s
	Brachiopoda gen. et sp. indet.	0	0	0	6	0	su, na, s
	?*Protathyris* sp.	0	0	2	9	9	su, na, s
	Cingulodermis sp.	0	0	0	12	0	su, na, s
	Arduspirifer arduennensis	0	0	2	0	1	su, na, s
	Quadrithyris termierae	0	0	0	0	1	su, na, s
Strophomenata	?*Dagnachonetes sp.*	0	0	0	1	0	su, nu, s
Bivalvia	Bivalvia ind. 1	0	0	10	0	0	?
	Panenka humilis	0	0	5	1	0	si, fu, m
	Panenka hollardi	0	0	0	3	4	si, fu, m
	Panenka princeps	0	1	0	0	0	si, fu, m
	Panenka sp. 1	0	1	0	0	0	si, fu, m
	Panenka obsequens	3	0	0	0	0	si, fu, m
	Neklania cf. *resecta*	0	1	0	0	0	si, fu, m
	Neklania cf. *obtusa*	0	0	1	0	0	si, fu, m
	Jahnia sp.	0	0	1	0	0	si, fu, m
	Jahnia aff. *conscripta*	0	5	0	0	0	si, fu, m
	Patrocardia evolvens evolvens	0	0	0	0	1	su, fa, s
	Patrocardia excellens sp.	0	0	0	0	10	su, fa, s
	Patrocardia tarda	0	0	2	2	16	su, fa, s
	Mytilarca cf. *chemungensis*	0	0	0	0	1	su, fa, s
	Mytilarca sp.	0	0	2	0	0	su, fa, s
	Actinopteria cf. *decussata*	0	0	11	0	0	smi, fa, s
	Grammysioidea sp.	0	0	0	0	3	si, fa, s
	Nuculoidea grandaeva	0	0	0	1	79	si, fu, m
	Eonuculoma babini	0	0	0	0	2	si, fu, m

Class	Species	S-D boundary	early Lochkovian	late Lochkovian	Pragian	early Emsian	Mode of life
	Palaeoneilo emarginata	0	0	0	2	59	si, fu, m
	Nuculites celticus	0	0	0	0	5	si, fu, m
	Cucullella triquetra	0	0	0	0	52	si, fu, m
	Phestia rostellata	0	0	0	0	149	di, fu, m
Rostroconchia	*Bohemicardia bohemicus*	0	0	0	1	0	smi, nu, s
Hyolitha	*Orthotheca* sp.	0	0	0	3	66	su, nu, s
Machaeridia	Machaeridia 1	0	0	0	1	0	si, fs, m
	Lepidocoleus rugatus	0	0	0	0	5	si, fs, m
Amphigastropoda	aff. *Coelocyclus* sp. nov.	0	0	0	1	0	su, fs, g
	Sinuitina sp.	0	0	0	0	5	su, fs, g
	Crenistriella sp.	0	0	0	0	8	su, fs, g
Gastropoda	Gastropoda ind. 1	0	0	20	0	0	su, fs, g
	Gastropoda ind. 2	0	0	0	4	0	su, fs, g
	Gastropoda ind. 3	0	0	0	2	5	su, fs, g
	Gastropoda ind. 4	0	0	3	0	0	su, fs, g
	Gastropoda ind. 5	0	0	4	0	0	su, fs, g
	Gastropoda ind. 6	0	0	34	0	0	su, fs, g
	Spirina sp.	0	0	0	1	0	su, fs, g
	Oriomphalus multiornatus gen. et sp. nov.	0	0	0	7	0	su, fs, g
	Australonema sp. nov.	0	0	0	2	0	su, fs, g
	Eotomarioidea ind. 1	0	0	0	1	0	su, fs, g
	Eotomarioidea ind. 2	0	0	0	1	0	su, fs, g
	Paraoehlertia sp.	0	0	0	1	0	su, fs, g
	Umbotropis sp.	0	0	0	2	0	su, fs, g
	Eohormotomina restisevoluta gen. et sp. nov.	0	0	0	2	0	su, fs, g
	Rihamphalus gracilis	0	0	0	5	0	su, fs, g
	aff. *Tychobrahea* sp.	0	0	0	1	0	su, fs, g
	Loxonematoidea ind. 1	0	0	0	7	0	su, fs, g
	Loxonematoidea ind. 2	0	0	0	3	0	su, fs, g
	Palaeozygopleura sp. nov	0	0	1	14	0	su, fs, g
	Palaeozygopleura sp.	0	0	0	0	34	su, fs, g
	Pleurotomarioidea ind., new genus?	0	0	0	2	0	su, fs, g
	Lukesispira pulchra	0	0	0	0	9	su, fs, g
	Planitrochus tardus	0	0	0	0	12	su, fs, g
	Platyceratidae ind. 1	7	0	0	0	0	p, fu, c
	Orthonychia sp.	0	0	0	1	0	su, fs, c
Cephalopoda	Orthocerida ind. 1	21	0	0	0	0	p, fs, pr
	Orthocerida ind. 2	0	0	0	4	0	p, fs, pr
	Orthocerida ind. 3	0	0	0	1	0	p, fs, pr
	Orthocerida ind. 4	0	0	0	1	0	p, fs, pr
	Orthocerida ind. 5	0	0	1	0	0	p, fs, pr
	Endoplectoceras sp.	0	0	0	1	0	p, fs, pr
	Pseudendoplectoceras lahcani	0	0	1	1	0	p, fs, pr
	Bohemojovellania sp.	0	0	3	0	0	p, fs, pr
	Tafilaltoceras adgoi	0	0	0	1	0	p, fs, pr
	Pseudorthoceratidae ind. 1	0	0	1	0	0	p, fs, pr
	Geidoloceras ouaoufilalense	0	0	0	24	0	p, fs, pr
	Subdoloceras atrouzense	0	0	0	46	0	p, fs, pr
	Subdoloceras engeseri	0	0	0	40	0	p, fs, pr
	Spyroceras cyrtopatronus	0	0	0	6	0	p, fs, pr
	Spyroceras latepatronus	0	0	0	1	0	p, fs, pr
	Spyroceras patronus	0	0	0	3	0	p, fs, pr
	Spyroceras sp.	0	0	0	0	9	p, fs, pr
	Cancellspyroceras loricatum	0	0	0	6	0	p, fs, pr
	Arthrophyllum vermiculare	0	0	0	63	13	p, fs, pr
	Murchisoniceras murchisoni	0	0	0	0	96	p, fs, pr
	Infundibuloceras brevimira	0	0	0	0	18	p, fs, pr
	Neocycloceras sp.	0	0	0	0	1	p, fs, pr
	Michelinoceras sp.	0	0	0	1	0	p, fs, pr
	Orthocycloceras tafilaltense	0	0	0	3	0	p, fs, pr
	Orthocycloceras sp.	0	0	0	0	26	p, fs, pr
	Tenuitheoceras secretum gen. et sp. nov.	0	0	0	1	0	p, fs, pr
	Tibichoanoceras sp.	0	0	0	1	0	p, fs, pr
	Arionoceras kennethdebaetsi sp. nov.	0	0	0	1	0	p, fs, pr
	Adiagoceras sp.	0	0	0	2	0	p, fs, pr
	Anaspyroceras sp.	0	0	0	1	0	p, fs, pr
	Harrisoceras sp.	0	0	0	1	0	p, fs, pr

Bulletin of Geosciences • Vol. 89, 1, 2014

Class	Species	S-D boundary	early Lochkovian	late Lochkovian	Pragian	early Emsian	Mode of life
	Angeisonoceras reteornatum	0	0	0	11	0	p, fs, pr
	Temperoceras aequinudum	0	0	0	3	0	p, fs, pr
	Temperoceras sp. 1	0	0	122	0	0	p, fs, pr
	Temperoceras sp. 2	0	0	0	0	36	p, fs, pr
	Temperoceras ludense	0	0	0	10	0	p, fs, pr
	Sphaerorthoceratidae	0	0	0	1	0	p, fs, pr
	Plagiostomoceras culter	0	121	0	0	0	p, fs, pr
	Plagiostomoceras hassichebbiense	0	0	0	0	7	p, fs, pr
	Plagiostomoceras sp.	0	0	0	2	0	p, fs, pr
	Hemicosmorthoceras sp.	0	0	0	1	0	p, fs, pr
	Bactritidae ind.	0	0	0	1	0	p, fs, pr
	Devonobactrites obliquiseptatus	0	0	0	0	1604	p, fs, pr
Placodermi	Brachythoracid placoderm	0	0	0	0	5	p, ff, pr
Acanthodii	*Machaeracanthus* cf. *peracutus*	0	0	0	0	18	p, ff, pr

APPENDIX I-E

A new species of *Tiaracrinus* from the latest Emsian of Morocco and its phylogeny

Published in *Acta Palaeontologica Polonica* 59 (2014)

A new species of *Tiaracrinus* from the latest Emsian of Morocco and its phylogeny

CHRISTIAN KLUG, KENNETH DE BAETS, CAROLE JUNE NAGLIK, and JOHNNY WATERS

Klug, C., De Baets, K., Naglik, C.J., and Waters, J. 2014. A new species of *Tiaracrinus* from the latest Emsian of Morocco and its phylogeny. *Acta Palaeontologica Polonica* 59 (1): 135–145.

We describe a new species of the unusual crinoid *Tiaracrinus*, *T. jeanlemenni* sp. nov. from the latest Emsian of the famous mudmound locality Hamar Laghdad, Morocco. It differs from the previously known species in the higher number of ribs and the vaulted rib-fields, which is corroborated by the comparison of simple quantitative characters and ratios as well as by the results of a cluster analysis and a Principal Component Analysis. Based on the new material and the published specimens, we discuss the phylogeny of the genus and suggest that *T. oehlerti* and *T. moravicus* represent the ancestral forms of this small clade.

Key words: Crinoidea, mudmounds, phylogeny, morphometry, symmetry, Devonian, Morocco.

Christian Klug [chklug@pim.uzh.ch] and Carole J. Naglik [carole.naglik@pim.uzh.ch], Paläontologisches Institut und Museum, Universität Zürich, Karl Schmid-Strasse 4, CH-8006 Zürich, Switzerland;
Kenneth De Baets [kenneth.debaets@fau.de], GeoZentrum Nordbayern, Fachgruppe PaläoUmwelt, Universität Erlangen, Loewenichstr. 28, D-91054 Erlangen, Germany;
Johnny Waters [watersja@appstate.edu], Department of Geology, Appalachian State University, ASU Box 32067, Boone, NC 28608-2067, USA.

Received 30 November 2011, accepted 4 June 2012, available online 6 June 2012.

Introduction

Palaeozoic echinoderms produced a wealth of unusual thecal morphologies, which are hard to interpret in terms of taxonomic assignment and/ or functional morphology. Although this is particularly true for Early Palaeozoic clades (e.g., Sumrall and Wray 2007), it still holds true for some Devonian forms, for example pyrgocystid edrioasteroids (e.g., Bather 1915; Dehm 1961; Holloway and Jell 1983; Klug et al. 2008; De Baets et al. 2010), some crinoids (e.g., Schmidt 1934; Bohatý 2011) or late blastozoans (e.g., Dehm 1934; Rahman and Lintz 2012). Crinoids show their highest disparity in the Ordovician, but disparity remains high until the end of the Devonian (Foote 1995). Several areas of the Palaeozoic crinoid morphospace have not been reoccupied in the Mesozoic (Foote 1999).

In recent years, we have discovered the first two specimens of the genus *Tiaracrinus* in Morocco. This genus is usually thought to be restricted to Early (Lochkovian) to Middle Devonian (Eifelian; see Le Menn 1987; Prokop 1987; Haude 2008), but Kříž (1992) reported some in open nomenclature from the Late Silurian (Ludfordian,). *Tiaracrinus* is peculiar for the following reasons: (i) the calyx shows a tetramerous symmetry; (ii) so far, it has not been found with arms, although some unusual arm structures have been assigned to the genus (see further); (iii) the theca has four fields with epispires, giving it a blastozoan appearance.

Species of *Tiaracrinus* based on calices were first described in the 19th century. Schultze (1866) introduced the genus with the type species *T. quadrifrons* in his monograph on the Middle Devonian echinoderms from the Eifel Mountains. Soon thereafter, two more species of *Tiaracrinus* were described, *T. oehlerti* Schlüter, 1881 and *T. rarus* (Barrande, 1887). In the 20th century, two additional species were published based on calices, *T. tedraedra* Jaekel, 1901 and *T. moravicus* Ubaghs and Bouček, 1962. Two species based on limbrachoids, unusual arm structures, have been recently assigned to *Tiaracrinus* with some reservation (*T.*? *obtusibrachialis* Haude, 1993 and *T.*? *aceribrachialis* Haude, 1993). Hauser (2008: 1) listed the latter two species as *nomina dubia*. Additional specimens in open nomenclature were reported from the Ludfordian, Lockovian, Pragian and Emsian of the Czech Republic (Prokop 1987; Kříž 1992; Prokop and Petr 2002).

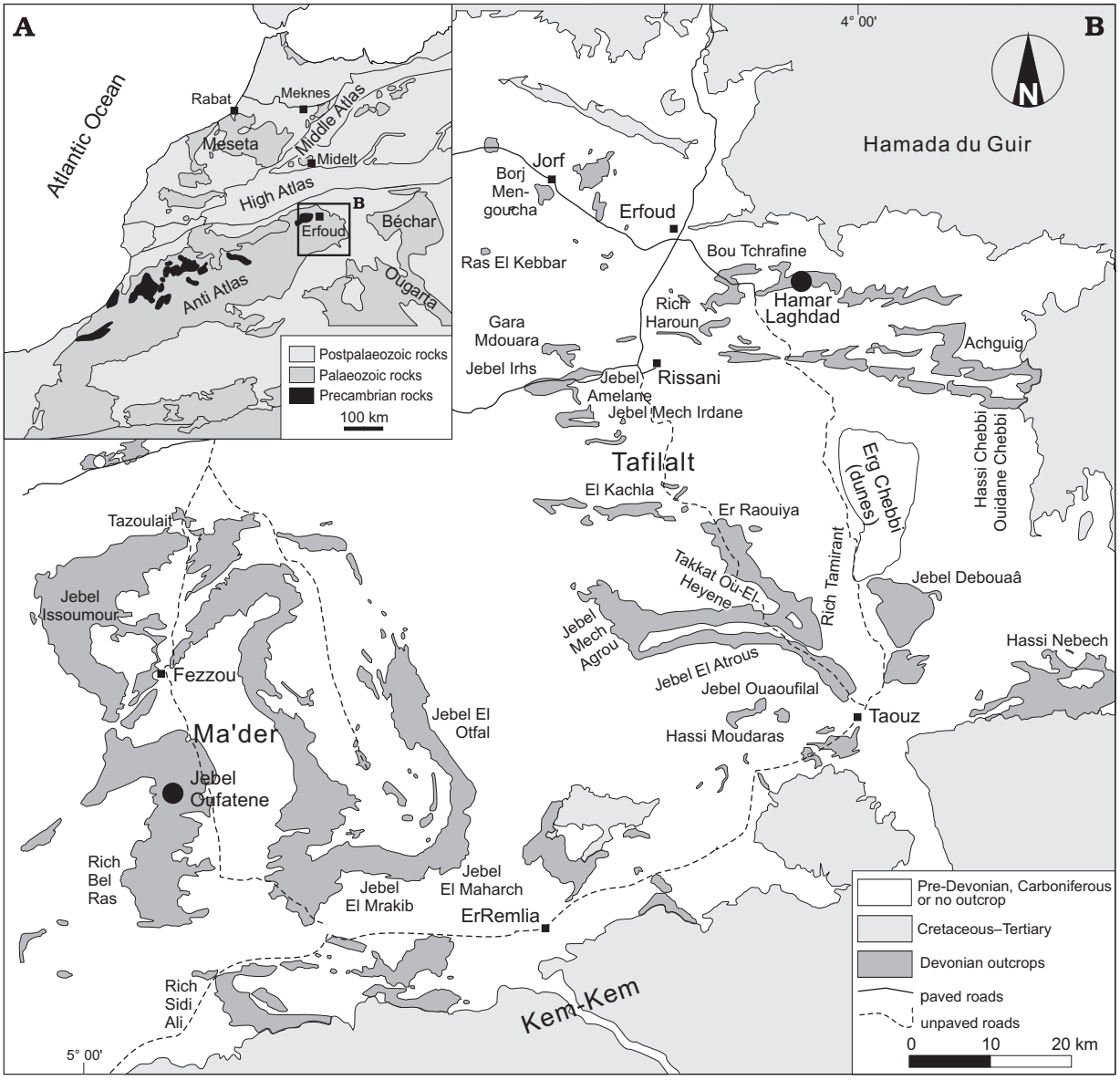

Fig. 1. Geological map (modified from Klug 2002) of the eastern Anti-Atlas showing the two localities that yielded *Tiaracrinus*.

In this study, we describe and illustrate the first two specimens of *Tiaracrinus* from the Early Devonian of Morocco. We discuss ontogenetic changes within this group as well as its phylogeny.

Institutional abbreviations.—GFCL, collection of D. Le Maître, Laboratoire de Géologie de la Faculté Catholique de Lille, France; LPB, Laboratoire de Paléontologie de Brest, France; PIMUZ, Paläontologisches Institut und Museum, Universität Zürich, Switzerland.

Other abbreviations.—PCA, Principal Component Analysis.

Material

So far, only two specimens of *Tiaracrinus* have been found in the Moroccan eastern Anti-Atlas by us. Both specimens are of latest Emsian age and were found at the southern edge of Jebel Oufatene (PIMUZ 29741) and at the "red cliff" in Hamar Laghdad (PIMUZ 29739; Fig. 1). Both specimens are stored at the Paläontologisches Institut und Museum at the University of Zurich. Both specimens (Fig. 2) are slightly corroded but well preserved otherwise. The specimen from Hamar Laghdad is slightly better preserved, probably due to

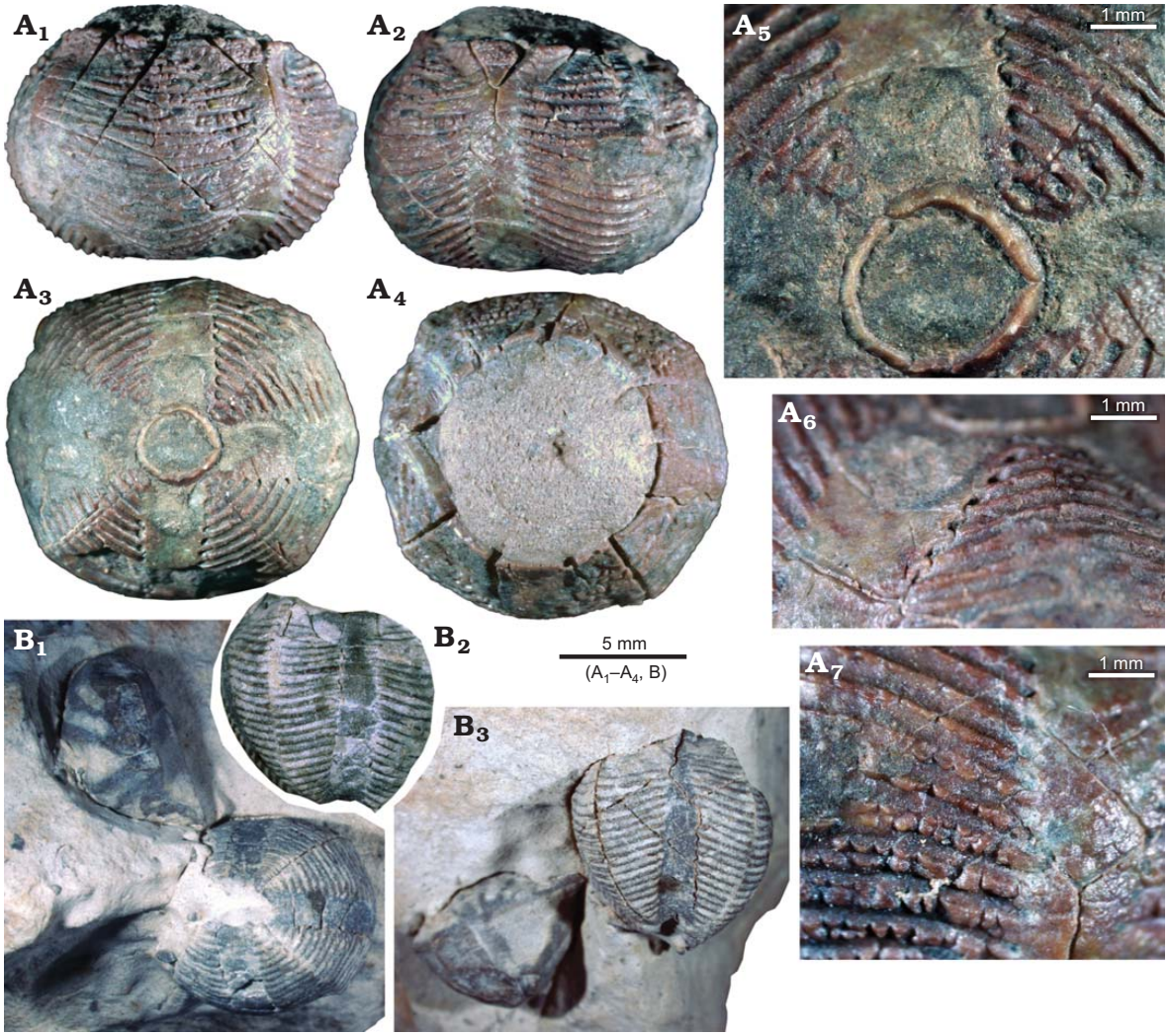

Fig. 2. Zophocrinid crinoid *Tiaracrinus jeanlemenni* sp. nov., probably late *Polygnathus patulus* Conodont Biozone, late *Anarcestes lateseptatus* Ammonoid Biozone, latest Emsian, Early Devonian, eastern Anti-Atlas Morocco. **A**. PIMUZ 29739, holotype, "Red cliff" at Hamar Laghdad, Tafilalt. Lateral views (A_1, A_2), showing the radial channel and the rib-fields; note the ornamentation in the channel near the oral surface in A_2. Aboral view (A_3), note the small cross section of the trimeral basals and the low rim around it. Oral view (A_4), note the ornamentation in the channel near the oral surface. Detail of A_3 (A_5), note the epispires and the uniform thickness of the ribs. On the top right, the subtle striation is faintly visible between the ribs. Oblique view of the aboral side (A_6), showing the epispires. Due to weathering, the ribs obtained a tuberculate ornament (A_7). **B**. PIMUZ 29741, paratype, Jebel Oufatene, Maïder. Aboral view (B_1), the rib-fields are less vaulted and the cross section of the calyx less quadrate than in the holotype; the fossil on the top left is a spiriferid. Lateral views (B_2, B_3), showing the narrow ribs and the smooth surface of the radial channels; in the lateral aspect it looks like the radial channel is tapering towards the oral side of the cup.

a partial silicification. Holdfast, stem, brachials, arms and oral plates are not preserved in both specimens.

PIMUZ 29739, the larger specimen, was collected from scree at the "red cliff" (Klug 2002; N 30.82453°, W 4.90210°) at Hamar Laghdad in the Tafilalt region. Hamar Laghdad is situated about 18 km ESE of the town Erfoud (Fig. 1). Hamar Laghdad has become world-renowned for its mud-mounds, some of which being completely exhumed, some others are still more or less covered by the overlying sediments (e.g., Roch 1934; Massa et al. 1965; Hollard 1974; Alberti 1982; Brachert et al. 1992; Wendt 1993; Belka 1994, 1998; Bultynck and Walliser 2000; Aitken et al. 2002; Berkowski 2006; Cavalazzi et al. 2007). As far as palaeontology is concerned, this locality yielded highly diverse trilobite associations (e.g., Alberti 1969, 1982; Klug et al. 2009), abundant cephalopods (Töneböhn 1991; Klug 2001, 2002; Klug et al. 2009) includ-

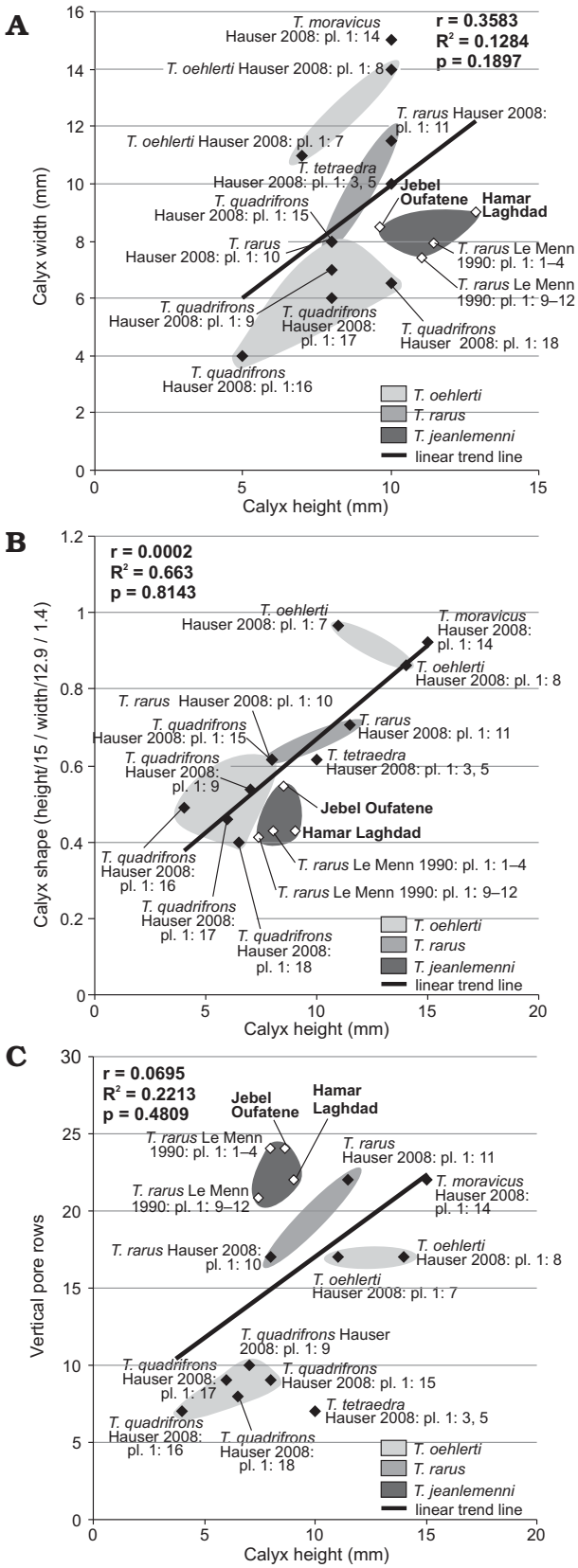

Fig. 3. Bivariate plots with various measurements and ratios of some published (Le Menn 1190; Hauser 2008) and the two newly described specimens of *Tiaracrinus*. See the methods chapter for definition of the parameters. **A**. Calyx width vs. calyx height; note the clear sepration of taxa. **B**. Calyx shape vs. calyx height. **C**. Number of pore rows vs. calyx height. As in A, the new taxon is also well separated from the existing taxa. The linear trendline probably reflects an ontogenetic trend. Open squares mark the values of the new species *T. jeanlemenni* sp. nov., solid squares mark all other species.

ing ammonoids infested by parasites (De Baets et al. 2011) as well as many blastozoans, crinoids (sometimes encysting corals: Berkowski and Klug 2012), brachiopods, rugose corals specialised on vent habitats (Berkowski 2004, 2006, 2008, 2012, Belka and Berkowski 2005), locally favositids in rock-forming numbers and large bivalves (*Panenka*, *Patrocardia* and similar forms). The specimen PIMUZ 29739 was collected from marl containing limestone nodules and layers of latest Emsian age. These layers contain ammonoids of the genera *Amoenophyllites*, *Anarcestes*, and *Chlupacites* (Klug et al. 2009). Immediately below these marl beds, a claystone succession of late Emsian age is present, which overly the massive mudmound limestone, also of Emsian age. The latter limestone contains *Mimagoniatites fecundus*, thus confirming their basal Dalejan age (e.g., Klug et al. 2009). Above the marl, the layers become increasingly limy. At the base of the limestone, a dark nodule layer contains abundant *Foordites veniens* (Klug 2002; Klug et al. 2009). Diagenesis and taphonomy of the red cliff are discussed in Klug et al. (2009).

PIMUZ 29741 is somewhat smaller and was found at the southern edge of Jebel Oufatene (Fig. 1; compare Hollard 1974; Massa et al. 1965). This specimen is slightly deformed, probably due to compaction of the sediment. However, this deformation is minimal. We tested this by taking high and low estimates of the measurements. Therefore, we think that the overall proportions are reasonably well preserved. This is additionally corroborated by comparing the superficial visual similarities and differences of the measured specimens with PIMUZ 29741 with the clustering of forms in the PCA and in the cluster analysis (see the methods chapter). It was collected from a trench where locals had dug for late Emsian trilobites (N 30.824532°, W 4.90210°). Jebel Oufatene is about 14 km S of Fezzou in the Maïder region (eastern Anti-Atlas, Morocco). According to Kaufmann (1998), the entire Emsian is about 100 m thick in this area. The Dalejan (late Emsian) is represented by a thick claystone and clayey marl sequence, which displays increasing carbonate content near its top. For a sedimentological basin model of the Maïder Basin: see Döring (2002).

Methods

In order to distinguish between the species of this genus based on morphological differences, we produced bivariate plots (Fig. 3), a Principal Component Analysis (PCA; Fig. 4)

Table 1. Values used in the principal component and cluster analyses. Most of the values were taken from Hauser (1997, 2008). Values with some uncertainty are given in bold.

Specimen	Width oral surface (mm)	Calyx width (mm)	Calyx height (mm)	width pore fields (mm)	Stem width (mm)	Epispire rows (number)	Width-size class	Height-size class	Curvature	Stem to calyx-ratio	Row-ratio	Shape
Hamar Laghdad	8.7	12.9	9	9.3	3	22	1.000	0.600	0.674	0.233	0.917	0.436
Jebel Oufatene	5	9.6	8.5	5.3	2.3	24	0.744	0.567	0.521	0.240	1.000	0.590
Tiaracrinus moravicus Hauser 2008, pl. 1: 14	8	10	15	4	1.9	22	0.775	1.000	0.800	0.190	0.917	0.938
Tiaracrinus oehlerti Hauser 2008: pl. 1: 7	5	7	11	2.5	1.7	17	0.543	0.733	0.714	0.243	0.708	0.982
Tiaracrinus oehlerti Hauser 2008: pl. 1: 8	7.5	10	14	4	2.8	17	0.775	0.933	0.750	0.280	0.708	0.875
Tiaracrinus quadrifrons Hauser 2008: pl. 1: 9	6.7	8	7	4.5	1.5	10	0.620	0.467	0.838	0.188	0.417	0.547
Tiaracrinus quadrifrons Hauser 2008: pl. 1: 15	6	8	8	5	1.4	9	0.620	0.533	0.750	0.175	0.375	0.625
Tiaracrinus quadrifrons Hauser 2008: pl. 1: 16	3.5	5	4	3.7	1	7	0.388	0.267	0.700	0.200	0.292	0.500
Tiaracrinus quadrifrons Hauser 2008: pl. 1: 17	5.2	8	6	4.5	**1.5**	9	0.620	0.400	0.650	0.188	0.375	0.469
Tiaracrinus quadrifrons Hauser 2008: pl. 1: 18	**6**	10	6.5	5.5	**1.5**	8	0.775	0.433	0.600	0.150	0.333	0.406
Tiaracrinus rarus Hauser 2008: pl. 1: 10	4.5	8	8	4.5	1	17	0.620	0.533	0.563	0.125	0.708	0.625
Tiaracrinus rarus Hauser 2008: pl. 1: 11	5.8	10	11.5	7	1.5	22	0.775	0.767	0.580	0.150	0.917	0.719
Tiaracrinus tedraedra Hauser 2008, pl. 1: 3,5	7	10	10	6.5	2	7	0.775	0.667	0.700	0.200	0.292	0.625
Tiaracrinus rarus Le Menn 1990: pl. 1: 1–4	8	11.5	8	8	1.5	24	0.891	0.533	0.696	0.130	1.000	0.435
Tiaracrinus rarus Le Menn 1990: pl. 1: 9–12	8.3	11.1	7.4	6.2	1.5	21	0.860	0.493	0.748	0.135	0.875	0.417

Correlation matrix

PC	Eigenvalue	% variance
1	1.84232	48.308
2	1.18509	31.075
3	0.435917	11.43
4	0.223277	5.8546
5	0.119034	3.1212
6	0.00807011	0.21161

and a Cluster Analysis (Fig. 5) using PAST (Hammer at al. 2001) based on the following six characters (Table 1):

Calyx width size class (based on the largest width): The largest specimen was set as 1.

Calyx height size class: The largest specimen was set as 1.

Curvature of the calyx walls, calculated by dividing the largest width of the oral surface (assumed to be more or less identical with the diameter of the oral edge of the radial circlet) by the maximum width of the calyx.

Stem to calyx-ratio: The ratio between the diameter of the facet of the most proximal nodal columnal and the diameter the maximum width of the calyx.

Row ratio: The number of epispire rows divided by the maximal number of epispiral rows of all known specimens.

Shape: The values of character 1 (width size class) divided by those of value 2 (height size class).

The standardisation was made for several purposes: (i) standardisation reduces the bias caused by differences in dimensions of the respective parameter; (ii) it eliminates the bias in scaling errors in those cases, where morphometric values were taken from the literature. We thus performed a PCA on the correlation matrix. The intraspecific variability is mainly caused by differences in ontogenetic trajectories (see Fig. 3) and, to a minor degree, by preservational biases such as the differences between internal moulds versus specimens that preserve the skeleton.

In the bivariate plots (Fig. 3), which were made using Excel, trendlines are given, which are supposed to show the predominant ontogenetic trend (correlation with calyx height, i.e., size). These were also produced with Excel.

The choice of specimens is based on their availability and preservation mainly. Not many well-preserved specimens of *Tiaracrinus* are sufficiently well documented and show all characters needed for our analyses, hence the low number of data.

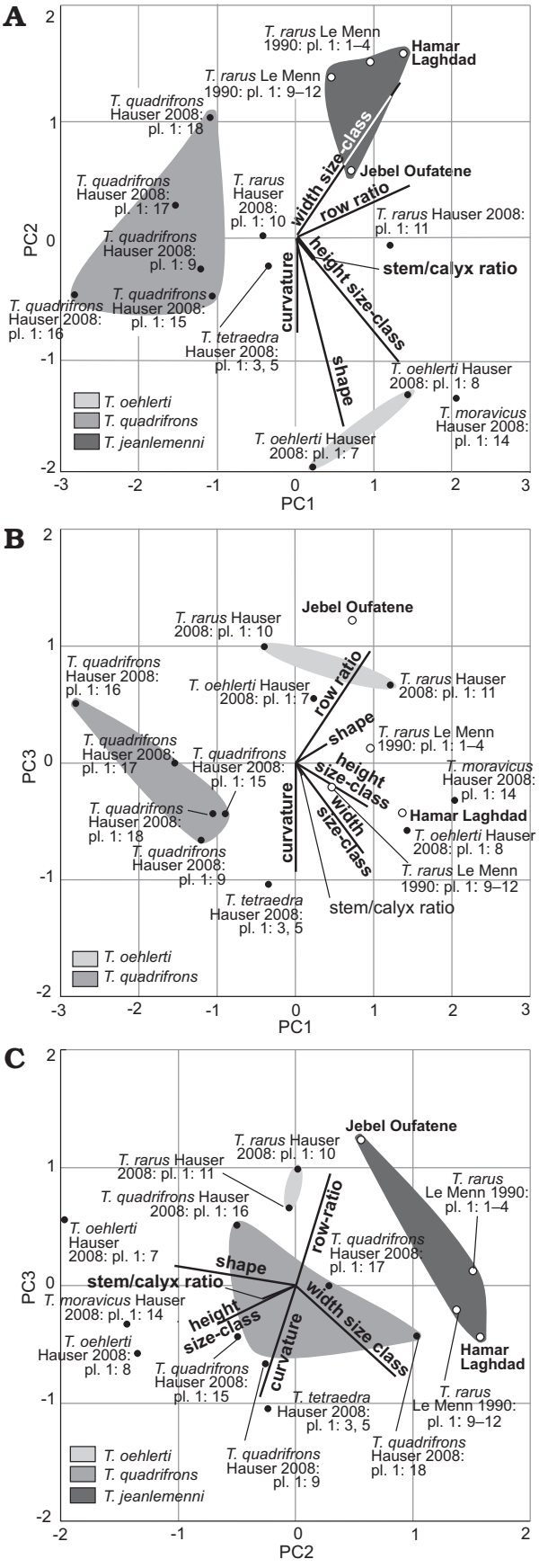

Fig. 4. PCA of some published (Le Menn 1190; Hauser 2008) and the two newly described specimens of *Tiaracrinus* (see Table 1). See Methods for definition of the parameters. **A**. Plot of principal components 1 and 2; note, how the new species separates well from the previously known ones. **B**. Plot of principal components 1 and 3. **C**. Plot of principal components 2 and 3; again, the new species is morphologically separated from the others. Open circles mark the values of the new species *T. jeanlemenni* sp. nov., solid squares mark all other species.

Systematic palaeontology

Phylum Echinodermata Klein, 1754

Class Crinoidea Miller, 1821

Order Disparida Moore and Laudon, 1943

Superfamily Belemnocrinaceae Miller, 1883

Family Zophocrinidae Miller, 1892?

Type genus: *Zophocrinus* Miller, 1891.

Discussion.—In spite of the overall similarity in cup-shape and the organisation of the oral surface, it still appears questionable to include morphologically quite different genera such as *Zophocrinus* and *Tiaracrinus* in the same family. As far as we understand, the evolution or evolutionary reduction of epispires is probably not fully understood. We therefore keep this historical family assignment in agreement with the Treatise (Moore et al. 1978) as well as crinoid experts such as Le Menn (1990) and Hauser (2008).

Genus *Tiaracrinus* Schultze, 1866

Type species: *Tiaracrinus quadrifrons* Schultze, 1866, original designation; Stínava near Plumlov, Moravia, Czech Republic, Emsian, Early Devonian.

Species included: *Tiaracrinus moravicus* Ubaghs and Bouček, 1962; *Tiaracrinus oehlerti* Schlüter, 1881; "*Staurosoma rarum*" Barrande, 1887; *Tiaracrinus quadrifrons* Schultze, 1866; *Tiaracrinus tedraedra* Jaekel in Lotz, 1901; *Tiaracrinus jeanlemenni* sp. nov.; "*Triaracrinus*" sp. (sic!) Kříž, 1992.

Discussion.—Initially described as a crinoid, *Tiaracrinus* was occasionally attributed to the Rhombifera (Blastozoa) by some early palaeontologists (Jaekel 1899, 1918; Bather 1900). Subsequently it has been consistently assigned to the crinoids (e.g., Frech 1902; Springer 1926; Bassler 1938; Moore et al. 1978; Le Menn 1990; Haude 1993; Hauser 2008). This confusion was probably largely related with its peculiar symmetry, the possible absence of arms and the presence of pores (epispires) on the theca. Here, we briefly discuss these features, their possible implications and problems associated with them:

(i) Symmetry: *Tiaracrinus* has three basals and four radials, thus determining the tetrameral symmetry of the calyx (Le Menn 1990). The oral surface is rarely preserved but has been discussed in detail by Le Menn (1990). The calyx shows five different plate numbers per circlet in the calyx. The base shows three plates while the cup is tetrameral. On the oral surface, 13 fields with brachial platelets and eight interoral fields can be seen, which surround the five oral plates (Le Menn 1990).

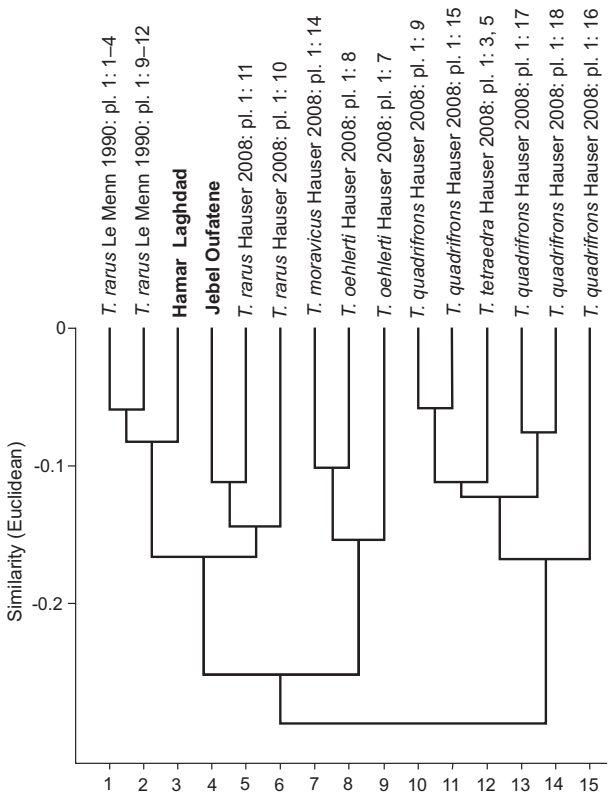

Fig. 5. Cluster analysis (Euclidean, paired group) of some published specimens and the two newly described specimens (see Table 1). The cluster on the right including *Tiaracrinus quadrifrons* and *Tiaracrinus tetraedra* is supported by the bootstrap (at 500 replicates; 59%with past); the *Tiaracrinus oehlerti* and *Tiaracrinus moravicus*-group (59 and 64%) and the *Tiaracrinus jeanlemenni* and *Tiaracrinus rarus*-group (62 and 72%) are also reasonably well supported. See also the methods chapter for definition of the parameters.

(ii) Arms: *Tiaracrinus* is commonly found without arms and has been described in the Treatise on Invertebrate Paleontology (Moore et al. 1978: 562) as follows: "Arm facets obscure or absent. Arms and columns unknown". Later, Haude (1993) assigned limbrachoids from the Middle Devonian of Germany to this genus. He discussed the problems of the systematic position of this genus: "Immerhin ist die Theka so ungewöhnlich gebaut, dass selbst bedeutende Kenner der Pelmatozoen wie Bather (1900: 57) und Jaekel (1918: 99) *Tiaracrinus* zu den Cystoiden stellten. (An einem Cystoiden wären im übrigen die Limbrachoide wesentlich leichter als [biseriale] versteifte Brachiolen zu interpretieren.)" [Translation: "After all, the theca is constructed in such an unusual way that even important adepts of the pelmatozoans such as Bather (1900: 57) and Jaekel (1918: 99) have assigned *Tiaracrinus* to the cystoids. (On a cystoid, by the way, the limbrachoids would be much easier to interpret as stiffened [biserial] brachioles.)"]

Le Menn (1990: 163) also discussed this issue: "Le nombre de bras demeure difficile à établir" [Translation: "The number of arms remains difficult to identify"]. While Le Maître (1958a–c) had suggested 18 arms based on 18 ditches on the oral surface, Le Menn (1990) thinks that these ditches were formed by erosion. The latter author discussed the possibilities of five or eight arms, based on the number and arrangement of oral, interoral, and brachial plates. It appears like this question has to stay unanswered until a complete, articulated specimen is found.

(iii) Pores on the calyx: *Tiaracrinus* displays four fields with epispires (Fig. 2). These epispires have been interpreted as representing a plesiomorphic character by Guensburg and Sprinkle (2007: 287): "Crinoid respiratory folds, for instance, are symmetrical internally and externally, whereas rhombiferan internal folds are extended forming interior bulges. Folds of most crinoids occur at triple junctures of plate corners, whereas those of rhombiferans cross plate sides."

The origin of the type material is unknown according to Hauser (2008), but Le Menn (1987) described similar specimens from the Saint Céneré Formation (Pragian) of the "Tranchée de la voie Sablé"; Massif Armoricain (France).

Stratigraphic and geographic range.—Species of *Tiaracrinus* are recorded from: the Emsian of Plumlov (Moravia, Czech Republic), the late Emsian (according to Prokop 1987) of Koňeprusy (Bohemia, Czech Republic), the Freilingen Formation (Eifelian) of Nollenbach (Eifel, Germany), the Greifensteiner Kalk (near Emsian–Eifelian boundary) of Greifenstein (Lahn-Dill-Kreis, Germany), the Amerboh Group (late Emsian) of the eastern Anti-Atlas (Morocco), the Kopanina Formation (Ludfordian, Silurian) of Mušlovka quarry (Bohemia, Czech Republic).

Tiaracrinus jeanlemenni sp. nov.

Fig. 2.

1990 *Tiaracrinus rarus* (Barrande, 1887); Le Menn 1990: 162, pl. 1.

Etymology: After Jean Le Menn, honouring his work on Palaeozoic echinoderms and his thorough description of the genus in Africa.

Type material: Holotype: PIMUZ 29739, a well-preserved calyx but lacking the oral surface. Paratypes: PIMUZ 29741, GFCL 2152–2153, LPB 16795.

Type locality: "Red cliff" at Hamar Laghdad (eastern Anti-Atlas, Morocco).

Type horizon: Probably late *Polygnathus patulus* Conodont Biozone, late *Anarcestes lateseptatus* Ammonoid Biozone, latest Emsian, Early Devonian (Bultynck and Walliser 2000; Klug 2002).

Diagnosis.—*Tiaracrinus* with a more or less spherical calyx, with four very broad rhomboid radial rib-fields, which are strongly vaulted and which carry a large number of slender ribs (>20), a small and narrow radial ring, narrow and with slightly concave radial channels.

Description.—For the description of the Algerian specimens see Le Menn (1990). The two new Moroccan specimens are described below. Specimen PIMUZ 29739, holotype (Fig. 2A). The specimen preserves only the broad subglobular calyx and measures 9 mm in height and maximally 12.9 mm in

width. At the oral surface, the width of the calyx is reduced to 8.7 mm, but the oral surface is not preserved. The radial rib-field is up to 9.3 mm wide and it carries up to 22 ribs with pores at the end. In some parts, the ribs carry tubercles, but this might be due to weathering. The four radial channels form a perfect cross when seen from the aboral side. Specimen PIMUZ 29741, paratype (Fig. 2B). This calyx also lacks the oral surface, arms, and the stem. With a calyx height of 8.5 mm, this specimen is only 9.6 mm wide and therefore more slender than the holotype and the Algerian specimens. Although this specimen is slightly deformed, this difference in shape is probably original rather than a taphonomic artefact. At the oral surface, it measures only 5 mm while the other three specimens measure 8 mm or more. The ribs in the diamond-shaped rib-field appear finer but are more numerous (24) than in the other specimens. The radial channels also form a perfect cross when seen from the oral side and the rib-fields form a right angle where the channels meet.

Discussion.—Le Menn (1990) listed the five species *Tiaracrinus moravicus*, *T. rarus*, *T. quadrifrons*, *T. soyei*, and *T. tedraedra*. His assignment of the three Algerian calices to Barrande's (1887) species *T. rarus* was based on the globular calyx with the large number of ribs and the rhomboid rib-fields, which are similar to the European species *T. rarus*. Both the bivariate plots (Fig. 3) and the PCA-plots of principal component 1 and 2 as well as of principal component 2 and 3 (Fig. 4) revealed, however, that all specimens of the new species plot in a field separate from those of *T. rarus* and the other species. By contrast, both in the cluster analysis (Fig. 5) and in the plot of principal component 1 and 3 (Fig. 4), the specimen from Jebel Oufatene (PIMUZ 29741) falls in the field of *T. rarus*.

The results of this cluster analysis (Fig. 5) of 15 specimens revealed three pairs of species, which plot in the same respective clusters (see also the phylogeny chapter). In this analysis (Fig. 5), *T. rarus* is the sister species of *T. jeanlemenni*. This is also supported by the PCA (especially the principal component 3, i.e., the width size-class and the row ratio) and the bivariate plots (Figs. 3, 4). The separation of *T. jeanlemenni* from *T. rarus* is based mainly on the higher number of pore rows (Fig. 3C) and the lower height to width ratio in the new species.

Morphologically, the Algerian specimens (Le Menn 1990: pl. 1: 1–12) strongly resemble PIMUZ 29739 from Hamar Laghdad, while the slightly smaller specimen PIMUZ 29741 from Jebel Oufatene looks slightly different (Fig. 2). The question arises, whether this last mentioned specimen belongs to a separate species because it has more ribs with epispires than the other four specimens and the calyx is more slender, which might, however, be due to the slight traces of compaction or due to intraspecific variability (which cannot be quantified due to the low number of available specimens). It resembles *T. rarus* in the narrower oral surface but it differs from this Bohemian species in the adorally converging radial channels. Nevertheless, most of its measurements and values (Fig. 3; pore rows in relation to size, height in relation to width) plot very close to the other specimens assigned to the new species (Fig. 3, 4), and therefore we conclude that it belongs to the new species and simply represents a morphological variant.

Stratigraphic and geographic range.—Late Emsian of the eastern Anti-Atlas (Morocco) and Monts d'Ougarta (Algeria).

Growth

As already pointed out by Le Menn (1990: 165), some of the characters of *Tiaracrinus*, such as the number of ribs, vary through ontogeny. The correlation of calyx width and height in the bivariate graph of Fig. 3A is not significant ($r = 0.358$, $R^2 = 0.128$, $p = 0.1897$), which is probably due to the fact that the graph depicts specimens from several species. Evaluation of a possible correlation with single species is, however, not possible at this point because of the lack of material and thus data. In spite of the lack of data, it is still clear that with increasing height, the width is also increasing, apparently to differing degrees in different species, but this hypothesis requires much more material to be tested. The number of ribs and epispires increases more or less constantly through ontogeny (Fig. 3B; $r = 0.0695$, $R^2 = 0.2213$, $p = 0.4809$), namely from 7 to 10 in *T. quadrifrons* from a calyx height of around 4 to around 8 mm, and in *T. rarus* from 17 to 22 at heights from about 8 to 11.5 mm, although the new species has more ribs than representatives of the other species at comparable sizes. We have printed a linear trendline to these epispire row-data, although the distribution of data points vaguely suggest an exponential correlation; the number of specimens and thus data is too low to draw conclusions on the exponential increase in row number. Nevertheless, a nonlinear increase in epispire rows would not be surprising since the volume of a sphere (and the calyx of *Tiaracrinus* is nearly spherical) also increases exponentially when compared to diameter (calyx height) increase; an exponentially growing body would probably have an exponentially growing respiration, hence the possibly exponential increase in epispire rows. The variation in strength of the ribs and size of the epispires within one specimen appears to be low (compare Hauser 2008: pl. 1).

Phylogeny

Some of the relationships within the genus are undoubtedly as proposed by Le Menn (1990). Accordingly, *T. oehlerti* and *T. moravicus* with their elongate and slightly ornamented calices represent a small monophylum (supported by the results of our cluster analysis in Fig. 5). Intrageneric variability is dominated by the significant ontogenetic increase in the number of epispire rows. A possible correlation between calyx width and height through ontogeny lacks statistical support, which is probably due to the low amount of data.

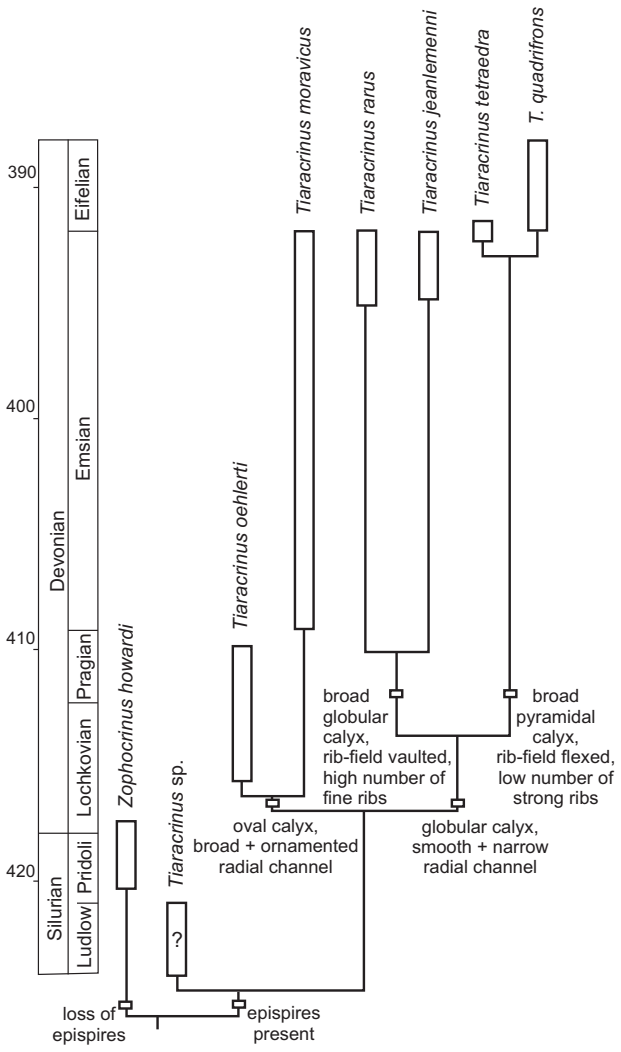

Fig. 6. Reconstruction of the phylogeny of the species of *Tiaracrinus*, based on their morphology and stratigraphic occurrences. Devonian timescale after Kaufmann (2006). All ranges of species lack precision and are thus indicated by open boxes.

Alternatively, as proposed by Hauser (2008: 2), *T. oehlerti* and *T. moravicus* could be conspecific and were assigned to different species because of differences in preservation. The same question is open with respect to *T. tedraedra* and *T. quadrifrons*, two superficially similar species with profoundly different preservation (Hauser 2008: 5), which also form one cluster. *T. jeanlemenni, T. rarus*, *T. tedraedra*, and *T. quadrifrons* share the broader calyx with the narrower radial channels and might thus be closely related (see Fig. 3).

The question arises, which of the various kinds of morphology represents the more plesiomorphic state. The age (Pragian to earliest Eifelian) of most of the reasonably well-known species does not differ significantly. Since *T. oehlerti* appears to be the oldest of the better known species, we suggest that the morphology with the elongate calyx and the more ornamented radial channels represent the more ancestral morphology (Fig. 6). At least the calyx shape is more similar to the genus *Zophocrinus*, which is one of the few genera in the same family according to the crinoid Treatise (Moore et al. 1978). Remarkably, all the other genera assigned to the Zophocrinidae lack epispires. Following Guensburg and Sprinkle (2007: 287), the presence of epispires in crinoids can be considered as a plesiomorphic character and thus, the morphology of *Zophocrinus* and *Parazophocrinus* would be more derived, if we accept the taxonomy of Moore et al. (1978). By contrast, it could be argued that the *Tiaracrinus*-lineage had evolved convergently, an assumption, which is less parsimonious. For a test of this latter hypothesis, material and data are not available at this point. Such material would have to show a transition between the epispire-free *Zophocrinus* and early *Tiaracrinus* with epispires, for instance with a very low number of rows.

Conclusions

Based on the higher number of ribs in the rhomboid rib-fields and the globular calyx-shape, we describe the new species *Tiaracrinus jeanlemenni* sp. nov., which resembles the Czech species *T. rarus*. The species pair *T. jeanlemenni* sp. nov. and *T. rarus* differs from the other *Tiaracrinus* species in the greater number of more narrow epispire rows and from the pair *T. oehlerti* and *T. moravicus* in the more globular calyx with the more narrow radial channels. Morphometric analyses (PCA and Cluster Analyses) support the closer relationships between the species pairs *Tiaracrinus jeanlemenni* sp. nov. and *T. rarus*, between *T. tedraedra* and *T. quadrifrons*, as well as between *T. oehlerti* and *T. moravicus*. In the cases of the latter two pairs, two explanations are at hand: Either, (i) *T. tetraedra* and *T. moravicus* represent junior synonyms with the type materials of both species-pairs being differently preserved or (ii) all four species, are closely related to the respective other species of the two species-pairs, representing two two-species monophyla. Based on their younger age and the much higher than wide calyx (reminiscent of the outgroup-genus *Zophocrinus*), we interpret the species-pair *T. oehlerti* and *T. moravicus* as the most plesiomorphic one within the genus, from which the other four species are derived.

Acknowledgements

The Moroccan colleagues of the Ministère de l'Energie et des Mines (Rabat and Midelt) benignly provided permits for the field work and for the export of samples. We greatly appreciate the work of the reviewers Elise Nardin (University of Toulouse, Toulouse, France) and Gary D. Webster (Washington State University, Pullman, USA), who put an unusual effort into their highly detailed reviews, thereby improving the manuscript significantly. We thank the Swiss National Science foundation for financial support of the field work (Project numbers 200021-1139561, 200020-25029, and 200020-132870).

References

Aitken, S.A., Colom, J.C., Henderson, C.M., and Johnston, P.A. 2002. Stratigraphy, paleoecology, and origin of Lower Devonian (Emsian) carbonate mud buildups, Hamar Laghdad, eastern Anti-Atlas, Morocco, Africa. *Bulletin of Canadian Petroleum Geology* 50: 217–243.

Alberti, G.K.B. 1969. Trilobiten des jüngeren Siluriums sowie des Unter- und Miteldevons. I. Mit Beiträgen zur Silur−Devon – Stratigraphie einiger Gebiete Marokkos und Oberfrankens. *Abhandlungen der Senckenbergischen Naturforschenden Gesellschaft* 520: 1–692.

Alberti, G.K.B. 1982. Der Hamar Laghdad (Tafilalt, SE Marokko), eine bedeutende Fundstelle devonischer Trilobiten. *Natur & Museum* 112: 172–182.

Barrande, J. 1887. *Système Silurien du centre de la Bohéme. I: Recherches paléontologiques, Classe des Echinodermes, Sec. 1: Ordre des Cystidées 7*. 233 pp. Published by the author, Praha.

Bassler, R.S. 1938. Pelmatozoa Paleozoica. *In*: W. Quenstedt (ed.), *Fossilium catalogus*, *I(83): Animalia.* 194 pp. W. Junk, Gravenhage.

Bather, F.A. 1900. The Pelmatozoa—Cystidea. *In*: E.R. Lankester (ed.), *A Treatise on Zoology*, *3: Echinodermata*, 38–77. A. & C. Black, London.

Bather, F.A. 1915, 1916. Studies in Edrioasteroidea. VI. *Pyrgocystis* n. g. *Geological Magazine, new series* 6 (2): 5–12, 49–60.

Belka, Z. 1994. Dewońskie budowle węglanowe (Carbonate buildups) Sahary Środkowej i ich związek z podmorskimi źródłami termalnymi (Carbonate mud buildups in the Devonian of the Central Sahara: evidences for submarine hydrothermal venting). *Przegląd Geologiczny* 5: 341–346.

Belka, Z. 1998. Early Devonain Kess-Kess carbonate mud mounds of the eastern Anti-Atlas (Morocco), and their relation to submarine hydrothermal venting. *Journal of Sedimentary Research* 68: 368–377.

Belka, Z. and Berkowski, B. 2005. Discovery of thermophilic corals in an ancient hydrothermal vent community, Devonian, Morocco. *Acta Geologica Polonica* 55: 1–7.

Berkowski, B. 2004. Monospecific rugosan assemblage from the Emsian hydrothermal vents of Morocco. *Acta Palaeontologica Polonica* 49: 75–84.

Berkowski, B. 2006. Vent and mound rugose coral associations from the Middle Devonian of Hamar Laghdad (Anti-Atlas, Morocco). *Geobios* 39: 155–170.

Berkowski, B. 2008. Emsian deep−water Rugosa assemblages of Hamar Laghdad (Devonian, Anti−Atlas, Morocco). *Palaeontographica* 284: 17–68.

Berkowski, B. 2012. Life strategies and function of dissepiments in rugose coral *Catactotoechus instabilis* from the Lower Devonian of Morocco. *Acta Palaeontologica Polonica* 57: 391–400.

Berkowski, B and Klug, C. 2012. Lucky rugose corals on crinoid stems: unusual examples of subepidermal epizoans from the Devonian of Morocco. *Lethaia* 45: 24–33.

Bohatý, J. 2011 Revision of the flexible crinoid genus *Ammonicrinus* and a new hypothesis on its life mode. *Acta Palaeontologica Polonica* 56: 615–639.

Brachert, T., Buggisch, W., Flügel, E., Hüssner, H., Joachimski, M.M., and Tourneur, F. 1992. Controls of mud mound formation: the Early Devonian Kess-Kess carbonates of the Hamar Laghdad, Antiatlas, Morocco. *Geologische Rundschau* 81: 15–44.

Bultynck, P. and Walliser, O.H. 2000. Emsian to Middle Frasnian sections in the northern Tafilalt. *In*: A. El Hassani and A. Tahiri (eds.), Moroccan meeting of the Subcommision on Devonian Stratigraphy (SDS)-IGCP 421 Excursion Guidebook. *Notes et Mémoires du Service Géologique du Maroc* 399: 11–20.

Cavalazzi, B., Barbieri, R., and Ori, G.G. 2007. Chemosynthetic microbialites in the Devonian carbonate mounds of Hamar Laghdad (Anti-Atlas, Morocco). *Sedimentary Geology* 200: 73–88.

De Baets, K., Klug, C., and Plusquellec, Y. 2010. Zlichovian faunas with early ammonoids from Morocco and their use for the correlation between the eastern Anti-Atlas and the western Dra Valley. *Bulletin of Geosciences* 85: 317–352.

De Baets, K., Klug, C., and Korn, D. 2011. Devonian pearls and ammonoid-endoparasite coevolution. *Acta Palaeontologica Polonica* 56: 159–180.

Dehm, R. 1934. Untersuchungen an Cystoideen aus dem rheinischen Unterdevon. *Sitzungsberichte der bayerischen Akademie der Wissenschaften mathematisch-naturwissenschaftliche Abteilung (München)* 1934: 19–43.

Dehm, R. 1961. Über *Pyrgocystis* (*Rhenopyrgus* nov. subgen.) *coronaeformis* Rievers aus dem rheinischen Unter-Devon. *Mitteilungen der bayerischen Staatssammlung für Paläontologie und historische Geologie (München)* 1: 13–17.

Döring, S. 2002. *Sedimentological evolution of the late Emsian to early Givetian carbonate ramp in the Mader (eastern Anti-Atlas, SE-Morocco)*. 116 pp. Unpublished Ph.D. thesis, Tübingen, http://tobias-lib.uni-tuebingen.de/volltexte/2002/560/.

Foote, M. 1995. Morphological diversification of Paleozoic crinoids. *Paleobiology* 21: 273–299.

Foote, M. 1999. Morphological diversity in the evolutionary radiation of Paleozoic and post-Paleozoic crinoids. *Paleobiology* 25 (Supplement): 1–115.

Frech, F. 1902. *Lethaea Geognostica oder Beschreibung und Abbildung der für die Gebirgs-Formationen bezeichnendsten Versteinerungen. I. Theil: Lethaea palaeozoica & Tab; Echinodermen*, 144–146. Schweizerbart, Stuttgart.

Guensburg, T.E. and Sprinkle, J. 2007. Phylogenetic implications of the Protocrinoida: Blastozoans are not ancestral to crinoids. *Annales de Paléontologie* 93: 277–290.

Hammer, Ø., Harper, D.A.T., and Ryan, P.D. 2001. PAST: Palaeontological statistics software package for education and data analysis. *Palaeontologia Electronica* 4 (1): 1–9.

Haude, R. 1993. Limbrachoide, ungewöhnliche Arme der bisher "armlosen" exotischen Seelilie *Tiaracrinus* (Devon; Rheinisches Schiefergebirge). *Göttinger Arbeiten Geologie und Paläontologie* 58: 87–96.

Hauser, J. 1997. *Die Crinoiden des Mitteldevon der Eifler Kalkmulden*. 274 pp. Published by the author, Bonn.

Hauser, J. 2008. *Revision von* Tiaracrinus *(Crinoidea, Cladida) aus dem Paläozoikum der Eifel und dem Sauerland (Rheinisches Schiefergebirge), Massiv Armoricain (Frankreich), Böhmen (Tschechien) und Nord-Afrika (Algerien),* 1–8. Published by the author, Bonn.

Hollard, H. 1974. Recherches sur la stratigraphie des formations du Dévonien moyen, de l'Emsien supérieur au Frasnien, dans le Sud du Tafilalt et dans le Ma'der (Anti-Atlas oriental). *Notes et Mémoires du Service Géologique du Maroc* 264: 7–68.

Holloway, D.J. and Jell, P.A. 1983. Silurian and Devonian edrioasteroids from Australia. *Journal of Paleontology* 57: 1001–1016.

Jaekel, O. 1899. Referat über: Ch. Wachsmuth & Fr. Springer: The North American Crinoidea Camerata. *Neues Jahrbuch für Geologie und Paläontologie* 1899: 374–383.

Jaekel, O. 1901. *Tiaracrinus tedraedra* n. sp. *In*: H. Lotz (ed.), *Pentamerus*-Quarzit und Greifensteiner Kalk. *Jahrbuch Königlich Preussischer geologischer Landesanstalten* 21: 77.

Jaekel, O. 1918. Phylogenie und system der Pelmatozoen. *Paläontologische Zeitschrift* 1: 1–28.

Kaufmann, B. 1998. Facies, stratigraphy and diagenesis of Middle Devonian reef- and mud-mounds in the Mader (eastern Anti-Atlas, Morocco). *Acta Geologica Polonica* 48: 43–106.

Kaufmann, B. 2006. Calibrating the Devonian Time Scale: A synthesis of U-Pb ID-TIMS ages and conodont stratigraphy. *Earth Science Reviews* 76: 175–190.

Klein, T. 1754. Ordre naturel des oursins de mer et fossiles, avec des observations sur les piquants des oursins de mer et quelques remarques sur les bélemnites. 235 pp. C.J.B. Bauche, Paris.

Klug, C. 2001. Life-cycles of Emsian and Eifelian ammonoids (Devonian). *Lethaia* 34: 215–233.

Klug, C. 2002. Quantitative stratigraphy and taxonomy of late Emsian and Eifelian ammonoids of the eastern Anti-Atlas (Morocco). *Courier Forschungsinstitut Senckenberg*, 238: 1–109.

Klug, C., Kröger, B., Rücklin, M., Korn, D., Schemm-Gregory, M., De Baets,

K., and Mapes, R.H. 2008. Ecological change during the early Emsian (Devonian) in the Tafilalt (Morocco), the origin of the Ammonoidea, and the first African pyrgocystid edrioasteroids, machaerids and phyllocarids. *Palaeontographica A* 283 (1, 2 Lfg.): 1–94.

Klug, C., Schulz, H., and De Baets, K. 2009. Red trilobites with green eyes from the Early Devonian of the Tafilalt (Morocco). *Acta Palaeontologica Polonica* 54: 117–123.

Kříž, J. 1992. Silurian field excursions: Prague Basin (Barrandian), Bohemia. *National Museum of Wales, Geological Series* 13: 1–111.

Le Maître, D. 1958a. Contributions à l'étude des faunes dévoniennes d'Afrique du Nord, 1: Echinodermes. *Bulletin du Service de la Carte Géologique de l'Algérie (n. s.)* 20: 113–154.

Le Maître, D. 1958b. Crinoïdes du Dévonien d´Afrique du Nord. *Comptes Rendus sommaires Société Géologique de France* 14: 344–346.

Le Maître, D. 1958c. Le genre *Tiaracrinus* Schultze. *Comptes Rendus de l'Académie des Sciences Paris* 246: 1068–1071.

Le Menn, J. 1987. Nouveaux échinodermes des schistes et calcaires du Dévonien inférieur du Basin de Laval (Massif Armoricain, France. *Geobios* 20: 215–235.

Le Menn, J. 1990. Les calices du genre *Tiaracrinus* (Crinoidea, Inadunata) dans l'Emsien d`Algérie et du Massif Armoricain. *Geobios* 23: 161–167.

Lotz, H. 1901. *Pentamerus*-Quarzit und Greifensteiner Kalk. *Jahrbuch Königlich Preussischer geologischer Landesanstalten* 21: 64–80.

Massa, D., Combaz, A., and Manderscheid, G. 1965. Observations sur les séries Siluro-Dévoniennes des confins Algéro-Marocains du Sud. *Notes et Mémoires, Compagnie Française des Pétroles* 8: 1–187.

Miller, J.S. 1821. A natural history of the Crinoidea or lily-shaped animals, with observation on the genera *Astria, Euryale, Comatula,* and *Marsupites*. 150 pp. Bryan & Co, Bristol.

Miller, S.A. 1883. *The American Palaeozoic Fossils. A Catalogue of the Genera and Species, with Names of Authors, Dates, Places of Publication, Groups of Books in which Found, and the Etymology and Signification of the Words, and an Introduction Devoted to the Stratigraphical Geology of the Palaeozoic Rocks: Echinodermata, 2. Edition*, 247–334. Privately published, Cincinnati.

Miller, S.A. 1891. The structure, classification and arrangement of American Palaeozoic crinoids into families. *Indiana Department of Geology & Natural History, 16th Annual Report* (for 1888, 1889): 302–326.

Miller, S.A. 1892. *North American Geology and Palaeontology. First Appendix*, 665–718. Western Methodist Book Concern, Cincinnati.

Moore, R.C. and Laudon, L.R. 1943. Evolution and classification of Paleozoic crinoids. *Geological Society of America, Special Papers* 46: 1–153.

Moore, R.C., Lane, N.G., Strimple, H.L., and Sprinkle, J. 1978. Order Disparida. *In*: R.C. Moore and C. Teichert (ed.), *Treatise on Invertebrate Paleontology, Part T: Echinodermata 2*, T520–T564. Geologial Society of America and University of Kansas, Boulder, Lawrence.

Prokop, R. 1987. The stratigraphical distribution of Devonian crinoids in the Barrandian area (Czechoslovakia). *Newsletter on Stratigraphy* 17 (2): 101–107.

Prokop, R.J. and Petr, V. 2002. Survey of echinoderms and a new ophiocistioid *Branzoviella talpa* gen. et sp. n. (Echinodermata, Ophiocistioidea) in the Lower Devonian, Lochkov Formation of the Barrandian area, Czech Republic. *Bulletin of the Czech Geological Survey* 77: 237–240.

Rahman, I.A. and Lintz, H. 2012. *Dehmicystis globulus*, an enigmatic solute (Echinodermata) from the Lower Devonian Hunsrück Slate. *Paläontologische Zeitschrift* 86: 59–70.

Roch, E. 1934. Sur des phénomènes remarquables observés dans la région d'Erfoud (confins algéro-marocains du Sud). *Association Études de la Géologie Méditerranéenne Occidentale* 5: 1–10.

Schlüter, C. 1881. Bau der Gattung *Tiaracrinus*. *Sitzungsberichte der niederrheinischen Gesellschaft in Bonn am 8. Juni 1881 Bonn*, 210–212. Niederrheinische Gesellschaft, Bonn.

Schmidt, W.E. 1934. Die Crinoiden des rheinischen Devons, I. Teil: Die Crinoiden des Hunsrückschiefers. *Abhandlungen der preussischen geologischen Landesanstalt (Berlin), Neue Folge* 163: 1–149.

Schultze, L. 1866. Monographie der Echinodermen des Eifler-Kalkes. *Denkschrift Königlichen Akademie der Wissenschaften, mathematisch-naturwissenschaftlichen Classe* 26: 113–230.

Springer, F. 1926. American Silurian crinoids. *Smithsonian Institute Publication* 2871: 1–239.

Sumrall, C.D. and Wray, G.A. 2007. Ontogeny in the fossil record: diversification of body plans and the evolution of "aberrant" symmetry in Paleozoic Echinoderms. *Paleobiology* 33: 149–163.

Töneböhn, R. 1991. Bildungsbedingungen epikontinentaler Cephalopodenkalke (Devon, SE−Marokko). *Göttinger Arbeiten zur Geologie und Paläontologie* 47: 1–114.

Ubaghs, G. and Bouček, B. 1962. Sur la présence du genre *Tiaracrinus* Schultze (Crinoidea) dans le Dévonien inférieur de Moravie (*Tiaracrinus moravicus* n. sp.). *Sborník Ústředního ústavu geologického (Oddíl paleontologický)* 27: 41–50.

Wendt, J. 1993. Steep-sided carbonate mud mounds in the Middle Devonian of the eastern Anti-Atlas, Morocco. *Geological Magazine* 130: 69–83.

APPENDIX II

Other collaborations (abstracts)

Intraspecific variation of phragmocone chamber volumes throughout ontogeny in the modern nautilid *Nautilus* and the Jurassic ammonite *Normannites*

Amane Tajika[1], Naoki Morimoto[2], Ryoji Wani[3], Carole Naglik[1] and Christian Klug[1]

[1] Paläontologisches Institut und Museum, Universität Zürich, Zürich, Switzerland
[2] Laboratory of Physical Anthropology, Graduate School of Science, Kyoto University, Kyoto, Japan
[3] Faculty of Environment and Information Sciences, Yokohama National University, Yokohama, Japan

ABSTRACT

Nautilus remains of great interest to palaeontologists after a long history of actualistic comparisons and speculations on aspects of the palaeoecology of fossil cephalopods, which are otherwise impossible to assess. Although a large amount of work has been dedicated to *Nautilus* ecology, conch geometry and volumes of shell parts and chambers have been studied less frequently. In addition, although the focus on volumetric analyses for ammonites has been increasing recently with the development of computed tomographic technology, the intraspecific variation of volumetric parameters has never been examined. To investigate the intraspecific variation of the phragmocone chamber volumes throughout ontogeny, 30 specimens of Recent *Nautilus pompilius* and two Middle Jurassic ammonites (*Normannites mitis*) were reconstructed using computed tomography and grinding tomography, respectively. Both of the ontogenetic growth trajectories from the two *Normannites* demonstrate logistic increase. However, a considerable difference in *Normannites* has been observed between their entire phragmocone volumes (cumulative chamber volumes), in spite of their similar morphology and size. Ontogenetic growth trajectories from *Nautilus* also show a high variation. Sexual dimorphism appears to contribute significantly to this variation. Finally, covariation between chamber widths and volumes was examined. The results illustrate the strategic difference in chamber construction between *Nautilus* and *Normannites*. The former genus persists to construct a certain conch shape, whereas the conch of the latter genus can change its shape flexibly under some constraints.

Subjects Developmental Biology, Evolutionary Studies, Marine Biology, Paleontology, Zoology
Keywords Ammonoidea, Nautilida, Intraspecific variability, Sexual dimorphism, Growth, 3D reconstruction, Jurassic, CT scan, Cephalopoda

Submitted 19 June 2015
Accepted 18 September 2015
Published 6 October 2015

Corresponding author
Amane Tajika,
amane.tajika@pim.uzh.ch

Academic editor
Laura Wilson

Additional Information and Declarations can be found on page 24

DOI **10.7717/peerj.1306**

How to cite this article Tajika et al. (2015), Intraspecific variation of phragmocone chamber volumes throughout ontogeny in the modern nautilid *Nautilus* and the Jurassic ammonite *Normannites*. **PeerJ 3:e1306; DOI 10.7717/peerj.1306**

Swiss J Palaeontol (2013) 132:23–44
DOI 10.1007/s13358-012-0050-y

Taphonomy and palaeoecology of the green Devonian gypidulid brachiopods from the Aferdou El Mrakib, eastern Anti-Atlas, Morocco

Lorena Tessitore · Mena Schemm-Gregory · Dieter Korn · Ferdinand R. W. P. Wild · Carole Naglik · Christian Klug

Received: 27 August 2012 / Accepted: 11 December 2012 / Published online: 12 February 2013

Abstract On Aferdou El Mrakib, a large reef mound in the Maïder region (Anti-Atlas, Morocco), thick-shelled gypidulids of two genera are locally very abundant. Like *Stringocephalus* in the shallow water limestone formations in Germany, these Moroccan brachiopods of the genera *Devonogypa* and *Ivdelinia* often display greenish shells. By analysing these shells by EDX, it turned out that the colour was possibly caused by impurities of Fe^{2+}-ions. The concentration varies, indicating that the colour is less dependent on the concentration than on shell thickness, because only the thickest parts of the shells appear green and thin-shelled forms never display the green colour. There is also some indication that the Fe content increases towards deeper shell layers (further away from the surface). In addition, we examined the quality and spatial distribution of sublethal injuries in over 200 specimens of *Devonogypa* and *Ivdelinia*. Shape, spatial distribution on the shells, and abundance of the sublethal injuries support the hypotheses that (1) the injuries had several causes, (2) some of these were inflicted by predators, probably cephalopods, and (3) many fractures and deformations might have been caused by the brachiopod shells hitting each other in dense populations in agitated water. The existence of dense clusters, built by the association of members of both genera or of only one taxon, is corroborated by the patchy occurrence of these brachiopods.

Keywords Brachiopods · Taphonomy · Palaeoecology · Reef-mounds · Devonian · Morocco

Electronic supplementary material The online version of this article (doi:10.1007/s13358-012-0050-y) contains supplementary material, which is available to authorized users.

L. Tessitore (✉) · C. Naglik · C. Klug
Palaeontological Institute and Museum, University of Zurich, Karl Schmid-Strasse 4, 8006 Zurich, Switzerland
e-mail: lorena.tessitore@uzh.ch

C. Naglik
e-mail: carole.naglik@pim.uzh.ch

C. Klug
e-mail: chklug@pim.uzh.ch

M. Schemm-Gregory
Centro de Geociências da Universidade de Coimbra, Largo Marquês de Pombal, 3000-272 Coimbra, Portugal
e-mail: Mena.Schemm-Gregory@dct.uc.pt; Mena.Schemm@gmx.de

D. Korn
Museum für Naturkunde, Leibniz-Institut für Evolutions- und Biodiversitätsforschung, Humboldt-Universität, Invalidenstraße 43, 10115 Berlin, Germany
e-mail: dieter.korn@mfn-berlin.de

F. R. W. P. Wild
Anorganisch-chemisches Institut, University of Zurich, Winterthurerstrasse 190, 5087 Zurich, Switzerland
e-mail: fwild@aci.uzh.ch

Birkhäuser

N. Jb. Geol. Paläont. Abh. 281/3, 247–266
Stuttgart, September 2016

Article

Neptunian dykes in the Devonian carbonate buildup Aferdou El Mrakib (eastern Anti-Atlas, Morocco) and implications for its growth

Lorena Tessitore, Carole Naglik, Kenneth De Baets, Thomas Galfetti, Christian Klug

With 9 figures and 2 tables

Abstract: Aferdou El Mrakib is the largest single carbonate buildup in the eastern Anti-Atlas, Morocco. Its sediments are intersected by several Neptunian dykes. Herein, we compare their facies, spatial arrangement and the associated fauna to that of Neptunian dykes from other mound localities in Morocco and elsewhere in order to assess their origin as well as that of the mound. One of the studied dykes is filled with pisoids. Its facies suggests some kind of seep origin, but the carbon and oxygen isotopic values have only slightly negative signatures, which might be diagenetic, thus prohibiting further interpretation. Nevertheless, the unique occurrence of pisoids at a depth of c. 50 metres below the mound surface within a dyke is herein interpreted as supporting the presence of a source with a considerable discharge.

Key words: Morocco, Devonian, Maïder Basin, carbonate buildups, Neptunian dykes, pisoids.

DOI: 10.1127/njgpa/2016/0598

www.schweizerbart.de
0077-7749/2016/0598 $ 5.00